IDENTIFICATION OF ANATOMICAL PREDICTORS OF LANGUAGE RECOVERY AFTER STROKE WITH DIFFUSION TENSOR IMAGING

Forkel, Stephanie Jacqueline

Awarding institution:
King's College London

Take down policy

If you believe that this document breaches copyright please contact librarypure@kcl.ac.uk providing details, and we will remove access to the work immediately and investigate your claim.

Institute of Psychiatry at The Maudsley   **King's College LONDON**   **King's College Hospital NHS**
NHS Foundation Trust

Doctoral dissertation submitted to the Department of Neuroimaging at the Institute of Psychiatry, King's College London, University of London, England,

United Kingdom.

Specialisation in Clinical Neuroimaging

IDENTIFICATION OF ANATOMICAL PREDICTORS OF LANGUAGE RECOVERY AFTER STROKE WITH DIFFUSION TENSOR IMAGING

Doctoral dissertation submitted by

Stephanie Jacqueline Forkel

Date of Birth 8th July 1985

First academic supervisor:	Prof. Steve Williams
Second academic supervisor:	Prof. Declan Murphy
Academic co-supervisor:	Dr. Marco Catani
Clinical supervisor:	Prof. Lalit Kalra
Examination committee:	Dr. Alexander Leff (UCL, London)
	Dr. Thomas Barrick (ULU, London)

Submission Date: 30th August 2013

Viva Date: 17th December 2013

'Illness is the night-side of life, a more onerous citizenship. Everyone who is born holds dual citizenship, in the kingdom of the well and in the kingdom of the sick. Although we all prefer to use only the good passport, sooner or later each of us is obliged, at least for a spell, to identify ourselves as citizens of that other place.'

Susan Sontag

Dedicated to my patients, my mother and the late Andrew Millar

During the course of this study you all had to exchange your passports, some temporarily some for good and one even had to return his. I am thankful most of you regained your citizenship and honour having had the pleasure of meeting you.

DISCLAIMER & PERMISSION TO USE

Disclaimer

Reference in this dissertation to any specific commercial products, process, or service by trade name, trademark, manufacturer, or otherwise, does not constitute or imply its endorsement, recommendation, or favouring by the University of London. The views and opinions of the author expressed herein do not state or reflect those of the University of London.

Permission to use

In presenting this dissertation, in partial fulfilment of the requirements for a PhD degree from the University of London, I agree that the Libraries of this University may make it freely available for inspection.

I further agree that permission for copying of this dissertation in any manner, in whole or in part, for scholarly purposes may be granted by the professors who supervised my dissertation or, in their absence, by the Head of the Department in which my work was done.

It is understood that any copying or publication or use of this dissertation or parts thereof for financial gain shall not be allowed without my written permission. It is also understood that due recognition shall be given to the author and to the University of London in any scholarly use which may be made of any material in this dissertation.

_____

Stephanie J. Forkel, MSc

ABSTRACT

Background Stroke-induced aphasia is associated with adverse effects on quality of life and the ability to return to work. However, the predictors of recovery are still poorly understood. Anatomical variability of the arcuate fasciculus, connecting Broca's and Wernicke's areas, has been reported in the healthy population using diffusion tensor imaging tractography. In about 40% of the population the arcuate fasciculus is bilateral and this pattern is advantageous for certain language related functions, such as auditory verbal learning (Catani et al. 2007).

Methods In this prospective longitudinal study, anatomical predictors of post-stroke aphasia recovery were investigated using diffusion tractography and arterial spin labelling.

Patients An 18-subject strong aphasia cohort with first-ever unilateral left hemispheric middle cerebral artery infarcts underwent post stroke language (mean 5±5 days) and neuroimaging (mean 10±6 days) assessments and neuropsychological follow-up at six months. Ten of these patients were available for reassessment one year after symptom onset. Aphasia was assessed with the Western Aphasia Battery, which provides a global measure of severity (Aphasia Quotient, AQ).

Results Better recover from aphasia was observed in patients with a right arcuate fasciculus [beta=.730, t(2.732), p=.020] (tractography) and increased fractional anisotropy in the right hemisphere ($p<0.05$) (Tract-based spatial statistics). Further, an increase in left hemisphere perfusion was observed after one year ($p<0.01$) (perfusion). Lesion analysis identified maximal overlay in the periinsular white matter (WM). Lesion-symptom mapping identified damage to periinsular structure as predictive for overall aphasia severity and damage to frontal lobe white matter as predictive of repetition deficits.

Conclusion These findings suggest an important role for the right hemisphere language network in recovery from aphasia after left hemispheric stroke.

ACKNOWLEDGEMENTS

I am deeply indebted and eternally grateful to my mother, **Dr. Carola Forkel.** You are remarkably strong and brave and I am profoundly obliged for everything you did. Every minute we can spend together I savour. You started my passion for science when you did your PhD and it has stayed with me ever since. Thank you for being such a great mum and for never ever giving up the fight.

In tiefster Dankbarkeit meiner Oma, **Heidemarie Kranich**. Du hasst Danksagungen, daher hier nur das Allerwichtigste: Du bist eine enorm starke Frau und ich bin stolz darauf Deine Enkelin zu sein. Danke für Alles.

A massive thanks to my London and Munich girls**!** I am truly blessed to have you all in my live!

Meinen tiefsten Dank an **Manuela L. Pfeiffer.** Danke, dass Du Familie bist und nicht nur in jeder Situation die richtigen Worte findest sondern auch immer da warst!

Tanja Jäckle, ich danke Dir für die pinken Wolken in meinem Leben, die unzähligen Brez'n-Stunden und dafür, dass unsere Stadt immer unsere Bank haben wird. Danke, dass Du Teil meiner jeden Welt bist.

Vera D'Almeida, you truly are my life advisor and my situation would be very different now if it weren't for you. I thank you from the bottom of my heart for everything my dearest! (You do know that mentioning your name here justifies another box of Millie's ;-))

Chloe Morris (Langlois) thanks for brightening up my days in so many ways! Your lovely persona and amazing support was ever so valuable and helpful. Be assured that I am honestly happy for you whatever you decide to do.

Dr. Anne, danke für Dein stets sonniges Gemüt, die Spontanbesuche und die vielen Knusperflocken!

Lucie Eisenmayer, **Antonia Beermann**, und **Maike Kummerhoff**. Danke, dass Ihr mich stets aufgenommen habt und München dank Euch immer mein zuhause geblieben ist.

Andrew Millar, you taught me about the strength, the grace and the agony that comes with the law of impermanence. Milles mercis for believing in love the way you did. You are deeply missed.

PUBLICATIONS

Peer-reviewed articles

Forkel SJ. Heinrich Sachs (1863-1928). *Journal Neurology*, in press

Forkel SJ, Thiebaut de Schotten M, Dell'Acqua F, Kalra L, Murphy D, Williams S & Catani M. Anatomical predictors of aphasia recovery: a tractography study of bilateral perisylvian language networks *Brain,* doi: 10.1093/brain/awu113

Forkel SJ, Mahmood S, Vergani F & Catani M. Sach's atlas on the white matter of the human occipital cortex *Cortex*, in press

Forkel SJ, Thiebaut de Schotten M, Kawadler JM, Dell'Acqua F, Danek A, Catani M. Anatomy of fronto-occipital connections from early blunt dissections to contemporary neuroimaging. *Cortex doi: 10.1016/j.cortex.2012.09.005*.

Vergani F, Mahmood S, Morris CM, Mitchell P & **Forkel SJ**. Intralobar fibres of the occipital lobe: A post mortem dissection study *Cortex, doi:10.1016/j.cortex.2014.03.002*

Catani M, Dell'Acqua F, Bizzi A, **Forkel SJ** et al., Beyond cortical localisation in clinico-anatomical correlation. *Cortex* 48(10):1262-87. 2012

Thiebaut de Schotten M, Dell'Acqua F, **Forkel SJ,** et al. A Lateralized Brain Network for Visuo-Spatial Attention. *Nature Neuroscience* 18;14(10):1245-6. 2011

Catani M, Craig M, **Forkel SJ**, et al. Altered integrity of perisylvian language pathways in schizophrenia: relationship to auditory hallucinations. *British Journal of Psychiatry* 15;70(12):1143-50. 2011

Book chapters & published conference contributions

Catani M, **Forkel SJ**, Thiebaut de Schotten M. Asymmetry of white matter pathways in the brain. In The Two Halves Of The Brain: Information Processing In The Cerebral Hemispheres (Eds, Hugdahl, K & Davidson, RJ). *MIT Press*. 2010

Forkel SJ, et al. Lateralisation of the arcuate fasciculus predicts aphasia recovery at 6 months. *Procedia Social and Behavioral Sciences* 23:164-166. 2011

Sürer F, **Forkel S**, et al. Towers of Hanoi and London on a tablet-PC Correlations with other executive tests. *Aktuelle Neurologie* 34:122. 2007

TABLE OF CONTENTS

LIST OF FIGURES

LIST OF TABLES

LIST OF ABBREVIATIONS & ACRONYMS

5-HT	Serotonin
ACA	Anterior cerebral artery
AcomA	Anterior communicating artery
ADC	Apparent Diffusion Coefficient
AF	Atrial fibrillation
AICc	Corrected Akaike Information Criterion
AQ	Aphasia Quotient
AS	Anterior segment of the arcuate fasciculus
B0	Main magnetic field
B1	Second magnetic field
BA	Brodmann area
BOLD	Blood-oxygen-level-dependent effect
Ca^{2+}	Calcium
cASL	Continuous arterial spin labelling
CBF	Cerebral Blood Flow
CCEP	Cortico-cortical evoked potential
CI	Confidence interval
Cl^-	Chloride
CSF	Cerebral spinal fluid
CT	Computer tomography
CVLT	California Verbal Learning Test
D	Diffusion coefficient
df	Degrees of freedom
DTI	Diffusion Tensor Imaging
DWI	Diffusion-weighted Imaging
e.g.	Exempli gratia, for example
ECA	External carotid artery
ECG	Electrocardiogram
EEG	Electroencephalography
ELAN	Early left anterior negativity
EPI	Echo-planar imaging
ERP	Event-related potential
et al.	Et alii, and colleagues

Etc.	Et cetera, and things like that
EV	Explanatory variable
FA	Fraction anisotropy
FAT	Frontal Aslant Tract
FID	Free induction decay
FLAIR	Fluid attenuated inverse recovery
fMRI	Functional Magnetic Resonance Imaging
FOD	Fibre orientation distribution
FOF	Fronto-occipital fasciculus
FSE	Fast spin echo
FSL	FMRIB Software Library
few	Familywise error
G	Gramm
GCS	Glasgow Coma Scale
GE	General Electronics (MRI scanner manufacturer)
GLM	General Linear Model
GM	Grey matter
G_x	Frequency-encoding gradient
G_y	Phase-encoding gradient
G_z	Slice-encoding gradient
H_0	Null hypothesis
H_2O	Water molecules
HARDI	High Angular Resolution Diffusion Imaging
HASU	Hyperacute stroke unit
i.e.	Id est, that is
IAP	Intracarotid amobarbital procedure (also known as WADA test)
ICA	Internal carotid artery
ICD-10	International Statistical Classification of Diseases *and Related Health Problems*, 10th Revision
ICH	Intracranial haemorrhage
ID	Identification number, identifier
IES	Intraoperative electrical stimulation
IFG	Inferior frontal gyrus
iFOF	Inferior fronto-occipital fasciculus
ILF	Inferior longitudinal fasciculus
IPL	Inferior parietal lobe
JSTOR	Digital library of academic journals, books, and primary sources

K-S	Kolmogorov-Smirnov Test of normality
KCH	King's College Hospital
KCL	King's College London
L	Left
LH	Left hemisphere
LI	Laterality Index
LOOCV	Leave-one-out-cross-validation
LS	Long segment of the arcuate fasciculus
LSD	Fisher's least significant difference
MCA	Middle cerebral artery
MD	Mean diffusivity
MdLF	Middle longitudinal fasciculus
MGN	Middle geniculate nucleus
min	Minute
ml	Millilitre
mm^2	Square millimetre
mm^3	Cubic millimetre
mmol	Millimoles
MNI	Montreal Neurological Institute
MRI	Magnetic Resonance Imaging
ms	Millisecond
n	Number of participants/patients
n/a	Not applicable
Na^{2+}	Sodium
NHS	National Health Service in the UK
NIHSS	National Institute of Health Stroke Scale
NMR	Nuclear magnetic resonance
no	Number
NPM	Non-parametric mapping programme
O	Oxygen
P	Percentage
p	Page
p	Significance level
PCA	Posterior cerebral artery
PcomA	Posterior communicating artery
PD	Proton density
PET	Positron emission tomography

Pre-SMA	Pre-supplementary motor area
PS	Posterior segment of the arcuate fasciculus
PubMed	US National Library of Medicine
PWI	Perfusion-weighted imaging
R	Right
R&D	Research & Development
rCBF	Regional cerebral blood flow
REC	Research Ethic Committee
RF	Risk Factor
RF	Radio frequency
RGB	Red-green-blue colour coding
RH	Right hemisphere
ROI	Region of Interest
rtPA	Recombinant tissue plasminogen activator
s	Second
SAH	Subarachnoidal haemorrhage
SCOPUS	Digital library of academic journals, books, and primary sources
SD	Spherical deconvolution
SD	Standard deviation
sFOF	Superior fronto-occipital fasciculus
SLF	Superior longitudinal fasciculus
SLSR	South London Stroke Register
SMA	Supplementary motor area
SNR	Signal-to-noise ratio
SPGR	Spoiled Gradient Echo
SPM	Statistic Parametric Mapping
SPSS	Statistical Package for the Social Sciences
STG	Superior temporal gyrus
SVD	Small vessel disease
T	Tesla
T1	Longitudinal relaxation
T2/T2WI	Transverse relaxation/ T2-weighted imaging
TBSS	Tract-Based Spatial Statistics
TE	Echo Time
TIA	Transient ischemic attack
TR	Relaxation Time
UCL	University College London

UK	United Kingdom
US	United States
VBM	Voxel-based morphometry
VLSM	Voxel lesion-symptom mapping
Voi	Volume of interest
VPL	Ventral posterior lateral nucleus
WAB-R	Western Aphasia Battery revised
WHO	World Health Organisation
WM	White matter

CHAPTER 1   FROM POST MORTEM TO IN VIVO DISSECTIONS

'It is a tragedy that so many of us learn so little from history

that could guide us now and in the future.'

(William Fields & Noreen Lemark, 1989)

An introduction to the history of connectional anatomy (white matter) in general, and the asymmetry of the perisylvian network in particular, will be given below. This chapter is adopted from a book chapter that I jointly authored with Marco Catani and Michel Thiebaut de Schotten in 2009.

Most of the 19th and 20th century white matter (WM) literature is only available in German hence my main contribution to this chapter was the research and translation of the historic literature.

A digital literature review was conducted using Internet databases (i.e. PubMed, SCOPUS, and JSTOR). To ensure a thorough search no exclusion criteria were applied and multiple combinations of keywords were used. English keywords included: arcuate fasciculus or bundle, white matter; German keywords involved: Associationsbündel, Bogenbündel, Markfasern, Ungenannte Marksubstanz. Additionally, hand-searched original reports from the 19th century were obtained from historical collections of several London-based libraries, such as the Institute of Psychiatry at King's College London (Meynert's and Wernicke's books), the British Library (Burdach's books), and the Royal Society in London (Reil's *Archiv für die Psychiatrie*), as well as several Germany-based university libraries including the Anatomical Institute at Ludwig-Maximilians-Universität in Munich (Burdach's books). Where available private libraries of the three authors were reviewed as well. Original reports were translated by German and French native speakers, namely Stephanie Forkel and Michel Thiebaut de Schotten. Anatomical validity of the translations was discussed with and reviewed by Marco Catani.

Sections of the book chapter that relate primarily to commissural (i.e. corpus callosum and anterior commissure) and projection pathways (i.e. cortico-spinal tract) have been exempt from this thesis chapter and only the association (i.e.

uncinate, inferior fronto-occipital, and arcuate) pathways are discussed here. Chapter images have been replaced with more educative images that were only produced after its publication. For a comprehensive introduction to the history and the asymmetry of all white matter pathways, please see the corresponding publication (Catani et al. 2010).

1.1   Introduction

> *"Here are eight instances in which the lesion was in the posterior third of the third frontal convolution. This number seems to me to be sufficient to give strong presumptions. And the most remarkable thing is that in all the patients the lesion was on the left side. I do not dare draw conclusions from this.*
>
> *—Paul Broca (1863)*

With these words, from a short report of a series of patients with acquired speech deficits, begins the modern period of the study of cerebral asymmetry. Despite Broca's reticence to draw any conclusion from his clinical–anatomical observation, his words clearly allude to a concept that has stood the test of time: the asymmetrical distribution of functions in the human brain. In later writings, Broca not only vehemently defended his idea of left lateralisation of speech but also initiated the discussion on the anatomical correlates of cerebral dominance (Finger 1994). This became an intensely growing field of research where anatomists focused their attention on either macroscopic (e.g., volume of gyri) or microscopic (e.g., cytoarchitectonic) differences between the two hemispheres.

However, a handful of researchers faithful to their belief on the importance of brain connections have tried to explain cerebral dominance in terms of white matter asymmetry. Their efforts were often been limited to speculation, as the availability of reliable methods to trace connections in the human brain have been lacking for decades.

Recent developments in magnetic resonance imaging (MRI) have introduced new methods, based on diffusion imaging tractography that can reconstruct white matter trajectories in the living human brain (Basser et al. 2000; Le Bihan 2003) (please see imaging chapter for details). The resultant influx of information on human connectional anatomy derived from tractography is likely to fill the gap in our anatomical knowledge of human brain connections and reinvigorate models of

cognition based on asymmetrical distribution of large-scale networks (Catani & Thiebaut de Schotten 2008).

Hence, the subject matter of this chapter is an overview of the hodological (pathway-based) approach to cerebral dominance and its historical context, with a special focus on the perisylvian networks.

Last, we present preliminary contributions from diffusion imaging tractography to increase our knowledge of the anatomy of the perisylvian networks, its heterogeneity in the healthy population, and possible functional and behavioural correlates of different patterns of lateralisation. […] One outcome of this review will be to highlight the merits of the hodological approach to cerebral dominance, and its modern pursuit with diffusion imaging tractography.

1.2 Early Hodological Approaches to Higher Cognitive Functions and Cerebral Dominance

The seventeenth century was a time of great accomplishments in the brain sciences, where anatomists called for a more realistic model of brain function(s) than one tied to the pineal gland and spirits flowing from the ventricles into the hollow nerves (C. Smith 2007a).

For the first time, distinct anatomical features of the brain surface were highlighted (e.g., lateral fissure as the most prominent cleft of the cerebral hemisphere) and the anatomy of previously unknown structures described in some details (e.g., corpus striatum). Others, such as Nicolaus Steno (1669), began to draw attention to the complexity of the fibre system:

> *We need only view a dissection of that large mass, the brain, to have ground to bewail our ignorance. On the very surface you see varieties which deserve your admiration: but when you look into its inner substance you are utterly in the dark, being able to say nothing more than that there are two substances, one greyish and the other white, which last is continuous with the nerves distributed all over the body. […] If this substance is everywhere fibrous, as it appears in many places to be, you must own that these fibres are disposed in the most artful manner; since all the diversity of our sensations and motions depend upon them. We admire the contrivance of*

the fibres of every muscle, and ought still more to admire their disposition in the brain, where an infinite number of them contained in a very small space, do each execute their particular offices without confusion or disorder. (Translated in Stirling (1902)*, p. 32)*

Despite these early anatomical achievements, new findings on the anatomy of white matter and novel ideas about the functional correlates of brain connections were not forthcoming.

Throughout the eighteenth century, the development of physiological methods to study the nervous tissue allowed the formulation of theories of nerve conduction as scientists moved away from "fluidist" or "vibratory" explanations and began to experiment with electricity. This was an important development, although it resulted in the shifting of attention from human to animal anatomy and from the central nervous system to peripheral nerves.

The emergence of the hodological theme as a central component of neurological and psychiatric thinking took place in the nineteenth century and can be attributed to the confluence of two developments: the extension of neuroanatomical research from a description of surface morphology to the dissection of the subcortical tracts, and the spread of 'associationist' models of cognitive functions from the realm of psychology to that of neurology and psychiatry (Catani & Mesulam 2008b). An obvious conduit for this convergence was the identification of white matter pathways.

Below, we review the pioneering anatomical work of Johann Christian Reil and Karl Friedrich Burdach, which led to the discovery of most association tracts of the human brain. We then introduce the work of Theodor Hermann Meynert and his 'associationist' school, which had a profound influence across countries, continents, and centuries. In the final section of this first part, we discuss the disconnection paradigm derived from 'associationist' theory and Hugo Liepmann's model of cerebral dominance based on the asymmetry of large-scale sensory-motor networks for praxis.

1.3   The Discovery of the Association White Matter Tracts

The first development pivotal to the emergence of the hodological approach to brain function was the identification of association tracts connecting distant regions within the same cerebral hemisphere. Several anatomists made important contributions to this field, but Johann Christian Reil and Karl Friedrich Burdach (see **Figure 1**) stand out for the originality of their findings and the far-reaching influence of their writings.

In 1788 Johann Christian Reil became professor at the University of Halle and director of the Clinical Institute at the age of 29 (Scharf 1960; Steffens 1815). In 1795 Reil founded the first physiology journal in Germany, namely the *Archiv für die Physiologie,* which he used as a vehicle for many publications about anatomy and physiology, including his own description of cortical and subcortical brain structures (Reil 1809a; Reil 1812b). His anatomical discoveries were derived from the development of a method based on the soaking of the brain in alcohol (initially he used brandy) that made it more suitable for dissection (Reil 1808). This method allowed him to reveal the course of the white matter bundles running beneath the major convolutions of the human brain (see **Figure 1**).

JOHANN REIL (1809, 1812)	KARL BURDACH (1822)	NOMINA ANATOMICA (1987)
Ungenannte Marksubstanz	Bogenbündel (arcuatus)	Arcuate fasciculus
Hakenförmiges Markbuendel	Hakenbündel (unciformes)	Uncinate fasciculus
Stratum von Längenfasern	Längenbündel (longitudinalis inferior)	Inferior longitudinal fasciculus
Bedeckte Bänder	Zwingen (cingula)	Cingulum

Johann Christian Reil (1759-1813)

Karl Friedrich Burdach (1776-1847)

Figure 1   The discovery of the association tracts of the human brain

The table shows the correspondence between Reil's original terms in German (Reil 1812b; Reil 1809b; Reil 1812a), Burdach's German and Latin terminology (Reil 1809b; Burdach 1822) and the names used in contemporary international nomenclature (Meyer 1970; Commitee 1989). A, B) The development of a method based on the soaking of the brain in alcohol that made it more suitable for dissection led Reil to discover the major association white matter tracts of the human brain. C, D) Burdach confirmed the findings of Reil and

introduced a novel nomenclature for the main association tracts that remains almost unchanged in the current international nomenclature.

Among the tracts that Reil identified were the medial curving fibres within the cingulate gyrus (i.e. *Bedeckte Bänder* or *Längenbänder)* (Reil 1812b) and the lateral arching connections coursing beneath the perisylvian fronto-parieto-temporal gyri that he described as the unnamed white matter substance (i.e. *Ungenannte Marksubstanz*) (Reil 1812a). Other tracts that he identified on the most ventral part of the brain are the hooked-shaped fibres behind the insula (i.e. *Hakenförmiges Markbuendel*) (Reil 1809c) and a longitudinal bundle between the occipital and temporal lobes (i.e. *Stratum von Längenfasern*) (Reil 1812b). Reil illustrated and commented on the presence of these tracts on both hemispheres and their possible role:

> *Each hemisphere is an independent organ and forms a closed loop in its own; both loops flow into each other through the mentioned structures [arcuate and uncinate].*
> (Reil 1809b)

Reil's findings were confirmed a decade later by Karl Friedrich Burdach, who was conferred doctor in medicine in Leipzig in 1799 and received a professorship for anatomy, physiology, and forensic medicine in Dorpat in 1811 (Meyer 1970). Here he commenced his anatomical dissections of the brain that he continued after moving to Königsberg as director of the Anatomical Institute. His studies culminated in the *Vom Baue und Leben des Gehirns;* a three-volume textbook containing confirmatory dissections of Reil's findings and his own original descriptions of some previously unidentified tracts, including the fibres connecting the occipital to the frontal lobe, later identified as part of the inferior fronto-occipital fasciculus (Curran 1909) (**Figure 2**). He also used Latin names for the major tracts, which became widely adopted and still remain almost unchanged in the current international anatomical nomenclature (see **Figure 1**).
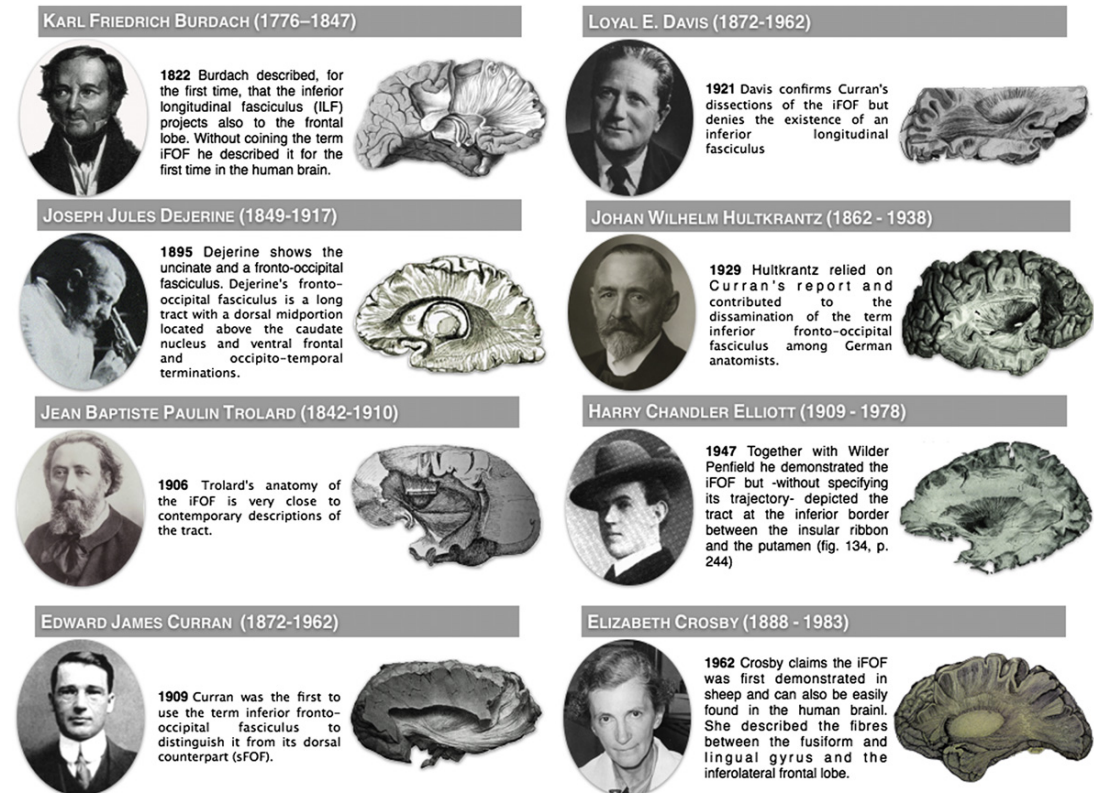
Figure 2   Seminal historical contributions to the anatomy of the inferior fronto-occipital fasciculus in the healthy human brain. Taken from Forkel et al. (2012)

Both, Reil and Burdach, were fascinated by Schelling's natural philosophy, which inspired their functional interpretations and speculative reflections (Meyer 1970). However their functional inferences were either dismissive of the role of the association tracts (e.g., Reil) or based on erroneous physiological speculations (e.g., Burdach):

> *The core [of the brain] is constituted by the organizations of the crus cerebri [Hirnschenkel] and the corpus callosum [Balken]. These together with the gyri and the grey matter seem to be the fundamental component of the brain; everything else seems to be just connection and transduction apparatus.* (Reil 1809a)

> *Fantasy is warm and lively; organically linked to blood circulation and can therefore be excited by the fast change of blood, resulting in a stronger tension in the brain. Reason in contrast is cold and cautious; any tempestuous movement is hostile to it [...]. The longitudinal system [association fibres] is more closely*

> *linked to the blood vessels [...] its alert activation causes*
> *more blood to be drawn to the vascular plexus [...]. The*
> *transverse [commissural] system on the contrary is in no*
> *special relation to the vascular system.* p.338, *Burdach*
> *(1826)*

This theoretical vacuum left the field open to the triumph of cortical 'localisationist' theories and the fierce antilocalisationist opposition based on holistic stances. One would have to wait until the second half of the century for the emergence of the hodological theme following the spread of 'associationist' models of cognitive functions from the realm of psychology to that of neurology and psychiatry (James 1890; Meynert 1885; Wundt 1904). According to the associationist doctrine, the formation of concepts, the recall of memories, the naming of objects, and even the spontaneous and voluntary initiation of movement, required the associative convergence (or integration) of information from multiple sources. The association tracts seemed to be the ideal anatomical substrate for such a theory.

1.4   Meynert's Associationist Theory of Brain Function

The idea of association has roots in Aristotle's writing and has been passed down the centuries from Epicurus through Hobbes to Hartley (Glassman & Buckingham 2007).

However, the credit for the formulation of an associationist theory grounded on anatomy falls to a psychiatrist known by his contemporaries as the great brain anatomist, Theodor Meynert, who was then Professor of Nervous Diseases and Director of the Psychiatric Clinic in Vienna. He took an original position with regard to the explanation of brain function and mental disorders (Catani & ffytche 2005). He first rejected contemporary theories of predisposition, which became the psychiatric the theory of moral insanity:

> *As regards to the theory of predisposition, and more*
> *particularly the doctrine of hereditary, which has been carried*
> *to the extreme of assuming the existence of innate idea, and*
> *which in clinical medicine, has led to the erroneous theory of*
> *moral insanity, I have deemed it necessary to criticise, in its*
> *proper connections, Darwin's theory of the inheritance of*
> *acquired faculties, as has been done before me by other*

> German authors, among them DuBois-Reymond and Weissman. It is taking altogether too simple a view of things, to regard morality as one of man's talents, and as a definite psychical property, which is present in some persons and lacking in others. (Meynert, 1885, preface, viii).

Thus, "dissatisfied with the statistical method, which laid inordinate stress upon hereditary predisposition to disease," Meynert resolved for an anatomical approach to mental disorders:

> In view of the necessity of starting from anatomical facts, I have endeavoured, in every case, not only to give due weight to the structure of the brain as the fundamental basis for the various forms of disease, but have endeavoured, with the same end in view, to insist upon and to explain every visible symptom exhibited by the patient. (Meynert, 1885, preface, vii)

Meynert's ambitious clinical research program aimed to establish the anatomical bases not only of mental disorders but also of specific symptoms; the success of its realization depending entirely on the deep anatomical knowledge of the human brain.

In 1884 he published (in German) *Psychiatry—Clinical Treatise on Diseases of the Forebrain based upon a study of its structure, functions, and nutrition*, impelled by the conviction of a need for a "scientific" treatise on mental disease. The title is a direct attack on the "science of psychiatry [that] has been too largely subjective" and refers "to the fundamental studies [of structure] indispensable to an understanding of the clinical manifestations of mental disease" (Meynert, 1885, p. Vi). The first volume of the *Treatise*, which Heinrich Sachs translated and published in English the year after (Meynert 1885), contains Meynert's description and classification of the main white matter tracts of the brain (see **Figure 3**). Before him, other anatomists such as Vieussens, Vicq d'Azyr, Reil, Burdach, and Gall had described differences in origin, course, and termination of fibres, but Meynert was the first to put forward an orderly classification of white matter fibres into three groups.
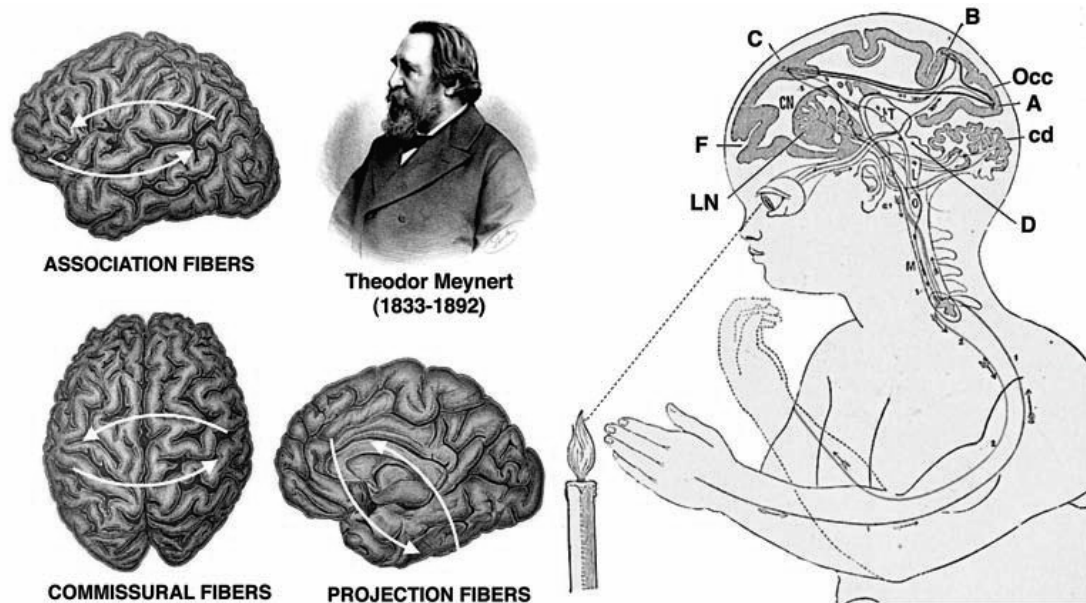
Figure 3   White matter classification after Meynert and his explanation of limb movement

Meynert used this diagram as an example to explain his associationist theory applied to the mechanism of an unconscious movement of the arm. A flame has injured a child's hand and the hand is therefore withdrawn as a reflex. The visual image of the flame, the painful sensation and the sensation of the reflex movement will also be conveyed to cortical centres (A and B). 'Since centre C is connected with [the other sensory centres] the child need not actually burn his hand again before guarding against the flame; but the memory of the flame and of its effect (through association with the centre in which the painful sensation has been stored), will suffice, through the one or the other of these associations, to initiate a movement which will put the arm beyond the reach of the flame.' A. Part of the visual cortex; B. Part of the cortical centre for cutaneous sensation; C. A centre in the for sensations of innervation; cd. Cerebellum; CN. Caudate nucleus; D. Mesencephalon; F. Frontal cortex; L. Pons Variolii; LN. Nucleus lenticularis; M. Medulla oblongata, terminating with a cross-section of the cervical spinal cord; O. Medulla oblongata; Occ. Occipital cortex; hT. Thalamus opticus. On the right black connections correspond to association fibres, blue, centripetal projection fibres and red centrifugal projection fibres.

The first group consisted of *projection* fibres, the ascending or descending pathways arising and terminating in the cortex, the second of *commissural* fibres, which connected cortex in both hemispheres (interhemispheric), and the third of *association* fibres, which connected cortical regions within a hemisphere (ipsilateral). He further subdivided the association tracts (or "fibrae propriae") into two groups, the *U-shaped* and the *long association bundles*, according to their cortical projections and the length of their subcortical course:

> *The U-shaped bundles of the cortex do not necessarily*
> *extend simply from one convolution to one next adjoining, but*
> *they may skip one, two, three, or an entire series of*
> *convolutions, and may thus join convolutions which are*

> *united among themselves to a convolution lying at some distance from these. The shortest fibrae propriae lie nearest to the cortex; the longest at the greatest depth, and are separated from the cortex by other intervening fibrae propriae, the length of which increases gradatim from the surface inward. (Meynert, 1885, p. 39)*

Once he had laid down the anatomical foundations of the model Meynert defined a specific role for each group of connections.

First Meynert extended Bell's division of the sensory ascending (centrifugal) and motor descending (centripetal) tracts of the spinal cord to the brain, thus considering the projection fibres, the major communication system between specialized cortical regions and peripheral sensory organs and muscles. Then he added a layer of complexity to the model by introducing the association fibre system:

> *In examining the structure of the hemispheres, and remembering that different, distinctly limited and functionally separated portions of the cortex receive impressions from the various senses, we may naturally infer that the association-bundles, the fibrae propriae of the cortex, which form anatomical connections between the different cortical regions, effect the physiological associations of the images which are stored in these various parts. (Meynert, 1885, p. 153)*

Thus, in this model, the cortex, through its projection and association connection system, becomes a place not only for sensation and motor response but also for higher cognitive functions and complex behaviours such as "logical functions" (e.g., *Schlussprocess*, Induction), "recollection," "learning," and "initiation of conscious movement" (see **Figure 3**).

Meynert was an outstanding neuroanatomist of international repute who attracted young doctors eager to learn anatomy from all over Europe and North America. Among them were Carl Wernicke, Sergei Korsakoff, Auguste-Henri Forel, Paul Flechsig, Bernard Sachs, and Sigmund Freud. Although Meynert used his

neuroanatomical findings to develop a theory of psychological function, which had profound influence on the early development of psychiatry, it was one of his most talented students, Carl Wernicke, who brought the associationist model to the clinic by applying the disconnection paradigm to explain neurological and psychiatric disorders.

1.5 Disconnection Syndromes and Early Hodological Theories of Hemispheric Dominance

Carl Wernicke (1848–1904) was born in Tarnovitz, which was in those days a town in Prussian Upper Salesia but is now in Poland. He read medicine in Breslau (Wraclaw) where he undertook most of his studies except for a six-month period in Vienna with Meynert (Keyser 1994). Wernicke was greatly influenced by his teacher's Associationist theory, and in his doctoral dissertation "*Der aphasische Symptomencomplex*" he postulated that if higher cognitive functions arise through associative connections, disorders of higher function must derive from their breakdown.

On the basis of this corollary he explained a disconnection syndrome that was to become the prototype for all others — conduction aphasia (*Leitungsaphasie)*, characterised by normal comprehension and intact verbal fluency but impaired repetition due to a lesion of the fibres connecting Broca's and Wernicke's areas (Wernicke 1874).

In Breslau Wernicke established one of the most important associationist schools. The disconnection paradigm was meanwhile applied not only to aphasia but also to other neurological (e.g., associative agnosia) (Lissauer 1890) and psychiatric (e.g., schizophrenia) (Wernicke 1906) disorders. However, it soon became evident that the disconnectionist paradigm *per se* was not sufficient to explain the association between certain manifestations and localisation of lesion in one hemisphere (i.e. lateralisation of symptoms). Surprisingly, Wernicke explained the lateralisation of language disorders by postulating the existence of specialised language centres in the left hemisphere. Similarly, Jules Dejerine when describing a disconnection syndrome characterized by inability to read but preserved writing, namely pure alexia, localised the centre specialised for reading in the left angular gyrus. It was one of Wernicke's students, Hugo Liepmann (**Figure 4**), who put forward an alternative explanation for the hemispheric dominance: the anatomical lateralisation of connections.

Hugo Liepmann joined Wernicke's clinic as an assistant in 1895 and carried the Breslau associationist doctrine to Berlin when he left four years later (Goldenberg 2003). Here he developed an interest in the motor system, which led him to propose a disconnectionist account of goal-directed movement disorders — the apraxias. Liepmann's theory of apraxia, first published in 1900, was based on his case study of a 48-year-old imperial counsellor (*Regierungsrat*) who was admitted to the Berlin psychiatric service with a diagnosis of mixed aphasia and dementia (Liepmann 1900). Although his spontaneous movements were normal (e.g., using a spoon while eating), a striking feature of the patient was that when asked to perform or copy gestures with his hand (e.g., point to your nose) or manipulate imaginary objects (e.g., show how you use a harmonica), he did so in an absurd fashion. Since the patient was able to understand the command, had no visual impairment, and had no evidence of paralysis, Liepmann formulated a network model for praxis (see **Figure 4**) and then hypothesised a disconnection of visual, auditory, and somatosensory areas from motor areas to explain the symptoms displayed by the counsellor:

> *I do not think there is a praxis centre, or even that it is located […] in the supramarginal gyrus. I never postulated that the apraxia of the counsellor is only due to a lesion in the supramarginal gyrus or that this is true for all cases of apraxia. In my case report I have postulated an interruption of the sensory-motor region of the right extremities from the most important cortical regions of both hemispheres, and thought that in this case the evidence is the disruption of the white matter of the supramarginal gyrus and the callosal connections from the other side. And I was right as the autopsy confirmed. (Liepmann, 1908, p. 77)*

Liepmann generalised his conclusions to all cases of apraxia for which he postulated a disconnection mechanism at different segments and nodes of the network and speculated on the leftward asymmetry of the praxis networks to explain the higher frequency of left hemisphere lesions in these patients:

> *Eupraxic movement results from the collaboration of many brain regions with the hand area. Lesions to the cortical regions and especially their connections with the hand centre*

> *at different points can impair praxis. […] Especially the left*
> *hemisphere hand centre including its connections to the rest*
> *of the brain in particular in the same hemisphere is*
> *irreplaceable; therefore, lesions to the left hemisphere are*
> *disastrous for praxis of all extremities. (Liepmann, 1908, p. 77)*

Unlike his predecessors, Liepmann took an original position to explain the neurobiological underpinnings of left-hemisphere dominance for praxis. His model does not imply the existence of a left-dominant cortical area for complex movement control.

Ct, temporal cortex, Co, Occipital cortex;
Cp, parietal cortex; Ci
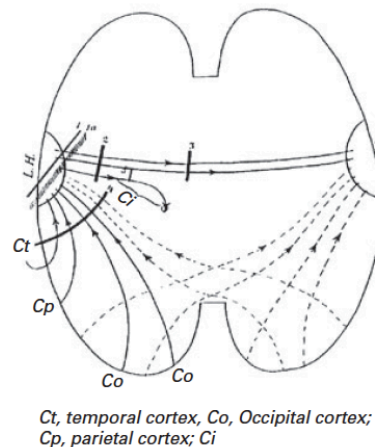
Figure 4   Hugo Liepmann and his diagrammatic explanation of the network underlying praxis and apraxia syndrome

Instead, left dominance for praxis is considered the result of an asymmetrical distribution of the sensory-motor pathways: "The contralateral connections are of subordinate importance as compared to the link of the left hand area with the rest of the brain." Liepmann added that *his diagram is not only relevant to apraxia,* as if it could also explain other lateralised syndromes. However, Liepmann's explanation was highly speculative in the absence of experimental evidence to support his claims. For a review, see Goldenberg (2003).

If the associationist school and the disconnectionist paradigm were to replace cortical localisationism in the neurology clinics, anatomical support was urgently needed.

1.6   Association Tracts

The *uncinate fasciculus* is the main association tract between the anterior temporal lobe and the inferior orbitofrontal cortex and is considered part of the extended limbic system. Pathology involving the uncinate fibres and its cortical projections has been associated with several symptoms including memory impairment, language deficits, and neuropsychiatric syndromes (Mega et al. 1997). The asymmetry of the volume and density of fibres of the uncinate fasciculus has been revealed in only one study using microscopy on human brains. The uncinate fasciculus was asymmetrical in 80% of subjects, containing on average 30% more fibres on the right than the left hemisphere (Highley et al. 2002). Voxel-based morphometric (VBM) studies of the white matter region containing uncinate fibres (i.e. anterior floor of the external capsule) are contrasting with both leftward (Hervé et al. 2006) and rightward (Good et al. 2001) asymmetry reported.

The *arcuate fasciculus* is a large association tract connecting perisylvian areas of the frontal, parietal, and temporal lobes. The arcuate fasciculus is involved in higher cognitive functions showing various degrees of functional lateralisation such as language, visuo-spatial processing, and social behaviour.

MRI has been used for VBM studies of the arcuate fasciculus. In general, the white matter regions containing fibres of the arcuate fasciculus are larger on the left compared to right (Hervé et al. 2006). However, there is also some evidence for regional differences in the asymmetry within different segments of the arcuate fasciculus, with most ventral regions being larger on the left and dorsal regions being larger on the right (Good et al. 2001). Furthermore, an increase in white matter density in the left arcuate fasciculus during childhood and adolescence has been reported (Paus et al. 1999). In a recent study, Blanton et al. (2004) documented significant gender differences in the white matter of the left inferior frontal gyrus (IFG), a region containing anterior projections of the arcuate fasciculus: boys but not girls showed a linear age-related increase in the white matter volume in this region. It remains to be determined whether such differences are to be attributed to only the arcuate fasciculus or other tracts connecting perisylvian regions. This is an issue that has been partially resolved with diffusion-tensor imaging (DTI) tractography.

DTI has been applied to study the in vivo asymmetry of the larger association tracts.

Büchel et al. (2004) used VBM and found higher left fractional anisotropy (FA) in a region corresponding to the arcuate fasciculus. Opposite results were reported by Park et al. (2004) with higher FA in the right arcuate fasciculus compared to the left. They also found lower FA on the left hemisphere for the uncinate and inferior and superior longitudinal fasciculus but reduced FA in the right cingulum compared to the right. Higher FA was also found in the left superior longitudinal fasciculus compared to the right (Makris et al. 2005), and the uncinate fasciculus (Kubicki et al. 2002; Rodrigo et al. 2007). […]

Wakana et al. (2004) dissected the major association tracts in 10 healthy subjects and found greater volume for the left superior longitudinal fasciculus, inferior longitudinal fasciculus (ILF), and cingulum.

Our own data confirm a leftward FA asymmetry for the arcuate fasciculus (**Figure 5**). […]. How these interindividual anatomical characteristica might relate to function will be elaborated on in the next section.
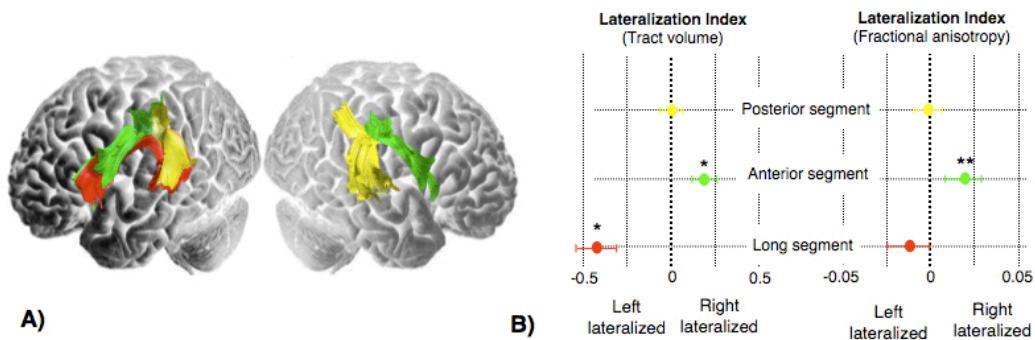
Figure 5   Arcuate fasciculus lateralisation in the healthy population

The arcuate fasciculus (sensu strictu) is significantly left-lateralised in the population. When the tract is separated into its three segments, the posterior segment (yellow) is bilateral whereas the anterior segment (green) is right-lateralised and the direct connection between Broca's and Wernicke's area (red) is left lateralised. $T(39) = 3$, $p < .01$.

1.7   Asymmetry of Perisylvian Pathways and Behavioural Correlates

The first tractography studies applied to the perisylvian pathways showed that the anatomy of the arcuate fasciculus is more complex than previously thought (Catani et al. 2005; Parker et al. 2005).

In addition to the long direct segment connecting Wernicke's area with Broca's territory (i.e. the arcuate fasciculus *sensu strictu*), there is an indirect pathway

consisting of two segments, an anterior segment linking Broca's territory with the inferior parietal lobule (Geschwind's territory), and a posterior segment linking the inferior parietal lobule with Wernicke's territory (Catani et al. 2005). This arrangement not only supports the more flexible architecture of parallel processing (Mesulam 1990) but also is in keeping with some of the classical neurological models of aphasia, contemporary models of verbal working memory (Baddeley 2003), and recent functional neuroimaging findings (Jung-Beeman 2005; Sakai 2005).

Additional support for the existence of the three perisylvian segments of the 'arcuate fasciculus' comes from other DTI studies (N. Lawes et al. 2008), human intraoperative electrocorticography (Matsumoto et al. 2004), functional connectivity (Schmithorst & Holland 2007), post mortem dissections (N. Lawes et al. 2008), and experiments in homologous parts of the monkey brain (Deacon 1992).

Tractography is also revealing unexpected findings about the projection of the arcuate fasciculus, whose cortical terminations extend beyond the classical limits of Wernicke's and Broca's areas to include part of the posterior middle temporal gyrus and middle and precentral frontal gyrus, respectively (Catani et al. 2005). More anterior and ventral portions of Broca's territory seem to be connected to posterior temporal and occipital regions through the uncinate and the inferior fronto-occipital fasciculus (IFOF) of the ventral pathway system (Anwander et al. 2006; Barrick et al. 2007). Finally tractography applied to language pathways highlights the importance of the inferior parietal cortex as a separate primary language area with dense connections to classical language areas through the indirect pathway. Geschwind's territory corresponds to Brodmann's areas 39 and 40, and although its importance as a linguistic region has been recognized for some time, the exact role of this area is still largely unknown (Catani et al. 2005) (see Chapter 2).

After adolescence, the degree of lateralisation of the long segment is quite heterogeneous.

An extreme degree of leftward lateralisation is observed in approximately 60% of the normal population (see **Figure 6**) (Catani et al. 2007). The remaining 40% of the population show either a mild leftward lateralisation (~20%) or a bilateral, symmetrical pattern (~20%). Similar results are reported for left-handed subjects (Hagmann et al. 2006; Vernooij et al. 2007). Of particular interest is the report of a gender dimorphism with respect to the lateralisation of the long segment, with

females more likely to have a bilateral pattern compared to males (see **Figure 6**) (Hagmann et al. 2006; Catani et al. 2007).
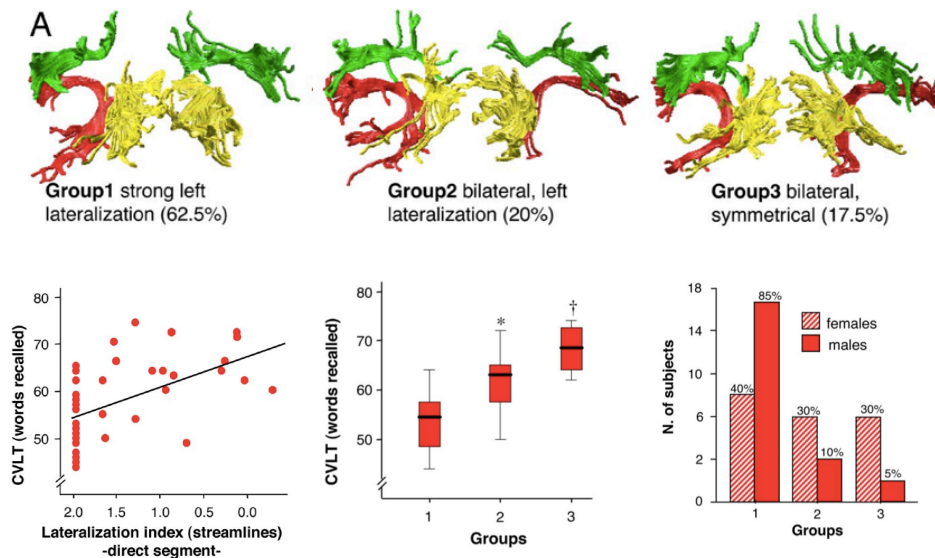
Figure 6   Inter-individual arcuate lateralisation and correlation with the California Verbal Learning Test (CVLT)

An important question is the extent to which structural differences between the two hemispheres correlate with functional lateralisation and whether the anatomical lateralisation of language pathways reflects differences in language performance. Preliminary studies combining DTI tractography and functional Magnetic Resonance Imaging (fMRI) show no correlation between the lateralisation of the arcuate volume and the degree of functional lateralisation as determined by fMRI during tasks of verbal fluency, verb generation, and reading comprehension (Powell et al. 2006; Vernooij et al. 2007). However, when extracting the fractional anisotropy along the entire arcuate fasciculus, these values are lateralised and seem to correlate better with the functional lateralisation as demonstrated in healthy individuals (Powell et al. 2006) and in patients with temporal lobe epilepsy (Rodrigo et al. 2007). This might imply that it is not the mere anatomical lateralisation but microstructural indices that might best correlate with function.

There are also preliminary findings showing that an extreme left lateralisation of the direct long segment is associated with poorer performance on a complex verbal memory task that relies on semantic clustering for retrieval (i.e. the California Verbal Learning Test, CVLT). The correlation remained significant after splitting the group according to gender, suggesting that the main determinant of CVLT performance is the anatomy (symmetry) of the language pathways, not the gender. Overall, these

findings support the notion that lateralisation of language to the left hemisphere is an important aspect of human brain organization, but paradoxically a bilateral representation might ultimately be advantageous for certain cognitive functions.

1.8   Conclusions

Although the hodological approach to cognition has a long history, the study of tract lateralisation is (surprisingly) still at its infancy. If the lack of methods suitable for anatomical studies of connections in the living human brain can in part justify this gap in knowledge, the complete absence of data on the monkey brain, for which powerful axonal tracing techniques are indeed available, is even more surprising.

For decades, anatomical drawings of tracts have been passed on to the anatomical textbooks of the next generation, and often the presence of those tracts in both sides of the brain was taken for granted. The recent flourishing of techniques based on diffusion imaging suggests that this leap of faith may not necessarily be true for tracts underlying unique human abilities. Clearly, we need a research program that sets off from the footsteps of the 'great neuroanatomists' of the nineteenth century, leading us to address those questions that for too long have remained unanswered.

Now, with unprecedented access to the connectivity of living human brain we can compare asymmetry of connections across species, formulate novel neuropsychological models based on anatomical findings on laterality, and take into account inter-individual variability within the spared hemisphere to predict recovery in patients with brain disorders.

(Full publication can be found in Hugdahl & Westerhausen 2010).

CHAPTER 2   APHASIA

'The theory of aphasia is the most difficult area of neurology'

(Luria, 1977)

People have an estimated 30.000 words encoded in their verbal memory, which they actively[1] use for communication. During a conversation 250 milliseconds are required to identify a heard word (regardless of the identification of context) (Marslen-Wilson & Tyler 1980). This elucidates the highly time-locked and efficient language processing needs of the human brain. Perceiving and producing connected speech are automatic for most people and the enormous cerebral computational effort is rarely appreciated unless the system produces errors (e.g., in the form of 'Freudian' mistakes in healthy people or aphasias in patients). The brain generates and integrates sentences made from phonological (sound), syntactical (grammatical) and semantic (meaning) information. If this neural system is severely impaired, for example, in aphasia patients who lose the ability to articulate or comprehend language, the identification of words (heard or to be produced) is disrupted and people lose the ability to communicate; often with devastating consequences for their private and professional lives. Hence I will next give an introduction to our current understanding of aphasia - including its causes, a brief discussion of aphasia assessments, and a historical account of aphasiology. The main focus, however, will be on stroke-induced (i.e. acquired) aphasias – as this is the topic of this thesis. This will be complemented by a selective review of the different methods used to determine the neural basis of language.

---

[1] The breadth of vocabulary expands with the years of education. It is estimated that the active vocabulary, meaning the words that are expressed in everyday speech, of an average English speaker contains 30,000 content words (Alekoumbides 1978; Levelt 1989). Passive vocabulary, i.e. the words that are understood but not expressed in everyday language, are vastly exceeding this number (Mariën et al. 2004; Seashore & Eckerson 1940; Müsseler & Prinz 2002).

2.1   Definition of Aphasia

The term *aphasia* was introduced by Trousseau in 1864 in his article poignantly entitled 'On aphasia, a sickness formerly wrongly referred to as aphemia'. Aphemia was the term introduced and preferred by Broca. For terminological discussion between Trousseau and Broca see (Ryalls 2003). Aphasia derives from the Greek word for language combined with the *a* prefix, meaning 'without language' (Greek ἀφασία). Various definitions have been proposed throughout the centuries, each reflecting the theoretical constructs of their time. Today's definition may henceforth be seen as a 'working definition' that is again likely to change over the next centuries: Aphasia is a disturbance of the reception and/or expression of language, in which the construction of words and sentences is marred by errors of form, content, and grammar (ICD-10); this loss or deterioration of verbal communication is due to an acquired lesion of the nervous system (Basso & Cubelli 1999).

It was noticed early in history that aphasia is a language disorder, and not a speech disorder (i.e. sensorimotor impairments of the articulatory apparatus such as dysarthria). Language disorders can affect all domains of language and contribute to impairments in writing (dysgraphia), reading (dyslexia) or in comprehension and/or articulation of continuous speech (dysphasia). Expressive deficits can arise from word finding difficulties (anomia), production of unintended words (paraphasia), loss of grammatical structure (agrammatism), inability to repeat auditory presented words, reduced verbal (categorical and lexical-phonemic) fluency, and the loss of intonation (aprosody). All of these symptoms can be expressed in isolation or combination. Depending on the impairment pattern, different taxonomies have been proposed which will be discussed below.

2.1.1   Causes of aphasia

Aphasias are, without exception, caused by cerebral pathology suffered through accident or disease at any given point in life. Two main groups can be distinguished: congenital and acquired aphasias. The latter group is defined as an acquired loss of language function after having gained eloquence. This loss of function can be induced by neurodegeneration (e.g., primary progressive aphasia (Mesulam 1982), trauma or cerebrovascular events).

Cerebrovascular aphasia, in contrast to neurodegenerative aphasia, is characterised by sudden loss of expressive and/or receptive language. Within the acquired language dysfunctions stroke-induced aphasia constitutes 80%, followed by traumatic brain injury with 10%, brain tumours (7%), infections and hypoxia (each 1%) (Wehmeyer & Groetzbach 2010). Acquired aphasias can be ascribed to lesions of the left hemisphere in the majority of cases. The left hemisphere is considered language dominant or eloquent in approximately 95% of the right-handed population and interestingly for a majority of left-handers as well (see **Table 1** for early cortical stimulation data and for a review see (Alekoumbides 1978). Crossed aphasias, where a right hemispheric lesion induces aphasia symptoms in right-handed patients are rare but do occasionally occur. These patients tend to recover well (Mariën et al. 2004).

Table 1   Hemispheric localisation pattern stratified for handedness.

Data taken from the early intraoperative cortical stimulation studies by Penfield and Roberts (1959).

	Left hemisphere (%)		Right hemisphere (%)	
Handedness	Total	Aphasic (%)	Total	Aphasic (%)
Right	157	115 (73.2)	196	1 (0.5)
Left	18	13 (72.2)	15	1 (6.7)
Total	175	128 (73.1)	211	2 (0.9)

Even though the definition of aphasia does not specify the lesioned hemisphere, the neuroscience community has generally been working under the assumption that the left hemisphere is language dominant. The left middle cerebral artery (LMCA) irrigates most of the left hemispheric cortical and subcortical areas (details in Chapter 4). Vessel occlusions and ruptures can cause a spectrum of language impairments. Cortical infarcts within this territory are seldom restricted to merely cortical regions and tend to reach beyond the damage to the convexity. This might account for complex forms of language dysfunctions that reach beyond the symptoms one would expect from a cortical lesion. Damage to subcortical nuclei and white matter connections can likewise cause language deficits especially when

the thalamus, basal ganglia, internal capsule and/or the perisylvian[2] white matter connections are affected (Luria 1966; Kertesz 2007; Cappa 1997; Nadeau & Crosson 1997; Duffau, Leroy, et al. 2008a; Crosson et al. 1986; Friederici 2006). Lesions to these structures, especially the thalamus, result in '*fluent but paraphasic output sometimes deteriorating to jargon […] and at least impairment in comprehension*' p. 301, (Crosson et al. 1986). Subcortical aphasias are similar to cortical aphasias in their clinical presentation but are generally transient (Kertesz 1988a).

2.1.2   Aphasia symptoms and taxonomy

Since the early 19th century, where the primary symptom was loss of articulation (Broca's definition) and/or comprehension (Wernicke's definition), the symptomatology of aphasia has been subject to a proliferation of nomenclature and fine-grained taxonomy. The currently defined symptoms will be described with examples in **Table 2**, all of which can appear in isolation or in co-presentation.

---

[2] Perisylvian refers to all cortical and subcortical structures adjacent to the lateral fissure, also referred to as Sylvian fissure. This includes the superior (and middle) temporal gyri, the inferior parietal lobe and the inferior and middle frontal gyri.

Table 2   Aphasia Syndromes: definitions with examples

Symptoms	Specifics	Definition	Example
Automatic speech	Echolalia	Automatic repetition of sentences and sounds of another person	'How did you end up in hospital?' 'Yes, how did I end up in hospital?'
	Perseveration	Unintentional (and often inappropriate) repetition of previously activated word or sentence part	'I have a book and even a book with me'
	Set phrases	Meaningless phrases	'yes, most certainly'
	Stereotypes	Repetitive phrase (word, sentence) that is adequate to the context but fixed.	'I can't so this. But I am…no I wanted ehm.. no I can't do this'
	Automatism/ recurring utterances	Repetitive phrase (word, sentence) that is not semantically/syntactically adequate to the context	'yes yes yes'
Agrammatism		Telegraphic style of speech marked by: one to two word sentences, stopping, emission of functional words	'first ehm unconscious I was and…my husband… ehm…called…and then yes the ambulance so ehm…driving hospital…'
Paragrammatism		Confused incomplete use of grammatical structures ('word salad'). Often long and complicated sentences due to: Duplication of sentence elements and clauses	'I wanted to in the evening my wife called'; 'I loved playing football for the club loved playing'
Paraphasias	Semantic	Range of output errors, including substitution, addition, duplication, omission, and transposition of linguistic units.	e.g., Pear instead of apple
	Phonemic	Errors involving individual phonemes (consonant or vowel sounds) within words. More complex errors involving transposition, omission, addition, or duplication of phonemes also occur.	e.g.,appe, aple
	Conduit d'approche	Self-corrective approach whereby the target word is approached by step-wise semantic/phonologic approaches	'The story about the strike no ehm not struck ehm stroke yes that's it, that was some time ago'
	Conduite d'écart	Self-corrective approach whereby the target word is lost by step-wise semantic/phonologic approaches	'The story about the strike no ehm not string ehm stage ah you know'
Neologism	Semantic	Semantic manipulation until the word becomes unrecognisable	e.g. 'The smoodle pinkered and that I want to get him round' for "The poodle needs to go out so I will take him for a walk"
	Phonologic	Phonologic manipulation of a word until it is not recognisable any more	e.g. planker for comb
Suprasegmental[3] deficit	Logorrhoea	Incoherent talkativeness often with diminished prosody (i.e. monotonous speech) and affect-deprived	'Did you had a stroke?' 'Oh well , you know the story about the stroke well if that was that easy. You know in my job I can do whatever I want and that is good and bad but most the time is not much effort, if you know what I mean…'
Anomia	Deficits of word meaning	Haltering speech where a target word is not available and is often substituted with another word	'I then go to ehm I go to…the cinema no not the cinema so I go to…ah doesn't matter'
	Deficits of word form activation	Tip-of-the-tongue phenomenon where the target word is known but cannot be formed correctly	'I went with my muh, no what am I saying, not with my mum but wil my yes sest no not brother but similar…'

---

[3]Segmental features of language are semantic, syntactic and articulatory processes; whereas suprasegmental are additive features such as prosody and affect. A hemispheric specialisation was suggested for both components (see below).

Based on these symptoms different classifications have been proposed, some of which are anatomically based whereas others are purely hypothetical. Recently, Ardila (2010) suggested a revised taxonomy based on contemporary neuroimaging data (**Table 3**). Although his efforts were recognised as novel, this new taxonomy was not adopted in the research community as it still relied on previously described categories with no added value for clinical practice (Marshall 2010). Different approaches can be utilised to achieve a classification of clinical symptoms into homogenous groups of patients. The usefulness and adequacy of such approaches are discussed later in this chapter. Depending on the applied method the number of aphasia type clusters may range between two to eight (**Table 3**). Three main classification approaches will be discussed below and a selective overview of six taxonomies is provided in **Table 3**. A historical appreciation of earlier accounts can be found in (Lecours, Lhermitte, et al. 1983b; Roch Lecours et al. 1992).

Table 3   Taxonomy of aphasia (selected approaches).

(Luria 1966)	(Benson & Geschwind 1971)	(Kertesz & Phipps 1977)	(Hecean & Albert 1978)	(André Lecours, Lhermitte, et al. 1983b)	(Ardila 2010)
Efferent motor	Broca	Broca	Agrammatic	Broca	Primary (central) aphasias: Broca-type (non-fluent)
Sensory	Wernicke	Wernicke	Sensory	Wernicke type I	Wernicke-type (fluent)
Afferent motor	Conduction	Conduction	Conduction	Conduction	
Dynamic	Transcortical motor	Transcortical motor	Transcortical motor	Aspontaneity	Secondary (peripheral) aphasias:
n/a	Transcortical sensory	Transcortical sensory	Transcortical sensory	Wernicke's type II	Conduction aphasia
n/a	Isolation language area	Isolation	n/a	n/a	SMA aphasia
Semantic amnestic	Anomic	Anomic	Amnestic	Amnestic	Dysexecutive aphasia:
n/a	Global	Global	n/a		
n/a	Aphemia	n/a	Pure motor	Pure anarthria	Extra-Sylvian (transcortical motor)

SMA, Supplementary motor area

The first classification approach to be discussed is based on the onset time of symptoms and postulates four classifications: 1) hyperacute aphasia within 72 hours

after symptom onset, 2) acute aphasia within the first four to six weeks of onset, followed by 3) post-acute aphasia after six weeks and before 12 months and 4) chronic aphasia if symptoms remain beyond 12 months of symptom onset. According to this approach acute aphasias are not classified based on symptoms but merely based on the time interval post symptom onset to account for the symptom fluctuation in the first few weeks (Biniek 1997). This fluctuation is currently considered to result from many factors, including for example reperfusion (Croquelois et al. 2003) (see Chapter 4 for more detail). Spontaneous remission has been estimated to be as high as 30% within the first six weeks of onset (Ferro et al. 1999). It is important to note, however, that the time frames to stratify hyperacute, acute, and chronic phases vary considerably in the stroke-aphasia literature. Acute and chronic aphasias are very different on many sociobiological levels. In terms of pathophysiology the functional deficit in acute aphasia extends beyond the structural damage due to an area of transient swelling. In the chronic stage compensation and reorganisation might lead to partial recovery of function. Neuropsychologically, the acute stage is often characterised by comorbid impairments of attention, affective symptoms and impaired perception of the newly acquired deficits. In chronic aphasia, compensation and reorganisation of cognitive processes are evident and most patients will have acquired coping strategies. In terms of social acceptance, the acute phase is characterised by an aphasic patient being perceived as ill and in need of support. Chronic aphasia on the other hand is often seen as a disability and patients are often exposed to socially inadequate reactions towards their impairments.

The second, most commonly used, classification is based on an individual's spontaneous speech output and verbal fluency to distinguish between fluent and non-fluent aphasias. Non-fluent aphasias are characterised by hesitant and haltering expression with great effort and five word length utterances on average (Huber et al. 1983; Kertesz 2007). In contrast to the time-locked classification this approach is applicable to the acute and the chronic phase and therefore allows for cross-sectional and longitudinal comparison. This method is also reflected in the pioneering work of Weisenburg and McBride (1935) where the authors popularised the distinction between expressive (often used as equivalent to non-fluent) and receptive (often used as equivalent to fluent) aphasia - as well as in the 19th century dichotomy of motor and sensory aphasias. All of these terminologies are still used today in the literature and the clinical arena.

The third classification follows from the Huber and Poeck's school and is based on cluster analysis over the symptom catalogue (Huber et al. 1983). Four symptom complexes and four special forms of aphasia are classified using this approach. A cluster of symptoms whose association is more frequent than chance is referred to as a syndrome. The four main aphasia syndromes are: global, Broca, Wernicke and amnestic aphasia. Each of these syndromes is defined via a specific symptom pattern with intact or impaired naming, repetition, comprehension and fluency abilities.

More anatomically-driven classifications distinguish between cortical aphasia (i.e. Broca/Wernicke aphasia) and subcortical aphasia (i.e. conduction and transcortical aphasias) (Nadeau & Crosson 1997); whereas other models distinguish between anterior and posterior lesion locations to determine the type of aphasia.

In conclusion, aphasias can be classified based on; i) their duration (time after onset), ii) fluency, iii) their anatomical lesion, or iv) according to syndromes -with the latter being the most common. There are, however, patients that do not fit into specific taxonomies (due to mixed symptoms or neuroanatomically inconsistent lesions). Also, the usefulness of taxonomical classification is debatable (Caramazza & Badecker 1991; Caramazza 1984). First, it has been shown that in about 15% of Broca aphasia patients, Broca's area was not actually damaged (Basso et al. 1985). Second, patients are transient between the groups in about 9% of cases after four months of onset and 16% of cases within seven months (Huber et al. 1983). Third, the main symptoms (i.e. agrammatism, paraphasias etc) are in themselves ill defined without a common diagnostic cut-off (Kolk & Heeschen 1990). Fourth, the taxonomy of aphasia according to main symptoms is strictly empirical and only reflects a statistically co-occurrence of a set of symptoms. Fifth, within the clinical setting and to establish therapy goals, a classification is not always necessary or useful, as the taxonomy does not imply to what extent these symptoms impact on a patient's daily life. Nonetheless, for research purposes, clustering of homogeneous groups is important for between group comparisons. Also, in the clinical arena the use of descriptive syndrome complexes facilitates and accelerates the communication between professionals.

In summary, the usefulness of taxonomical classification has therefore to be considered in the context of the specific aim of a study, therapy plan or clinical setting.

2.1.3   Comorbid conditions

Suffering from aphasia entails physiological ramifications (i.e. medical and sensomotory problems), psychological, and psychopathological consequences. Clinically, aphasias are commonly accompanied by a variety of symptoms such as: neglect (inattention to one side within the intra- and extrapersonal space); hemianopsia (half field blindness); double vision (diplopia); anosagnosia (unawareness of illness); apraxia (impaired movement sequences); agnosia (impaired object recognition); amnesia (memory impairments); drowsiness; inattention (motor and sensory and affecting the intra- and/or extrapersonal space); altered affect (increased anxiety, increased frustration, post stroke depression) and poor impulse control; executive functioning deficits; and sleeping problems. In addition, altered affect needs to be considered in language studies - as depression can significantly impact on task performance and is a common comorbidity post stroke (with one third of patients suffering from depression within the year after symptom onset (Hackett et al. 2005; Sturm et al. 2004). Whilst some of these affective symptoms are transient others may remain for longer and reciprocally interact with aphasia symptoms. These factors should be carefully obtained and systematically investigated in future studies.

2.1.4   Clinical profile of aphasia

Stroke-induced aphasias resolve naturally within the succeeding months of symptom onset in approximately 30% of patients (Ferro et al. 1999). The exact nature of this recovery, its speed and duration, as well as beneficial and adverse contributing factors are not fully understood yet. Studies suggested that recovery may reach beyond the currently assumed time window and might still be measurable after two years (Nicholas et al. 1993). The current consensus is however, that maximal recovery occurs within the first three months and thereafter plateaus between six to twelve months with only minor subsequent improvements (Basso 1992; Lendrem & Lincoln 1985; Ferro et al. 1999; Enderby et al. 1987).

2.1.4.1 Incidence and prevalence

Estimates of newly diagnosed post stroke aphasia (incidence) and estimates of diagnosed stroke-induced aphasia at a given point in time (prevalence) vary considerably depending on the applied diagnostic criteria of aphasia, chosen assessment battery, study design, sample size, and the investigated population (i.e. age restrictions due to catchment area, country specific etc.). It is estimated that between 20-38% of stroke patients will develop aphasia as a sequel to the stroke (Pedersen et al. 1995; Wade et al. 1986; Kauhanen et al. 2000; Brust et al. 1976; Engelter et al. 2006). When comparing several studies in the literature the range of patients developing aphasia seems even wider than the suggested 30% (see **Table 4**). Furthermore, a sex shift for the occurrence of aphasia was reported which disappears once corrected for the stroke frequency between the sexes (Kertesz & Sheppard 1981). It should also be considered that aphasic syndromes fluctuate considerably within the first weeks after symptom onset and the first three months are considered the critical window where most improvements can be seen (Biniek 1997; Enderby et al. 1987). Over the course of time the fluctuation reduces and after 12 months a change in classification is unlikely (Laska et al. 2001). The timing of assessment is therefore a critical factor to consider.

Table 4   Incidence of aphasia after stroke

	Study duration (years)	Recruited centres	Total strokes seen	Total no aphasia	% Aphasics from total seen	Methods
(Brust et al. 1976)	3	1	850	177	20.8	Review of medical notes
(Pedersen et al. 1995)	2	1	881	335	38.0	Stroke scale, CT
(Bogousslavsky et al. 1988)	6	1	1000	307	30.7	Review of medical notes
(Dickey et al. 2010)	4	12	3207	1131	35.3	Clinical and behavioural data
(Hier et al. 1994)	3	4	1805	458	25.4	Clinical data, CT
(McDermott et al. 1996)	2.5	1	456	39	8.6	WAB, CT or MRI
(Engelter et al. 2006)	1	4	269	80	29.7	NIHSS, CT or MRI, Dopplers, ECG
(Miceli et al. 1981)	10	1	390	241	61.8	Review of medical notes
(Wade et al. 1986)	2.5	96	545	131	24.0	Review of medical notes
(Enderby et al. 1987)	ukn	1	117	19	16.2	FAST aphasia screening
(Kauhanen et al. 2000)	1	1	106	36	34.0	WAB, CT, clinical data, psychiatric screening
(Laska et al. 2001)	1.5	1	106	36	34.0	CT, stroke scale

CT=computer tomography, WAB=Western Aphasia Battery, MRI=magnetic resonance imaging, NIHSS=National Institute of Health Stroke Scale, ECG=electrocardiogram, FAST= Frenchay Aphasia Screening Test

2.1.4.2 Prognostic criteria

Various demographic, neurological and medical factors have been discussed as contributors towards recovery. However, testing those factors in isolation can be difficult as they often interact or are not quantifiable with current measures (Code 2001). Demographic, clinical, lesion and language factors have been discussed in the literature with varying conclusions regarding their positive influence on occurrence (Hier et al. 1994), severity (Basso et al. 1980), and fluency of aphasia (Brust et al. 1976; Basso et al. 1980; Basso et al. 1987). Other studies did not show significant influences (Pedersen et al. 1995; Habib et al. 1987; Kertesz & Sheppard 1981).

2.1.4.2.1   Demographical factors

Age at symptom onset, sex, and educational level have all been considered as contributing factors. A common finding is that anterior lesions resulting in Broca and

conduction aphasia are more common in younger patients and posterior lesions resulting in comprehension deficits in older patients (Eslinger & A. Damasio 1981; Laska et al. 2001; Harasymiw et al. 1981; Obler et al. 1978; Ferro & Madureira 1997; McDermott et al. 1996; Miceli et al. 1981). Age is a confounding contributor whereby young stroke patients have better chances of recovery (Kertesz & McCabe 1977). The evidence is however not straight forward and some studies suggested that age might selectively affect distinctive aphasia types (Lendrem & Lincoln 1985; Kertesz & Poole 1974; Pedersen et al. 2004). Advanced age is further associated with comorbid deficits and the putative disadvantageous role for recovery might not be age *per se*.

Sex differences have been previously reported by some authors - with women being less likely to develop aphasia as compared to men; however this association is mainly lost when the authors control for the occurrence of stroke between the sexes (Abu-Zeid et al. 1975). Otherwise no significant sex differences were described (Kertesz & McCabe 1977; Kertesz & Sheppard 1981; Pedersen et al. 2004; Engelter et al. 2006; Ferro & Madureira 1997; Miceli et al. 1981). Age and sex are therefore no independent predictors of recovery in most studies (Hier et al. 1994; Brust et al. 1976; Engelter et al. 2006; Inatomi et al. 2008; Lazar et al. 2008; Pedersen et al. 1995). The influence of educational levels has also been considered - with conflicting results - but there is significant evidence that education is not a strong predictor of recovery (Ferro et al. 1999; Miceli et al. 1981).

2.1.4.2.2   Clinical factors: Post onset time, clinical comorbidities, clinical severity

Recovery is maximal within the first six months, with most improvements seen in the initial three month after the stroke (Pedersen et al. 1995). Thereafter the curve plateaus with minor improvements still to be seen (Nicholas et al. 1993). Owing to the fact that until recently no objective clinical assessment of stroke severity was available only limited data is accessible on the influence of clinical ramifications. The introduction of the National Institute of Health Stroke Scale (NIHSS, see **Appendix B**) (Brott et al. 1989) across countries has changed this drastically. The NIHS scale provides a measure of clinical severity of stroke at three time points and assesses the level of consciousness, signs of neglect, sensory-motor functions with a very brief language test. The lower the initial clinical impairment (i.e. lower NIHSS score) the better the expected outcome (Inatomi et al. 2008). Further factors considered relevant for aphasia outcome are hypertension, diabetes, incontinence

and arterial fibrillation. However, their predictive value seems low (Bogousslavsky et al. 1988; Enderby et al. 1987). Further and more standardised studies are needed.

2.1.4.2.3   Lesion factors: type, size and location

A focal lesion (as caused by ischemic stroke) has less negative impact on initial severity and long-term recovery than diffuse brain damage (i.e. haemorrhage). The predictive value of lesion location and size is usually stratified according to aphasia types. The definition of lesion size is currently undergoing changes due to methodological advances (i.e. perfusion imaging and diffusion-weighted imaging (DWI) lesion delineation) that allow clinicians and researchers to investigate not only the core stroke but the brain tissue that has been affected by limited perfusion post stroke but may be salvageable (Sztriha et al. 2011). Lesion size can be measured using different imaging contrasts (computed tomography or MR-based sequences such as T1- weighted, diffusion-weighted or perfusion-weighted), all of which may yield different results. Generally, lesions restricted to one cortical area are associated with relatively good recovery compared to lesions extending into the underlying white matter and/or surrounding structures where less improvements are seen (Ferro et al. 1999). Whilst some studies reported on lesion size as a independent predictor (Kertesz et al. 1979; Pedersen et al. 1995), other did not replicate these findings (Laska et al. 2001; Inatomi et al. 2008; Murdoch 1988; Lazar et al. 2008).

2.1.4.2.4   Language factors: initial symptom severity and aphasia type

Initial severity of aphasia has been identified as an independent predictor (Ferro et al. 1999; Pedersen et al. 2004; Kertesz & McCabe 1977; Laska et al. 2001; Lazar et al. 2008; Kertesz 1988b); Initially more severe patients recover less (Kertesz & McCabe 1977; Laska et al. 2001). In a retrospective study, initial comprehension abilities were indicative of long-term outcome for articulation and comprehension alike (Lomas & Kertesz 1978). This study has to be considered carefully though as it was shown that naming and fluency recovery is often slower and incomplete whereas comprehension and repetition of simple tasks recover first (Ferro et al. 1999). The aphasia type has often been shown to be associated with recovery (Kertesz & McCabe 1977; Ferro et al. 1999; Lomas & Kertesz 1978; Kertesz & Sheppard 1981; Kertesz 1988b). It is indicated that anomia and conduction aphasias have a better outcome, whereas transcortical and Broca aphasias and,

even more so, Wernicke and global aphasias were associated with worse prognoses (Ferro et al. 1999). This finding has to be carefully evaluated against the background of confounding variables, including age-related atrophy, subclinical dementia, and mortality rates (i.e. mortality may be higher in the older group and thereby drive the appearance of an age-related aphasia type).

In conclusion, age and gender are not generally considered to be predictive for recovery - whereas the initial aphasia severity is. Also lesion location and extent should be considered carefully and the chosen delineation (i.e. is the penumbra included or excluded) should be made clear.

2.2   Clinical assessment and diagnosis

Aphasia is not seen as a uniform disorder and the assumed model of language functioning based on either clinical, physiological, psycholinguistic, or anatomical constructs, influences the choice of assessment (Benton 1967; Swindell et al. 1984). Further factors have to be taken into consideration such as the intent of assessment for clinical or research purposes and the desired sensitivity and specificity of the assessment (i.e. screening vs. full battery). Today's test libraries hold a wealth of aphasia assessments that are all based on different conceptualisations and each of them has their own advantages and disadvantages; some of which will be discussed here. Taxonomical classification for example is pivotal for research purposes but less relevant for clinicians and therapists as discussed in the conclusion to subchapter 2.1. A comparison of two main batteries shows that the Boston Diagnostic Aphasia Examination classifies only 60% of patients according to a syndrome category (the remaining patients are mixed), whereas the Western Aphasia Battery categorises every patient. This rigid categorisation may sometimes wrongly classify patients or attribute one patient to two different categories. Early approaches of European pioneers in aphasiology still provide the foundations of these instruments such as the paper test by Marie (1883), the hand-eye-ear test by Head (1926), and Geschwind's repetition task (Geschwind 1971). All of these forerunners recognised the need for standardised assessments. A landmark study by Weisenburg and McBride assessed, for the first time, an aphasic group in comparison to a control group with a patchwork of standardised tools (Weisenburg & McBride 1935). Today's test instruments are essentially refinements and extensions of the 1930's approach tailored to test more recent theoretical and constructional standards, such as standardisation (i.e. normalisation against a healthy population and rigid application manuals), reliability

(i.e. reproducibility across settings and examiners), and construct validity (i.e. measuring what you want to measure).

2.2.1   Theoretical explanations of language errors in aphasia

Each school of thought has a different explanation to where the origin of language errors lies. For example, some believe it to originate from the inability to access the memory of words; others believe that the linguistic knowledge to produce and comprehend language is lost upon cerebral damage. Depending on this conceptualisation, clinical assessments would either test for memory functions or linguistic knowledge. It is hence pivotal to be aware of the underlying test theory of the assessments used. Hence, some theories on the cause on language errors in aphasia are discussed hereafter.

Thinking disorder

As we will see in the historical part of this chapter, aphasia was initially seen as a thinking/ memory disorder and was often considered to have originated from intellectual deficits (Kussmaul 1877). With Broca's (1861) description this idea was however already lacking substance as it was thenceforth shown that patients could present with isolated aphasia and still be able to function in daily life with no intellectual impairments.

Loss of linguistic knowledge

This approach assumes that aphasia is a result of the loss of language knowledge, which can either affect isolated faculties of language (e.g., use of grammatical forms) or affect all input and output domains of language (production, comprehension, and reading/writing) (Goodglass & Kaplan 1983). A complete loss of language faculties may explain global aphasia and an isolated loss, for example selectively for syntax, may explain agrammatism and Broca's aphasia (Berndt & Caramazza 2008; Bonhoeffer 1902). According to this theory, aphasia can only be cured when this knowledge is re-acquired.

Access impairment

The all-or-nothing approach of the previous concepts would not account for transient aphasia and anomia (word finding difficulties), which can be better

explained with an intermittent lack of access (Weigl & Bierwisch 1970). In this case the patients' competence is intact but the execution is impaired (Berndt & Caramazza 2008). This can also be seen in the tip-of-the-tongue phenomenon in healthy people. When aphasic patients are given a choice of words similar to the target word they can most often reject the distractors and select the target word; an indication that the word concept is intact. Patients additionally benefit when semantic or phonemic clues are provided, meaning that when for example an object is shown and the patient cannot name it, it might be beneficial to provide semantic clues (i.e. words that are commonly used in combination with the object) or phonemic cues (i.e. proving the sound of the first syllable of the target word) (Kotten 1997). Furthermore, it was suggested that it might be the automatic language processes that are impaired where, due to the high temporal demands of continuous speech production and comprehension, a swift access to linguistic knowledge is not possible. Syntax seems not to be the only domain where impaired access can be seen and this concept was further extended to non-lexical processing (Friederici 1985).

Economy of effort

Contrary to the concept of loss of language knowledge, this non-linguistic theory hypothesises that agrammatism/Broca aphasia is the result of the economy of effort, a strategy embraced by the patient (consciously or unconsciously) to adopt the difficulties he experiences in speaking. According to this theory, patients 'learn' to avoid difficult words or sentence structures and embrace an agrammatic but systematic style of communication. Empirical evidence however seems to contradict this hypothesis as for example, providing cues does not significantly improve agrammatism in patients (Goodglass & Kaplan 1983).

Adaptation hypothesis

'*The basic assumption here is that agrammatic (telegraphic) speech results from the strategic choice for elliptical expressions.*' p. 221, (Kolk & Heeschen 1990). This means that the patient chooses to avoid certain grammatical structures and words that would be problematic. Such avoidance strategies include, for example, low speech rate and a reduced variety of grammatical forms. This implies that the patient is aware of his/her deficits and draws on cognitive avoidance strategies (Salis & Edwards 2004; Kolk & Heeschen 1990). In this theory the assumption is

that syntactic competence is still given however the computational resources needed to create complex sentences are reduced.

These above mentioned hypotheses (non-linguistic/ linguistic) tried to explain the emergence of aphasic errors. All hypotheses have in common that they stimulated experimental investigations. It is however important to be aware of these different conceptualisations when choosing an assessment as each test strongly depends on the underlying theory and will assess language and/or language impairment accordingly. Although some explanations seem more plausible than others, currently none of these hypotheses have been falsified (yet).

2.2.2   Overview assessments

Many different instruments are available to formally or informally assess aphasia. However, there is no test battery that can capture the complexity of a language disorder with a single number and every test has to be sensitive towards the assessed population (e.g., children vs. adults). Comprehensive standardised assessment batteries classify the type and severity of aphasias whereas all standardised tests (screenings, short assessments, informal assessments) examine the classical language domains (i.e. fluency, naming, repetition, comprehension, vocabulary). Some tests are only intended for screening purposes whereas others are designed for holistic assessments (see **Table 5** for an overview of representative assessments, also see (Salter et al. 2006) for a review of screening tools).

All batteries assess spontaneous speech (e.g., story telling), repetition (i.e. words to sentence level repetition), auditory comprehension (e.g., sequential commands), and naming (i.e. object naming); other (supplementary) dimensions may or may not be present, according to the theoretical orientation of the authors. The wide range of tasks will ensure that other disorders (e.g., motor speech problems, such as dysarthria) are diagnosed and determine the nature and severity of the language problem. Examiners are commonly advised to record suprasegmental features, such as prosody and affect even though these are barely officially tested. The differences between batteries are primarily their terminology, internal organisation, the tested modalities, and the level of linguistic complexity and item difficulty (Lendrem & Lincoln 1985; Spreen & Risser 2003; Kertesz & Poole 1974; Spreen & Strauss 1998; Pedersen et al. 2004; Lezak et al. 2004; Murray & Coppens 2011). The choice of test is at the discretion of the clinician or researcher and is commonly

influenced by clinical factors, such as the severity of the presented impairment and the post-onset time, but also by personal factors, such as the level of proficiency in assessments, the theoretical background and sometimes the country of origin of the examiner.

Table 5   Commonly used language screening tests and assessments (taken from (Turgeon & Macoir 2008).

Box 1.1   Most representative assessment instruments according to types of assessment

Bedside and screening tests
- Reitan, R.M. (1991). *Aphasia screening test*. Tucson, AZ: Reitan Neuropsychology Laboratory.
- Whurr, R. (1996). *The aphasia screening test* (2nd edn). San Diego, CA: Singular Publishing Group.

Comprehensive examinations
- Goodglass, H., Kaplan, E., & Barresi, B. (2001). *Boston diagnostic aphasia examination*. Philadelphia, PA: Lippincott, Williams & Wilkins.
- Helm-Estabrooks, N. (1992). *Aphasia diagnostic profiles*. Chicago, IL: Riverside Publishing.
- Kay, J., Lesser, R., & Coltheart, M. (1992). *Psycholinguistic assessments of language processing in aphasia (PALPA)*. Hove, England: Lawrence Erlbaum Associates.
- Kertesz, A. (2006). *Western aphasia battery revised*. San Antonio, TX: Harcourt Assessment.

Assessment of specific aspects of language
Auditory and reading comprehension
- Brookshire, R., & Nichols, L.E. (1993). *The discourse comprehension test*. Minneapolis, MN: BRK Publishers.
- De Renzi, E., & Vignolo, L. (1962). The Token Test: A sensitive test to detect receptive disturbances in aphasics. *Brain*, *85*, 665–678.
- LaPointe, L.L., & Horner, J. (1998). *Reading comprehension battery for aphasia*. Austin, TX: Pro-Ed.

Semantic processing
- Howard, D., & Patterson, K.E. (1992). *The pyramids and palm trees test*. Oxford: Harcourt Assessment.

Naming
- German, D.J. (2000). *Test of adolescent and adult word finding* (2nd edn). Austin, TX: Pro-Ed.
- Kaplan, E., Goodglass, H., & Weintraub, S. (2001). *Boston naming test* (2nd edn). Philadelphia, PA: Lippincott, Williams & Wilkins.

Syntax
- Bastiaanse, R., Edwards, S., & Rispens, J. (2002). *The verb and sentence test*. Toronto: Harcourt Assessment.

Writing
- Hammill, D.D., & Larson, S.C. (1996). *Test of written language* (3rd edn). Austin, TX: Pro-Ed.

Assessment of functional communication
- Frattali, C.M., Thompson, C.K., Holland, A.L., Wohl, C.B., & Ferketic, M.M. (1995). *Functional assessment of communication skills for adults*. Rockville, MD: American Speech-Language-Hearing Association.
- Holland, A.L., Frattali, C.M., & Fromm, D. (1999). *Communication activities of daily living* (2nd edn). Austin, TX: Pro-Ed.

2.2.3   In Detail: Western Aphasia Battery revised (WAB-R)

In the Western Aphasia Battery revised (WAB-R) (Kertesz 2007), Andrew Kertesz employed a mathematical approach to classification of profile characteristics. A set of measurable objective, precise, and reproducible classifications is defined through an optimal set of aphasiac clusters (Kertesz & Phipps 1977). Based on this conceptualisation the WAB-R generates diagnostic classifications useful for the clinical and research arena alike. The test measures the patient's level of performance as a baseline and a function over time, to provide a comprehensive assessment of the patient's assets and deficits based on a rigid taxonomy and through determining the severity of aphasia. The test is aimed at English-speaking adults with acquired neurological disorders.

The battery necessitates the use of additional materials (pen, watch, ball, book, matches etc.), which impacts on its usability in the clinical setting if the patient is not mobile and/or no access to an assessment room in the vicinity is given. The WAB-R

has two forms (assessment form and supplementary reading/writing form) and each is composed of four sections (spontaneous speech, auditory comprehension, repetition, naming, reading, writing, apraxia, visuo-spatial/constructional/calculation), containing a total of 32 tasks (see **Appendix C**). A global score for each section can be calculated and cut-off scores are provided. The scoring of the first form provides the Aphasia Quotient (AQ), a measure of symptom severity that ranges between 0-100, whereby scores above an AQ≥93.8 are considered as normal language function (Pedersen et al. 2004; Swindell et al. 1984). Each of the individual subtasks tests a specific language processing stage or the integrity of stored information by confronting the patient with spoken and written words, sequential instructions and various objects as well as demanding eloquent and/or graphic output.

As discussed before, clinical assessments are limited in their scope of complexity due to time limitations on the one hand and the lack of appropriate measurement scales on the other. The WAB-R does not test every instance of complex neurolinguistic models but provides a good overview of verbal and written comprehension and production.

Spontaneous speech is assessed with two tasks designed to elicit conversational speech to measure functional communication, information content, speech fluency, lexical access, paraphasias and grammatical competence.

Auditory comprehension is measured through three tasks by confronting the patient with relational prepositions (i.e. put the pen on the other side of the book), increasingly complex syntactical constructions and increased sentence length (yes/no questions and sequential commands). Yes/No questions are given with relations to personal orientation (i.e. 'is your name Smith?'), environmental orientation (i.e. are the lights on in this room?) and more abstract general questions (i.e. 'does it snow in July?'). This leads to increased syntactical complexity but semantically consistent difficulty. The auditory word recognition task detects category-specific loss of comprehension for objects, colours, numbers, letters, and body parts. This task also allows us to infer Gerstmann's syndrome (finger agnosia, left/right confusion, acalculia, and agraphia) associated with an inferior parietal angular lesion (Gerstmann 1940). The auditory comprehension span task is designed to be the most difficult task within the WAB-R and crucial for diagnostics (Kertesz 2007). All test items are kept within the working memory span and are presented with increasing complexity.

The *repetition* task requires the patient to repeat single words and sentences of increasing length and complexity and varying probability (e.g., low and high frequency words such as pen vs. government). These items are also kept within the working memory span to reduce memory and executive deficit interferences. This task is used to distinguish between conduction and transcortical aphasia. The last three test items are to be highlighted. 'Delicious freshly baked bread' is intended as the oral agility item; Geschwind's repetition item 'no ifs, ands' or buts' requires only monosyllabic repetition and the final item contains all letters of the alphabet: 'Pack my box with five dozen jugs of liquid detergent'.

The *Naming and Word Finding* task only determines the severity but not the type of aphasia within this assessment. The naming of 20 objects (provided by the examiner as part of the assessment) measures the lexical access. The word fluency task (category) measures lexical access and components of executive symptoms (i.e. perseveration) along with lexical/semantic fluency. The final two tasks measure word finding abilities within a contextual setting (automatic lexical access in over-learned sentences) and more spontaneous speech but within a controlled setting. Examples would be 'roses are red, violets are…?' for the contextual setting and 'where can you buy stamps?' for the spontaneous speech. The resulting aphasia syndromes according to the WAB-R are summarised and explained in **Table 6** together with their frequency.

The WAB-R can be utilised to establish a variety of measures and determine the taxonomical group for each patient. First the raw scores for each subtest are compiled and composite section scores (spontaneous speech, auditory verbal comprehension, repetition, naming and word finding) are calculated according to the directions in the record form 1 (see appendix). All composite section scores are then scaled to comparable levels with scores ranging between 1 and 10 (note: it is note clearly stated by the author of the assessment but spontaneous speech is considered separate here for information content and fluency and is hence entered unchanged into further arithmetic). These scaled section scores are then added together to obtain a composite scaled section score (max 50). Assuming the percentage of normal function is 100% the cumulated section scores (max score 50) need to be multiplied by two (Kertesz & Poole 1974). The result is the Aphasia Quotient (AQ), which serves as an indicator of functional severity of speech disturbance (Figure 4). Likewise this score is used as numerical measure of improvement over time.

Raw scores are mainly used to distinguish fluent and non-fluent aphasias. Together with the scaled composite section scores these are expended to determine aphasia types (i.e. taxonomy). The AQ on the other hand is merely a measure of severity and cannot be employed to infer an aphasia type. The AQ can be stratified to obtain five severity groups, which were adopted within the present work.

Raw Scores & Composite Section Scores (CSS)

Section: Spontaneous Speech (SS–CSS, max 20)
Information content (max 10)
Fluency, grammatical competence & paraphasias (max 10)

Section: Auditory Verbal Comprehension (AVC-CSS, max 200)
Yes/no questions (max 60)
Auditory word comprehension (max 60)
Sequential commands (max 80)

Section: Repetition (R–CSS, max 100)
Repetition (max 100)

Section: Naming & Word Finding (NaWF–CSS, max 100)
Object naming (max 60)
Word fluency (max 20)
Sentence completion (max 10)
Responsive speech (max 10)

Scaled Composite Section Scores (sCSS, max score 50)

sCSS Spontaneous Speech = SS–CSS (max 20)
sCSS Audit. Verb. Comprehension = AVC–CSS/20 (max 10)
sCSS Repetition = R–CSS/10 (max 10)
sCSS Naming & Word Finding = NaWF–CSS/10 (max 10)

Aphasia Quotient (AQ)

50 (max total sCSS value) * 2 = AQ (0 – 100)

Fluency

Global
Broca
Isolation
Transcortical motor
Wernicke
Transcortical sensory
Conduction
Anomic

Non-fluent

Fluent

Aphasia Type

Normal language: AQ ≥ 93.8
Mild aphasia: AQ ≥ 75
Moderate aphasia: AQ = 51-75
Severe aphasia: AQ = 26-50
Very severe aphasia: AQ = 0-25

Aphasia Severity

Figure 7   Rationale behind the revised Western Aphasia Battery raw scores, composite section scores (CSS), scaled composite scores (sCSS), and the Aphasia Quotient (AQ). The raw and composite scores are used to derive one of eight aphasia types (stratified by fluency); whereas the AQ is an indirect measure of five distinct classes of severity.

For clarification on how to implement the scoring system I want to introduce a thought experiment at this point. To derive an aphasia type (i.e. taxonomical classification), one determines where a patient's score falls within the range of each subtest criterion. For example, to arrive at a classification of Broca's aphasia the fluency raw score must below 4. For the same patient the comprehension score must fall between 4-10, repetition must be less than 8, and the naming score must be between 7 and 9. Values of fluency represent the Fluency, Grammatical Competence and Paraphasias raw score; whereas values for comprehension,

repetition, and naming represent the scaled composite sections scores used to determine the AQ (see WAB-R manual for details). Patients might have a similar pattern for three out of these four measures but if they are without the range on one of the scales they will be classified with another aphasia type. If one were to consider a similar patient to the example above but only assume that the naming section score falls below 7, that patient would derive a global aphasia type. Likewise patients with different recovery patterns might present with a similar number in their AQ scores whilst the underlying recovery within each section might be different. This however is mostly relevant when investigating the change in scores rather than the absolute scores at baseline and follow-up.

Table 6   Aphasic syndromes classified within the WAB-R and their incidence within the standardisation cohort from Kertesz (1977).

Fluency	Syndrome	Classification	%
Fluent Normal or excessive quantity of speech; paraphasic substitutions, circumlocutions, jargon, and echolalia could be features	**Wernicke**	Characterised by impaired comprehension and paraphasias; at times jargon, circumlocutions, and unawareness of speech deficit	15
	Transcortical sensory	Characterised by poor comprehension but relatively good repetition and fluent spontaneous speech	7
	Conduction	Characterised by good comprehension and poor repetition, with phonemic paraphasias and word retrieval difficulties; at times, groping and verbal approximations	9
	Anomia	Word-finding difficulties; impairment or inability to recall words	29
Non-fluent Slow effortful speech; ability to initiate speech, quantity, and prosody are affected	**Broca**	Primarily expressive, characterised by scant, hesitant, effortful, agrammatic and paraphasic spontaneous speech; at times, slightly better repetition, relatively good comprehension and often, verbal apraxia. Reading aloud is poor, but reading comprehension is often good, writing is affected similar to speech	17
	Global	Severe involvement of both expressive and receptive language, characterised by stereotypic repetitive utterances, lack of gestural, written or oral communication, and almost entirely absent verbal comprehension	16
	Transcortical motor	Characterised by reduced spontaneous speech but relatively good comprehension and repetition	4
	Isolation/ mixed transcortical	Results from the isolation of the speech area from other association areas of the brain; only repetition remains and comprehension and output are impaired	3

It should be noted here that the WAB-R does not assess lexical-phonemic fluency most commonly assessed with generating lists of words that share the same initial letter (for Anglophone assessments this is typically a list of words for the letters F, A, and S as these are the most common initial letters of the language). Fluency of speech is sensitive to socioeconomic demographic factors with a gender effect past the age of 55 years and a general decline in both sexes over the age of 70 years; an effect that seems to affect semantic fluency (e.g., list of animals) more than phonemic fluency (e.g., list of F words) (Benton et al. 1994; Troyer 2000). These deficits are not sufficient to classify a type of aphasia (Kertesz 2007; Kreindler et al. 1980). Lexical-phonemic fluency is more difficult than semantic categorical fluency

for most people but this was shown to be inverse for neurodegenerative patients (Lezak et al. 2004). Given the different nature and potentially different anatomical correlates for both fluency tasks we added a lexical-phonological task to the assessment (FAS word lists).

The WAB-R serves to test theoretical characteristics sufficiently (Spreen & Risser 2003), but does not recognise qualitative aspects of the patient's performance (i.e. visual search in the room, gestures, or suprasegmental language aspects). The WAB-R has been subjected to three main criticisms. The first is the intermittent diagnostic mismatch between classifications made by clinicians and classification based on the assessment (G. Davis 1993; Swindell et al. 1984); disparities that may be related to the neglect of qualitative behavioural observations. Second, the WAB-R has a rigid taxonomical system that does not allow for mixed aphasias (Spreen & Risser 2003). Third, the validation was obtained from veterans, a population where the sex ratio is heavily weighted towards men of certain age and the possibility of some degree of post-traumatic impairments cannot be excluded.

CHAPTER 3 ANATOMY OF LANGUAGE

'Anatomy is destiny'

(Sigmund Freud)

The anatomy of language is intimately related to the study of the loss of language (i.e. aphasia as defined above). The classical clinico-anatomical approach infers a functional specialisation of an area by examining the deficits that follow damage to this area (co-localisation of function); however, this approach was later criticised as not inferring the localisation of function but rather picturing the location of deficits. The quest for language in the brain was hence driven by the loss of language and aphasiology (study of aphasia) and has seen the rise and fall of many theories. To gain an understanding of the development of theories and methodologies in language research it is important to understand where the field has come to at the present day and how the current ideas are still influenced by early theories. An extensive review is beyond the scope of this work and only a selective review of important contributions (to the field in general or stroke-induced aphasia in particular) will be discussed (for a review see Tesak (2008), Finger (1994), and Code (2010).

3.1 Early Theories (Prior to the 19th century)

The 19th century is often considered the birth period of aphasiology thanks to the seminal contribution of Broca (1861) and Wernicke (1874). A link between brain damage and loss of language function was, however, already suggested in ancient Egyptian (Edwin Smith Surgical Papyrus, written in the 17th century Before Christ, and containing the earliest reference to the brain in human records) and Indian (Samhitas) medical writings (Finger 1994; Kandel et al. 2000). These single case reports are based on head trauma patients that presented with some sort of language difficulties. This led to the vague assumption of the importance of the brain in language. Whilst the Dark and Middle ages did not contribute much to the science of aphasiology, various patients have been reported and theories have been developed from the renaissance onwards (Critchley 1970).

Language was considered a faculty of memory, located within the fourth cerebral ventricle (Tesak & Code 2008). Aphasia was consequently considered a memory disorder caused by damage (e.g., exceeding phlegm, injury) to the fourth ventricle. A seminal contribution was published by Johannes Schenk von Grafenberg in the 16th century where von Grafenberg i) rejected the medieval ventricular theory (but not the idea that language belongs to the memory faculty), ii) compiled 16 case reports of language disorders and iii) realised that aphasia is not a speech disorder (motor impairments of the speech apparatus) but a language disorder (central language functions) (Tesak & Code 2008).

Before the end of the 17th century, publications were only brief reports and deficient of essential details. This was to change with the early detailed reports of stroke-induced aphasia (Finger 1994).

The 18th century is of central relevance to the development of aphasiology due to i) the realisation that there are different aphasia types and ii) the first conceptualisation of aphasia as a lexical memory problem rather than a general memory problem and iii) the recognition of the clinico-anatomical association between stroke and aphasia as published by Morgangi (1761). Gesner's language amnesia paper (1789) was the most detailed contribution thus far and was centred on a patient that today's classification would characterise as Wernicke-type aphasic (i.e. fluent speech with neologism and non-sense words). Gesner reported the isolated language deficits with other higher cognitive functions being intact and therefrom concluded that language was a selective disorder of memory (Tesak & Code 2008).

In conclusion, prior to the 19th century language was already considered a brain function and aphasia, even though not defined as such yet, was described in a series of patients. The clinico-anatomical observations already acknowledged the link between head trauma and cerebrovascular events with aphasia and language still considered a memory function (located in the fourth ventricle). The favourable politico-medical environment and methodological advances laid the foundations for the great discoveries of the 19th century that were about to change our understanding of aphasia profoundly.

3.2   19th century

This century is marked by i) the serious systematic study of aphasia, ii) the first post mortem accounts in an attempt to map language in the brain, which cumulated in the birth of aphasiology as a dedicated field of science and established the left hemisphere as the language dominant half of the brain. The different theories are described in some detail below.

3.2.1   Localisations theories

Craniology (later called phrenology by Gall's student Spurzheim) is a topographic doctrine coined by the German physician and anatomist Franz Joseph Gall (1764-1828). This school established the hypothesis that cranial prominences are indicative of underlying brain development and that these specific cortical areas expand with superior functioning. Gall mapped 27 faculties distributed over the skull and located language behind the orbit (**Figure 8**B). The reasoning behind this idea being that verbal memory was located in the frontal lobe and people with excellent verbal memory abilities would develop this particular brain region more extensively than others, which in turn would result in the orbits being pushed forward (e.g., bulging eyes) (Zola-Morgan 1995).

Although phrenology is no longer given serious consideration by the scientific community and often seen as pseudoscience, it however cannot be neglected that at a time where in vivo neuroimaging was not yet available, Gall's intent to associate circumscribed cranial regions with cognitive function was very influential and established the foundations of localisation theory, the most influential theory that was to drive neurosciences and psychology to the present day (Temkin 1947; Finger 1994; Eling 1994; York 2009).
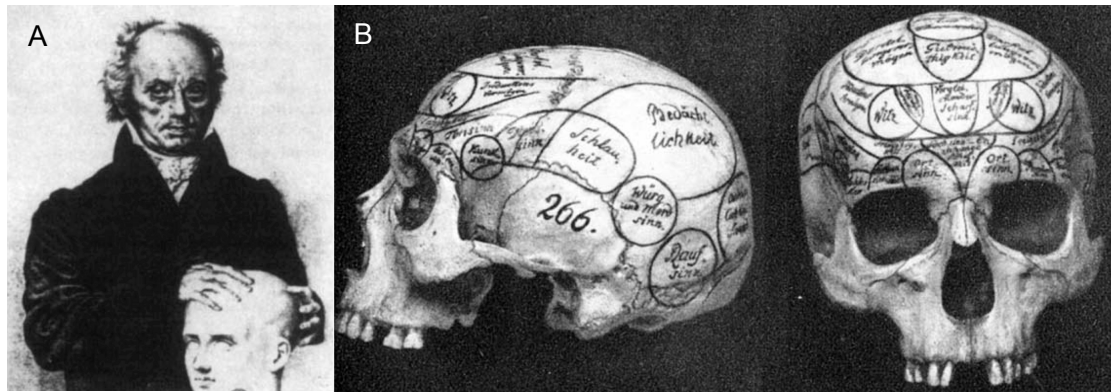
Figure 8   Phrenology - Franz Gall and an original skull

A Franz Joseph Gall examining a skull (from (Haymaker 1953)) **B** Skull with Gall's hand-written functional areas (from (Wolfgang & Michael 2008)) from Gall's collection of 300 human and 120 cat skulls.

Seeking more validated methods the phrenologist-turned experimental scientist Jean-Baptiste Bouillaud amassed a total of over 500 cases of language pathologies (Finger 1994), introducing for the first time a multi subject language study. Owing to his and other experiments in animals and lesion observations in man, language was already ascribed to the anterior lobes (Head 1926; Finger 1994). This assumption was countered with reports of double dissociation, where damage to the frontal lobes did not result in language deficits and likewise damage to other lobes did. Bouillaud took up this challenge and proposed one of the most famous bets in neurosciences: '*Herewith I offer 500 francs to anyone who will prove me with an example of a deep lesion of the anterior lobes of the brain without a lesion of speech*', which he paid for in 1865 when Velpeau presented an eloquent frontal lobe tumour patient (Finger 1994).

The 'revolution' for neurolinguistic sciences was looming in the 1860s when Paul Broca, in reaction to the debate, emphasised the superiority of clinical lesions over cranial protrusion examinations in the quest for functional brain regions and consolidated the localisationist approach (**Figure 9**C,D). In this approach a lesion to one area will cancel the functions executed by this area. In his five years of active contributions to aphasiology Broca reported the post mortem examination of one of the most famous cases in neurosciences, Monsieur Lebourgne also known as 'Tan' (only syllable the patient was able to utter). Broca's patient presented with isolated language deficits (not able to speak but understand) and at autopsy a critical region for language production was identified within the lateral aspect of the left inferior

frontal gyrus close to the Sylvian fissure. Broca herewith confirmed Bouillaud's localisationist claim of the frontal lobe harbouring language. After having studied another eight patients with a similar lesion and symptoms, Broca formulated the theory of language lateralisation in 1864, ascribing articulated speech to the left hemisphere (Kandel et al. 2000; Tesak & Code 2008). The superiority of the left hemisphere was also supported, in Broca's view, by neurodevelopmental studies demonstrating that the sulci of the left hemisphere formed before the right (Anon 2003; André Lecours, Lhermitte, et al. 1983b).

Gustave Dax, on behalf of his father Marc Dax, claimed the primacy of the formulation of the left-hemispheric dominance theory but historically lost the conflict owing to Broca's already established status amongst the medical profession (Finger 1994). Broca's aphasiology had resonance in the UK and attracted famous followers such as John Hughlings Jackson, William Ogle, Henry Bastian, Frederic Bateman and Byron Bramwell, which all added to aphasiology (for details see (Tesak & Code 2008)).
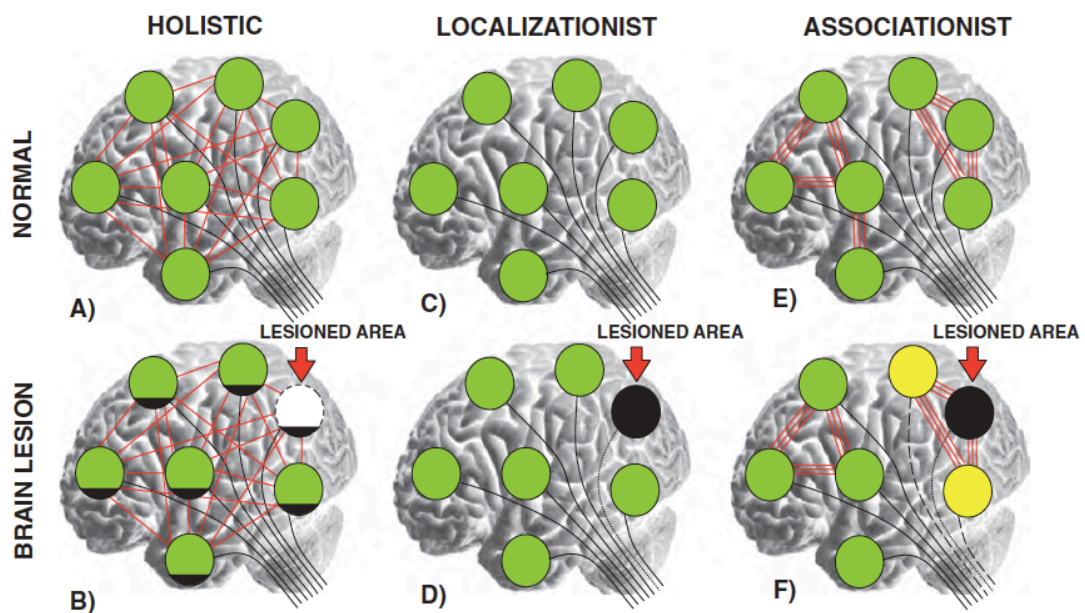
Figure 9   Three schools of thought of brain function and consequences of cortical lesions

 A,B Holistic approaches believe function is homogeneously distributed across the cortex and a lesion to one region will affect other regions to the same extend. **C,D** Localisationists consider a function to be carried out by a discrete independent cortical region. If this region is damaged the function is lost. **E,F** Associationist believe some areas to be interconnected and commonly provide a certain function. A lesion to a cortical area will hence affect the associated areas but leave others intact resulting in partial dysfunction (Catani & Thiebaut de Schotten 2012).

3.2.2 Holistic approach

Before the localisation theory was established, the holistic approach prevailed between the 1820s-70s. In an attempt to map and isolate the location of functions within the brain the French physiologist Flourens systematically removed Gall's functional areas in the animal brain (Kandel et al. 2000). It should be considered at this point that from today's perspective early ablation and stimulation methods were rather crude and not suited to the introduction of focal brain damage (Riese & Hoff 1951). Flourens' conclusion did not support a phrenological approach and he claimed that a lesion to a specific area would affect the rest of the brain homogeneously, a principal called *cortical equipotentiality* (Tesak & Code 2008; Kandel et al. 2000) (**Figure 9**A, B).

3.2.3 Associationist studies

Theodor Meynert laid down the foundations of the first theory of language when he formulated his *fibre theory* and postulated the dichotomous brain, with the rostral part executing motor and the caudal part sensory functions (please see Chapter 1). Neither agreeing with the mosaic of phrenological functional areas nor the opposing view that mental functions are homogeneously distributed across the cortex, Meynert's student Carl Wernicke took a combined approach. He believed core functions to be localised within focal areas (i.e. the perirolandic regions had been described as motor and sensory areas); whereas higher cognitive functions are distributed within large-scale networks (**Figure 9**E). Wernicke adopted and integrated his mentor's theories into his idea of a connected language network, when he described a language-relevant comprehension locus in the temporal lobe (previously described by Meynert) and developed the first (associationist) anatomical model of language (**Figure 10**A). This was to become the classic doctrine in aphasiology:

> *'The whole area of the first convolution circling the Fossa Sylvii together with the insular cortex serves as speech centre; and thus the first frontal convolution, because it is a motor area, is the centre of motor images, the first temporal convolution, because it is sensory, the centre for sound images; the fibrae propriae joining in the insular cortex constitute the connecting psychic arc'.*
> (1874, translated in *(Tesak & Code 2008)*)

Within this ingenious brief paragraph Wernicke defined the anatomy of language for the next decades and introduced the pivotal concept of a connection between two distant language areas (according to Wernicke mainly relevant for language

acquisition), which was later claimed to be the arcuate fasciculus by Dejerine. Wernicke further established the fact that aphasias presented with linguistic differences and considered four types of aphasias based on his model. His name later became eponymous with sensory aphasia (a temporal lesion resulting in a loss of word concepts and hence fluent but non-sense talk) and associated with conduction aphasia (disconnection between Broca and Wernicke areas).
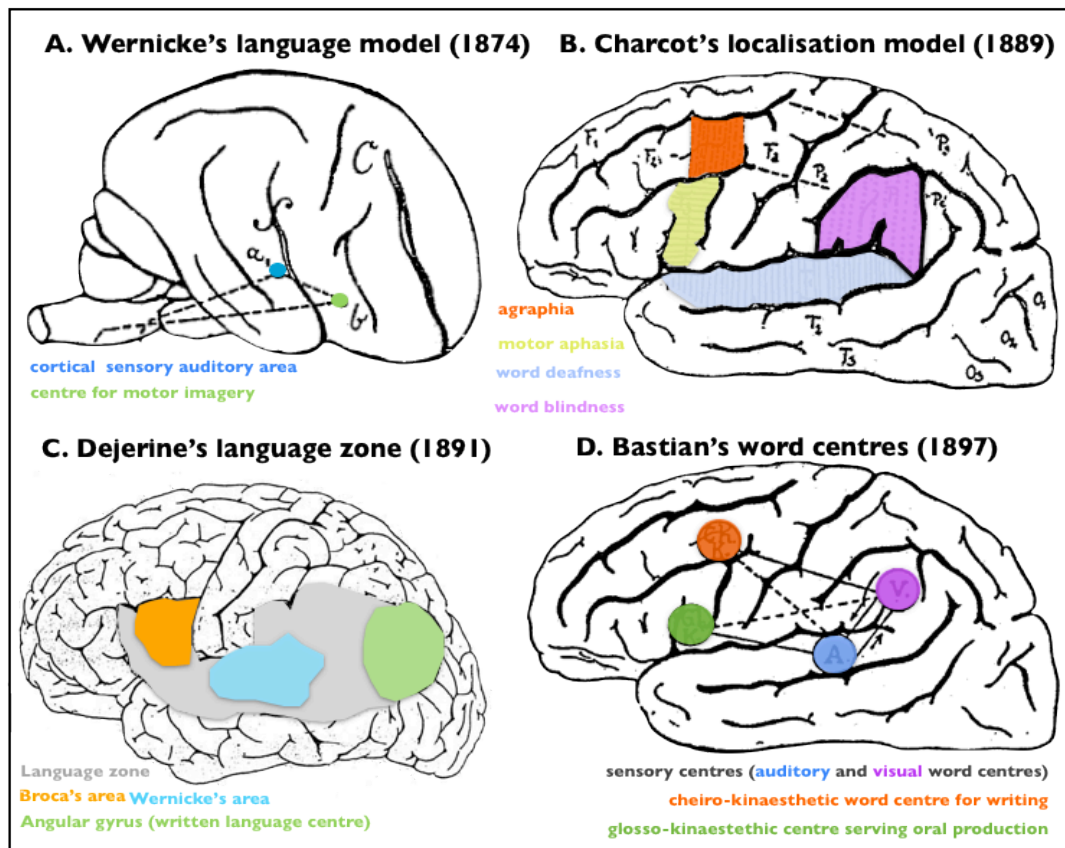
Figure 10   19th century anatomical associanists language models based on clinical observations

A Wernicke's model of language production is the first associanists anatomical model including a as the central terminal of the acoustic nerve and b as the centre for motor imagery in the inferior frontal lobe. For reading and writing the model was extended to a centre for graphic motor imagery in the middle frontal gyrus and a centre for visual letter imagery (not shown here). **B** Charcot's cortical localisation of aphasia, agraphia and word deafness/blindness (1889; adopted from (Tesak & Code 2008)). **C** Dejerine's language zone encompasses the frontal, temporal and inferior parietal lobe as well as specialised areas. **D** Bastian's diagram showing the approximate sites of the word centres, two of which are receptive and two are expressive in nature. Solid lines represent customary routes for stimuli whereas dotted lines occasional routes (modified from (Bastian 1897)).

The Meynert-Wernicke model, even though far ahead of its time from today's perspective, was critiqued for having made the mistake '*of plotting the centres in specific areas of the brain. The localisation of elementary functions of language is*

not mature enough for this' (Kussmaul 1877, translated in Tesak 2008). The next 100 years would see a wealth of neuropsychological and neuroanatomical models of language functions.

One such approach was Lichtheim's expansion of Wernicke's model by the dimension of a concept area conveying meaning rather than considering language to be a pure sensorimotor function. Lichtheim postulated a connected concept-motor-sensory language system and described corresponding clinical symptoms for all possible disconnections within this system (see Chapter 1 and Chapter 2 for details). He added transcortical motor and sensory aphasias to the Broca-Wernicke model. Lichtheim did not anatomically localise the concept area but considered it to be '*a common function of the entirety of sensory areas instead*' (1885, in Tesak & Code 2008); a view that was to be revisited by Norman Geschwind in the 20th century.

The relevance of further language areas beyond the receptive-expressive regions became more evident and subsequent studies tried to map them. Charcot, thought giver to students such as Freud, Marie and Dejerine, agreed with Broca that the motor language centre and further suspected lesions of the middle frontal gyrus would result in agraphia, lesions to the superior temporal gyrus (STG) would produce word deafness and a lower parietal lobe lesion would cause word blindness (**Figure 10**B). Dejerine (1885), diverging from his mentor's approach, defined a *language zone*, an aggregation of specialised cortical areas (Broca's, Wernicke's and the angular gyrus) respectively responsible for production, auditory and written comprehension (**Figure 10**C).

In the UK, Bastian (1898) had anticipated Wernicke's findings but did not publish his theories until 19 years later and hence was credited with limited recognition. Bastian produced one of the first connectional diagrams of the brain where he aimed to integrate speech, auditory and writing areas with the motor pathways of the hand and tongue, a model that closely resembles Charcot's model (**Figure 10**D). Bastian can also be credited for his detailed description of word deafness and word blindness (Bastian 1887). Aphasia, according to Bastian, is the result of hemispheric white matter damage and whilst linguistic functions are impaired other cognitive domains remain intact. In normal language function, he believed in the interaction between four language areas, two receptive and two expressive in nature. Bastian is nowadays primarily known for his description of word deafness and word blindness rather than his aphasia work. Anecdotally, he became the object of disparagement after claiming a precise circumscribed lesion in one of his

patients that was then found to have damage within the entire left middle cerebral artery territory. Interestingly, Bastian attributed aphasia recovery to right hemispheric plasticity: '*In many cases where recovery from different kinds of speech defects occurs (the nature of which I need not now particularise) we are compelled to assume that centres and commissures in the right hemisphere gradually undergo further organisation, so as to compensate for the destruction of corresponding structures in the left hemisphere.*' p. 85-86, (Bastian 1897)

One famous opponent of the associative Wernicke-Lichtheim model was Sigmund Freud, who developed his own (non-anatomical) model and classification system. Freud's (1891) objection was that i) clinically patients often present with a spectrum of deficit rather than complete loss of language and ii) that the model predicts forms of aphasia (i.e. isolated loss of repetition) that has not been seen and are unlikely to exist.

Many neuroscientists followed the associationist approach (i.e. Kussmaul and Charcot), but their contributions only marginally expanded or modified the classical Wernicke-Lichtheim model and some were reluctant to anatomically anchor the localisation of language/aphasia.

In conclusion, linguistic neurosciences in Europe have seen confrontation between three prevailing schools of thought: i) localisationists, ii) holistics and iii) associationists. These schools disagreed on i) where language is located in the brain (discretely localised within the frontal lobes, homogenously throughout the brain or organised in parallel networks) and ii) which methods are most adequate to study brain functions (clinical observation and case studies or repeatable experimental animal studies). Regardless of the affinity between all protagonists, a tremendous contribution to the understanding of the clinico-anatomical relationship has been provided and profoundly redefined our understanding of the anatomy of language.

3.3   20th century

The evolution of aphasiology came to an abrupt halt during World War II that led to a scientific shift from central Europe to other countries (e.g., US) and the emphasis transferred from basic sciences to rehabilitation owing to the large number of brain injured aphasic soldiers in the aftermath of the war. This development necessitated elaborated assessments, which were provided by Weisenburg and McBride (1935).

They were the first to provide standardised tests and a new approach to working with patients, yet their assessments were very much aligned to previous approaches (spontaneous production, naming, repetition, comprehension).

Systematic clinico-anatomical data were accumulated by Luria who published his monograph *Traumatic Aphasia* in 1947 (English translation 1970), a compilation of data acquired from war injuries. He took an intermediate position to the 19th century schools and associated damaged tissue with loss of function and applied his own aphasia taxonomy:

> *'There is no doubt, however, that the archaic concepts [late 19th century ideas] used in present-day clinical practice are grossly obsolete. No one thinks any longer that "centres" of sensory speech and motor speech really exist, least of all, a "centre of notions". Nor can anyone nowadays believe that the defect underlying conduction aphasia is an anatomical disruption between the "centres" of sensory and motor speech. In short, the theoretical approach to the forms of aphasia just mentioned can no longer withstand criticism'.*
> p. 130, (Luria & Hutton 1977)

Luria believed that only investigation from the inside (i.e. post mortem) or from the outside (i.e. observing the symptomatology) was not sufficient and needed the intermediate step of systematic clinico-psychological assessment (Luria & Hutton 1977). Anatomically, Luria highlighted the perisylvian region (inferior frontal, superior temporal and superior marginal/ angular gyrus) with an extension to the superior frontal lobe.

The associationism revival came in the 1960s with the American neurologist Norman Geschwind, who reinvestigated the Wernicke-Lichtheim model and advanced the model by highlighting the disconnection syndromes. Geschwind's efforts on the clinical description of disconnection syndromes attracted many scholars in subsequent decades, who further complemented his work (Mesulam 1990; ffytche & Catani 2005; Catani & ffytche 2005) (**Figure 11**). According to Geschwind many methods (animal models, intraoperative stimulation, brain tumours, head trauma) have been used to study language but all with inherent limitations; to him the best method was the stroke model even though '*fully suitable cases of this type are not common*' yet it has the advantage of 100 years worth of experience and delimited areas of brain damage (Geschwind 1970). Geschwind conceptualised the significance of the inferior parietal region as secondary

(intermodal) association area[3]: *'The situation in man is not simply a slightly more complex version of the situation present in the higher primates but depends on the introduction of a new anatomical structure, the human inferior parietal lobule, which includes the angular and supramarginal gyri, to a rough approximation areas 39 and 40 of Brodmann'* (p. 273, (Geschwind 1965b)). To Geschwind this area is the intermodal integration area of the brain where all other association cortices project to and the middle and posterior region of the superior temporal gyrus (Wernicke's area, roughly BA22) reciprocally projects to the angular gyrus (indicated as 'parietotemporal' cortex in **Figure 11**).
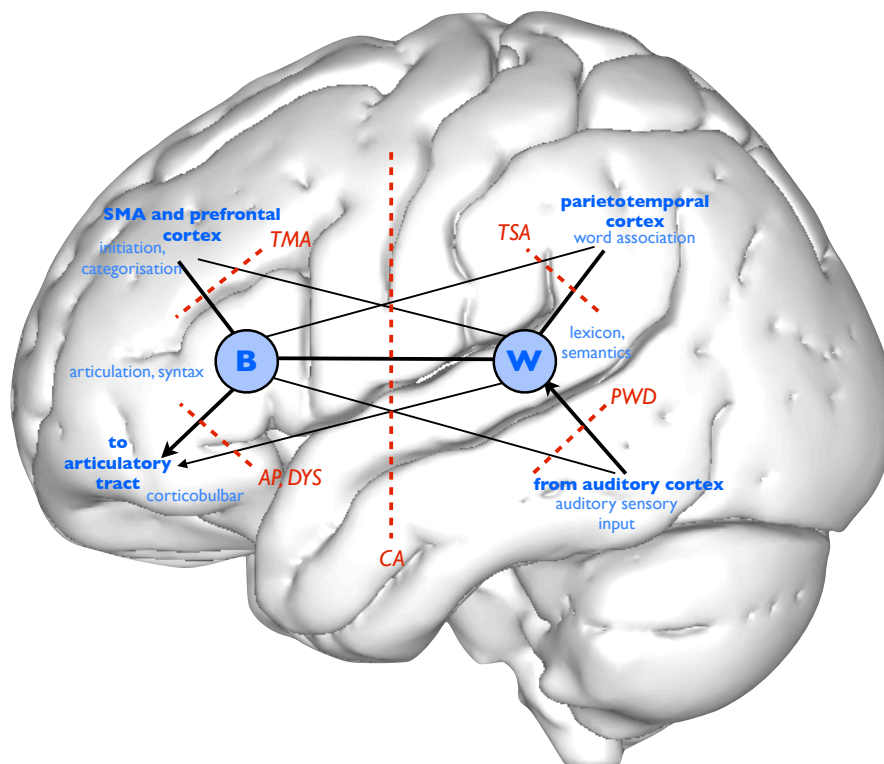
Figure 11   Neoclassical language network

Schematic clinico-neuroanatomical model of aphasia where bold blue highlights cortical regions and light blue describes the most commonly associated function of these areas. Red represents the aphasias and where a disconnection can be assumed (red dotted lines). Black lines indicate connections between cortical language areas (blue). Red lines indicate neural lesions with corresponding aphasia types. SMA, supplementary motor cortex; B, Broca; W, Wernicke, TMA, transcortical motor aphasia; TSA, transcortical sensory aphasia; AP, aphemia; DYS, dysarthria; PWD, pure word deafness; CA, conduction aphasia. The right hemisphere (not shown here) is relevant for communicative impact of spoken language (emotional-attitudinal prosody and paralinguistics processes) in this model. A right-hemispheric disconnection will hence results in aprosodia. Modified from (Mesulam 1990).

---

[3] Secondary association area as defined by Geschwind is an evolutionary new area receiving most afferent input from adjacent association areas with few thalamic connections.

Wernicke can be considered as the first to associate the connection between Broca's and Wernicke's areas with language function. Initially, however, he believed both regions are connected through fibres of the external capsule (1874). It was von Monakow who first identified the arcuate fasciculus as the pathway interconnecting Broca's and Wernicke's area, a view later adopted by Wernicke (1908). Damasio and Damasio (1980) investigated CT imaging from six patients and concluded that the arcuate fasciculus is consistently lesioned but mostly together with the left cortical regions of the auditory complex, the insular region and the supramarginal gyrus.

The complexity of this language network increases when further considering reading capacities that require a connection to visual areas and right hemispheric linguistic processes (e.g., prosody, affect) that depend on information transmission via the corpus callosum.

In conclusion, research in the 20th century re-defined not only the structural and functional anatomy of the language network but also demonstrated that aphasiology is a field of research at the intersection of multidisciplinary neurosciences including neurology, cognitive psychology, linguistics, physiology and speech pathology.

3.4   Beyond Broca's area and the arcuate fasciculus

Inconsistencies in the classical clinico-anatomical model have been highlighted ever since the first language model was proposed (Bateman 1870; Poeppel & Hickok 2004; Luria 1958; Sondhaus & Finger 1988) and problems with the identification of 'Broca's area' permeate the history of aphasia beginning with the notion that by the time of death Leborgne was aphasic for already 21 years which would have changed the appearance of his lesion and the observation that patients with a lesion to Broca's area often present without the corresponding symptoms or likewise a remote lesion can cause these symptoms (Basso et al. 1985; Dronkers 2000; Murdoch 1988; Basso 2000; Fridriksson et al. 2007; Alekoumbides 1978).

One possible explanation accounting for unusual cases and second-stage recovery[4] was introduced by von Monakow (1905) in the form of diaschisis[5] together with his

---

[4] First stage recovery accounts for the recovery from acute physiological effects, such as haemorrhage, cellular reactions and chemical alternations. Second-stage recovery reaches well into the post acute and chronic stages.

claim that '*gyral regions that have been associated with aphasic language disorders have been considered too narrowly by far up to now, and namely as far as the long association fibre tracts, commissures, and their areas of destination and origin respectively*' (Tesak & Code 2008). Supporting evidence was later stated by Mohr et al. (1978) who provided a comprehensive review of cases since the year 1820, taking into account neuroradiological, clinical and neuropsychological material and concluding that a Broca-like aphasia can result from a lesion to any part of the upper division of the middle cerebral artery, this includes the operculum, the inferior parietal lobe (ILP), the insula and subcortical structures (see **Figure 20** in Chapter 4). Von Monakow also realised that stroke lesions albeit often having a well-defined core extend far beyond the visible borders of the lesion, a phenomenon today referred to as the lesional penumbra. This assumption was also brought forward against Broca who never performed cross-sections of his post mortem specimens (Marie, 1922). Thanks to non-invasive neuroradiology methods including computerised tomography (CT) and magnetic resonance imaging (MRI), the famous case of Broca was re-examined and it was shown that the lesion extended well beyond 'Broca's area' into the deep white matter (**Figure 12**) (Signoret et al. 1984; Dronkers et al. 2007). Aphasiology may have been very different if the method of fibre dissection would have been applied to early investigations.

---

[5] Diaschisis describes a long-distance effect where a dysfunction of brain structures in other vascular territories (i.e. remote to the lesion), that are functionally linked with the lesioned region, is caused by imbalance of inhibitory or excitatory neurotransmission (Hagoort 2005; Stemmer & Whitaker 2008; Fadiga et al. 2006).

Coronal cut at 32 mm: lesion affecting the IFG extensivley.

CT

Coronal cut at 44 mm: lesion to the precentral gyrus, operculum, insula,   STG (bevore Hesch'ls gyrus)

Corical lesion to the inferior frontal lobe with further softenenign of adjacent cortical areas described by Broca (1861).

MRI

Lesion extends into GM of IFG, inferior parietal lobe and anterior superior temporal lobe with further subcortical involvement (claustrum, putamen, globus pallidus, caudate head, internal capsule) and vast white matter damage (i.e., fronto-parietal network)

Figure 12   Neuroradiological images of Broca's famous patient

Both methods showed the lesion dramatically extending subcortically. The upper panel shows the CT scans; the lower panel the MR scans of the same brain. IFG = Inferior frontal gyrus, GM = Grey matter, STG = Superior temporal gyrus. Modified from (Signoret et al. 1984; Dronkers et al. 2007).

The dispute over the definition of Broca's area as a motor (Broca) or sensory area (Bastian 1887) or neither (Flechsig), together with the accumulation of "unusual cases" went so far that some claimed Broca's region may not be language-specific at all (Hagoort 2005; Fadiga et al. 2006). Other proposed candidate functions of Broca's included hierarchical structure building (Friederici 1985), semantic retrieval (Badre & Wagner 2002), and selection of competing alternatives (Thompson-Schill 2005).

In conclusion, the anatomical areas and their associated functions have expanded over the centuries. According to Broca the posterior third of the inferior frontal gyrus

is associated with articulated speech, whereas current research indicates that i) an extended network serves language functions and that ii) a more complex clinical presentation can be seen upon infarction of Broca's area. Tesak and Cohen (2008) concluded their historical review with the notion that '*Broca's area and its syndrome endure into the twenty-first century, and so do some of their mysteries, despite the ingenious methods we can devise to probe the anatomy […] and the experimental tasks we can invent to explore*' the resulting impairments. Some of these 'ingenious' methods will be discussed below.

3.4.1   Cyto-, receptor-, and myelooarchitecture

Cytoarchitectonics

Classically, sections of brain tissue were sliced, stained up and then visually investigated for distinctiveness in their grey matter (GM) thickness, form and size of areas, number of horizontal laminations, relative laminae thickness, arrangements of cells and cell types (e.g., size), cell density, and staining affinities. It was later assumed that cytoarchitectonic areas are functionally discrete in electrophysiological studies as well (e.g., (Luppino et al. 1991)). A neat overlap was shown for basic sensorimotor functions but not for higher cognitive functions.

Broca's area (sensu strictu) largely coincides with the cytoarchitectonic Brodmann areas (BA) BA44/45 and BA47 or macroscopically the opercular, triangular and orbital part of the inferior frontal gyrus (Amunts et al. 1999; Aboitiz & García 1997; Lieberman 2002; Gannon 2010; Stemmer & Whitaker 2008; Amunts & Zilles 2012) (**Figure 13**A). Wernicke's area is classically located at the posterior superior temporal gyrus, caudally to Heschl gyrus, where the primary auditory cortex (BA 41) is located.

Microscopically, however Wernicke's area is ill defined and '*over time, both the functional and anatomical boundaries of 'Wernicke's area' have become so broad as to be meaningless*' p. 83, (Wise et al. 2001). The anatomical boundaries were placed in the tempero-parietal cortices including associative auditory cortex (BA22), lateral occipito-temporal area (BA37), angular (BA39) and supramarginal gyri (BA40), primary auditory cortex (BA41/42), and planum temporale (BA22). The planum temporale has a consistently reported leftward asymmetry (Galaburda et al. 1987; Geschwind & Levitsky 1968; Kakeshita 1925; Wada et al. 1975), which is already apparent after the 29th week of gestation (Wada et al. 1975).
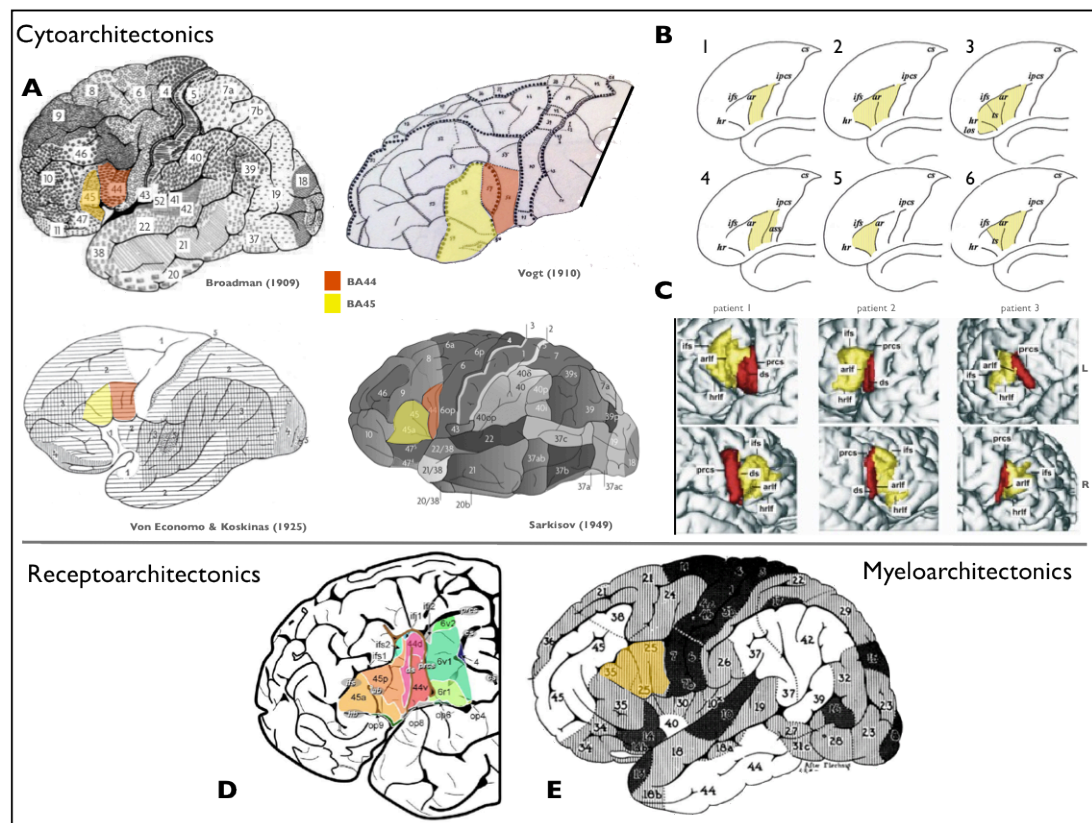
Figure 13   Cyto-, receptor-, and myeloarchitectonic definitions of 'Broca's area'

A Classical cytoarchitectonic maps **B** Schematic diagram of macroscopic definitions of Broca's area with pars opercularis (1), pars opercularis and triangularis (2), opercularis, triangularis and orbitalis (3), opercularis and precentral gyrus (4), triangularis (5) and opercularis and posterior half of the Pars triangularis (6) (Keller et al. 2009). **C** Interindividual variability shown with left and right hemispheric 3D reconstructions in three post mortem brains after histological preparation (Amunts et al. 1999). **D** Recepto-architechnic definition of 'Broca's area'. Parcellation of an extended Broca's area based on receptorarchitecture segregating BA45 rostro-caudally into an anterior (45a) and posterior part (45b) and parcellating BA44 dorso-ventrally with a further extension to area BA6 (Amunts et al. 2010). **E** Myelogenic map of Flechsig (modified by Bonin) indicating early maturation (black), intermediate (grey) and latest maturations (white). Number coding corresponding to sequential maturation (1-44) (Fuster 1995).

The term 'Broca's are/region' has not been used consistently in the literature, where BA44 and BA45 have both been indicated in isolation, together, or with the additional regions BA47 (orbital inferior frontal gyrus) and/or BA6 (inferior precentral gyrus) (Keller et al. 2009; Foundas et al. 1998) (**Figure 13**B). Depending on the choice of parameters (e.g., staining dye) different sets of cortical areas were recognised (i.e. Brodmann's 52 areas; Vogt's 200 areas). In a review on Broca's area, Keller et al. (2009) summarised the various anatomical locations used as reference for 'Broca's area' in different studies and concluded that there is a dissociation between cytoarchitectonically and functionally defined Broca's areas in

the left and right hemisphere (**Figure 13**B). The authors appreciate that more often than not a leftward asymmetry was reported in cytoarchitectonic studies but conclude that due to methodological limitations and variations there *'is currently no convincing explanation to associate the left-right asymmetry of Broca's area with the lateralisation of language'* (p. 29). Prior to this cross-study variability review, Amunts et al. (1999) investigated the intersubject asymmetry of surface anatomy. The authors reconstructed 3D volumes of BA44/45 in three subjects and collected histological tissue probes. They were able to show that the surface anatomy varies considerably across subjects, and as a consequence so does Broca's area (**Figure 13**C).

Brodmann's definition of boundaries was based on visual inspection and hence observer-dependent and does not necessarily match other more detailed cytoarchitectonic maps (e.g., Vogt, 1910; Sanides, 1962; Ngowayang, 1934; Von Economo and Koskinas, 1925; **Figure 13**A). Brodmann used a single staining method that selectively identified cell bodies and neglected the sulci and deep brain structures. Additionally, the posterior inferior frontal gyrus is a region of intimately located cytoarchitectonic areas and the difference in identified areas between studies may be a direct result thereof. Brodmann's cytoarchitectonical parcellation of the cortex (even though today's best known due to its incorporation in the atlas of Talairach and Tournoux 1988), was not the only, and maybe not the best attempt to identify distinguishable brain regions.

Meynert (1885) was the pioneer on cytoarchitectonics. He introduced the concept of the six cortical layers (molecular, outer granular, pyramidal, inner granular, spindle cell layer, medullary) for most of the cerebrum with a few caudal areas presenting with additional layers. This discovery is the foundation of cytoarchitectonics and was further developed over the next century. In an early attempt to correlate physiological to histological function, Campbell published his beautiful textbook containing comparative cross anatomy and histological human studies (A. W. Campbell 1905; ffytche & Catani 2005; Macmillan 2012) (**Figure 14**C). For the temporal lobe Campbell distinguished three areas: auditory-sensory, auditory psychic and common temporal area. The auditory-psychic area (caudal three fifths of the superior temporal gyrus) harbours the centre for 'word deafness'. 16 years after Brodmann, Von Economo and Koskinas published a monumental textbook including 112 micrographs. Based on Nissl staining, they defined 54 fundamental cytoarchitectonic areas and their atlas was readily adopted in the field of animal research but tragically failed to gain recognition within the human neurosciences

(Triarhou 2007) (**Figure 14**A). Von Economo and Koskinas considered sensory, motor, amnestic and insular aphasia associated with distinct cortical areas.

Another functional cortical map was provided by Kleist who employed the clinico-anatomical approach on World Ward I injury victims to map the deficits and further associated these findings with cytoarchitectonics. Kleist identified perisylvian areas relevant for sentence and word articulation and comprehension together with regions for names, reading and writing (**Figure 14**B).

In conclusion, cytoarchitectonic mapping of Broca's area sensu strictu revealed considerable intersubject variability for its location and boarders (Amunts et al. 1999; Keller et al. 2009; Keller et al. 2007).

Figure 14   Functional localisation map of the left hemisphere based on architectonics

Coloured areas are relevant for language processing in both models but are not necessarily equivalent between A and B. **A** Corresponding functions of the cortical parcellation according to von Economo and Koskinas (1925). **B** Kleist's functional correspondence for cytoarchitectonic subdivision**.**

3.4.2 Receptorarchitectonics

It was further suggested that receptor boundaries more clearly than cytoarchitectonic boundaries may cluster functionally distinct regions, given that neurotransmitters could elicit inhibitory or excitatory responses. Using receptoarchitectonics (distribution of receptor binding sites of classical neurotransmitters), Zilles et al. (2002) demonstrated interlaminar and regional differences for receptor distribution between areas 44 and 45 and surrounding areas. Investigating classical transmitters (glutamate, gamma aminobutric acid, serotonin, and noradrenaline), the authors showed, for example, that BA45/44 could be subdivided rostro-caudally and dorso-ventrally with regards to the receptor binding sites for glutamate and serotonin (5-HT). The glutamate receptor is highly concentrated in the rostral part and more lowly concentrated caudally of BA45. 5-HT on the other hand, has high binding sites dorsally and low binding sites ventrally in BA44 (**Figure 13**D). This subdivision withstands comparative anatomy studies (Petrides and Pandya, 2001) and has also been implicated in fMRI studies where, for example, the most ventro-posterior part of BA44 was activated during syntactic tasks (Indefrey & Levelt 2004) and the dorsal pars opercularis in phonological tasks (Heim & Friederici 2003). These studies collectively indicate a more fine grained parcellation of Broca's area on the one hand and on the other a putative extension to neighbouring areas such as the premotor area BA6 at the ventral precentral gyrus, dorso-lateral prefrontal areas BA9 and BA46, area BA47 at the orbital part of the inferior frontal gyrus, and the anterior insula (**Figure 13**D). Receptoarchitectonic analyses of the temporal cortex are not yet available, but studies are ongoing (Friederici 2011).

Myeloarchitectonics

The pioneer Paul Flechsig developed the method of myelinogenesis, whereby the myelin sheath at different developmental stages is stained up (instead of cell bodies as in cytoarchitectonics). Applying this method systematically, Flechsig and his scholars (e.g., Oskar Vogt) derived a myeloarchitectural map of the human brain, which Flechsig separated according to an early myelinating primitive zone (for all sensorimotor cortices), and an association zone that myelinates last (**Figure 13**E). Considering the localisation of the language network (sensu strictu) the eloquent regions are harboured within the intermediately myelinating zone; if the extended network is considered, the regions coincide with the late myelinating brain.

The conclusion from these studies may be, as Chris McManus allegedly put it when asked, what he believes we know for sure: '*Probably, Broca's original observation that the vast majority of patients who have unilateral damage to their brain, if it's on the left, lose speech. That's the only thing I think is clear from the whole literature*" (p. 165, 1988).

3.4.3   Intracarotid amobarbital procedure (IAP) or WADA test

'*The Wada test […] has been a major source of knowledge concerning the lateralisation of language functions*' (Geschwind, 1970). Intracarotid injections of amobarbital (IAP, commonly called the *WADA test* giving credit to Juhn Wada who first developed it) have been performed for clinical purposes since 1949, when it was noted that a direct intracarotid injection of an anaesthetic agent produces a transient ipsilateral paralysis of hemispheric function without the interruption of vital functions. This approach has since become the gold standard for pre-surgical language lateralisation determination (Wada 1949; Wada & Rasmussen 1960). Injection into the language dominant hemisphere causes a dense transient aphasia for 2-3 minutes, followed by few minutes of milder aphasic symptoms. As a precautionary measure EEG is recorded simultaneously to document functional contralateral changes but also monitor possible overflow of the anaesthetic (Emde Boas van 1999). Given the invasiveness of the WADA test, it is not without controversy and it has been suggested that advanced non-invasive functional neuroimaging methods may supersede it in clinical practice (Desmond et al. 1995; Binder et al. 1996; Yetkin et al. 1998; Abou-Khalil 2007). However, some studies implied that the methodological coherence is greater for the frontal lobe than for the temporal lobe (Lehéricy et al. 2000) and believe fMRI is not yet validated enough to replace the WADA test in the clinical arena (Rutten et al. 2002). Ross et al. (1988) reported that upon left internal carotid artery (ICA) injection their patients became densely aphasic. When the right hemisphere was infused patients lost the ability to impart affect onto their speech. Right hemispheric modulation of suprasegmental (e.g. prosody, affect) language components has been reported several times using different psychophysiological methods (Bowers et al. 1987; Weintraub et al. 1981; Larsen et al. 1978; Shapiro & Danly 1985; Benowitz et al. 1983). Ross and Mesulam (1979) highlighted the relevance of the right fronto-parietal opercula in language modulation. The authors conclude that anterior circulation lesions (see **Figure 22** in Chapter 4) cause loss of affective prosody but also imply it may be an

affective motor not a comprehension deficit (i.e. patients understand affect but cannot produce it themselves).

Two approaches are employed to calculate lateralisation. One method purely measures the duration of muteness (i.e. speech arrest) after left (L) and right (R) hemispheric injection and obtains a laterality index based on the formula LI = (L-R) / (L+R). The other approach is based on a language assessment before and during the procedure yielding the percentage (P) of correct answers under anaesthesia (P_L-P_R) (Benbadis et al. 1998). Even though both approaches seem clinically acceptable a validation study showed that the obtained scores from both methods do not correlate; a correlation was however shown between the percentage of correct performance and language lateralisation as defined with fMRI (Benbadis et al. 1998). The WADA test is invasive and brings about various neurosurgical risks and, in most patients, the limitations of this method outnumber the benefits, given the availability of non-invasive neuroimaging methods. The most striking limitations are the following: i) the angiographic procedure is invasive and complications have been reported (Dion et al. 1987; Stemmer & Whitaker 2008), ii) complementary methods (e.g., intraoperative cortical mapping) are needed to precisely demarcate language localisations, iii) the interpretation of the test relies on a 'normal' arterial anatomy, which is not necessarily given in a patient and iv) the test is approximately 3.7 times more cost intensive than fMRI (Binder et al. 1996; Medina et al. 2004).

3.4.4   Intraoperative electrical stimulation (IES)

During intraoperative electrical stimulation the mapping of functional (elucidating an obvious response when stimulated) and non-functional (no obvious response upon stimulation) areas is performed prior to the potential re-section of brain tissue. Two effects can be seen upon stimulation, either an evoked behavioural change or an interference with on-going behaviour (Ojemann 2003). A low-frequency stimulation is directly administered to specific parts of the brain and the patient is then engaged in tasks (i.e. naming task for the testing of eloquent areas). If the patient loses the capacity to perform the task when a specific area is stimulated, this brain tissue is considered functional. This method is commonly applied in tumour resections and epilepsy surgery to maximise the resection of pathological tissue whilst minimising language deficits after surgery. The application of direct electrical stimulation to the

brain as means of mapping the cortical functions in humans dates back to the year 1874 (De Witte & Mariën 2012).

The first to use this method to provide in vivo evidence for Broca's area as a language region was the American neurosurgeon Wilder Penfield, when he performed IES of the '*forbidden territory*' resulting in speech arrest during an object naming task in epileptic patients:

> *'Mapping the speech area. Forbidden territory. […] In the beginning it was our practice to refuse radical operation upon the dominant hemisphere unless a lesion lay anteriorly in the frontal lobe or posteriorly in the occipital lobe. Like other neurosurgeons, we feared that removal of cortex in other parts of this hemisphere would produce aphasia. The left temporal lobe and the fronto-centro-parietal areas were considered to be devoted to mechanisms of speech, and aphasia literature gave no clear guide as to just what might and what might not be removed with impunity. But patients continued to present themselves in increasing number with focal epilepsy […]. Many of these patients were not aphasic. And so we were emboldened gradually to make more and more excisions within the forbidden territory.' p. 103,(Penfield & L. Roberts 1959).*

A summary of the electrical stimulation literature compiled by Lecours (1983b) and based on Penfield's work compares the resulting language impairments upon stimulation of the left and right hemispheric cortical areas and thalamic pulvinar (**Table 7**).

Table 7   Electrical stimulation in cortical and subcortical structures and resulting language impairments.

Colour-coding implies a gradient from greater to lesser (blue-green-yellow) intensity of observed phenomena. *Palialia: rapid repetition of the same segment, usually a syllable.*

		Vocalisations	Slurring	Palialia	Arrest	Hesitation	Naming — Anomia	Naming — Perseveration	Naming — Verbal paraphasias
Left hemisphere	Inferior half of postcentral gyrus	green	green	green	green	green			
	Inferior half of precentral gyrus	blue	green	blue	blue				
	Ventral lateral nucleus		green	green	green	?	green	green	
	Penfield's SMA	green	green	green	green	green	green	green	
Classical language zone	Broca				blue	blue	blue	blue	blue
	Wernicke			green	green	green	blue	blue	blue
	Inferior parietal lobe					green	blue	blue	blue
	Pulvinar						green	green	Misnaming
Right hemisphere	Inferior half of postcentral gyrus	green	green		yellow	yellow			
	Inferior half of precentral gyrus	blue	green		yellow	yellow			
	Ventral lateral nucleus		green	green	yellow	?			
	SFG caudal internal third	green	green	green	green	green			
	Pars opercularis					yellow			
	Caudal half of STG and MTG								
	Inferior parietal lobe								
	Pulvinar								

This schematic summary indicates that certain functions, such as vocalisation and slurring, occur without lateral predominance; whereas other functions, such as naming, are strongly left lateralised.
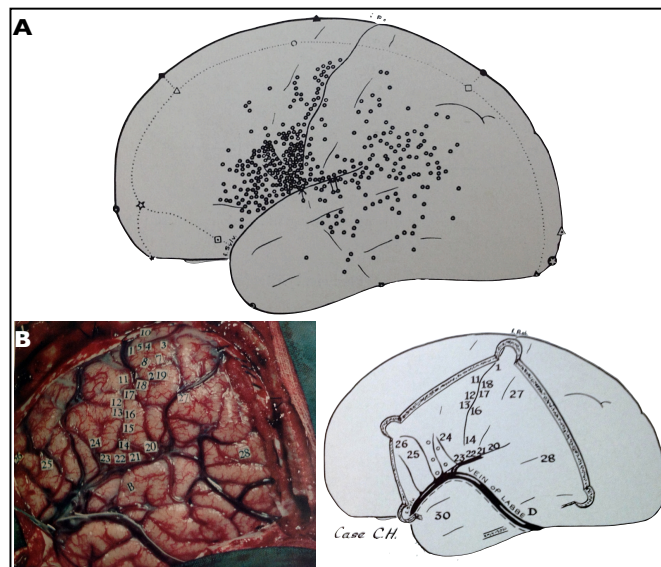
Figure 15   Intraoperative electrical cortical stimulation (Penfield & L. Roberts 1959)

A Cortical map of areas that interfere with speech upon electrical stimulation (individual disturbances include speech arrest, hesitation and slurring of speech, distortion and repetition of words and syllables, confusion with number counting, inability to name with retained ability to speak, perseverations). B Case C.H. Photograph and corresponding

drawing of the left hemisphere as exposed at surgery. Stimulation of electrodes at 26-8 produced aphasic interference with speech. 23-4 elicited anarthria (motor speech arrest).

Penfield's pioneering explorative work identified a detailed cortical language-associated region map (**Figure 15**). This work was complemented by Schaeffler et al. (1993) who replicated the speech arrest upon inferior frontal gyrus stimulation and furthermore implied that coinciding comprehension deficits for higher-level auditory and visual instructions are induced, a finding that has been observed in other studies as well (e.g. Papathanassiou et al. 2000).

In recent years, this method was employed for various functional anatomical studies (Bello et al. 2008; De Witt Hamer et al. 2011; Ellmore et al. 2009; Leclercq et al. 2010; Henry et al. 2004; Duffau 2005; Duffau et al. 2005; Duffau, Peggy Gatignol, et al. 2008b; Duffau, Leroy, et al. 2008a; Duffau, Denvil, et al. 2002b; Duffau, Capelle, et al. 2002a; Maldonado et al. 2011; Mandonnet et al. 2007; Matsumoto et al. 2004; Matsumoto et al. 2011). Duffau et al. (2002a) compared their intraoperative mapping with pre-surgical MR images and implied the following functional anatomy. Upon stimulation of the subcallosal bundle[6] language was no longer initiated; stimulation of the periventricular white matter resulted in dysarthria and the stimulation of the arcuate and insular connections induced conduction aphasia symptoms. In a later study Duffau et al. (2009) specifically investigated the functional role of the uncinate fasciculus for language and concluded that the uncinate is not a language-specific tract but is relied upon for some linguistic information. Bello et al. (2008), for the first time using a 3 Tesla (T) MR scanner, showed that pathways remain unchanged only in small tumours but dislocate, infiltrate or disconnect in larger tumours. Stimulation of individual tracts resulted in phonemic (superior longitudinal fasciculus, here considered as a branch of the arcuate) and semantic paraphasias (the inferior fronto-occipital and uncinate). De Witt Hamer et al. (2011) investigated the putative language tract, middle longitudinal fascicle (MdLF, detailed below) (Makris et al. 2009) and reported that neither upon stimulation nor removal of large parts of the tract were language deficits (transient nor long-term) induced and concluded that '*the MdLF is not essential for language in humans*' (p.967).

---

[6] Here defined as '*a white matter area surrounding the lateral angle of the frontal horn containing a pathway through which fibers pass from the cingulate gyrus and supplementary motor area to the caudate nucleus*' (p.210). Further references can be found in Schmahmann and Pandya (2006) and Forkel et al. (2012).

A slightly different approach was employed by Matsumoto et al. (Matsumoto et al. 2004; Matsumoto et al. 2011). This method is based on invasive monitoring with subdural electrodes by inserting a grid of electrodes over a defined patch of cortex and was developed to electrically track the cortico-cortical connections for epileptic spike propagation. The gird allows stimulating cortical tissue through subdural electrodes, and recording the cortical evoked potentials that emanate from distant cortical regions. The first language study employing this method demonstrated three results: (i) that connections were site specific, meaning that a stimulation at Broca's area elicited cortico-cortical evoked potentials (CCEPs) over the lateral parieto-temporal area, whereas, stimulation at the face motor area just posterior to Broca's area elicited a more anterior CCEP distribution in the postcentral gyrus; (ii) the connections between the anterior (i.e. Broca territory) and posterior (i.e. Wernicke territory) language areas were electrophysiologically bidirectional, meaning that stimulation of anterior language areas evoked potentials in posterior language areas and vice versa and (iii) the distribution of evoked potentials indicated the existence of a large posterior language network distributed over the lateral parieto-temporal cortex, such as supramarginal gyrus and posterior part of the superior and middle temporal gyri, surrounding the previously recognised core region of this area (Matsumoto et al. 2004).

Multimodal approaches (i.e. combining MR-based imaging with IES) have yielded interesting results. Leclerq et al. (2010) report an overlap of 81% between IES mapping and MR-based white matter pathway reconstructions. Furthermore, articulatory deficits and paraphasias were induced with arcuate stimulation; whereas the inferior fronto-occipital fasciculus was only associated with semantic paraphasias. Sarubbo et al. (2012) reported the multistage resection (here over the course of four years) of Wernicke's area due to a left temporal tumour inducing transient language deficits in a right-handed woman. The pivotal observation in this patient is that during her first surgery Wernicke's territory was spared, as it was established to be a functional area. Three years later, however, it was possible to remove the very same area due to an apparent utilisation of ipsi- and contralateral cortices to perform eloquent functions. Ellmore et al. (2009) matched approximately 79% of their stimulation map with MR-based white matter pathway reconstructions of essential eloquent areas, all intimately located to the arcuate fasciculus. The authors conclude that MRI can be utilised to predict the cortical language areas for surgical interventions. By far one of the most comprehensive multimethodological studies investigated epilepsy patients with a WADA test to determine hemispheric

language dominance, electrostimulation of anterior-posterior language cortices, and invasive monitoring with subdural electrodes (Matsumoto et al. 2004). The authors found that stimulating the anterior language area elicited cortico-cortical evoked potentials in the temporo-parietal cortices, in the middle and posterior part of the superior temporal gyrus, the middle temporal and supramarginal gyrus. This pattern of activity nicely fits to purely anatomical observations described within this chapter.

Despite these exciting findings, inherent methodological limitations have to be considered. Firstly, IES can only be applied to a limited clinical population (mostly tumour and epileptic patients) where the anatomy is resected and therefore population-wide generalisation is limited. Secondly, the interpretation of brain structures depends on the a priori conceptual framework of the surgeon and on the en vogue terminology (i.e. the arcuate fasciculus was equated to i) the superior longitudinal fasciculus (today considered as a fronto-parietal network) (Dejerine, 1885) and ii) the superior fronto-occipital fasciculus (Onufrowicz 1887). Third, intersubject variability in the location of eloquent areas is considerable and seems to be associated with age, gender and premorbid language skills of the patient (Ojemann 2003). The abovementioned studies do emphasise the coherence between MR-based imaging and intraoperative mapping; however, these results have to be evaluated on a patient-by-patient basis. The advantages of this combined approach are a decreased duration of surgery, reduced patient fatigue, and less intraoperative seizures (Bello et al. 2008; Thiebaut de Schotten & Bartolomeo 2011).

In conclusion, intraoperative mapping advanced our understanding of the language network and emphasised the importance of connectional anatomy. Based on the above studies, it might be assumed that the arcuate fasciculus (for articulation) is part of an extended language network that further includes pathways such as the inferior fronto-occipital fasciculus (for semantics) and the superior longitudinal fasciculus (for phonemics). This model, however, awaits multimodal validation.

3.4.5   Structural and functional neuroimaging studies

3.4.5.1   Structural MR-based Diffusion-weighted imaging tractography (DTI)

Anatomically, Johann Christian Reil (1812) provided the first known pictorial description of fibres connecting the inferior frontal gyrus and the superior temporal gyrus by arching around the Sylvian fissure. He identified a group of fibres running deep in the white matter of the temporal, parietal, and frontal regions closely surrounding the Sylvian fissure. Unaware of the significance of these fibres Reil entitled them as *unnamed white matter* and chose the show them in the right hemisphere (see Catani and Mesulam, 2008a). Ten years later Karl Friedrich Burdach replicated Reil's extensive anatomical work and introduced Latin names for all structures previously described. He designated these perisylvian fibres collectively as fasciculus arcuatus, owing to the arching shape of the longest most medial fibres (Burdach 1822). The anatomy of the arcuate fasciculus has since been found to be more complex than initially anticipated. Jules Dejerine (1895) believed that these fibres were composed primarily of short U-shaped associative fibres connecting adjacent perisylvian areas.

A landmark study in modern arcuate anatomy was based on DTI tractography (see Chapter 5) and reported that the arcuate fasciculus does not purely interconnect inferior frontal and superior temporal gyri, as was classically believed, but is constituted of a parallel indirect connection to the inferior parietal lobe (Catani et al. 2005). The inferior parietal region has previously been indicated as putative multimodal association area (Geschwind 1965b). The direct connection (long segment) extends from the posterior inferior frontal gyrus to the posterior superior and middle temporal gyrus. The indirect segments run between i) the inferior frontal and inferior parietal gyri (anterior segment) and ii) inferior parietal and temporal gyri (posterior segment). The authors report considerable variability of the temporal terminations and the size of all three segments across subjects, but they were able to reconstruct the pathways in all participants. Furthermore, the long segment was shown to reach beyond the language areas sensu strictu, with rostral terminations within the inferior and middle frontal as well as the inferior precentral gyri (BA39,40) and the indirect segments projecting more caudally; a finding that complements the previously discussed rostro-caudal segregation of Broca's area (chapter 3.4.1), and that will reappear below (see Paulesu 1997). Two years later, the same group re-investigated the arcuate anatomy and this time included the right hemispheric perisylvian connections (Catani et al. 2007). In this study the authors demonstrated an interhemispheric pattern of arcuate lateralisation across subjects and further

showed a correlation with verbal learning based on semantic association. The task performance was best in participants with the most bilateral arcuate anatomy. The authors also reported gender differences (for details see paragraph 1.7).

Glasser and Rilling (2008) segregated the arcuate into two segments: one connecting the posterior frontal lobe (BA6, 44) with the posterior superior temporal gyrus (BA22), and one projecting from frontal regions (BA6, 9, 45) to the middle temporal gyrus (BA21, 37) (**Figure 16**A). The authors reported both segments to be left lateralised and implied a functional segregation whereby the dorsal branch is associated with phonological processing and the more ventral branch with lexical-semantic processes. Makris et al. (2009) reported a middle longitudinal fasciculus (MdLF), a tract the authors believed to run within the superior temporal gyrus, connecting the temporal pole to the inferior parietal lobe (angular gyrus). The authors suggested, based on the cortical terminations of the MdLF, that it is associated with language function. As we have seen in the previous subchapter, however, more recent stimulation studies of tissue along the trajectory of the MdLF, as well as the resection of large parts of it, did not elicit any language deficits (De Witt Hamer et al. 2011). Frey et al. (2008) segregated the connection of opercular and triangular inferior frontal gyrus based on experimental evidence from monkey research and claimed that the opercular region is connected to inferior parietal lobe (IPL) through the superior longitudinal fasciculus (branch III). This connection has been demonstrated in the comparative literature (Thiebaut de Schotten, Dell'Acqua, et al. 2012b). The authors reported that the triangular region projects anterior to the Heschl's gyrus via the external/extreme capsule and further claim that the superior temporal gyri connections project dorsally to Broca's area to BA6 and 8 (**Figure 16**A). Overall, these results are coherent with animal studies but lack validation with human dissections. The authors do however briefly discuss that they were able to find an arcuate with a resemblance to previous post mortem and in vivo reports (when placing their regions of interest differently). The 'classical' arcuate was indeed connecting the posterior superior temporal gyrus to the inferior frontal opercular and triangular areas though favouring a connection to pars opercularis. A temporo-parietal connection was also described which is attributed to the MdLF as described before. Kaplan et al. (2010) considered only a horizontal portion of the arcuate fasciculus, which the authors claim is difficult to differentiate from the third branch of the superior longitudinal fasciculus (SLFIII), and reported it selectively connects the supramarginal gyrus to the caudal inferior frontal gyrus (opercular and

ventral premotor area) but not to the more rostral triangular part. This result was shown for both hemispheres.

Anwander et al. (2006) parcellated Broca's area based on its anatomical connectivity. The authors report a segmentation into three regions BA44, 45 and deep frontal operculum with the more caudal-dorsal (BA44, inferior precentral gyrus) regions being connected to the posterior language areas through the arcuate/SLF and more anterior-ventral regions (BA45) through a ventral system passing through the external/extreme capsule. Similarly, Frey et al. (2008) parcellated Broca's area into BA44 and BA45 based on connectivity to IPL and the superior temporal region.

A more recent study, dedicated to the shorter intralobar frontal lobe connections, showed that the pars opercularis (and, to a minor extent, the pars triangularis and precentral gyrus) is connected to the anterior supplementary and pre-supplementary motor area (pre-SMA) in the superior frontal gyrus through the *frontal aslant* tract (FAT) and further identified a range of fronto-insular tracts (Catani, Dell'Acqua, Vergani, et al. 2012b), a finding that is in agreement with earlier anatomical (N. Lawes et al. 2008; Oishi et al. 2008) and clinical studies where stroke patients with a corresponding lesion presented with articulatory planning deficits (i.e. motor squeal of articulation) (Dronkers 1996). It should be noted here that even though all studies used in vivo tractography the underlying methods vary considerably in their approaches and reconstructions (i.e. deterministic and probabilistic diffusion tensor imaging, spherical deconvolution (SD), and q-ball imaging).
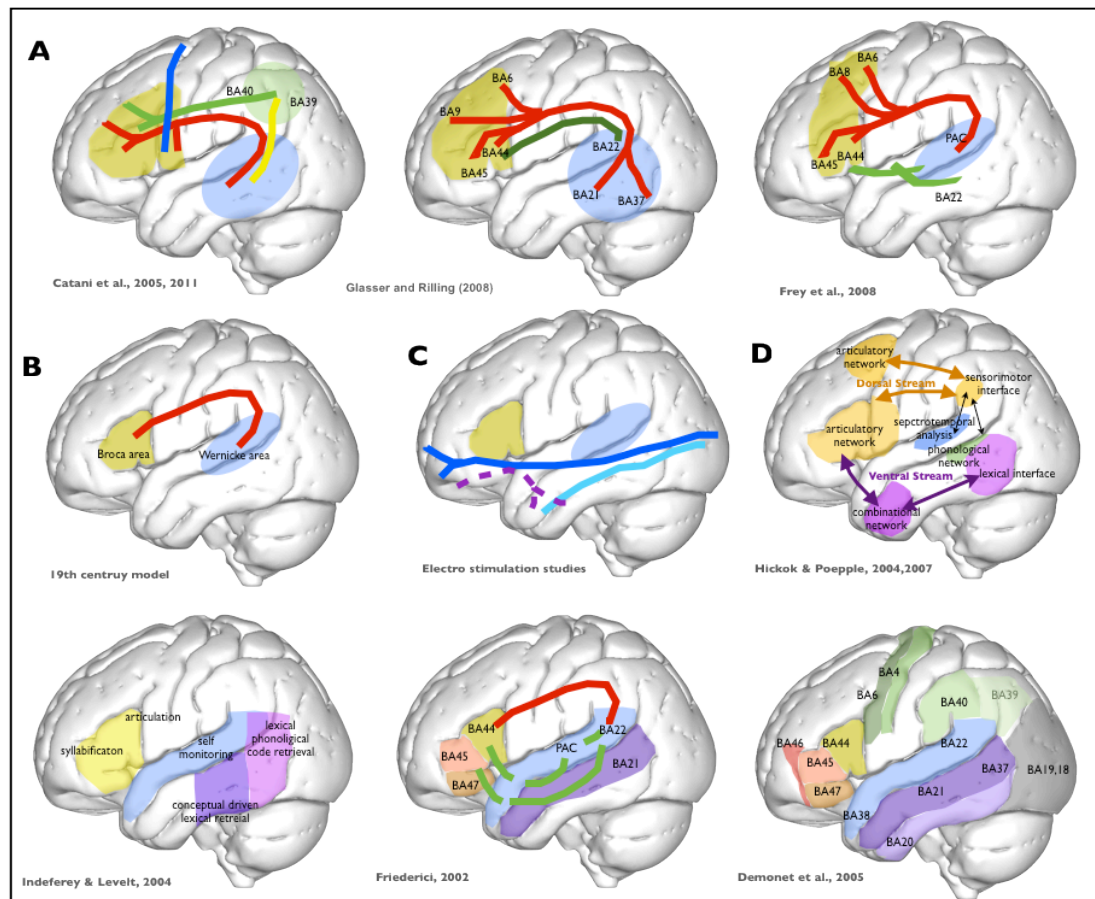
Figure 16   Multimodal approaches to define the anatomy of language

Cross-methodological comparison of in vivo tractography (A), tomography (D) and electrostimulation (C) of perisylvian network in comparison with the classical model. **A** Different classifications of the language network in the living human brain based on MR-based diffusion tractography. **B** Classical 19th century post mortem model. **C** Electrostimulaton. **D** functional tomography studies.

3.4.5.2 Functional imaging (EEG, fMRI, PET)

3.4.5.2.1 Electroencephalogram (EEG)

EEG was the first neuroimaging method used to correlate language functions with neuroelectrical measures (scalp voltages). The potential of EEG was discovered in the 1950s once it became evident that stimulus-dependent measureable parameters (amplitude, latency, and skull topography) could be extracted from a time series of changes in electrical brain activity recorded from the skull before, during and after an event of interest. Event-related potentials (ERPs) are produced by endogenous stimuli (i.e. emotions and anticipations of a person) as well as exogenous stimuli (i.e. response task). In language studies, event-related potentials are time-locked to stimuli presentation and differ systematically with manipulations

to phonology, semantics and syntax. Three event-related potentials have been implicated as relevant for language processing (**Figure 17**). One surrogate measure is the early left anterior negativity (ELAN, negativity peak around 200ms), first described by Friederici et al. (1993), that has been associated with phrase structure violations (e.g., 'The students enjoyed Bill's of review the play') (Hahne & Friederici 1999; Lau et al. 2006). A second later occurring slightly right-lateralised negativity, N400 (between 200-600ms), is best recorded over the centro-parietal lobe (Kutas & Federmeier 2011) and has been associated with lexico-semantic integration (Friederici 2002; Kutas & Federmeier 2011; Steinhauer & Friederici 2001). A late centro-parietal positivity (P600 or syntactic positive shift) has been elicited with obvious syntactic violations (grammatical anomalies or incongruences such as 'The patient met the doctor while the nurse with the white dress shows the chart during the meeting') that necessitate sentence revision or within syntactically complex sentences (Friederici et al. 1993; Osterhout et al. 1994; Kaan et al. 2000). Its topographical location is characterised by the syntactic operations involved in the building of complex sentences and retrieval processes that influence the latency and amplitude of the P600 response (Gouvea et al. 2010). This model has a strong modular character whereby auditory sentence comprehension (sentence production is not specifically considered here) is processed along a sequential three-step cascade.

Methodologically, EEG provides the advantage of being applicable to healthy and clinical populations alike. On the downside EEG is lacking the spatial resolution that is needed to locate language processes to anatomical structures and networks. Additionally, language ERPs are best seen in violation paradigms, which may not produce language-specific responses but categorical violation-specific responses. Attempts to combine EEG with other imaging methods to circumvent this problem or advanced EEG method with improved spatial resolution have been attempted but are not yet readily applicable.
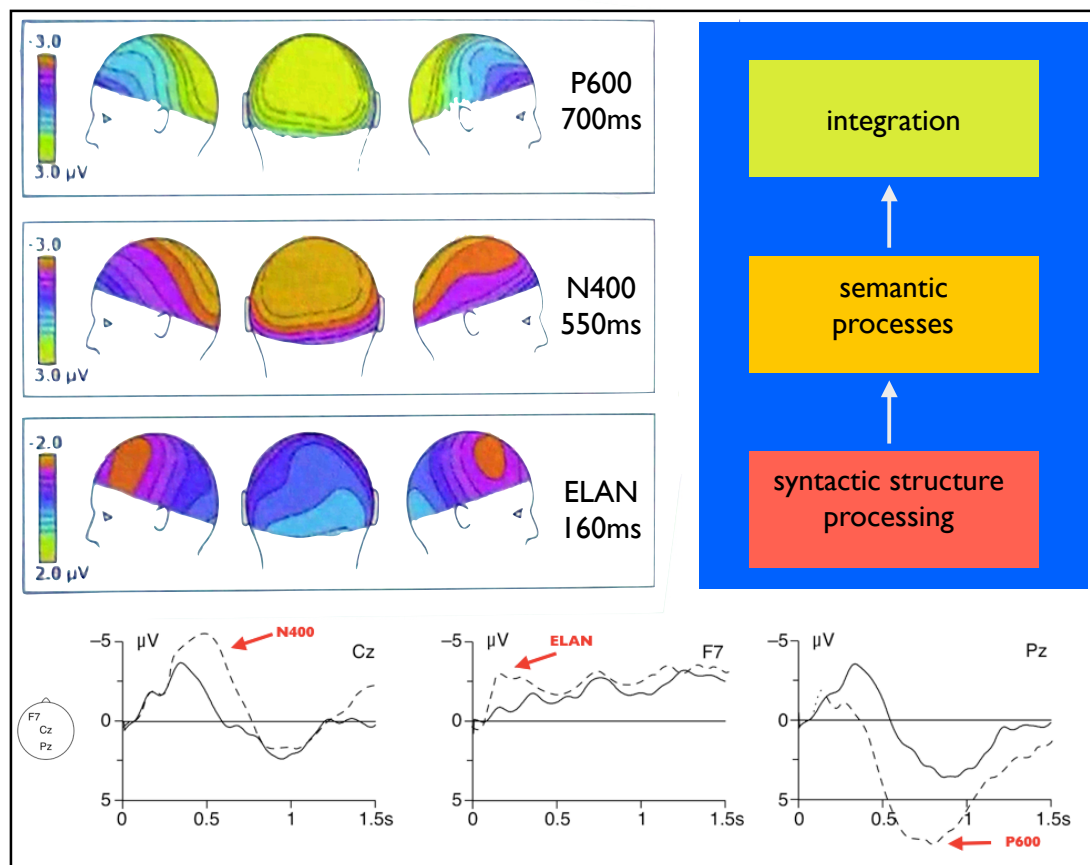
Figure 17   Electroencephalogram event related potentials representing language processes

P600 for integration processes, N400 for semantic processes, and early left anterior negativity (ELAN) for initial syntactic structural processes. These potentials are best elicited within violation paradigm studies, here represented as solid lines for correct conditions and dotted lines for semantic/syntactic violations (modified from (Friederici 2002; Friederici 1985)).

3.4.5.2.2 Positron emission tomography (PET) and functional magnetic resonance imaging (fMRI)

It was only in the late 1980s that a Nature publication highlighted the usability of PET in language research (Petersen et al. 1988). Nowadays considered as the typical functional imaging methods, PET and fMRI have been the methods of choice for many years to investigate the human brain in vivo during task and rest periods and a plethora of articles has been published in established journals. See (Cabeza & Kingstone 2001), for a comprehensive review. Functional methods are based on the task-dependent blood oxygen (O) level changes induced by a certain area's increased demand for oxygen and nutrition due to altered performance needs. This increased oxygen level can be measured through modulation of regional cerebral blood flow (rCBF), or extracted as an fMRI signal called blood-oxygen-level-

dependent (BOLD) effect. PET or perfusion MRI are most commonly utilised to directly correlate mental operations with indices of brain activity.

Recent language models incorporate functional neuroimaging data. All of these models, however, highlight different aspects of language, namely lexical processing (Price 2010), integration of linguistic structures (Friederici 2002), continuous speech perception (Hickok & Poeppel 2007), and articulation (Indefrey & Levelt 2004).

Dual stream model by Hickok and Poeppel

Poeppel and Hickock (2000) elaborate on their dual-pathway model, derived from imaging, deficit-lesion, and electrophysiological data. Within this model the pathways originating from the superior temporal gyrus extend along a dorsal parieto-frontal route to interface auditory-articulatory representations of speech and along a temporo-parieto-occipital route for lexical-semantic mapping. Auditory stimuli are initially processed bilaterally within the superior temporal gyrus and sulcus. Further processes are separated along two routes: a bilateral ventral route (ventrolateral superior temporal gyrus to inferior and medial temporal gyrus) for comprehension and "meaning mapping" and a left-hemispheric dorsal route (inferior partial lobe to inferior frontal gyrus) for phonologic-articulatory mapping (**Figure 16**D). This model was functionally extended by Saur et al. (2008) and Saur et al. (2010) who suggested that the dorsal route is relevant for higher phonological processes (e.g., repetition of pseudo words) and the ventral stream is implicated in comprehension.

Language comprehension and syntax

Angela Friederici (2002) argued in favour of a bilateral temporo-frontal network for auditory comprehension. Within this model the temporal cortices subserved identification of syntactic and semantic input whereas the frontal lobes are relevant to build relations between them.

In the left hemisphere, the anterior part of the superior temporal gyrus is relevant for the identification of syntactical information and the middle temporal gyrus is relevant for semantic content identification. In the right hemisphere, processing of suprasegmental information (i.e. prosody) activates the posterior part of the superior temporal gyrus. The relation between the syntactic and semantic information is then formed in the frontal lobe in BA44 and operculum and BA45/47. From EEG studies

it is apparent that syntactic identification precedes semantic identification, i.e. a syntax-first model, but all processes of auditory sentence comprehension have to be integrated at a later processing stage to fully understand spoken language. Anatomically this model is placed within the traditional framework wanting the inferior parietal extension, and the notion that Broca's area is language-relevant (locus of syntax) but not language-specific as other tasks activate this region as well.

Functional imaging reviews

In a review of functional imaging and stimulation studies, Indefrey and Levelt (2004) proposed a time-locked five stage model for articulation and comprehension that anatomically translates into lexical access and retrieval within the middle and superior temporal gyrus and syllabification in the posterior inferior frontal cortex, and articulation in the inferior precentral and postcentral gyrus. This model, however, did not highlight the parietal lobe as language-relevant (**Figure 16**). These studies complement and challenge the classical language and aphasia model (for review see (Démonet et al. 2005; Vigneau et al. 2006) reviewing 1992-2006, (Friederici 2011) reviewing 1993-2011, (Price 2010) reviewing 2009, and (Price 2012) reviewing 1992-2011).

The pioneering work in the field of functional language studies (with PET) was provided by Petersen et al. (1988) where a functional anatomical model was established. The authors favoured a parallel processing cascade, whereby perceived words (either visually or auditory) engage separate modality-specific areas, with a common and parallel access to articulatory and semantic information. Most interestingly is the authors' interpretation of Broca's area:

> *'The left Sylvian regions are near Broca's area; a region often viewed as specifically serving language output. But Sylvian activation was also found in the right hemisphere, and this bilateral Sylvian activation was also found when subjects were instructed to simply move their mouths and tongues, arguing against this region as language-specific' (p. 587)*

They further allocated semantic processing to the left ventrolateral inferior frontal gyrus (BA47) and articulatory processes along the frontal motor system. This study was replicated and extended by Wise et al. (1991) who demonstrated that the classical Wernicke's area is the only temporal lobe region whose activation is independent of the rate of presentation of auditory stimuli.

Most recent meta-analyses (Vigneau et al. 2006; Price 2012; Price 2000; Friederici 2011; Démonet et al. 2005; Turken & Dronkers 2011) showed that phonological, syntactic and semantic processes grossly follow the gyral surface architecture and even though mostly distinct, partially overlap locally. The anterior superior temporal gyrus is activated by all three modalities. Phonological processes seem to be propagated within the posterior-dorsal aspects of the frontal and temporal lobes; whereas semantic and sentence-level analysis was ascribed to the pole and middle portion of the middle temporal gyrus. The pars opercularis and ventral triangularis of the frontal lobe are associated with semantic and syntactic processes. This study further concludes on a functional rostro-caudal segregation of the inferior frontal gyrus as it was proposed by various individual studies whereby the triangular area is more associated with semantic processes and the opercular areas with phonological processes (Buckner et al. 1995; Zatorre et al. 1996; Nixon et al. 2004; Bookheimer 2002).

3.4.6   Hemispheric asymmetries in language-related pathways

Functional lateralisation (and with it hemispheric specialisation) is often quoted as a cardinal achievement in human brain development that is crowned by the evolution of language. The lesion-deficit approach of Broca and Wernicke promoted the left hemisphere as being language-dominant. Most experimental work on hemispheric specialisation originated from the study of epileptic patients undergoing surgical section of the corpus callosum (interhemispheric white matter connection) for seizure control, the famous 'split-brain' patients. These patients provided the unique opportunity to study hemispheric functions rather independently from the input and interaction with the other hemisphere. Based on a series of investigations, Gazzaniga et al. (1981) concluded that for language, the left hemisphere is dominant for expressive functions whereas the right hemisphere is only capable of comprehension with minimal syntactic processing. Phonetic processing was tested, for example, with an auditory dichotic test where stimuli are presented to one ear at a time and the patient is instructed to transcribe the heard message. This was only possible for stimuli presented to the left hemisphere (transcribed with the right hand) but not for stimuli presented to the right hemisphere (transcribed with the left hand).

However, these are selective case reports that often are warrant of pre-surgical hemispheric language dominance information and can therefore be marvelled at for their excellent experimental neuropsychological complexity but allow limited generalisation for language lateralisation.

Another source of information originates from lesion-deficit studies and the subsequent recovery from brain lesions, such as in stroke. In this context it has long been hypothesised that undamaged neighbouring cortical areas as well as homotopic contralateral cortical areas might compensate for some of the lost function in the language dominant hemisphere (Roch Lecours et al. 1983a). Nearly 30 years ago it was still speculation that the influence of the right hemisphere varies dependent on the degree of functional language lateralisation; a hypothesis that was not testable with the available methodology but has since been validated (Matsumoto et al. 2008). The early, yet invasive, gold standard to define language lateralisation used to be through the injection of sodium amytal (as described in 3.4.3). However, if applied to stroke patients with a left hemispheric lesion the deficits would be equivalent to the symptoms of bilateral lesions.

In recent years, functional MRI and tractography has been used to study the laterality of language and the underlying connectional anatomy. In one such study Powell et al. (2006) examined 10 right-handed healthy volunteers showed a bilateral, yet left dominant, lateralisation for language functions with a corresponding pattern for the tractography of the inferior frontal gyrus to the superior temporal gyrus connection. Yet, no significant correlation was found between the volumetric lateralisation of the arcuate fasciculus and the degree of functional lateralisation for verbal fluency, verb generation and reading comprehension. Interestingly, functional lateralisation correlated with the lateralisation of the fractional anisotropy of the arcuate fasciculus. In a similar study design, only this time using deterministic instead of probabilistic tractography, the leftward asymmetry of the arcuate fasciculus was replicated in right- and left-handed healthy participants by Vernooij et al. (2007) who further reported a correlation with the number of streamlines of the arcuate fasciculus and functional asymmetry. In the same year, Catani et al. (2007) reported on the asymmetry of the arcuate fasciculus as shown with deterministic tractography and provided two pivotal observations, (i) across the population the degree of asymmetry is variable between individuals and (ii) that a more bilateral representation of the arcuate fasciculus is indicative of better task performance on the CVLT. In this study, individuals were clustered into three groups. The first group only had the arcuate fasciculus in the left hemisphere; the second group presented strong leftward asymmetry but had right-hemispheric connections whereas the third group was completely bilateral. Unfortunately this study is devoid of functional measurements and it is therefore not clear for which aspects of language the

laterality pattern might be most important. Matsumoto et al. (2008) replicated these asymmetry findings in 24 patients with focal lesion or epileptic focus. In this study the WADA test was used to determine the unilateral language dominance and the results showed that the direct fronto-temporal connection of the arcuate fasciculus was significantly lateralised to the dominant hemisphere. Another patient-based study investigated 30 left-hemispheric chronic stroke patients with residual language impairments and identified that the extent of damage to the left arcuate fasciculus was predictive of the residual impairments (Marchina et al. 2011). The authors did the same analysis with the uncinate fasciculus and the external capsular system, which had no predictive significance. What these studies highlight however is (i) the importance of the right hemisphere for language functions and possibly recovery, (ii) the gap between strong unilateral functional representation and a common bilateral structural representation.

In conclusion, post mortem and especially in vivo imaging studies have expanded and re-fined our understanding of the anatomy of language. Various imaging methods (in vivo and lesion-deficit) suggest that Broca's area is not a homogeneous entity but can be parcellated into sub-regions, such as the dorsal/ventral opercularis area relevant for syntax and the anterior and posterior triangular area relevant for semantics. It has to be noted that, albeit advanced, these methods still have their limitations. Electrocortical recordings and tomography methods are complementary yet at the same time in striking opposition in terms of their temporal and spatial resolution. Skull recordings are most apt for time-locked responses but the activation cannot be precisely located on the cortex or subcortical structures; whereas tomography has a good spatial resolution but several seconds of hemodynamic delay in signal generation which does not allow it to pick up delicate signals such as the language-specific positivities and negativities (ELAN, N400, P600). The fMRI signal was further shown to be influenced by endo- and exogenous factors including age, gender, motivation, literacy, task difficulty, response modality (e.g. vocal, motor, thought), motion artefacts, paradigm dependency (e.g. word or sentence level), morphing into Talaraich space (for detailed review see Démonet et al. 2005).

The paramount conclusion concerning the neuroanatomy of language can only be that although some of the first lesion-deficit findings have never been totally

invalidated (e.g., the involvement of Broca's area in speech production and the left superior temporal gyrus in auditory verbal comprehension) our understanding expanded tremendously over the course of the 20th century owing to the rapid advances of in vivo imaging methods. Considering the abovementioned studies, it seems that the language network relies on quintessential language-relevant areas within a large-scale network that selectively activates/co-activates core regions (i.e. semantics activate area BA45, phonological processing is restricted to the dorsal aspect of BA44). Not only does current research suggest an expanded left hemispheric network but also the influence of the right hemisphere has come under close scrutiny with the present understanding being that suprasegmental components of language are generated, modulated and processed by the right hemisphere. Despite the impression that multi-imaging methods provide converging evidence we have to bear in mind that '*infinitesimally tiny physical forces that occur in the brain (which are presumed to be associated with elements of language) must (1) be tremendously magnified and then (2) radically transformed into something the reader can see*' p57, (Stemmer & Whitaker 2008). Results therefore have to be scrutinised against the underlying methodological approach it was obtained with.

Anatomically, the network of language is determined by cortical and subcortical structures. All perisylvian structures lie within the vascular territory mainly supplied by the middle cerebral artery. The next chapter will detail the underlying vascular supply to all language relevant areas in the brain and investigate how an interruption to the blood supply can cause aphasias.

CHAPTER 4 STROKE

'The cortex is not infinitely adaptable. If it were, every stroke patient would recover completely'

(Seung 2012)

4.1 Short history of stroke

A clinical description of stroke, or as it used to be called apoplexy, is available from early writings by Hippocrates:

> *'The healthy subject is taken with sudden pain; he immediately loses his speech and rattles in his throat. His mouth gapes and if one calls him or stirs him he only groans but understands nothing. He urinates copiously without being aware of it. If fever does not supervene, he succumbs in seven days, but if it does he usually recovers' (translated in (Clarke 1963).*

In the tradition of the Greek medicine of humours (yellow bile, blood, phlegm, black bile) that are each attributed to earthy resources (fire, air, water, earth) and associated with certain qualities (hot, cold, dry, moist), apoplexy was considered to be caused by accumulated cooled-off black bile. Hence, a feverish patient was thought to be recovering because fever would warm the blood and black bile (Finger 1994). Still, most patients died within a week. The Swiss physician Jakob Wepfer reported in his monograph 'historiae apoplecticorum' (1759) on 21 stroke patients with detailed medical histories and post mortem accounts. He described the blood vessel system in detail and recognised that apoplexy can have two causes, namely blockage of the internal carotid and vertebral arteries or rupture of blood vessels, and that these occur at certain preferential areas of rupture. The importance of the carotid arteries is also represented in its name, which originates from the Greek word 'karos', meaning 'deep sleep' and implies that any impediment to the blood flow to the brain results in unconsciousness (Fields & Lemark 1989).

The definition of apoplexy, however, was still vague and by no means exclusive to what we would refer to as stroke these days as patients with sudden loss of limb sensation and uncoordinated movements were often categorised under apoplexy:

> *'[…] In any disorder in which the patient suffered sudden loss of consciousness and died shortly thereafter, this diagnosis was no doubt also invoked. Thus acute myocardial*

infarction and pulmonary embolism, as well as acute non-vascular cerebral events, would
be included in what we can more correctly call the apoplectic syndrome' p.302, (Clarke
1963).

However, being a scholar of his time, Wepfer's explanation was that if vessels are blocked then life spirits are hindered from entering the brain and from being transformed into soul spirits (spiritus animalis); whereas if vessels are ruptured soul spirits are hindered from entering the periphery. Predisposing causes for stroke according to Wepfer were cold weather, storms, laziness, and spicy food.

Giovanni Battista Morgagni, when in his eighties, defined two causes of apoplexy: i) serous, ii) sanguineous (i.e. haemorrhagic). With this clinico-pathological opus in epistolary form, the '*challenge of unsolved problems seriously enters the medical literature*'. To Morgagni the '*proximate cause' of either a sudden diminution of the internal motions performed in the brain, to wit, when we move, think, or perceive ... yet there are many and various causes that bring it about, some of which entirely escape the notice of the senses'* p.118, (Schiller 1970).

The association between blood and stroke was already recognised in Morgagni's times and even though Morgagni provided a dichotomous aetiology, apoplexy became associated with haemorrhage only. In the UK, Bayle described calcification and plaques in cerebral arteries, especially in the elderly:

> *'It is very common in examining the brain of persons who are considerably advanced in life,*
> *to find the trunks of the internal carotid artery upon the side of the sella turcica very much*
> *diseased, and this disease extends frequently more or less into the small branches. The*
> *disease consists of bony or earthy matter being deposited in the coats of the arteries, by*
> *which they loose a part of their contractile and distentile powers, as well as of their*
> *tenacity.' From Morbid Anatomy, 1793 in (Gruber-Gerardy et al. 2005)*

Only in 1820 did the French physician Rostan claim 'softening of the brain' (i.e. 'diminution of cohesion in the tissues' according to his mentor Andral) to be the most common cerebral lesion and refused inflammation as the cause whilst still lacking the evidence of vessel occlusions. Arteriosclerosis (hardening of the arteries) was first mentioned in 1829 by the physician Johann Lobstein. He '*described the arterial thickening and that 'yellow puree-like, uneven, knobby matter, perfectly similar to the surface of those bones affected with osteosclerosis'; it was not 'phlogistic', i.e. not inflammatory, but I can neither give its cause nor its effect*' p.123, (Schiller 1970). The link between hardening of the arteries resulting in softening of brain tissue was not recognised yet. Still adhering to the inflammatory doctrine, Cruveilhier already recognised the relevance of cardiac blood clots:

'Also the cretaceous changes […] in the arteries of old women at the Salpetriere have not escaped me. Are they not sometimes, with their shrunken lumen, the cause of arterial occlusion –both through themselves […] and through the arteritis obliterans that some times follows. […] It was extremely likely that fragments would be thrown towards the extremities in a great number of cases […] also from the right ventricle into the pulmonary circulation' p.125, (Schiller 1970).

Cruveilhier's phenomenon was later described by Virchow (1847), who coined the term emboli for these fragments (**Figure 18**). With the postulations from Virchow's thrombogenesis, the knowledge of spreading of emboli, and the knowledge of arteriosclerotic changes, much of our knowledge today was already established some 150 years ago. Virchow's work on problems of vascular and inflammatory pathology was continued and expanded by his scholar Cohnheim, who introduced the concept of 'cerebral infarct' through his arterial wax globules injection studies. With this method he engineered emboli that result in either ischemic necrosis (due to cessation of nutritional supply) or haemorrhage. These experiments were done in the frog.
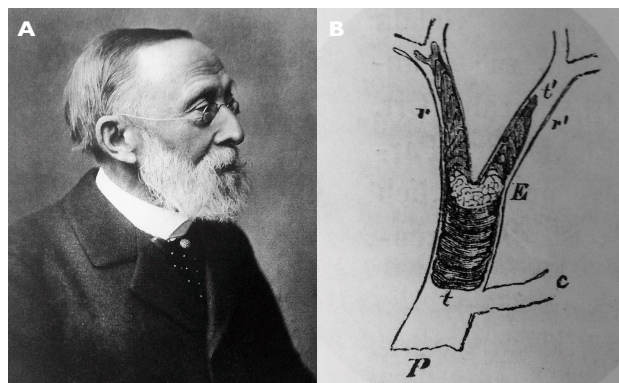
Figure 18   Photograph of Virchow and his idea of thrombogenesis (1862) (in (Gruber-Gerardy et al. 2005)

In Austria in the 1840s, '*Rokitansky had presumably performed more autopsies than any single man before him. As to haemorrhagic apoplexy Rokitansky insisted on a novel concept: its close mechanical association with heart disease. Many apoplexies were due to congestion, or dilatation of the right ventricle. Haemorrhage, more importantly, may secondly be related to hypertrophy of the left ventricle and hence to an increased 'impulse' p.126,* (Schiller 1970). Hypertension was not easily measured at this time and the most applicable treatment of stroke was bleeding. It

was only in the second half of the 19th century that sphygmographs were manufactured to measure systolic blood pressure (Gruber-Gerardy et al. 2005). The influence of hypertension towards arteriosclerosis was described in the early 20th century.

Stroke terminology is influenced by philosophical and medical constructs. The Greek term 'apoplexia', means 'struck down by violence' and mirrors the fact that a patient develops sudden paralysis and change in well-being. The term still implies some celestial force reflecting the philosophy of that time. Stroke (or stroke of apoplexy) was used as a synonym for apoplectic seizure as early as the 16th century and is a fairly literal translation of the Greek term (similarly for French *coup de sang*, and German *Schlaganfall*). The use of the expression 'cerebrovascular accident' has been widely abundant owing to the fact that stroke is not considered as accidental but usually has underlying diagnosable causes and some strokes may be preventable if those cause and risk factors (RF) were recognised and controlled early on (Hankey 2007).

The term embolus was used prior to Virchow but not in the sense he used it in his work nor similar to the current understanding (Schiller 1970). Paul of Aegina in the seventh century coined the term hemiplegia which is still in use (Schiller 1970).

Even though stroke seems well-understood today, these advances have been rather recent and much knowledge was gained from the advent of in vivo neuroimaging. Some concepts have been deducted by clinicians for centuries and were statistically validated in controlled large cohort studies more recently (e.g., the importance of hypertension and the efficacy of aspirin); whereas other concepts did not stand the test of time (e.g. unrestrained laughter as a cause of stroke).

4.2   Definition of stroke

The current clinical World Health Organisation (WHO) definition of stroke is '*a focal (or at times global) neurological impairment of sudden onset, and lasting more than 24 hours (or leading to death) and of presumed vascular origin*' p. 11, (ManualWorld Health Organization 2006). Within this definition the symptom duration beyond 24 hours is crucial as focal neurological symptoms resolving within 24 hours are defined as transient (short-term) ischemic attacks (TIA). The WHO defined this time frame in 1978 not on the grounds of documented time courses but rather due to the uncertainty about its course. Most TIA symptoms, even though they can last for up to 24 hours, do resolve within 30 minutes. If symptoms persist beyond 24 hours a

focus of ischemic infarction can be detected using certain neuroimaging contrasts or at autopsy (Mohr 2004). The critical differentiation is therefore based on pathological tissue changes, whereby brain tissue will infarct (as is the case of stroke) or blood flow is quickly restored not rendering the tissue permanently (as is the case for a TIA). The presence of a TIA increases the risk of future stroke.

4.3   Epidemiology of stroke

The study of the distribution and causes of stroke within the population and in particular within south London has yielded congruent results but with varying frequency estimates. Epidemiological studies are heterogeneous in design and outcome measures used, ICD criteria are regularly revised and catchment areas for a defined population may have changed. These and other factors directly impact on the obtained results (which vary) and the numbers presented in this thesis are to be interpreted as current estimates.

4.3.1   Incidence, prevalence, and mortality

Incidence. The stroke incidence for south London can be estimated from the South London Stroke Register (SLSR), a registry spanning over 7 years of first-ever strokes in a multi-ethnic urban population of 271,871 inhabitants (63% white, 28% black, 9% other ethnical background) (see for example (Stewart et al. 1999; Addo et al. 2011; Wolfe 2002; Markus et al. 2007; Hajat et al. 2011; Mohan et al. 2009). The risk of first-ever stroke, and the type of stroke, varies considerably internationally and between socioeconomic groups - with an increased risk and higher incidence of small vessel occlusions amongst black individuals, Hispanics, Pacific Islanders and Asians (Hajat et al. 2011). Within the south London population the annual age-adjusted incidence rate (total ischemic strokes not stratified by aetiology) per 100.000 was 101.2 (95% CI 82.4 to 122.9) in men and 75.1 (95% CI 59.1 to 94.1) in women, yielding a 34.75% excess in men (Hajat et al. 2011). The risk of stroke increases with age and approximately one in four men, and one in five women aged 45 years, can expect to have a stroke if they reach the age of 85 years (Wolfe 2000). The evaluation of stroke incidence within South London (stratified by age) is shown in a global geographical comparison in **Figure 19**.
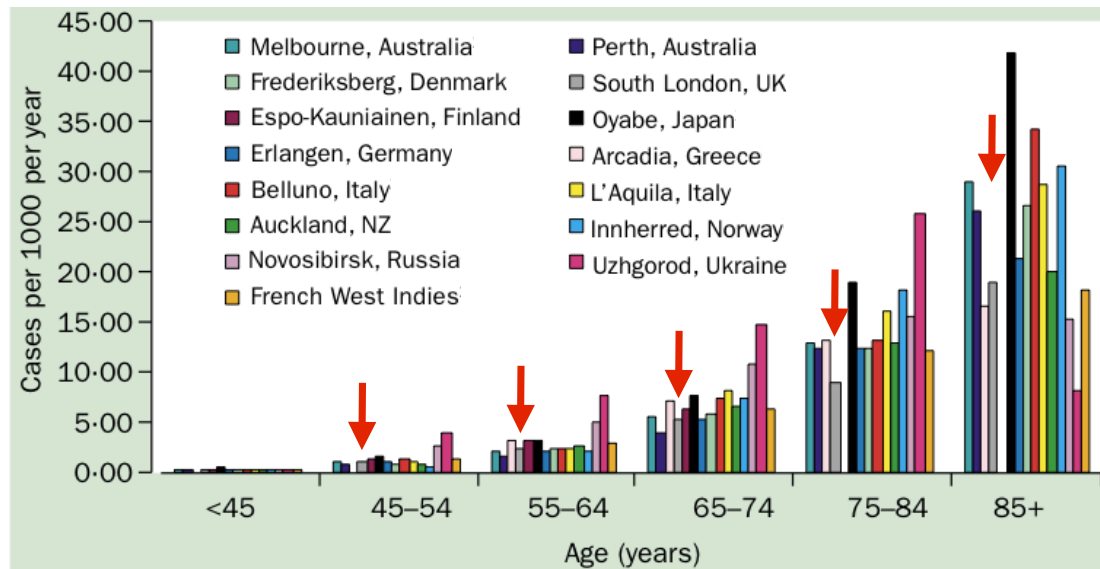
Figure 19   Annual stroke incidence rate stratified by age and country per thousand cases

All stroke types included. South London incidence rate is indicated by red arrow (from (Feigin et al. 2003).

Prevalence. A review of nine population-based studies (for New Zealand, US, Netherland, UK, Bolivia, Papua New Guinea, China, and Italy) yielded an age-standardised prevalence for people over the age of 65 years of between 46.1-73.3 per thousand people, with men ranging between 58.8-92.6 and women between 32.2-61.2 (Feigin et al. 2003).

Mortality. Stroke is currently the second leading cause of death in the UK and worldwide, accounting for an estimated 4.5 million deaths worldwide with an estimate of nine million survivors (Wolfe 2000; Mathers et al. 2009). The average age-adjusted stroke mortality ranges between 50-100 per hundred thousand people per year in developing countries (Donnan et al. 2008). For our South London recruitment centre (King's College Hospital (KCH), Camberwell, Greater London) specifically, the mortality rate amongst the admission to the stroke unit was on average 6.08% (range 1.2-15.1%) over a period of six months (July to December 2009).

4.3.2   Risk factors

Risk factors for stroke and predisposing conditions can include modifiable environmental factors (e.g., smoking, diet) and non-modifiable factors (e.g., demographics, genes; **Table 8**. Certain predisposing factors (e.g., elevated blood pressure) are common to both stroke types, whereas others may be more relevant in the aetiology of haemorrhages rather than ischemia or vice versa.

Table 8   Risk factors of stroke stratified according to their modifiability (from (Goldstein et al. 2006).

Non-modifiable RFs	Modifiable RFs	Modifiable lifestyle factors
• Age	• Hypertension	• Weight
• Sex	• Atrial fibrillation (AF)	• Physical activity
• Ethnic background	• Diabetes mellitus	• Substance misuse
• Family history	• Hyperlipidaemia	• Smoking
• Previous strokes	• Non-valvular AF	• Oral contraceptive

4.3.2.1   Demographic factors

Ethnic background, advanced age, and sex have been consistently shown to contribute significantly to the risk of stroke (Stewart et al. 1999; Hajat et al. 2011; Markus et al. 2007; Cox et al. 2006; Feigin et al. 2003; Lawes et al. 2004). Stroke can happen at any time in life but advancing age brings higher incidence rates for hypertension, atrial fibrillation and other risk factors. Geographical differences in stroke risk are consistently shown in the literature, such as described above and shown in **Figure 19**.

4.3.2.2 Previous stroke and transient ischemic attacks (TIA)

Between 15-23% of strokes are preceded by a transient ischemic attack (TIA) (Lovett et al. 2003; Giles & Rothwell 2007). The immediate risk of reoccurrence within the first week after a stroke is reported to be between 1-12.8% (Johnston et al. 2000; Giles & Rothwell 2007). Reliable predictors of patients at high risk are still needed (Hill et al. 2004) and the annual incidence for stroke reoccurrence was estimated to be between 4-14% (Hier et al. 1991; Davis et al. 1987). The reoccurrence risk is tightly linked to clinical treatment and patient compliance. For example, in an investigation of two cohorts with atrial fibrillation (AF) over a period of six years Mant et al. (2007) showed that the cohort on anticoagulation treatment (e.g., warfarin) had a lower incidence of strokes compared to the cohort on

antiplatelet treatment (e.g., aspirin). Within the anticoagulation group (n=488) 24 participants suffered from a primary stroke (1.8% risk per year) whereas in the antiplatelet group (n=485) 48 events were registered (3.8% risk per year; Relative Risk warfarin vs. aspirin 0.48, 95% CI 0.28–0.80, p=0.0027). The cost and benefits of anticoagulation treatment has to be evaluated on a patient-specific basis because it seems significantly to reduce the risk of stroke occurrence but requires high patient compliance in terms of regular blood tests and has an increased risk of bleeding (Mant et al. 2007; EAFT 1993).

4.3.2.3   Hypertension and atrial fibrillation (AF)

Hypertension is the prime independent risk factor for strokes (ischemic and haemorrhagic) across both sexes and all age groups. Hypertension occurs in most adult populations and an estimated two thirds of strokes are attributable to elevated blood pressure levels (Lawes et al. 2004).

Table 9   WHO classification of systolic hypertension in relation to increased risk of stroke

Staging	Range	Risk
Normal	<130mmHg	
Stage 1	140-159mmHh systolic	2x
Stage 2	≥160mmHg	3x
Stage 3	≥180mmHg	3x

This increase in risk is dependent on the magnitude of elevated blood pressure; with groups suffering from essential hypertension at stage 2 or 3 demonstrating a three-fold risk (Mohr 2004; Wolf et al. 1991; P. H. Davis et al. 1987) (**Table 9**). Both forms of hypertension (systolic, diastolic) increase the risk but elevated systolic blood pressure appears to be a more robust predictor (Mohr 2004; Pedelty & Gorelick 2007; MacMahon et al. 1990). Controlling blood pressure can reduce the initial risk and risk of reoccurrence by 36% for the subsequent 5 years of hypertensive treatment (Simon 1991).

Often co-incident with hypertension is arrhythmia (e.g., AF), which has been acknowledged to predispose to stroke with an estimated seventeen fold risk increase for valvular AF and six fold increase for non-valvular AF (Pedelty &

Gorelick 2007; Wolf et al. 1991). For each advancing decade of age the incidence of AF nearly doubles (Wolf et al. 1991) and AF-induced strokes are associated with higher mortality rates, larger infarct size, and increased disability (Pedelty & Gorelick 2007).

4.3.2.4   Blood chemistry

Abnormalities in cholesterol, low and high density lipoproteins, elevated homocysteine, and triglycerides have been investigated as contributing factors. Lipid levels have come into focus following the advent of successful stroke prevention with statin agents, which lower lipid levels by inhibiting 3-hydroxy-3-methylglutaryl coenzyme A reductase. Increased high-density lipoprotein has been found to reduce the risk of ischemic stroke (Sacco et al. 2001). The relationship between cholesterol and stroke seems more complex. Research indicated that reduced levels of cholesterol (<4.1mmol/l) increase the risk for intracerebral haemorrhages (Torbey & Selim 2007; Mohr 2004); whereas increased total cholesterol seems to be associated with an increased risk of ischemic stroke (Pedelty & Gorelick 2007).

4.3.2.5   Diabetes mellitus

The relative risk for stroke in diabetics (type I and II) has been estimated to be between 1.5-3.0 after accounting for other risk factors (e.g., blood pressure elevation) (Barrett-Connor & Khaw 1988). Thromboembolic strokes seem to have the strongest relation with diabetes (Abbott et al. 1987). Poor diabetes management and longer disease duration further increase the risk additionally (Roehmholdt et al. 1983).

4.3.2.6   Lifestyle factors

Smoking puts people at an estimated higher risk for stroke of 1.5–2 times with a dose-dependent (i.e. heavy smokers are at higher risk than light smokers) and sex-dependent distribution (i.e. smoking women are at higher risk compared to smoking men) (Shinton & Beevers 1989).

Alcohol influences stroke risk, especially for haemorrhagic stroke, in a dose-dependent fashion following a J-shaped function (Sacco et al. 1999). This curve

suggests beneficial effects of minor alcohol consumption and devastating effects in heavy drinkers. Alcohol may influence the stroke risk in various ways such as elevated blood pressure, cardiac arrhythmias, and reductions in cerebral blood flow.

Dietary habits such as consumption of whole grains, fish, fruit and vegetables have been related to general health and reduced incidence of stroke (Mohr 2004).

Physical activity has been shown to reduce stroke incidence, especially in men (Abbott et al. 1987; Mohr 2004). Abdominal obesity in both sexes, and especially in younger patients, was implicated as a contributing factor when the waist-hip ratio was greater than 0.93 in men and 0.86 in women (Suk et al. 2003).

Oral contraceptives have been implicated to increase stroke risk by 2.75 in women, especially beyond the age of 35 years and even more so in combination with other risk factors such as smoking and hypertension. This is due to enhanced clotting based on an increase in platelet aggregation and by the alteration of clotting factors favouring thrombogenesis (Mohr 2004; Gillum et al. 2000). The risk seems to be dose-dependent with low oestrogen content (less than 50μg) not appearing to increase the risk (Petitti et al. 1996).

4.3.2.7 Seasonality

The influence of cold weather was already suspected as a risk factor at Galen's times (Schiller 1970). A winter excess of stroke has now been documented in several studies but heterogeneous effects of weather on stroke occurrence are reported (Rothwell et al. 1996; Magalhães et al. 2011; van Rossum et al. 2001). Seasonal effects have been described with stroke incidence peaking in the winter (Myint et al. 2007), followed by spring (Turin et al. 2008), autumn and summer (Haberman et al. 1981). Not only seasonal changes have been related to the incidence and mortality of stroke but also daily meteorological changes, such as rapid (within 24-48 hours) temperature drops or increases and changes in the atmospheric pressure (Jimenez-Conde et al. 2008). Interestingly, atmospheric pressure drops are more likely to cause ischemic strokes whereas an increase is more likely to cause haemorrhages (Jimenez-Conde et al. 2008), which may partially explain the difference in seasonal incidence.

The relationship between stroke and meteorological variables is however incredibly complex; for instance, changes in causative and secondary factors have to be taken into account, such as behavioural changes over the seasons and/or in relation to daily weather (Kasper et al. 1989) that might alter blood pressure, dietary habits, and alcohol intake to name but a few.

4.3.3   Health care costs

An estimated 2-4% of the total health care costs worldwide are attributed to stroke; the UK figure suggest that stroke accounts up to 5% of the total National Health Service (NHS) costs - with an annual expenditure of £8.9 billion for primary (e.g. hospitalisation, scanning etc.) and secondary care (e.g., unemployment, therapy) (Donnan et al. 2008; Saka et al. 2009).

4.4   Cerebral blood supply

Extracranially, the common carotid arteries have two divisions, the external carotid arteries (ECA, supplying face and scalp) and the internal carotid arteries (ICA, supplying the anterior three-fifths of cerebrum, hence called anterior circulation). The posterior two-fifths of the cerebrum, as well as the cerebellum and the brain stem are supplied by the vertebral arteries that unite at the level of the brain stem to form the basilar artery (posterior circulation). At the ventral aspect of the brain, branches of the ICAs and the basilar artery anastomose to form the Circle of Willis, which surrounds the suprastellar cistern and lies below the hypothalamus and third ventricles. Rostrocaudal the circle gives rise to the following arterial branches bilaterally: anterior cerebral artery (ACA), anterior communicating artery (AcomA), middle cerebral artery (MCA), posterior communicating artery (PcomA), and posterior cerebral artery (PCA). Each artery is irrigating a circumscribed cerebral area and occlusion therefore leads to focal damage to a specific region (**Figure 20**A).

The ACA supplies the olfactory bulb and tract, gyrus rectus, and medial orbital gyrus, corpus callosum, cingulate gyrus, medial frontal gyrus, and paracentral lobule. The parietal ramifications are responsible for the precuneus (Stefani et al. 2000). The MCA irrigates the medial aspect of the Sylvian fissure (M1 segment[7]),

---

[7] The horizontal segment extending between the origin of the MCA to the bi-/trifurcation (or genu).

the insular (M2 segment[8]), the frontal operculum (M3 segment[9]) and the cortical convexity (M4 segment[10]) (Pai et al. 2007) (**Figure 20**B). The PCA irrigates ventrotemporal regions (uncus, fusiform gyrus) and medial occipital areas (cuneus, precuneus, splenium, lingual gyrus) (**Figure 20**A/B).
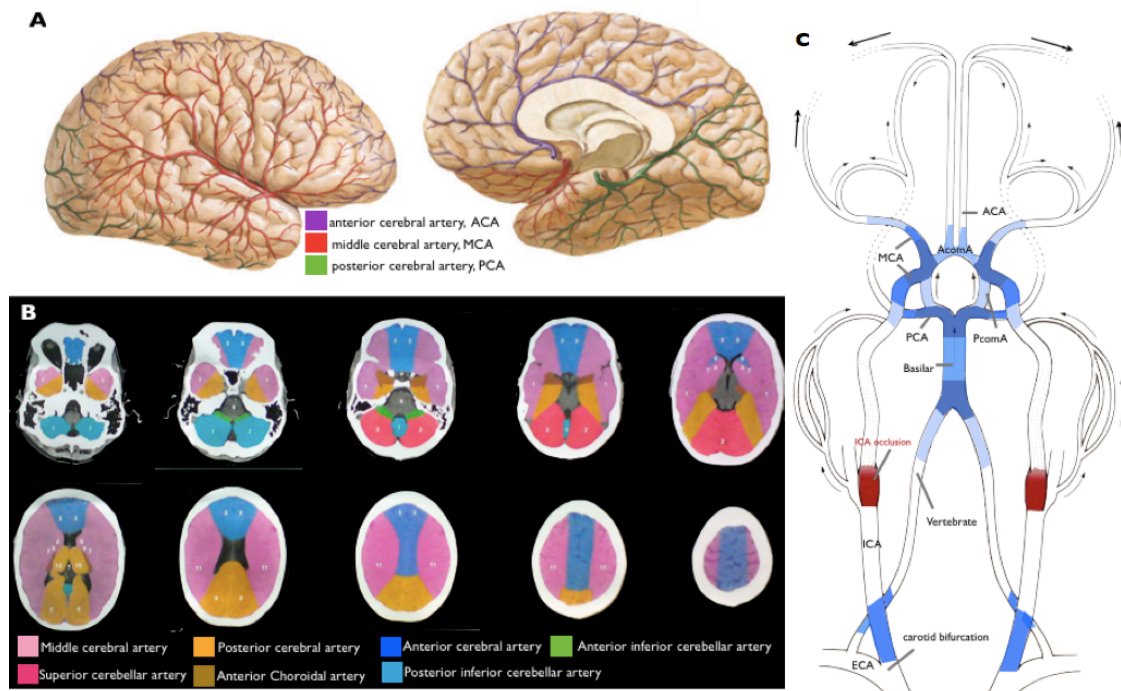
Figure 20   Intracranial cerebral arterial blood supply

A Depicts the blood supply to the lateral convexity and the medial aspects of the brain (modified from the Netter atlas). **B** Shows axial brain slices colour accordingly to the specific vessel supply to subcortical and cortical territories. Modified from (Tomandl et al. 2003; Kloska et al. 2007). **C** Demonstrates the origin of the cerebral blood supply from the extracranial carotid artery that is then bifurcation into the external carotid artery (ECA) and the internal carotid artery (ICA). At the level of the pontine brain stem the vertebrate arties are joint as basilar artery. Branches of the ICA and the basilar anastomose to form the Circle of Willis. The circle gives raise the following arterial branches: anterior cerebral artery (ACA), anterior communicating artery (AcomA), middle cerebral artery (MCA), posterior communicating artery (PcomA), and posterior cerebral artery (PCA). Panel C figure also demonstrates occlusions (red, blue with varying frequency) and the compensational mechanism of collateral flow. Modified from (Mohr 2004).

Occlusions and ruptures can happen to any of the larger vessels and their small branches but certain arterial locations are more prone, such as bifurcations (**Figure 20**C). Blockages can be caused by thrombolism (e.g., stationary clot), embolism (e.g., detached clot), and stenosis (vessel narrowing of >70% is considered

---

[8] The insular segment runs over the insular and divides into 6-8 major branches.
[9] The sylvian segment extending between the insular and the lateral cerebral fissure.
[10] The cortical branches extending ramifications over frontal, parietal and temporal lobes.

haemodynamically significant) (**Figure 21**). Occlusions within the ICA sometimes allow for haemodynamic compensation through collateral blood flow via the ACA (A1 segment), the posterior communicating artery, or both within the Circle of Willis (**Figure 20**C, occlusion indicated in red).
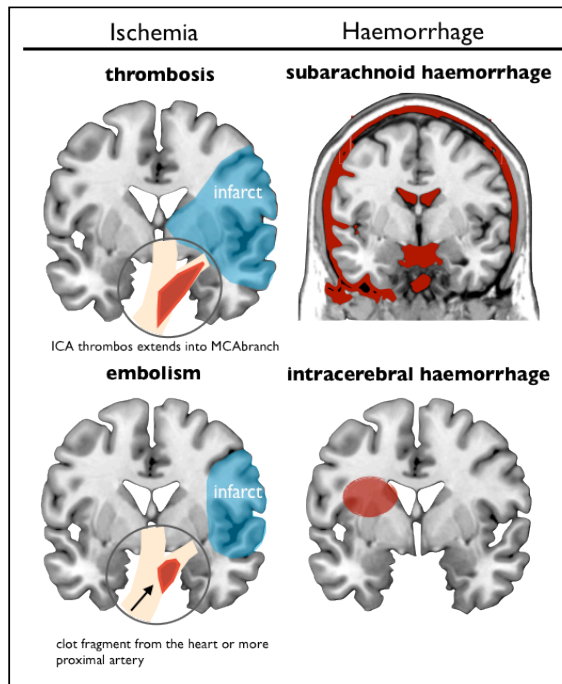
Figure 21   Types of ischemic and haemorrhagic strokes.

4.5   Pathophysiology and clinical manifestations of stroke types

Arterial occlusion resulting in ischemic stroke constitutes approximately 84% of strokes, whereas haemorrhages contribute to approximately 16%. Clinically, a stroke is often described by means of the affected artery (e.g., MCA stroke) and entails focal negative (i.e. loss of function) neurological symptoms such as motor symptoms (e.g., hemiparesis, dysphagia, ataxia), speech and language disturbances (e.g., dysphasia, dysgraphia, dysarthria), sensory symptoms (e.g., hemianopia, paresthesia), vestibular symptoms (e.g., vertigo) as well as behavioural/cognitive symptoms (e.g., amnesia, disorientation) (**Figure 22**). A specialist can, in general, infer the neuroanatomical location of a stroke from their patients presenting with focal symptoms. For example, unilateral weakness is associated with a lesion to the corticospinal tract, clumsiness frequently with a cerebellar lesion, unilateral sensory loss typically affects the spinothalamic tract and double vision the occulomotor pathways. An apt clinical diagnosis of stroke, depending on the post onset time and experience of the clinician, is estimated in 80-85% of cases (Group 1997).

Site of occlusion	Lateral lesion extent	Medial lesion extent	Common symptoms associated with this lesion
			Contralateral gaze palsy, hemiplegia, hemisensory loss, hemispatial neglect, head and eye deviations hemianopsia, global aphasia (dominant hemisphere), aprosody and anosognosia (non-dominant hemisphere)
			Contralateral severe motor hemiplegia, hemisensory loss, transcortcial motor/sensory aphasia (dominant hemisphere), neglect, sopor, hemianopia
			Contralateral weakness and sensory loss of face and hand, conduction aphasia (dominant hemisphere), constructional dyspraxia (non-dominant hemisphere)
			Contralateral hemiplegia, hemisensory loss, gaze palsy, hemineglect with motor dominance (non-dominant hemisphere), bucco-facial/limb ideomotor apraxia, Broca aphasia (dominant hemisphere)
			Contralateral hemianopsia or upper quadrant anopsia, Wernicke aphasia (dominant hemisphere), constructional dyspraxia and difficulty comprehending emotional prosody and hemineglect with sensory predominance (non dominant hemisphere)
			Incontinence, contralateral hemiplegia, transcortical aphasia, limb dyspraxia
			Contralateral weakness of lower limb, hip, food and shoulder. sensory loss lower limb, transcortical aphasia, limb dyspraxia
			Primary visual deficits including visual field loss, visual agnosia, Balint syndrome, prosopagnosia, palinopsia, micropsia/macropsia, disorders of reading, disorders of colour vision, memory impairment, motor dysfunction

Figure 22   Schematic arterial occlusions and the corresponding cerebral damage and symptoms

Schematic arterial occlusions, their resulting cerebral damage (lateral and medial view) and commonly associated symptoms for the middle cerebral (blue), anterior cerebral (red), and posterior cerebral (green) arteries. Adopted from (Mohr 2004).

4.5.1 Ischemia

The aetiopathogenesis of most cerebral ischemia results from one or more of the following five mechanisms: embolization from the heart into brain vessels (e.g. due to myocardical infarction, mitral valve damage etc.); arterial stenosis; decreasing of systemic blood pressure; thromboembolism of large vessels; and decreased cardiac output (e.g., due to myocardial contractility, substantive haemorrhage etc).

Thrombotic occlusions commonly occur at arterial bifurcations. Stenosis precipitated by turbulent blood flow, atherosclerosis, and platelet adherence can cause blood clots to form. Less common causes, often seen in younger patients, are cervical artery dissection, essential thrombocythaemia, polycythaemia, sickle cell anaemia, protein C deficiency, and substance misuse (Carroll & Chataway 2006). The vasculature can be occluded by emboli (loose blot clots) originating most commonly from the heart (cardioembolic) but also from extracranial arteries or through right-to-left shunts. Mural emboli and platelet aggregates are most commonly embolised to the brain. Embolic material is however rather unstable and spontaneous recanalization is evident in approximately 52% of MCA (stem and branch) occlusions within 48 hours post onset (Mohr 2004).

Ischemia is a potentially reversible altered state of brain physiology and biochemistry subsequent to cessation or restriction of blood flow delivery resulting in a drop below the normal values (cortex, 0.8ml/g/min; white matter, 0.2ml/g/min). The brain may be protected against a focal disturbance of the blood supply by the collateral vessels (**Figure 20**C). Anastomotic connections between the carotid and vertebral arteries provide a collateral system able to compensate for the occlusion of up to three of these arteries. If however perfusion pressure drops to critical levels, ischemia develops, progressing to infarction if the constriction endures. The critical threshold for failure of neuronal electrical function is below 30% of the normal blood flow, and below 10% for the failure of energy metabolism and ion pumps, which results in the breakdown of cell membrane integrity (Astrup et al. 1981). This cascade is triggered by the halt of neuronal protein synthesis, the cessation of electrical activity and finally the interruption of cell membrane integrity leading to neuronal death. In recent years, drugs to restore perfusion have been developed (see 4.6). The infarct size partially relies on the integrity of the collateral blood supply.

The concept of an ischemic penumbra has gained increasing attention recently, even though the theory has been around for centuries (see 4.1). Penumbra describes an area of reduced blood flow (between 0.10-0.23ml/g/min) where

functional activity of neurons is suppressed (low cerebral blood flow and electrical failure) although metabolic activity for maintenance (cellular homeostasis) of structural integrity of the cell is preserved (high oxygen extraction fraction, OEF and cerebral metabolic rate of oxygen, $CMRO_2$) (Kumar et al. 2010). The neurons within this area may remain viable for several hours after symptom onset due to the collateral supply and the area tends to decrease over time. '*The extent of the ischemic penumbra is time-dependent. It decreases over time by gradual recruitment into the core, and represents a key target for therapeutic intervention*' p.15, (Kumar et al. 2010) (**Figure 23**C).

Focal cerebral ischemia due to blood flow deprivation initiates a complex pathophysiological ischemic cascade resulting in excitotoxicity, peri-infarct depolarisation, inflammation and eventually apoptosis ('programmed cell death'). All of these steps are potential targets for therapeutic interventions.

With supply depletion, the membrane potential cannot be maintained and neurons and glia cells depolarise. As a result, voltage-dependent calcium (Ca^{2+}) channels become permeable leading to the release of excitatory glutamate whilst energy-dependent processes are impeded (e.g., postsynaptic neurotransmitter uptake), leading to excess accumulation of glutamate in the extracellular space (**Figure 23**B). Likewise, the activation of glutamate receptors leads to Ca^{2+} and sodium (Na^+) influx. This glutamate-mediated over-activation results in cellular influx of Na^+, chloride (Cl^-), and water. The ensuing oedema affects the local perfusion and has potentially remote effects due to increased intracranial pressure, vascular compression, and herniation. Excess intracellular calcium initiates various injurious enzymatic pathways, such as proteases, lipases, and endonucleases together with the release of cytokines. Calcium accumulation within the mitochondria, which initially partially sequester calcium, is correlated with enhanced free radical production, which in turn leads to membrane disruptions (fluidity and permeability) and damage to the cytoskeletal integrity. This cascade of second messenger activation, free radical production, and hypoxia triggers the expression of proinflammatory genes (Dirnagl et al. 1999). This is followed by peri-infarct spreading depolarisation that facilitates the gradual expansion of the core region into the penumbra. The inflammatory response engulfs residual cells and within six hours post onset, astrocytes become hypertrophic, whilst microglial cells assume a morphology that is typical of activated microglia. Within a day of a MCA occlusion the microglial reaction is well developed in the ischaemic brain, particularly in the penumbra (Dirnagl et al. 1999).
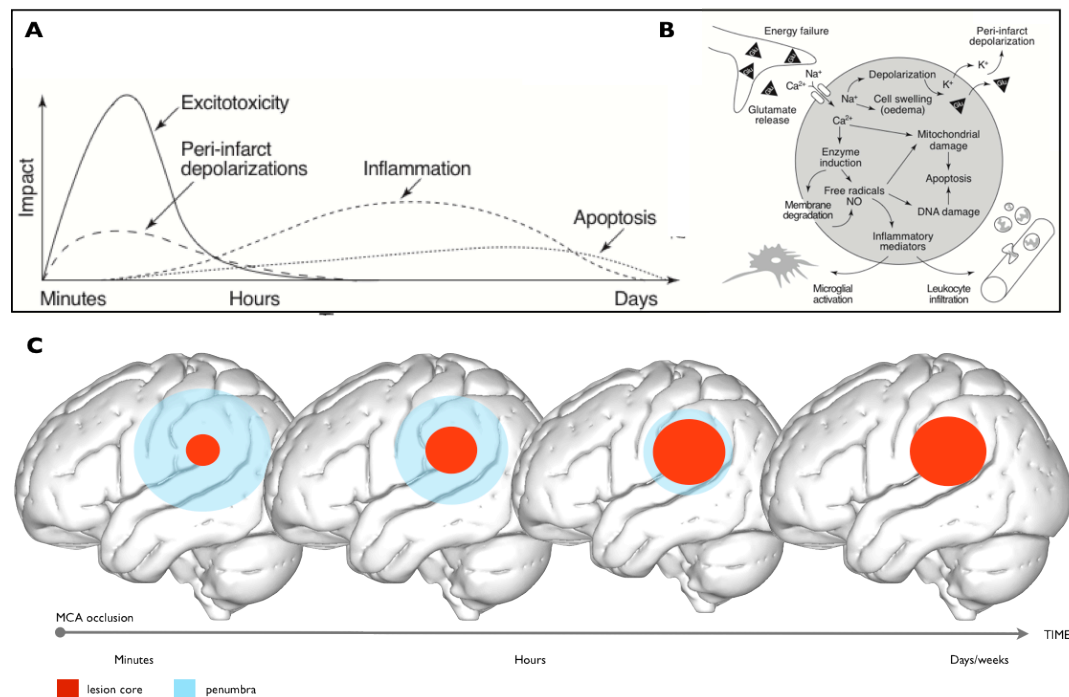
Figure 23   Ischemic cascade and penumbral evolvement over time

A shows the time-dependent dynamic influences of excitotocity, peri-infarct depolarisation, inflammation and apoptosis. **B** shows the intra- and extracellular signalling cascade initiated by the ischemic insult (from (Katramados & Vareals 2007; Dirnagl et al. 1999)). **C** shows the schematic dynamic evolvement of stroke core and penumbra following a middle cerebral artery (MCA) occlusion. Adapted from (Dirnagl et al. 1999).

4.5.2   Haemorrhage

Intracranial haemorrhage may affect the brain parenchyma classified as intracerebral haemorrhage (ICH) or the surrounding meningeal spaces classified as subarachnoidal haemorrhage (SAH) (**Figure 21**).

Primary ICH accounts for an estimated 10-15%, whereas SAH accounts for 5% of strokes in western countries. In Asia and amongst Afro-Caribbean the proportion is estimated to be between 30-40%. ICH is the result of bleeding from an arterial source directly into brain tissue. The primary loci are subcortical structures such as the putamen (35-50%), white matter (~30%), thalamus (10-15%), and pons (5-12%) (Mohr 2004); These areas are predominantly supplied by small deep arterial branches (50-200μm). The principal causes of primary non-traumatic ICH is arterial hypertension and amyloid angiopathy, whereas secondary ICH can be caused, for example, by intracranial aneurysms, arteriovenous malformations, intracerebral tumour, arterial dissection, substance misuse (Hankey 2007; Carroll & Chataway 2006). Hypertension-induced strokes commonly affect the basal ganglia, thalamus,

brain stem and cerebellum whereas secondary ICH more frequently affects lobar regions (Carroll & Chataway 2006). SAH is caused by the rupture of an intracranial saccular aneurysm in 80% of cases. Although abrupt in onset the stroke is frequently a manifestation of underlying long-standing unidentified processes (Katramados & Vareals 2007). Upon symptom onset patients tend to present with reduced levels of consciousness, nausea, and headache.

4.6 Acute treatment: Recombinant tissue plasminogen activator (rtPA) and endovascular thrombectomy

The ischemic cascade described above (chapter 4.5.1) can be altered in some cases by the intravenous or intra-arterial administration of an enzymatic agent, a genetically engineered version of naturally occurring tissue plasminogen activator manufactured via recombination biotechnology (from bacteria) and is therefore called recombinant tissue plasminogen activator (rtPA). rtPA is a protein that activates the enzyme plasminogen and it causes fibrinolysis to dissolve the occlusive blood clot by breaking the cross-linked fibrin mesh. This renders the clot soluble and further enzymatic processes can resolve it to resume cerebral perfusion and supply of oxygenated blood. Recent investigations focus specifically on the penumbral region as the tissue is affected by the occlusion but may still be salvageable. Perfusion computer tomography (CT) imaging has proven to be a good tool for estimating penumbral tissue by demonstrating a mismatch between the extent of the core region and the hypoperfused tissue. Early recanalisation is beneficial for functional outcome and mortality rates (Smith 2007b).

More recently it was shown that rtPA has a substantial efficacy when given within a maximum of 4.5 hours post onset, especially for distal thrombi (Latchaw et al. 2009); however, the odds of a favourable outcome decreased thereafter and may even be harmful after a certain period of time (Hacke et al. 2008). The benefits of an extended treatment window within selected cohorts is currently under investigation, for example at King's College Hospital (KCH) (Sztriha et al. 2011). London is covered through eight hyperacute stroke centres with KCH covering a catchment area of 1.5 million people. The KCH records between 2008 and 2010 show a rise in rtPA treatments from 25% of all admissions in January 2008 up to 41% in July 2010. In general, it was shown that aphasic stroke patients are more likely to receive thrombolysis treatments (Engelter et al. 2006).

The guidelines of thrombolysis treatment are still stringent and lengthy, and the licence of the drug contains numerous restrictions. Investigations are underway to answer to the following difficulty: '*The burning question is no longer whether thrombolysis is effective, but in whom it is effective, in whom it is ineffective and in whom it is dangerous*' p. 240, (Hankey 2007).

Some patients are ineligible for rtPA treatment for various reasons, such as late presentation to the hospital or increased risk of symptomatic haemorrhage due to the blood thinning properties of the rtPA. In a subset of these patients a mechanical approach to remove the occluding thrombus might be considered. This treatment is based on the introduction of microcatheters into the vessel, that are used to guide the wire to occlusion site and allow for the thrombus to be removed either through suction or withdrawal. This is referred to as mechanical thrombectomy. Historically this method was introduced for coronal vessels and was pioneered by the German physician Werner Forssmann who conducted a self-experiment whereby he introduced a catheter from his antecubital vein in the elbow into the right atrium (Forssmann 1929). The incentive for this endeavour was the need for intracardiac injections for cardiac resuscitation at a time where direct cardiac injections were more often than not fatal. Forssmann changed speciality after being made redundant for his 'cavalier' approach but subsequently received a Nobel Prize in 1956 [jointly awarded to André Cournand and Dickinson W. Richards] "for their discoveries concerning heart catheterization and pathological changes in the circulatory system" (http://www.nobelprize.org).

Recanalisation of cranial vessels can be achieved via proximal or distal mechanical endovascular neurothrombectomy in some patients by means of a so-called stent-retriever. In contrast to stents the retriever is only temporarily introduced into the vessel. The differentiation between distal and proximal approaches is the location of the applied force on the thrombus. Proximal devices apply the force at the base of the thrombus where the catheter tip is placed into the clot and a blood-thinning drug is directly administered locally (aspiration catheters). This breaks down the blood clot that can then be sucked away through the microcatheter. Distal devices propagate the tip of the microcatheter past the thrombus to be unsheathed behind it, and thereby applying the force to the distal base of the thrombus and removing the clot by withdrawing the catheter (coil-like devices). Microcatheters are also used to place stents, which are mesh tubes inserted into a vessel to ensure it cannot close up again. In the absence of human in vivo comparative studies, a comparative swine study described the proximal approach to be superior in application speed, in

the ability to repeat attempts, and low complication rate; whilst distal approaches are superior in the removal of thrombotic material but with an increased risk of thromboembolic events and vasospasms (Gralla et al. 2006). Mechanical thrombectomy was seen to be beneficial in some patients due to its wide time frame of application, the treatment success and the low risk of symptomatic haemorrhages as well as the reduced mortality after treatment (Versnick et al. 2005; Nogueira et al. 2012).

In conclusion, stroke and its associated risk factors have been clinically well circumscribed for a long time. More recently, international comparative studies showed that underlying genetics, geography, and comorbid disorders might influence the occurrence and severity of stroke symptoms. The exact nature of recovery is yet to be elucidated, especially for higher cognitive functions. In recent years thrombolysis is the only available acute treatment that has yielded compelling positive results for functional short and long-term outcome after stroke. However, questions still remain to be answered regarding the general applicability of the treatment, treatment alternatives and predictive factors for recovery.

CHAPTER 5   MR-BASED NEUROIMAGING

'The tendency to reify language into something material is perhaps nowhere more subtly treacherous than when imaging techniques are applied'

(Rodden and Stemmer, 2006)

5.1   General principles of Magnetic Resonance Imaging (MRI)

In the imaging sciences, the first wave of enthusiasm was elicited by the discovery of x-rays by the German physicist Wilhelm Conrad Roentgen (1898). For the first time in the history of medicine it was possible to investigate the internal human body in vivo whereas before only post mortem examinations had allowed the study of the internal anatomy and pathological alterations. Nowadays, computer tomography (CT) or magnetic resonance imaging (MRI) are the most commonly used techniques for neuroimaging, which are particularly apt for neuroscience research and clinical applications due to their high resolution and timely acquisition whilst having minimal side effects.

'*No other technique [than MRI] has proven to be so uniquely flexible and dynamic*' p. 291, (Toga et al. 2000). MRI has revolutionised our approach to neurosciences by allowing the investigation of neuronal tissue in vivo and non-invasively (in most cases) with a relatively high spatial resolution. The concept of nuclear magnetic resonance (NMR) was simultaneously and independently discovered in the mid-1940s by Bloch (1946) and Purcell (1946), for which they shared the Nobel Prize. However, it was not until 1973 that the possibility of obtaining images with magnetic resonance (MRI) based on the NMR phenomenon was first described (Lauterbur 1973; Mansfield & Pykett 1978) and only in the 1980s that MRI emerged as a clinically useful diagnostic tool for stroke (Bydder et al. 1982; Ramadan et al. 1989; Brant-Zawadzki et al. 1983). MRI has since been employed for structural, functional, pharmacological and perfusion investigations, angiographies, MR elastographies and many more. The past 40 years have witnessed the increase in field strengths of scanners, new contrast weighting and improved spatial resolutions. Below, the basics of MRI will be explained (on a conceptual rather than quantitative level) followed by a methodological introduction to diffusion-weighted imaging (DWI) and

tractography. These methodological concepts are then discussed in the light of stroke and aphasia research.

5.1.1 General principles of MRI and basic pulse sequences

The human body is composed of copious water molecules (H_2O), which consist of two hydrogen atoms (H) and one oxygen atom (O). At the centre of hydrogen atoms is a positively charged proton (H^+) that contains spin, causing it to precess, around its own axis. This nuclear spin is represented as a three-dimensional vector in a coordinate system (x, y, z) (**Figure 24**A). Protons generate a minute magnetic field due to their spin and positive charge (magnetic dipole vector) and are therefore sensitive to environmental magnetic fields. In the absence of an external applied magnetic field, magnetic dipoles such as the hydrogen atom have no preferred orientation. In the presence of a magnetic field spins start to precess around the magnetic field. This phenomenon is referred to as Larmor precession. The spins precess about B_0 at a frequency v defined by the Larmor equation:

$$v = \gamma B_0$$

with v being the frequency of precession, γ is the gyromagnetic ratio (with a value of 4257Hz/gauss pro proton), and B_0 is the magnitude of the magnetic field.

5.1.1.1 Main magnetic field (B0) and radiofrequency pulses

MRI utilises these natural magnetic properties of the human body and their interaction with radio waves to obtain images. MRI scanners are strong magnets that create a magnetic field. The main magnetic field of the MRI scanner is a strong and static field referred to as B_0 and aligned to the z-axis, typically defined to point along the bore of the scanner. A suitable magnetic field in MRI depends on two prerequisites, namely the field uniformity (homogeneity) and the field strength. Homogeneity over space and time allows us to obtain images that are independent of the type of scanner used or where the head is positioned within the bore. The field strength is the magnitude of the static magnetic field generated by the scanner and is measured in units of tesla (T), which equals 10,000 Gauss. Homogenous and stable field strengths are available in the range of 1.5 to 11T for human use, and up to 24T for animal use. Common scanner strengths for humans, however, range

between 1.5-3T in the clinical arena and up to 7T for research purposes. Patients are placed at the centre of the magnetic field (isocentre) and the protons contained within brain tissue become polarised aligning themselves either parallel or antiparallel with the external main magnetic field B_0 (**Figure 24**B); with a slight excess in parallel alignment.

This alignment to B0 along the z-axis can be manipulated by excitation via the application of radio frequency pulses (RF), which momentarily creates a second magnetic field (B_1). Excitation means that the total magnetisation vector formed by the spins (i.e. their total alignment) is tilted out of alignment with B_0 (e.g., away from the longitudinal magnetisation along the z-axis towards the x-y plane), either perpendicular (90°, also known as the transverse magnetisation) or antiparallel (180°) (**Figure 24**C). Technically, any angle rotation of the net magnetisation vector into the transverse plane can be achieved; depending on the duration and amplitude of the RF pulses applied. The amount of tilting is denoted as the flip angle θ. When this RF excitation terminates, protons realign with the main magnetic field B_0 by emitting energy. The time it takes to reach their original orientation (i.e. realign) can be measured with MRI.

The radiofrequency pulses are generated and received by electromagnetic coils, or radiofrequency coils, that produce and gather electromagnetic fields at the resonant frequencies of the atomic nuclei (Larmor frequency) within the static magnetic field. The coil is placed around the head of the participant. The signal recovered by the coil depends on the type of coils used (surface or volume coil, phased array) which impacts on the spatial coverage and sensitivity.

These surrounding receiver coils are detecting currents, generated by placing a participant in a strong static magnetic field and exciting its atomic nuclei through RF pulses. These detected currents are the MRI signal but are devoid of spatial information and are thus not sufficient to reconstruct an image. To add the spatial information magnetic gradients need to be introduced.

This third set of magnetic fields, called the magnetic field gradients otherwise often simply referred to as gradients, are auxiliary gradients superimposed upon B_0 and applied along the x, y, z coordinate system. Separate gradient coils that can modify the strength of the magnetic field along specific directions, by either increasing or decreasing the strength, recover the spatial information (details below). Thus far we assumed that the static magnetic field of the scanner is homogeneous, which in reality is unfortunately rarely true. To correct for this a final set of coils, so called

shimming coils, are in place. The shimming coils can generate compensatory magnetic fields to correct the inhomogeneity in the static magnetic field.
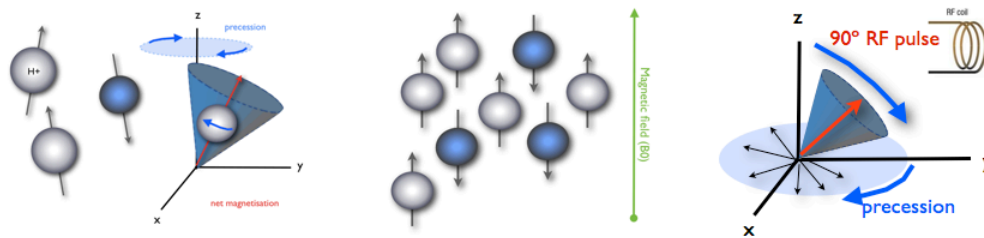
Figure 24   Physical concept of Magnetic Resonance (MR)

A Random thermodynamic precession motion of hydrogen protons around their own axis. **B** When a person is introduced to the magnetic field of a MRI scanner (B_0), protons align to the main magnetic field. **C** This coherent alignment can be manipulated via the application of a radio frequency (RF) pulse through the RF coil. This tilts protons away from B0 towards a higher energetic level.

5.1.2   Longitudinal and transverse relaxation

Application of a B1 field orthogonal to B_0 causes the nuclear magnetisation vector to be flipped away from the longitudinal (z) axis onto the transverse (x-y) plane (**Figure 24**C). When the applied B1 field is switched off, the magnetisation in the x-y plane reduces due to three factors: i) transverse relaxation (T2), ii) longitudinal relaxation (T1), and iii) variation in the B_0 field (i.e. B_0 inhomogeneity). These MR signals are detected through the radiofrequency coil and do not remain stable for a very long time. During signal reception the transverse magnetisation rapidly loses coherence (transverse decay), and the longitudinal magnetisation slowly recovers (longitudinal recovery). These signal changes are referred to as relaxation. The relaxation time (TR; i.e. the time between excitation and realignment back to B_0) is characterised by T1 (longitudinal) and T2 (transverse) relaxation as explained below and in **Figure 25**.

The longitudinal recovery ranges in the order of a few hundreds of milliseconds to a few seconds, and is hence considered relatively slow compared to the transverse signal decay. Atoms of different cerebral tissues recover at different times, based on how the tissue dissipates energy, which allows for tissue differentiation based on T1 recovery time (**Figure 25**, left). Depending on how fast the next RF pulse is applied the T1 signal might have fully recovered or might still be recovering. The delay between the applications of two pulses in the same volume is referred to as the

repetition time (TR). T1-weighted images have a short TR (300-800 milliseconds) emphasising the effects of T1 relaxation on the image.
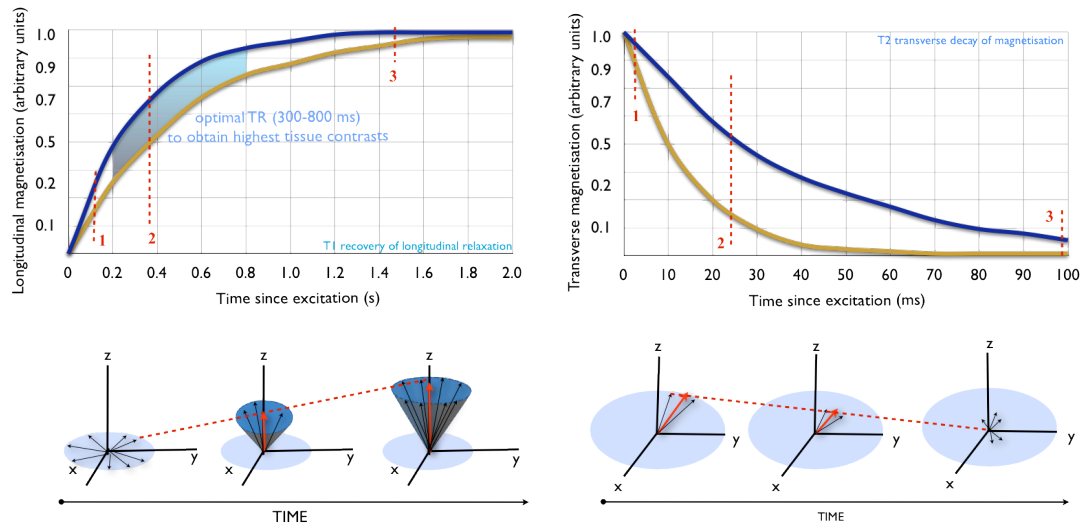
Figure 25   Longitudinal (T1) and transverse (T2) relaxation

The upper panel shows the recovery of net magnetisation (left) and the decay of transverse signal (right) in two different tissue types (blue and orange). The relaxation times are tissue-dependent and the time point of imaging is therefor crucial (dashed lines, 1-3). This is exemplified for both relaxations where at time point 1 no differentiation between tissue types is possible, at time point 2 the tissue contrast is very high and at time point 3 the tissue contrast is again low (consider the different time scales (*s*/*ms*) in this model). By adjusting these time points images can be weighted towards the T1 or T2 contrasts. The lower panel depicts the conceptual relaxation (in correspondence with upper panel) with reference to the coordinate system.

T2-weighted imaging on the other hand measures the signal decay (or loss of coherency between precessions) within the transverse plane (x-y plane; **Figure 25**). Here the net magnetisation reflects the vector sum of various individual spins and the magnitude is therefore dependent on the underlying coherence, meaning that the greater the coherence the greater the net magnetisation. Over time the magnetisation along the transverse plane reduces due to the local field interactions of nuclei rendering them to spin at different frequencies. This randomisation of spins (or dephasing) leads to a reduced vector sum along the x-y plane and results in a loss of image signal occurring with a time constant known as T2. Additionally, spatial inhomogeneities in the magnetic field can also influence the spins by exposing them to different magnetic fields over time. This results in some spins precessing faster than others. The combination of spin-spin interactions and additive field inhomogeneities is described by the time constant T2*. Both T2 contrasts are related yet T2 decay is always longer than T2* decay.

T2-weighted images allow a long time (~100-500 milliseconds) between excitation and signal collection, which ensures high tissue contrast, and a long TR (>1 second) to ensure T1 contrast is not dominant in the image signal as the longitudinal recovery is almost complete. The duration of signal decay in tissue where water can freely move (e.g., ventricular system) is longer than in restrictive tissue (e.g., axonal structures).

5.1.3   Spin Echo effect

As described above MR images are acquired by a fine tuned on-off interaction of radiofrequencies in a prescribed sequence, referred to as *pulse sequence*. This pulse sequence determines the image contrast, its resolution, and quality. After a RF pulse is applied, net magnetisation is flipped onto the transverse plane and over time spins begin to dephase (as described above).

If a pulse of resonant radio frequency close to the Larmor frequency of the nuclear spins is induced and the net magnetisation is flipped onto the transvers plane the initial very fast decaying signal is the so–called free induction decay (FID).

This dephasing is elicited by different precessing speeds of spins. In order to realign them to each other, a second RF pulse is applied at a given time (*t*) after the initial excitation to eliminate spin dephasing. This so-called refocusing RF pulse flips the spins in the perpendicular plane to the main magnetic field (i.e. 180 degrees), which aligns the faster precessing spins behind the slower precessing spins. Assuming constant conditions, all spins will re-phase at a given time (*2t*). This moment of spin coherence is referred to as *spin echo*. The time between the first RF pulse and the formation of the echo is referred to as the echo time (TE) and is defined as twice the time (*t*) between the two RF pulses (*2t*).
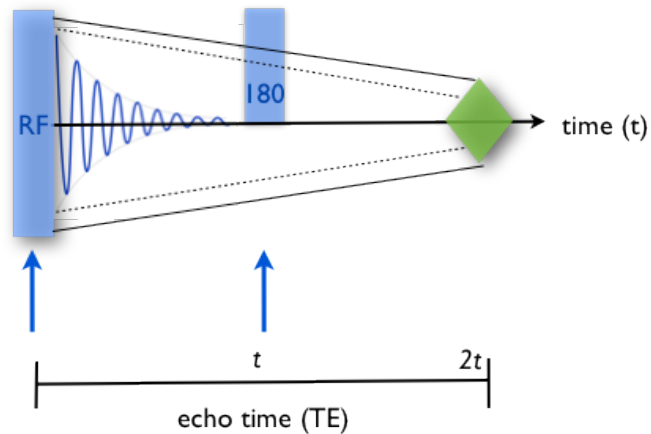
Figure 26   Spin Echo Imaging (schematic).

Sequences that utilise refocusing pulses are indicated as spin echo pulse sequences, whereas those that do not are denominated as gradient echo sequences. Manipulating the TE and TR parameters (TE/TR) will change the obtained imaging contrasts towards a T1 or T2-weighted image (see below).

5.1.4   Image generation

5.1.4.1.1   Slice selection (gradients)

All atomic nuclei exposed to an excitation pulse will contribute to the signal detected in the coil. A first step towards image generation is therefore the slice selection. As mentioned before, the spatial information is added to the image by the application of auxiliary magnetic field gradients, that are spatially varying magnetic fields superimposed upon B_0. The precession frequency is proportional to the strength of the magnetic field. Given that the gradients vary spatially they cause atoms to spin at different rates in different spatial locations (**Figure 27**). Therefore, this spatial specificity can be used to select different image components of different frequencies and generate a spatial map thereof.

Selective excitation of spins within that particular slice but not other spins within the probed tissue is the pivotal step to slice selection. This selectiveness is achieved by matching the radio frequency excitation pulse and the precession frequency of the spin within the slice. Excitation of spins occurs when the RF is applied at the

Larmor frequency. In the presence of a linear gradient, the Larmor frequency changes along the gradient (**Figure 27**). A slice of spins is excited with an orientation perpendicular to the applied gradient. Slice selection is therefore the result of the simultaneous application of a linear magnetic field gradient and an RF pulse.
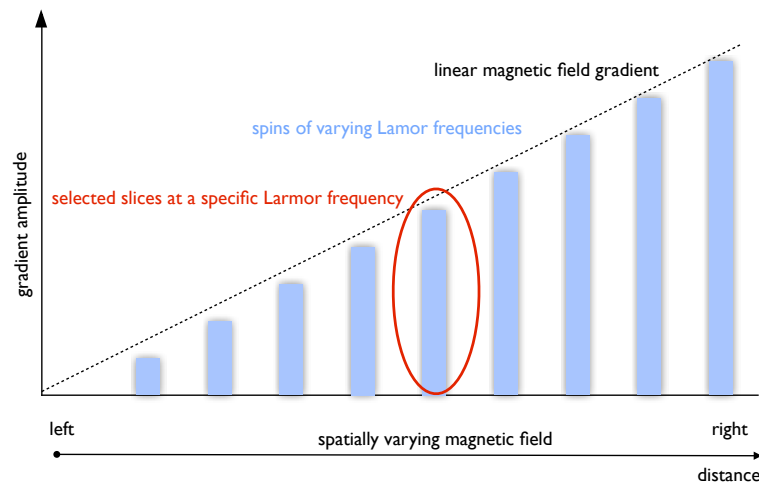
Figure 27   Magnetic field Gradient (Gz) application for slice selection

Obtaining the spatial information as described above will however only provide a 1D image. Given that the brain is a three-dimensional organ, spatial information has to be resolved in three directions, which requires at least three gradients applied along the three axes of the coordinate system as described below (**Figure 28**).
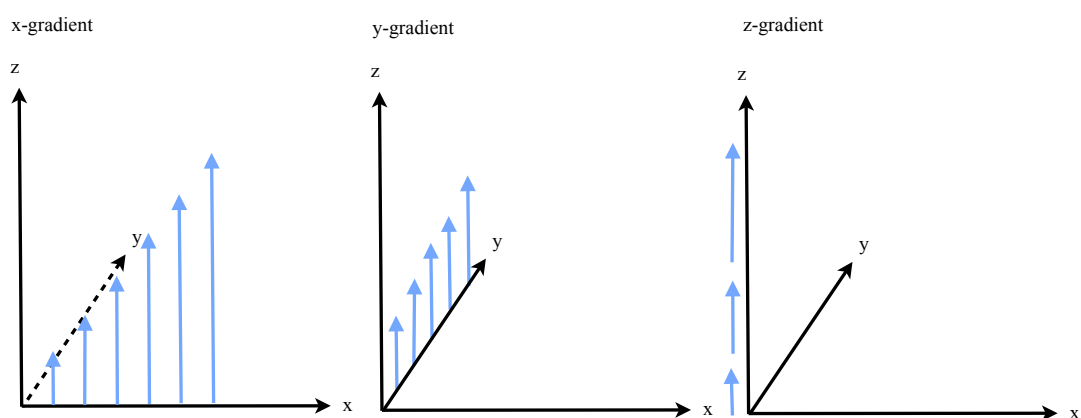
Figure 28   Resolving spatial information in three dimensions

Resolving spatial information through the use of orthogonal gradients. Adapted from (Huettel et al. 2009)

The systematically spatially varying magnetic field strength is utilised to select a specific brain slice (plane) by exciting or refocusing the spins perpendicular to the gradient. The thickness of the excited slice depends on the frequency bandwidth of the RF pulse and the strength of the gradient.

Slice selection produces a 2D slice of the brain. The remaining dimensions need to be resolved in order to create a 3D brain image. This is achieved by introducing additional gradients onto the selected slice that cause spins at different locations to precess at different rates owing to the spatially varying strength of the gradient. This allows us to obtain the individual spin contributions to the signal. This pattern of radiofrequency pulses produces a complex MR signal that can then be resolved with the Fourier transformation. The mathematical foundations of image formation are beyond the scope of this chapter but follow the Fourier transformation.

5.1.4.1.2   Frequency encoding

Is the additional linear magnetic gradient present during the data acquisition causing the precessional frequencies of spins to change linear over space, this is referred to as the frequency-encoding gradient (usually indicated as G_x). The signal is encoded into different frequencies depending on their position toward the frequency-encoding gradient. In the presence of the gradient, the protons will have distinct precession frequencies, at one end of the slice protons precess faster than the protons at the other end, and the measured frequency reflects the position along the frequency-encoding gradient. If for example the gradient is applied left to right (x-axis) the spins on the left will have higher resonance frequency than the tissue on the right; this measured frequency thus reflects the position along the frequency-encoding gradient. Signal processing tools can dissolve these different frequencies and thereby map the physical distances between imaged structures.

5.1.4.1.3   Phase coding

Upon slice selection, all excited spins contribute to the MR signal. All protons within the single two-dimensional slice are processing at the same rate allowing the conclusion that there are protons within the slice but not where exactly they are located therein. To disentangle the individual contributions of spins additional gradients are applied along the two in-plane directions (x-y plane) defining the excited slice. This causes the spins at different spatial locations to precess at different times. The application of magnetic gradients within a slice involves two

intertwined processes, referred to as frequency encoding and phase encoding. These two gradients must be applied sequentially.

The phase-encoding gradient (usually referred to as G_y) is typically applied perpendicular to the slice-encoding gradient as a linear spatial variation, prior to the data acquisition period (read-out) and allows spins to accumulate differential phase offsets over space (**Figure 29**). The phase is 'the angle made by the transverse magnetisation vector with respect to some fixed axis in the transverse plane' p. 256, (Bernstein et al. 2004).
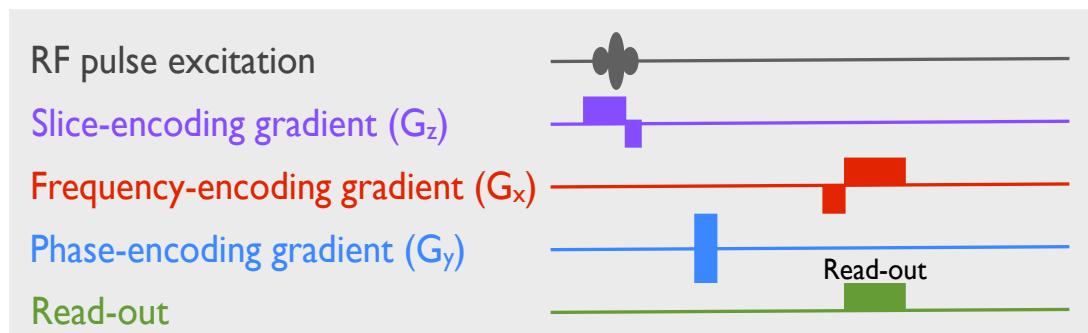
Figure 29   Pulse sequence elements necessary for phase and frequency encoding within a selected slice

The RF pulse is needed to excite protons and an initial slice selection is applied at a specific Larmor frequency. Additional linear magnetic field gradients are applied to obtain spatial information along the x-y plane of the reference frame. The phase encoding gradient usually proceeds the frequency encoding gradient, which is applied during the period of data acquisition (read-out). Adopted from (Huettel et al. 2009).

5.1.4.1.4   Echo-planar imaging (EPI)

In 1976 the British physicist Peter Mansfield proposed a technique that allows for the collection of an entire image slice at once, by sending one RF pulse followed by rapid alterations of the magnetic field gradients during signal recording. This technique has been introduced as echo-planar imaging (EPI) and allowed for ultrafast image acquisition that improved the feasibility of clinical MR imaging. EPI is the fastest acquisition method for MRI but compromises spatial resolution. EPI is the primary method of acquiring diffusion-weighted data as it significantly reduces data corruption through motion artefacts in robust DW images (Jones & Cercignani 2010). The issues around motion artefacts and how to further reduce them will be discussed in more detail in the study-specific chapter of this thesis. On the other hand, the rapid read-out in EPI increases the risk of eddy current effects and susceptibility effects (commonly in the temporal lobes) (Jones & Cercignani 2010). These issues can be partially corrected for during the data pre-processing stages.

The reconstruction of the obtained complex signal into an image lies beyond the scope of this chapter.

5.1.5   Structural imaging contrasts

5.1.5.1 T1-weighted imaging

T1-weighted imaging is based on the mechanism whereby nuclei, which received energy through RF pulses, dissipate that energy to their adjacent environment and return to their equilibria along B_0. This realignment leads to the gradual recovery of net magnetisation along the longitudinal z-axis (**Figure 25**). On T1-weighted images cerebral spinal fluid (CSF) is hypointense (i.e. dark), fat appears hyperintense (i.e. bright), grey matter has less intensity than white matter (i.e. it appears darker), and chronic ischemic lesions appear hypointense (**Figure 30**).

5.1.5.2 T2- weighted and T2*-weighted imaging

The T2-weighted image has its maximal signal intensities in fluid rich regions of the brain, such as the ventricles (**Figure 30**). Regions with slow T2 relaxation time are hyperintense on the obtained image. CSF is consequently hyperintense, fat barely has a signal, grey matter appears brighter than white matter, and ischemic lesions and oedema appear hyperintense. In this contrast it might be difficult to distinguish a lesion from normal CSF, especially for smaller lesions.

5.1.5.3 Fluid Attenuated Inversion Recovery (FLAIR)

An image contrast that is better suited to distinguishing between CSF and lesions is FLAIR imaging (Hajnal et al. 2001). The CSF signal is nulled in these images by the application of an initial RF pulse (inversion pulse) prior to the standard imaging pulses. This renders the CSF signal almost entirely suppressed and it appears dark on the final image, whereas lesion tissue will appear hyperintense as on the T2-weighted (**Figure 30**). This contrast is therefore well suited to detect lesions in border zones of different tissue types, such as cortical and periventricular lesions. In the stroke arena, FLAIR, even though slightly longer in acquisition time, is often used in preference to a standard T2-weighting, as haemorrhages and arterial occlusion are also shown as hyperintense and are therefore readily detectable.

5.1.5.4 Proton density map (PD)

Proton density, or sometime referred to as spin density, reflects the concentration of MRI-visible protons in cerebral tissue (**Figure 30**). The majority of protons (i.e. hydrogen nuclei) are present in all tissue water (e.g., the cerebral spinal fluid). The cerebral white matter also contains numerous non-aqueous protons (30% of white matter protons). PD-weighted contrasts are therefore tissue-dependent. The net magnetisation in proton density-weighted contrasts reflects the contribution of all spins within each voxel and provides an image representing the number of protons within each voxel. To maximise the PD contrast, the T1 and T2 contrasts are minimised by manipulating the TE and TR windows, with a short TE to minimise the T2 losses whilst a long TR to minimise T1 losses.

Distinctive tissue types (grey and white matter, cerebral spinal fluid, and abnormal tissue) will relax differently after excitation resulting in varied signal responses. The MR image represents a display of these spatially localised signal intensities where the difference in amplitudes of the released energy from the various tissue types translates into different contrasts in the images (i.e. hypo- or hyperintense).
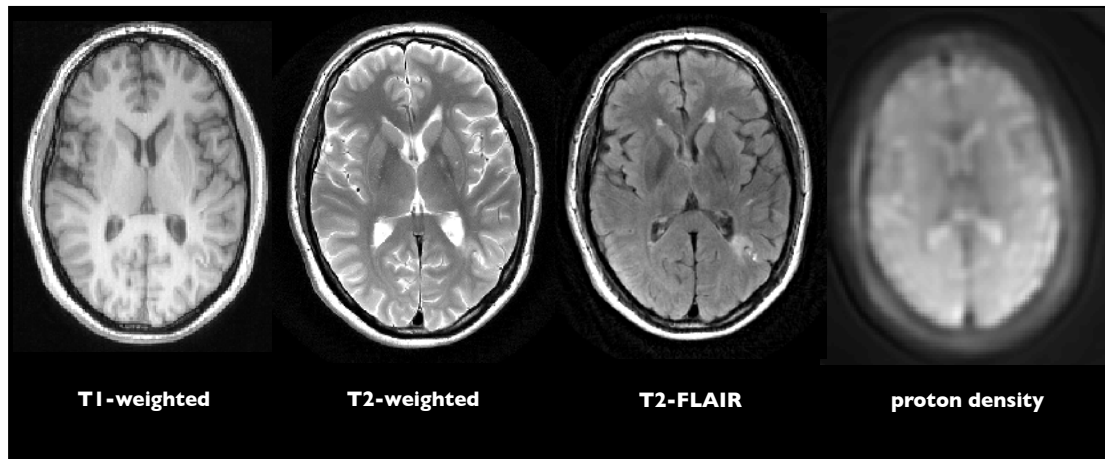
Figure 30   Common structural imaging contrasts

T1-weighted, T2-weighted, T2 FLAIR, and proton density maps (PD). Images are taken from study data.

5.1.6   Physiological pulse sequences

Whilst conventional sequences provide purely anatomical information, more recently implemented sequences can extract functional and physiological information. These include various contrasts of which the following two will be discussed in detail below as they have been employed for the study at hand: perfusion-weighted imaging (PWI) and diffusion-weighted imaging (DWI).

5.1.6.1 Perfusion-weighted Imaging (PWI)

The brain is in constant demand for oxygen and nutrition, which are provided through the bloodstream. This irrigation of cerebral tissue via hematologic delivery is referred to as perfusion. Perfusion, defined as the volume of blood travelling through a tissue mass over time, is tissue-dependent: grey matter perfusion is approximately 60mL/100g/min and white matter is about 20 mL/100g/min (Huettel et al. 2009).

Until recently, cerebral perfusion was only measurable by H20-15 PET or by injecting exogenous intravascular contrast agents (e.g., gadolinium) into the blood stream. The resulting signal attenuation is proportional to the amount of contrast agent present within the voxel. A recent non-invasive MR advance uses radio frequency pulses to electromagnetically "label" arterial blood water as an endogenous diffusible tracer to measure the absolute cerebral blood flow (CBF) (D. Roberts et al. 1994) (**Figure 31**). This method is thus referred to as arterial spin

labelling (ASL) and can be acquired via pulsed or continuous labelling (Detre & Alsop 1999; Alsop & Detre 1998); the latter (cASL) was used in the study at hand. Continuous ASL saturates spins in upstream blood within the carotid arteries of the neck through RF labelling with magnetic inversion. The labelled blood then travels to the brain and enters the imaging slice. A second set of images is acquired in the absence of the labelled blood. The difference between those two sets of images is the absolute blood flow, as all other tissues should be similar (**Figure 31**).

Regardless whether the ASL was acquired pulsed or continuous, the labelling of blood alters the longitudinal magnetisation selectively. To obtain a maximal signal difference between the two sets of acquired images (labelled and non-labelled), a short TE is necessary to minimise signal loss due to T2 and T2* relaxation effects.

Even though this method is still in its infancy, and rarely clinically applied, its spatial and temporal resolution and non-invasiveness outperform previously used methods, such as PET (Wong et al. 1999). A handful of studies have investigated the comparability of ASL to previously used invasive methods and have provided converging evidence that ASL correlates if not supersedes these methods (Chalela et al. 2000; Deibler, Pollock, Kraft, Tan, Burdette & Maldjian 2008a; Deibler, Pollock, Kraft, Tan, Burdette & Maldjian 2008b).
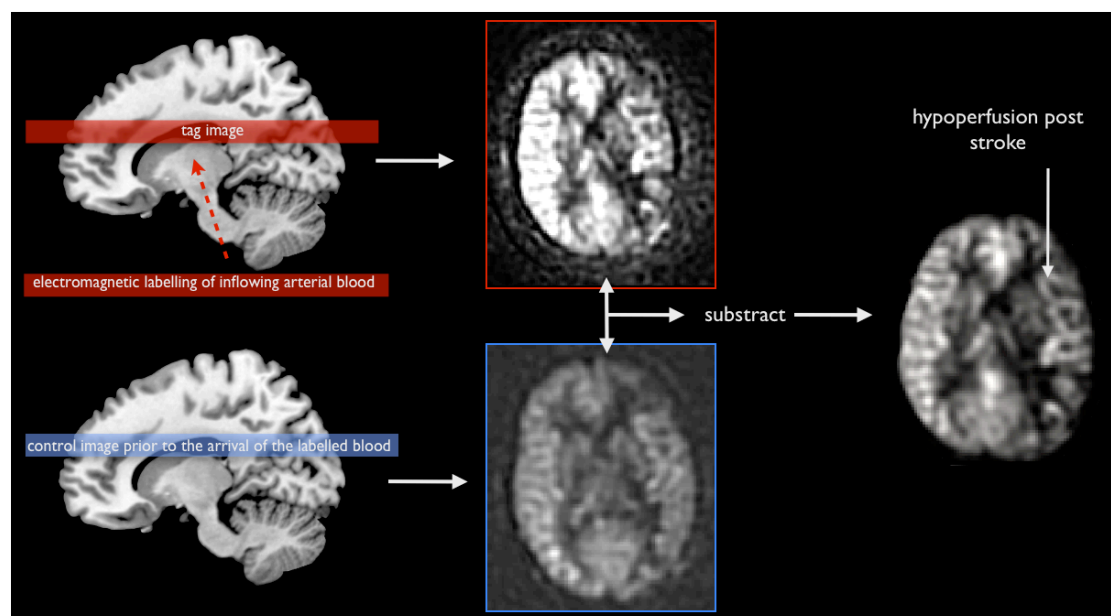
Figure 31   Continuous arterial spin labelling (cASL)

The panel depicts the schematic methodological cascade for continuous ASL with the demonstration of a post stroke left middle cerebral artery territory hypoperfusion (radiological view, i.e. left is shown on the right; own data taken from the same patients as in **Figure 30**).

5.1.6.2 Diffusion-weighted imaging (DWI)

The advantages of MRI scanning in ischemia have been recognised since the 1980s (Brant-Zawadzki et al. 1985), however, the T1 and T2 contrast of the lesion evolves during the first 12-24 hours which leads to inaccurate measures and is often reported negative (i.e. as normal) in the acute phase (Mohr et al. 1995). Diffusion sensitive images were shown to be superior over conventional contrast for the early post-ictal hours (Moseley et al. 1990; Baird & Warach 1998). This discovery was crucial as the first six hours are considered as the period with the greatest therapeutic opportunities for treating ischemia (e.g., thrombolysis treatment). Additionally, the development of Echo Planar Imaging (EPI) allowed for a fast whole-brain acquisition time and thereby reduced some artefacts (induced for example by head movements) and improved the feasibility of rapid acute clinical scanning (Stehling et al. 1991; Mansfield & Pykett 1978).

DWI is based on the measurement of the displacement of water. In a free medium, the displacement of water molecules obeys a three dimensional Gaussian distribution over a given time; meaning that water molecules travel randomly but equally in all direction over a distance that is statistically defined as the diffusion coefficient (D).

$$\langle r^2 \rangle = 6D\Delta$$

Where r^2 is the mean-squared displacement of particles
during a diffusion time Δ, and D is the diffusion coefficient.

D depends on the size of the molecules as well as the nature (e.g., viscosity) and temperature of the environment. This phenomenon is often referred to as *Brownian motion* (or 'diffusion') paying credit to the first scientist to have observed it in a Petri dish (Jones 2008; Le Bihan et al. 2006). If water molecules were not hindered by cellular structures (e.g., cell membranes, cytoskeleton, macromolecules) they would diffuse at an equal rate in all directions in a given time (isotropic diffusion). DWI measures this displacement of water over time within a three-dimensional space, such as the imaged voxel (volumetric pixel). MR images are made sensitive to diffusion by the application of two gradient pulses, the so-called diffusion gradients whose duration and separation can be manipulated. Whereas the first applied gradient labels the protons in space along a specific direction defined by the gradient, the second gradient detects nuclei that have changed location during the defined time interval (i.e. diffused). This displacement of water molecules can be

measure along different directions by applying varying diffusion gradients. The signal attenuation of diffusion-weighted images measured along a gradient direction is quantitatively related to the degree of phase variation and therefore to the amplitude of the displacement distribution. On diffusion-weighted images CSF therefore appears hypointense and ischemic tissue appears hyperintense (due to reduced parenchymal diffusion). The level of induced sensitivity to diffusion generated by the imaging sequence is referred to as the b-value; a value that can be manipulated to optimise sequence acquisition (Jones et al. 2002). The higher the b-value, the higher the sensitivity to diffusion (Le Bihan 2012). Mathematically, the b-value is proportional to the square of the applied gradient strength (Basser & Oezarslan 2009).

$$b = \gamma^2 G^2 \delta^2 (\Delta - \frac{\delta}{3})$$

Where γ is the constant (cyromagnetic ratio), δ represents the duration of the gradient, Δ the separation of gradient and G the amplitude of different gradients.

5.1.6.3 Apparent diffusion coefficients (ADC) maps

In neuronal tissue, the above-described molecular displacement differs from the Brownian motion due to the presence of cellular obstructions. These reduce diffusion distances unevenly in the three-dimensional space as compared to free water. The water molecule movements in brain tissue are hindered and the measured diffusion coefficient appears reduced compared to free water and is hence referred to as apparent diffusion coefficient with the acronym ADC (Le Bihan et al. 2006; Le Bihan et al. 1986). DWI provides information about tissue structure and intra/extracellular space through ADC maps that can account for motion and partial volume effects[11] in imaged voxels (Le Bihan et al. 1986). During the acute phase ischemia lesions appear hypointense (i.e. dark) on ADC maps due to the reduction in the displacement of water that leads to reduced signal attenuation. This is quite the opposite of DWI images where the lesion appears hyperintense (i.e. bright). The appearance of the lesion on ADC maps changes over time whilst the ischemic cascade is evolving (cytotoxic oedema, vasogenic oedema, tissue necrosis); during this period the ADC signal normalises and then becomes elevated

---

[11] Partial volume effect refers to the fact that within one imaged voxel (in this study the voxels are 2.4x2.4x2.4mm) might contain not only one single type of tissue but more than one (i.e. grey and white matter, white matter and CSF, different types of white matter etc).

in the chronic stages of ischemia (Warach et al. 1995; Warach et al. 1996; Welch et al. 1995).

In early studies of diffusion it was noted that the contrast in ADC maps was orientation-dependent (i.e. it varies depending on the direction of measurement) (Chenevert et al. 1990; Doran et al. 1990; Moseley et al. 1990). The directional dependency was shown to result from the diffusion anisotropy reflecting the intrinsic structural anisotropy of biological tissue (Basser et al. 1994). The anisotropy is mainly determined by the presence of intact and organised cell membranes that hinder water diffusion along a specific direction.

These imaging contrasts (conventional and physiological) should be used in combination and applied to stroke patients to improve diagnosis (Schellinger et al. 2010). For example, using DWI and FLAIR in combination reduces the partial volume effect of CSF whilst increasing the lesion contrast (Latour & Warach 2002; Lansberg et al. 2001). '*As a rule of thumb, DWI hyperintensities without T2 or FLAIR changes implies reduced ADC and can be taken as evidence of acute ischemic injury*' p.463, (Mohr 2004).

5.2   Image quality

5.2.1   Signal-to-noise-ratio (SNR)

The image quality depends on various factors, amongst which the signal to noise ration is rather crucial. Signal is here considered as meaningful changes in some quantity; whereas noise is considered as irrelevant sources of variability. Noise originates, amongst other sources, from different spatial and temporal sources, such as the inhomogeneity of the main magnetic field, thermal molecular motion within the human body, and the various relays within the measuring chain of the scanner (e.g., coil, magnet, and receiver).

The ratio between the relevant and the irrelevant signal, called signal-to-noise ratio (SNR) determines the quality of the final image, i.e. the more noise, the less signal, the worse the image and vice versa.

5.2.2   Imaging artefacts

Various artefacts can affect MR images and either originate from the participant or the equipment. Two main types of artefacts can compromise image quality and are induced by the participant, namely bulk motion artefacts (i.e. head movements) and

physiological motion (i.e. cardiac pulsation). Whereas head movements can partially be corrected post-acquisition, pulsation artefacts cannot. To reduce the likelihood and amplitude of motion artefacts the participant has to be comfortable and the head should be padded appropriately during the acquisition. To decrease pulsation artefacts, sequences can be acquired gated to the cardiac cycle. Pulsation artefacts are mainly introduced by the systolic part of the cardiac cycle (Poncelet et al. 1992) and are most prominent in regions closely linked to the arterial and CSF system, for example, the periventricular regions. Diffusion measures will be explained later on in this chapter but it should be highlighted already that pulsation artefacts influence diffusion measures and various tensor indices: i) increase the apparent diffusivity (Turner et al. 1990) and ii) have detrimental effects on the trace (Pierpaoli et al. 2003), fractional anisotropy, fibre orientation, and tractography results (Jones & Pierpaoli 2005).

The second source of artefacts originates from the imaging equipment. For example, rapid alternation of strong gradient pulses induces so-called eddy currents in electrically conductive assemblies of the MRI scanner (Jones 2008; Le Bihan et al. 2006). These currents can originate in any conductive part of the scanner and are gradient amplitude and duration dependent. Eddy current-induced distortions can render the images contracted, dilated or overall shifted. In conventional contrasts these currents tend to self-cancel. Various pre-acquisition steps can be implemented to ameliorate interferences (i.e. self-shielded gradient coils etc.) but also in the processing stage correction methods are available. Eddy current distortions are slice-specific and can therefore be corrected on an individual basis; for example, by normalising the image to a reference such as the B_0 scan or discarding spurious, single images from the data set.

5.3   Advanced MR Imaging

5.3.1   Diffusion tensor imaging (DTI)

Simultaneously with Moseley's (1990) report on the advantages of DWI in acute stroke imaging in cats, it was noted that the properties of water diffusion depend on the underlying anatomical structure (Chenevert et al. 1990; Doran et al. 1990; Le Bihan 1995). For example, in the ventricles water can freely move in all directions; if however, the water molecules are constrained within axons diffusion is facilitated parallel to the axonal direction and hindered perpendicular to it (**Figure 32**). This property is referred to as anisotropic (restricted motion) and isotropic (equal motion)

diffusion and forms the basis of diffusion tensor imaging tractography that allows visualisation of white matter connections in the living human brain.
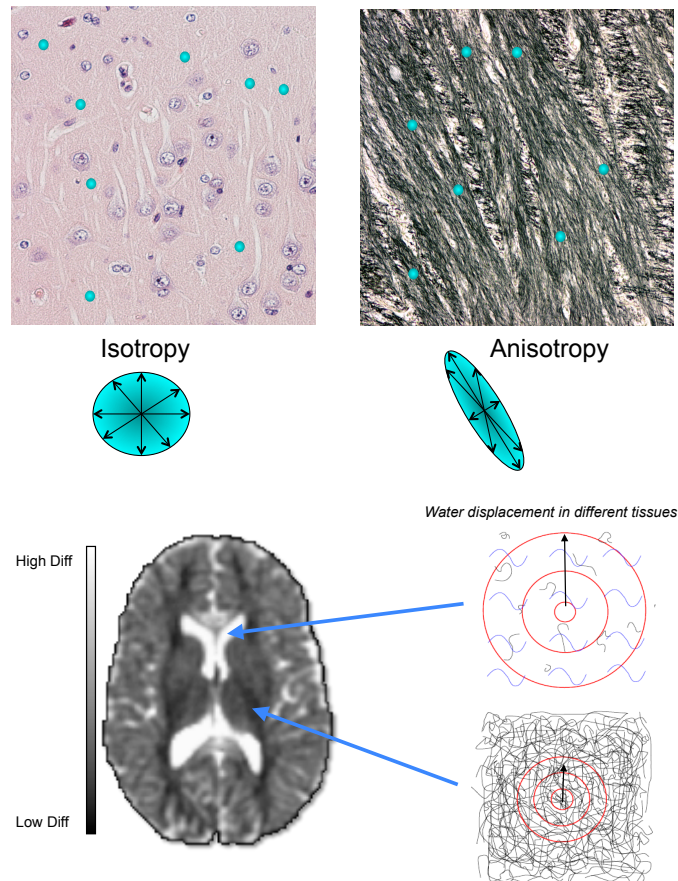
Figure 32   Concept of tissue-specific water diffusivity

The upper panel depicts water movement in an unconstrained tissue environment (isotropic diffusion) and in restrictive tissue (anisotropic diffusion) (courtesy of Dr. Bizzi). The lower panel exemplifies this principle on a brain image where the water displacement is high in the ventricles and low in brain tissue (courtesy of Dr. Alexander).

5.3.1.1 Diffusion tensor model

As previously described the ADC is orientation-dependent in a way that the more structurally anisotropic the tissue will be, the more the ADC will be dependent on the measured direction (Kontis et al. 2009). Here, for the first time, diffusion tensor imaging provides a 3D model of water diffusion that can also describe anisotropy. Within the diffusion tensor model it is assumed that the displacement of water is unequal along measured directions. Whereas diffusion of free water can be described as spherical (due to the equal displacement in all directions) the diffusion tensor is often described as ellipsoid (due to the unequal displacement) (**Figure 32** and **Figure 33**). This ellipsoid is defined through six parameters. Three mutually orthogonal eigenvalues, commonly denoted by λ_{1-3}, that define diffusivity along the

principal axes of the ellipsoid; whilst the orientation of the diffusion is defined by the eigenvectors, commonly denoted by v_{1-3} (**Figure 33**). The orientation of the tensor is parallel to the principal eigenvector (v_1) and the principal eigenvector is in turn associated with the largest eigenvalue (λ).

The tensor can be estimated from a series of DWI by linear regression (Basser & Le Bihan 1992) (**Figure 33**A). Given that the aforementioned six parameters (λ_{1-3}, v_{1-3}) define the tensor a minimum number of six DWI's and one non-DWI (b0) image are required to estimate the tensor; often in research studies more than 60 directions are applied. A detailed description of tensor estimation methods lies beyond the scope of this work and can be found in Jones (2009).
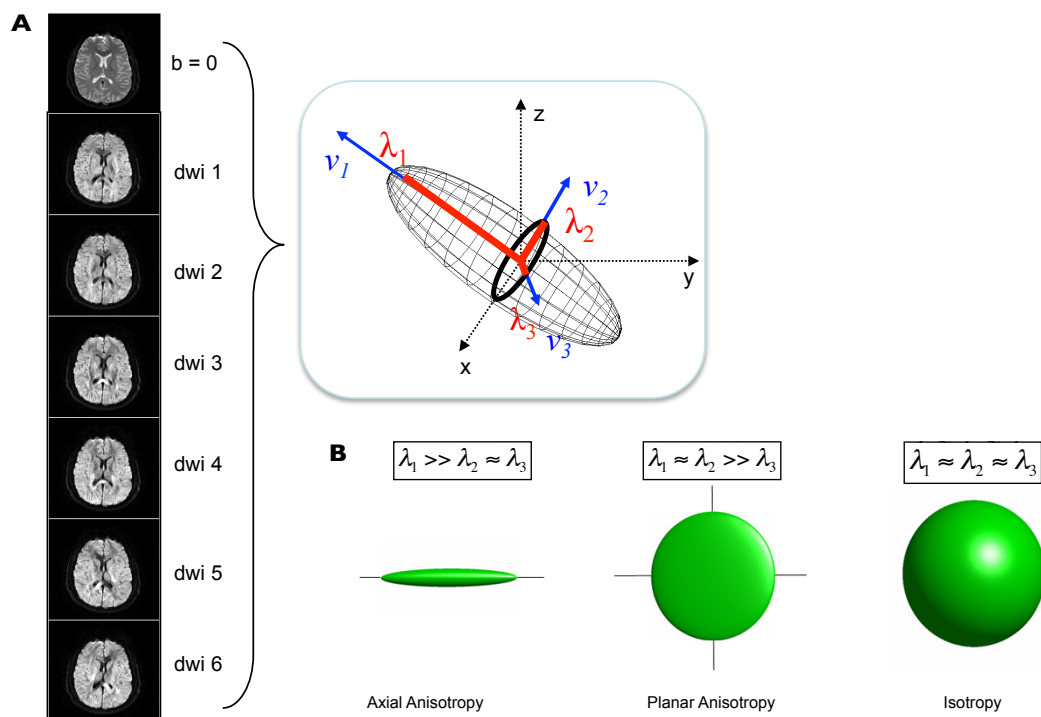
Figure 33   Tensorial ellipsoid and its relation to isotropy/ anisotropy

Dwi1 to dwi6 relates to a series of diffusion-weighted images (dwi) from which the tensor is estimated. v_{1-3} denotes eigenvectors, λ_{1-3} denotes eigenvalues, x,y,z denotes laboratory reference frame (Courtesy of Dr. Dell'Acqua).

5.3.1.2 Tensor-derived parameters

5.3.1.2.1 Trace or Mean diffusivity (MD)

The trace of the diffusion tensor is equal to the sum of the three eigenvalues ($\lambda_1+\lambda_2+\lambda_3$). The averaged trace can be considered as mean diffusivity (MD; **Figure 34**). In clinical studies (acquisitions with a b-value $\leq 1500\,\text{smm}^{-2}$) the MD was shown to be rather homogeneous throughout parenchyma (Jones 2009; Pierpaoli & Basser

1996). This reduces the distinctness of anatomical structures but does not confound the detection of diffusion abnormalities, such as an acute ischemic lesion (Lythgoe et al. 1997). MD is therefore a useful clinical surrogate measure of diffusion deficits.
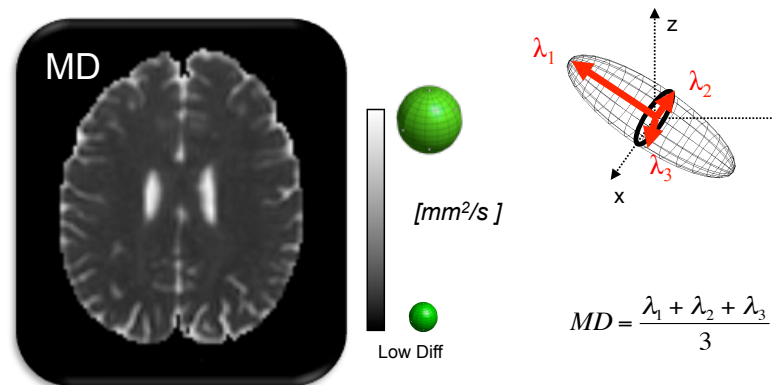
Figure 34   Average trace/ mean diffusivity

Trace and mean diffusivity (MD) with corresponding tensor and mathematical equation (courtesy of Dr. Dell'Acqua)

5.3.1.2.2 Diffusivity along ellipsoidal axes

The diffusivity measured along the principal axis (λ_1) is referred to as axial diffusivity (also called longitudinal or parallel diffusivity). The average of diffusivities along the two orthogonal axes (λ_2, λ_3) is denoted as radial diffusivity. The application of these measure is however still debated, as the direction and magnitude of the eigenvalue/eigenvector system relies on physical measures that are sensitive to noise, influenced by the estimated tensor ellipsoid and potentially by underlying pathologies (Wheeler-Kingshott & Cercignani 2009).

5.3.1.2.3 Fractional Anisotropy (FA)

Mathematically, the variance of all three eigenvectors (ν_{1-3}) about their mean is normalised by the overall magnitude of the tensor (Jones 2009). The resulting FA index represents the fraction of the tensor that can be attributed to anisotropic diffusion. The normalised FA value designates free diffusivity (i.e. unhindered isotropic) with the value 0; and constrained diffusion (i.e. anisotropic along one axis only) with the value 1.

On FA maps graded signal intensities represent these FA values, whereby grey matter and CSF (where diffusivity is relatively unrestricted, i.e. isotropic) appear dark, while white matter appears bright, and voxels with a high degree of parallel

structures, such as within the corpus callosum, appear the brightest (Jones 2008) (**Figure 35**).
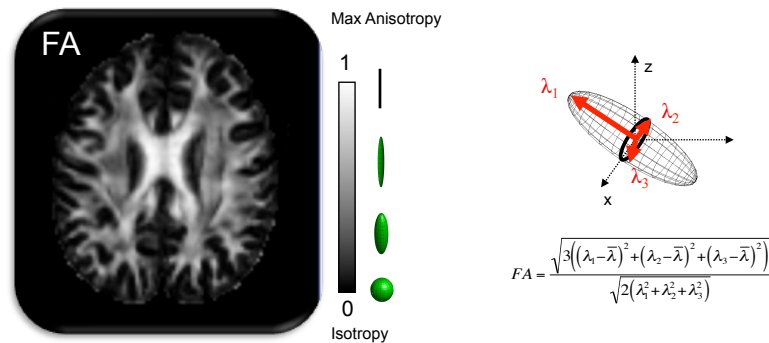
Figure 35   Fraction anisotropy (FA)

FA map with corresponding tensor and equation (courtesy of Dr. Dell'Acqua)

It has been noted above that it is possible to infer fibre orientation from DWI and ADC maps when the structures are predominantly aligned to the principle axes (x, y, z). These values are however dependent on the orientation. The direction of highest diffusivity, defined as the eigenvector associated with the largest eigenvalue, is on the other hand a robust measure for fibre orientation (Jones 2009). Based on this, colour-coded FA maps were developed where the orientation of fibres along the three axes is represented by three colours (Pajevic & Pierpaoli 1999). Within this scheme interhemispheric connections (i.e. commissures) are denoted in red, ipsilateral longitudinal connections (i.e. associations) are represented in green, and ascending/descending connections (i.e. projections) are shown in blue (**Figure 36**). These maps are thus sometimes referred to as red-green-blue (RGB) maps.

$$(R,G,B) = FA(|v_{1x}|, |v_{1y}|, |v_{1z}|)$$
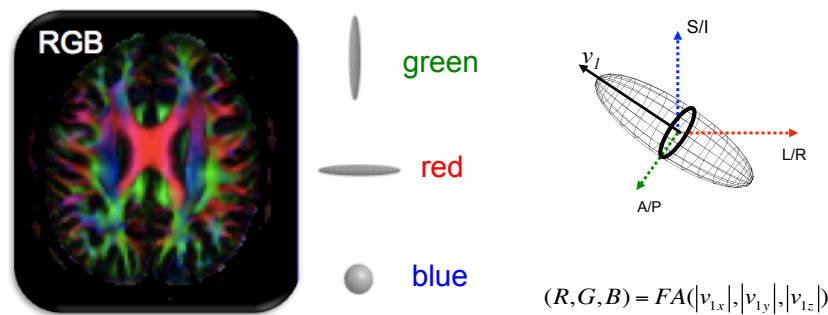
Figure 36   Red-Green-Blue (RGB) colour-coded FA map

RGB colour-coded FA map with corresponding tensor and equation (courtesy of Dr. Dell'Acqua)

Table 10   Commonly used diffusion-derived measures. From (Ciccarelli et al. 2008).

	Explanation
Tract volume	The volume of the tractography-derived tract (mm³ or cm³)
Fractional anisotropy (FA)	A measure of the deviation from isotropy that shows the degree to which the diffusion tensor is "anisotropic". High FA is found in the brain regions that contain white matter fibres because the water molecules move more easily parallel to the fibres
Mean diffusivity (MD)	The mean molecular motion, independent of tissue directionality
Parallel diffusivity	Diffusivity parallel to the axonal fibres (axial diffusivity)
Radial diffusivity	The diffusivity perpendicular to the axonal fibres, which is calculated from the mean magnitude of diffusion along two perpendicular directions that are orthogonal to the overall maximum diffusion direction
Voxel-based connectivity	An index provided by the probabilistic tractography algorithms at each single voxel that indicates the probability of a connection to the starting point

5.3.2   Diffusion Tensor Imaging (DTI) Tractography

Two classes of algorithms are available for tractography, namely deterministic and probabilistic. Deterministic tracking approaches of streamline propagation can be initiated at multiple starting points, usually at obligatory passages sometime referred to as 'bottleneck' passages. The tensor within each voxel is then estimated and the streamlines are pieced together voxel by voxel based on the principal direction within each voxel (Conturo et al. 1999; Mori & van Zijl 2002; Mori et al. 1999). Tracking is usually constrained by angle and fractional anisotropy thresholds (e.g., α=45°, FA ≥0.15); these parameters are set (often arbitrarily) to prevent streamlines turning back on themselves in successive tracking steps and to ensure that the principal eigenvector is well defined and the uncertainty in principal eigenvector is reduced (Jones 2008). Probabilistic tractography propagates various trajectories from a given starting point (or 'seed point') (Koch et al. 2002; Behrens, Woolrich, et al. 2003b), instead of a single trajectory as it uses deterministic tracking. This

results in a map visualising the probability that certain voxels are connected to the starting point (Kaden et al. 2007). Probabilistic tracking termination is also achieved through the restriction of angular deviation between successive propagation steps to avoid the tracts looping back onto themselves (Behrens, Johansen-Berg, et al. 2003a; Behrens, Woolrich, et al. 2003b).

The current study is based on the deterministic approach, which is discussed below.

Based on the local and discrete estimation of the main fibre orientation within one voxel, it is possible to apply algorithms that can follow the direction across voxels and unite them if certain prerequisites are sufficiently obeyed (such as no abrupt curvatures or a drop in FA; **Figure 37**). '*Originated in the late 1990s, the purpose of fibre tracking or 'tractography' is to infer the three-dimensional trajectory of anisotropic structures in tissue by piecing together discrete (voxel-based) estimates of the underlying continuous fibre orientation field*' p. 942, (Jones 2008). The underlying assumption is that the prevailing direction of diffusion (i.e. the eigenvector associated with the largest eigenvalue) within each voxel aligns with the principal fibre orientation (Basser et al. 1994). Based on this assumption the direction of maximal diffusion is propagated across adjacent voxels (**Figure 37**). Two subjective thresholds are used to constrain the tractography reconstruction of white matter pathways. If, for example, the angle would exceed a 45° angle the algorithm would stop the propagation at this voxel, as such a sharp curvature is assumed rather unlikely (angle threshold). A second threshold is defined based on FA values (0 isotropic, 1 anisotropic), the FA threshold will be usually set to 0.2, which limits the reconstruction to areas of high anisotropy. The propagation will terminate whenever FA values are reduced below the previously defined threshold. This FA reduction is likely to occur in regions of multi-fibre orientations and voxels of mixed tissues (i.e. grey and white matter boarder). The investigator decides upon these two thresholds during the preprocessing of the data and defines a step size for the propagation based on the resolution of the data.
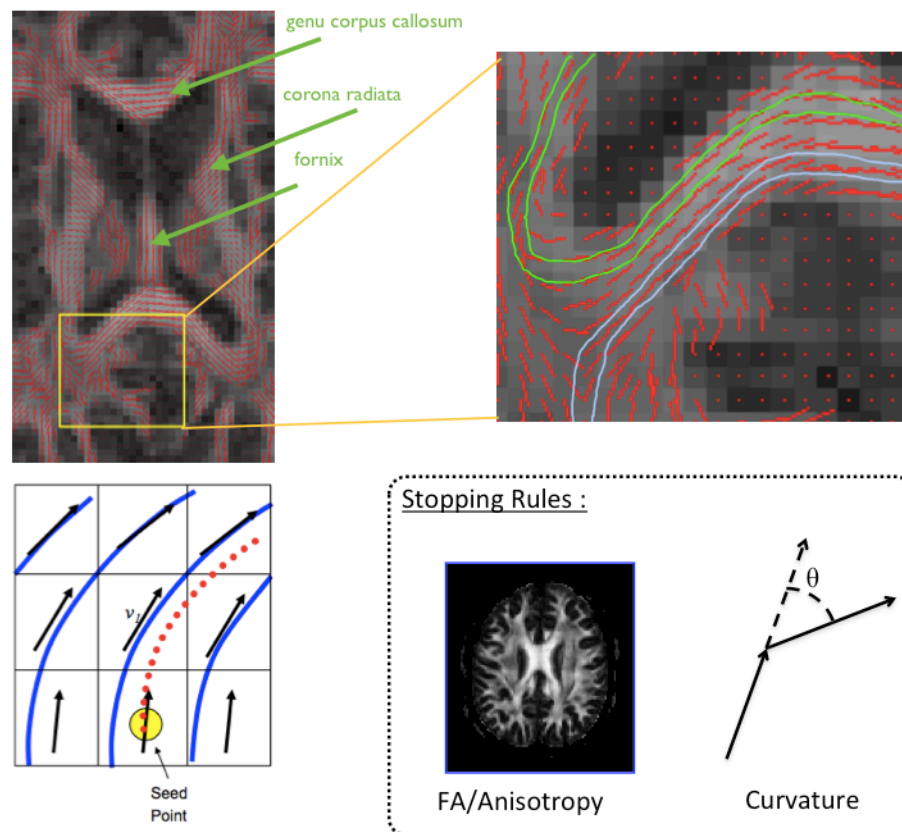
Figure 37   Voxelwise propagation and stopping rules

Voxelwise propagation underlying tractography and propagation stopping rules (i.e. FA and angular threshold)

Using deterministic tracking software, virtual in vivo dissections of white matter pathways can be achieved, whereby one or multiple regions of interest (ROIs) are selected and streamlines passing through these regions are visualised. When multiple regions of interest are used (as is the case for most white matter pathways) streamlines are visualised that obey Boolean logic filtering; meaning that the use of multiple ROIs allows for the following combinations: i) streamlines passing simultaneously through ROI1 and ROI2 are visualised (A+B), ii) streamlines passing through ROI1 and not through ROI2 are visualised (A-B), or iii) streamlines passing through ROI1 and ROI2 but not ROI3 are visualised (A+B-C) (Conturo et al. 1999; Catani et al. 2002; Wakana et al. 2004; Mori & van Zijl 2002; Catani & Thiebaut de Schotten 2008) (**Figure 38**).

It is important to emphasise at this point that the reconstructions are a visualisation of the water diffusivity direction and not axonal structures per se.
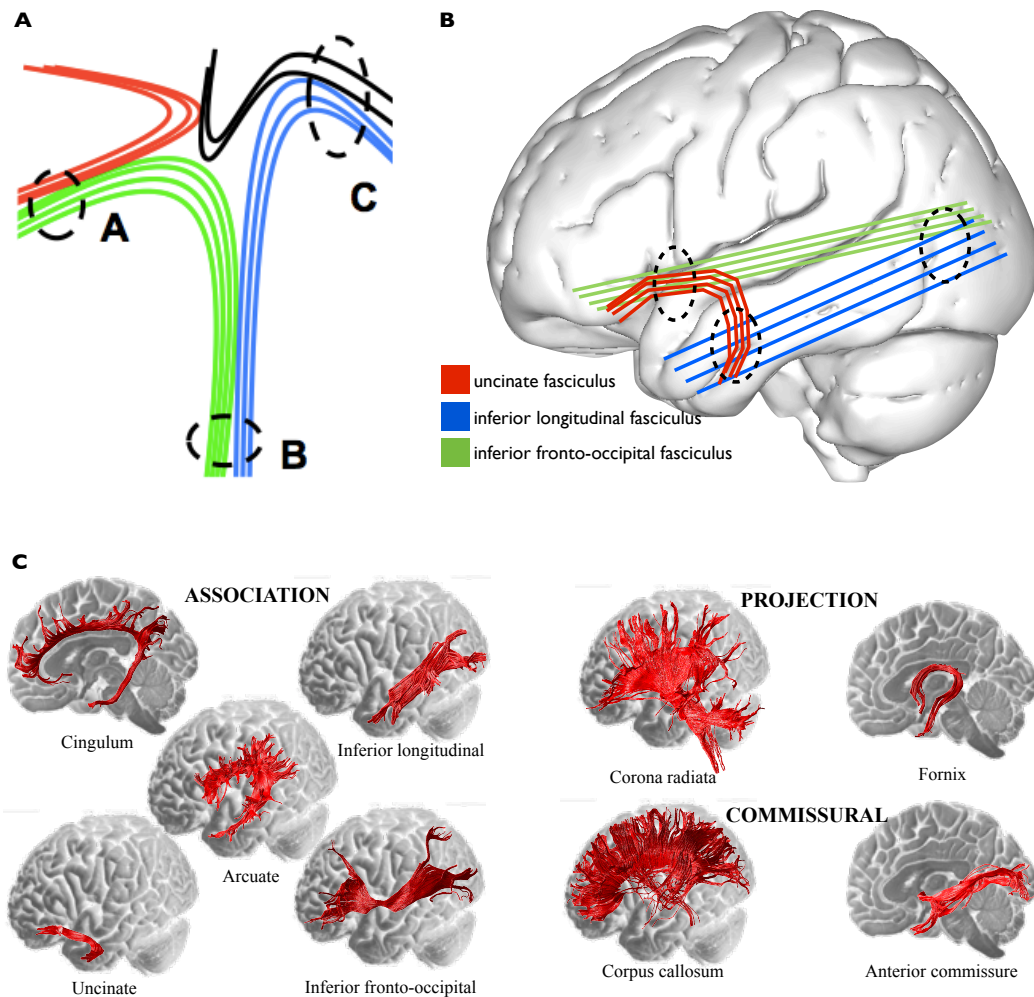
Figure 38   Boolean logic and Boolean logic filtering

Panel **A** depicts schematically the concept of Boolean logic. Taken from (Catani et al. 2002). **B** Application of Boolean logic in the brain, exemplified with the ventral network pathways. **C** depicts all major white matter pathways in the human that can be dissected applying Boolean logic filtering from (Catani & ffytche 2005).

5.3.3   Limitations of the tensor model

The deterministic approach, as the name implies, is a more rigid and conservative approach to tractography than the probabilistic approach. Deterministic tracking only produces one tract that is the most likely reconstruction, whereas probabilistic tracing visualises all possible propagations starting from a ROI. Hence, deterministic tractography does not provide a margin of certainty, even though uncertainty is associated with each estimate of the principal eigenvector (v_1) (Jones 2003). This is most relevant for areas of multi-fibre orientation, grey matter, and CSF (Jones 2003; Jones 2008; Mori & van Zijl 2002). Furthermore, because ε_2 and ε_3 are constrained to the plane orthogonal to λ_1 and the principal eigenvector (v_1) is

parallel to the fibre orientation the tensor model cannot provide information about the orientation of additional fibres within a voxel. This makes tractography based on the tensor model prone to artefactual reconstructions that are mainly due to the inability to separate crossing fibres, which in turn can generate false positives (i.e. non-existent tracts) and false negatives (i.e. absence of truly existing tracts) (Dell'Acqua & Catani 2012). Diffusion-derived measures, such as FA, are dependent on the SNR and become increasingly overestimated with lower SNR (Pierpaoli et al. 1996). FA, the main surrogate measure of tract integrity used in the literature, is however voxel-specific rather than tract-specific. FA reductions within a voxel can result from multi-fibre crossing, touching, or 'kissing' and from partial volume effects. This necessitates advanced algorithms or the consideration of novel diffusion models (Dell'Acqua & Catani 2012; Jones 2010). Multi-fibre orientation models, such as spherical deconvolution, can overcome some of these limitations (as discussed below).

5.3.4 Spherical deconvolution (SD)

Recently, the development of spherical deconvolution provided an algorithm that resolves multiple fibre orientations within voxels, where DTI classically choses the average direction of a voxel (**Figure 39**). This algorithm is based on the postulation that the signal obtained from different white matter structures can be translated into a three-dimensional signal profile (Dell'Acqua et al. 2012). The multipeak shape of the spherical function provides the number of distinct fibre orientations within a voxel, the fibre orientation, and weight of each fibre component. This method is therefore useful to resolve multifibre orientations in complex white matter regions that typically occur in complex organisms.
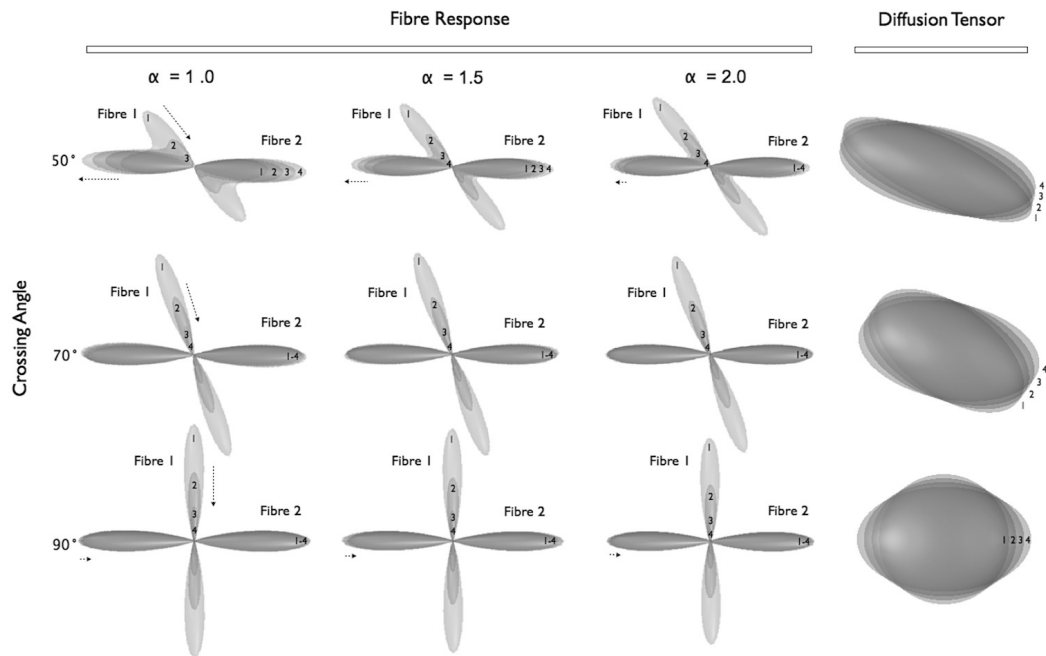
Figure 39   Simulation results from SD and DTI algorithms

This figures demonstrates the reconstruction of two crossing fibres at different crossing angles (50°, 70°, and 90°) using spherical deconvolution (SD, here shown under fibre response) and Diffusion tensor imaging (DTI). Taken from (Dell'Acqua et al. 2012)

In conclusion, magnetic resonance imaging enables the non-invasive in vivo study of neuronal tissue in both health and pathology. Various MRI techniques have been developed and/or improved in recent years (e.g., in terms of field strength and the use of rapid imaging techniques together with improved signal-to-noise ratios that can provide high contrast differentiation between tissue types). Also, recent advances in physiological contrast, such as diffusion and perfusion-weighted imaging, have paved the way to studying the living human brain.

5.4   Stroke-specific neuroimaging

CT scanning is the so-called 'gold standard' for acute stroke assessments due to its availability and the possibility to scan patients regardless of the presence of ferromagnetic devices or implants. Even though CT brain scans are still common as a primary imaging source to establish the presence of cerebral haemorrhage prior to thrombolysis treatments, the use of MRI for diagnostic purposes and management of acute stroke is rapidly growing. This is due to the proportion of negative CT scans during the early evaluation of ischemia, the superior sensitivity of MRI in the detection of lacunar strokes, and the ability to obtain various imaging

contrasts simultaneously. The disadvantages of MR imaging compared to CT scanning are: i) decreased availability, ii) higher costs, iii) longer scanning times, and iv) contraindications, which limit its utility in some patients (e.g. those patients with metallic implants, claustrophobia, and/or marked obesity cannot be scanned). The advantages on the other hand are: i) higher image resolution, ii) rapid detection of ischemic changes (in the order of minutes), and the iii) availability of multi-contrast acquisitions (e.g., DWI and PWI) as previously discussed.

As noted above (please see Chapter 4), the ischemic cascade results in the breakdown of the cellular membrane integrity. Within the core region of the infarct, the critically reduced blood flow leads to the failure of the Na^+/K^+ pump and a subsequent increased influx of sodium (anoxic depolarisation) that results in the loss of ion homeostasis and promotes intracellular water accumulation (cytotoxic oedema) (Srinivasan et al. 2006). Subsequently, the blood-brain-barrier becomes increasingly compromised and this results in an efflux of serum proteins and intravascular water from endothelial cells into the extracellular space –which in turn-lead to vasogenic oedema (Kahle et al. 2009). Intracellular water accumulation is therefore considered a surrogate marker of impending cell death. The swelling of the infarct is usually at its maximum within 3-5 days post stroke, and gradually subsides over the course of the following two weeks. The accumulation and confinement of water within the intracellular space results in restricted water diffusion. Diffusion-weighted imaging is highly sensitive to the diffusion of water molecules and can therefore detect intracellular accumulation of water within minutes. This diffusion slowing (i.e. cytotoxic oedema) results in a hyperintense signal (i.e. bright) on the DW image. Within the penumbral region, the blood flow restriction has not yet reached critical levels to sufficiently impede performance of the Na^+/K^+ pump. The diffusion-weighted signal of the penumbra is therefore usually normal. However, the penumbra can be estimated and visualised with perfusion-weighted (PW) methods (e.g., ASL, PET, perfusion CT) and then it can be overlaid on the diffusion-based ADC maps. The mismatch between diffusion and perfusion imaging contrasts is seen as an MRI marker of the penumbra. However, only a handful of studies have investigated the relationship between penumbra and aphasia recovery (please see section 5.5 below for full details). In brief, acute stroke lesion volume (as measured with diffusion-weighted imaging) is associated with subsequent clinical stroke severity as assessed using the NIHSS (Lövblad et al. 1997). Further, some have reported that clinical recovery can be predicted by

combining clinical factors (such as stroke severity and delay between symptom onset and treatment time), with diffusion-weighted parameters (Baird et al. 2001).

5.4.1   Dynamic MRI signal changes in stroke (pseudonormalisation)

Ischemic changes influence the signal contrasts (as described above). Given the dynamic nature of the ischemic cascade, the obtained image signals are variable over time (see **Figure 40**). On T2-weighted images the ischemic damage is best appreciated after 12-24 hours of symptoms onset, when the infarcted area becomes hyperintense. After a variable period - ranging from one to four weeks - the signal attenuation reduces. The DWI signal meanwhile increases in the hyper acute and acute stages with maximal signal changes within the first post-ictal week. The elevated DWI signal reduces after approximately three weeks. The ADC signal decreases immediately post-ictal with its nadir within 24 hours (Moseley et al. 1990; Pierpaoli et al. 1996; Pierpaoli & Basser 1996). This drop is related to the shift of extracellular to intracellular water accumulation (Warach et al. 1992; Moseley et al. 1990; Siesjö 2008). Hereafter the signal stabilises for 3-5 days and then progressively increases to become elevated in the chronic stage (Albers 1998). This signal progression has also been related to the cascade of underlying histopathological changes (vasogenic edema, loss of cell membrane integrity, gliosis, cell death) (Welch et al. 1995). Due to the temporary coexistence of cytotoxic edema (decreased diffusion) and vasogenic edema (increased diffusion) the ADC signal will appear normal within 1-4 weeks after onset before the signal chronically elevates (Bodini & Ciccarelli 2009). This period is referred to as pseudonormalisation as the imaged tissue is damaged whilst being characterised by a normal appearing ADC. During this period the lesion appears hyperintense on DWI (owing to the T2 component on the DWI), isointense on ADC, and elevated on T2-weighted imaging (Copen et al. 2001). The progressive ADC signal elevation thereafter mirrors the accumulation of extracellular water, tissue cavitation, and gliosis. Further, not only total lesion size follows specific temporal path - sub compartments also do this. This implies that the lesion tissue is heterogeneous (Warach et al. 1997) and that different ADC intensities indicate different temporal stages of tissue evolution towards infarction (González et al. 1999).

The time window of pseudonormalisation of the ADC signal can occur as early as two days post onset in patients treated with thrombolysis (Marks et al. 1999). The ADC progression is also related to patient age and lesion aetiology (Copen et al. 2001). In this study by Copen et al., ADC transition in signal intensity seemed to

increase earlier in the older patients and in nonlacunar strokes. These results suggest the possibility that for younger and lacunar stroke patients the therapeutic window might increase.
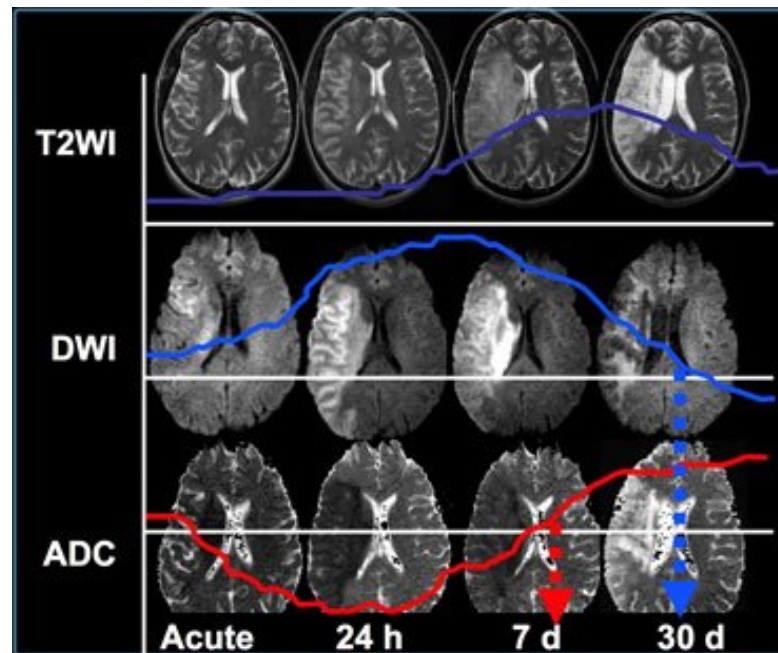
Figure 40   Pseudonormalisation of imaging signals

Pseudonormalisation of imaging contrasts. T2-weighted imaging (T2WI) detects ischemic damage the earliest after 12-24 hours post onset, the signal then increases and stabilises again after a period of about 30 days. Diffusion-weighted imaging is highly sensitive to early changes in stroke and lesions can be appreciated as hyperintense signal alterations within minutes after onset. The signal intensity reduces over time. The apparent diffusion coefficient (ADC) drops within minutes of onset and reaches its nadir within 24 hours. Thereafter the signal increases. Modified from (Lansberg et al. 2001; Wu et al. 2011).

Due to the time-locked progression of the ADC signal it is possible to estimate the infarct age. A similar effect can be seen on CT scans. Within two to three weeks post onset the so-called 'fogging-effect' occurs whereby the hypodense infarct gradually (but only temporarily) increases in density and sometimes becomes isodense before eventually becoming hypodense again (Becker et al. 1979; Chalela & Kasner 2000). Knowledge of these effects is pivotal for the aging of an infarct and for the correct interpretation of the imaging results.

5.5   Neuroimaging in aphasia

Neuroimaging has helped the field of aphasia leap beyond the classical clinico-anatomical observations (Catani, Dell'Acqua, Bizzi, et al. 2012a). Perfusion and diffusion weighted contrasts, as well as diffusion tensor tractography, have provided new insights into the anatomy and recovery from aphasia. However, especially for the realm of language, and in our case aphasia research, the best method has to be chosen for the purpose of investigation. **Table 11** details the commonly used imaging methods in language research whilst highlighting their strengths and weaknesses.

Table 11   Imaging methods utilised in language research including their advantages and disadvantages. From (Stemmer & Whitaker 2008)

Technique	Method and/or measures	Spatial/temporal resolution	Invasiveness/ discomfort to subject	Loudness	Availability	Monitary cost	Unique advantages	Unique disadvantages
EEG, ERP	Bioelectric activity (fluctuating voltage changes detected at scalp)	Centimeters/ milliseconds	Non-invasive/very little (more tolerant to movement than, e.g., fMRI)	None	High	Low	Good temporal resolution, ready availability, ease of recording	Low spatial resolution
fMRI	Relative change in deoxyhemoglobin; blood-oxygen-level-dependent (BOLD) effect	Millimeters/1–5 s	Non-invasive/moderate: strict movement restrictions, narrow quarters	Very high	Limited	High	Good spatial resolution	High magnetic field; loud; low temporal resolution
DTI	Application of specific radiofrequency and magnetic field-gradient pulses to track the movement of water molecules in the brain	Millimetres/–	Non-invasive/moderate: strict movement restrictions, narrow quarters	High	Limited	High	Good spatial resolution	Loud; movement restrictions
PET	Intravenously injected radioactive tracer; perfusion; glucose metabolism; oxygen utilization	Millimeters/about 90 s	Invasive (radioactive tracer)/moderate: no head movement, narrow quarters	None	Very limited	Very high	Ability to measure brain metabolism + pharmacodynamics	Poor temporal resolution; exposure to radioactivity; limited to short tasks
MEG/MSI	Biomagnetic activity (magnetic fields measured by superconductive detectors and amplifiers at scalp)	Millimeters at cortex (less precise for deep sources)/ milliseconds	Non-invasive/little: strict movement restriction	None	Extremely limited	Very high	Excellent temporal and good cortical spatial resolution	Detects only dipoles oriented tangentially to the skull but not radially
rTMS	Application of rapidly changing magnetic fields to specific areas of the brain leading to excitation or inhibition of neuronal cells	Centimeters/–	Invasive (application of magnetic stimulus)/ moderate to high (possible headache)	Low	Limited	Low	Ability to induce "virtual, temporary lesions"	Possible headache; in very rare cases epileptic seizure
NIRS (optical imaging)	Changes in the brain's oxygen absorption based on optical properties of hemoglobin; concentration of deoxyhemoglobin, oxyhemoglobin, total hemoglobin	Millimeters/ milliseconds	Non-invasive/very little (more tolerant to movement than fMRI)	None	Limited	Low	Low costs combined with excellent temporal and very good spatial resolution; tolerant to movement	Limited depth penetration (maximum of about 5 cm)
ES (ESM)	Application of electrical current directly to the surface of the brain. Induces a local temporary "lesion" that disrupts normal function	Millimeters/ milliseconds	Very invasive: brain penetration	None	Extremely limited	High (surgery costs; technique itself low cost)	"Gold standard" of spatial and temporal resolution	Brain bleeding, infection

DTI: diffusion tensor imaging; EEG: electroencephalography; ERP: event-related potentials; ES: electrocortical stimulation; ESM: electrocortical stimulation mapping; fMRI: functional magnetic resonance imaging; MEG: magnetoencephalography; MSI: magnetic source imaging; NIRS: near-infrared spectroscopy (also referred to as optical imaging); PET: positron emission tomography; rTMS: repetitive transcranial magnetic stimulation.

Perfusion studies have indicated that lesion size is not the pivotal contributor but rather the extent of hypoperfusion (i.e. penumbra), which explained the fluctuations in language proficiencies in acute aphasia. The penumbral extent and its relation to aphasia was investigated in detail by Hillis et al. (2006) who demonstrated that post stroke naming deficits improved with reperfusion. In addition to the 'classical areas', this study emphasised the importance of reperfusion of the left midfusiform gyral region (BA37) that was consistently shown to be hypoperfused in patients with naming deficits. The relevance of reperfusion to post stroke language recovery were previously shown with MR-based imaging (Fridriksson et al. 2002) and PET imaging (Cappa et al. 1997). The extent of hypoperfusion was further identified as a better predictor of neurological severity post stroke than lesion size (Barber et al. 1998; Beaulieu et al. 1999; Chalela et al. 2000). Ochfeld et al. (2010) further showed that the time of assessment is relevant as hypoperfusion and infarction of BA44/45 is associated with Broca aphasia in the acute stages but less so in chronic stages. The author related this finding to connectional rearrangements and cognitive mechanisms to cope with the functional loss.

In the first week following a stroke, however, the fluctuations in language abilities and between syndrome classifications as well as spontaneous recovery have been related to the restoration of blood flow to hypoperfused areas. For instance Hillis et al. (2002) examined the reperfusion of ten Brodmann areas (10, 18-20, 22, 37-40, 44, 45) with both PWI and DWI. They found that reperfusion of area BA22, i.e. the classical Wernicke's area, is most commonly associated regaining the capacity to understand spoken language. Also Croquelois et al. (2003) used perfusion CT and DWI and focussed on the three frontal gyri, the superior and middle temporal gyri, basal ganglia and inferior parietal lobe as well as the insular and external capsule region. The authors showed that if penumbral tissue within these regions evolves into infarction aphasia scores deteriorated whereas if penumbral tissue was reperfused the aphasia scores improved for repetition, spontaneous speech, and comprehension. These studies highlight the importance of early reperfusion of stroke damaged cortical areas for long term language recovery.

Nonetheless, the relevance of subcortical structures and connections between language-relevant cortical areas were also thought to be likewise important. Only in recent years, the 19th century hypothesis of the connectional anatomy of language could be investigated using Diffusion tensor imaging (DTI) tractography. DTI allows non-invasive in vivo investigations of anatomical connections between identified language areas. The first acute aphasia group comparison study by Breier et al.

(2008) investigated the three surrogate pathways of language (superior longitudinal fasciculus (SLF), arcuate fasciculus (AF) and uncinate fasciculus) in 20 patients assessed at least one month post stroke (mean 22 months±24 months, range 1–72 months). The arcuate is considered a subcomponent of the SLF in this study and whenever the authors refer to it they mean the vertical segment (i.e. the connection between Geschwind's and Wernicke's territory). The authors reported reduced FA in the superior longitudinal and arcuate fasciculi. When correlated with the Western Aphasia Battery the SLF was associated with repetition deficits only, whereas the arcuate was associated with repetition and comprehension deficits. Repetition deficits were associated with the SLF and AF regardless of the damage to cortical areas; however, comprehension was not independent of cortical damage to the superior temporal gyrus. No correlations were found for the uncinate fasciculus. These findings are in line with the 19th century hypothesis that damage to the arcuate fasciculus will manifest in conduction aphasia, marked by intact expression and reception of language with poor repetition as the conduction between the receptive and the expressive areas is interrupted.

Hosomi et al. (2009) retrospectively reported on 13 stroke patients assessed within two days of admission. The authors did not replicate FA differences between a control group, non-aphasic stroke patients and aphasic patients. In contrast, the authors found reduced volume of the left arcuate, which was the strongest predictor for the presence of aphasia at the time of discharge. Another study investigated the lesion load of the arcuate as predictor by using an atlas approach (Marchina et al. 2011). Lesion maps of chronic aphasics (≥11 months post onset) were tested against atlas-based percentage overlay maps. The authors showed that the amount of damage to the arcuate fasciculus is a good predictor of articulation impairments (rate of speech, content). Lesion sizes as well as the ventral pathways were shown not to be predictive.

In brief, these studies used various indices to identify the role of white matter pathways for language and/or language impairment after stroke. The consensus from these studies is that the arcuate fasciculus has been consistently shown to be relevant for intact language and likewise, damage to the arcuate was shown to be associated with language impairment. Further, no other pathway in the left hemisphere has yielded similar results (e.g., uncinate fasciculus).

Whilst these studies agree on the importance of the arcuate fasciculus for language in stroke, methodological limitations within each study as well as differences

between these studies have to be considered. These aspects shall be discussed later (see Chapter 12).

In conclusion, neuroimaging is contributing to our understanding of post stroke neuronal changes and functional recovery. Structural and functional imaging (i.e. T1/T2/FLAIR and fMRI) have already corroborated a wealth of studies that generated informative but not yet conclusive evidence towards the recovery of aphasia. The newly developed physiological imaging (i.e. perfusion and diffusion weighted) has opened up the field for novel investigations and a fostered understanding of recovery. Only a handful of studies are yet available that implement these techniques in aphasiology.

CHAPTER 6   METHODS

'Truth in science can be defined as the working hypothesis best
suited to open the way to the next better one.'

(Konrad Lorenz)

This chapter provides a point of reference for the reader to the specific objectives of the study, a description of the patients studied and the materials and methodologies used as well as an introduction to the statistical rational.

6.1   Aims

The principle aim of this study was to use diffusion tensor imaging (DTI) tractography in hyperacute stroke patients to investigate the underlying a priori white matter anatomy. DTI allows examination of the arcuate fasciculus, connecting frontal and temporal language areas, as well as the degree of lateralisation of this tract. In stroke imaging however the left hemisphere measures are altered due to the ischemic changes and hence no laterality will be calculated here in relation to DTI measures. Moreover, the influence of the presence of the arcuate on the right hemisphere in relation to language task performances was primarily investigated in this study. This research was complemented by the study of perfusion changes in the acute and chronic stages with a non-invasive MR-based method, called arterial spin labelling.

6.2   Objectives

The specific objectives of this thesis will be divided into categories based on the methods used to investigate the question.

General hypotheses (H):

H1: Classical anatomical and demographical factors (e.g., lesion factors and patient-specific factors) are independent predictors of baseline and longitudinal aphasia severity.

Methods: A prediction includes the directionality between variables and hence a regression model is necessary to investigate this hypothesis. Classical predictors will be added as independent variables and aphasia severity at baseline and six months after symptom onset will be defined as dependent variables. This method allows teasing apart the individual contribution of these factors towards aphasia severity within the model.

H2: Clinically, patients who received thrombolysis seem to recover their language functions better and within a shorter time interval compared to non-thrombolysed patients. Hence, the hypothesis is that thrombolysed patients recover better.

Methods: Limited literature is available on thrombolysis and aphasia recovery trajectories. It has however been reported that aphasic patients are more likely to receive thrombolysis treatment (Engelter et al. 2006). The information if the treatment was administered will be obtained from the clinical notes and be coded binary (thrombolysis given vs. not given). An independent t-test will be performed to identify the mean differences between the two patient groups. Given that this is a preliminary study and this hypothesis emerged after the study commenced, the groups are not balanced and no *a priori* power calculations were conducted. However, given the high number of thrombolysed patients at King's College Hospital it was of interest to investigate the influence of treatment within our sample. To this end, we will conduct a power analysis to identify the strength of our results or, if applicable, define the number of patients needed for future studies to investigate this question further.

Lesion analysis hypotheses:

H3: Damage to cortical language areas, including the left inferior frontal and superior temporal gyrus, has been shown to be critical for language deficits. We therefore expect the maximum lesion overlay in our group to encroach on these regions.

Methods: Lesions will be delineated on each patient's native structural scan (T1-weighted) and will then be brought into a common reference space (MNI). From the normalised lesions binarised percentage lesion overlay maps will be calculated with an automated software package and manually in FSL.

H4: Based on the literature, one can assume that lesion locations will predict behavioural impairments as follows: lesions to the inferior frontal gyrus will be associated with altered fluency, lesions to the posterior temporal gyrus will be associated with comprehension deficits. In addition we expect that lesions along the

arcuate fasciculus will be associated with repetition deficits and extended lesions will be associated with an overall reduction in the aphasia quotient, reflecting a global impairment. We therefore expect a lesion-symptom analysis to map the deficits accordingly.

Methods: Two programmes are available to conduct lesion-symptom mapping, NPM within mricron (Rorden et al. 2007) and matlab-based VLSM (Bates et al. 2003). Both programmes follow a similar rationale but apply slightly different test statistics (for discussion see (Rorden et al. 2007; Medina et al. 2010). Inputs needed for either of these programmes are the lesion maps for each patient (obtained from the previous analysis) and the corresponding scores on the language assessment. The scaled composite section score for repetition and the subscore from the word fluency and word finding section will be employed in parallel with the global composite score of severity (Aphasia Quotient). In addition to this classical approach a new method will be implemented (recently described in (Thiebaut de Schotten, Tomaiuolo, et al. 2012b) whereby the lesion overlay maps are overlaid onto probability maps provided within a DTI atlas from healthy subjects (available from www.natbrainlab.com) to determine the degree of involvement of each segment of the arcuate fasciculus and other language-related tracts. These values will then be entered into a regression model to establish if the damage to a given tract is predictive of language deficits.

Tractography-based hypotheses (DTI with a supplementary SD approach):

H5: Given the presence of the lesion only on the left hemisphere we have different expectations for the ipsilateral and contralateral language regions. In the left hemisphere we intend to use tractography to quantify the damage to the language tracts by measuring tract-specific indices, whereas in the right hemisphere we expect tractography to show the intact anatomy of the three segments of the arcuate fasciculus.

Methods: Diffusion data will be pre-processed to reduce possible motion and equipment-induced artefacts to then obtain scalar maps (e.g., fractional anisotropy map). Whole brain tractography will be performed and the arcuate fasciculus will be virtually dissected in alignment with previous publications. A three regions of interest approach will be employed to obtain all three segments. For each segment tract-specific indices will be extracted (e.g. volume occupied by the streamlines, FA, MD, etc.). These measurements will be used to test the following hypothesis.

H6: Previous studies have implied that the lesion load to the arcuate fasciculus is predictive of language impairments (Marchina et al. 2011). We therefore expect to see a gradient of deficiency dependent on the degree of disconnection of the three segments.

Methods: A recently introduced method, called trackwise hodological lesion-deficit analysis (Thiebaut de Schotten, Tomaiuolo, et al. 2012b) will be employed. This method utilises a probabilistic tractography atlas as background for the individual lesions of each patient. When a patient's lesion overlapped on a voxel with a

probability above chance level (i.e. >50%) the tract is considered disconnected. The resulting values are then entered into a regression model with the aphasia quotient at baseline and follow-up as dependent variables.

H7: The direct connection between the inferior frontal gyrus and the superior temporal gyrus has traditionally been associated with repetition deficits. However, until recently this hypothesis was not testable due to the lack of methods for performing white matter dissections in stroke patients. Tractography can be used to investigate this aspect. Building on previous clinical and anatomical studies we expect to observe that damage to the long segment of the arcuate fasciculus, i.e. the direct connection between the superior temporal and inferior frontal gyri, is associated with repetition deficits.

Methods: Methodologically, the relation between repetition deficit and tractography indices will be investigated including the lesion load to the long segment of the arcuate fasciculus as possible predictor and the repetition scaled composite section scores of the WAB-R as dependent variable in a regression analysis. Whilst controlling for demographical variables, such as age and gender. This analysis will be run for the baseline and longitudinal repetition deficits.

H8: Based on previous literature it was shown that 60% of people are strongly left lateralised for the arcuate fasciculus, whereas 40% demonstrate streamlines in the right hemisphere. Likewise, it has been reported that about 30-40% of stroke patient will recover their language functions post stroke (please see introduction to thesis for details). The hypothesis is that those two groups might overlap and that recovery might be facilitated by the presence of a right hemisphere arcuate fasciculus. We therefore expect to observe patients with a larger volume of long segment streamlines within the right hemisphere to reach higher scores on the WAB-R after six months compared to patients with smaller long segments in the right hemisphere.

Methods: The main analysis will be a regression model including classical predictors and the volume of the arcuate fasciculus as predictors of aphasia severity at baseline and longitudinally. To isolate the contribution of the volume of the long segment, the regression model will take into account demographical patient data (age, sex) and lesion factors (i.e. lesion size) at the first level. The second level will introduce the arcuate volume. This method will allow us to disentangle the change in significance, if any, that the long segment is accountable for. Where both models are significant the goodness of fit will be established using the Aikake Information criterion (AIC).

H9: During the course of the study we had the opportunity to re-scan some patients, which will allow for longitudinal comparison. Functional plasticity has been previously described in the literature alongside dynamic peak activation shifts post

stroke (Saur et al. 2006; Schaechter et al. 2006). Further, the literature has described Wallerian degeneration following stroke, which will lead to white matter degeneration. Anisotropy metrics, such as FA, are sensitive to Wallerian degeneration (Pierpaoli et al. 2001; Thomalla et al. 2004; Mukherjee 2005). A decrease in FA, which results from a decrease in the major eigenvalue and increase in the minor eigenvalues, can be detected within a fortnight of symptom onset (Thomalla et al., 2004). We therefore expect to see a reduction in FA within the three segments of the arcuate fasciculus at the second scanning time point compared to the acute scan.

Methods: Anisotropy and structural metrics will be extracted for all patients from both scanning session and will be compared across time using a paired t-test where the data is Gaussian and a Wilcoxon signed-rank test where this assumption is violated.

H10: This analysis is supplementary to the main aim of the study. There has been a growing body of literature that an extended language network is orchestrating various linguistic functions. According to the literature two pathways, besides the arcuate fasciculus, are especially relevant. These include the inferior fronto-occipital fasciculus (iFOF) as part of the "ventral stream" (Saur et al. 2008; Forkel et al. 2012) that is mainly implicated in semantic functions (Duffau et al. 2002). The other pathway is the Frontal Aslant Tract (FAT) that has been implicated in motor planning and speech initiation (Catani et al. 2012).

Methods: Given that both pathway systems (i.e., iFOF and FAT) are interwoven within dense fibre populations (i.e. the iFOF is merging with the uncinate anteriorly and the inferior longitudinal fasciculus posteriorly and the FAT is mingling with the three branches of the superior longitudinal fasciculus, the lateral projection of the corpus callosum and the cingulum) DTI is likely to provide only partial reconstructions of these pathways. Hence, a Spherical Deconvolution (SD) approach will be implemented for this part of the analysis. Given that SD is a non-tensorial model that is not restricted by the fractional anisotropy measures tracking within the left hemisphere should produce anatomically consistent reconstructions. To this end, it is also possible to calculate laterality indices and aim to replicate what has been shown previously in the literature in healthy brains. As above the FA and volume of these tracts will be obtained and entered into a correlation analysis with a) the overall aphasia severity and specific section scores of the WAB-R. For example, the iFOF measures were correlated with semantic fluency measures.

Perfusion-based hypotheses (pCASL approach):

H11: Considering that ischemic stroke causes an occlusion and hence reduced blood flow to cortical areas, it can be assumed that hypoperfusion will lead to functional deficits. We therefore expect to observe left hemispheric perfusion deficits, which are predictive of the overall aphasia severity.

Methods: Firstly, the native cerebral blood flow (CBF) maps and the structural T1-wighted images will manually set to their image origin (coordinate [0, 0, 0]) situated on the anterior commissure. Secondly, images will be segmented and normalised (unified segmentation). Thirdly, the perfusion map and the grey matter map of each patient will be co-registered in SPM. Rigid-body registration transformation parameters will be estimated for moving the ASL into alignment with the smoothed GM image, and subsequently applied to the ASL image. The resultant perfusion image will be normalised to standard (MNI) space using the normalisation parameters obtained during the unified segmentation process. In order to remove extracerebral signal, the normalised perfusion images will be masked using the SPM image calculator (ImCalc) (80% probability of being brain). Perfusion values will be extracted from the final images as the global perfusion mean across each hemisphere.

H12: Hilis et al., 2001 reported that hypoperfusion in critical language areas is predictive of language deficits. We therefore hypothesised that in our data hypoperfusion within language areas is also predictive of language impairments in a way that hypoperfusion within Broca's area will affect fluency and hypoperfusion within Wernicke's area will affect comprehension measurements.

Methods: Pre-processing of perfusion maps is identical to the above. To obtain the perfusion within each cortical language region the *Anatomy* toolbox will be used with predefined probability maps of each region. These ROIs will be applied to each hemisphere in each patient and the mean perfusion within each region will be extracted using the FSL tool fslstats to extract the mean for nonzero voxels. These measures are then correlated with the scaled composite section scores of the WAB-R.

6.3 Participants

Patients with left hemisphere stroke and language impairment were recruited from the hyper acute stroke unit (HASU) at King's College Hospital, London between 2009 and 2012. Patients were screened within three days of admission using the Western Aphasia Battery Bedside Screening (WAB-R). Inclusion criteria were: (1) right-handedness, (2) first ever infarct, (3) presence of aphasia, (4) no previous neurological or psychiatric history, (5) medically stable to tolerate ambulance transport, (6) no MRI contraindications and (7) native English speaker. Eligible patients underwent comprehensive language assessment within 10 days of symptom onset (mean 5±5 days) and MRI scanning within two weeks, except for two patients who were scanned at day 20 and 24 after admission[12] (overall mean 10±6 days). Six months after admission patients were re-invited for a language

---

[12] The medical status of these two patients excluded earlier assessments.

assessment (mean 200±55 days). One subject had to be excluded after full assessment and scan due to a later non-stroke diagnosis (acute disseminated encephalomyelitis). The patient was excluded from all analyses. None of the patients had died over the course of this study. Eighteen patients fulfilled the inclusion criteria and completed the baseline assessment (12 males; mean age 63±39 years; age range 28-87 years). Two patients (subject 14 and 16) did not attend the follow-up assessment thus sixteen patients completed the follow-up assessment (10 males; mean age 60±17 years; age range 28-87 years) (please see **Table 13** in Chapter 7). All patients or their next of kin gave written informed consent. The study was approved by the Wandsworth Research Ethical Committee (09/H0803/95) and the local research and development committee (KCH1700).

6.4   Study design

All patients were screened with the brief WAB-R bedside screening to assess suitability for this study. If deemed suitable, the complete WAB-R assessment was administered to the extent possible depending on the medical condition of the patient and the in-patient duration (hospital target is set at three days) together with an MRI scan at the earliest possibility.

Patients were followed-up after six months post onset and reassessed with the full language test. Some patients kindly made themselves available for a one year scan and a repeated language screening (**Figure 41**).
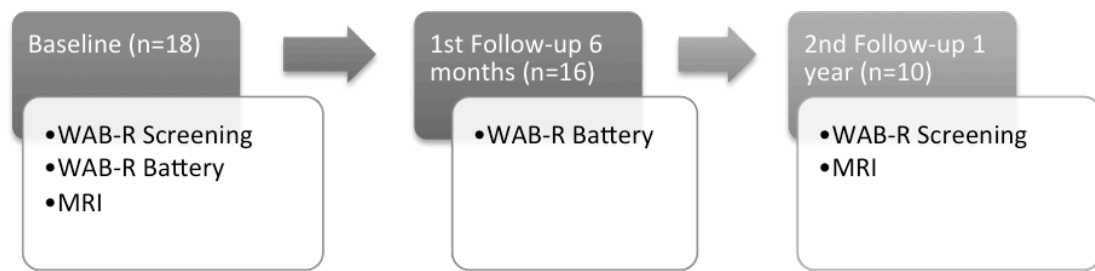
Figure 41   Study design

Western Aphasia Battery Revised (WAB-R) and received an MRI scan. 16 patients were reassessed for their language function after six months and 10 patients were rescanned and screened after one year.

6.5   Recruitment status and study impediments

Across London 131 HASU beds are available, allocated between eight London hospitals (London 2009). The numbers of HASUs and available beds fluctuated during the period of this study due to regular re-evaluations by the South London Cardiac and Stroke Network. For King's College Hospital the number of beds varied between 12-19 over the recruitment period. The recruitment from a HASU poses several logistical obstacles, which will be briefly mentioned with an account of how they were accommodated within the study (**Table 12**). The outlay of the local facilities necessitated ambulance transport for patients between the HASU and the MRI scanning facility. This delicate logistical chain caused delay and in some instances cancellations of scanner slots. During the course of this study the National Health Service (NHS) hospital allocation system changed (with effect on the 19th July 2010). This resulted in a patient influx to the HASU and resulted in higher demands for repatriation. The evolution of recruitment is plotted against the expected recruitment and screening efforts (**Figure 42**).

Table 12   Recruitment complications and implemented solutions.

Obstacle	Resulting problem(s)	Solution employed
Porter HASU - transport lounge	Delayed pick up of patients from the ward	Porter booked in advance and pick up time was confirmed again
Ambulance transport	- Booking 72 hours prior to transport required - Allocation of 3 hours slots for pick ups (for a 9am scan the patient had to be ready at 6am) - Delayed arrival which resulted in the need to cancel some scanning slots - Patients were erroneously left at the KCL radiology department regardless written instructions to the Centre for Neuroimaging Sciences - Pick up time after the scan was often 3 hours, which could mean the patient was occupied for a total of 7 hours with no guidelines on fluid restrictions or a possibility to rest. - Transport restricted to workdays and office hours, i.e. between 9am-4pm - Due to high transport demands the jobs were often delegated to subcontractors with no adequate clinical competency - Driving personnel ill trained to deal with patient's needs or drive not adequately for wheelchair transports (e.g., aphasic patients got shouted at for not giving directions).	I waited with the patients during the 3 hours slot and accompanied every return transport to provide directions to drivers to ensure that the patient feels comfortable and arrives at the correct location. I filed two complaints to the transport services regarding the inappropriate driving style, inability to follow written directions and the driver's rapport with the patients. All complaints were officially followed up but without further results.
Scanner availability	- Slots bookable according to transport availability, i.e. only workdays between 11-2pm - Need to obtain clinical notes to prove absence of ferromagnetic metal - Slots are usually booked/cancelled in advance which does not suit a hyper acute clinical study where it is not possible to plan patient availability	Late cancellation slots were booked were possible and 'slot sharing/swapping' with another study was attempted. For the medical history the next of kin and GP were engaged and relevant notes were faxed directly to radiographers where possible.
Patient mobility	Patient mobility was often restricted due to the presence of post stroke hemiparesis without personnel trained on safe patient mobilisation.	Future stroke studies should be equipped with a *Rotastand* for patients to independently move from the chair to the bed or have a dedicated trained person allocated to the project.
Repatriation	Patients are repatriated to their local hospitals within the target of three days. Unless ethical approval for the other hospitals were available the patient cannot be recruited back for further assessments (i.e. scanner slots were needed within three days)	Ethical approval was extended to further sites that were most commonly repatriated to. Future studies should attempt a comprehensive south London study approval within the stroke network (approval of each hospital is needed separately currently).

HASU, hyper acute stroke unit; KCL, King's College London
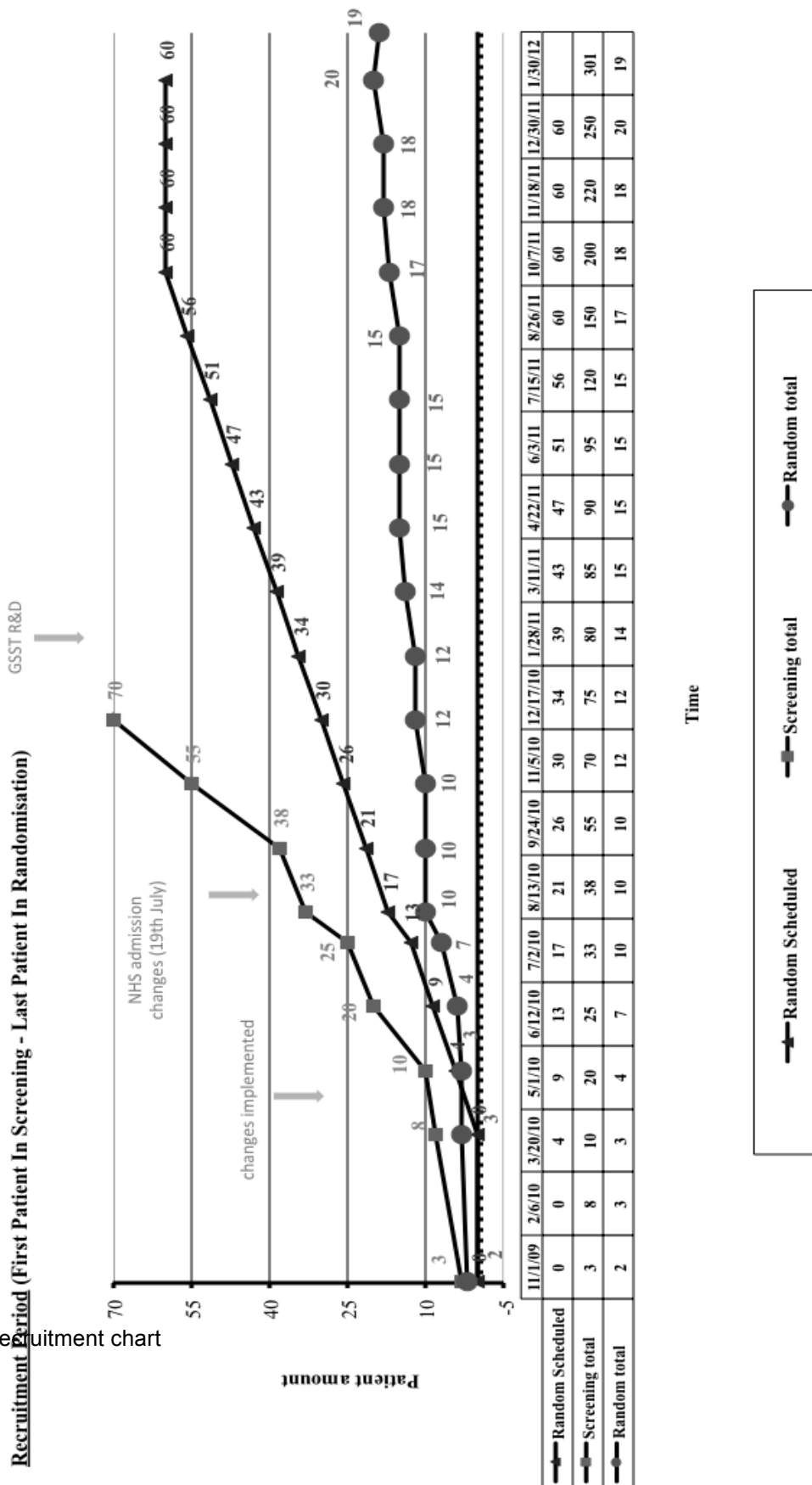
Figure 42   Patient recruitment chart

6.6   Data acquisition

6.6.1   Language assessment

Language function was assessed with the Western Aphasia Battery Revised (WAB-R) (Kertesz 2007). All patients were assessed with the WAB-R bedside screening (3.44±3.29 days, range 1-15 days), followed by a full examination with the comprehensive battery to the extent possible within the demands of a hyperacute ward (5.44±4.69 days, range 1-17 days). Assessments were regularly conducted in the presence of a speech and language therapist. At follow up (199.87±54.71 days, range 127- 229 days) patients were re-assessed with the same version of the battery. One year post stroke ten patients volunteered to be re-assessed with the WAB screening and re-scanned.

6.6.2   Neuroimaging acquisition protocol

6.6.2.1   Conventional structural imaging

The scanning protocol included the following structural scans: T2-weigthed images (36 slices, TE = 83 ms, TR = 5000 ms, slice thickness = 3 mm, matrix = 512x512x26, FOV = 24 cm, flip angle = 90 degrees), T2 Fluid Attenuate Inverse Recovery (T2-FLAIR) (36 slices, TE = 166 ms, TR = 10 sec, slice thickness = 5 mm, matrix = 320x320, FOV = 24 cm, flip angle = 90 degrees), and SPGR T1-weighted images (>100 slices, TE = 2.8 ms, TR = 7 ms, slice thickness = 1 mm, matrix = 256x256x196, FOV = 28 cm, flip angle = 20 degrees). These scans were subsequently used as reference images for classical lesion analysis or for co-registration purposes as described below.

6.6.2.2 Diffusion-weighted imaging (DWI)

Diffusion data was acquired using a High Angular Resolution Diffusion Imaging (HARDI) protocol optimised for subjects with high risk of movement during the scan. The total amount of acquired DWI data was twice that of the standard protocol to allow sufficient data to accommodate the presence of severe motion (standard: 32 directions + 4 b_0 scans, this protocol: 60 directions + 7 b_0). The 60 DW directions were then further randomly reordered as described in Cook et al. (2007) to distribute motion artefacts uniformly across the whole spherical sampling.

MRI-DWI data sets were acquired using single shot echo-planar imaging (EPI) on a 3T GE scanner (General Electric, Milwaukee, US) with a standard 8-channel head coil for signal reception. The acquisition was cardiac gated to avoid acquisition

along the systolic phase and hence reduce pulsation artefacts (Jones & Pierpaoli 2005). Diffusion-weighted axial slices were obtained using the following parameters:

Data was acquired with the following parameters: voxel size 2.4 x 2.4 x 2.4 mm, matrix = 128 x 128, field of view = 307 x 307 mm, 60 slices, 1 average, TE = 93.4 ms, b-value = 1500 s/mm^2, 60 diffusion-weighted directions and 7 non-diffusion-weighted volumes, using a spin-echo single-shot echo-planar imaging (EPI) sequence with an ASSET factor of 2. Peripheral gating was applied with an effective TR of 20/30 R-R interval.

This acquisition rendered the data compatible with different analyses such as standard diffusion tensor tractography (DTI) and Spherical Deconvolution tractography techniques (Dell'Acqua et al. 2010; Dell'Acqua et al. 2012).

After the first two data acquisitions it became apparent that acute stroke patients cannot tolerate the original DTI sequence of approximately 17 minutes. To make the scan more tolerable for the patients and to reduce subject movements the DTI sequence was split in two shorter scans of 33 directions (29 DWI + 4 b$_0$) and 34 directions (31 DWI+ 3 b$_0$). Here, the timings for the peripheral gating were fine tuned for the specific protocol thus reducing the total scan time to approximately 8.15 minutes and 8.32 minutes for each scan (detailed scanning time dependent on heart rates can be found in Appendix A. Cardiac Gating Protocol). Since the implementation of the split sequence, no major motion artefacts were detected upon visual inspection of the data in the FMRIB Software Library package (FSL, http://www.fmrib.ox.ac.uk/fsl/).

6.6.2.3 Arterial spin labelling (ASL)

To assess regional tissue perfusion, pseudo-continuous arterial spin labelling (pCASL) was acquired as described in Handley et al. (2013).

Image acquisition

A previously optimised perfusion acquisition (Howard et al., 2012) was employed for the current study with the following details: rCBF measurements were made using a pulsed-continuous arterial spin labelling technique (pCASL, Dai et al., 2008). Arterial blood was labelled using a train of Hanning radio frequency (RF) pulses of 500µs duration, with an inter-pulse gap of 1500µs and a total labelling duration of 1.5 seconds. A train of gradient pulses of similar duration and repetition rate (each followed by a refocusing lobe) accompanied the RF train to achieve flow-driven

adiabatic inversion. The maximum gradient amplitude under the Hanning pulses and the average gradient intensity over the RF train duration were 9mT/m and 1mT/m, respectively. These values satisfy the adiabatic condition for inversion and place the first aliased labelling plane away from the excitation bandwidth of the Hanning pulse (Dai et al., 2008). In the control phase, the sign of alternate Hanning pulses was reversed, and the amplitudes of the gradient pulses were adjusted so that the magnetization transfer effects of the pulse are compensated whilst achieving no net inversion of arterial spins.

After a post-labelling delay of 1.5s, the image was acquired with a 3D Fast Spin Echo (FSE) spiral multi-slice readout. This delay has been found to be appropriate to minimize vascular artefacts (Howard et al. 2011). To minimise blurring, the spiral acquisition was very short (4ms), and the required resolution was achieved with 8 spiral interleaves (TE 32ms/TR = 5500ms; ETL = 64). Images were acquired at a 48x64x60 matrix on an 18x24x18cm field of view and reconstructed to a 256^2 in plane matrix, resulting in a nominal spatial resolution of 1x1x3mm. Three pairs of tagged-untagged images were collected. Selective saturation of the image slab was applied at 4.3s before acquisition; selective inversion was applied 3s before acquisition with further non-selective inversions at 1.5s, 764ms, 334ms and 84ms before imaging. This repeated inversion achieved successful suppression of the background static tissue signal, thus maximizing the sensitivity to blood perfusion.

Following the three arterial spin labelling (ASL) control-label pair averages, images were acquired with the same imaging sequence but with inversion recovery preparation instead of ASL. One sequence with saturation of 4.3s and then an inversion at 1650ms before imaging was used to create a fluid suppressed image. A second sequence with saturation at 4.3s and then inversion at both 2408ms and 511ms was also acquired to create a fluid and white matter suppressed image. For both these sequences, the receiver gain was automatically lowered by 21 dB relative to the ASL sequence to avoid receiver saturation. These images were used to help quantify blood flow from the ASL as described below.

Flow Quantification

For quantification of flow, the sensitivity of the image was calibrated to water at each voxel (Alsop and Detre, 1996; Buxton et al. 1998; Williams et al. 1992). By means of a neighbourhood maximum algorithm to avoid regions with partial volume

of suppressed fluid, a low-resolution sensitivity map was created. This map was calibrated for water sensitivity by assuming the tissue was predominantly white matter with a water concentration of 0.735gm/ml (Herscovitch and Raichle, 1985) and a T1 of 900ms, and using the equations for inversion recovery signal attenuation. This calibration produced a sensitivity map (C) equal to the fully relaxed MRI signal intensity produced by one gm of water per ml of brain. With this co-registered sensitivity map (C), CBF was calculated at each voxel using the equation specified in Howard et al. 2012.

The whole ASL pulse sequence, including the acquisition of calibration images, was performed in 6:08 minutes.

6.7   Data pre-processing

A detailed pre-processing protocol, including the used terminal commands, is available as **Appendix D.** A conglomerate of software packages was employed for data processing analyses, including standard neuroimaging software, such as Statistical Parametric Mapping (SPM, http://www.fil.ion.ucl.ac.uk/spm/), FMRIB Software Library package (FSL, http://www.fmrib.ox.ac.uk/fsl/), MRICROn (http://www.mccauslandcenter.sc.edu/mricro/mricron/), ExploreDTI (http://www.exploredti.com/), and in-house softwares matlab-based StarTrack (www.natbrainlab.com).

6.7.1   DTI pre-processing

6.7.1.1   Concatenation

Since the new split diffusion sequence has been introduced no major motion related artefacts have been recorded after visual inspection of the data. This procedure however necessitated an additional initial pre-processing step to combine (*concatenate*) both acquisitions. After converting the scanner-native DICOM files into NIFTI files (*dcm2nii* from mricron) both acquisitions as well as the corresponding b-value (*.bval) and b-vectors (*.bvec) were available. These files were then combined using a matlab-based script to obtain a single NIFTI file, containing all 60 diffusion-weighted directions and seven non-diffusion-weighted images.

6.7.1.2 Artefact correction

To reduce the presence of motion artefacts during the acquisition the patients were bedded as comfortably as possible with extra padding between the coil and the head to avoid involuntary movement. Additionally, during the post-processing long-term motion artefacts were corrected with ExploreDTI motion artefact correction and the additional gradient table rotation (www.exploredti.org). Equipment-induced artefacts (i.e. eddy currents) were corrected with ExploreDTI through iterative affine correction to the non diffusion-weighted scan. For each patient the data quality was visually inspected. Patients with more than two corrupted volumes on the scan slice would have been excluded.

6.7.1.3 Diffusion tensor tractography

Whole brain tractography was performed by selecting as seed voxels all brain voxels with fractional anisotropy (FA) >0.2. Streamlines were propagated with a step-size of 1mm, using Euler integration and b-spline interpolation of the diffusion tensor field (Basser et al. 2000). Where FA<0.2 or when the angle between two consecutive tractography steps was larger than 45° tractography was stopped. Using a matlab-based script the data was then exported to TrackVis (www.trackvis.org) for virtual dissections and volume measurements of white matter pathways according to Catani et al. (2008).

6.7.1.4 Spherical deconvolution tractography

Spherical deconvolution was chosen to estimate multiple orientations in voxels containing different populations of crossing fibres. The input data was the acute and chronic diffusion weighted scans as *matlab* converted files (.mat) and already corrected for motion and eddy current distortions. A modified (damped) version of the Richardson-Lucy algorithm for spherical deconvolution (Dell'Acqua et al. 2010) was employed using the Software StarTrack (http://www.natbrainlab.com). Algorithm parameters were chosen as described in (Dell'Acqua et al. 2012). A fixed fibre response corresponding to a shape factor of $\alpha = 1.5 \times 10^{-3}$ mm^2/s was chosen (Dell'Acqua et al. 2013), the number of iterations of the deconvolution algorithm was 400, the damping parameter for the damped Richardson Lucy SD algorithm regularisation (n) was 0.06 (the higher the value the lower the risk of false positive reconstructions) Propagation step size was 0.5, angle threshold was set to 45°.

Fibre orientation estimates were obtained by selecting the orientation corresponding to the peaks (local maxima) of the fibre orientation distribution (FOD) profiles. To exclude spurious local maxima, we applied an absolute and a relative threshold. A first "absolute" threshold was used to exclude small local maxima due to noise or isotropic tissue. This threshold is 3 times the amplitude of a spherical FOD obtained from a gray matter isotropic voxel. A second "relative" threshold of 8% of the maximum amplitude of the FOD was applied to remove the remaining local maxima with values greater than the absolute threshold (Dell'Acqua et al. 2010). Visual data quality check was done according to the guidelines and an interim result is shown in **Figure 43**.

In order to automate some steps of the tractography dissection, regions of interest (ROIs) based on previous reports (Catani et al. 2007; Thiebaut de Schotten et al. 2008; Thiebaut de Schotten, Dell'Acqua, et al. 2011a; Thiebaut de Schotten, ffytche, et al. 2011b) were defined on the *MNI152* template provided within FSL.

For each participants Convergence Maps from Richardson-Lucy Spherical Deconvolution Algorithm were registered to MNI152 template provided within the FMRIB Software Library package (FSL, http://www.fmrib.ox.ac.uk/fsl/) using Advanced Normalisation Tools (http://www.picsl.upenn.edu/ANTS/), which combine affine with diffeomorphic deformations (Avants et al. 2008; Klein et al. 2009). The inverse deformation was then applied to the ROI defined in the MNI152 in order to bring them to the native space of every participant. Individual dissections of the tracts were then visually inspected and corrected.
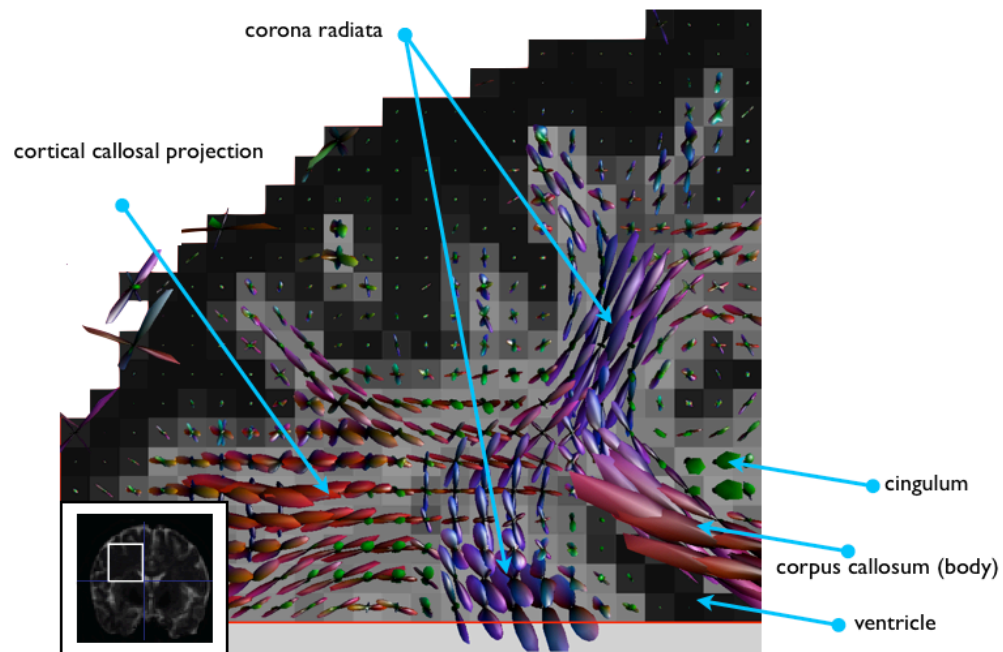
Figure 43   StarTrack© reconstruction of multifibre orientation

StarTrack© reconstruction of multifibre orientation in the white matter of the dorsal superior and middle frontal gyrus. The highlighted area visualises pathways approaching the convexity. In this fibre-dense white matter area close to the cortex one can appreciate the crossing of the callosum (red), the corona radiata (blue-purple) and the superior longitudinal fasciculus (green). Own data shown.

6.7.2   Arterial spin labelling (ASL) pre-processing

ASL data acquisition was attempted in all 19 patients, however, at baseline four patient data sets (subjects 02, 06, 11, 12) were acquired without ASL due to time restrictions during the scanning session. One patient (subject 01) needed to be excluded from further analysis due to the presence of substantial movement artefacts. This leaves a total of 14 datasets to be analysed at baseline.

Longitudinally, 10 patients returned after 12 months of symptom onset and ASL sequences were acquired, with one acquisition being not suitable for further analysis due to the endogenous tag still being accumulated in the artery (**Figure 44**). Hence baseline data of 14 patients and follow-up data of nine patients was available for analysis.
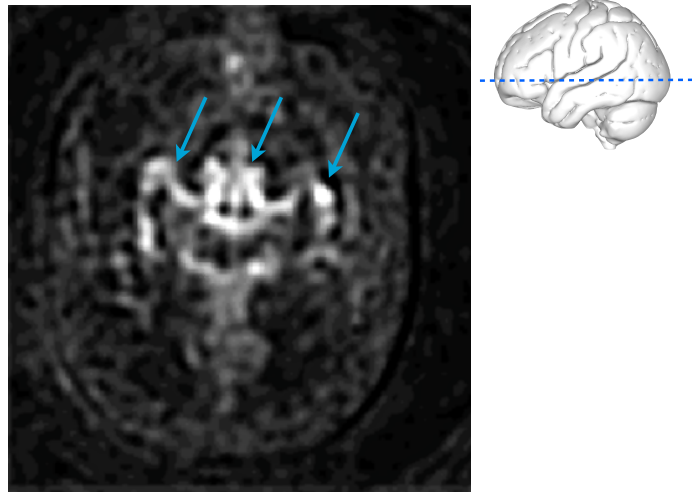
Figure 44   Cerebral Blood Flow (CBF) map for subject 06's one year scan

The tag still remains in the bilateral branches of the middle cerebral artery (MCA). Due to the tag still being in the artery at the time of imaging this subject had to be excluded from further perfusion analysis.

Firstly, the native cerebral blood flow (CBF) maps and the structural T1-weighted images were manually reoriented using SPM so that the image origin (coordinate [0, 0, 0]) was situated on the anterior commissure.

Secondly, the Clinical Toolbox (http://www.mccauslandcenter.sc.edu/CRNL/clinical-toolbox) was employed to segment and normalise (i.e. unified segmentation) the structural images. The advantage of this toolbox is that it is specifically developed for clinical scans and can handle lesioned data well.

Thirdly, the perfusion map and the grey matter map of each patient were co-registered in SPM. This process involved smoothing (6mm kernel) the segmented gray matter (GM) image, from segmentation, to create a target for registration, which more closely resembled the distribution of signal within the perfusion image. Rigid-body registration parameters were estimated for moving the ASL into alignment with the smoothed GM image, and subsequently applied to the ASL image. The resultant perfusion image was then normalised to standard (MNI) space using the normalisation parameters obtained during the unified segmentation process. In order to remove extracerebral signal, the normalised perfusion images were masked using the SPM image calculator (ImCalc) (80% probability of being brain). The final masked perfusion map was smoothed with a kernel of 8 mm. In an attempt to be very conservative and only include grey matter whilst excluding white matter, the final images were re-masked to only include grey matter (minimum 30%

probability of being grey). Previous studies (e.g., Howard et al., 2012) used a masking of 20%, which was still overly inclusive for our cohort.

Fourthly, given the nature of unilateral lesions in our cohort the individual contribution of each hemisphere to the perfusion values should be evaluated and hence the masks were dichotomised into left and right hemispheres; this was achieved by splitting the MNI template (MNI152_T1) at the hemispheric midline using fslmaths and binarising both resulting masks in fsl. These binarised masks were applied to the grey matter thresholded perfusion maps and the global perfusion values for each hemisphere in each patient were extracted using fslstats.

Finally, the same method was applied to extract the perfusion within each region of interest. Anatomical ROIs in MNI-template space were derived from the Juelich probabilistic histological atlas. Based on *a priori* information regarding brain regions related to language, ROIs were created for pars opercularis (Broca_44), pars triangularis (Broca_45) (Amunts et al. 1999; Amunts et al. 2004), inferior parietal lobe (IPL_PF, IPL_PFcm, IPL_PFm, IPL_PGa) (Caspers et al. 2008; Caspers et al. 2006), and the posterior superior temporal gyrus [STG_Te10, STG_Te11, STG_Te3]. The mean of the 20% voxels with greatest CBF values was computed (Mitsis et al. 2008) as a summary measure. ROIs were extracted from each individual CBF map acquired for each participant at each session (i.e., baseline and one year post stroke); these data were used to examine temporal variation in regional CBF response between the sessions. In addition, group comparison analyses were conducted based on the extracted ROIs for each hemisphere at each session (Howard et al. 2011) (see script in appendix).

6.8   Un-anticipated acquisition differences and their resolutions

Three participants (01, 02, 14) had more complex pre-processing requirements due to unanticipated dissimilarities in the acquisitions, which could be resolved as described below.

6.8.1.1   Un-split sequences (subject 01 and 02)

The diffusion datasets for subject 01 and 02 were acquired with the initial DTI sequence (full set of 60 directions acquired in on sequence). Only after these first two patients were acquired the need and possibility to split the DTI sequence into two parts to considerably reduce motion artefacts was discussed and subsequently implemented (details described above in 6.7.1). Due to the concatenation step the

results from all patients are a single NIFTI file including the 60 directions and 7 non-diffusion weighted images.

6.8.1.2   Acquisition with wrong gradient table (subject 14)

The first 30 directions of the DW scan for subject 14 was acquired with the correct gradient table but the second scan was acquired with the gradient table for the first scan as well, which rendered 30 directions unusable (**Figure 45**, upper and middle left panel). The data set was reprocessed and corrupted directions were rejected (**Figure 45**, bottom panel).
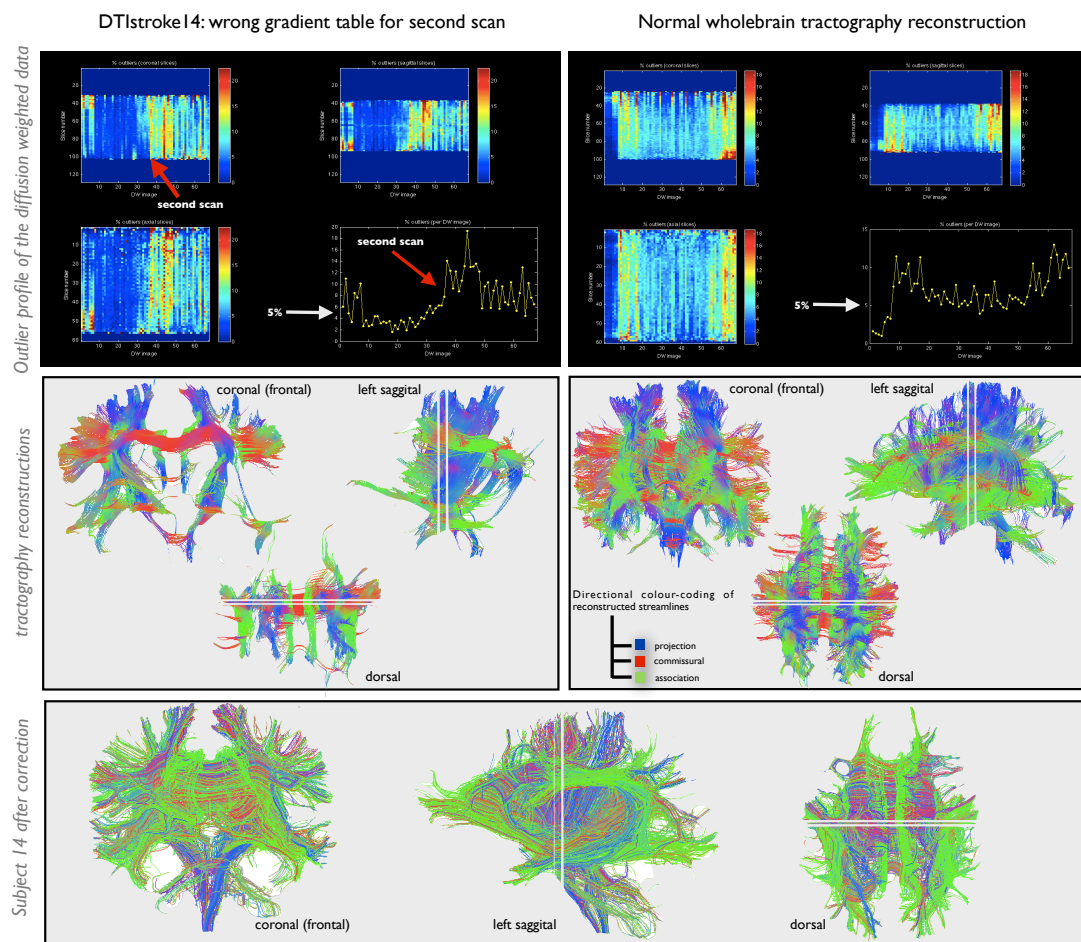
Figure 45   Subject 14 (left) in comparison with non-corrupted data set (right)

The upper panel shows the outlier profile for subject 14 and a comparison data set. It can be appreciated that the profile of subject 14 has an increased error rate due to a wrong gradient table applied during the acquisition. The percentage of outliers within the diffusion-weighted image usually centres around 5% and the level of noise within the acquisition is equally spread across the acquisition. The outlier profile comparison between a successful scan and the corrupted acquisition of subject 14 clearly shows that i) the level of noise increases significantly between the two scanning sets and ii) the percentage of outliers vastly exceeds the 5% mark with peaks as high as approximately 19%. The left middle panel shows the

resulting whole brain tractography reconstructions before correction. The lower panel shows the corrected results for subject 14 after corrupted directions were discarded.

6.9   Data processing

6.9.1   Lesion analysis

For each patient the structural scan were examined and anatomical landmarks were identified (Nieuwenhuys et al. 2008; Naidich et al. 2001; Türe et al. 1999). Once the anatomy was acknowledged the lesion location was defined for every patient and a list summarising the locations is provided in the results (**Table 17** in Chapter 7). An example is given below of how structures and lesions were identified (**Figure 46**).
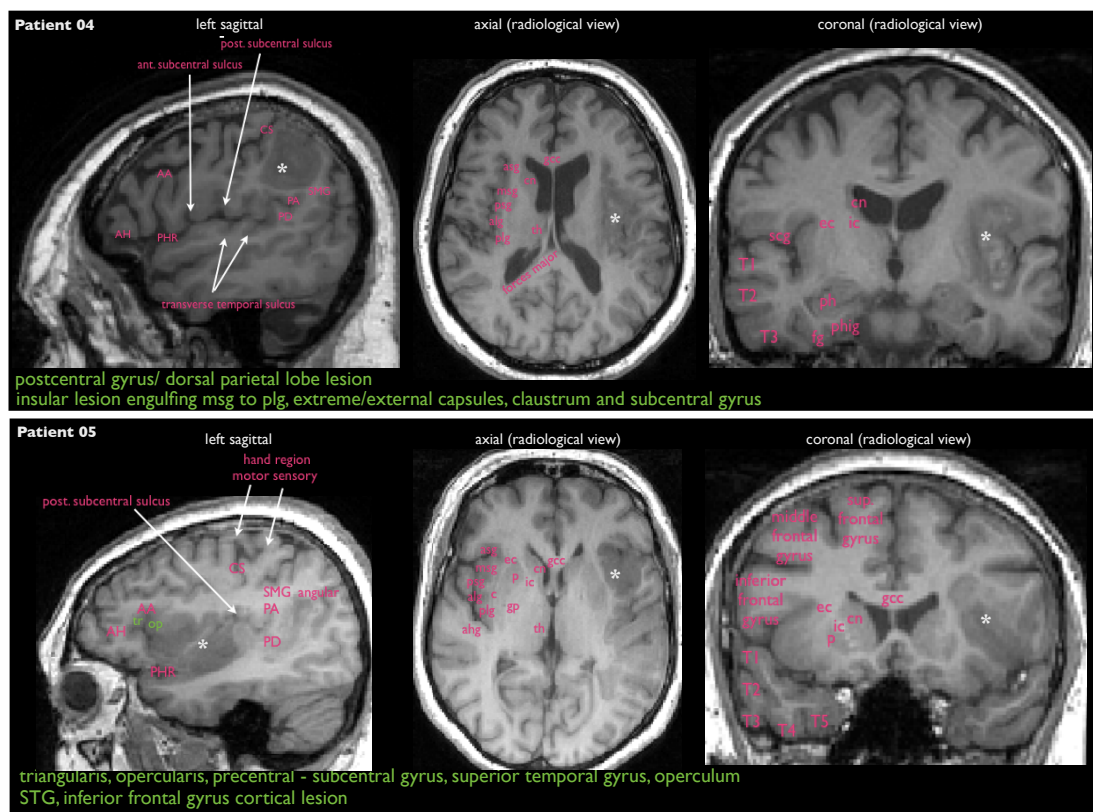
Figure 46   Exemplified lesion identification on structural scans (here patients 04, 05)

This method was applied to all patients in this study. Anterior ascending ramus [AA}, anterior horizontal ramus [AH], posterior horizontal ramus [PHR], posterior ascending ramus [PA], posterior descending ramus [PD], central sulcus [CS], anterior short insular gyrus [asg], middle short insular gyrus [msg], anterior long insular gyrus [alg], posterior long insular gyrus [plg], caudate nucleus [cn], thalamus [th], internal capsule [ic], external capsule [ec], subcentral gyrus [scg], superior temporal gyrus [T1], middle temporal gyrus [T2], inferior temporal gyrus [T3], fusiform gyrus [fg], parahippocampal gyrus [phig], pes hippocampi [ph], triangularis [tr], opercularis [op], supramarginal gyrus [SMG], genu corpus callosum [gcc], putamen [p], globus pallidus [gp].

For the group level analyses one of 18 patients had to be excluded, as no T1-weighted scan was acquired leaving a total cohort of 17 patients for the acute and

15 patients (two failed to complete the follow-up assessment) for analyses at the chronic point.

In a first step, native coronal T1-weighted images were re-sliced axially and co-registered to the corresponding T2-weighted image (*coreg*) and thence skull stripped with the *bet* function in FSL. Stripped axial T1-weighted images were then normalised to a common reference space (Montreal Neurological Institute, MNI). The lesions were manually delineated on the axially re-sliced native T1-weighted images in FSL. The transformation matrix obtained in the previous normalisation step was applied to the lesion volume to normalise the lesion volume to the MNI space.

In a next step, lesion overlay percentage maps were obtained by binarising (i.e. given a value of 0 or 1 to each voxel) the normalised lesion volumes and overlaying them in the MNI space.

Step 1: Obtain lesion volume in MNI space

fsl-based

mricron-based
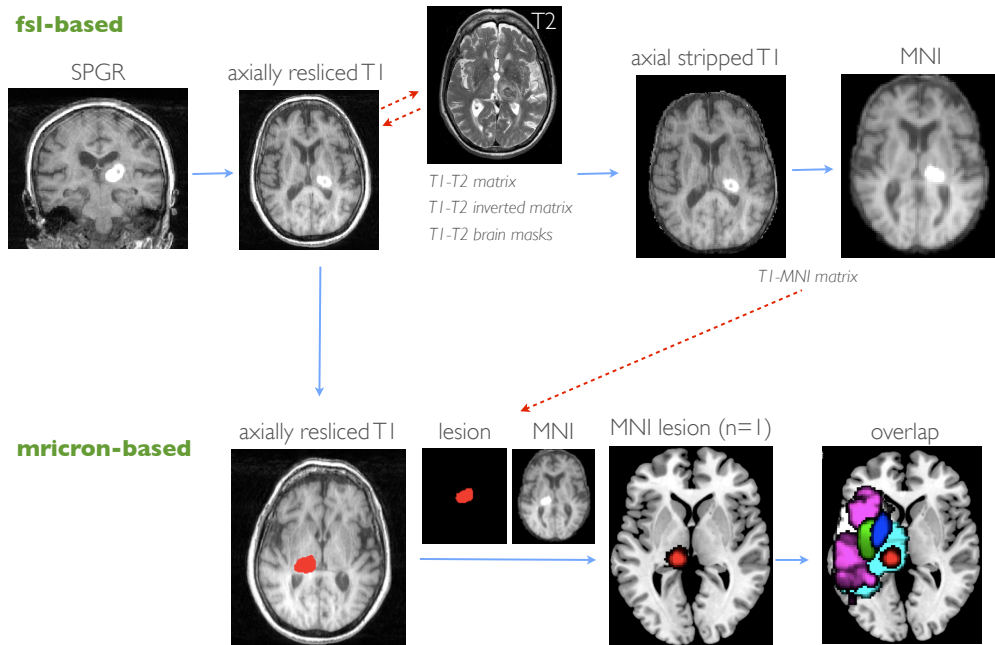
Step II: Lesion overlay percentage maps

all fsl-based
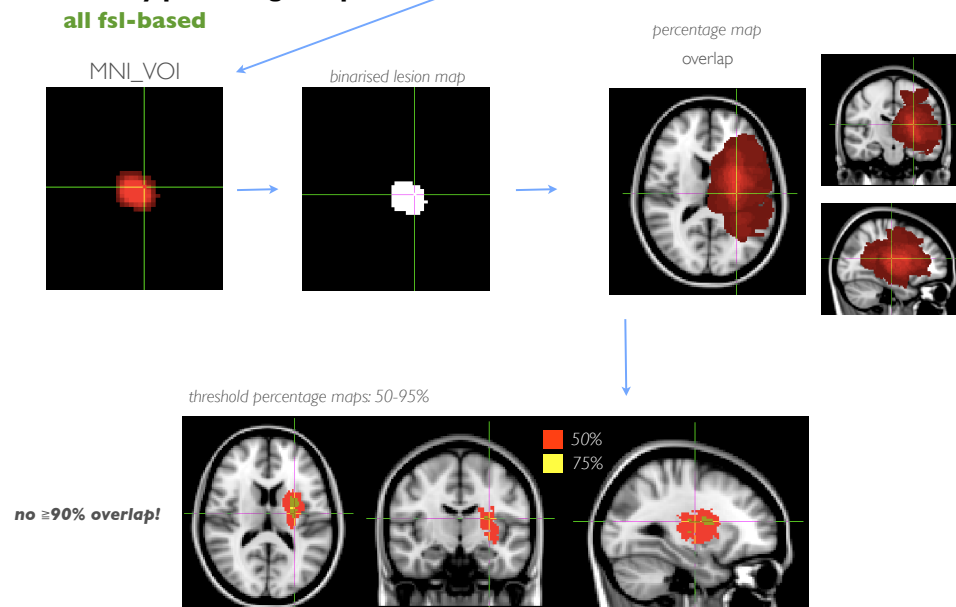
Figure 47   Lesion analysis cascade – initial steps

Step 1 provides the lesion of all patients plotted onto an MNI template. Step 2 provides a simple lesion overlay percentage maps (own data). The data shown is taken from left hemispheric stroke patients with the lesions being shown either in radiological or neurological view depending on the programme used for visualisation.

6.9.2   Advanced lesion analysis

6.9.2.1 Voxelwise 'topological' lesion-deficit analysis

To identify voxels within the brain that have a significant effect on behaviours a voxel-base lesion-symptom mapping approach was implemented (Bates et al. 2003; Rorden, Karnath, et al. 2007b). This will allow identifying those cortical regions between all patients that indicate that the presence of a lesion to these specific regions has little (cold colours) or considerable (warm colours) effects on the language performance (such as the overall severity and repetition impairments).

This advanced lesion analysis was performed as linear regression analysis with the non-parametric mapping programme (NPM) and a voxel lesion-symptom mapping tool (VLSM) implemented in mricron, a method less sensitive to outlier profiles compared to other software packages (Rorden, Bonilha, et al. 2007a). The normalised lesions defined on T1-weighted images were converted into volumes of interest (*.voi) using the conversion tool in mricron and a binary map was created. The a priori minimum lesion density threshold was set to 10%, which means that statistics will only be computed for voxels that are damage in more than 10% (most commonly within our sample size this is equal to two patients) of the patients. Statistically, the continuous deficit analysis was performed that is based on the Brunner Munzel test. This rank order test requires at least 10 observations in each group whilst its power is assumed to be stronger than a t-test where the assumptions for parametric test are violated (as is often the case in behavioural observations) (Rorden, Karnath, et al. 2007b; Brunner et al. 2002). The multiple comparison problem implicit in the standard voxel-by-voxel hypothesis testing framework was accounted for with permutation testing within the voxel-based lesion-symptom mapping approach (Nichols et al. 2002). Permutation tests can be used to control for multiple comparisons in neuroimaging studies and are significance tests based on resamples drawn at random from the original data. Methods, such as VLSM, allow for permutation testing, at some computational expense, to determine a critical cluster size threshold (p < .005), based on commonly 1000 random permutations of the data (Kimberg 2007).

6.9.2.2 Trackwise 'hodological' lesion-deficit analysis

A recently published DTI atlas (Thiebaut de Schotten, ffytche, et al. 2011b) was used to describe the pattern of disconnection induced by each lesion at the individual level. This MNI-based atlas provides a colour-coded probability for each voxel belonging to a specific tract whereby blue represents a threshold of p<0.05,

green is set to 50% of people having a tract in this voxel, yellow represents 75%, and red indicates that a voxel belongs to this tract in 90% of the population. When a patient's lesion overlapped on a voxel with a probability above chance level (i.e >50%) the tract was considered disconnected (**Figure 48Error! Reference source not found.**). Values were assigned to each colour: blue=1, green=2, yellow=3, red=4. Hence, only lesion load above 2 (i.e. above chance) were considered as disconnected.

Statistical Package for the Social Sciences (SPSS Inc, Chicago, Ill) was used to compute regressions in order to identify the tracts whose lesion had a predictive value, after excluding confounding factors such as the lesion size. A first logistic regression used five independent variables: lesion volume (continuous measure), age (continuous measure), gender (categorical), and the disconnection of each segment (long segment, anterior segment, posterior segment). The regression aimed at identifying whether these four variables were able to predict the recovery of language function post stroke. All track-wise hodological lesion-deficit results were subjected to Bonferroni correction for multiple comparisons.
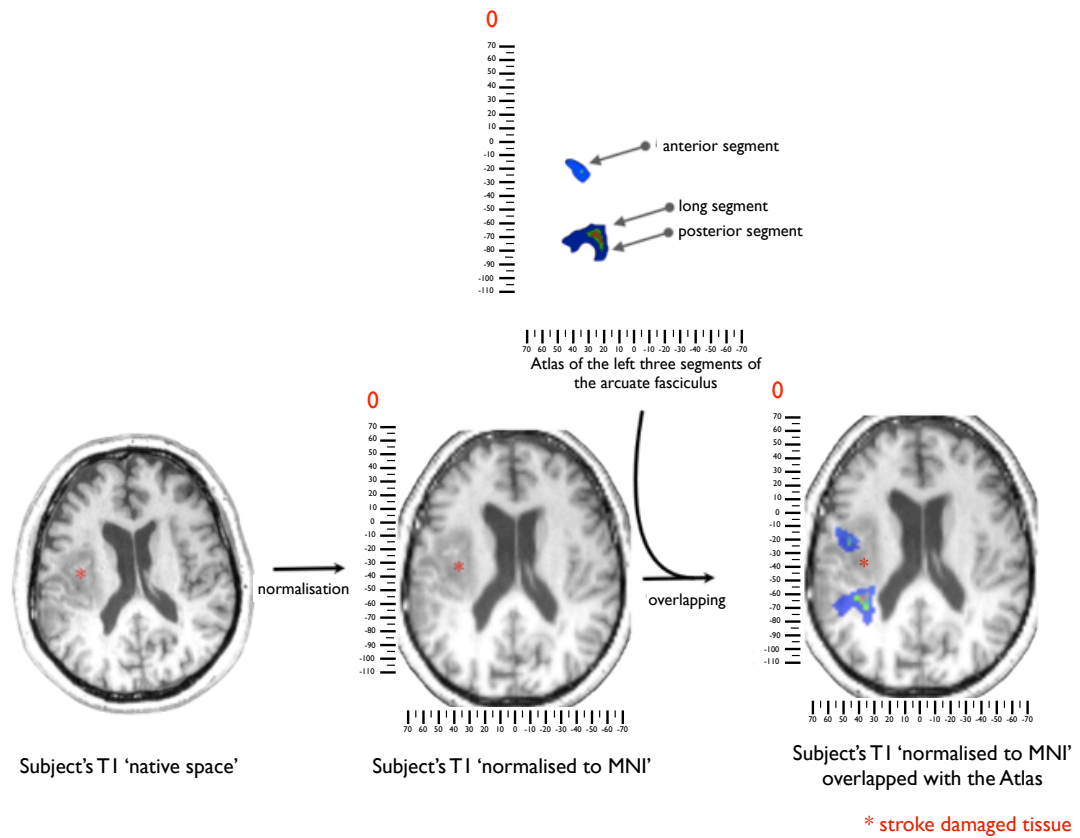
Figure 48   Trackwise hodological lesion-deficit approach

The native T1-weightes image is transformed from the native space into the MNI space and an MNI-based atlas is used as an overlay on the normalised image of the patient (own data shown). MNI normalised white matter atlas available from www.natbrainlab.com

6.10 DTI Analyses

6.10.1 Inter-rater variability

To ensure internal reliability two anatomists used TrackVis (www.trackvis.org) for virtual dissections and volume measurements of the three segments of the right arcuate fasciculus.

6.10.2 DTI tractography reconstructions

The arcuate fasciculus is connecting the temporal, parietal and frontal lobes via the dorsal route. The temporo-frontal direct connections as well as the two indirect connections between the angular gyrus and the frontal and temporal lobe were dissected using TrackVis. The ventral network connecting the occipital, temporal and frontal lobes is comprised of i) the uncinate fasciculus, connecting the anterior temporal lobe to the ventrolateral frontal lobe, ii) the inferior longitudinal fasciculus connecting the occipital and temporal lobes, and iii) the inferior fronto-occipital fasciculus, a long-range connection between the occipital and frontal lobe. Additionally, the recently described frontal aslant tract was dissected that is interconnecting Broca's area with the supplementary motor area (Catani, Dell'Acqua, Vergani, et al. 2012b).

The acquired dataset was compatible with tensorial and non-tensorial tractography methods, the latter that can partially resolve fibre crossing, such as spherical deconvolution (SD; see 6.6.2.2). The dataset was therefore additionally analysed for SD tractography, which allows for the visualisation of the fronto-parietal network (superior longitudinal fasciculi I-III). For each of these pathways the volume was extracted by means of number of streamlines as well as voxel count, radial and axial diffusivity, fractional anisotropy (FA) and mean diffusivity (MD). These surrogate measures were exported and analysed in IBM SPSS 20 (http://www-01.ibm.com) and R (www.R-project.org).

Arcuate fasciculus

The arcuate fasciculus was dissected using a three region of interest approach. The restrictive cortical approach according to Catani et al. (2005) was employed with sagittal cortical ROIs placed within the frontal, parietal and temporal lobes (**Figure 49**). The arcuate fasciculus is the candidate pathway for language-relevant functions.
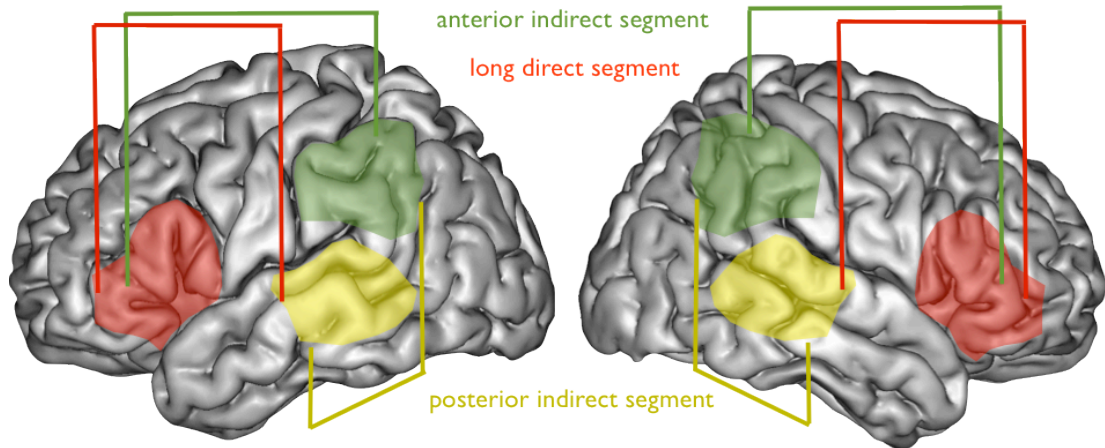
Figure 49   Region of Interests (ROIs) for the three segments of the arcuate fasciculus

Three ROI are placed on the lateral convexity of the left and right hemisphere. By combining the adequate ROIs the long direct segment, anterior and posterior segment of the arcuate fasciculus can be reconstructed.

Ventral network: inferior fronto-occipital fasciculus (iFOF)

The ventral network was delineated using the approach and the regions of interest detailed in (Forkel et al. 2012). Two ROIs, delineated on coronal planes, were used to dissect the fronto-occipital connections (**Figure 50**). An occipital region was placed on the white matter of occipital lobe posterior to the parieto-occipital sulcus and the temporo-occipital notch. One anterior ROI was defined on the white matter of the frontal lobes and delineated on the white matter of the external/extreme capsule. All streamlines between occipital and ventral frontal ROIs were labelled as iFOF.
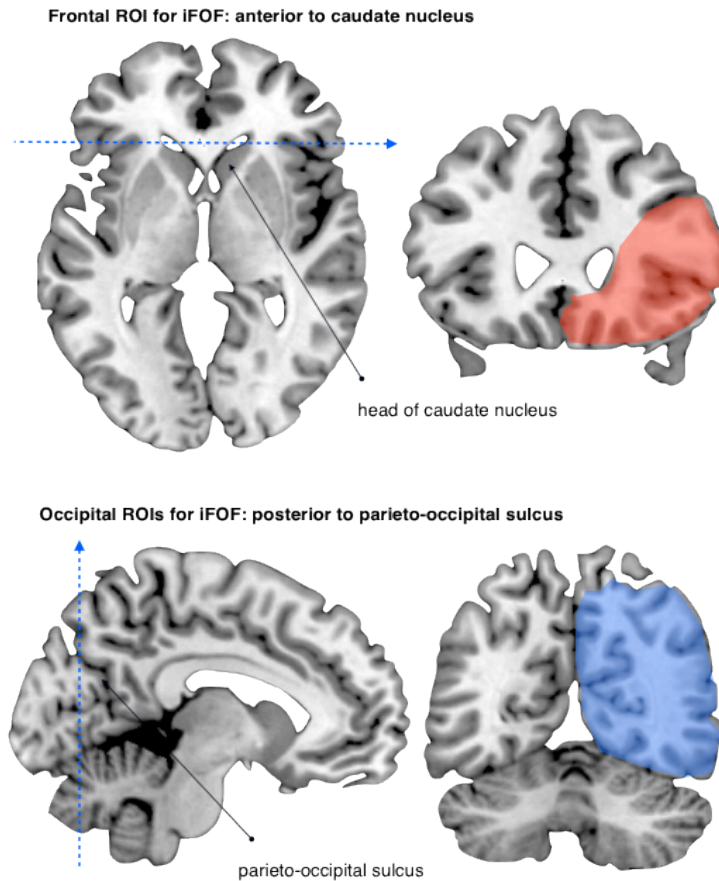
Figure 50   ROIs for the inferior fronto-occipital fasciculus

Adopted from the supplementary material in (Forkel et al. 2012)

Frontal aslant tract (FAT)

The frontal aslant tract was dissected with one ROI in the inferior frontal gyrus and the second ROI around the supplementary motor area as described in Catani et al. (Catani, Dell'Acqua, Vergani, et al. 2012b) (**Figure 51**). The FAT was implicated as candidate pathway for the initiation of articulation and motor components of articulation.
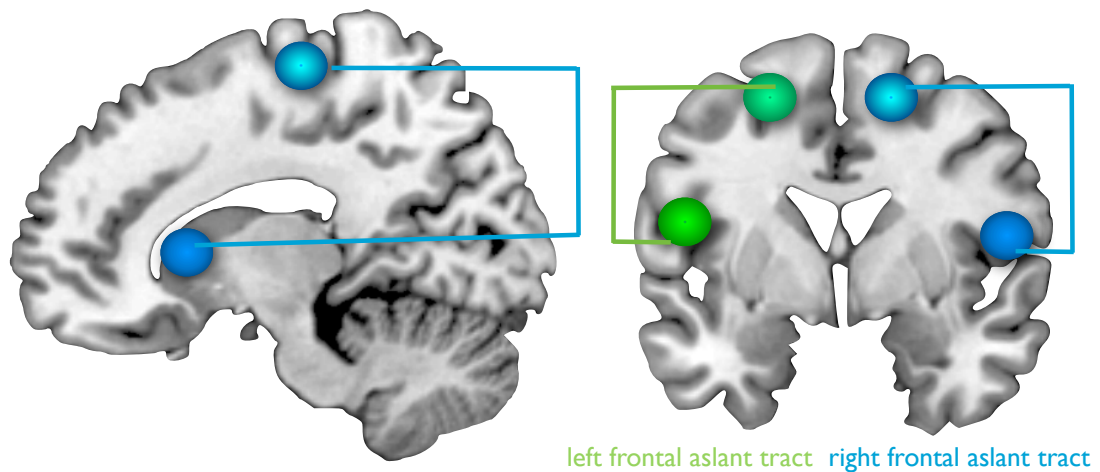
Figure 51   ROI for the frontal aslant tract (FAT)

A sphere is placed in the supplementary and pre-supplementary motor area and a second sphere is placed in Broca's area. On the sagittal plane the impression might arise that the ROI was placed on the caudate nucleus. This was not the case but in order to visualise both ROIs at the same time in this plane, the visualisation of the overlay brain had to be sliced at this specific point (as can be appreciated when comparing to the coronal slice on the right).

6.10.3 Right hemispheric volume

Given that the left hemisphere was affected by the stroke a reconstruction of pathways cannot be entirely trusted on methodological grounds and additionally the degree of damage varies within the left hemisphere. It is therefore not advisable to calculate a laterality index (LI) as the commonly used equation relies on the volume of the left and right hemispheric arcuate fasciculus alike (Seghier 2008):

$$LI = \frac{right\ hemisphere\ arcuate\ -\ \text{left}\ hemisphere\ arcuate}{right\ hemisphere\ arcuate\ +\ \text{left}\ hemisphere\ arcuate}$$

Instead, I embraced another approach whereby the volume of the right hemisphere is extracted (explained below) and the volume of the arcuate fasciculus is normalised to the hemisphere volume. This approach controls for the simple fact that a bigger hemisphere might have a bigger arcuate fasciculus.

The computation was done in FSL (Smith et al. 2004) through linear registration of the native T1 image (1mm) onto the FSL T1 template (1mm). Prior to the registration, the native T1 image was first skull stripped (*bet*) with the fractional intensity default threshold of 0.5.

In a second step an inclusive brain mask of the right hemisphere was hand drawn in mricron (**Figure 52**). *fslmaths* was then employed to mask the normalised skull

stripped T1 images and *fslstats* allowed to extract the volumetric measurements of each right hemisphere.

To investigate the relationship of the right hemispheric volume and the long segment of the arcuate fasciculus (LS) in the right hemisphere, a correlation analysis was conducted.

| skull stripped T1 image | normalised stripped T1 image | right hemispheric brain mask |
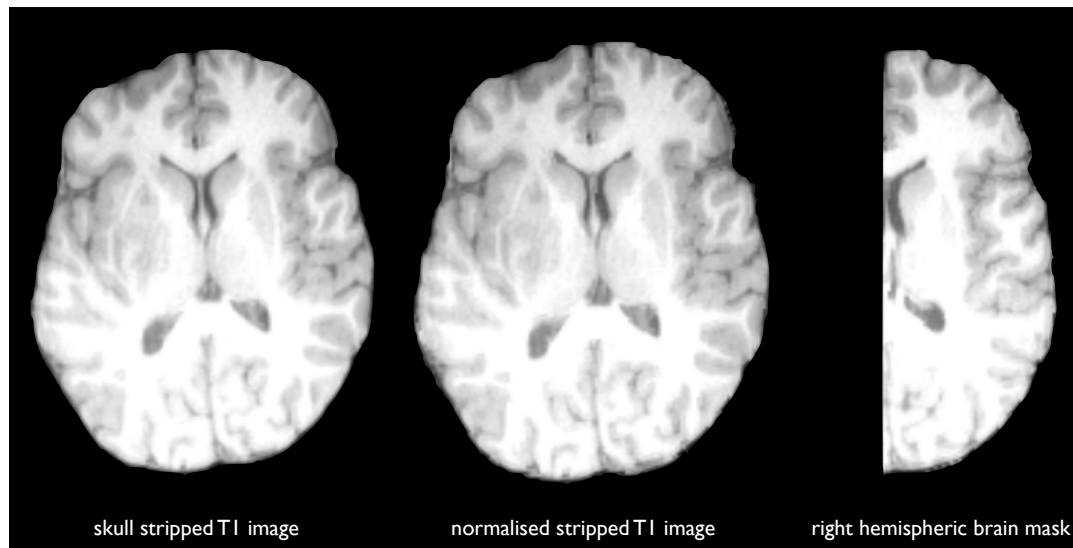
Figure 52   Process of extracting right hemispheric volumes

Native T1 images (first image) were co-registered and skull stripped with the FSL T1 MNI template and normalised to the standard space (second image). A right hemispheric brain mask was then applied (third image) and the hemispheric volume was extracted (own data shown).

6.11 Tract-Based Spatial Statistics (TBSS)

Tract-Based Spatial Statistics employs non-linear registration and generates a whole brain white matter skeleton (S. M. Smith et al. 2004; S. M. Smith et al. 2006; S. M. Smith et al. 2007). TBSS has some advantages over voxel-based morphometry methods (VBM) and tractography. In comparison to VBM, TBSS overcomes the alignment problems. Also it is an automated method that can be used to investigate the whole brain (rather than individual tracts as with tractography). No detailed a priori neuroanatomical knowledge is required (S. M. Smith et al. 2009). TBSS relies on a group mean fractional anisotropy (FA) map that is skeletonised to represent the centres of all fibre pathways, which are common to all subjects within the studied cohort (**Figure 53**A).

The previously described DTI pre-processing provides FA maps for each patient. These maps were extracted using MATLAB-based ExploreDTI (*export to nii* function). Individual FA maps where then aligned to a common target using non-

linear registration (FNIRT) and an average FA map was created (**Figure 53**B). The mean FA map was then skeletonised through "thinning" (**Figure 53**C). In a next step the individual normalised FA map is projected onto the skeleton to account for residual misalignment from the first step. A FA skeleton map is then available for each subject. Subsequent voxelwise statistics are applied across subjects on the skeleton-space FA data. Each step is clearly explained in the FSL tutorial on TBSS (http://www.fmrib.ox.ac.uk/fslcourse/lectures/practicals/fdt/index.htm#tbss).
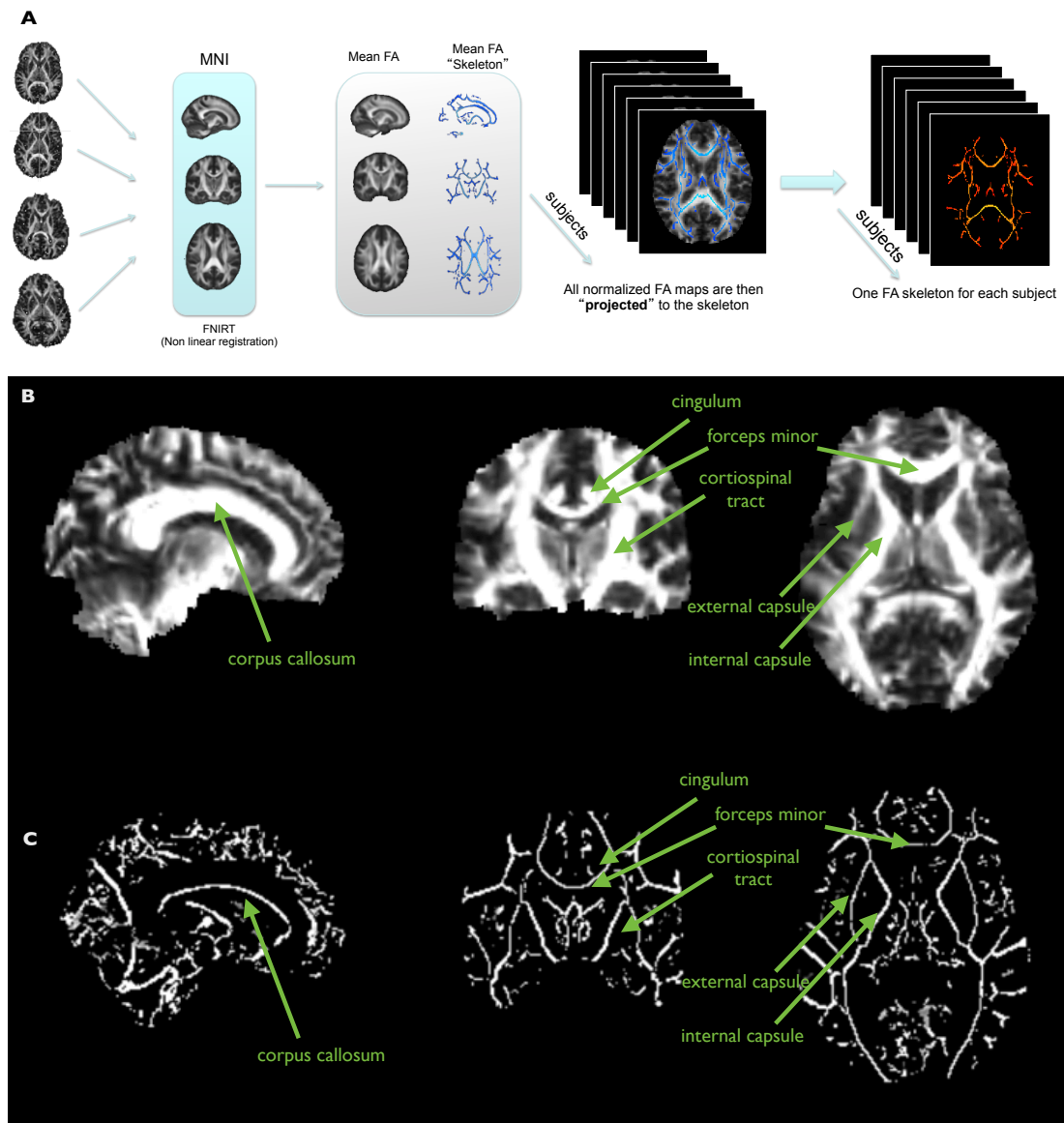
Figure 53   TBSS analysis cascade

A Cohort FA maps are first normalised to MNI and averaged to create a mean white matter skeleton of the group. The individual normalised FA maps are then projected onto the skeleton and the individual white matter skeleton can be extracted (courtesy of Dr. Dell'Acqua). **B** Averaged fractional anisotropy (FA) map with anatomical landmarks (own data). **C** Skeletonised white matter map (own data).

Two TBSS analyses were conducted. In both cases, FA maps were pre-processed as described above and then submitted to a general linear model (GLM) analysis.

The data was statistically analysed in FSL using randomise (http://fsl.fmrib.ox.ac.uk/fsl/fslwiki/Randomise). This permutation method is used for thresholding statistical maps where the null distribution is not known (hence non-parametric testing). This modelling and interference can be achieved by using a standard general linear model (GLM) design setup (Nichols & Holmes 2002). Methodological rational behind the GLM analysis is available here: http://fsl.fmrib.ox.ac.uk/fsl/fsl4.0/feat5/glm.html. This is the recommended approach by the TBSS manual and the used terminal commands including explanations can be found in Appendix D. UNIX commands

The first model was a single-group average with additional covariate analysis (for methodological details please see the manual: http://fsl.fmrib.ox.ac.uk/fsl/fslwiki/GLM#Single-Group_Average_with_Additional_Covariate). Subjects were attributed to a group (the acute FA maps) and additional demographic and behavioural measurements (i.e. language recovery, age, sex, thrombolysis and lesion size) were available. These measures were treated as covariates and were defined as explanatory variables (EVs) in the model. Values are always entered 'demeaned' into the analysis; this means the value of interest is subtracted from the group mean.

The aim of this analysis was to test for the regression of FA changes (in- or decrease) and language recovery at six months.

The second model accounted for FA changes between the baseline scans the second scan one year later. The difference between those two FA maps was calculated and the resulting subtraction map was analysed with regards to the predictive value for language recovery.

The aim was to test whether longitudinal FA changes might reflect behavioural changes (as in improved language functions). Nine data sets were entered into the analysis.

Here, the chronic FA maps were registered onto the acute FA maps of each subject to reduce the effect of different head orientations during acquisition and have both images in the same reference space. This was achieved with FSL flirt with the acute image being the reference (see Appendix D. UNIX commands). The registered chronic FA map was then subtracted from the acute FA map using FSLmaths (**Figure 54**).

Individual Subject Subtraction Map
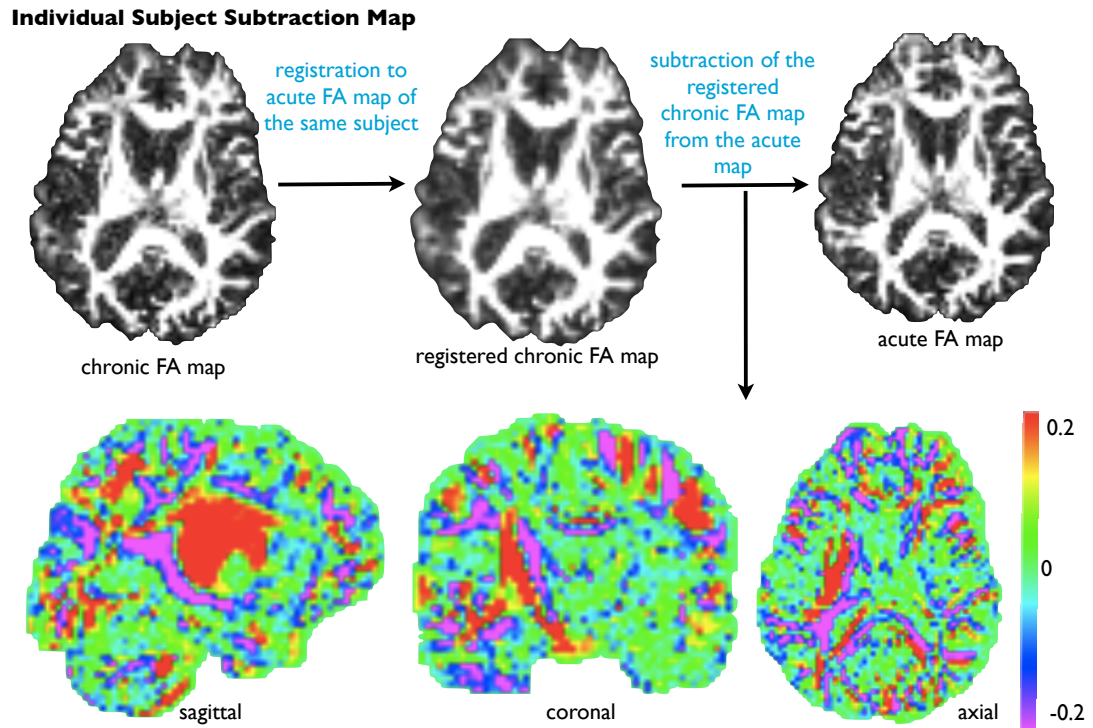
Figure 54   Advanced TBSS comparison between acute and chronic imaging

The chronic fractional anisotropy (FA) map is registered to the corresponding acute FA map (same patient, different time points of scanning). The resulting registered chronic map is then subtracted from the acute FA map, generating a FA difference map. Colour coding 'spectrum' was chosen to highlight changes in FA (increase= red, decrease= blue). Positive values (red) indicate FA increases, neutral values (green) indicate no FA changes, and negative values (blue) indicate FA decrease. Own data shown.

The resulting maps were averaged. In a next step the acute and chronic FA maps were summed up and divided by two to create the group average FA image of which the skeleton was created. The skeleton was then applied to the subtraction maps (**Figure 55**). A skeleton of the subtraction maps is not obtainable as these maps only depict the difference between the two time points of scanning and therefore do not contain a full skeleton. Hence the group average FA maps were used and the skeleton was then re-applied to the subtraction maps.

The data was submitted to a classical TBSS analysis using a study specific template and an FA threshold of 0.2.
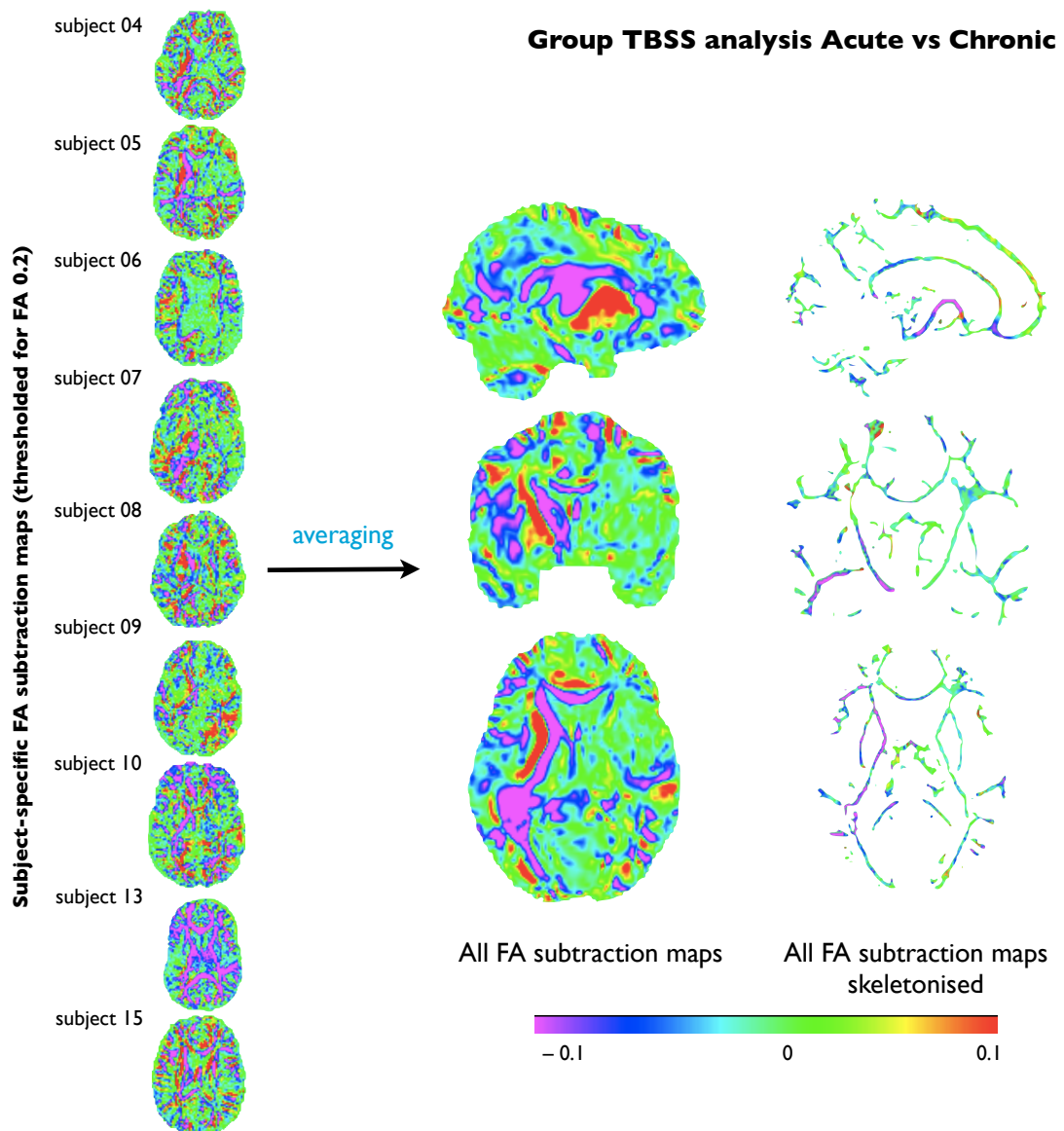
Figure 55   Group TBSS analysis for chronic vs. acute subtraction FA maps

The left panel shows individual FA map subtraction maps. The middle panel shows the group average FA subtraction map. A FA skeleton was obtained from the group FA maps (acute+chronic/2) and then applied to the subtraction maps providing the skeletonised FA map of subtraction. Positive values (red) indicate FA increases, neutral values (green) indicate no FA changes, and negative values (blue) indicate FA decrease. Own data shown.

To setup the design the following parameters were defined. The input was set to 9, as nine data sets were available for acute and chronic comparisons. Five EVs were defined as, EV1: age, EV2: sex, EV3: lesion size, EV4: thrombolysis, and EV5: aphasia quotient difference between chronic and acute testing.

The contrast of interest was defined as positive or negative regressions between behavioural performance (i.e. difference in language score chronic vs. acute) and longitudinal FA changes (see **Figure 56**, C1 and C2). This means that where FA

increases the aphasia score increases (positive) and where the FA decreases the aphasia score decreases (negative).
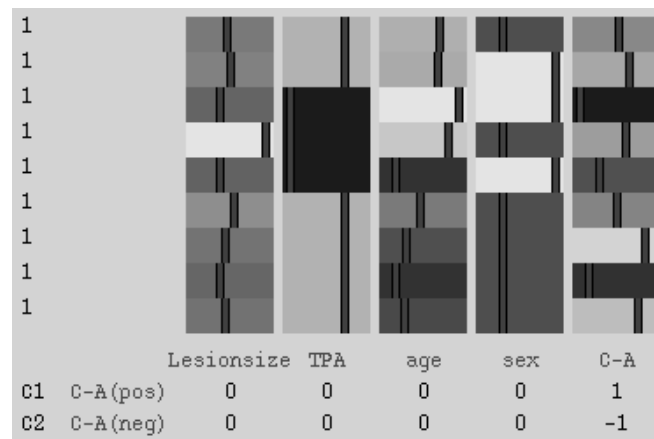
Figure 56   General Linear Model (GLM) for language recovery (C-A)

The left side represents the number of inputs (i.e. patient data sets), which were nine in this study. The bottom panel shows the contrast vectors for positive (C1) and negative (C2) interaction with the recovery variable 'C-A' (chronic aphasia quotient–acute aphasia quotient).

6.12 ASL region of interest analyses

Regional cerebral blood flow differences were investigated in a priori language areas sensu strictu in the left and homologous areas in the right hemisphere, including Broca's are (BA44/45), Wernicke's area (BA22), and the inferior parietal lobe. This analysis was conducted in SPM8 using the Anatomy toolbox to obtain a priori defined regions of interest in the normalised space. Mean values of cerebral blood flow in cortical target areas were extracted using fslmaths (see Appendix D. UNIX commands).

6.13 Statistical analysis

Statistical analyses were partially conducted in IBM SPSS 20 (www.ibm.com/software/analytics/spss/) and some advanced analysis was calculated using the open source software R (http://www.r-project.org/). In the results chapter below the use of R will be clearly stated, otherwise conventional SPSS analysis was conducted. Data was tested for normal distribution and where ever normal distribution could be assumed parametric tests were applied, whereas in cases where it could not be assumed non-parametric tests were used.

Relationships of categorical variables were analysed with chi^2 test and for continuous variables with Pearson's correlation.

Relative importance of potential predictors of aphasia recovery were analysed with multiple linear regression and logistic regression analyses.

It will be highlighted in the results if corrected or uncorrected values are shown. When it is indicated that Bonferroni corrected values are displayed for multiple comparisons the correction was based on the following rational.

If, for example, three indicators of behaviour are given (i.e. language is assessed as auditory comprehension, spontaneous speech, and repetition) and three indicator of anatomy are given (i.e. the three segments of the arcuate), 3x3=9 correlations can be calculated. The general null hypothesis (H0, no difference/association) can therefore be rejected nine times. Testing the null hypothesis over multiple comparisons has hence a bigger chance of rejecting the null hypothesis as if only one test of significance was applied (accumulation of α/Type I error). Assuming that the multiple comparisons entail m comparisons (in this example it would be 9) each test would be calculated with the corrected α error level α', where α'= α/m. In order to reject the null hypothesis a test of significance needs to reach the corrected level of α'=0.05/9=0.0055 (Bortz 2005).

The neuroimaging data was, unless stated otherwise or in circumstances were it is commonly not applied (e.g., DTI), subjected to multiple comparison corrections. Multiple comparisons correction is pivotal as the probability of making a Type I error increases when performing multiple statistical tests. This can be a significant concern especially for voxel-based studies, which typically involve testing across a multitude of voxels. The standard approach in fMRI is controlling for the family-wise error rate (FWER), or the probability of making one or more Type I errors amongst all tests. Achieving this control normally entails accepting an increased risk of Type II error. However, Bonferroni correction, the commonly used procedure for FWER control, is conservative for dependent comparisons (i.e. acceptance of higher Type II error). Lesion data, such as was used in the current stroke study, is liable to be a particularly affected by Bonferroni correction because of the inherent spatial coherence of lesion maps. Lesions tend to present in contiguous voxels whereby the condition of one voxel is strongly predicted by that of its adjacent voxels (i.e. voxels are not independent given that if one voxel is lesioned the neighbouring voxel has a chance of being lesion as well). Commonly used alternatives for this stringent approach (especially in fMRI studies) are the Gaussian Random field theory, False Discovery Rate (FDR), and permutation testing. Amongst these methods FDR and permutation testing have been advocated for lesion analyses (Rorden et al, 2007; Medina et al, 2010; Kimberg 2007; Rorden et al, 2004). False

discovery rate, as the name implies, provides a method for adjusting the expected proportion of false positives among voxels. FDR is more lenient than the Bonferroni method, which comes with greater power and increased rates of Type I error.

Decisions on statistical test were determined based on the rational shown in **Figure 57**. Statistical results are reported in compliance with the conventional thresholds for the probability values reflecting the strength of evidence against the null hypothesis (H_0): p=0.05 for significant results, p=0.01 for very significant results, and p=0.001 for highly significant results.
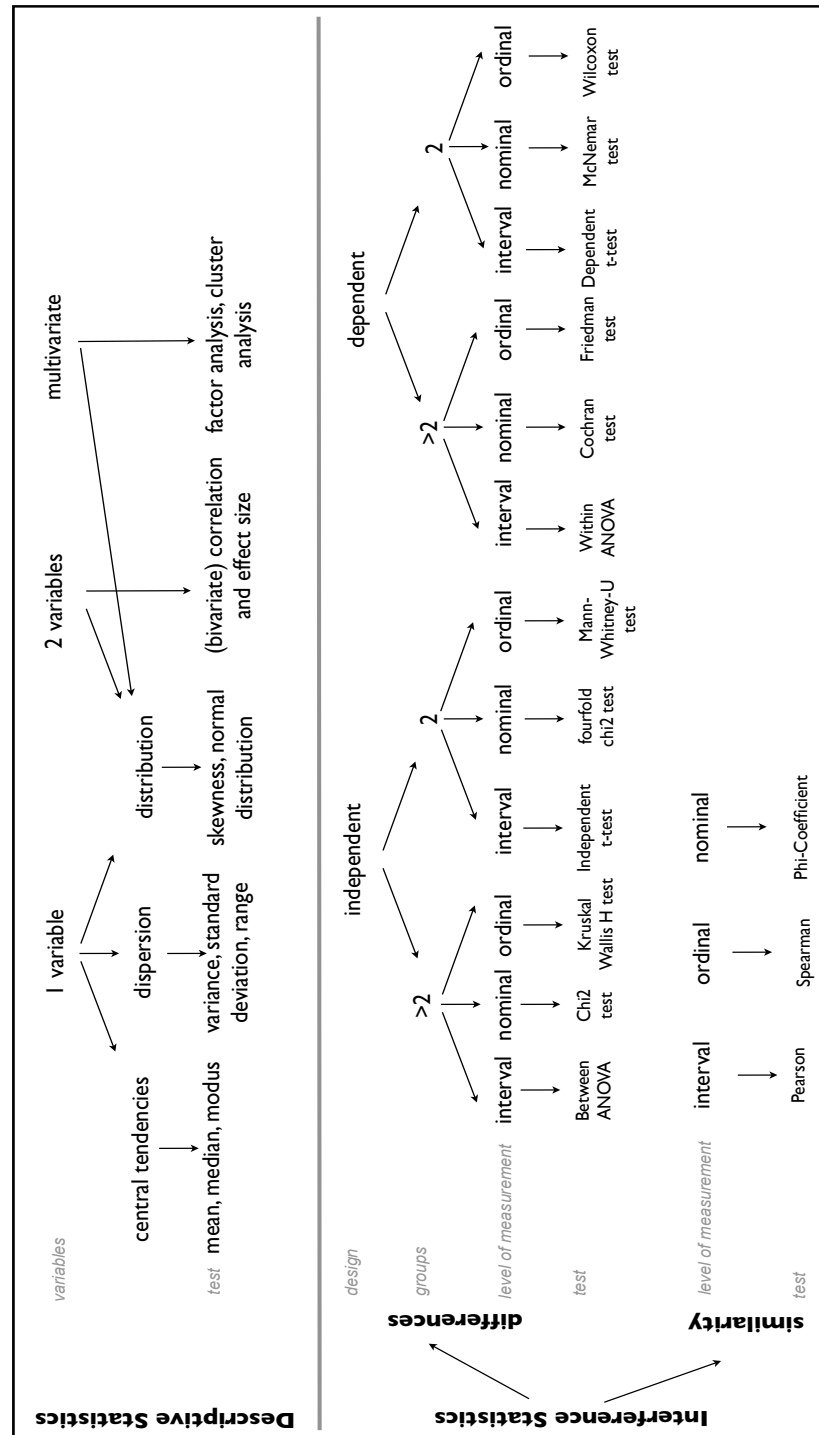
Figure 57   Statistical decision diagram

Depending on the data at hand one test is more reasonable than the other, i.e. if a variable has identified outliers the mean will be biased towards them and the use of the median might be more applicable. A pivotal step in descriptive statistics is the test for normality, which will influence the subsequent interferential statistics. The lower panel shows the decision pathways for test of similarity and differences based on design (independent vs. dependent groups), number of groups (≥2), and level of measurement (continuous, dichotomised or ranks). Post-hoc tests are not considered here though they were applied in the analyssi. Adopted from (Kuehberger 2006).

CHAPTER 7   BASELINE ASSESSMENTS

'Medical statistics are like a bikini: what they reveal is suggestive,
but what they conceal is vital.'

(Prof. Aaron Levenstein in his farewell lecture, 1981)

For easier reading, the results were separated in three chapters according to each assessment. Hence, the first subchapter addresses the results from the baseline assessment; the second subchapter is dedicated to the follow-up results at six months, and the third subchapter details the results after one year. A chapter with supplementary analysis and a chapter with case reports of selected patients of interest complement these main chapters.

To avoid confusion, the study design should be briefly mentioned again at this point. The baseline assessment included a screening, full language assessment and a MRI scan. The follow-up assessment, conducted six months after admission to the stroke unit, only involved a repeat of the language assessment. After one year from symptom onset, some patients were re-scanned and administered a repeated language screening.

The current subchapter is dedicated to the investigation of our initial baseline measures and their potential correlation with aphasia severity and specific language subscales.

7.1   Patients

18 first-ever left-hemispheric stroke patients with complete baseline assessment (12 males; mean age 63.39 years±18.44 years; age range 28-87 years) were included in this study (**Table 13** for individual demographics).

7.2   Demographics, language, lesion, and clinical factors

Demographical data. A correlation analysis showed that age and sex are not significantly associated with initial aphasia severity (age: r=.65, *p*=.797; sex: r=.045, *p*=.858; please see **Table 13** for raw data).

Possible gender differences were analysed with an independent *t-test* analysis. No gender differences were established for aphasia severity ($t_{(16)}$= −.087, *p*=.93). The two categorical variables sex and fluency were also not significantly related (Fischer's exact *p*=1.0).

ID	Sex	Age[1]	Ethnicity	rTPa	Aphasia type (screening)	Aphasia type (Baseline)	Aphasia type (Follow-up)	Baseline severity (AQ)	Longitudinal severity (AQ)	Infarct volume (nr of voxels)	DoA-screen (days)	DoA-BAQ (days)	DoA-MRI (days)	DoA-FAQ (days)
01	F	87	White British	Yes	Wernicke	Anomic	Recovered	75.90	95.20	2634	3	8	9	148
02	M	28	White Irish	No	Global	Transcortical motor	Recovered	45.00	96.20	123495	8	8	6	229
03[B]	M	72	White Irish	Yes	Transcortical motor	Transcortical motor	Anomic	67.00	81.40	6575	2	2	10	175
04[B]	M	70	White British	Yes	Broca	Broca	Anomic	42.00	91.90	15531	3	5	5	193
05[B]	F	69	White British White	Yes	Broca	Global	Anomic	11.50	73.30	20382	1	5	5	183
06[B]	F	81	British	No	Wernicke	Anomic	Anomic	79.50	87.90	2735	2	5	24	194
07[B]	M	75	White British White	No	Wernicke Transcortical motor	Wernicke	Wernicke	15.40	73.50	82635	5	5	7	188
08[B]	F	44	British Black	No		Broca	Anomic	58.40	87.20	1173	2	3	4	215
09[B]	M	59	Caribbean White	Yes	Broca	Broca	Anomic Transcortical motor	32.80	81.00	28779	3	17	11	217
10[B]	M	50	British Black	Yes	Global	Global		4.70	83.10	11705	2	1	4	221
12	F	71	Caribbean White	Yes	Broca	Global	Anomic	21.6	69.70	46002	3	5	11	206
13[B]	M	44	British British	Yes	Broca	Anomic	Recovered	79.16	95.60	3434	1	1	20	180
14*	M	86	White White	Yes	Conduction	Conduction	n/a	60.83	n/a	7756	2	2	2	n/a
15[B]	M	49	British British	Yes	Broca	Broca	Anomic	19.20	89.20	11234	15	6	15	378
16*	M	89	White White	Yes	Broca	Global	n/a	17.60	n/a	8261	2	17	17	n/a
17	M	79	British White	No	Broca	Broca	Anomic	59.00	81.10	411	2	2	15	183
18	F	44	British Indian	Yes	Broca	Broca	Broca	6.03	92.20	10801	3	3	9	127
19	M	44	British	Yes	Anomic	Anomic	Anomic	78.30	92.30	5666	3	3	8	161
MEAN(SD)		63.39(18.44)									3.44(3.29)	5.44(4.69)	10.11(6.00)	199.87(54.71)

[1] Age is shown in years
* No longitudinal data available
B) Follow-up assessment at one-year post stroke is available
F: female, M: male, rTPA: thrombolysis, DoA: date of admission, AQ: Aphasia Quotient, MRI: magnetic resonance imaging

Table 14   WAB-R scaled composite section scores and raw scores stratified by gender.

	BASELINE			
	♀		♂	
	n	Mean (SD)	n	Mean (SD)
Total AQ score (0-100)	6	42.19(13.50)	12	43.42(7.41)
AQ scaled composite section scores				
Spontaneous speech (0-20)	6	8.33 (3.07)	10	7.20(1.50)
Comprehension (0-10)	6	6.03(.94)	10	5.50(.915)
Repetition (0-10)	6	4.30(1.25)	10	3.73(1.25)
Naming (0-10)	6	4.02(1.39)	10	2.56(.92)
Raw scores				
Information content (0-10)	6	4.83(1.38)	10	3.90(1.02)
Fluency (0-10)	6	3.17(1.72)	10	3.10(0.90)
Comprehension (0-60)	6	39.00(5.90)	10	42.30(5.74)
Auditory recognition (0-60)	6	38.33(6.14)	9	40.11(5.74)
Sequential commands (0-80)	6	43.33(11.37)	9	37.11(8.51)
Repetition (0-100)	6	42.00(12.48)	10	37.30(12.51)
Naming (0-100)	6	28.00(9.13)	10	16.80(6.84)
Semantic fluency (0-20)	6	2.33(1.31)	9	1.22(0.60)
Phonemic fluency (extra)	5	0.60(0.60)	7	2.43(1.38)
Sentence completion (0-10)	6	5.17(2.04)	9	4.56(1.22)
Responsive speech (0-10)	6	4.33(1.96)	9	4.00(1.24)

Language factors. At baseline, 12 patients were classified with non-fluent aphasia (i.e. Broca-type) and six patients were classified with fluent aphasia (i.e. Wernicke-type). Independent t-test analysis revealed that the non-fluent aphasia group was associated with a lower (i.e. more severe) baseline severity than fluent aphasias ($AQ_{non-fluent}$=32.08±21.85, AQ_{fluent}=64.85± 25.23; $t_{(16)}$= 2.85, p=.011). The was no age difference between non-fluent (60.33±17.953 years) and fluent (69.50±20.206 years) groups ($t_{(16)}$= −.994, p=.335).

The overall aphasia severity (AQ) was significantly correlated with all subscales of the WAB-R except for comprehension (**Table 15**), which is to be expected given that these measures constitute the overall aphasia quotient (see introduction).

Table 15   Correlation between baseline WAB-R raw scores and the total AQ at baseline.

WAB-R raw scores	Baseline AQ
Content	r=.830**
Grammar	r=.684**
Comprehension	r=.381, *ns*
Auditory word recognition	r=.645**
Sequential commands	r=.531*
Repetition	r=.861**
Naming	r=.763**
Fluency (semantic)	r=.851**
Fluency (phonemic)	r=.745**
Sentence completion	r=.882**
Responsive speech	r=.927**

** Correlation is significant at 0.01 level (2-tailed)
* Correlation is significant at 0.05 level (2-tailed)
ns, Correlation is not significant
AQ, Aphasia Quotient

The individual subscales of the WAB-R were entered into a regression analysis to investigate whether their influence on the baseline severity is independently predictive. The linear multiple regression model defined the baseline aphasia severity as dependent variable and included four continuous baseline variables: the WAB-R scaled composite section scores for spontaneous speech, naming, comprehension, repetition, and semantic fluency. The baseline model was significant ($F_{(4,11)}$=130.179, p<.000) and revealed repetition (β=.324, t(4.696), p<.001), spontaneous speech (β=.410, t(5.024), p<.000) and naming (β=.273, t(3.060), p<.011) as predictors for the initial severity.

Taxonomical classification changes were also recorded as is shown in **Figure 69**. It is apparent that in the time between the bedside screening and the full baseline assessment many patients regained some of their language capacities, which is for example represented by a marked by the transition from severe to milder forms of aphasia. For example, patients classified as anomic increased between the time of screening (5.56%) and baseline (22.22%); likewise the number of patients with Broca's aphasia decreased (screening 50%, baseline 33.33%).

Six months after symptom onset most patients were classified as anomic (68.75%), and three patients (18.75%) made a full recovery in terms of their language

functions (i.e. AQ≥93.8). The remaining 12.5% included one conduction aphasia patient and one transcortical motor aphasia patient.

Aphasia severity, gender and mean age of each taxonomical group is detailed below in **Table 16**. Only one patient each was classified as Wernicke or conduction aphasia.

Table 16   Baseline taxonomy stratified by of aphasia severity (AQ), gender breakdown and age.

		AQ		Male	Age	
	n (%)	mean	SD	%	mean	SD
Global	4 (22.2)	13.85	7.379	50	69.75	15.945
Broca	7 (38.9)	35.12	19.673	71.4	55.57	14.223
Transcortical motor	2 (11.1)	56	15.556	100	50	31.113
Wernicke	1 (5.6)	15.4	.	100	75	.
Conduction	1 (5.6)	60.83	.	100	85	.
Anomia	3 (16.7)	78.5	2.271	33.3	76	14.177
Total	18 (100)	40.27	26.162	66.7	64.22	17.758

Lesion factors. A Kolmogorov–Smirnov test for normality showed that lesion size is not normally distributed in our sample ($D_{(18)}$=.297, p<.000), hence non-parametric tests were used to further investigate the influence of lesion size. A Spearman correlation between lesion size and the initial severity was highly significant (r= –.637, *p*<.004). This negative correlation implies that bigger lesions are associated with a lower AQ score, which means more severe language impairments. Lesion size was not markedly different between sexes (U=44.00, *p*=.494).

Clinical factors. The surrogate measure of clinical severity was the NIHSS, a 15-item neurologic examination ranging from 0-30, whose scores were normally distributed within this sample ($D_{(17)}$=.140, *p*=.20). The NIHSS scores in our sample were obtained on admission (i.e. not simultaneously with the language assessments) and ranged from 1-27 with a mean score of 12.38±8.11. Stroke severity was not significantly different between sexes (NIHSS♀ 10.33±9.4, NIHSS♂ 14.55±7.75; $t_{(15)}$=-.995, *p*=.336). Stroke severity was not correlated with the initial

language severity (r=−.059, *p*=.822). A scatterplot of the NIHSS scores against the baseline severity (AQ) indicates a curvilinear U-shaped association (**Figure 58**).
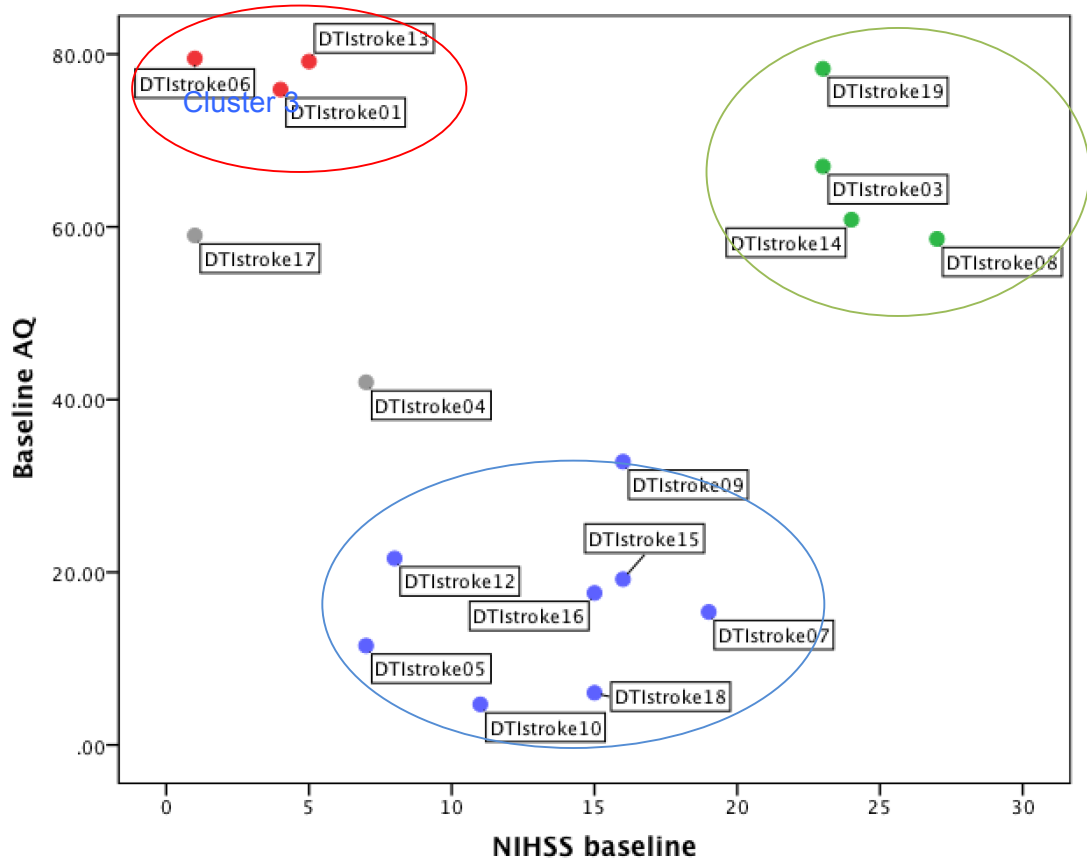
Figure 58   Scatterplot of baseline stroke severity (NIHSS, 0-30) against baseline aphasia severity (AQ, 0-100)

Red dots indicate patients with relatively good language and minimal stroke severity. This group is mainly constituted of anomic patients. Grey dots indicate two Broca patients. Blue dots indicate the more heterogeneous aphasia group with severely impaired language and severe stroke impairments. Green dots indicate patients with very severe stroke symptoms and moderate language impairments.

Looking at the scatterplot of stroke severity against the baseline language severity, the cluster with the high AQ and low NIHSS (**Figure 58**, red) includes all but one patient that were classified as anomic aphasias on the baseline assessment (**Table 13**). Patients 04,17 were both Broca aphasics (**Figure 58**, grey). The low AQ-mid range NIHSS cluster comprised of a heterogeneous aphasia group: Global (4), Broca (3), Wernicke (1) aphasias (**Figure 58**, blue). The cluster scoring high on both scales included: anomia (1), transcortical motor, conduction, and Broca aphasias (**Figure 58**, green). The Broca patient in the last cluster is the only Broca

patient in the sample who was initially classified as 'transcortical motor' on the screening (**Table 13**).

In a next step, group lesion overlay maps were calculated for each cluster indicated in red, blue and green in the scatterplot (**Figure 59**). Upon visual inspection it can be appreciated that group 1 (i.e. red cluster) has its maximal overlay in the posterior arm of the internal capsule bordering onto the posterior thalamus and the posterior lentiform nucleus; whereas the extent of maximal overlay is much bigger in group 2 (i.e. blue cluster), reaching from the middle frontal gyrus down to the middle portions of the temporal lobe encompassing the basal ganglia, thalamus, capsules, and genu corpus callosum. For group 3 (i.e. green cluster) the maximal overlay is in the subcortical structures including the putamen, the globus pallidus, the internal capsule, the posterior lateral aspects of the thalamus, and the caudate nucleus (**Figure 59**).
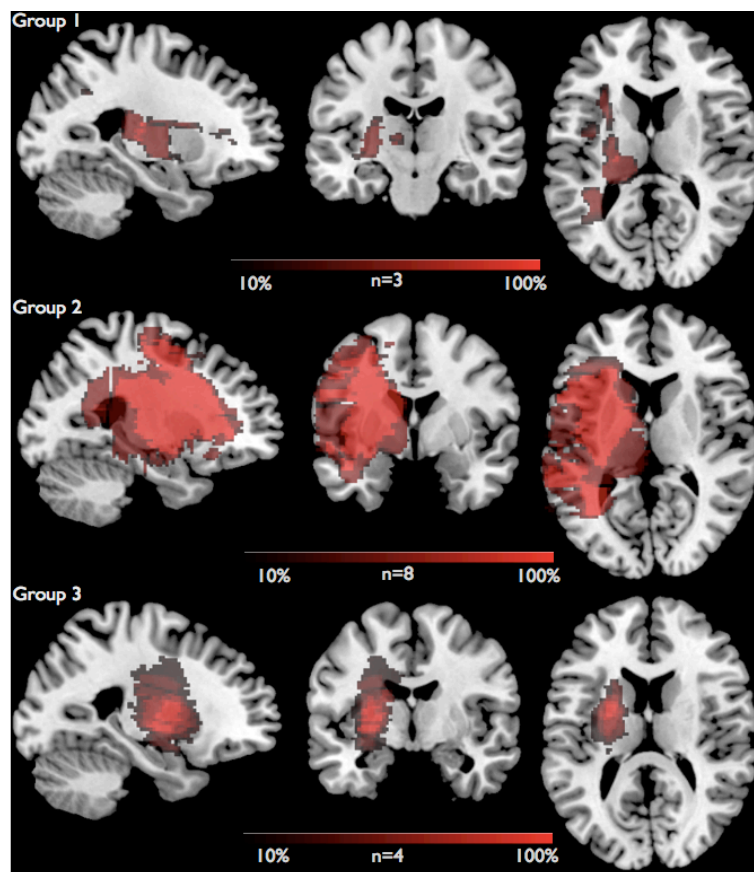
Figure 59   Lesion overlapping for the baseline NIHSS-AQ groups shown in figure 59

Other relevant clinical measure besides stroke symptom severity is the presence of small vessel disease (SVD) as determined by radiological report. SVD was obtained

categorically and an independent t-test revealed no differences between the group with SVD and without for the initial aphasia severity (SVD=56.10±27.98, no-SVD=34.67±24.63; $t_{(16)}$=−1.708, p=.107).

7.3   Structural MR imaging

7.3.1   Visual lesion analysis on MR imaging contrasts (T2 FLAIR, DWI, ADC)

All images were processed for visualisation by converting the original DICOM files obtained from the 3T MRI scanner into software readable files (i.e. NIFTI or ANALYZE). The diffusion-weighted images (DWI) and apparent diffusion coefficient (ADC) maps are automatically obtained from the pre-processing steps for diffusion tensor imaging tractography as described in the methods chapter (subchapter 6.7.1).

A summary of relevant neuroimaging scans of all patients (n=18) is provided in **Figure 60**. This figure shows that i) a lesion and lesion extent are easier identified on DWI over other structural imaging contrasts and ii) that lesion evolution can be staged based on the appearance on ADC contrast were lesions are either hyper- or hypointense.

The signal intensity of the ADC maps suggests a spectrum from strongly hypointense to strongly hyperintense. This reflects the varying delay of scanning times after symptom onset (see **Table 13**). As described in the neuroimaging chapter (subchapter 5.1.6.3), the ADC measure drops immediately after vessel occlusion rendering the ischemic region hypointense. This initial signal drop is followed by an apparent signal normalisation (pseudonormalisation) and subsequent signal elevation. It can be appreciated that patient 10 presents with hypointense ADC signal whilst patient 14 presents with an elevated ADC signal. This indicates that the evolution of the lesioned tissue progressed to different stages in those two thrombolysed patients at the time of scanning.

A summary of the anatomical locations of visually identified lesions together with their frequency is shown in **Table 17**. The most commonly lesioned areas are the frontal lobe gyri and subcortical structures. The corresponding scans can be found

in **Figure 60**. Given the two-dimensionality of the brain scans presented herein, the extent of some lesions cannot be entirely appreciated.

Table 17   Lesion location summary (n=18) stratified by lobar and subcortical structures

Region of Interest (left hemisphere)	Total patients	Patient ID
FRONTAL LOBE		
Inferior frontal gyrus	6	02,10,15,16,17,18
Middle frontal gyrus	5	02,03,15,16,18
Superior frontal gyrus	3	02,06,15
Operculum	5	04,05,09,10,15
Precentral gyrus	3	12,15,16
PARIETAL LOBE		
Post central gyrus	1	04
Inferior lobus	1	05
TEMPORAL LOBE		
Superior temporal gyrus	3	03,07, 13
Middle temporal gyrus	1	13
Anterior temporal gyrus	1	10
Insular anterior/posterior	9/6	03,04,05,06,09, 13,16,17,18/04,06,08,09,13,18
OCCIPITAL LOBE		
	n/a	n/a
SUBCORTICAL STRUCTURES		
Putamen	10	02,03,07,08,09,10,13,14,18,19
Globus pallidus	9	02,03,07,08,10,13,14,18,19
Caudate nucleus	5	02,03,13,14,18
Thalamus	2	01,18
External capsule	5	03,13,14,18,19
Internal capsule (posterior arm)	7	01,04,08,13,14,18,19
Corona radiata	7	04,07,08,09,17,18,19
Periventricular abnormalities	4	06,07,10,16
Small vessel disease	5	01,03,06,07,16
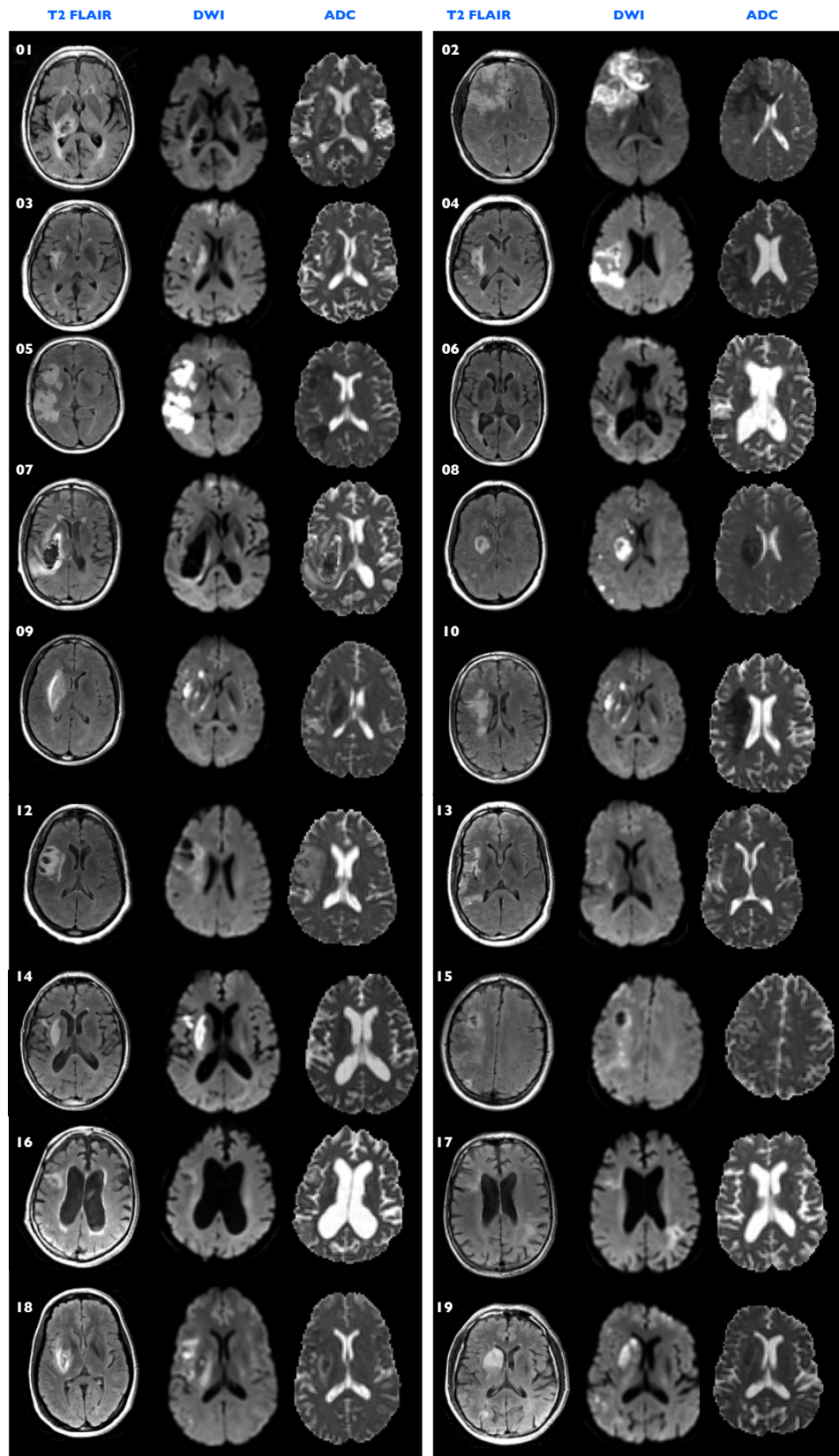
Figure 60   Native, acute stage MRI contrasts of individual subjects (n=18)

All scans are shown in axial plane at the level of maximum infarct volume for each patient and hence the slice level might differ between patients

7.3.2   Advanced lesion analysis

7.3.2.1 Voxelwise 'topological' lesion-deficit analysis

For group comparison, lesion analysis was performed in 17 patients (one of the 18 patients had to be excluded as no T1-weighted image was acquired).

As a first step, percentage overlay maps were calculated from all 17 subjects using mricron. This analysis demonstrated that the most consistent overlay was in the inferior frontal gyrus, the internal and external/extreme capsules, the claustrum, the putamen, the medial thalamic nuclei, and the peri-insular white matter (**Figure 61**).
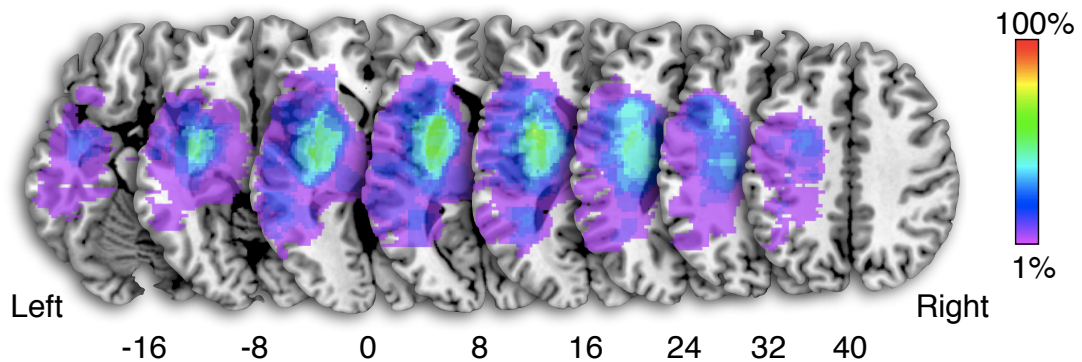
Figure 61   Percentage lesion overlay map (0-100%) for the acute phase

This figure demonstrates the lesion overlay of all recruited subjects. The highest overlay is seen in the peri-insular white matter of the external/extreme capsules and internal capsule, the claustrum, striatum and lateral thalamus. At the cortical level the lesion overlay was highest in the insula and the perisylvian cortex..

In the next step, a regression analyses was performed to identify lesion topology that might be predictive of a) overall aphasia severity and b) repetition deficits at baseline.

This was achieved with a non-parametric mapping (NPM) linear regression lesion analysis based on a voxel-based lesion-symptom mapping approach as detailed in Chapter 6. The NPM regression analysis only took into account regions that were damaged in at least 10% of the patients.

The first model was defined to identify the voxel associated with more severe aphasia at baseline. Hence, baseline severity of aphasia was set as the dependent variable and the following four regressors were added into the model: stroke severity (continuous), age (continuous), gender (dichotomous), and thrombolysis treatment (dichotomous). The regression revealed the highest predictive values in the white matter of the middle and inferior frontal gyri and the anterior insular ribbon

(**Figure 62**). This result suggests that lesions to this area are predictive of initial aphasia severity at baseline.
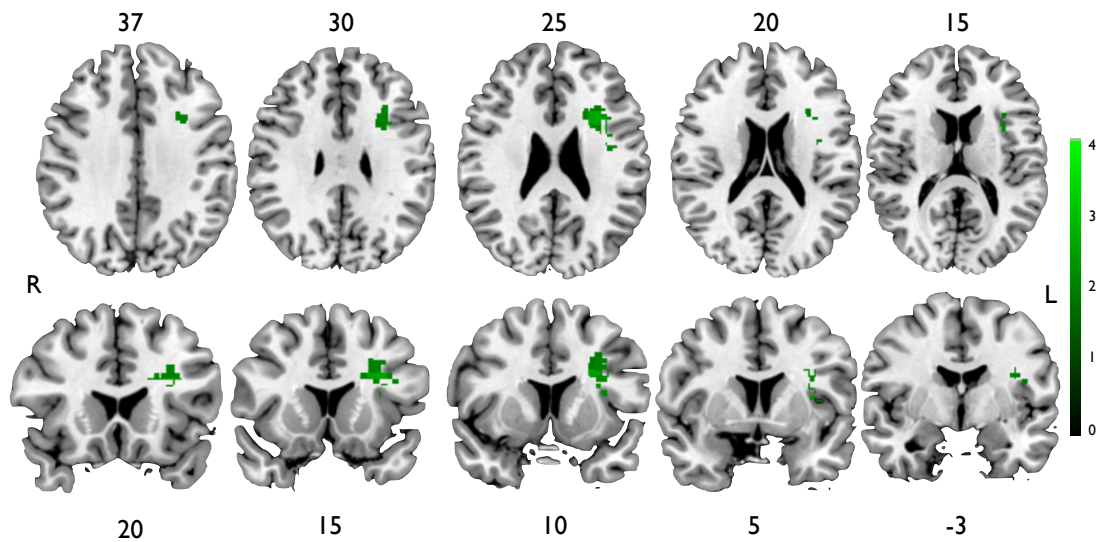
Figure 62   Lesion-symptom analysis for aphasia severity at baseline

The results shown are correct for confounding variables as defined in the above paragraph. The shown results are z-transformed (reflected in the scalar colouring) with a significance level of *p*<.001. Results shown are corrected for multiple comparisons with permutation testing.

The second model investigated the relation between repetition impairment at baseline and relevant voxels. Baseline variables entered into the model were the repetition score together with age, sex, thrombolysis and stroke severity (NIHSS). The results indicate that lesions to the white matter of the middle and inferior frontal gyri, peri-insular regions as well as the temporal stem are predictive of initial repetition deficits at baseline (**Figure 63**).
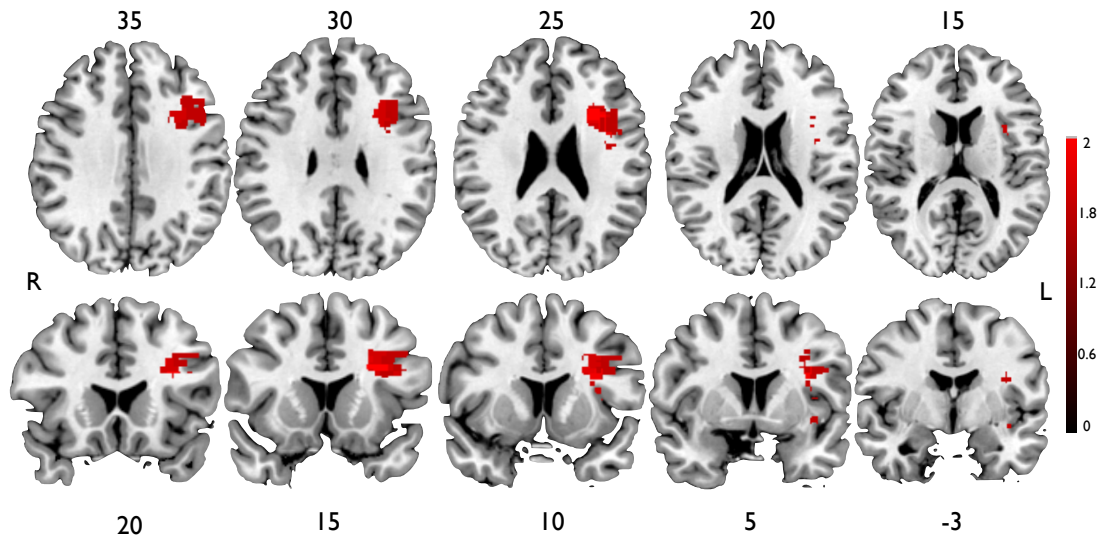
Figure 63   Voxel-based lesion-symptom mapping for repetition deficits and corresponding voxels

The results shown are correct for confounding variables as defined in the above paragraph. The shown results are z-transformed (reflected in the scalar colouring) with a significance level of *p*<.05. Results shown are corrected for multiple comparisons with permutation testing.

7.4   DTI analysis

7.4.1   DTI Atlas-based 'hodological' analysis

As a first step, the aforementioned atlas (available online: www.natbrainlab.com) was used as overlay on the acute lesion maps **Figure 61**. This approach has been used in our recent publications (Catani, Dell'Acqua, Bizzi, et al. 2012a; Thiebaut de Schotten, Tomaiuolo, et al. 2012c). This approach identified that in the acute stage, all perisylvian pathways had a minimum overlay with the group lesion map of 2%. However, the lesion overlay maximum (up to 90%) was centred on the anterior and long segment in particular. However the overlap often reaches much higher percentages (**Figure 64**). The affected pathways are the left-hemispheric inferior fronto-occipital fasciculus, the anterior commissure, the internal capsule and all three segments of the arcuate fasciculus, corpus callosum, cingulum, inferior longitudinal fasciculus and the left fornix.
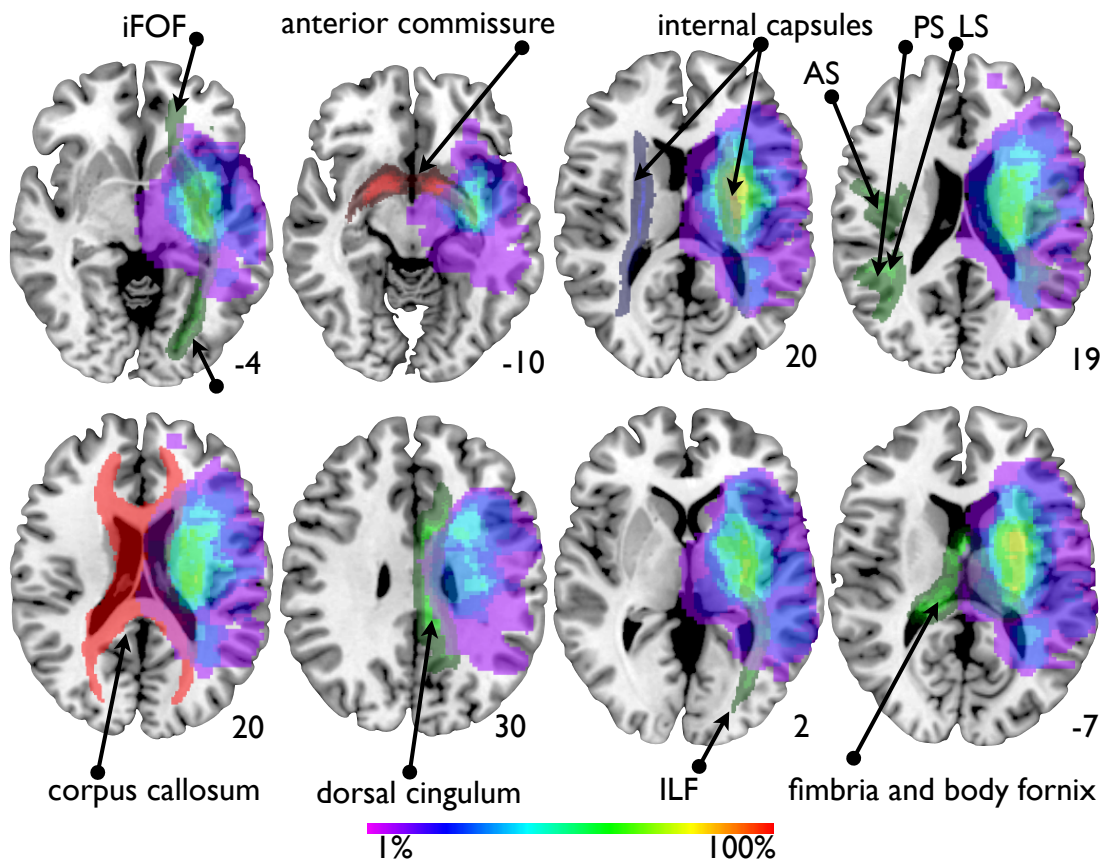
Figure 64   DTI Atlas overlay on acute left-hemispheric lesion percentage maps
(n=17)

The colour coding of pathways is in accordance with the directional FA-colour coding
(red=commissures, green=association, blue=projections). iFOF, inferior fronto-occipital
fasciculus; AS, anterior segment; PS, posterior segment; LS, long segment; ILF, inferior
longitudinal fasciculus. Where tracts cannot be appreciated on the lesioned hemisphere they
are shown on the right hemisphere for reference (internal capsule and arcuate segments).

It can be assumed from the lesion location that the fronto-parietal connections,
namely superior longitudinal fasciculi (SLFs), were damaged as well, however, they
are not reconstructable with DTI and no atlas is yet available online for overlay
investigations. The SLF has been implicated in visuo-spatial attention (Thiebaut de
Schotten, Dell'Acqua, et al. 2011a).

7.4.2   Perisylvian pathway reconstructions

Individual DTI reconstructions of the three arcuate segments were dissected in all
patients (n=18) with three males and one woman presenting without the left anterior
segment (patients 04, 07, 12, 15), two males without right long segment (patients
10, 17), and one male without right posterior segment (patient 14) as well as one
woman without left long segment (patient 12; **Figure 65**).

dorsal view   left-lateral view   right-lateral view
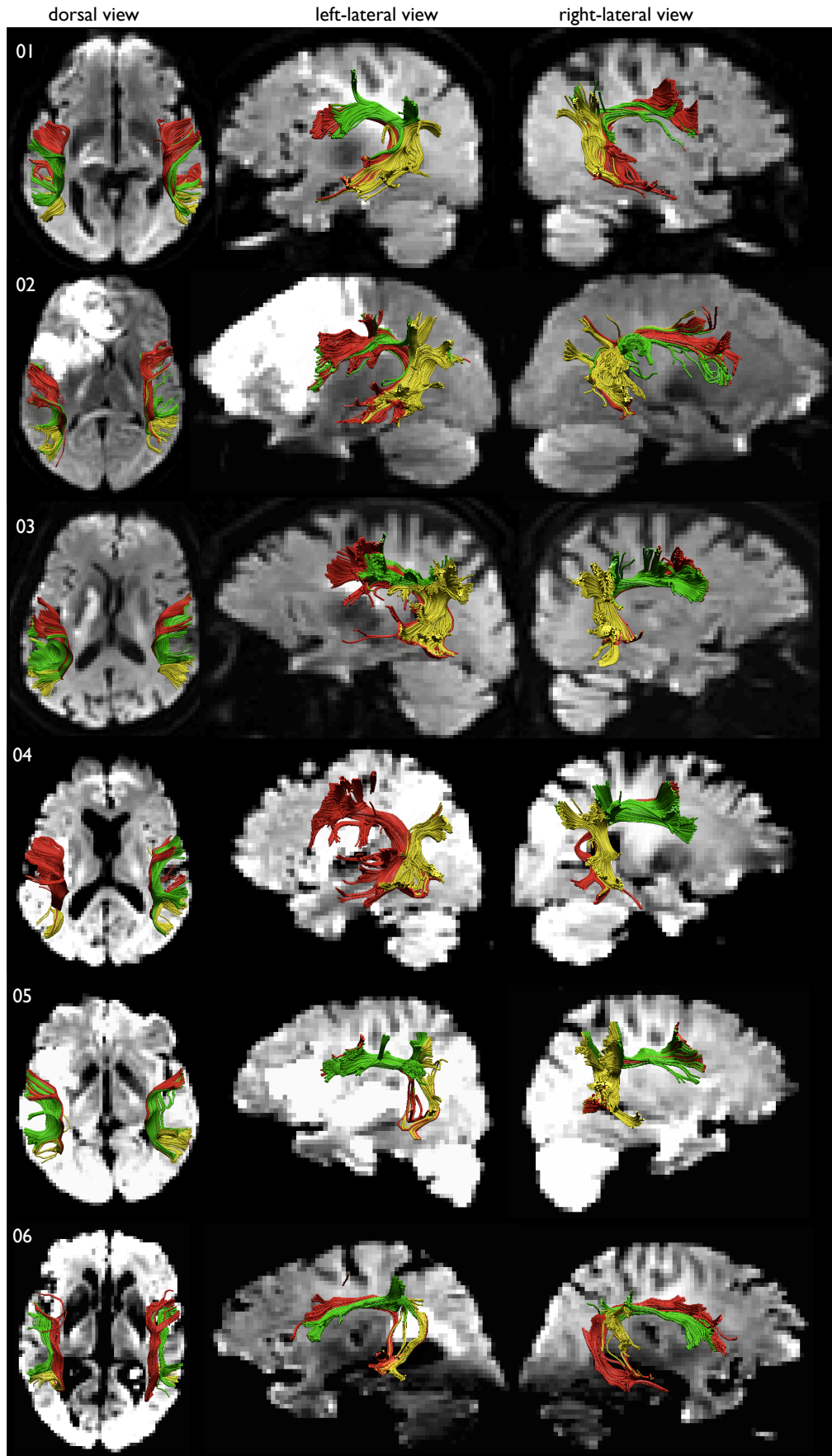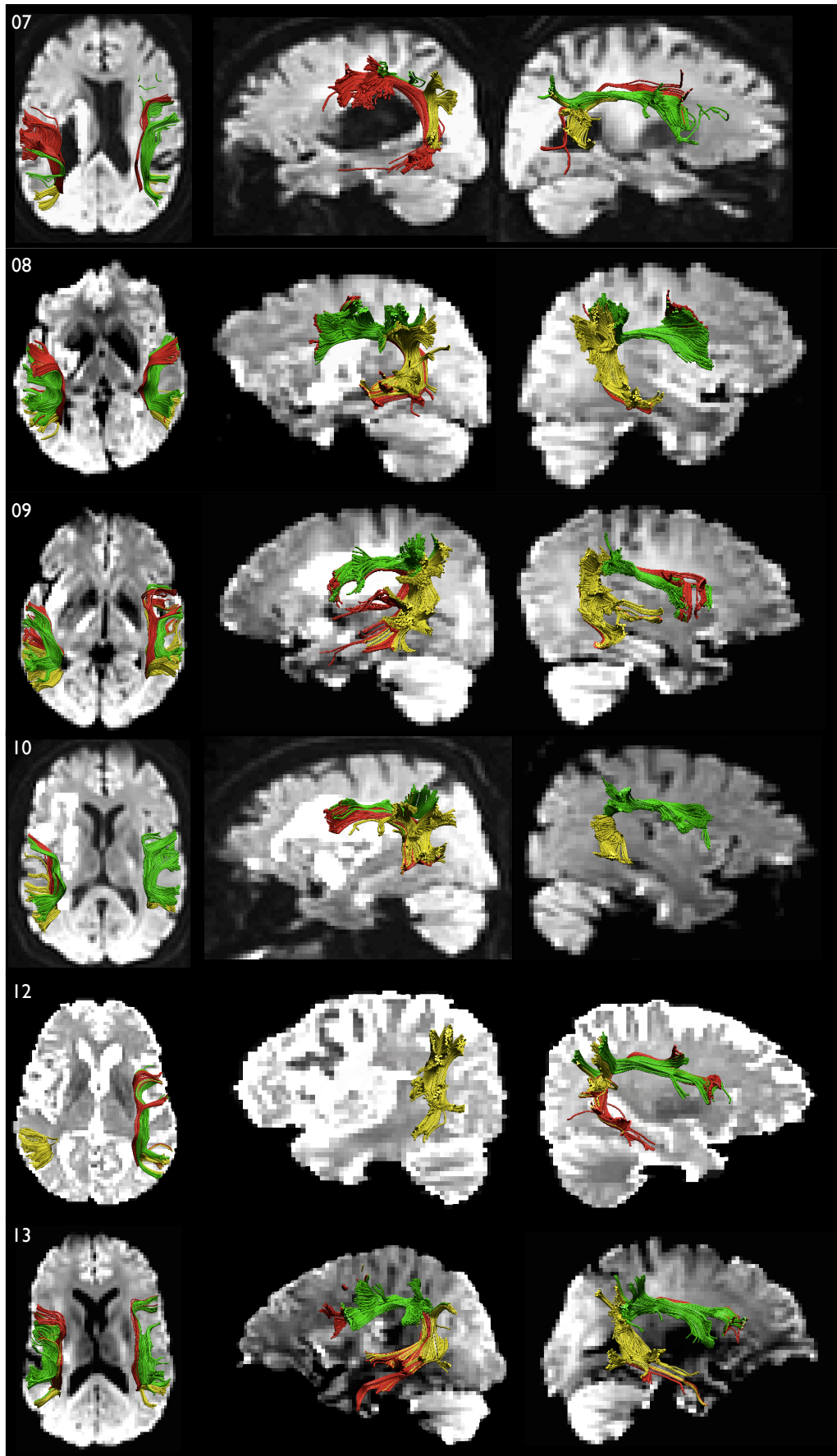
See overleaf.

See overleaf.
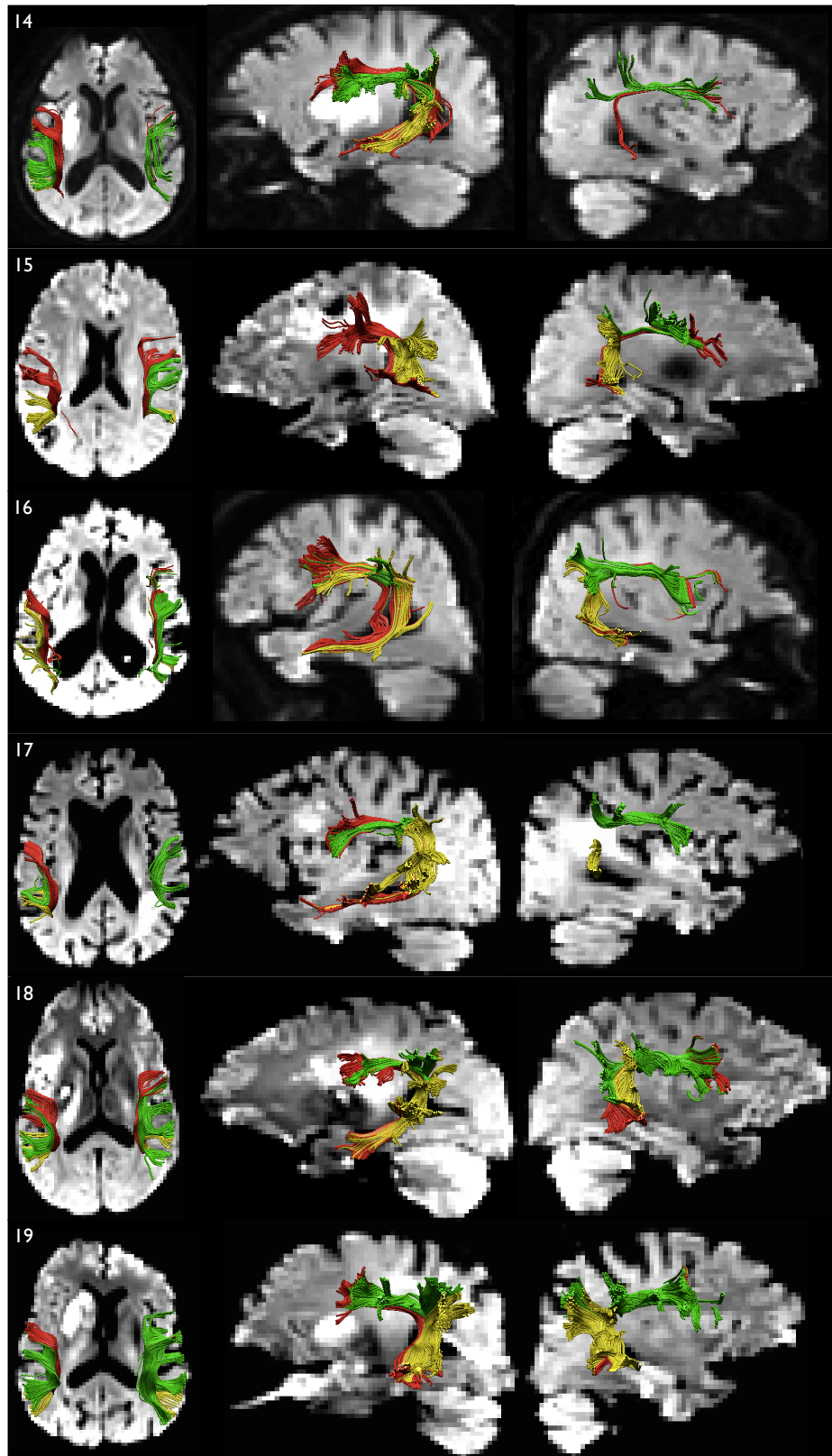
Figure 65   DTI reconstruction of the three segments of the arcuate fasciculus

Individual diffusion tensor imaging (DTI) tractography reconstructions of the anterior (green), posterior (yellow) and long segment (red) of the left and right arcuate fasciculus post stroke. The arcuate is shown in all patients (n=18) in the dorsal, left-lateralised, and right-lateralised

view. The background image is the native diffusion-weighted scan of each individual patient to facilitate the identification of the lesion and to identify whether the lesion is encroaching on the perisylvian pathways.

7.4.2.1 Indices of microstructure analyses

Measures obtained from the dissections of the three segments in the left and right hemisphere as shown in **Figure 65** were correlated and compared with regards to the behavioural data and possible gender differences.

7.4.2.1.1 Trace or Mean diffusivity (MD)

Independent t-test analyses between the sexes as well as between the thrombolysis groups revealed no differences in mean diffusivity in any of the segments (**Table 18**).

Table 18   Independent t-test for mean diffusivity in the three arcuate segments.

Mean Diffusivity in segments		n	Mean (SD)	*t*	df	*p*
Left Anterior segment (L_AS)	*Female*	5	.000725(.000875)	.411	13	.688
	Male	10	.000710(.0000604)			
	No rtPA	5	.000709(.0000552)	−.222	13	.823
	rtPA	10	.000718(.0000759)			
Right Anterior segment (R_AS)	*Female*	6	.000726(.0000763)	.242[1]	6.2	.766
	Male	12	.000718(.0000372)			
	No rtPA	5	.000735(.0000495)	.739	16	.471
	rtPA	13	.000715(.0000527)			
Left Posterior segment (L_PS)	*Female*	6	.000696(.0001228)	−1.065	16	.303
	Male	12	.000744(.0000723)			
	No rtPA	5	.000785(.0000960)	1.725	16	.104
	rtPA	13	.000706(.0000833)			
Right Posterior segment (R_PS)	*Female*	6	.000726(.0000477)	.711	16	.487
	Male	12	.000662(.0002118)			
	No rtPA	5	.000725(.0000171)	.609	16	.551
	rtPA	13	.000668(.0002057)			
Left Long segment (L_LS)	*Female*	5	.000689(.0001081)	−.075	15	.941
	Male	12	.000693(.0000848)			
	No rtPA	5	.000737(.0000829)	1.415	15	.178
	rtPA	12	.000672(.0000872)			
Right Long segment (R_LS)	*Female*	6	.000706(.0000609)	.839	15	.414
	Male	12	.000631(.0002120)			
	No rtPA	5	.000561(.0003170)	−.961[1]	4.0	.390
	rtPA	12	.000698(.0000449)			

[1] Levene's test for equality of variance was significant hence the adjusted *t* and *p* values were used.

At baseline, the WAB-R scaled composite section score for spontaneous speech positively correlated with the mean diffusivity in the left anterior and long segment (r=−.62, *p*=.024; r=−.56, *p*=.031). However, none of these correlations survived multiple comparison with the adjusted p value *p*=.0041.

7.4.2.1.2 Diffusivity along ellipsoidal axes (radial and axial diffusivity)

Independent t-test analyses between the sexes as well as between the thrombolysis groups revealed no differences in perpendicular diffusivity in any of the segments (**Table 19**).

Table 19   Independent t-test statistics for perpendicular diffusivity in the three arcuate segments.

Perpendicular Diffusivity in segments		n	Mean (SD)	*t*	df	*p*
Left Anterior segment (L_AS)	*Female*	5	.000567(.0000978)	.783	14	.447
	Male	11	.000502(.0001728)			
	No rtPA	5	.000511(.0000483)	.504	14	.622
	rtPA	11	.000509(.0001833			
Right Anterior segment (R_AS)	*Female*	6	.000537(.0000826)	.155[1]	6.6	.882
	Male	12	.000532(.0000466)			
	No rtPA	5	.000553(.0000680)	.874	16	.395
	rtPA	13	.000526(.0000555)			
Left Posterior segment (L_PS)	*Female*	6	.000551(.0001037)	–.763	16	.457
	Male	12	.000581(.0000646)			
	No rtPA	5	000625(000911)	1.97	16	.066
	rtPA	13	.000550(.0000645)			
Right Posterior segment (R_PS)	*Female*	6	.000564(.0000603)	.768	16	.454
	Male	12	.000509(.0001671)			
	No rtPA	5	.000571(.0000479)	.812	16	.429
	rtPA	13	.000511(.0001620)			
Left Long segment (L_LS)	*Female*	6	.000436(.0002299)	–.800[1]	5.4	.457
	Male	12	.000513(.0000676)			
	No rtPA	5	.000553(.0000779)	1.25	16	.231
	rtPA	13	.000462(.0001538)			
Right Long segment (R_LS)	*Female*	6	.000504(.0000592)	1.215	16	.242
	Male	12	.000405(.0001918)			
	No rtPA	5	.000387(.0002205	–.815	16	.427
	rtPA	13	.000458(.0001438)			

[1] Levene's test for equality of variance was significant hence the adjusted *t* and *p* values were used.

At baseline no correlations were evident between perpendicular diffusivity and overall language severity (L_AS: r=.15, *p*=.642; R_AS: r=.14, *p*=.663; L_PS: r=.187,

p=.561; R_PS: r=−.194, *p*=.545; L_LS: r=.304, *p*=.337; R_LS: r=.568, *p*=.054). Likewise, no correlations were found with the scaled composite section scores of the WAB-R.

For axial diffusivity, independent t-test analyses between the sexes as well as between the thrombolysis groups revealed no differences in any of the segments (**Table 20**). At baseline, no correlations were found between the initial axial diffusivity and language severity (L_AS: r=.345, *p*=.272; R_AS: r=.412, *p*=.183; L_PS: r=.210, *p*=.512; R_PS: r=−.136, *p*=.673; L_LS: r=.307, *p*=.331; R_LS: r=.303, *p*=.339).

Table 20   Independent t-test statistics for axial diffusivity in the three arcuate segments

Axial Diffusivity in segments		n	Mean (SD)	t	df	p
Left Anterior segment (L_AS)	*Female*	6	.000868(.004312)	.67	16	.948
	Male	12	.000854(.0004079)			
	No rtPA	5	.001025(.0000802)	1.729[1]	13.7	.206
	rtPA	13	.000795(.0004605)			
Right Anterior segment (R_AS)	*Female*	6	.001104(.000656)	.432	16	.671
	Male	12	.001092(.0000553)			
	No rtPA	5	.001100(.0000450)	.207	16	.839
	rtPA	13	.001094(.0000629)			
Left Posterior segment (L_PS)	*Female*	6	.000985(.0001750)	−1.325	16	.204
	Male	12	.001071(.0001013)			
	No rtPA	5	.001104(.0001358)	1.260	16	.226
	rtPA	13	.001018(.0001274)			
Right Posterior segment (R_PS)	*Female*	6	.001049(.0000420)	.622	16	.543
	Male	12	.000969(.0003090)			
	No rtPA	5	.001031(.000616)	.364	16	.720
	rtPA	13	.000982(.0002973)			
Left Long segment (L_LS)	*Female*	5	.001020(.0001440)	−.427	15	.675
	Male	12	.001053(.0001397)			
	No rtPA	5	.001106(.0001032)	1.244	15	.233
	rtPA	12	.001017(.0001448)			
Right Long segment (R_LS)	*Female*	6	.001111(.000732)	.722	15	.482
	Male	11	.001009(.0003379)			
	No rtPA	5	.000910(.0005111)	−.835[1]	4.0	.450
	rtPA	12	.001101(.0000562)			

[1] Levene's test for equality of variance was significant hence the adjusted *t* and *p* values were used.

7.4.2.1.3 Fractional Anisotropy (FA)

Independent t-test analyses between the sexes as well as between the thrombolysis groups revealed no differences in fractional anisotropy in any of the segments (**Table 21**).

At baseline, no correlations were found between overall aphasia severity (AQ) and fractional anisotropy in any of the segments (L_AS: r=−.116, *p*=.749; R_AS: r=−.09, *p*=.805; L_PS: r=.00, *p*=1.0; R_PS: r=−.119, *p*=.744; L_LS: r=.00, *p*=.999; R_LS:

r=.253, *p*=.481). No correlation was found between FA and the WAB-R scaled composite section scores.

Table 21   Independent t-test statistics for fractional anisotropy measures in the three arcuate segments

Fractional Anisotropy (FA)		n	Mean (SD)	*t*	df	*p*
Left Anterior segment	*Female*	5	.393346(.0631921)	.32[1)]	5.0	.976
	Male	10	.392389(.0313735)			
	No rtPA	5	.393906(.0338705)	.075	13	.941
	rtPA	10	.392109(.0474167)			
Right Anterior segment	*Female*	6	.449996(.0509789)	.123	16	.904
	Male	12	.446966(.0484112)			
	No rtPA	5	.432450(.0692605)	−.848	16	.409
	rtPA	13	.453947(.0386805)			
Left Posterior segment	*Female*	6	.365534(.0529254)	−.654	16	.523
	Male	12	.379759(.0384978)			
	No rtPA	5	.355889(.0688308)	−.834[1)]	4.5	.446
	rtPA	13	.382375(.0283341)			
Right Posterior segment	*Female*	6	.391011(.0487201)	.449	16	.659
	Male	12	.366701(.1262992)			
	No rtPA	5	.374259(.0737695)	−.013	16	.990
	rtPA	13	.375015(.1182965)			
Left Long segment	*Female*	5	.415359(.0470804)	−.816	15	.427
	Male	12	.436157(.0481750)			
	No rtPA	5	.425218(.0455957)	−.263	15	.796
	rtPA	12	.432048(.0499468)			
Right Long segment	*Female*	6	.475814(.0351361)	.462	15	.651
	Male	11	.446770(.1496651)			
	No rtPA	5	.403598(.2263959)	−.745[1)]	4.0	.497
	rtPA	12	.479281(.0273152)			

1)   Levene's test for equality of variance was significant hence the adjusted *t* and *p* values were used.

7.4.2.1.4 Volumetric measures (number of voxels)

A partial correlation between the overall aphasia score at baseline and volumetric measures of all segments controlled for lesion size, thrombolysis, age and sex showed no significant association **Table 22**).

The four scaled composite section scores and the additional raw scores for fleuncy of the WAB-R were entered into the partial correlation analysis (**Table 22**). After correction the following association was significant. Comprehension was positively correlated with the right long segment.

Table 22   Partial correlations (uncorrected) between volume of the three segments and the overall baseline aphasia severity (B_AQ) and four scaled composite section scores and the additional raw score for fluency of the WAB-R

		B_AQ	SS	Comp	Rep	Nam	SF	PF
Anterior segment (AS)								
Left AS	Corr.	.406	1.09	−.003	.441	.447	.171	−.220
	p	.150	.735	.993	.151	.145	.595	.570
	df	12	10	10	10	10	10	7
Right AS	Corr.	.237	.601	−.001	.194	.465	.449	.727
	p	.414	.039	.998	.545	.128	.144	.027
	df	12	10	10	10	10	10	7
Posterior segment (PS)								
Left PS	Corr.	-.056	−.140	.093	.266	.216	−.301	−.464
	p	.848	.664	.774	.403	.501	.342	.209
	df	12	10	10	10	10	10	7
Right PS	Corr.	.235	.177	.247	.327	.383	.189	.047
	p	.418	.583	.438	.299	.219	.556	.905
	df	12	10	10	10	10	10	7
Long segment (LS)								
Left LS	Corr.	.185	.246	.532	−.002	.022	.194	.240
	p	.527	.441	.075	.994	.945	.546	.533
	df	12	10	10	10	10	10	7
Right LS	Corr.	.529	.595	.818	.436	.299	.591	.433
	p	.052	.041	.001*	.156	.346	.043	.245
	df	12	10	10	10	10	10	7

Control Variables: Thrombolysis, age, sex, lesion size
B_AQ, baseline aphasia quotient; SS, spontaneous speech; Comp, comprehension; Rep, repetition; Nam, naming; SF, semantic fluency; PF phonemic fluency
* Bonferroni corrected p-value is $p \leq 0.001$

CHAPTER 8   FOLLOW-UP ASSESSMENT (6 MONTHS)

This subchapter investigates the correlation between behavioural and neuroimaging data collected at baseline and the severity of aphasia at six months after symptom onset.

8.1   Patients

16 patients kindly made themselves available for a longitudinal language assessment (10 males; mean age 60.38 years±17.26 years; age range 28-87 years; **please see Table 13 in Chapter 7**). Two male patients (14,16) withdrew and no longitudinal data are available. Information from their families suggests that they made a full functional recovery.

8.2   Longitudinal language assessment

The very same version of the WAB-R used at baseline was re-administered after six months and measures of aphasia severity and the performance on the 32 subscales of the WAB-R were obtained (**Table 23**). Out of the 16 patients who returned, 81.25% of patients were still aphasic according to WAB-R criteria. Three patients recovered fully (AQ≥93.8).

Table 23   WAB-R scores six months from stroke stratified by gender.

	LONGITUDINAL (6 months)			
	Females		**Males**	
	n	Mean (SD)	n	Mean (SD)
Total AQ score (0-100)	6	84.25(4.23)	10	86.53(2.39)
AQ subscales				
Spontaneous speech (0-20)	6	16.00(1.53)	10	16.50(0.87)
Comprehension (0-10)	6	8.98(0.49)	10	9.43(0.15)
Repetition (0-10)	6	9.08(0.31)	10	8.92(0.34)
Naming (0-10)	6	8.07(0.51)	10	8.42(0.30)
Individual tasks				
Information content (0-10)	6	8.00(1.07)	10	8.90(0.28)
Fluency (0-10)	6	8.00(1.00)	10	7.60(0.62)
Comprehension (0-60)	6	57.00(1.55)	10	59.10(0.46)
Auditory recognition (0-60)	6	58.83(0.65)	10	59.00(0.37)
Sequential commands (0-80)	6	63.67(7.89)	10	70.60(2.75)
Repetition (0-100)	6	90.83(3.12)	10	89.20(3.41)
Naming (0-100)	6	51.50(2.95)	10	54.60(1.80)
Semantic fluency (0-20)	6	11.17(2.06)	10	9.90(1.55)
Phonemic fluency (extra)	5	13.00(5.19)	10	10.20(2.76)
Sentence completion (0-10)	6	8.33(0.62)	10	10.00(n/a)
Responsive speech (0-10)	6	9.67(0.33)	10	9.70(0.21)

Demographical data. A correlation analysis showed that aphasia severity at six months is not significantly associated with age and sex respectively (age: r=–.39, p=.15; sex: r=.09, p=.74).

Possible gender differences were analysed with an independent *t-test* analysis. At follow-up, no significant differences in aphasia severity were observed (AQ$_\male$=86.5±7.5; AQ$_\female$=84.3±10.4; $t_{(14)}$=–.510, p=0.62). Also, no significant gender difference was observed in scores on the WAB-R subscales.

Lesion factors. A Kolmogorov–Smirnov test for normality showed that lesion size was not normally distributed (D$_{(18)}$=.297, p<.000), hence non-parametric tests were

used to further investigate the influence of lesion size. No significant association was observed between initial lesion size and aphasia severity after six months (r= −.276, *p*=0.30).

Clinical factors. Initial stroke severity (NIHSS) was not correlated with the longitudinal aphasia severity (r=−.044, *p*=.877).

The potential influence of clinical and demographic baseline measures to predict aphasia severity at six months was investigated with a two-stage hierarchical multiple regression analysis. Two subsequent models were defined whereby the aphasia severity six months after symptom onset was defined as the dependent variable.

The following admission measures were defined as independent variables: baseline AQ (continuous), stroke severity (NIHSS, continuous), age (continuous), sex (dichotomous), and in the second model thrombolysis treatment (dichotomous) was added.

The first-stage hierarchical regression model was not significant (R^2=.532, $F_{(4,10)}$=2.838, *p*=.082) and the second-stage model where thrombolysis treatment was added was also not significant (R^2=.556, $F_{(5,9)}$=2.254, *p*=.137) with no significant increase in the predictive power of the model (53% to 56%; *p*=.500).

Other relevant clinical measure besides stroke symptom severity is the presence of small vessel disease (SVD) and thrombolysis treatment (rtPA).

SVD was obtained categorically and an independent t-test revealed no differences between the group with and without SVD for longitudinal aphasia severity (AQ: SVD=85.23±8.07, no-SVD=85.94±9.08; $t_{(14)}$=.157, *p*=.878).

For thrombolysis, independent t-test analyses showed no difference between the thrombolysed and non-thrombolysed groups in relation to their longitudinal aphasia severity (rtPA(n=11): 85.18±8.455, No- rtPA (5): 85.9±8.839; $t_{(14)}$=−.153, *p*=0.881).

No significant difference was observed for patients that received thrombolysis and those that did not with regards to their aphasia severity after six months (rtPA (n=11): 85.90±8.84, No- rtPA (n=5): 85.18±8.46; $t_{(14)}$=−.153, *p*=.881). Likewise, no difference was recorded in their percentage gain (rtPA (n=11): 415.74±585.86, No-rtPA (n=5): 117.58±150.04; $t_{(14)}$=−1.102, *p*=.289).

A univariate analysis of variance with repeated measure was used to investigate whether significant changes occurred between the two time points of assessment (baseline/ follow-up) with the presence of thrombolysis treatment as the between-subject factor. This analysis shows that the factor time is significant ($F_{(1,14)}$=34.678, p<.000) with no significant influence of treatment (i.e. rtPA) ($F_{(1,14)}$=.836, p=.376; **Figure 66**).

A power calculation revealed that the critical t-value of t=1.654 would be reached for a one-sided independent t-test with an effect size of 0.5, a significance level of α=0.05 with a sample size of 176 total participants (88 in each group). Further interference on the influence of thrombolysis can therefore not be undertaken within this study.

The identification of significant differences necessitates a much larger cohort, however, primary analysis indicates that patients receiving thrombolysis have lower AQ scores at baseline (i.e. more language impairment), a steeper recovery slope, and slightly better recovery compared to the non-thrombolysed group. These tendencies await further confirmation within a large clinical trial.
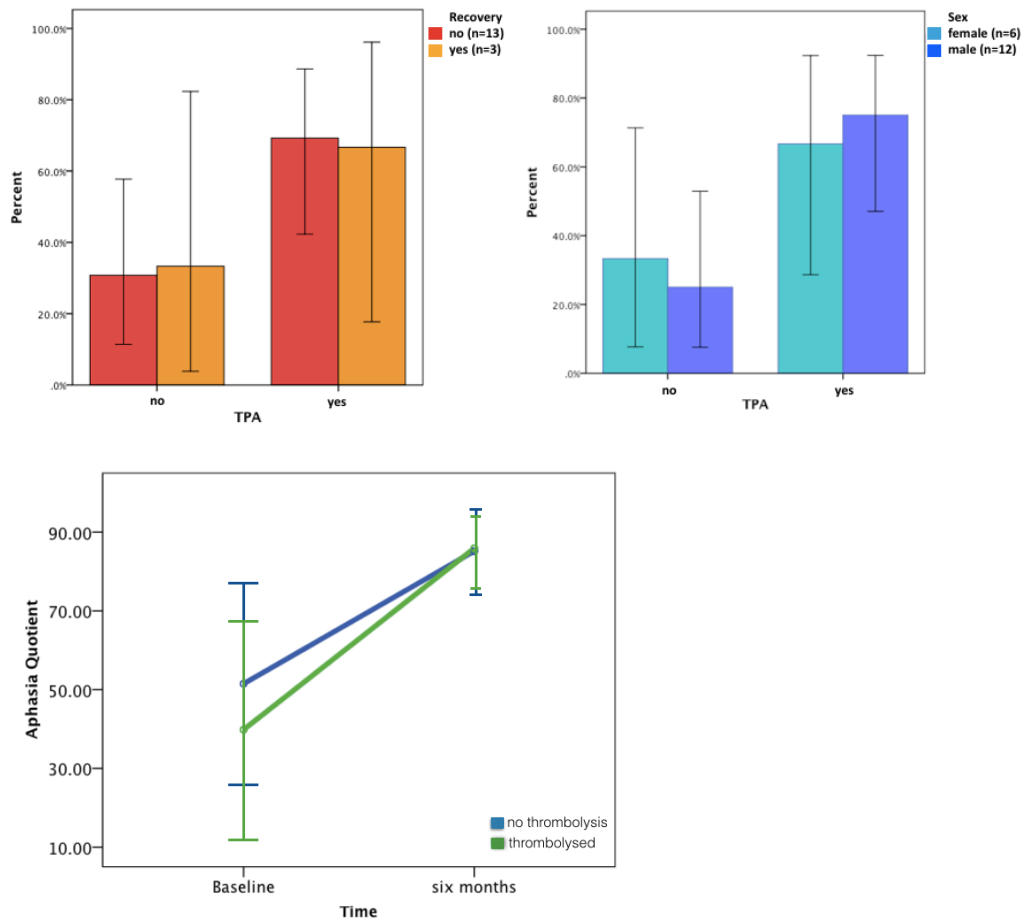
Figure 66   Thrombolysis treatment (TPA) in the present cohort

The bar graphs visualise the percentage of recovered patients (top left) and the gender distribution (top right) within the thrombolysis groups. Recovery is defined as an absolute AQ score at six months above 93.8. The lower panel shows the repeated measures ANOVA plot for the baseline against the follow-up assessment with the in-between factor thrombolysis. The means and standard deviations are shown.

8.3   Comparison of baseline and longitudinal aphasia severity

On average, a significant improvement was observed between the two assessments ($AQ_{Baseline}$=43.48±28.00, $AQ_{6-months}$=85.68±8.44; $t_{(15)}$=− 6.759, p<.001).

All patients improved compared to the baseline assessment but with a varying degree of recovery (**Figure 67**). To account for this spectrum of recovery the percentage of gain was calculated using the formula [(y-x)/x)*100] where y is the longitudinal severity and x is the baseline severity. This calculation yielded only positive values (as all patients improved).

1	very severe aphasia	0-25
2	severe aphasia	26-50
3	moderate aphasia	51-75
4	mild aphasia	75+
5	normal language	>=93.8
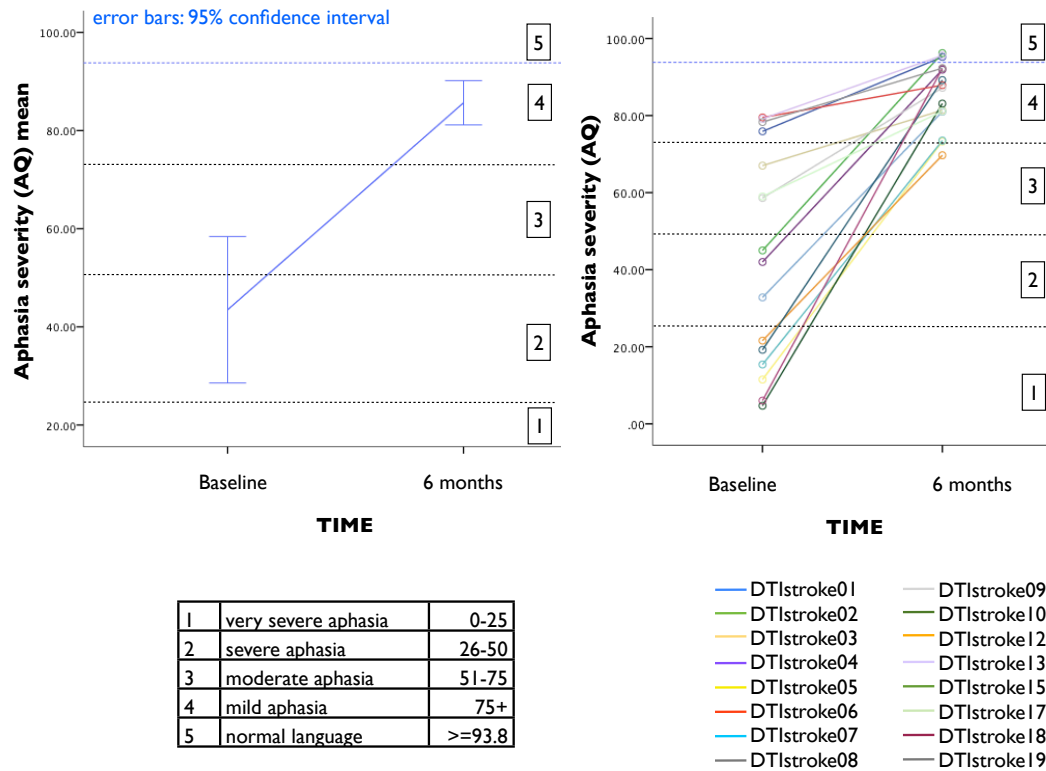
Figure 67   Mean and individual recovery curves

Mean (left) and individual (right) recovery curves between baseline assessment and six months follow-up (n=16). The left plot shows the group mean between the two time points in comparison to the individual curves on the right. 1–5 are the severity classifications according to the WAB-R manual. The blue dotted line indicates the cut-off for normal language functions (AQ≥93.8; AQ ranges between 0-100), which was reached by three patients six months after symptom onset.

Baseline aphasia severity was positively correlated with the longitudinal aphasia severity (r=.49, $p≤.054$) with the regression formula: *baseline AQ = 79.246 + 0.148* follow-up AQ*. The correlation coefficient (R^2) for the regression line is 0.241 (**Figure 68**, top).

Instead of looking exclusively at the absolute aphasia severity after six months, I investigated the percentage of gain for each patient. When plotting the percentage of gain over the baseline severity a curvilinear association was observed (**Figure 68**, bottom left). Parametric testing is not suitable for non-linear associations and the variable *percentage gain* was hence logarithmically transformed to linearise the data and to achieve a log-normal distribution. A regression model with both variables, the baseline severity as independent variable and the percentage in gain as dependent variable, was significant ($R^2=.524$, $F_{(1,14)}=16.888$, $p≤.001$) with the baseline severity as predictor (beta=−.739, $t(−4.109)$, $p≤.001$). The regression

function can be resolved with $y=(b0+b1(lnx1)+e)^2$, where b0 is the constant beta, b1 is the predictor beta and e is the error.
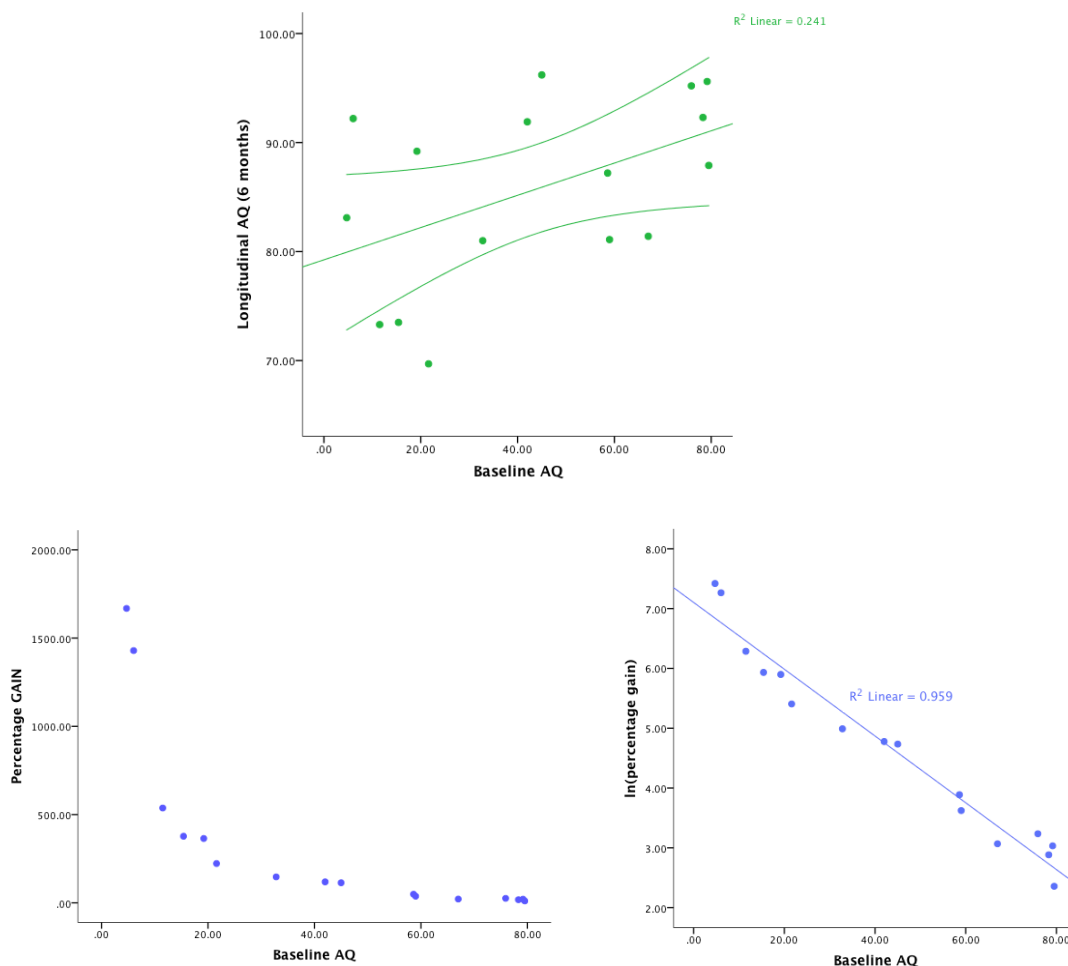
Figure 68   Relation between baseline severity and longitudinal severity

The top panel shows the raw data of longitudinal severity over baseline severity (AQ) with 95% confidence intervals (CI, curved lines). The bottom panels show the curvilinear association between percentage in gain ([(longitudinal AQ-baseline AQ)/baseline AQ)*100]) and baseline severity (left). Due to the non-linearity of the raw data a logarithmic transformation on the percentage of gain was conducted and the corresponding scatterplot is shown on the bottom right.

A median split (AQ=43) allowed us to compare 50% of patients that score on the lower and the higher end of the scale with regards to their percentage in gain. A significant improvement was observed for the patients with more severe aphasia at baseline (AQ<43; mean=608.10±599.48) compared to the patients with more moderate expressions of aphasia (AQ≥43; mean=37.02±11.75; $t_{(7.043)}$=−2.69, p≤.05).

At baseline, twelve patients were classified with non-fluent aphasia and six patients were classified with fluent aphasia. When comparing their longitudinal aphasia severity, no difference was observed ($AQ_{non-fluent}$ =84.209±8.119, AQ_{fluent} =88.900±9.149; $t_{(14)}$= −1.032, $p≤.319$).

The overall longitudinal severity was associated with the baseline auditory word recognition ability and the initial semantic fluency (**Table 15**).

Table 24   Correlation between baseline WAB-R subscales and the AQ at follow-up.

WAB-R baselines	6 month AQ
Content	r=.370,*ns*
Grammar	r=.377,*ns*
Comprehension	r=.276, *ns*
Auditory word recognition	r=.608*
Sequential commands	r=.348, *ns*
Repetition	r=.343, *ns*
Naming	r=.045, *ns*
Fluency (semantic)	r=.556*
Fluency (phonemic)	r=.545, *ns*
Sentence completion	r=.373, *ns*
Responsive speech	r=.320, *ns*

* Correlation is significant at 0.05 level (2-tailed)
ns, Correlation is not significant
WAB-R, Western Aphasia Battery; AQ, Aphasia Quotient

This relation was further investigated with a multiple linear regression analysis. The individual subscales of the WAB-R at baseline were entered into a regression analysis to investigate whether their influence on the longitudinal severity is independently predictive.

The linear regression model included six continuous baseline variables: the overall aphasia severity at baseline as well as the individual subscales: spontaneous speech, naming, comprehension, repetition, and semantic fluency. Bonferroni corrected significance threshold of p=0.0083 was applied. The model was not significant and none of the entered variables reached significance ($F_{(6,8)}$=1.579, p=0.268).

Taxonomical classification changes were also observed as is shown in **Figure 69**. Six months after symptom onset most patients were classified as anomic (68.75%), and three patients (18.75%) made a full recovery in terms of their language functions (i.e. AQ≥93.8). The remaining two patients were one Wernicke patient and one transcortical motor aphasia patient.

Screening (n=18)
3.44±3.29 days post admission

Baseline (n=18)
5.44±4.69 days post admission

6 months post onset (n=16)
199.87±54.71 days post admission

Broca   Transcortical motor   Wernicke   Conduction   Anomia   Global   Recovered
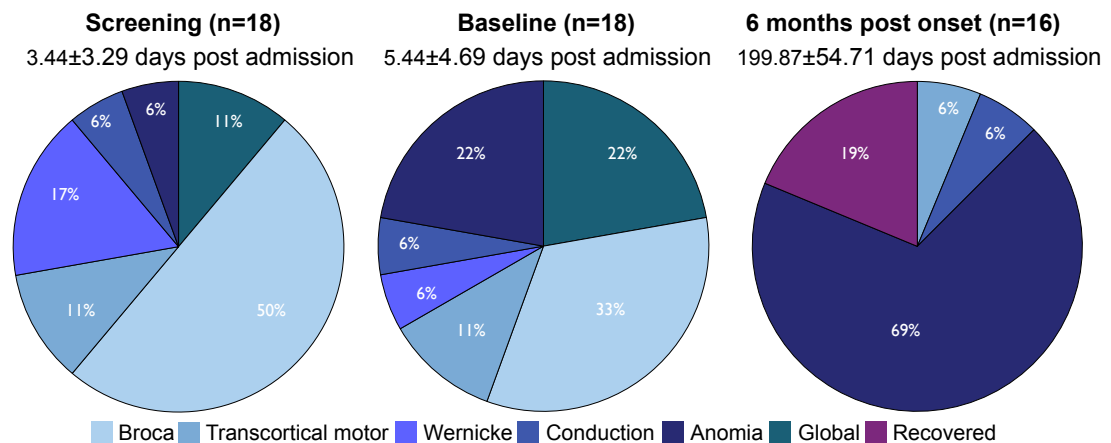
Figure 69   Taxonomical classification

This figures shows the taxonomical classification of all recruited patients at screening (on average 3 days post onset), at baseline (on average 5 days post onset), and at follow-up (on average 120 days post onset)

8.4   Voxelwise 'topological' lesion-deficit analysis

The non-parametric mapping (NPM) linear regression lesion analysis based on a voxel-based lesion-symptom mapping approach used at baseline was implemented again to investigate which voxels are predictive of longitudinal aphasia severity.

The NPM regression analysis only took into account regions that were damaged in a minimum of 2 patients (10%) of the patients (n=15).

Longitudinal severity of aphasia was set as dependent variable and the following four regressors were added into the model: stroke severity (continuous), age (continuous), gender (dichotomous), thrombolysis (dichotomous). The regression revealed the white matter of the middle and inferior frontal gyri, the white matter in the transition of the posterior superior temporal gyrus to the inferior parietal lobe (not shown in figure) and Heschl's gyrus as the areas that are predictive of longitudinal aphasia severity (**Figure 70**).
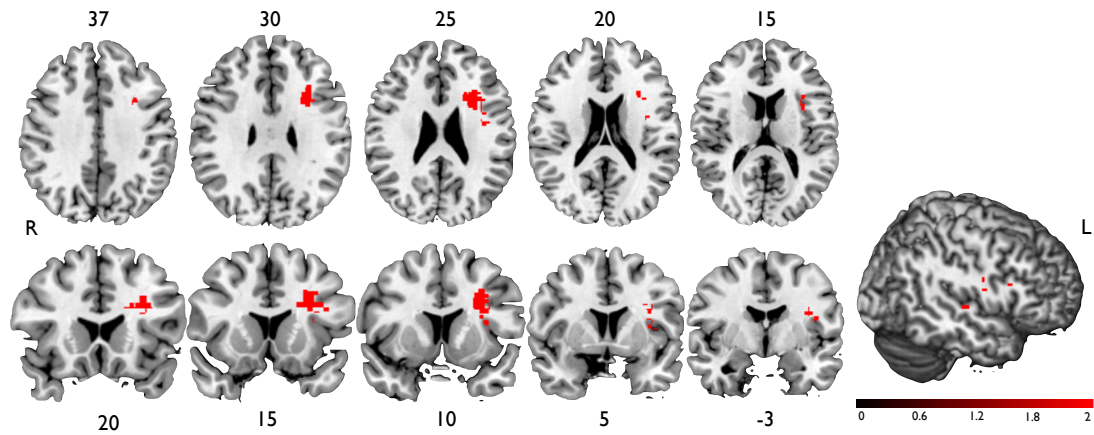
Figure 70   Voxel-based lesion-symptom mapping for the longitudinal aphasia severity. Results shown are corrected for multiple comparisons with permutation testing.

The results shown are corrected for confounding variables as defined in the above paragraph. The shown results are z-transformed (reflected in the scalar colouring) with a significance level of *p*<.001.

8.5   Trackwise 'hodological' lesion-deficit analysis

A key question of interest to this study was whether a disconnection of the arcuate fasciculus is predictive of longitudinal aphasia severity as was hypothesised since the 19th century.

These objectives were tackled by employing a novel hodological lesion-deficit analysis whereby an MNI-based atlas was used as overlay on study-specific MRI scans collected at baseline (see 6.9.2.2). Values representing the amount of damage to an arcuate segment were obtained for each patient and then binarised for when a tract was present in more than 50% of people, hence a score >2 (**Table 25**).

Table 25   Hodological lesion analysis

	"Lesion Load"			>50% chance of dissection		
ID	LS	AS	PS	LS	AS	PS
01	1	0	0	0	0	0
03	1	1	0	0	0	0
04	4	2	1	1	0	0
05	3	2	4	1	0	1
06	4	0	4	1	0	1
07	4	4	4	1	1	1
08	3	1	0	1	0	0
09	4	2	1	1	0	0
10	4	4	4	1	1	1
12	4	4	1	1	1	0
13	1	0	2	0	0	0
14	2	1	0	0	0	0
15	1	1	0	0	0	0
16	1	0	0	0	0	0
17*	0	0	0	0	0	0
18	4	1	0	1	0	0
19*	0	0	0	0	0	0

ID, identification of patients
LS, long segment of the arcuate fasciculus
AS, anterior segment of the arcuate fasciculus
PS, posterior segment of the arcuate fasciculus
(Note: Patient 2 is missing in this list as no T1-weighted image was acquired that could have been used for the overlay.)
*Patients where lesions are quantified as '0' did not show any lesion-arcuate overlap on their T1-weighted image, despite having a confirmed stroke lesion and presenting with aphasia.

A multiple linear regression analysis was conducted for each segment at a time. Aphasia severity at baseline and longitudinally (continuous) was separately defined as the dependent variable and lesion volume (continuous), age (continuous), gender (binary) and disconnection of each segment (binary[13]) as independent variables. None of the models identified the dissections of the three segments in the left hemisphere as predictors of aphasia severity at baseline or after six months (**Table 26**).

---

[13] A binary classification was used as the underlying lesion load coding (i.e. 0-4) cannot be considered linear and is defined normative.

Table 26   Trackwise hodological regression analysis for aphasia severity

	Baseline AQ		**Follow-up AQ**	
Model 1: Long Segment	$F_{(4,13)}$ = 1.575	*p* = .239	$F_{(4,11)}$ = 2.209	*p* =.135
Predictive variables entered				
Disconnection	B = –29.742	*p* = .054	B = –7.606	*p* = .093
Age	B = – 0.027	*p* = .940	B = –.232	*p* = .073
Sex	B = –11.648	*p* = .453	B = –2.306	*p* = .610
Lesion size	B = 0.000	*p* = .394	B = 0.000	*p* = .389
Model 2: Anterior Segment	$F_{(4,13)}$ = 1.173	*p* = .367	$F_{(4,11)}$ = 2.8	*p* =.079
Predictive variables entered				
Disconnection	B = –32.259	*p* = .105	B = –11.046	*p* = .045
Age	B = .129	*p* = .738	B = –.183	*p* = .139
Sex	B = 2.863	*p* = .837	B =1.271	*p* = .742
Lesion size	B = 0.000	*p* = .679	B = 0.000	*p* = .774
Model 3: Posterior Segment	Missing correlation			

In the next step, the ancillary question was addressed whether the classical hypothesis that Broca's and Wernicke's connections (i.e. long segment) is important for repetition can be demonstrated using DTI. To tackle the latter the WAB-R scale repetition was used, which assesses single word and sentence repetition, whilst including oral agility items, a sentence of only monosyllabic words, and a sentence with all letters of the alphabet (see Appendix C. Western Aphasia Battery Revised (WAB-R).

The same approach was employed to investigate if the lesion load to the long segment in the left hemisphere is predictive of repetition deficits at baseline. The model was not significant for the baseline repetition deficit (R^2=.324, $F_{(4,11)}$=1.317, *p*=.323) or the longitudinal baseline repetition deficit (R^2=.477, $F_{(4,11)}$=2.504, *p*=.103; **Table 27**).

Table 27   Trackwise hodological regression analysis for repetition

	Baseline AQ		Follow-up AQ	
Model 1: Repetition	$F_{(4,11)}$ = 1.317	p = .323	$F_{(4,11)}$ = 2.504	p =.103
Predictive variables entered				
Long segment disconnection	B = –4.299	p = .046	B = –5.919	p = .217
Age	B = – 0.010	p = .853	B = –.320	p = .029
Sex	B = –2.642	p = .217	B = –5.668	p = .261
Lesion size	B = –1.711E-005	p = .558	B = 0.000	p = .172

8.6 Right hemispheric perisylvian network (*paper under review*)

8.6.1 Inter-rater variability analysis

Two anatomists used TrackVis (www.trackvis.org) for virtual dissections and volume measurements of the long segment of the right arcuate fasciculus in all participants and achieved a high inter-rater reliability (r = 0.635; p<0.000). The second analyst was blinded to the symptoms of the patients and was only given the data set without further information apart from the presence of the lesion.

8.6.2 Volumetric analysis

In this study, our primary goal was to identify anatomical predictors of aphasia recovery. Hence, we limited our model to factors that could directly influence the anatomy of the three segments of the arcuate fasciculus. Previous studies have shown that amongst these factors are age (i.e. smaller arcuate in older patients; Bava et al., 2011; Lebel et al., 2011), gender (i.e. larger right arcuate in females; Catani et al., 2007; Kanaan et al., 2012; Inamo et al., 2011; Hsu et al., 2008), lesion size (i.e. smaller arcuate in larger lesions; Johansen-Berg & Behrens, 2006; Goldberg & Ransom, 2003; Ciccarelli et al., 2008), and level of education (i.e. higher education level might be neuroprotective; Stern et al., 1994; Ott et al., 1995; Letenneur et al, 1999; Brayne et al., 2010). Other studies have also shown baseline aphasia severity is predictive of longitudinal out come (Ferro et al., 1999; Pedersen et al., 2004; Laska et al., 2001; Lazar et al., 2007; Kertesz 1988b), which we were not able to include in our analysis. Previous studies show that baseline measurement fluctuations occur within a fortnight of symptom onset due to clinical-

physiological processes and the influence of psychodynamic mechanisms (Hillis et al., 2001; Hackett et al., 2005; Gottesman et al., 2010; Lazar et al., 2008). For this reason, baseline language measures in relation to longitudinal therapeutic goals are usually obtained after two weeks from onset to allow sufficient time for acute processes to settle. In the current study, baseline measures were obtained on admission (mean 5±5 days) and therefore are not reliable indices of language impairment. Indeed, in our sample severity of aphasia at baseline is not correlated with the language score obtained six months after (r(16)=.49, p>.05).

To determine which one of these variables (age, gender, lesion size, level of education) are most relevant to our data and to identify the best subset of variables explaining the dependent variable (i.e. longitudinal aphasia severity) they were introduced to a backward elimination analysis. This method places all possible variables, as identified from the literature or driven by a hypothesis, in the model and calculates the contribution of each of them. Their contribution is then compared against a removal criterion (here we used a probability value for the test statistic of p>0.001). The variable with the least contribution to the model is then removed and the reduced model re-estimated for the remaining variables. The contribution of the remaining variables is re-assessed in an iterative way until the model reaches statistical significance.

The resulting subset of variables was introduced into subsequent regression analyses. The primary analysis employed a hierarchical multiple linear regression. In this analysis, two subsequent models were defined with the longitudinal aphasia severity, defined as the absolute aphasia Quotient (AQ) value obtained after six months, as the dependent variable. The first-level model included the variable subset identified by the backward elimination, namely age, gender, and lesion size. In the second-level of the model the three segments index sizes were separately added to model.

Where both models were significant, the fit of each model was estimated by calculating the corrected Akaike information criterion for small sample sizes (AICc) (Akaike 1974; Hurvich & Tsai 1989). The AICc is a goodness of fit measure corrected for model complexity (i.e. penalising increasing number of predictors). We used this analysis to compare both levels of the regression models and to verify that the increase in predictive power of the second-level model is not merely driven by a higher number of predictors.

The secondary analysis addressed group differences between gender, fluent vs. non-fluent aphasia types (defined according to a cut-off of 4 on the WAB-R fluency scale), and thrombolysis groups (thrombolysed vs. non thrombolysed).

Statistical analyses were performed using *R* 2.15.1 software (www.R-project.org). Power analysis was conducted using the software package G*Power (http://www.psycho.uni-duesseldorf.de/abteilungen/aap/gpower3/).

Identification of previously established predictors of symptoms severity

Based on previous studies we considered age, gender, lesion size, and education as potential predictors of aphasia severity at 6 months (Eslinger & Damasio 1981; Laska et al. 2001; Ferro & Madureira 1997; McDermott et al. 1996). In addition these factors can also influence the anatomy of the white matter tracts (Lebel & Beaulieu 2009; Thiebaut de Schotten, Cohen, et al. 2012a). In order to confirm whether these factors significantly influence language outcomes in our dataset a backward regression analysis was conducted. This method introduces all potential variables into the model at once before subsequently eliminating each independent variable, starting with the variable with the smallest partial correlation coefficient. A conventional significance level of 0.1 was assumed for this analysis. The analysis shows that when all variables are included, the model is not significant for predicting longitudinal language outcomes ($R2=.605$, $F_{(4,9)}=3.448$, $p=.06$). The subsequent analysis removed education from the variables and the model become significant including only age, gender, and lesion size ($R2=.596$, $F_{(3,10)}=4.921$, $p=.024$). This result is in line with the literature where education has no strong evidence of being an independent predictor of long-term recovery (Ferro et al. 1999). Based on these findings age, gender and lesion size are good predictors of recovery in our dataset. This subset of variables was therefore taken into account for subsequent regression analyses.

Diffusion Tensor Imaging (DTI) tractography

The volume, defined as the number of voxels intersected by the streamlines of each segment, was extracted for the left and right hemispheres for each patient (**Table 28**).

Table 28 Volumetric measures (number of voxels) of all three segments in both hemispheres

ID	Left Hemisphere Volume 3 segments			Right hemisphere Volume 3 segments		
	LS	AS	PS	LS	AS	PS
1	533	283	529	920	360	381
2	1138	475	775	666	637	692
3	1191	610	894	545	633	778
4	1705	0	517	742	678	545
5	356	605	310	445	388	627
6	489	347	284	830	346	269
7	1234	104	327	285	765	378
8	861	851	811	432	626	750
9	736	552	1014	563	557	1015
10	488	397	796	0	720	374
12	0	0	699	672	482	300
13	959	786	581	439	743	660
14	880	660	440	161	399	0
15	830	0	589	385	347	339
16	780	242	669	380	643	448
17	659	232	765	0	378	112
18	532	287	623	582	841	293
19	622	496	569	206	1971	628

ID=identification number, AS=anterior segment, PS= posterior segment, LS=long segment

Left hemisphere. The hierarchical regression analysis showed that a model including age, gender and lesion size was predictive of longitudinal aphasia severity (R^2=.502, $F_{(3,11)}$=3.689, p=.047). The predictive value of the model improved but not significantly when the volume of the left long segment was included in addition to age, gender and lesion size (R^2=.623, $F_{(4,10)}$=4.138, p=.031; R^2 change: $F_{(1,10)}$=3.235, p=.102). Among the four variables entered only lesion size was an independent predictor [beta=−.630, t(−3.129), p=.011] of longitudinal aphasia severity.

The same analysis was repeated for the left anterior and posterior segments of the arcuate fasciculus and both models were not predictive (anterior segment index size: R^2=.541, $F_{(4,10)}$=2.943, p=.076; posterior segment index size: R^2=.577, $F_{(4,10)}$=3.411, p=.053). The result indicates that by taking into account all three

predictors the left hemispheric model can explain approximately 50% of the variability in language recovery. By adding the volume of the left long segment the model can explain 62% of the variability, which represents only a 12% increase in predicting value. Overall, this analysis indicates that in the left hemisphere the only independent predictor of longitudinal aphasia is the lesion size. It should be taken into consideration here, however, that the volume measurements of the left and right arcuate segments reflect two different anatomical properties of these fibres. In the right hemisphere the volume of the tracts reflects the anatomy of a pre-existing tract, which is unaffected by the stroke. By contrast, in the left hemisphere tract volume measurements are indicative of the residual fibres whose quantity depends on the amount of damage occurred in the middle cerebral artery territory. Hence, while the right tract measurements reflects the anatomical volume of the pre-existing arcuate the left tract volume is an indirect measure of lesion load specifically to the arcuate fasciculus. We therefore investigated if the lesion size and the volume of the left arcuate segments correlate, which was not the case for the left long segment nor the sum of the three segments in the left hemisphere (left long segment: $r(18)=.224$, $p=.372$; sum of left three segments: $r(18)=.078$, $p=.760$). Also when adding the sum of the three segment as a predictor to the regression model, the model did not explain the observed data (level 1(age, gender, lesion size): $R^2=.275$, $F_{(3,12)}=1.52$, $p=.260$; level 2 (addition of the left three segments: $R^2=.305$, $F_{(4,11)}=1.206$, $p=.362$; R^2 change: $R^2=.030$, $F_{(1,11)}=.467$, $p=.508$).

Right hemisphere. The hierarchical regression analysis showed that a model including age, gender and lesion size was not predictive of longitudinal aphasia severity ($R^2=.275$, $F_{(3,12)}=1.52$, $p=.260$). The predictive value of the model improved significantly when the volume of the right long segment was included in addition to age, gender and lesion size ($R^2=.568$, $F_{(4,11)}=3.62$, $p=.041$; R^2 change: $F_{(1,11)}=7.462$, $p=.020$). Of the four predictors only age [beta$=-.678$, $t(-3.087)$, $p=.010$] and the right long segment [beta$=.730$, $t(2.732)$, $p=.020$] were independent predictors. Gender [beta$=.505$, $t(1.920)$, $p=.081$] and lesion size [beta$=-.441$, $t(-2.04)$, $p=.066$] were marginally significant. For the right hemisphere the model that includes only age, gender and lesion size explains about 30% of the variance of language performances at 6 months ($R^2=.275$, $F_{(3,12)}=1.520$, $p=.260$). By adding the volume of the right long segment the model increases to 57%, which represents a statistically significant increase in predictive value.
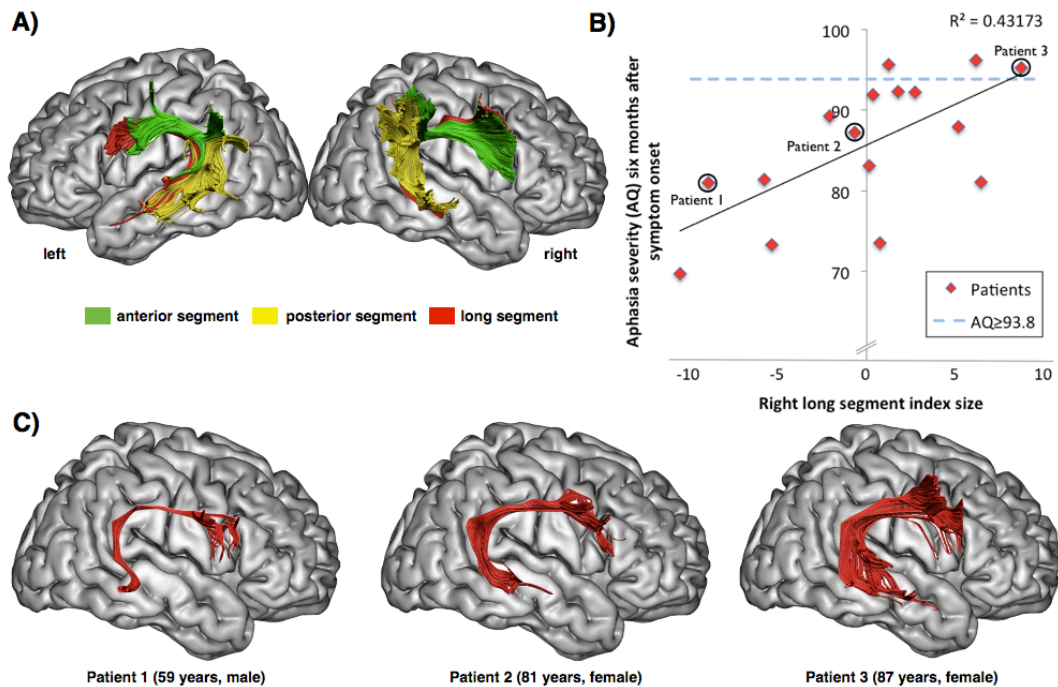
Figure 71   DTI reconstruction of right-hemispheric perisylvian language network

The top panel depicts the DTI reconstruction of the right hemispheric arcuate fasciculus in three left hemispheric stroke patients. The anterior segment (green) and the posterior segment (yellow) can be appreciated in all three patients. The long segment (red) connecting homologues of the perisylvian language areas is, however, missing in the first patient, slightly represented in the second and very prominent in the third patient. The lower left panel shows the regression plot for aphasia recovery and the standardized residuals for the right normalised long segment volume corrected for the regressors age, gender, and lesion size. The right lower panel shows the correlation plot for aphasia recovery at six months follow-up and the volume of the right long segment.

8.6.3   Indices of microstructure analyses

8.6.3.1 Trace or Mean diffusivity (MD)

Six months post onset, phonological fluency correlated with the mean diffusivity of the right anterior segment (r=–.52, p=.047). None of these correlations, however, survived multiple comparison with the adjusted p value *p*=.004.

A partial correlation between the overall aphasia score at follow-up correlated highly significantly with the mean diffusivity of the anterior segment in both hemispheres (r=.729, *p*=.040; r=.764, *p*=.027, two-tailed). These relations were further investigated in more detail using regression analyses.

8.6.3.2 Diffusivity along ellipsoidal axes (radial and axial diffusivity)

At six months post onset, no correlations were obtained between the initial perpendicular diffusivity in the three segments and the language assessments.

Independent t-test analyses between the sexes as well as between the thrombolysis groups revealed no differences in axial diffusivity in any of the segments. At six months post onset, no correlations were found between the initial axial diffusivity and the language assessments.

8.6.3.3 Fractional Anisotropy (FA)

Six months post onset, spontaneous speech marginally correlated with the fractional anisotropy of the left anterior segment (r=–.55, *p*=.054). Comprehension correlated with the FA of the left posterior segment (r=.61, *p*=.013). Phonologic fluency correlated marginally with the left long segment (r=.53, *p*=.052). None of these correlations, however, survived multiple comparison with the adjusted p value *p*=.0041.

8.7 TBSS

A TBSS analysis was conducted between the aphasia severity at six months as the dependent variable and the fractional anisotropy maps from the baseline scanning assessment. Age, gender, thrombolysis treatment, and lesion size were added as covariates to this analysis. The results indicated that reduced FA in the left temporal stem, temporal lobe and inferior frontal gyrus white matter is associated with poor recovery, whilst increased FA in the right middle frontal gyrus, the junction of the anterior limb of the internal capsule and the external/extreme capsules, cingulate gyrus, and parietal lobe seem to predict better recovery (**Figure 72**).
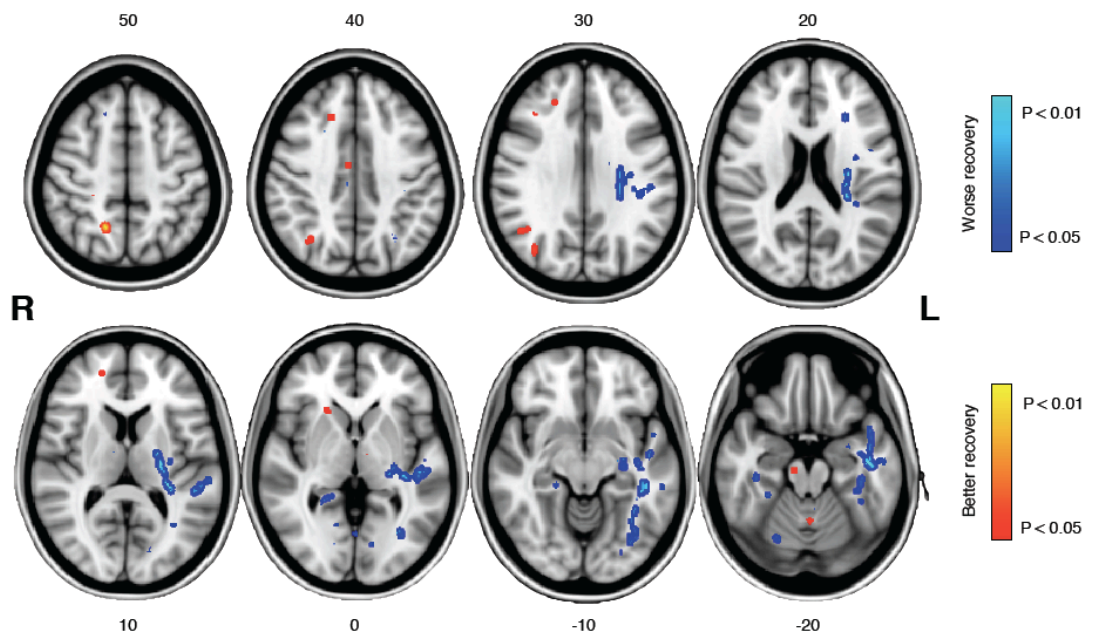
Figure 72   TBSS analysis of baseline FA values and longitudinal language recovery

Blue voxels represent areas of reduced fractional anisotropy (FA) values significantly associate with poor recovery; red voxels represent areas of increased fractional anisotropy (FA) values significantly associate with better recovery after six months. Contrasts are controlled for age, sex, thrombolysis, and lesion size (uncorrected for multiple corrections)

CHAPTER 9   CHRONIC ASSESSMENT (12 MONTHS)

This chapter is dedicated to the comparison between baseline and chronic neuroimaging data in relation to aphasia severity.

At one year, the WAB-R screening was repeated together with a repeat MRI scan utilising the same scanning protocol and equipment used for the first scan.

One year after symptom onset, none of the eighteen patients had died. Two patients relocated (Jamaica and Cheshire), two patients withdrew six months after onset, and one patient was hospitalised for another medical conditions. For three patients the one-year scan was not performed as this was outside the study collection period. Hence, a total of 10 complete datasets of one-year neuroimaging assessments were available (mean 408±47 days after symptom onset).

Out of those 10 first-ever stroke patients, nine (90%) were still aphasic to a varying degree. One patient was assessed to have Wernicke aphasia (patient 07), one patient was classified as transcortical motor aphasia (patient 10) and the remaining seven patients were categorised anomic (patient 03-06,08-09,15). One patient fully recovered (patient 13).

The chronic structural MR images can be seen in **Figure 73Error! Reference source not found.** and the connectional anatomy is available in **Figure 76**.
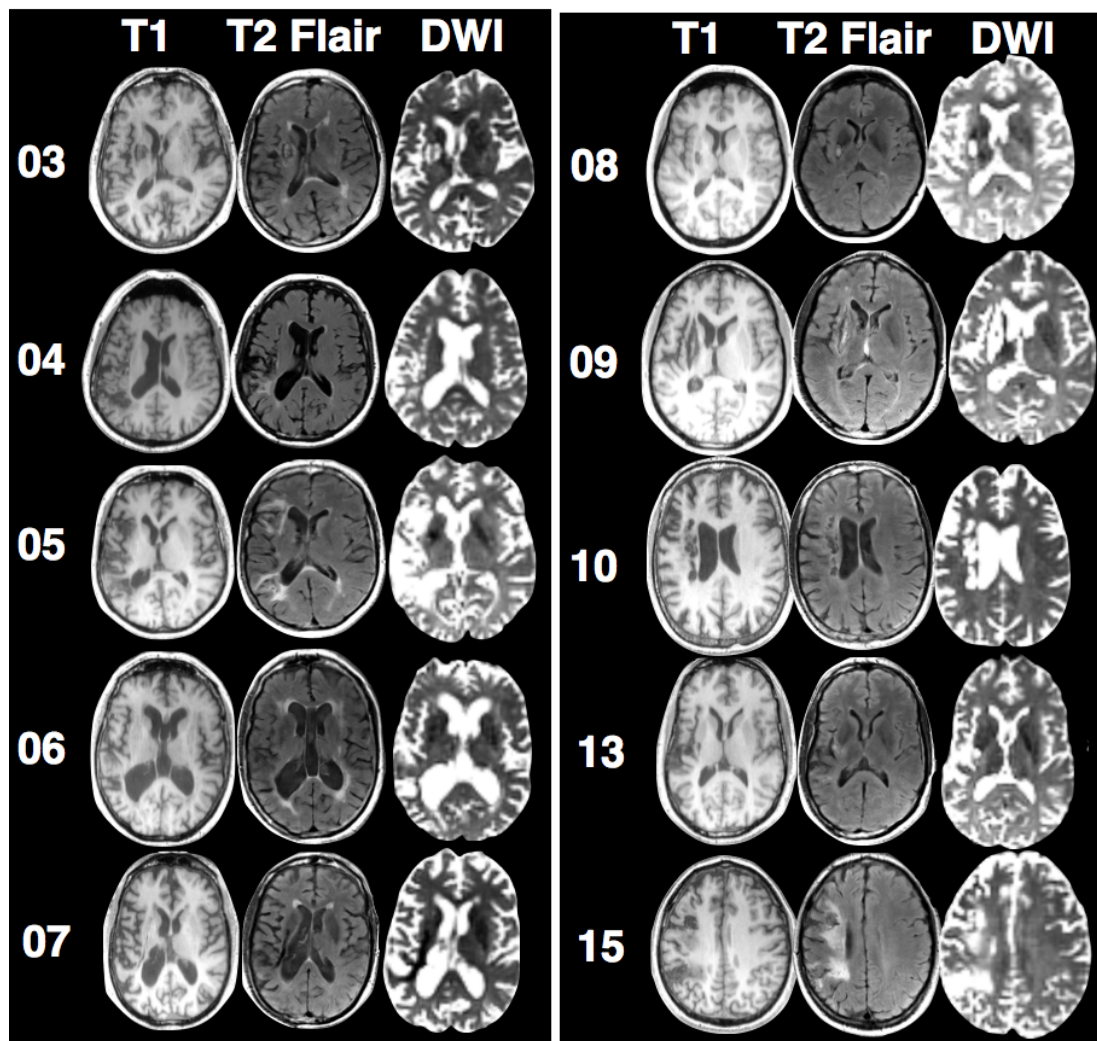
Figure 73 Native structural scans of patients assessed at the chronic stage

MRI contrasts shown are T1, T2, and T2 FLAIR. Red asterix indicates the stroke lesion. One patient (06B) has no asterix indicating the lesioned area in any of the contrast, as the stroke was not evident on conventional MR contrasts. In this subject, the hyperintense lesions on the T2-weighted images were deemed to be periventricular small vessel disease by a radiologist.

9.1   Lesion analysis

Lesion analysis was performed on the one year scans. The ROIs of the lesions were manually drawn on the native scans and then normalised to the MNI template. As seen above ten scans were available. However, only nine were used for lesion analysis, as the lesion in subject 06 was not identifiable on classical structural scans. (Note: Automatic lesion segmentation was also attempted with an SPM toolbox called automatic lesion identification 'ALI' (Seghier et al. 2008), which also failed to identify a lesion).

One can appreciate from the lesion overlay map in **Figure 74** that, in the chronic stages, the lesions were affecting all perisylvian regions. These include i) the superior temporal lobe (including Heschl's gyrus), ii) the inferior and middle frontal gyri, and to a minor extent the superior frontal gyrus, iii) deep brain nuclei (i.e. putamen, anterior caudate nucleus), iv) the three capsules (i.e. posterior arm of the internal capsule, external/extreme capsules), v) claustrum, and vi) the entire insular ribbon. The maximum overlay is located on the posterior short insular gyrus/anterior long insular gyrus, extending anterior-posteriorly along the insular ribbon between the middle short insular gyrus and the inferior periinsular sulcus, and medio-laterally between the insular ribbon and posterior globus pallidus (engulfing the extreme capsule, claustrum, external capsule, and putamen). Insular anatomic labelling is in accordance with Türe et al. (1999).
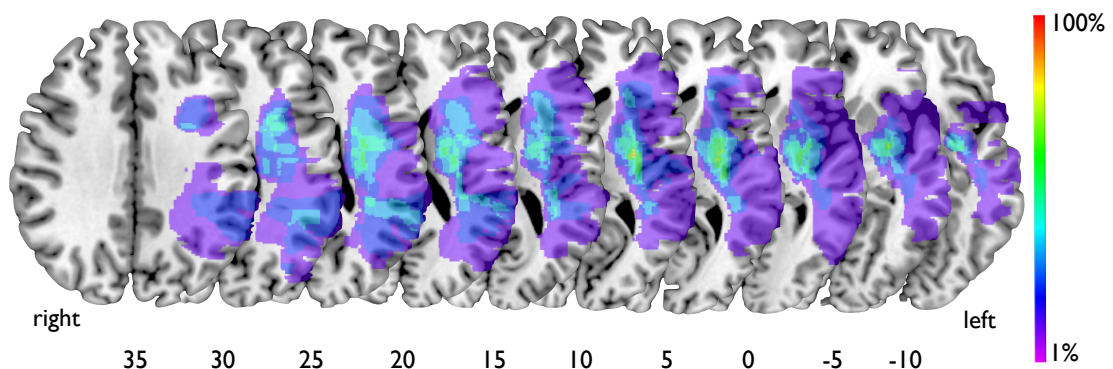
Figure 74   Percentage overlay map of chronic (12 months post onset) left-hemispheric lesions (n=9)

A Kolmogorov-Smirnov (K-S) test indicated that within this subsample of nine patients, lesion volume at baseline and one-year can be considered normally distributed (chronic: K-S Z=.673, *p*=.76; baseline: K-S Z=.823, *p*=.51). Paired parametric comparison between the baseline lesions and the chronic lesion volumes of this subgroup of nine patients, did not reveal a significant change in lesion size (*t*(8)=–0.377, *p*=.72) over the duration of one year. The mean comparison however indicates a slight reduction in lesion size over time: baseline lesion size was, on average, 20160 (±24937) voxels (equal to 279±344 ml)[14] compared to the average chronic size of 16365 (±15403) voxels (equal to 226±213 ml).

---

[14] Lesion volume was calculated according to the equation below. *Lesion volume=nr of lesioned voxels*volume of one voxel*. Volume of one voxel can be calculated through the voxel size 2.4x2.4x2.4 (mm^3) and was then convert to millilitre (ml).

Given the small number of observations, further symptom-lesion mapping (i.e. regression analyses) was not attempted due to the likelihood of over-fitting the data.

9.2   DTI Results

9.2.1   DTI Atlas-based analysis

As a first step the aforementioned atlas (www.natbrainlab.com) was used to overlay the chronic lesion maps onto. This analysis identified that, in the chronic stage, four left-hemispheric pathways were affected, namely the inferior fronto-occipital fasciculus, the anterior commissure, the internal capsule and all three segments of the arcuate fasciculus (**Figure 64**A).
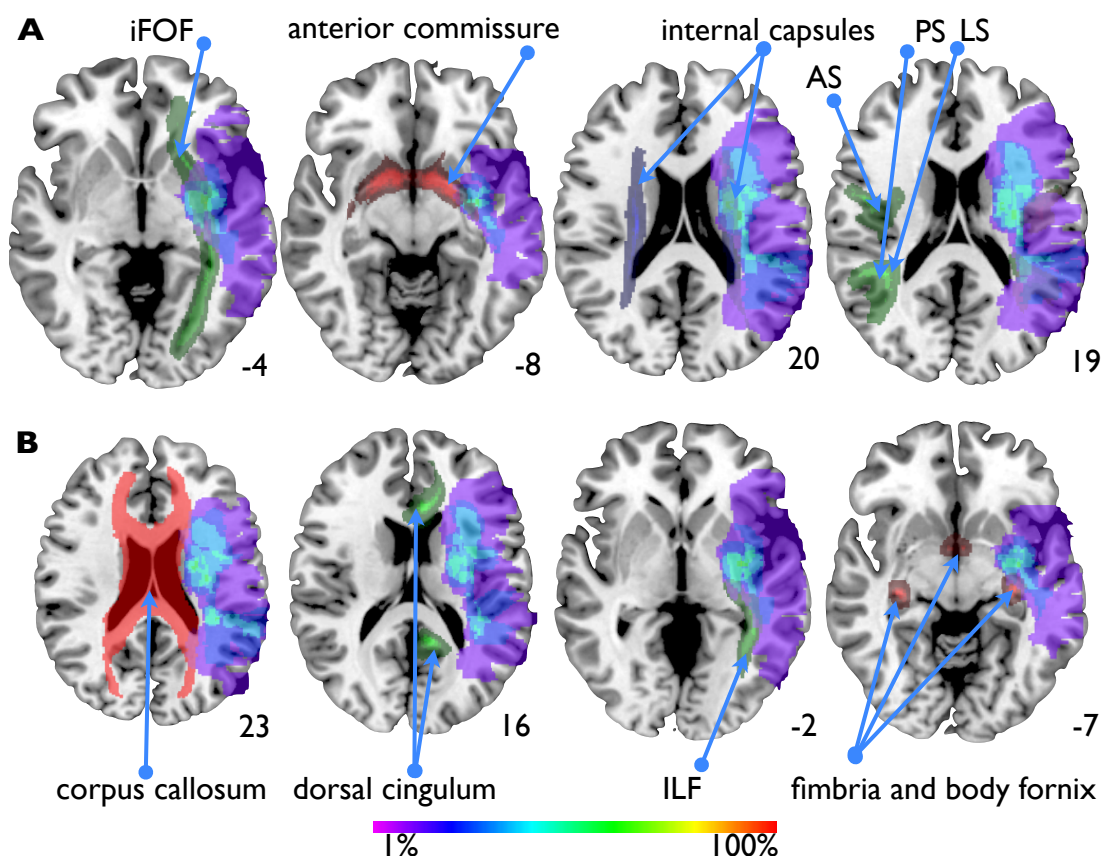
Figure 75   DTI Atlas overlay on chronic left-hemispheric lesion overlay percentage maps (n=9)

Panel **A** depicts the overlay of pathways affected by the chronic lesions. Panel **B** shows pathways that were not affected. The colour coding of pathways is in accordance with the directional FA-colour coding (red=commissures, green= association, blue=projections). The cingulum is represented in two parts as it is an arching tract and hence from a dorsal axial perspective the tract separates into two parts. Similarly, the fornix separates into its fimbria, and thus appears like a three-part structure from the dorsal axial view. iFOF, inferior fronto-occipital fasciculus; AS, anterior segment; PS, posterior segment; LS, long segment; ILF, inferior chronic fasciculus. Where tracts cannot be appreciated on the lesioned hemisphere

they are shown on the right hemisphere for reference (internal capsule and arcuate segments).

The corpus callosum (**Figure 64**B) is shown amongst the non-affected pathways, however, it should be considered that a DTI atlas was used here and therefore cortical projections of the corpus callosum cannot be visualised. Those cortical projections can however be considered as affected by the chronic lesions. This will be considered in more detail in Chapter 12. The dorsal and ventral (not shown here) parts of cingulum were not engulfed by the lesion at any point along their course; neither were the fornix (body and fimbria) and the inferior longitudinal fasciculus[15].

It can be assumed from the lesion location that the superior longitudinal fasciculi (SLF 1-3) were damaged as well, however, these are not reconstructable with DTI and no atlas is yet available online for overlay investigations (atlas in prep and will be available online www.natbrainlab.com).

In comparison to the lesion-atlas overlay at baseline, four pathways are no longer considered affected by the lesion, namely the corpus callosum (regardless its lateral projections), the cingulum, the ILF, and the fornix.

9.2.2   Perisylvian pathway reconstructions

To investigate the chronic changes in the white matter anatomy the dissection of the three arcuate segments was attempted again after one year of symptom onset and compared to the baseline measurements. Likewise, volumetric measurements were obtained for each dissected pathway.

Upon visual inspection, the dissections of the arcuate in the left hemisphere revealed substantial intra- and interindividual variability between the two time points (i.e. baseline vs. one-year post stroke). Obvious changes in the arcuate anatomy in the left and right hemisphere between the baseline and one-year dissections can be appreciated when comparing **Figure 60** in subchapter 7.3 and **Figure 76** in this chapter.

---

[15] The visualisation of axial slices does not demonstrate this fact nicely, however when all three planes (axial, sagittal, coronal) are available simultaneously, it is clear that those two tracts are unaffected.
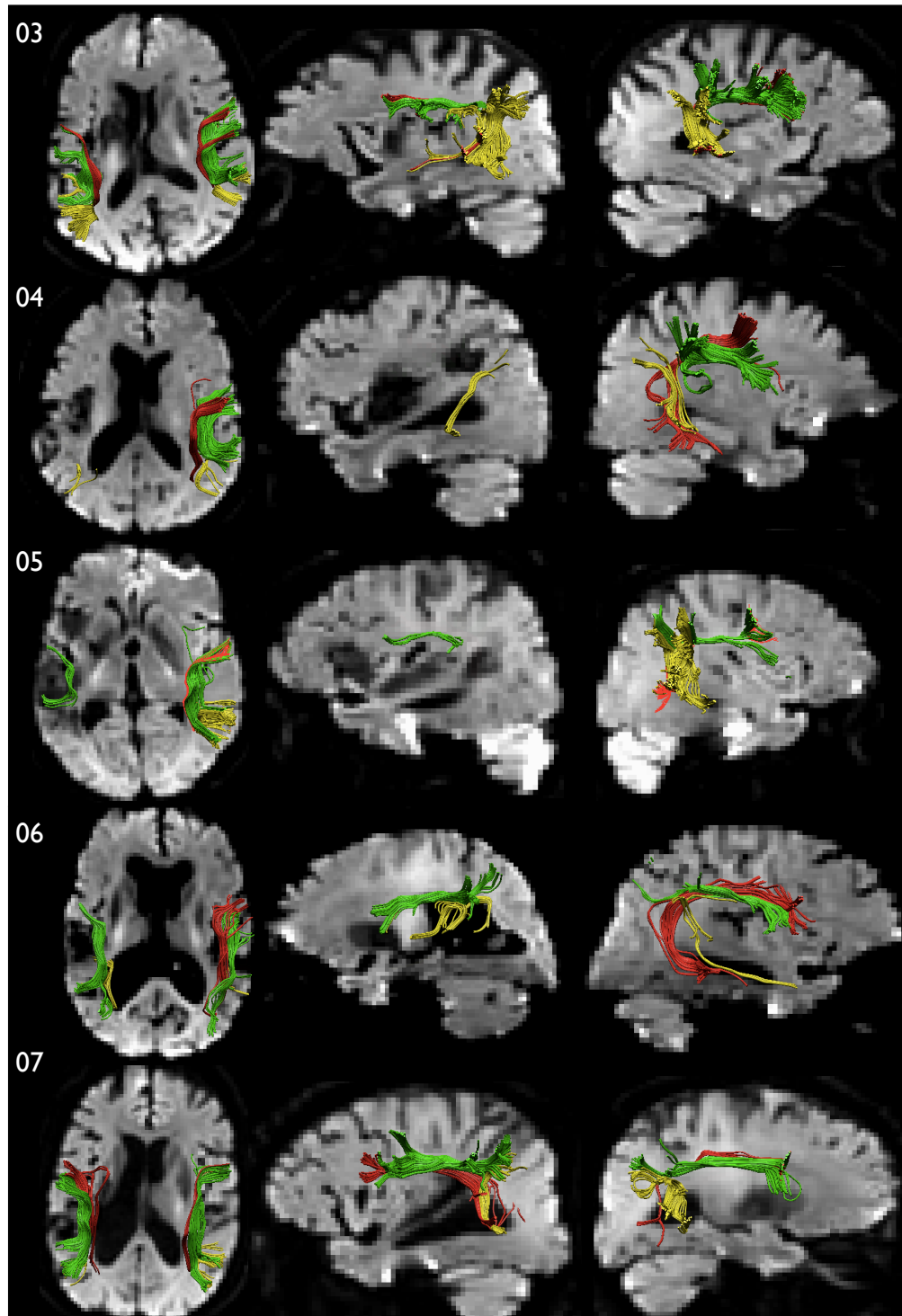
See overleaf.
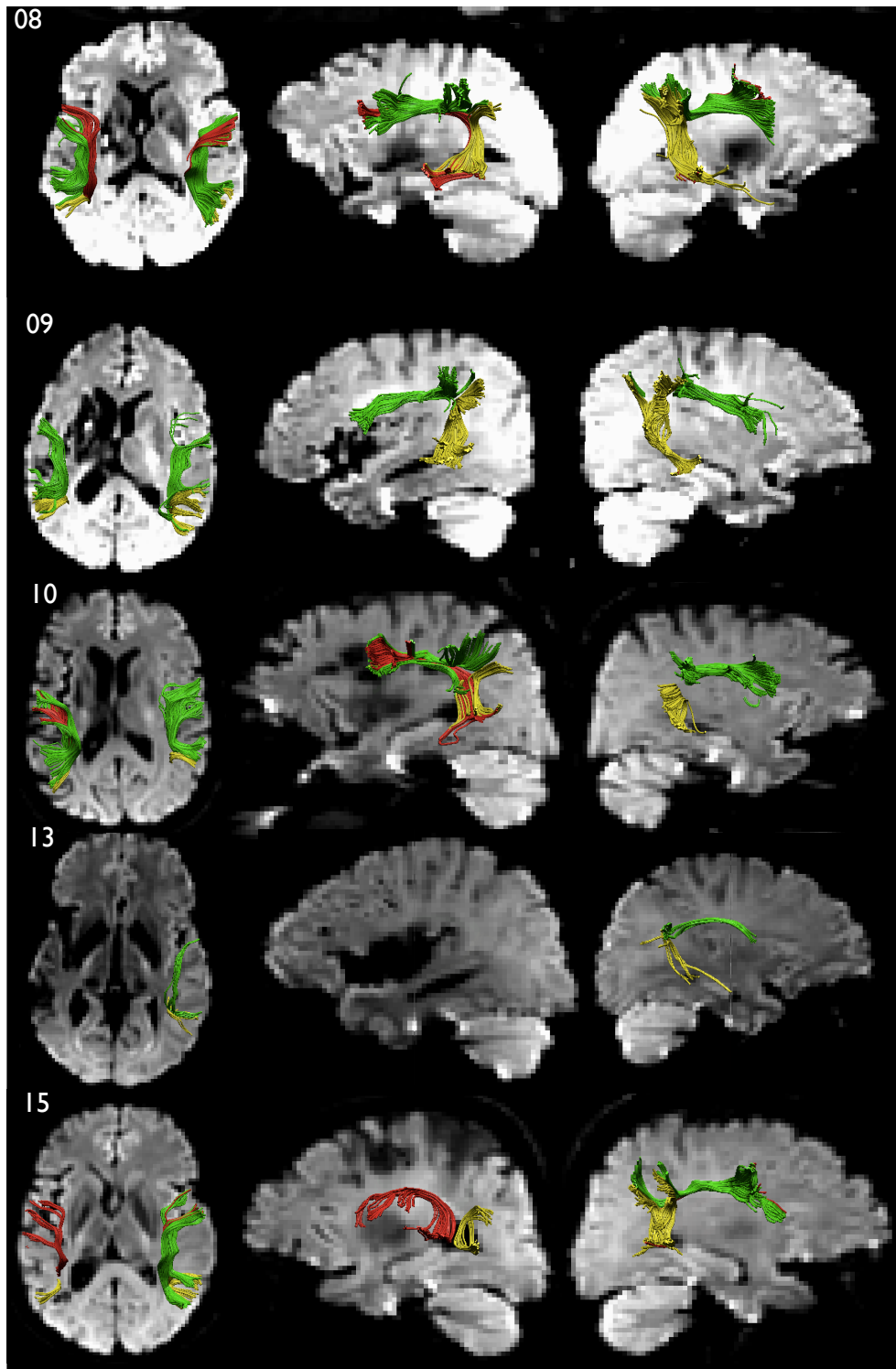
Figure 76   Bilateral DTI arcuate fasciculus reconstructions in chronic stroke

DTI tractography reconstructions show the anterior (green), posterior (yellow) and long segment (red) of the left and right arcuate fasciculus post stroke where dissection was possible. The arcuate is shown in the dorsal, left-lateralised, and right-lateralised view respectively (n=10). The background image shows the corresponding one-year native diffusion-weighted scan of each patient to facilitate the identification of the lesion and to identify whether the lesion is encroaching on the perisylvian pathways.

Beyond visual inspection, a paired *t-test* analysis revealed significant volumetric reduction in the posterior and long segment bilaterally, whilst the anterior segment did not seem to be affected (**Table 29**).

Table 29   Paired t-test comparisons between baseline and one-year volumes of the three segments.

		n	Mean (SD)	t	df	p
Anterior segment left	*Baseline*	10	425.20(310.15)	1.701	9	.123
	1 year	10	247.60(224.26)			
Anterior segment right	*Baseline*	10	580.30(163.76)	0.850	9	.417
	1 year	10	520.30(186.97)			
Posterior segment left	*Baseline*	10	612.30(259.30)	5.857	9	.000***
	1 year	10	224.40(241.58)			
Posterior segment right	*Baseline*	10	573.50(236.83)	3.949	9	.003**
	1 year	10	298.60(228.52)			
Long segment left	*Baseline*	10	884.90(410.07)	4.708	9	.001***
	1 year	10	202.70(214.13)			
Long segment right	*Baseline*	10	466.60(231.69)	3.898	9	.004**
	1 year	10	271.80(199.23)			

*** Significant at .001 level
** Significant at .01 level

When investigating the FA in all segments and both hemispheres, the FA is reduced in all segments; however, no significant changes can be detected apart for the long segment in the left hemisphere (**Table 30**). Here, a reduction in the mean FA across the entire length of the tract is apparent whilst the standard deviation (SD) is increased compared to the baseline measures.

Table 30   Paired t-test comparison between baseline and one-year fractional anisotropy (FA) changes in the three segments in both hemispheres.

		n	Mean (SD)	*t*	df	*p*
Anterior segment left	*Baseline*	10	.33(.17)	0.959	9	.363
	1 year	10	.29(.20)			
Anterior segment right	*Baseline*	10	.46(.04)	1.206	9	.259
	1 year	10	.43(.10)			
Posterior segment left	*Baseline*	10	.36(.05)	1.434	9	.185
	1 year	10	.28(.20)			
Posterior segment right	*Baseline*	10	.41(.04)	1.481	9	.173
	1 year	10	.36(.14)			
Long segment left	*Baseline*	10	.42(.04)	2.565	9	.030*
	1 year	10	.24(.22)			
Long segment right	*Baseline*	10	.45(.16)	1.467	9	.176
	1 year	10	.37(.21)			

* Significant at .05 level

9.3   Tract-based Spatial Statistics (TBSS) Results

FA maps were pre-processed, as described in the Chapter 6, and submitted to a general linear model (GLM) analysis. Here, chronic FA changes (i.e. from the baseline scan to the one-year scan) were investigated. The difference between those two FA maps was calculated and the resulting subtraction map was analysed with regards to its predictive value for language recovery.

The aim was to analyse whether chronic FA changes might reflect behavioural changes (e.g., improved language function). Nine data sets were entered into the analysis.

For the GLM TBSS analysis, *contrast 1* gives chronic>acute test (i.e. increase in FA over time) and *contrast 2* the chronic<acute test (i.e. decrease in FA over time), as fully corrected for multiple comparison across space results.

The results for *contrast 1* indicate that an increase in FA is primarily seen for the white matter of the right hemisphere (**Figure 77**). This increase is predictive of chronic aphasia severity with an increase in FA reflecting an improvement in the aphasia score (i.e. less severe).

An increase in FA is primarily detected within the white matter of the right hemisphere across all lobes (frontal, parietal and temporal) as well as in the sublobar commissural and projection white matter [i.e. corpus callosum (including

bilateral forceps minor), cortical spinal tract, corona radiata, and external/extreme capsules].

For *contrast 2*, no association between decreased FA and aphasia severity were observed. This lack of significance might reflect the variety in stroke lesions and different evolution of structural brain recovery.

Both contrasts are controlled for the influence of the following confounding variables: age, sex, thrombolysis, and lesion size. The influence of age on FA changes over life span haven been previously acknowledged (Pfefferbaum et al. 2000). The results are further corrected for multiple comparisons.
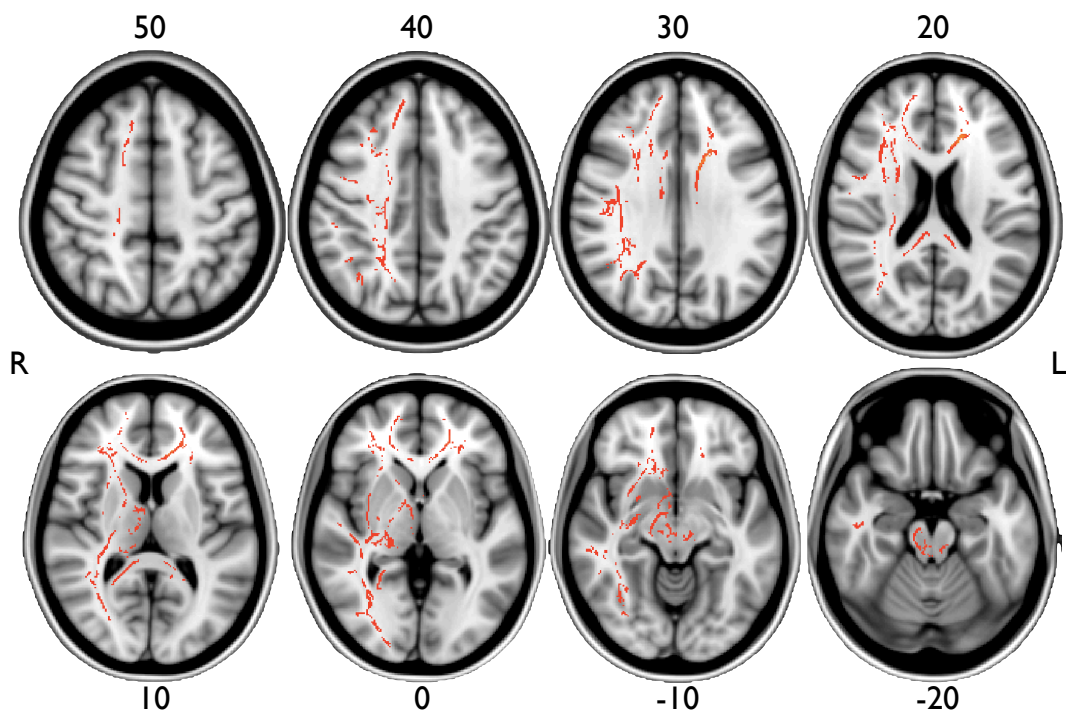
Figure 77   TBSS GLM analysis for chronic data, *contrast 1*

Red regions indicate areas where an increased FA positively correlated with improvements in language performance. This figure shows the result of *contrast 1* (chronic>acute FA) corrected for multiple comparisons thresholded to *p*<0.05 in MNI space. An increase of FA is evident in the white matter of the right hemisphere, including the temporal, parietal and frontal lobes, and the corpus callosum and cortical-spinal tract at the level of the medulla oblongata.

9.4   Continuous arterial spin labelling analysis

Perfusion data from 13 patients were available (**Figure 78**). Global perfusion values were extracted for each hemisphere in parallel with perfusion measures within the cortical language areas.
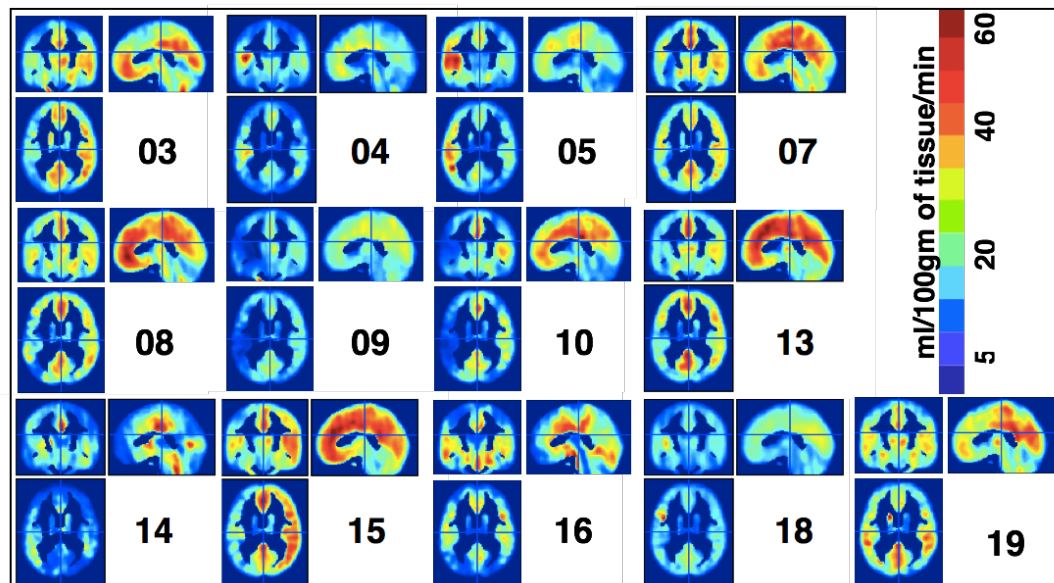
Figure 78 Grey matter thresholded (30%) normalised perfusion maps at baseline for 13 patients of our cohort shown in neurological view.

The first aim was to investigate if the left-hemispheric post-stroke perfusion can predict the language deficits at baseline or after six months. To this end, global perfusion measures within the left hemisphere of each patient (see table 2) were entered into a Pearson correlation analysis, after establishing that none of the measurements are significantly different from the normal distribution. This parametric analysis revealed no association between global left hemisphere perfusion post-stroke and baseline aphasia severity (r(13)= –0.211, *p*=0.489) or longitudinal aphasia severity (r(11)= –0.059, *p*=0.863). This suggests that the overall perfusion post-stroke is not predictive of the severity of aphasia.

The second aim was to replicate, if possible, results previously shown in the literature by Hillis et al., 2006. The authors of this study reported that hypoperfusion within Wernicke's was associated with initial comprehension deficits. Similarly, it was of interest if post-stroke perfusion within Broca's area might be associated with impaired articulation functions. To test this hypothesis perfusion within language ROIs was extracted and correlated with the four scaled composite subscale scores. The rationale for using these scores is that spontaneous speech and naming should tap into the articulatory functions assumed to involve Broca's region, whereas comprehension should be mediated via Wernicke's area. Repetition deficits have classically been ascribed to a lesion along the connection of both areas and will therefore be investigated in relation to both ROIs. Previous studies have

concentrated on left hemispheric perfusion. The same will be done here, however, the data for the right hemisphere is also shown for completeness (**Table 31**).

Perfusion within Broca's region did not yield a significant association with the scaled composite subscale score for spontaneous speech (BA44: $r(11)= -0.108$, $p=0.752$; BA45: $r(11)= -0.162$, $p=0.634$). Similarly, this cortical region was not associated with naming deficits (BA44: $r(11)= -0.159$, $p=0.640$; BA45: $r(11)= -0.170$, $p=0.618$). Similarly, perfusion with the superior temporal lobe was not correlated with comprehension deficits (STG_Te10: $r(11)= 0.154$, $p=0.651$; STG_Te11: $r(11)= 0.237$, $p=0.482$; STG_Te3: $r(11)=0.119$, $p=0.728$). Repetition deficits were not associated with perfusion measures in either frontal or temporal regions in our cohort (STG_Te10: $r(11)= -0.028$, $p=0.936$; STG_Te11: $r(11)= 0.058$, $p=0.866$; STG_Te3: $r(11)=-0.026$, $p=0.941$; BA44: $r(11)= -0.130$, $p=0.704$; BA45: $r(11)= -0.130$, $p=0.704$).

In conclusion, it was not possible to replicate the previously described finding of a hypoperfusion within Wernicke's area being predictive of the severity of word comprehension impairments. This discrepancy might be due to different methodological approaches in relation to the imaging methodology (i.e., exogenous vs. endogenous tracer), diverging perfusion measurements (i.e., relative delay in perfusion vs. average perfusion within ROI), different language assessments (non-standardised assessment vs. standardised battery), and sample size. Further considerations will be detailed in the discussion.

Table 31 Perfusion measures at baseline stratified by hemisphere. Values represent measures extracted from within cortical language regions of interest (ROI) and the global mean perfusion within each hemisphere. The underlying perfusion map was the 30% grey matter thresholded smoothed normalised cerebral blood flow map. All measurements represent ml/100gm of tissue/min.

ID	BA44	BA45	IPL_PF	IPL_PFcm	IPL_PGa	STG_Te10	STG_Te11	STG_Te3	GLOBAL	BA44	BA45	IPL_PF	IPL_PFcm	IPL_PGa	STG_Te10	STG_Te11	STG_Te3	GLOBAL
	Left Hemisphere									**Right Hemisphere**								
3	23.20	18.32	12.18	24.99	11.22	38.20	36.49	17.09	286.39	20.83	19.18	13.75	26.30	16.96	34.11	35.97	20.45	199.65
4	21.69	16.11	10.52	27.10	8.94	61.93	49.92	18.34	224.86	20.83	19.18	13.75	26.30	16.96	34.11	35.97	20.45	199.65
5	42.67	27.31	22.32	53.07	26.06	82.46	67.62	37.27	364.31	29.77	24.85	16.64	37.64	18.99	45.92	46.22	19.77	270.11
7	27.65	19.39	13.48	27.91	17.28	28.68	15.42	17.19	254.70	33.23	25.34	15.45	35.13	19.65	41.36	37.36	24.67	269.91
8	21.07	17.39	13.09	23.73	8.56	29.55	29.57	19.34	235.91	28.91	26.46	19.47	32.42	24.61	34.66	31.99	21.75	255.52
9	15.53	15.45	4.15	7.44	11.65	7.51	6.82	12.94	210.39	29.77	24.21	15.39	28.89	18.08	37.82	36.00	20.48	254.08
10	9.29	11.26	4.46	6.39	6.83	6.39	8.39	5.41	197.85	28.34	21.44	14.03	29.84	15.53	39.76	36.41	18.96	227.68
13	27.79	24.72	12.65	26.75	17.30	29.72	29.66	14.02	271.93	34.06	29.40	18.49	35.11	23.68	40.69	38.52	22.16	277.61
14	11.89	6.42	9.52	20.04	11.27	18.48	19.24	6.87	144.24	9.54	7.21	7.81	13.85	9.10	20.15	20.69	10.35	126.01
15	22.16	16.47	5.55	18.62	10.67	38.60	28.86	19.32	260.81	40.79	33.49	25.35	47.77	27.05	49.86	46.02	28.70	339.92
16	18.72	13.53	8.32	22.21	6.32	34.48	31.55	16.38	176.84	20.69	13.49	11.76	25.45	10.94	31.12	32.94	15.40	185.81
18	50.26	36.21	20.01	36.81	28.13	48.18	43.32	28.74	385.08	37.35	32.23	22.36	43.70	28.26	50.22	48.27	28.27	349.57
19	25.10	17.28	18.98	38.63	20.09	38.07	31.50	20.34	257.67	26.73	18.92	16.03	36.84	18.50	38.29	37.80	19.18	235.87
Min	9.29	6.42	4.15	6.39	6.32	6.39	6.82	5.41	144.24	9.54	7.21	7.81	13.85	9.10	20.15	20.69	10.35	126.01
Max	50.26	36.21	22.32	53.07	28.13	82.46	67.62	37.27	385.08	40.79	33.49	25.35	47.77	28.26	50.22	48.27	28.70	349.57
Mean	24.39	18.45	11.94	25.67	14.18	35.56	30.64	17.94	251.61	27.76	22.72	16.18	32.25	19.10	38.31	37.24	20.82	245.49

CHAPTER 10 SUPPLEMENTARY ANALYSIS (DTI AND SD)

'Once we accept our limits, we go beyond them'

(Albert Einstein)

The present study focussed on the relationship of the arcuate fasciculus and post stroke language recovery using diffusion tensor tractography. However, as discussed in the introduction to this dissertation, the arcuate fasciculus might not be the only pathway in the human brain that is involved in language processes. To account for the possibility that the inferior fronto-occipital fasciculus (iFOF) might be involved in language functions, especially semantic processing as suggested by Duffau et al. (2005), this fibre system was dissected and anatomical-functional correlations were computed.

Contemporary diffusion imaging methodology has some limitations (see subchapter 5.3.3). To overcome some of these restrictions and to be able to dissect a pathway, that is thought to be relevant for all motor aspects of language, an additional pre-processing with spherical deconvolution was conducted and the frontal aslant tract (FAT) was dissected.

Some of the findings presented in this chapter still await validation in patient cohorts and/or comparison data from healthy volunteers. Where comparison measures are available, they will be mentioned in the chapter.

10.1 Diffusion tensor imaging (DTI) analyses of the iFOF

The ventral system was dissected in the previously described patient sample. In patients where the lesion encompassed the external/extreme capsules, the inferior fronto-occipital fasciculus (iFOF) could only be partially dissected (for example in patient 18; **Figure 80**). For subject 14 the iFOF was not dissected, as the DTI did not reveal any connections between the frontal and the occipital lobes. This might be due to the incomplete data acquisition for this patient as discussed in Chapter 6. After the dissections were obtained, tract specific measurements, namely the tract volume (number of voxels) and the fractional anisotropy for each pathway, were extracted and entered into our statistical analyses.

For both measures a highly significant right-ward asymmetry was observed, indicating that the tract is bigger in the right hemisphere (to be expected given the presence of a lesion in the left) and that the fractional anisotropy is higher in the right hemisphere (to be expected given that the integrity of the pathway might be altered in the left hemisphere) (**Figure 79**, **Figure 80**).
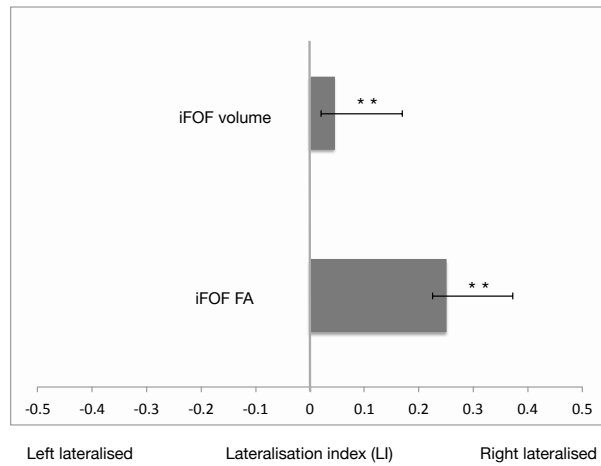
Figure 79   Laterality indices (volume and FA) of the iFOF
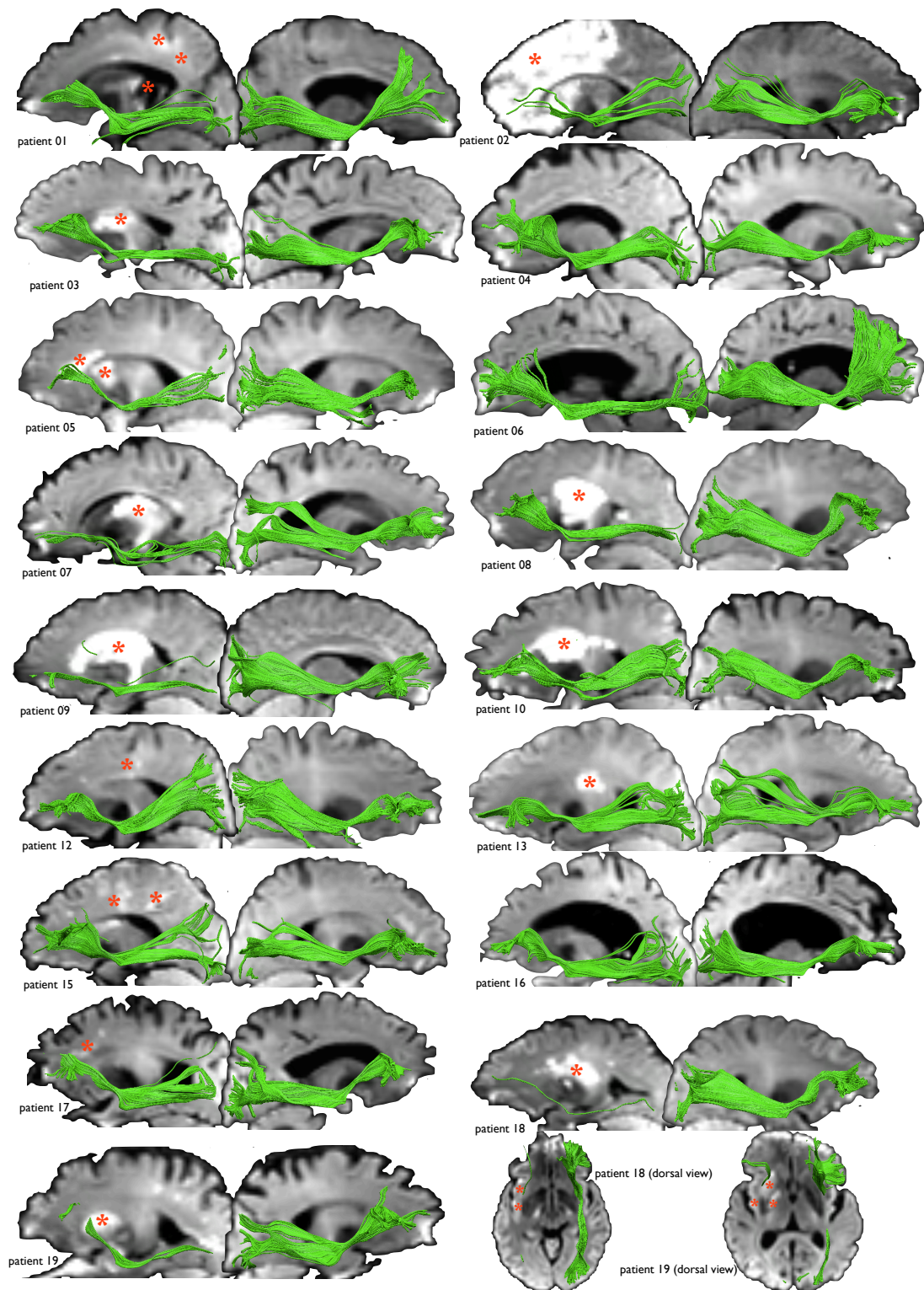
Figure 80   Bilateral inferior fronto-occipital fasciculus (iFOF)

This figure shows the DTI reconstructions of the iFOF in the presented stroke cohort overlaid on each patient's native diffusion-weighted image. The red asterix indicates the location of the lesions. The bottom right shows the dorsal view for patient 18 and 19 to better demonstrate the impact the lesion had on the pathway.

For comparison, the MNI-normalised anatomy of the inferior fronto-occipital fasciculus as seen in a healthy cohort is shown in **Figure 81**. The figure depicts the superior and inferior fronto-occipital fasciculus as obtained with spherical deconvolution tractography. The top panel shows an MNI-normalised three dimensional reconstruction of the pathways and the lower panel shows the percentage overlay maps where it can be appreciated that the iFOF has a consistent trajectory along its entire course and across subjects (for details please see the original publication). In the healthy population, the iFOF is right lateralised for number of streamlines (significantly) and for tract volume (not significantly); fractional anisotropy, however, is not significantly lateralised (Thiebaut de Schotten, ffytche, et al. 2011b). Hence, the highly significant right-lateralised asymmetry in fractional anisotropy in this stroke sample is either due to decreased left hemispheric FA or increased right hemispheric FA. Given the presence of a lesion in the left hemisphere in this stroke cohort, it seems more likely, however, that decreased left hemispheric FA values are driving this significant observation.
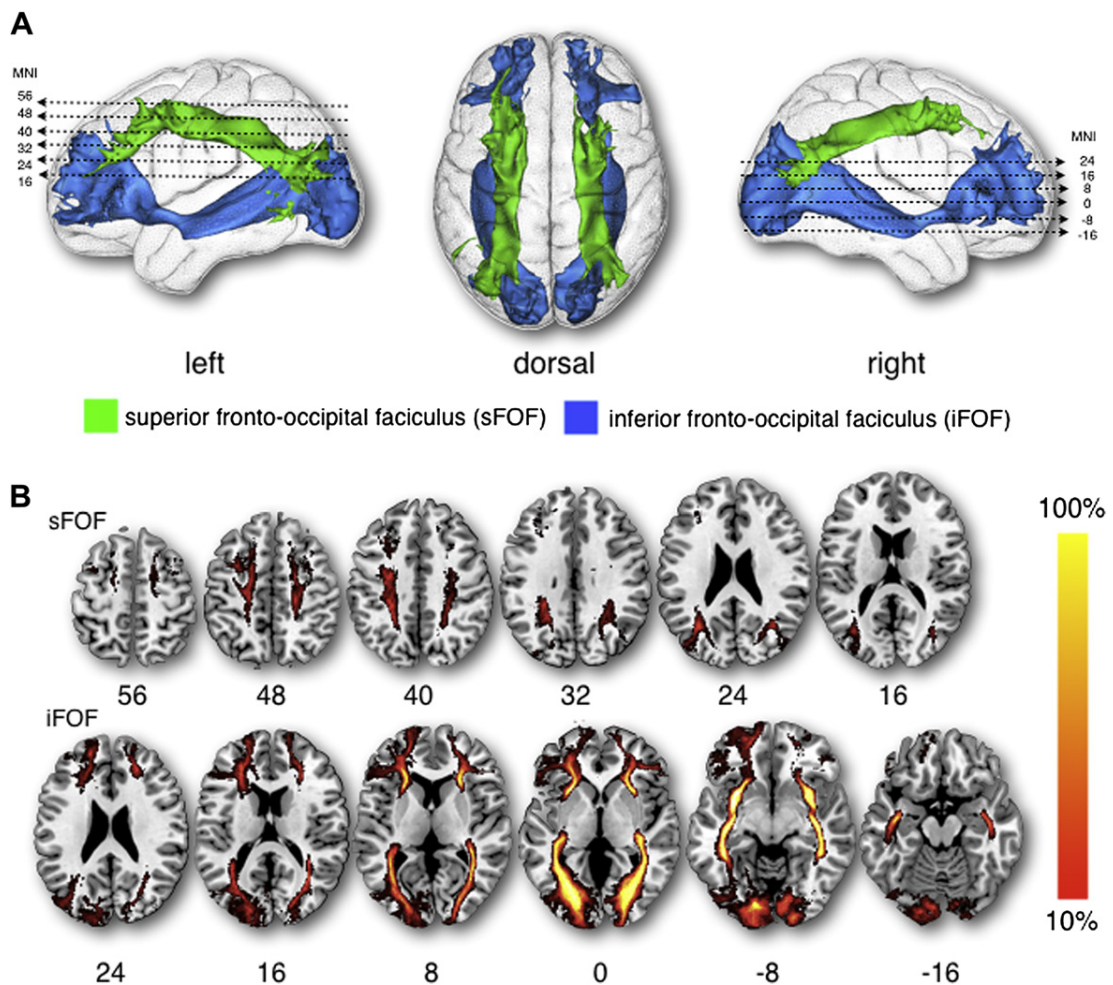
Figure 81   SD reconstruction of the superior fronto-occipital fasciculus (sFOF) and inferior fronto-occipital fasciculus (iFOF) in a healthy cohort as published in Forkel et al.

(2012) **A** 3D reconstruction of the normalised trajectory of the sFOF and iFOF. MNI coordinates are in correspondence with the MNI slices shown in panel B. **B** MNI-normalised overlay percentage maps of the sFOF (upper panel B, MNI 56-16) and the iFOF (lower panel B, MNI 24 to –16).

Despite earlier reports treating fractional anisotropy as non-Gaussian (Jones et al. 2005), all measures in our sample are normally distributed (**Table 32**).

Table 32   Test of normality of the IFOF tract specific measurements

		Fractional anisotropy		Volume (no of voxels)	
		Left	**Right**	**Left**	**Right**
n		17	17	17	17
Normal Parameters[a,b]	Mean	.4456	.4877	989.8235	1544.4706
	SD	.03855	.03322	465.02046	330.44707
Most Extreme Differences	Positive	.074	.104	.129	.125
	Negative	-.097	-.081	-.147	-.110
Kolmogorov-Smirnov Z		.402	.430	.608	.514

[a]. Test distribution is Normal.
[b]. Calculated from data.
SD, standard deviation

The volume as well as the fractional anisotropy was significantly higher in the right hemisphere relative to the left hemisphere (**Table 32** and **Table 33**).

Table 33   iFOF volume and fractional anisotropy in both hemispheres in the acute stage.

Inferior fronto-occipital fasciculus		n	Mean (SD)	*t(paired)*	df	*p*
Volume	*Left*	17	989.82(465.02)	-4.309	16	.001
	Right	17	1544.47(330.45)			
Fractional anisotropy	*Left*	17	.4456(.03855)	–3.673	16	.002
	Right	17	.4877(.03322)			

When investigating the association between the overall language performance indices from the WAB-R at baseline and after six months with the iFOF tract measurements, it can be observed that fractional anisotropy in the left hemisphere is correlated with the baseline severity of aphasia (r(17)=.522, *p*=.032). The right FA had a tendency to significance when correlated with baseline severity (r(17)=–.44, *p*=.076). The iFOF volume was not associated with severity at follow-up (left:

r(17)=−.012, *p*=.963; right: r(17)=.046, *p*=.860). At follow-up, fractional anisotropy was no longer correlated with the longitudinal severity of aphasia (left: r(16)=.330, *p*=.213; right: r(16)=−.036, *p*=.895). Tract volume was not associated with longitudinal severity (left: r(16)=−.015, *p*=.955; right: r(16)=.105, *p*=.70).

As discussed in the introduction (Chapter 3), the iFOF is hypothesised to be important for semantic language processes. As a surrogate language index from the WAB-R, I used semantic categorical word fluency (animals) to test for association with the inferior fronto-occipital fasciculus. At baseline, only the FA of the right iFOF correlated with the number of animals generated in one minute (r(15)=−.535, *p*=.04). At follow-up none of the iFOF measures were significantly associated with semantic fluency (**Table 34**).

Table 34   Correlation between semantic word fluency and tract specific measurements of the iFOF.

Inferior fronto-occipital fasciculus			n	r	*p*
Volume	*Baseline*	*Left*	15	−.105	.709
		Right	15	−.020	.942
	6 months	*Left*	16	.069	.799
		Right	16	.043	.875
Fractional anisotropy	*Baseline*	*Left*	15	.499	.058
		Right	15	−.535	.040*
	6 months	*Left*	17	.474	.064
		Right	17	−.195	.470

* Significant at the 0.05 level

It should, however, be noted here again that the semantic category word fluency task of the WAB has been previously criticised and its shortcomings have been discussed in the introduction to this dissertation (subchapter 2.2.3 and also Norman 1988).

The WAB-R subscales were further entered into a correlation analysis. For the baseline, the following associations were observed. Grammar and phonemic fluency (FAS words) were negatively correlated with the FA of the right iFOF

(grammar: r(16)=–.684, *p*=.004; FAS: r(12)=–.612, *p*=.035). This implies that the lower the FA in the right iFOF the better the grammar and phonemic fluency. Naming was marginally associated with the FA in the left iFOF (r(16)=.481, *p*=.06).

For the longitudinal assessment, all WAB-R subscales were tested against the iFOF measures and only single-word based object naming was positively correlated with the FA in the left iFOF (r(16)=.633, *p*=.008), indicating that the higher the FA of the left iFOF the better the object naming performance on the WAB.

10.2 Spherical deconvolution (SD) analysis of the FAT

This study benefitted from the use of contemporary diffusion imaging methodology. However, several limitations should also be acknowledged. Current DTI algorithms are prone to implicit limitations, including generating the presence of false positives (i.e. non-existing tracts) and false negatives (i.e. absence of truly existing tracts). These limitations have to be considered with caution, especially when endeavouring to extract quantitative measures within the lesioned hemisphere.

To address some of these shortcomings but also to take into account pathways that cannot be dissected using DTI, the present study was supplemented with an additional spherical deconvolution analysis that can partially overcome some of the abovementioned limitations whilst allowing us to investigate additional pathways that cannot be dissected using more conventional DTI in regions of high fibre density (i.e. fibre crossings >2). The in-house software *StarTrack* was used to conduct this analysis (for more details please refer to Chapter 6).

One tract that is particularly difficult to dissect with diffusion tensor imaging algorithms is the frontal aslant tract (FAT). In the healthy population, the FAT interconnects anterior supplementary and pre-supplementary motor areas (pre-SMA) of the superior frontal gyrus and the pars opercularis of the inferior frontal gyrus. This results in a lateral to medial trajectory of the pathway as can be seen in **Figure 82**D. Given its specific position in the frontal lobe, the FAT is located in an area of complex white matter anatomy. Here, various fibre populations are present including the medial and lateral projections of the corpus callosum, cortico-spinal tract, arcuate fasciculus, superior longitudinal fasciculus as well as other intralobar and cortical u-shaped fibres. Given this rich anatomy, reconstructing the FAT using conventional DTI is most difficult and for this purpose spherical deconvolution was implemented here. It can be seen in **Figure 82**E (yellow pathway) that the FAT is significantly left lateralised in the healthy population.
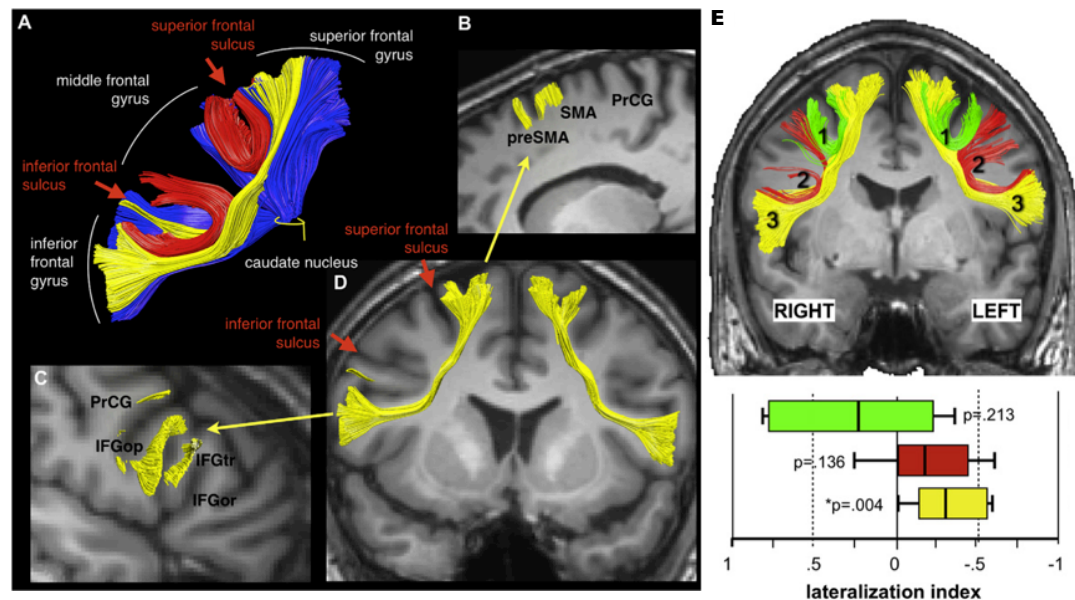
Figure 82   Anatomy and laterality of the frontal aslant tract

Anatomy (A–D) and lateralisation (E) of the frontal aslant tract (FAT) here shown in yellow. The figure above is shown in radiological view. Taken from (Catani, Dell'Acqua, Vergani, et al. 2012b).

In the present study, the frontal aslant tract was bilaterally dissected in all stroke patients available for this analysis (n=17). Paired t-test analysis showed that the volume of the FAT, measured as voxel count and track count, was found to be significantly left lateralised (no of voxel: $t_{(16)}$=3.486, p=0.003; track count: $t_{(16)}$=2.166, p=0.046). A laterality index (LI) was calculated based on the volume (voxel and tract count) grounded on the previously described formula (Right-Left/Left+Right). This aligns all subjects between the values of -1 and 1, where negative values indicate a left lateralisation. **Figure 83** shows the LI plot for voxel and track count lateralisation of the frontal aslant tract; both indices are left lateralised as described in the text. This lateralisation pattern is in line with the previous report for healthy volunteers (**Figure 82**).
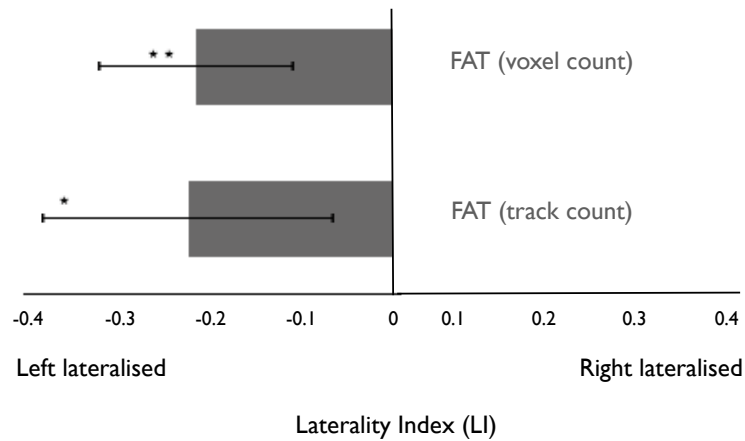
Figure 83   Lateralisation Index (LI) frontal aslant tract (FAT) with 95% confidence interval

At baseline, the FAT LI for track count had a tendency to significance when correlated with the overall baseline severity of aphasia ($r(17)=-.423$, $p=.09$) and a significant association was observed with word repetition ($r(17)= -.678$, $p=0.003$). No other significant correlations with subscales (i.e. naming, semantic and phonemic fluency, comprehension) were observed at baseline or after six months post onset.
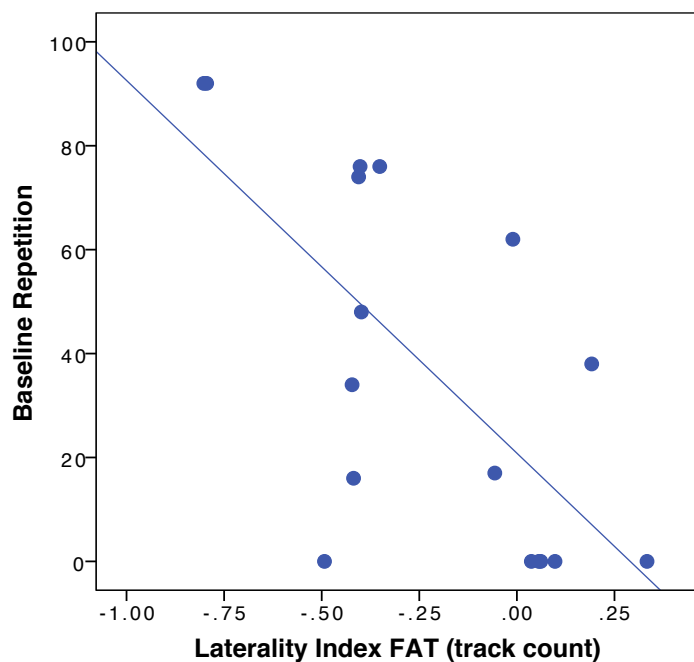
Figure 84   Scatterplot of volumetric laterality of the frontal aslant tract (FAT) against the repetition score at baseline

Given the observed correlation with repetition, this relationship was further investigated. For this, the sample was divided (median split) into high and low

performers on the repetition scale. When comparing the high and low performers on the repetition task at baseline, the high performers had a marginally significant larger FAT in the left hemisphere (**Table 35**). No differences were found for the right hemispheric FAT between the two groups (**Table 35**).

Table 35   Differences for high and low performer on the repetition scale in relation to the volume of the frontal aslant tract (FAT).

FAT volume (track count)	Repetition (median split at 34)	n	Mean (SD)	*t*	df	*p*
Left	*Low performer*	9	181.11(97.16)	–2.028	15	0.06
	High performer	8	274.75(92.50)			
Right	*Low performer*	9	166.00(110.40)	.768	15	.768
	High performer	8	148.13(135.44)			

In conclusion, this supplementary analyses demonstrated that the iFOF, as part of the ventral system, is strongly right lateralised in our sample. The FA of the left iFOF is positively correlated with the overall aphasia severity at baseline (i.e. better left FA less severe aphasia). The FA of the right iFOF is negatively correlated with semantic fluency, grammar, and phonemic fluency (i.e. higher right FA worse performance on the tasks). After six months, the FA of the left iFOF positively correlated with naming (i.e. better left FA better naming). Overall, it appears from this that higher FA of the right iFOF is less beneficial whereas higher FA values for the left iFOF are beneficial for language performance. How these measures related to the performance in healthy volunteers still awaits investigation.

Further, the frontal aslant tract was dissected in all patients and was strongly left lateralised as can be expected from the literature. The laterality of the FAT also correlated with repetition, indicating that the more left lateralised the FAT is the better the baseline repetition performance.

CHAPTER 11 CASE REPORTS (THREE PATIENTS)

'Neurology is learning stroke case by case'

(Anonymous)

Given the richness of the presented data set and the very complex nature of language impairments, it is worth looking at some patients on an individual basis. Even though group-level comparisons are important and pivotal for predicative analyses, some information is lost when pooling the data (Fedorenko & Kanwisher 2009; Steinmetz & Seitz 1991; Démonet et al. 2004). Hence, some of the patients within the sample discussed so far will be individually presented here and their deficits will be investigated in sight of the underlying anatomy.

A detailed patients' medical history (since admission to the HASU) will be given and the available imaging will be used to demonstrate the lesion and allude to possible compensation routes that would still allow the patients to perform the language functions they maintained or later regained. Within the current work, these compensatory routes are not provable but are the most likely routes according to my knowledge and in agreement with the literature.

11.1 Case report 1 (patient 01)

Case history

[4 Nov 2009] 87-year-old right-handed lady admitted to the hyperacute stroke unit at King's College London with a first-ever unilateral cardio-embolic stroke. On admission, her clinical examination yielded a Glasgow Coma Scale (GCS) score of 14, NIHSS score of 4 due to global aphasia and lack of orientation. The patient is an English native speaker with no previous medical history in neurology and/or psychiatry. She was thrombolysed within 35 minutes of arrival at the Accident and emergency department department. Post-thrombolysis the patient developed a thalamic haemorrhagic transformation. All language assessments were obtained post thrombolysis.

On admission, the stroke specialist in charge classified her as globally aphasic.

[7 Nov 2009] At the screening she presented with auditory verbal comprehension deficits (5/10), was not able to follow sequential commands (3/10), and slightly impaired repetition (6/10).

[12 Nov 2009] The baseline assessment identified a left-right confusion (though intact finger recognition), impaired repetition (76/100), impairments in sequential commands (41/80), naming and word finding difficulties (51/60), reduced semantic-categorical word fluency (4/20), and reduced spontaneous speech (16/20). The baseline assessment also included a memory assessment that identified working memory impairments on the spatial (forwards: 2/16, backwards: 1/14; age-corrected) and digit spans (forwards: 7/16, backwards: 1/14; age-corrected).

[1 April 2010] Six months post symptom onset, her naming was perfect with still reduced word fluency (15/20) and high-level impairments for repetition (84/100). The overall aphasia quotient was 95.2, and was hence classified as *recovered*.

On structural imaging a posterior thalamic lesion including the middle geniculate nucleus (MGN) was evident. The left MGN is primarily connected to the auditory cortex and the posterior thalamus is connected to the superior temporal and the inferior parietal cortices (**Figure 85**).

The conundrum here was that the patient initially presented with global aphasia and later Wernicke-type aphasia with a rather discrete lesion not affecting the convexity of the brain.
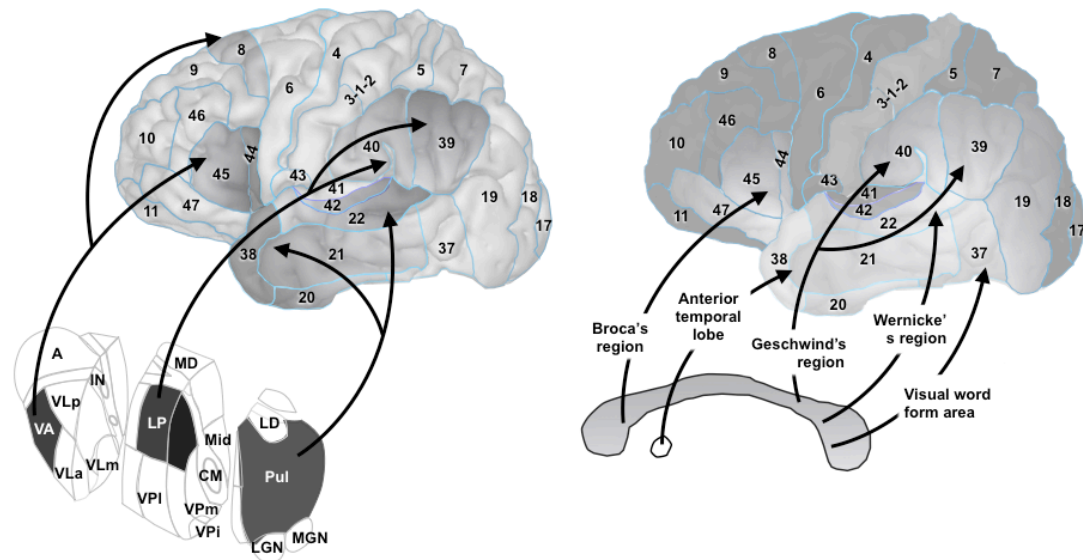
Figure 85   Thalamo-cortical connections and density of the interhemispheric connections

This figure shows the thalamo-cortical connections of language areas (BA22,40,39,44,45) and their interhemispheric connections. For the callosal connections, bright areas represent the areas that are less connected though the corpus callosum and dark areas are strongly connected. It can be seen that the language areas tend to be less connected compared to other cortical regions. Thalamic nuclei in the figure: A, anterior group; LGN, lateral geniculate nucleus; LD, laterodorsal; LP, lateroposterior; MD, mediodorsal; MGN, medial geniculate nucleus; Mid, midline; Pul, pulvinar; VA, ventral anterior; VLa, ventral lateral anterior; VLm, ventral lateral medial; VLp, ventral lateral posterior; VPi, ventral posterior inferior; VPl, ventral posterior lateral; VPm, ventral posterior medial; IN, intralaminar nuclei; CM, centromedian nucleus. Nomenclature based on (Morel et al. 1997). (Courtesy of Prof. Katrin Amunts and Dr. Marco Catani, in press).

However, when looking at the diffusion-weighted imaging a larger lesion, engulfing the arcuate fasciculus, can be appreciated (**Figure 86**). This demonstrates nicely the previously reported advantage that DWI can have over conventional imaging, especially in the acute stages of stroke.

The lesion, as seen on DWI, is impacting on the left arcuate fasciculus and might partially explain the patient's repetition deficits at the screening and baseline

assessment. Additionally, the lesion has damaged the middle geniculate nucleus of the auditory thalamus. This part of the thalamus is connected to the auditory cortex via projection fibres. These projections fibres have been consistently demonstrated in the monkey (Mesulam & Pandya 1973; Rauschecker et al. 1997) and the human brain using histological methods (Rademacher et al. 2002; Bürgel et al. 2006) and diffusion imaging (Behrens, Johansen-Berg, et al. 2003a; Berman et al. 2013).

In this patient, the auditory thalamus and its cortical projections are damaged/disconnected, not allowing auditory input to be relayed for further processing. Also, the frontal aslant tract was not dissectible in the left hemisphere using DTI, showing that the white matter connections reaching Broca's area (i.e. the arcuate fasciculus and the frontal aslant tract) were severely damaged.

In conclusion, the core of the stroke lesion is centred on the posterior thalamus in the left hemisphere. Extended damaged was evident on diffusion-weighted imaging identifying disconnections to the white matter reaching Broca's and Wernicke's territories (**Figure 87**).

T1–weighted imaging   **Diffusion–weighted imaging**

Diffusion tensor tractography of the arcuate fasciculus

dorsal view   left sagittal view   right sagittal view
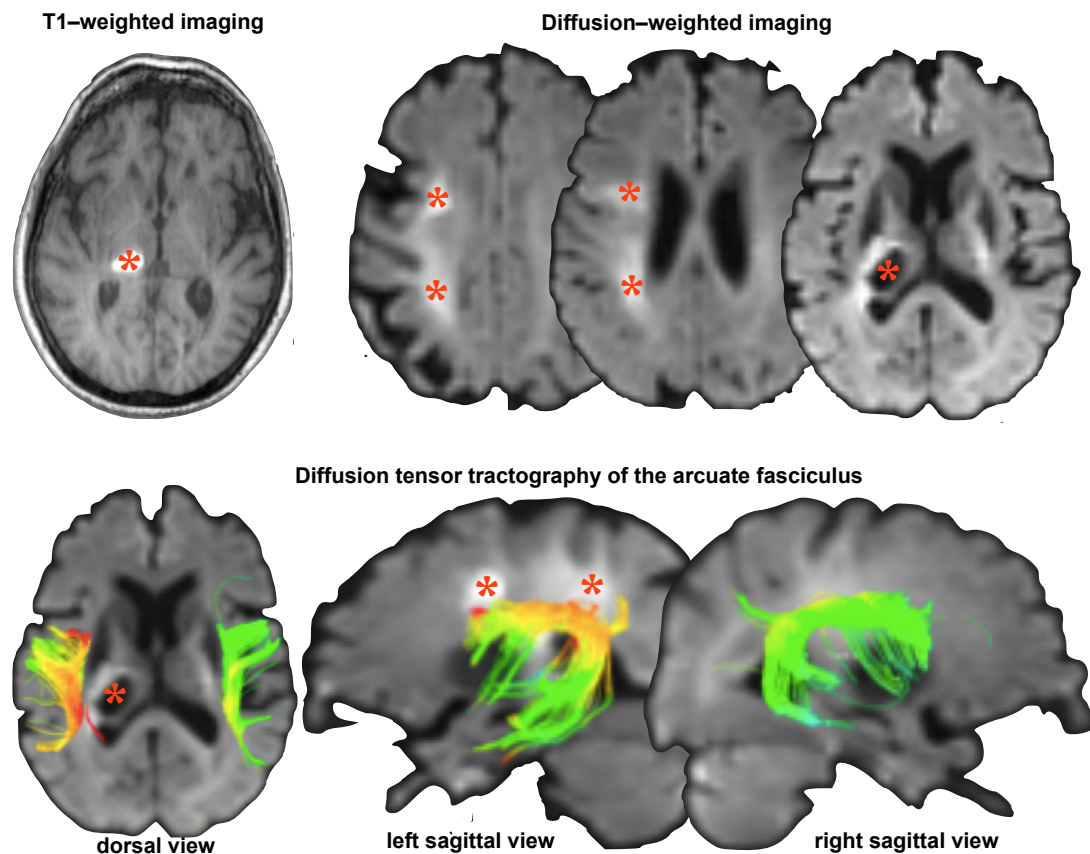
Figure 86   MRI contrasts for patient 01 and the bilateral arcuate anatomy

The top panel shows the T1-weighted structural scan with the left thalamic lesion (indicated as asterix) in comparison to lesion extent as shown on the diffusion-weighted imaging. The bottom panel depicts the reconstruction of the arcuate fasciculus as a whole (upper panel) and split into three segments (lower panel). The above image visualises the arcuate fasciculus (dorsal, left-lateral and right-lateral views) with the fractional anisotropy mapped onto the pathway. Visualisation is overlaid onto the patient's native diffusion-weighted image. The red asterix indicates the lesion.

Nevertheless, this patient was able to repeat words and short sentences in the presence of word finding difficulties at baseline. If we assume that auditory input is processed via the right MGN, the input could then be further relayed to the Wernicke homologues region in the right hemisphere. From here, there is a possibility of two different routes. The first would be to pass the information on to the ipsilateral Broca homologue area and from there utilise interhemispheric connections (possibly the genu of the corpus callosum) to propagate the processed information towards the left-hemispheric Broca region to then produce the verbal output (**Figure 87**).

Another possibility would be to pass on the information from the right Wernicke area via posterior commissural pathways to the left-hemispheric Wernicke area; From there, other pathways than the arcuate (e.g., uncinate, iFOF) might allow for the information to travel to further processing areas (**Figure 87**). Naming, especially semantic naming, has been implicated to be mitigated along the ventral network including the uncinate (Papagno 2011; Papagno et al. 2011; Heide et al. 2013) and the iFOF (Duffau 2008).

Damage to the auditory system for patient 01 and possible compensatory routes utilising the right hemispheric homologues areas and interhemispheric commissural pathways.
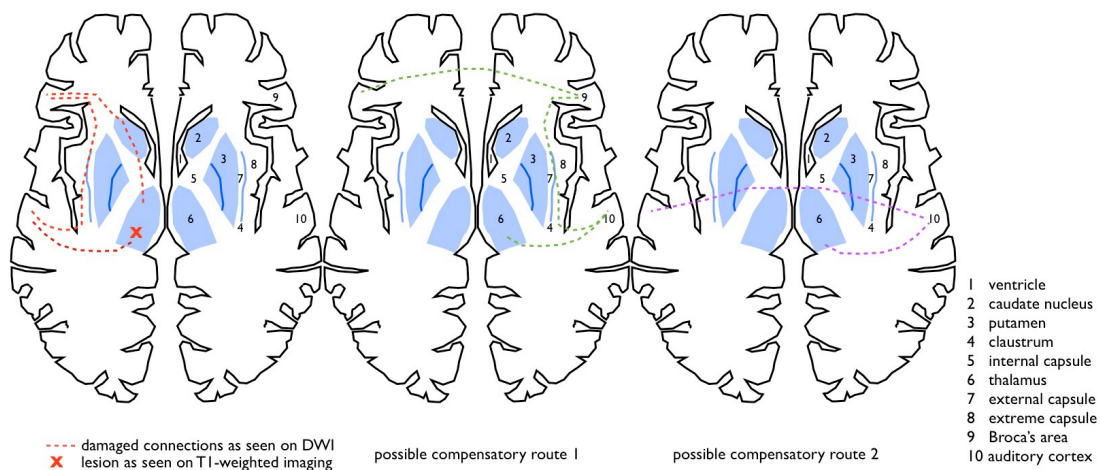
Figure 87   Damage and possible compensation for patient 01

11.2 Case report 2 (patient 02)

Case history

[8th November 2009] A 28-year-old right-handed man (electrician) was admitted to the HASU at King's College Hospital with a first-ever unilateral stroke presenting with dense right-sided hemiplegia, right-sided sensory loss and inattention, receptive dysphasia and expressive aphasia and behavioural problems. Patient was not thrombolysed due to the lack of a clear time of onset. On the imaging, it can be appreciated that the patient had a lesion to the left frontal lobe extending from the pole to the level of the anterior thalamus, whilst encompassing all cortical and subcortical structures of the left frontal lobe (**Figure 88**A). The perisylvian white matter affected

included the arcuate fasciculus, uncinate fasciculus, iFOF, and FAT.

[10th November 2009] On the initial screening, comprehension is variable but relatively good for simple commands (max. 2 words). Patient was able to repeat his own name but no other words. Automatic speech (counting, days of the week) was possible after priming. Patient prefers non-verbal communication but is inconsistent with gestures.

[16th November 2009] Unable to repeat letters but can repeat single words after semantic priming. No spontaneous speech. Auditory verbal comprehension intact for personal questions but not for abstract questions (45/60). Patient can follow two-stage commands inconsistently (35/80). Repetition good but with length effect (92/100). No object naming (1/60), no word fluency (1/20).

[26th June 2010] The patient made a full functional recovery with word fluency problems that were more severe for phonemic fluency. Spontaneous speech OK. Auditory verbal comprehension intact (60/60). Patient can follow sequential commands (80/80). Repetition good (98/100). Object naming OK (53/60). Reduced semantic word fluency (10/20) and impaired phonemic fluency (2).

At the time of reassessment he was on medication: 5mg Asprin (once a day), 40mg simvastatin (one a night), 4mg Perindopril (one a day), 200mg Dipyridamole (twice a day).
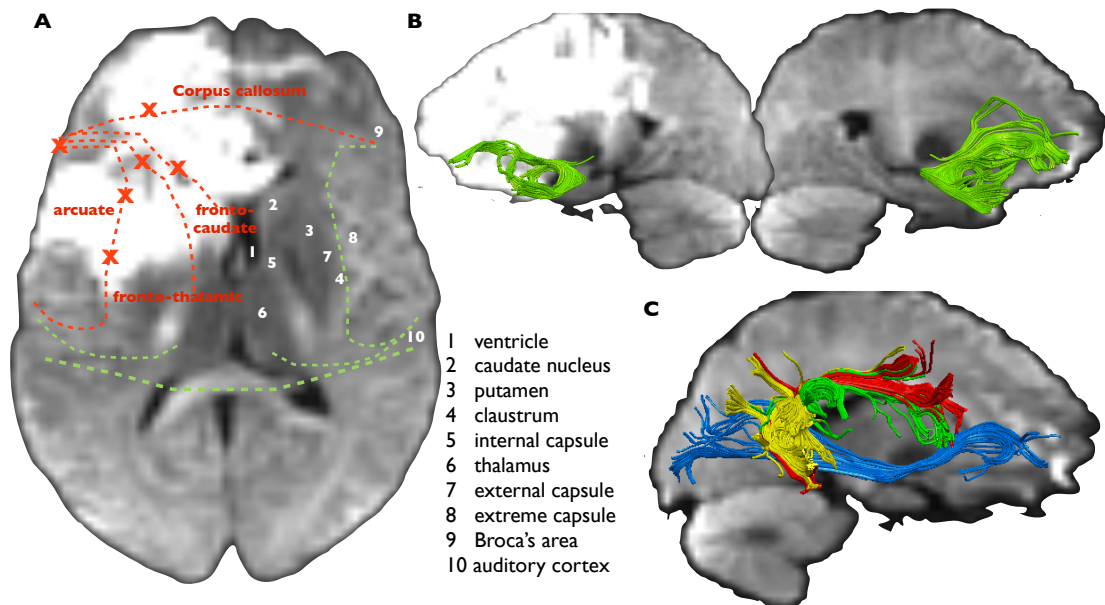
Figure 88   DWI Damage patient 02 and white matter connections

Figure **A** depicts the DWI of patient 02 as axial slice with the schematic diagram of damaged and intact connections. **B** shows the damage to the uncinate fasciculus in the left hemisphere that has reduced volume compared to the right uncinate fasciculus. **C** shows the right hemispheric Perisylvian white matter of the same patient.

In this patient, the uncinate fasciculus (connecting anterior temporal and inferior frontal cortices) is affected by the lesion and the left uncinate is hence reduced in volume (**Figure 88**B). This damage might account for the naming impairment in this patient. The first language function this patient recovered was the ability to repeat words. Given the size and location of his lesion this ability to repeat words is not likely to be performed by the left hemisphere but rather through the intact right hemisphere (**Figure 88**C). The potential of the right hemispheric homologues areas to perform repetition tasks has been previously shown with PET imaging (Ohyama et al. 1996). The right hemispheric pathways are not affected by the lesion apart from the lesion along the genu of the corpus callosum, which is likely to cause callosal degeneration in the right hemisphere. Also naming abilities after left-hemispheric damage have been identified for the right hemisphere (Fridriksson et al. 2009).

11.3 Case report 3 (patient 08)

Case history

[27th June 2010] A 43-year-old right-handed previously known hypotensive lady was admitted to the HASU at King's College

Hospital with a first-ever unilateral stroke, presenting with dense right-sided hemiparesis, sensory loss, neglect, and dysphasia. On admission, her clinical examination yielded a GCS score of 11 and an NIHSS score of 27. The patient was not thrombolysed (>5 hours). The clinical CT scan showed a striatocapsular infarct engulfing the left lentiform nucleus, posterior limb of the internal capsule, with extent into the corona (see **Figure 89** for lesion on DWI).

[29th June 2010] On the WAB-R screening, the patient was diagnosed with moderate transcortical motor dysphasia with reduced fluency (3/10), reduced spontaneous speech (6/10) and impaired naming (5/10).

[30th June 2010] On the full assessment the patient was diagnosed with moderate Broca's aphasia (AQ 58.6/100) with reduced semantic (2/20) and phonemic (0) fluency. Repetition was found to be extremely effortful (48/100) and only possible for single words.

[29th December 2011] Patient presented without neglect but remaining spams in right upper limb and left neck. On the language assessment, she was classified as mild anomic (AQ=87.2). Semantic (18/20) and phonemic (31) fluency improved remarkably. Naming (60/60) and repetition (98/100) intact. Spontaneous speech was still marked by object omissions, hesitations and shortened phrase length and an overall effortful speech. The patient reports having developed obsessive-compulsive disorder subsequent to suffering the stroke. At the time of reassessment she was on medication: 40mg fluoxetin-neuraxpharm (once a day), 2.5mg bendroflumethiazide (once a day), 75mg clopidogrel (once a day), 40mg simvastatin (one a night), 2.5mg ramapril (one a day), 10-20mg baclofen (three times a day).

dorsal view (arcuate fasciculus)   **coronal view (frontal aslant tract)**

left sagittal view (arcuate fasciculus)   **right sagittal view (arcuate fasciculus)**
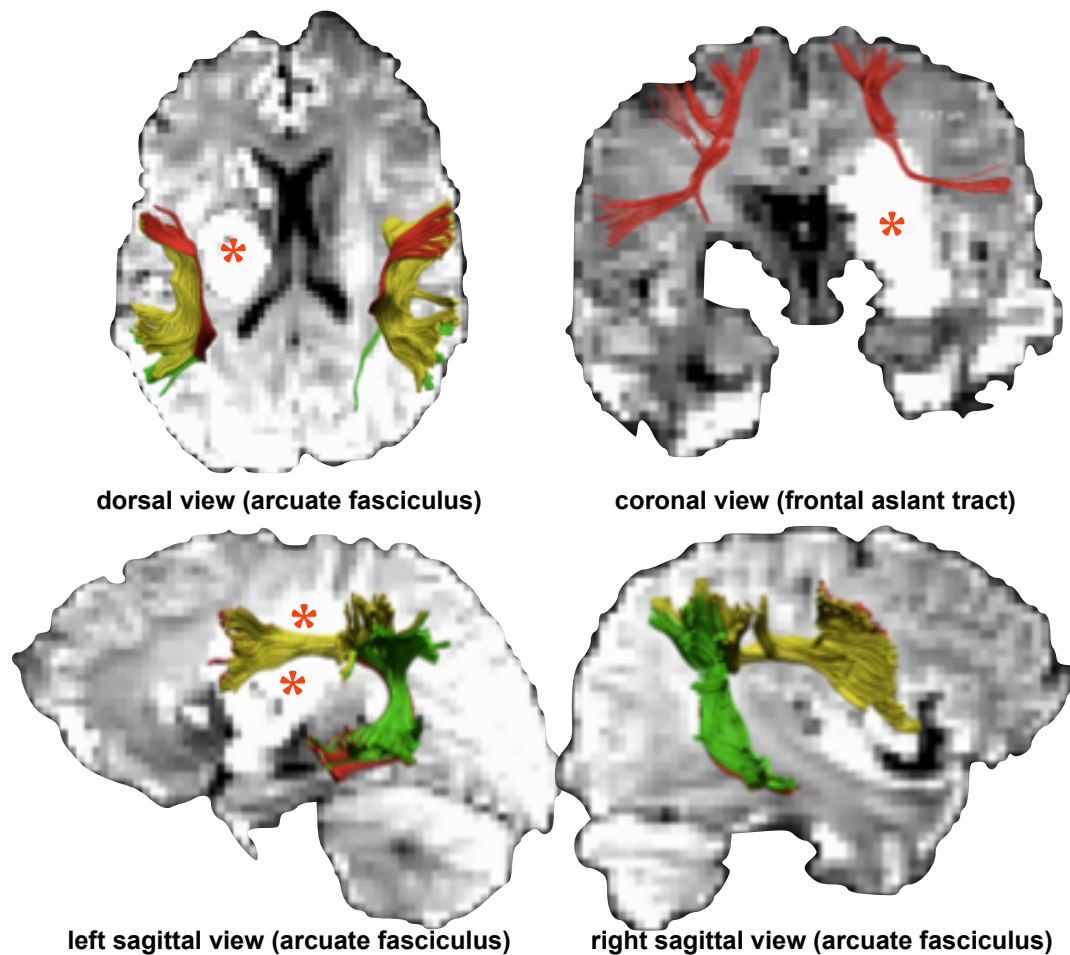
Figure 89   DTI reconstruction of the arcuate fasciculus and the frontal aslant tract
for patient 08

DTI reconstruction of the three arcuate segments shown in dorsal, left-lateralised, and right-lateralised view. The lesion on the left is bordering onto the medial aspects of the long segment but is not engulfing any of the segments. The coronal vies shows the dissection of the frontal aslant tract that is engulfed by the lesion in the left hemisphere. Visualisation is overlaid onto the patient's native diffusion-weighted image. The red asterix indicates the stroke lesion.

In this patient, the arcuate seemed unaffected, yet the FAT and the ventral pathways (uncinate fasciculus and iFOF) are affected by the lesion. The impact to the pathways connecting to the anterior temporal lobe might account for the object naming difficulties at baseline that later recovered as the lesion extend reduced. The core of the lesion is, however, encompassing the putamen, caudate, and thalamus, which might account for the word finding difficulties at baseline. The patient recovered her word finding capacity but her spontaneous speech was still marked by hesitancy, which might be explained by the interruption to the FAT (connecting Broca's territory to the supplementary motor cortex) on the one hand and the disconnection of fronto-striatal connections on the other. Lesions to these

subcortical structures have previously been implicated in aphasia (Mega & Alexander 1994; Jonas 1982; Nadeau & Crosson 1997; Cappa 1997; Alexander et al. 1987).

In conclusion, the above patients demonstrate that diffusion imaging can be a pivotal tool to define the extent of damage cause by a stroke. Clinical CT scanning often underestimates the true lesion size and therefore lesion-symptom mapping might not be accurate. Using DTI, I was able to show that language deficits might be explained by means of other mechanisms that are not immediately evident when examining the clinical images.

Further, from the analysis of the patients discussed here and from the remaining sample, it appears that subcortical structures and/or their connections are important for language functions. Based on the lesion locations and the deficits, it seems that single word comprehension relies on the connection between the auditory thalamus and the auditory cortex, whereas complex auditory comprehension involves the parietal lobe. Word fluency seems related to the subcortical structures (putamen, caudate and thalamus) and/or their connection. Semantic fluency relies on an intact connection between the anterior temporal lobe and the frontal lobe (i.e. uncinate). Confrontation object naming (i.e. verbal response to visually identified image) might be processed via the inferior longitudinal fasciculus (connecting occipito-temporal regions) for object recognition and then through the ventral (i.e. uncinate) or dorsal (i.e. arcuate) stream for object naming. Repetition, in the presence of the lesion to the left arcuate fasciculus, might be compensated ipsilateral via the uncinate fasciculus or contralateral through the right arcuate fasciculus. These observations are in correspondence with early aphasiology literature (Marie 1926).

CHAPTER 12   GENERAL DISCUSSION

'Science is not about finding the truth at all, but about finding better ways of being wrong. The best scientific theory is not the one that reveals the truth — that is impossible. It is the one that explains what we already know about the world in the simplest way possible, and that makes useful predictions about the future.'

(Schofield 2013)

Aphasia, in its entire complexity, has been systematically studied for over a century. Although some breakthrough achievements have been established, for example by identifying critical language-related areas, the nature of aphasia recovery remains vague. Nevertheless, continuous research concerning the aetiology and pathophysiology have fostered our understanding which can help to comprehend the nature of this often life-long language impairment and, where possible, the recovery therefrom. Several approaches have been used in the past to explore its aetiology, pathophysiology and recovery with the goal to optimise early intervention and therapy outcome. The following general discussion will bring together these approaches, discuss and integrate the main research findings and evaluate them critically.

To the best of the author's knowledge, this is the first report of an acute-to-chronic longitudinal DTI study investigating post stroke language recovery. Previous studies in the healthy population suggested that the arcuate fasciculus is related to language (Catani et al. 2007). Likewise, studies in aphasic patients showed that damage to the arcuate fasciculus (as in reduced FA or reduced number of streamlines in the left hemisphere) is a predictor of language deficits, especially for articulation, repetition, and comprehension (Breier et al. 2008; Hosomi et al. 2009; Marchina et al. 2011; Yamada et al. 2007). In this study, we also found the arcuate fasciculus to be a predictor of recovery, though given the methodological limitations (which were not considered in the previous clinical studies referenced) we focused on the unaffected contralesional hemisphere.

12.1 Use of diffusion MRI and tractography in the clinical arena

Since its introduction to the research arena in the 1990s, diffusion MRI and tractography have constant methodological advances. In addition, interpretation of the results has been refined, and novel indices of microstructural integrity have been described. In the past couple of years the gap to the clinical arena was bridged and DTI has been applied to a variety of neurological and psychiatric conditions (Maas & Mukherjee 2005; Ciccarelli et al. 2008).

Neurological diffusion MR studies included, for example, small vessel disease (Holtmannspötter et al. 2005; Patel & Markus 2011; O'Sullivan et al. 2005; de Laat et al. 2010), stroke (Mukherjee 2005; Chien et al. 1992; Sotak 2002; Warach et al. 1992; Keir & Wardlaw 2000; Gillard et al. 2001; Thomalla 2005), neurodegenerative diseases (Basser et al. 2000; Finger 1994; Le Bihan 2003; Acosta-Cabronero et al. 2010; Acosta-Cabronero et al. 2011; Greicius & Kimmel 2012; Y. Assaf 2008; Metzler-Baddeley, Hunt, et al. 2012a; Prodoehl et al. 2013; Ciccarelli 2007; Meijer et al. 2013; Inglese & Bester 2010; Pagani et al. 2007), epilepsy (Assaf et al. 2003), and traumatic brain injury (Shenton et al. 2012; Kinnunen et al. 2011).

Diffusion MR studies of psychiatric disorders include schizophrenia (Catani et al. 2011; Alba-Ferrara & de Erausquin 2013; Williamson & Allman 2012; Kanaan et al. 2009), autism (for a review see Travers et al. 2012), attention deficit hyper-activity disorder (for a review see van Ewijk et al. 2012), affective disorders (for a review see Sexton et al. 2009), and psychopathy (Craig et al. 2009).

Before the introduction of DTI into the clinic, it was applied in the healthy population. DTI in healthy people hence replicated previous post mortem dissections (Thiebaut de Schotten, ffytche, et al. 2011b; Yoshida et al. 2013; Lawes et al. 2008; Catani et al. 2007).

Taking all of these studies together, it is evident that diffusion MRI and tractography are sensitive to alterations in white matter architecture and microstructural changes that occur during brain maturation, normal aging, and pathology.

However, tractography cannot yet be considered as a fully validated clinical tool as methodological impediments are still being recognised (e.g., tract displacements in the presence of lesions and further issues that have been discussed throughout this dissertation). However, constant advances in diffusion methods and refined algorithms lead to shorter acquisition times and better data quality. These enhancements will allow DTI to be used as a clinical tool which, we hope, will be widely distributed across clinical facilities.

12.2 Main findings and discussion of the hypotheses

12.2.1 General hypotheses

12.2.1.1 'Classical predictors' and their relevance for aphasia severity

When comparing the baseline and follow-up assessments, all patients improved. At follow-up at six months post onset, the majority of patients were classified as anomic. The original WAB-R does not provide a score or category indicating normal language performance. The cut-off score used in this study originates from the work of Pedersen et al. (2004) and Swindell et al. (1984). Even though considerable improvements occurred, some patients were still perceptively dysphasic beyond anomia. This indicates that the WAB-R might not be sensitive enough to detect higher-level impairments. It should be noted here that no current test is ideal to assess language difficulties at baseline and the chronic stages alike (see also subchapter 2.2). Nonetheless, in order to have a comparable measure the same test should be used for both assessments.

In this study, aphasia severity at baseline and after six months was independent of age and gender. Also, no gender differences were observed for the recovery, which is in line with the literature (Kertesz & Phipps 1977; Pedersen et al. 2004; Engelter et al. 2006; Ferro & Madureira 1997; Hier et al. 1994; Brust et al. 1976; Lazar et al. 2008; Pedersen et al. 1995; Goldenberg & Spatt 1994).

The importance of lesion size and location has been debated in the literature (Kertesz et al. 1979; Pedersen et al. 1995; Laska et al. 2001; Inatomi et al. 2008; Lazar et al. 2008; Goldenberg & Spatt 1994; Plowman et al. 2012). In the current study, lesion size influences the initial aphasia severity but seemed to have less impact on longitudinal severity. The inconsistencies across previous studies might originate from different methodologies, where lesions are defined on CT, DWI, and PWI. Also the influence of hypoperfused tissue has only recently been taken into account and recent studies suggest that cerebral hypoperfusion might be a better indicator for aphasia severity than lesion size, especially in the acute stage (Fridriksson et al. 2002). This will be further discussed below (12.2.4).

Stroke severity, as obtained from the NIHSS, did not correlate with baseline or longitudinal severity in this study. This finding is in contrast to previous work where NIHSS was predictive of aphasia severity (Bruyn 1989; Inatomi et al. 2008; Fazio et al. 1973); One fact that might bias our observations is that the NIHSS score on admission was used to correlate with language assessments obtained at a later stage. These scores were not obtained by the research team but were taken from

the clinical notes. Hence, there is a possibility that differences in qualification might be present that could impede the subjectivity of the test (Schmülling et al. 2008). Other differences in comparison to previous studies were also noticed. For example, the study by Inatomi et al. (2008) used the NIHSS criteria for aphasia as well as measures obtained from non-standardised language tests. How these compare to the overall WAB-R score in our study is not clear. Further, patients with aphasia often remain disabled despite low NIHSS (Paolucci et al. 1998). Previous studies also showed a good correlation between NIHSS taken 24h from admission and acute imaging, such as DWI and PWI (Tong et al. 1998). In our study, only the initial NIHSS was available for all subjects but not the 24h score and the imaging was obtained at a later stage. A more detailed investigation of the NIHSS and WAB-R as well as imaging measures should be undertaken, given that the NIHSS is the most standardised form of acute stroke assessment adopted in clinical and research settings. A G*Power calculation indicated that our study would have needed a total sample size of 74 patients to detect a correlation between NIHSS and language scores with an effect size of $f^2=0.15$, alpha 0.05 and a power of 0.95. This indicates that we were significantly underpowered to draw meaningful conclusions from our NIHSS data.

12.2.1.2 Influence of thrombolysis

Previous studies reported on the beneficial effects of thrombolysis, such as reduced lesion size and functional recovery (Parsons et al. 2002; Saver et al. 2013). In this study by Parsons et al. (2002), patients had comparable initial lesion extent on DWI and PWI but differed at later imaging, where thrombolysed patients presented with smaller lesion extent. However, how thrombolysis affects aphasia and aphasia recovery is not clear. Acute stroke patients presenting with language impairments are more likely to receive the treatment and tend to present with smaller lesions 24h after treatment (Kremer et al. 2013). This is in line with the aforementioned study by Parsons et al. (2002) where thrombolysed patients tend to present with smaller lesions regardless of the presence of aphasia. The potential benefits of thrombolysis for aphasia recovery are not yet fully understood (Maas et al. 2012). During the course of our study, the rate of thrombolysis treatments was constantly increasing at KCH and amongst our baseline study participants the majority of patients had received rtPA (13/18). Even though tendencies were observed whereby thrombolysed patients seemed to have more severe aphasia at baseline and steeper recovery slopes, the current study is underpowered to draw any sound

conclusions from these data. Further, the availability of thrombolysis might be changing the lesion patterns observed. This means that, for example, in patients that would have had very large MCA infarct, a rapid resolution of the clot would facilitate reperfusion of distal cortical areas but might leave highly sensitive subcortical structures damaged. This is merely a working hypothesis that would need further testing in larger stroke cohorts.

In conclusion, several factors are influential in recovery from aphasia, but a strong predictor model has not been conceptualized based on patient-related or stroke-related factors.

12.2.2 Lesion-based hypotheses

Lesions were manually delineated on T1-weighted images for this study. However, results are different when using the less established approach of defining lesions on diffusion-weighted images. In this case, lesion extent is considerably larger than on T1-weighted MR imaging, especially in the acute stages. We decided to use the classical approach (i.e. lesion delineation on T1-weighted MR images) here for our results to be comparable, however, in the future DWI lesion extent should also be considered.

12.2.2.1 Commonly damaged brain structures and their implications for aphasia

A lesion overlay analysis at baseline revealed the highest overlay in our sample in the inferior frontal gyrus and the peri-insular nuclei and white matter. These peri-insular regions remain significantly affected at the chronic stage. It should be considered here that the chronic group is reduced compared to the baseline (9 vs. 18 patients) and hence the overlay is less powerful and more diverse. Nonetheless, these structures have been implicated in early literature on aphasia. The inferior frontal gyrus needs no further introduction as critical area for aphasic symptoms. Fewer consensuses is available for aphasia in cases of subcortical lesions.

The basal ganglia are primarily known for their involvement in motor function. However, they are closely connected to each other and cortical areas, including language-relevant cortices. The putamen, for example, has afferent connections to the motor, premotor, and supplementary motor cortices whilst its efferent

connections pass through the globus pallidus and the thalamus. The putamen has also been shown to be involved in cases of subcortical aphasia, i.e. where a lesion does not affect the convexity but only deep brain structures (Naeser et al. 1982; De Boissezon et al. 2005; Cappa 1997; Mega & Alexander 1994; Nadeau & Crosson 1997).

The head of the caudate nucleus, whose main afferent and efferent connections are with the prefrontal cortex, has been implemented in acute aphasia though these symptoms were transient within two weeks in most patients (Kumral et al. 1999). It has been suggested that the language deficits manifest when the caudate lesion extends to the anterior limb of the internal capsule (Damasio et al. 1982).

Subcortical aphasias have been criticised and were deemed artefacts originating from cortical hypoperfusion, remote cortical damage that is not apparent on clinical imaging, or thalamic disconnections (Nadeau & Crosson 1997; Nadeau 2008; Olsen et al. 1986; Hillis et al. 2002).

Thalamic lesions with effects on language have been reported for i) ischemic and haemorrhagic insults, ii) gliomas and iii) surgical lesions (thalamotomy) for treatment (Vallar et al. 1988; Jonas 1982; Bruyn 1989). The literature is, however, controversial – and especially with regards to the affected nuclei and the type of resulting dysphasia (Penfield & L. Roberts 1959; Crosson et al. 1986; Bruyn 1989). Lesions to thalamic nuclei most commonly affecting language function were reported as the pulvinar and ventralposterior lateral (VPL) nucleus (Lecours, Vanier, et al. 1983c; Bruyn 1989; Fazio et al. 1973). The degree of recovery amongst subcortical aphasia stroke patients varies substantially but symptoms are transient in most cases (Metzler-Baddeley, O'Sullivan, et al. 2012b; Vallar et al. 1988).

Thorough investigation of the relationship between the thalamus and language function were undertaken by Penfield and co-workers in the late 1950s to early 1960s (Jones et al. 2013; Penfield & Roberts 1959). Here, thalamo-cortical projections were considered equally, if not more important, than the ipsilateral association connections between language regions. The authors justify this based on the greater number of efferent and afferent thalamo-cortical connections to Broca's and Wernicke's areas as well as the inferior parietal lobe compared to the number of cortico-cortical connections between those areas (**Figure 90**B). This deduction on the connectional anatomy between those structures was mostly gained from electrical stimulation of the thalamus or therapeutic surgical destruction thereof.
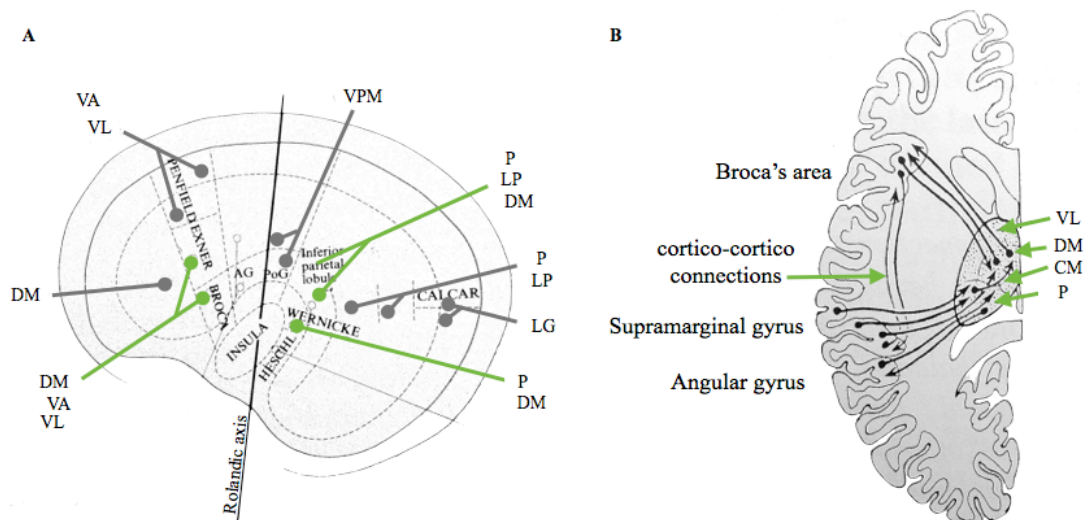
Figure 90   Thalamo-cortical connections between thalamic nuclei and language zone

This figures shows the thalamo-cortical connections of language areas according to Penfield (modified from (André Lecours, Vanier, et al. 1983c). **A** depicts the reciprocal connections between thalamic nuclei and the language cortex. The left hemisphere is here presented in a Mercator projection. **B** shows the reciprocal thalamo-cortical and cortico-cortical connections between the inferior frontal and inferior parietal lobe language areas. It is indicated here that the thalamo-cortical connections outnumber ipsilateral associative connections. VA, VL, VPM= ventral anterior, ventral lateral, and ventral postero-medial nuclei of the thalamus; LP= lateral posterior nucleus; P=pulvinar; DM= dorsomedial nucleus; LG=lateral geniculate body; MG=medial geniculate body; Calcar= axis of the calcarine fissure.

The thalamus is extensively connected to cortical areas and subcortical structures (**Figure 85**) and is therefore directly implicated in language functions. Thalamic aphasia is defined by anomia in spontaneous speech, impaired confrontation naming, and relatively normal grammar, articulation and repetition (Nadeau 2008). Thalamic aphasia is therefore predominantly a lexical-semantic impairment although syntactical impairments (i.e. agrammatism) have also been described (De Witte et al. 2006).

The selective involvement of the thalamus, without the basal ganglia, has been replicated for syntactic and semantic parameters of acoustically presented sentences using EEG recordings from deep brain structures (Wahl et al. 2008). The authors suggest that syntactic-semantic stimuli are processed along a thalamo-cortical network.

12.2.2.2 Investigation of lesion-symptom interaction with VLSM

The construct of modular functions of isolated cortical regions has been postulated for many decades and inevitably researchers and clinicians alike were eager to see if common areas are damaged in patients with certain dysfunctions. This ultimately resulted in a method today referred to as voxel-based lesion-symptom mapping (VLSM), whereby statistical analysis (e.g., Brunner Menzel test) are applied to identify brain voxels that are related or even predictive of certain deficits (Bates et al. 2003; Rorden, Karnath, et al. 2007b). As with any (neuroimaging) method VLSM is not flawless and still has some limitations that await to be conquered in the years to come (Rorden & Karnath 2004).

For our study, we first used VLSM to identify voxels that are predictive of the overall aphasia severity at baseline, and repeated this analysis for repetition deficits.

The analysis revealed that the voxels associated with overall aphasia severity at baseline lie primarily within the white matter of the middle and inferior frontal gyri with extension to the posterior superior temporal gyrus/ inferior parietal lobe and Heschl's gyrus. For repetition, similar regions were identified in the white matter of the middle and frontal gyri but with a wider medial-lateral extent and additional involvement of the temporal stem.

These findings are in agreement with the hodological literature as they coincide with the trajectory of the anterior and long segments of the arcuate fasciculus (Catani & Thiebaut de Schotten 2012); likewise, topological studies identified lesions to the inferior parietal/superior temporal lobes as crucial for repetition deficits (Anderson et al. 1999). Repetition in healthy volunteers was shown to activate superior temporal and premotor cortices bilaterally (for word lists and single words), or ipsilaterally (for non-word repetition) (Saur et al. 2008; Ohyama et al. 1996; Abo et al. 2004; Price et al. 1996). For aphasic patients, the pattern of activation is altered with some patients activating ipsilateral peri-infarct regions (Heiss et al. 1999); whereas other patients utilise the right hemisphere for repetition (Abo et al. 2004; Ohyama et al. 1996). Heschl's gyrus contains the primary auditory cortex and is therefore important for auditory comprehension. Previous studies have consistently reported a leftward asymmetry for Heschl's gyrus with regards to volume (Penhune et al. 1996; Penhune et al. 2003), surface area (Chiarello et al. 2004), length (Schneider et al. 2005), and its cytoarchitecture (Morosan et al. 2001). It was further shown that the increased left volume can be attributed to increased white matter rather than grey matter (Penhune et al. 1996) and to cellular layering (Hutsler & Gazzaniga 1996). Substantial inter-individual variability was also reported for this structure

(Abdul-Kareem & Sluming 2008; Leonard et al. 1998). This asymmetry is further replicated on a functional level, where it is suspected that the left is relevant for temporal resolution, whereas the right is relevant for spectral resolution (e.g., pitch) (Zatorre, Belin, et al. 2002a; Zatorre, Bouffard, et al. 2002b; Yoo et al. 2005). Bilateral damage to Heschl's gyrus results in cortical word deafness (Clark & Russell 1943). None of our patients had a bilateral lesion but the left Heschl's gyrus was affected in patients with repetition deficits.

12.2.3 DTI-based hypotheses

The central hypothesis of this study was that left-hemispheric stroke patients suffering with language impairments might recover better in the presence of a right-hemispheric long segment of the arcuate. Before considering this idea, related hypothesis had to be addressed first. These include i) the replication of the three segments in this clinical cohort and ii) whether the lesion load to the left arcuate in itself is predictive of aphasia severity. Further, the 19th century hypothesis that lesions along the arcuate cause conduction aphasia, i.e. isolated repetition deficits, was investigated. Finally, the central hypothesis was tackled, concentrating on the perisylvian white matter anatomy in the contralesional hemisphere.

12.2.3.1 Replication the three segments of the arcuate fasciculus bilaterally

In accordance with studies in healthy volunteers, the three segments were dissected bilaterally unless the lesions were directly encroaching on the tract. None of the diffusivity measures were significantly lateralised at baseline. After one year the volume was significantly reduced in all left hemispheric segments, apart from the anterior segment. FA was also selectively reduced in the left long segment.

12.2.3.2 Lesion load of the arcuate predictive of severity

The lesion load to the left arcuate fasciculus has been implicated as a predictor for language deficits, especially for articulation and naming impairments (Marchina et al. 2011) and repetition (Kummerer et al. 2013). The most commonly employed approach is atlas-based, however, different atlases have been used for different studies. For this study, arcuate lesion load was not predictive of aphasia severity at baseline or six months after symptom onset. This unexpected finding might be related to the lesions being drawn on T1-weighted images and hence the lesion

extent might have been underestimated. Further the lesion load classification was only obtained as a binary measure, which reduces the statistical possibilities of analysis. Consistent and well-established measures of lesion-load will need to be evaluated in future studies.

12.2.3.3 The role of the arcuate in repetition/conduction aphasia

The left arcuate fasciculus has long been the suspected culprit of conduction aphasia and/or repetition deficits (Geschwind 1970; Geschwind 1965a). In correspondence with the abovementioned lesion-symptom mapping for repetition, the voxels implicated as predictive for repetition deficits are located along the trajectory of the anterior and long segments of the arcuate. Therefore, the lesion load to the arcuate might predict repetition deficits. Surprisingly, the left arcuate lesion load was not predictive of repetition deficits at baseline or six months after symptom onset for our study. When comparing our results with the literature, the role of the left arcuate fasciculus for repetition and conduction aphasia has been questioned (Bernal & Ardila 2009), whilst other groups suspect inter-individual variability to account for negative results (Berthier et al. 2012; Steinmetz & Seitz 1991; Fedorenko & Kanwisher 2009). Other DTI studies did not quantify lesion load as such but reported on surrogate measures of damage that i) a reduction in the number of streamlines of the left arcuate is the strongest predictor of aphasia (Hosomi et al. 2009) and ii) reduced FA of the left arcuate is associated with repetition and comprehension deficits, whereby comprehension deficits are also related to damage to the superior temporal gyrus (Breier et al. 2008). Other non-DTI-based studies, however, did report correlations between lesion load (defined by atlas overlay) in arcuate areas and aphasia symptoms (Marchina et al. 2011; Kummerer et al. 2013).

12.2.3.4 Role of the Right hemisphere for language and aphasia recovery

We were able to demonstrate that patients with a larger long segment of the arcuate fasciculus in the contralesional right hemisphere recover better from aphasia regardless of gender, age and lesion size. This is a novel finding that is selective for the right long segment. In the healthy population, a bigger right-hemispheric long segment of the arcuate has been shown to be beneficial for language performance (Catani et al. 2007). How the right hemisphere is contributing to language functions and the recovery from aphasia is controversial (Selnes 2001). It has, however, been

suggested that recovery from aphasia may depend on the ability of the contralesional hemisphere to subserve language functions (Saur et al. 2006; Lee et al. 1984). Various language capacities have been shown to be performed or mediated by the right hemisphere. Using PET imaging, for example, repetition was related to right hemispheric activation (Ohyama et al. 1996). fMRI showed that semantic anomia in aphasia patients is associated with activations in the right hemisphere (Fridriksson et al. 2009; Raboyeau et al. 2008). Further, functional imaging studies, for example, indicate the right hemisphere for articulation related to suprasegmental aspects (i.e. prosodic and non-propositional) (Dogil et al. 2002; Ackermann & Riecker 2004; Kemeny et al. 2005; Zatorre, Belin, et al. 2002a). In general, receptive and expressive language processes can be carried out in part by the right hemisphere.

A strong dichotomisation between left-hemispheric and right-hemispheric functions is only applicable to adults, contrary to earlier beliefs (Kinsbourne 1975). Functional imaging has shown that in children both hemispheres are rather equally involved in linguistic functions (Moscovitch 1981; Friederici et al. 2011; Szaflarski et al. 2006). This age-dependent model of lateralisation assumes that language specialisation to the left hemisphere is obtained around pubescence (Szaflarski et al. 2006). This coincides with the maturation of myelination in language-related white matter at the same age (Pujol et al. 2006).

Language functions and their underlying anatomical substrates progressively lateralise towards the left hemisphere during development (Skeide et al. 2014; Holland et al. 2001; Amunts et al. 2003), with some language functions remaining predominantly being processed by the right hemisphere in adult life (Ross & Mesulam 1979; Weintraub et al. 1981). A recent fMRI study has shown that children up until the age of 10 years synchronically process semantic and syntactic information whereas adults process both separately and then integrate the information (Skeide et al. 2014). This is reflected in a progressively left lateralised activation (Skeide et al. 2014). How this functional segregation is exactly achieved, what it is triggered by and how both hemispheres interact in the healthy brain is still a matter of on-going research.

How exactly this functional segregation is achieved, what it is triggered by and how both hemispheres interact in the healthy brain is still a matter of on-going research. This applies even more so to the changes in functional activation and structural plasticity post stoke. Different suggestions about this complex dichotomisation and interaction were introduced to the linguistic community over the decades. For

example, the idea that the default setting is an inhibition from the left hemisphere over the right hemisphere for linguistic functions via interhemispheric commissures. In the presence of a left-hemispheric stroke, this inhibition is interrupted, and could lead to either unmasking of previously ready language capacities or reorganisation of right hemisphere language areas (Lindell 2006; Cappa 2000). This idea would also be supported by novel fMRI findings whereby a temporary left-to-right shift has been observed post stroke (Saur et al. 2006). The best aphasia recovery is seen in patients where this activation shift is temporary and returns to the left hemisphere. Another theory was that early sensory stages of processing are common to both hemispheres alike. For later processing however, specialised left and right hemispheric systems take over, whilst interhemispheric crosstalk via commissural pathways is still given (Moscovitch 1976; Moscovitch 1983; Moscovitch 1981). For this model, lesion site is important, as the site of the lesion will produce different symptoms.

Whether aphasia recovery materialises via recovery of lesioned tissue, ipsilateral or contralateral reorganisation, or ipsilateral or contralateral compensation has yet to elucidated.

12.2.3.5 Longitudinal plasticity of white matter structures

The important question of longitudinal recovery being related to structural plasticity was addressed with the one year repeat scan. The hypothesis was, that if anything were to change, we would expect an increase in structural connectivity as a representation of functional increase. This hypothesis had meanwhile gained foundation when a DTI-based study reported on plasticity (i.e. FA increase) in the left arcuate fasciculus when learning to read (Thiebaut de Schotten, Cohen, et al. 2012a). Overall, we observed an increase in FA in the right hemisphere related to improvements in aphasia severity using TBSS. At the same time, peak perfusion in the left hemisphere increased significantly after one year compared to the baseline perfusion measure as seen with cASL. Contrary to expectation, however, the DTI analysis showed a bilateral decrease in arcuate volume for the posterior and long segments. A selective FA reduction in the left long segment was observed. Given that significant overall FA changes were observed in the TBSS analysis but not the tract-specific DTI analysis, these changes might be explained by callosal degeneration, which would ultimately lead to increased FA in the right hemisphere as the number of streamlines within previously fibre-dense areas will reduce with

degeneration. The corpus callosum is the largest white matter tract in the human brain (Hofer & Frahm 2006; Aboitiz & Montiel 2003) and any lesion will necessarily affect callosal projections. Hence, an interhemispheric callosal degeneration could be expected and might partially explain the observed reduction in arcuate volume bilaterally. An interesting question that arises from this train of thought is the relation of the corpus callosum to hemispheric lateralisation in general and the arcuate fasciculus in particular. Ringo et al. (1994) put forward the controversial theory that larger brains impose a temporal limitation on conduction speed (i.e. larger brain, longer interhemsipheric transmission time), which is driving interhemispheric isolation and thereby hemispheric lateralisation. Aboitz et al. (Aboitiz & Montiel 2003) replicated the observed reduction in conduction speed with increasing interhemsipheric distances. In an earlier study, Aboitz et al. (1992b) reported on the relation of callosal fibres and 'language-gifted' cortex in relation to gender and observed gender-dependent 'pathway-specific decrease in interhemipsheric connectivity with increasing lateralisation' (p.154). Brain lateralisation of language cortices is here defined as anatomical asymmetries in Sylvian fissure length, which reportedly is a proxy of functional lateralisation (Aboitiz, Scheibel & Zaidel 1992a). The authors report a negative relationship (in men only) between the size of the isthmus (part of the corpus callosum) and language asymmetry, meaning that the bigger the isthmus the more left-lateralised language is (Aboitiz, Scheibel, Fisher, et al. 1992b). In the same paper, similar relations were reported for the anterior splenium in women. These gross anatomical measures have, however, been criticised and their relation to handedness and neuroanatomical structures are inconclusive (Beaton 1997). This debate might be revisited using advanced imaging methods to identify the direct relation between callosal fibres and perisylvian pathways.

12.2.3.6 Beyond the arcuate fasciculus

The arcuate fasciculus has been the primary language pathway ever since the two remote language areas have been described by Broca and Wernicke. However, with advanced understanding of the complex language system, a dual pathway network has been suggested in analogy of the visual dual stream system. As discussed throughout this dissertation, the 'ventral stream' has gained considerable attention over the past years. The inferior longitudinal fasciculus, connecting occipito-temporal cortices has been implicated for reading. Semantic processes have been implicated for the inferior fronto-occipital fasciculus and the uncinate

fasciculus, connecting anterior temporal pole and orbitofrontal cortex. These observations are based on indirect fMRI evidence (Saur et al. 2008), tract-based DTI evidence (Catani et al. 2013), and electrocortical stimulation (Duffau 2005). For a review see also Dick and Tremblay (2012).

In our study, FA of the right inferior fronto-occipital fasciculus (iFOF) was negatively associated with syntax and phonemic fluency at baseline and FA of the left iFOF was positively correlated with object naming at six months post onset. We further replicated the anatomy of the frontal aslant tract (FAT) and observed a positive correlation between laterality and word repetition, which is consistent with the literature available (Catani, Dell'Acqua, Vergani, et al. 2012b). The FAT is connecting Broca's area and pre-SMA and has hence should be involved in articulation processes. The results from these analyses are novel and await replication and validation in both healthy and clinical populations.

12.2.4 Perfusion-based hypotheses

It is important to note that we cannot speak of perfusion deficits as such, as there is no reference to previous perfusion values. Only a relative decrease or increase can be observed in relation to the surrounding and contralateral areas. Future studies might consider using corrected perfusion values, normalised to the perfusion in regions where little perfusion changes are to be expected.

Cortical and subcortical lesions have long been debated as the sole location and cause of deficits. More recently, it was suggested that the concept of subcortical aphasia might be revisited as no lesion is a pure subcortical lesion due to remote cortical hypoperfusion (Nadeau 2008; Hillis et al. 2002). Likewise, it was shown that hypoperfusion in language areas is related to aphasia and even more so reperfusion of those areas with aphasia recovery (Metter et al. 1990; A. Hillis et al. 2000; A. E. Hillis et al. 2006). Perfusion deficits have hence been suggested as the strongest predictor of aphasia severity (A. E. Hillis et al. 2001; Fridriksson et al. 2002). Also, overall initial bihemispheric metabolic depression has been described subsequent to stroke (Cappa et al. 1997). In this study, no association between perfusion measurements and language measures were observed. It was not possible to replicate the previously described finding of a hypoperfusion within Wernicke's area being predictive of the severity of word comprehension impairments. This discrepancy might be due to different methodological approaches in relation to the imaging methodology (i.e., exogenous vs. endogenous tracer),

diverging perfusion measurements (i.e., relative delay in perfusion vs. average perfusion within ROI), different language assessments (non-standardised assessment vs. standardised battery), and sample size. Further considerations will be detailed in the discussion of the limitations of this method below.

12.3 A hodotopic framework for clinico-anatomical correlation

The "hodotopic framework" was introduced in 2005 by Marco Catani and Dominic ffytche as an elaboration on Geschwind's disconnection model based on Wernicke's associationist's school (see introduction for details) and is summarised in **Figure 91**. In the figures a simplified large-scale network of cortical territories and white matter connections is represented. A series of specialised areas are connected by U-shaped association fibres to form a functional territory. These territories are connected by long white matter association tracts. This framework uses a new terminology to allow us to extend the model beyond classical neurological disorders of white matter disconnections and cortical deficits to include those involving white matter hyperconnectivity and cortical hyperfunction (e.g. epilepsy, schizophrenia).

"Hodotopic" reflects the dual contribution of specialised cortical areas (topos = place) and connecting white matter pathways (hodos = path) to higher cognitive functions. This framework includes the presence of "functional" epicentres, which are interconnected by white matter pathways, and implies that multiple areas are able to undergo the same function or that single areas are pluripotent.

Theories of aphasia can be divided into those emphasising dysfunction at specific brain locations (topological) and those emphasising dysfunction in the connections between brain regions (hodological). Classical examples would be a typical expressive aphasia with a lesion to the inferior frontal gyrus pars opercularis/triangularis (topological) and conduction aphasia with a lesion affecting the connections between inferior frontal gyrus and superior temporal gyrus (hodological). Both theories are guided by different methodologies (figure below). For example, a topological theory might rely on post mortem autopsies, functional magnetic resonance imaging or voxel-based morphometry (VBM). All of these techniques, directly or indirectly, allow us to infer a critical function performed by a specific cortical area. By contrast, hodological theories are mainly utilizing structural connectivity methods such as tractography but also mathematical methods based on functional connectivity. The latter does not necessarily imply an anatomical connection between two areas and might include dynamic causal modelling, EEG coherence analysis, structural equation modelling etc.

The most famous account of aphasia, which became known as the famous case "Tan", was interpreted by Paul Broca (1863) within a purely topological framework: *"Here are eight instances in which the lesion was in the posterior third of the third frontal convolution. This number seems to me to be sufficient to give strong presumptions. And the most remarkable thing is that in all the patients the lesion*

was on the left side. I do not dare draw conclusions from this". This observation was later replicated and expanded on by many others and most famously by Carl Wernicke. In contemporary neuroscience, functional neuroimaging studies of language consistently show activation of cortices relevant to the modality and content of the language paradigm, e.g. word production elicits activation in BA 44/45 and word comprehension studies activate mainly BA 22. In addition, as highlighted in the introduction, these regions largely coincide with classical intra-operative stimulation studies by Penfield and more recent perfusion studies by Hillis.

Although the evidence mentioned above provides strong support for the topological framework many cases are not accounted for within this model. This applies strongly to patients presenting, for example, with expressive aphasia with remote lesions outside the inferior frontal gyrus. Within the hodological framework these patients can be accounted for when assuming that a disconnection of a critical area to another causes the deficits. However, in the early 19th century connectional anatomy was only known through post mortem blunt dissections and animal models but not within the living human brain. This changed with the advent of diffusion-weighted imaging tractography. Many of these previously hypothesized mechanisms that cause higher cognitive function disruptions need to be revisited in the light of current methodological advances.

The current work is in line with the hodological framework and investigates the relation between cortical damage, white matter pathway damage and aphasia. In addition we wanted to explore the importance of the intact right hemisphere for language recovery. We observed that the volume of the long segment of the arcuate fasciculus in the right hemisphere (contralateral to the lesion) is an important predictive factor for recovery of language after stroke. The volume of the other segments in the right and left hemisphere was not correlated with recovery. In addition we have confirmed the importance of other predictive factors, including age, gender and lesion size. In particular, in our sample, lesion size in the left hemisphere is the strongest predictor of post stroke aphasia recovery after six months. Lesion size has previously been shown to play an important role in recovery through a variety of different mechanisms, including tissue neuronal repair, reperfusion of stroke tissue, and recruitment of peri-lesional spared areas (Croquelois et al., 2003; Heiss et al., 1999; Warburton et al., 1999). In larger lesions, compensation could also occur after recruitment of ipsilateral circuits not

previously concerned with language (Code, 2001; Crosson et al., 2007; Hillis and Heidler, 2002). An original finding of our study is the predictive value of tractography-derived measurements of tract volume in the right hemisphere. Specifically, the volume of the long segment connecting posterior temporal and inferior frontal regions is a good predictor of longitudinal recovery of aphasia after stroke.

This result indicates that different mechanisms might be at play across the two hemispheres. As inferred from the model, lesion size is predictive of long-term outcome regardless of our added DTI measures. However, in the right hemisphere model the classical predictors do not sufficiently predict recovery, but when DTI measures are added, the model significantly improves and can explain up to nearly 60% of the variance in language performances at follow-up.

Recent tractography imaging studies show that the arcuate is involved in auditory memory (Catani et al., 2007; López-Barroso et al., 2013) and may have a role in recovery after stroke (Tuomiranta et al., 2013). Lopez-Barroso et al. (2013) reported a correlation between higher performances in an auditory memory tasks for pseudo-words and strength of connectivity of the left long segment measured with both tractography (i.e. radial diffusivity) and functional connectivity (i.e. temporal correlation of BOLD response between the three peri-sylvian regions connected by the arcuate) in healthy people. The right long segments also play a role in auditory memory tasks based on semantic clustering strategies, where a larger volume of this segment is related to better performances (Catani et al., 2007). Furthermore, a recent single case study reported a woman with a stroke affecting the left arcuate fasciculus resulted in aphasia. After rehabilitation the patient was able to recover the ability to learn novel active vocabulary and the authors speculate that this was due to the presence of compensatory pathways in the right hemisphere (Tuomiranta et al., 2013).

This hypothesis is in line with previous PET and fMRI studies that indicated an important role of the right hemisphere for aphasia recovery after stroke (Cappa, 2000; Karbe et al., 1998; Saur et al., 2006). Two possible mechanisms have been suggested: unmasking of previously ready language capacities or reorganisation of right hemisphere language areas (Cappa, 2000). In both cases the presence of larger right long segment volume could facilitate direct cross-talk between right hemisphere homologues of Broca's and Wernicke's regions. Additionally, these studies revealed a dynamic activational shift to the contralesional hemisphere during recovery (Saur et al., 2006). This shift seems to be only advantageous for

recovery if of a temporary nature (Hillis, 2006; Saur et al., 2006; Szaflarski et al., 2013). Nonetheless, in such cases the right hemisphere appears to be able to temporarily adopt linguistic competence beyond the non-verbal aspects already been assigned to the non-dominant hemisphere (e.g. prosody, intonation, and affective content) (Ross et al., 1988; Turkeltaub et al., 2012). Our study suggests that these right-hemispheric language functions could be mediated by a specific portion of the arcuate fasciculus. Currently, it remains difficult to determine how a pre-existing right arcuate could facilitate functional recovery.
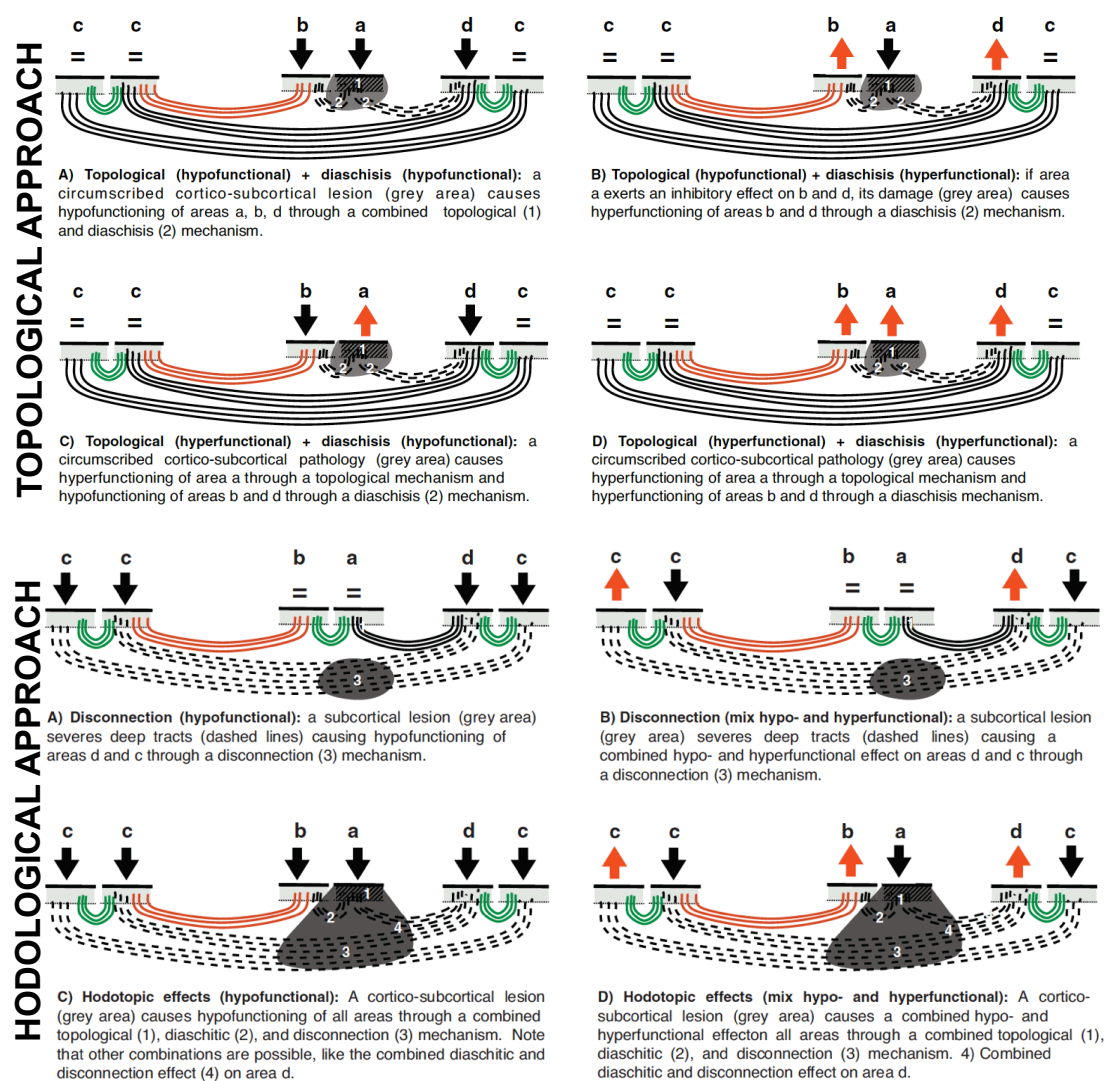
Figure 91   Topological   and   hodological   frameworks   for   clinico-anatomical correlation

Top panel: Topologic framework for clinico-anatomical correlation. Here the effects of a superficial cortical-subcortical lesion are described in terms of a combined topological effect and dischisis. Red arrows indicate hyperfunctioning areas, black arrows hypofunctioning areas. Bottom Panel: Hodotopic framework for clinico-anatomical correlation. A-B) The effects of a deep lesion on long tracts connecting distant areas. C-D) The effects of a cortico-subcortical lesion result in combined topological and hodological (diaschisis,

disconnection) dysfunction. Here the effects of a deep lesion are described in terms of a combined topological effect, disconnections and diaschisis. Red arrows indicate hyperfunctioning areas, black arrows hypofunctioning areas.

Cortical pathology

Figure 91 illustrates the different combinations of topological and hodological mechanisms. **Figure 91** relates to the pathology of a cortical area and its underlying U-shaped fibres, such as might be caused by localised vascular, neoplastic, epileptic, or neurosurgical lesions. Cortical pathologies may cause two kinds of topological dysfunction, either hypoactivity or hyperactivity within a damaged area. The dysfunction may go beyond the affected cortical site to include cortical regions connected (i.e. diaschisis). As for pure hodologically-based dysfunction, these remote effects will demonstrate either a metabolic diaschisis (e.g. reduced cerebellar metabolism for controlateral frontal lesions) or a dynamic diaschisis, only being apparent for tasks normally requiring both interconnected regions.

Subcortical pathology

The second mechanism relates to pure subcortical white matter lesions leading to cortical dysfunction (hyper- or hypofunctioning) through a hodological effect (i.e. disconnection) (**Figure 91**, bottom panel A, B). For some tasks this dysfunction may simply reflect the failure or excess of transfer of outputs from one area to another (Lichtheim's subcortical disconduction); however, for tasks requiring the simultaneous cooperation of cortical regions (e.g. synchronous bimanual coordination), one can consider the function itself to be distributed and the lesion is therefore disrupting or enhancing the function as a whole (Wernicke's subcortical disconnection). Whether for a serial or distributed task, the dysfunction of connected regions may only be apparent for those tasks requiring both connected areas, the function of each area individually being normal when they are part of a different network. For some 'irritative' lesions of the white matter the hodological effect could result in the hyperactivity of the entire network or a combined hyper- and hypofunctional effect.

Cortico-subcortical pathology

The third type of dysfunction involves both hodological and topological mechanisms

(**Figure 91** bottom panel C, D). In relation to deficits, this is the pattern most likely to be encountered clinically and would typically be caused by a large lesion. Here, the lesion involves both cortical and subcortical structures with superficial and deep white matter affected. In this case, combined topological and hodological effects produce widespread cortical dysfunction. Auditory hallucinations in schizophrenia provide an example of combined hodological and topological hyperfunction, with increased activation of Broca's, Wernicke's, and Geschwind's territory (Lennox et al. 2000) and indirect, diffusion tensor tractography evidence of decreased anatomical connectivity between these regions (Catani et al. 2011).

In general, the hodotopic framework adds clinically useful features to existing models, in particular, extending them beyond classical neurological deficits and disconnections to encompass a broader range of disorders. Of course, its main clinical usefulness will come not from the generalisations outlined above, but from its application to specific functional domains. At least in the short term, the future of the clinico-anatomical correlation method in neurology and psychiatry is likely to be shaped by advances that are currently unfolding in the field of imaging. In the past, lesions could only be referred to cytoarchitectonic atlases, which provided little information on white matter tracts (e.g. Talairach and Tournoux, 1988). As a consequence, the clinico-anatomical correlation method could only link specific deficits with a discrete cortical area. Today, lesions can be mapped onto both cytoarchitectonic and white matter atlases, the latter derived for example from diffusion MRI (Wakana et al. 2004) or post-mortem dissections (Bürgel et al. 2006). This adds a new layer of complexity to the correlation method by linking deficits to inferred dysfunction within distributed networks (Rudrauf et al. 2008).

Furthermore, we are now able to track pathways between distal cortical areas and obtain measurements of the microstructural integrity of white matter tracts in the living human brain. This allows the application of the clinico-anatomical correlation method outside the neurology clinic within the practice of functional psychiatry where a 'lesion' remains inferred, rather than demonstrable.

By combining diffusion MRI with other functional imaging methods we will be able to go beyond a one-to-one correspondence of lesion site and deficit and understand the precise mechanisms (i.e. hypofunctioning or hyperfunctioning areas) underlying a wide range of symptoms. Both topological and hodological explanations will be used to test specific hypotheses and generate unbiased interpretations. This is as true today as at its beginning, when, for example, one-sided interpretation of the anatomical correlates of speech arrest deficit brought into existence Broca's area

instead of Broca's fasciculus.

In summary, the current understanding of the anatomy of aphasia, from a topological (i.e. cortical) and hodological (i.e. connectional) point of view, is shown in **Table 36** (adapted from Catani, Dell'Acqua, Bizzi, et al. 2012a). When applying the topological and hodological approach to language and aphasia research the crucial areas and pathways for normal function and dysfunction can be defined (**Table 36**).

Table 36   Aphasia syndromes and their associated lesions

Aphasia syndrome	Topology		Hodology
	Anatomical structure	Cortical areas (BA)	
Wernicke	Superior temporal gyrus	42,22,37	PS, LS
Broca	Inferior frontal gyrus	6,44,45	AS, LS
Conduction	Parietal and frontal lobes	42,22,37	LS
Global	Left MCA territory	6,22,37,39,40,42,44,45	AS, PS, LS
Transcortical motor	Anterior-superior to Broca's area or thalamus	6,8,9,46	AS
Transcortical sensory	Posterior, temporal-occipital area	22,37	PS
Apraxia (orofacial)	Inferior frontal, insula, BG		AS, FAT

BA, Brodmann area; BG, basal ganglia; AS, anterior segment; PS, posterior segment; LS, long segment; FAT frontal aslant tract

12.4 Limitations of tractography and their ramifications for this study

This study benefited from the use of contemporary diffusion tensor imaging optimised for stroke patients. However, as previously mentioned (see also subchapter 5.3.3 in the introduction and Dell'Acqua and Catani 2012), DTI has some limitations that could affect the results obtained for this dissertation. The general advantages and limitations of DTI are summarised in **Table 37**.

Table 37   Advantages and limitations of DTI

Modified from the work of (Dell'Acqua & Catani 2012; Catani 2006; Campbell & Pike 2013; Jones et al. 2013).

Advantages	Limitations
In vivo	Limited spatial resolution (i.e. multi-tissue populations, partial volume effect)
Quantitative measurements	Validation is needed
Not destructive	A priori knowledge of white matter anatomy required
Non-invasive	Indirect anatomical method
Applicable to human and animal brain	Presence of artefacts (i.e. false positive and false negatives)
Hodological approaches to brain function/ dysfunction	Operator dependent (tractography algorithm)
Correlation with behavioural and other functional measures	Limited visualisation of bending, merging and crossing fibres
Applicable to large populations	Pitfalls when trying to combine it with other brain mapping tools
Time efficient	No differentiation between afferent and efferent connections
Multiple pathways within each subject	Low angular resolution

Albeit previous studies in healthy controls (Catani et al. 2007; Lebel & Beaulieu 2009; Yeatman et al. 2011; Häberling et al. 2013; Powell et al. 2006; Vernooij et al. 2007) and clinical cohorts (Hosomi et al. 2009; Yamada et al. 2007; Breier et al. 2008; Marchina et al. 2011; Matsumoto et al. 2008) reporting on the laterality of the arcuate fasciculus, it was a conscious decision to refrain from this analysis for the current study. In the acute stages of a stroke the neuroanatomy is altered due to infarction, ruptured cellular barriers, and the presence of peri-lesional oedema. All of these processes affect white matter anatomy. Due to the break down of neuronal structures one would hence expect to see an FA drop in the chronic lesioned hemisphere. The tensor model is FA-based and thus a reliable reconstruction of the altered anatomy is not given. Due to the lack of information from the lesioned hemisphere, no lateralisation index was calculated but rather the focus was on the interindividual variability within the contralesional hemisphere.

Furthermore, DTI is prone to produce false positive and false negative results as the tensor represents the average direction of water molecules within each voxel. In this study, it was at times difficult to judge – in the left hemisphere – if reconstructed

streamlines were true findings or false positives. The difficulty arises as the lesion is altering the structural arrangements causing white matter pathways to be displaced or interrupted. Least restrictions possible were applied during the reconstruction of streamlines. For example, minimal exclusion ROIs were implemented unless anatomical knowledge would dictate otherwise and visualisations were undoubtedly artefactual.

In pathologies where atrophic changes are evident, DTI is prone to cerebrospinal fluid-based partial volume artefacts, which are mostly affecting white matter structures close to the ventricles, i.e. the corpus callosum and the fornix (Metzler-Baddeley, O'Sullivan, et al. 2012b). These partial volume effects are more prone to alter diffusivity measures compared to anisotropy measures, whereby the first is elevated and the latter is decreased (Metzler-Baddeley, O'Sullivan, et al. 2012b; Pfefferbaum & Sullivan 2003). The pathways under investigation in this study are not closely related to the ventricles and should therefore be less affected by partial volume effects.

The arcuate fasciculus can be readily dissected using DTI. Other white matter tracts, however, cannot be visualised due to the inability of conventional DTI to resolve multi-directionality within a voxel. In such cases, a supplementary analysis was conducted employing spherical deconvolution to overcome this methodological limitation (Thiebaut de Schotten, Dell'Acqua, et al. 2011a; Dell'Acqua et al. 2012; Dell'Acqua & Catani 2012).

Given that this study is amongst the first to use DTI to investigate post stroke white matter changes in relation to language, some of the data presented here can only be compared to results obtained from control studies. DTI has only recently been introduced in clinical research and further validation studies are needed to establish consistency in the common changes associated with neuropathology (Yamada et al. 2009; Metzler-Baddeley, O'Sullivan, et al. 2012b; Campbell & Pike 2013).

Previous deterministic DTI studies of white matter anatomy in stroke are heterogeneous in their time of assessment post stroke (starting from two days up to two years post onset), their methodology (i.e. utilising a) standardised language assessments vs. a clinical diagnosis of aphasia; b) different scanners, c) different acquisition protocols), and their results (Roberts et al. 2003; Hosomi et al. 2009; Breier et al. 2008; Marchina et al. 2011; Campbell & Pike 2013). It should be considered here that changes in fibre attenuation, multi-directionality within sampled

voxels, and partial volume effects might influence FA values that are not tract specific but voxel specific (Dell'Acqua et al. 2012; Metzler-Baddeley, O'Sullivan, et al. 2012b; Jones et al. 2013). This may account for some discrepancies reported across studies. Whilst FA is the most widely used metric of anisotropy in research, its biological interpretation should be carefully conducted (Jones et al. 2013). The presence of pathological changes introduces another layer of complexity as measurements could be influenced by physiological evolution of damage and repair within the brain. This can lead to inconsistent FA measures and erroneous FA estimations. Further, a quantification of streamlines might be underestimated, as pathways are likely to be dislocated due to the presence of a lesion.

Diffusion tensor tractography is based on the estimation of maximal anisotropy within a given voxel to determine the tensor direction. In this study we employed a fractional anisotropy (FA) threshold of 0.2, which yielded anatomical consistent results. A FA threshold of 0.2 is one of the standard thresholds used in tractography studies as it preservers high anisotropy voxels corresponding to white matter regions whilst at the same time rejecting low anisotropy voxels where there is increased uncertainty in the tensor orientation or the voxel is likely not to contain white matter (e.g., grey matter and cerebrospinal fluid). Given the presence of neuropathology in this study (i.e. left hemispheric stroke), we also pre-processed the data set with an FA threshold of 0.15, however, we observed increased spurious streamline reconstructions without a significant improvement in the anatomy of the tract.

The primary objective of this study was to investigate the contralesional hemisphere (here right hemisphere) and refrain from tracking through lesioned tissue. An area of oedema commonly surrounds the core of a stroke lesion. In the presence of partial volume effects oedema can reduce the FA measurement in a given voxel and therefore streamlines might stop at the border of the lesioned area even though the white matter might still be present (i.e. false negative reconstruction). To suppress the effect of the oedema higher b-value acquisition, other fast diffusion component or multi-shell (e.g., multi b-value) approaches might be applied in the future. These are however more time consuming and hence not applicable for acute clinical populations at this point in time. These approaches can also be used to separate the contribution of different microstructural compartments, for example, fast diffusion intra- and extracellular diffusion (e.g., NODDI approach, Zhang et al., 2012).

In contrast to other available methods, such as probabilistic or advanced tractography the following information is relevant. Advanced tractography was used in this work at times to overcome some of the limitations of DTI as explained above. The main advantage of the Damped Richard-Lucy, as recently described by Parker et al. (2013), is that the number of false positive reconstructions is considerably lower compared to a standard constrained spherical harmonic deconvolution approach. As far as we know this method is providing a robust estimate of real fibre orientation while reducing the number of false positive reconstructions. Likewise, in the presence of extremely low anisotropy regions the algorithm is implementing adaptive regularisation levels to prevent the amplification of spurious components due to noise.

In relation to probabilistic tractography the following methodological comparison is important. *Seed-based tractography* is strongly affecting the number of streamlines and only visualises the streamlines from that specific seed region. Hence the number of streamlines visualised is strongly related to the size and location of the chosen region of interest (ROI). Shifting the ROI hugely affects the reconstruction both in probabilistic and deterministic approaches.

Whole brain tractography by contrast reconstructs all possible streamlines and then visualises the streamlines passing through a selected ROI. This approach is therefore less user-dependent than seed-based approaches. Unfortunately, probabilistic has more computational constraint for whole brain analyses and hence, for practicable applications, probabilistic can only be done as seed-based approach.

Probabilistic tractography

A measure of uncertainty within the data is calculated based on a chosen algorithm. Once the uncertainty is derived, the streamlining algorithm is run repeatedly to build up a pattern of possible pathways. The end result is a set of multiple pathways starting from the chosen seed, which is then conventionally summarised by assigning to each voxel the percentage of pathways, launched from the seedpoint, that pass through the voxel (Jones 2010; Jones & Basser 2004). It should also be considered that there are effects of distance on connection probabilities, whereby the confidence assigned to connections diminishes with increasing distance from the seed point (figure 3). This limitation impacts especially on the investigation of long-range interlobar (e.g., inferior fronto-occipital fasciculus) or interhemispheric (e.g., complete corpus callosum) connections.

Deterministic tractography, as the name implies, is a more rigid and conservative approach to tractography. Deterministic tracking only produces one tract that is the most likely reconstruction, whereas probabilistic tracing visualises all possible propagations starting from a ROI. This means that whole brain tractography is less examiner-dependent as all possible streamlines are generated. At the same time the ROIs are usually larger than in probabilistic tractography. However, deterministic tractography in contrast does not account for a measure of uncertainty as it is done in probabilistic algorithms. By the same token, probabilistic tractography is seed-based, which means that if the ROI is moved by a few voxels a different reconstruction will be visualised. Hence, probabilistic tractography is highly dependent and sensitive to ROI position.

12.5 Shortcomings of voxel-based statistical analyses

Voxel-based lesion mapping approaches are commonly used these days and date back to the early clinic-anatomical pioneers Paul Broca and Carl Wernicke. However, with the development of in vivo neuroimaging methods and the readily available software packages to perform such analyses, the current voxel-based approaches were scrutinised carefully.

Current methods for lesion overlap map analysis (Rudrauf et al. 2008; Thiebaut de Schotten, Tomaiuolo, et al. 2012b) involve calculating the number or proportion of patients with injury to each voxel in the brain. This can be done separately for behaviourally distinct groups (e.g., with and without some behavioural deficit) or anatomically distinct groups (e.g., frontal vs. occipital lesions). A more recent addition to this method is the voxel-based lesion-symptom mapping (VLSM) (Bates et al. 2003). The result of a VLSM analysis is a statistical map in which each voxel quantifies the difference in observed behaviour between patients with and without a lesion in that location. The underlying statistic is most commonly a permutated t-test or the Brunner-Menzel test (Rorden et al. 2007).

The following limitations need to be considered when interpreting these results. 1. Lesion overlay maps indicate areas of greatest overlap within a group of patients. However, one limitation is that only damage to brain voxels is considered (Mah et al., *Brain* in press). This closely resembles the problem that this overlap might be primarily due to the vascular anatomy, which renders certain areas (e.g., the insula) more vulnerable to damage than others. With such an assumption, some identified areas may not represent areas pivotal for lost/reduced functions but are simply

anatomically vulnerable regions (Mah et al., *Brain* in press). Nevertheless, these areas might be important for a given function either directly as a functional hub or indirectly as a relay knot or supporting area. 2. The nature of the method favours a selection bias whereby patients who present with transient deficits or small strokes are likely to be excluded. Most studies are conducted in chronic rather than acute stroke and hence only chronically affected patients are accounted for. 3. The area of damage is usually not restricted to the underlying functional modules or cytoarchitectonic areas (e.g. BA 44/45). Hence, a careful consideration across different methods is advisable. 4. In order to obtain a lesion overlay map all structural images have to be warped into common reference space. To this end the presence of a stroke, especially with different lesion extent, might introduce some alignment errors that might affect the registration and subsequently affect the results. 5. With the lesion overlay method only damaged areas are identified which are likely to correspond to the core of a stroke lesion. However, morphologically intact but functionally comprised areas are not taken into consideration. Hence, supplementing the voxel-based lesion mapping with perfusion measures is pivotal. 6. Lesion overlay methods do not provide good temporal resolution and no time course of the evolution of lesioned areas is considered.

These limitations are being discussed in the literature, however, there is still little consensus as to what the "gold standard" should be. Hillis et al. (2004) for example suggest scanning acute stroke patients regardless of their lesion size to overcome the selection bias. On the contrary, Rorden and Karnath (2004) argue to recruit chronic patients to overcome the problem of structural-functional mismatch.

The current study attempted to address these issues and consecutively recruited acute stroke patients (overcoming the selection bias for transient symptoms and small strokes) and followed them up six months after (overcoming the mismatch bias). Additionally, perfusion (to assess perfusion mismatch and whole brain hypo-/hyperperfusion) and diffusion imaging (to assess white matter damage) together with behavioural measures (to perform voxel-based lesion symptom mapping) were acquired to complement the lesion analysis.

12.6 Limitations of perfusion analyses

It is instructive to note that the mean amplitude of CBF in this cohort of acute stroke patients is at times low (approximately 20 – 30 ml/100gm of tissue/min), when compared to the mean grey matter perfusion values found in young, healthy adults

(approximately 50 ml/100gm of tissue/min) (Petersen et al. 2010). There are several reasons why this may be the case as is discussed hereafter.

Firstly, the raw CBF images of these subjects showed, in the majority of cases, substantial motion artefacts. This would have had a profound effect on the efficiency of labelling if the subjects moved in the region immediately below the cerebellum. However, the major contributing factor from the point of view of motion would have been caused by the 'blurring' of grey and white matter regions. Since the mean of grey matter is substantially lower (~ 20 ml/100gm of tissue/min for healthy, young subjects), the mean over the whole brain would have also been reduced.

Secondly, ASL is a subtraction technique with low Signal-to-Noise Ratio (SNR). The maximum perfusion induced differences in the MR signal in the order of 2%. As pointed out in the methods section, we collected three 'control-label' pairs to compute the CBF maps. Motion during the collection of the raw 'control' and 'labelled' images would have also reduced the mean value across all voxels.

Thirdly, in the presence of stroke it is likely that these subjects had abnormal blood velocity, which would have given rise to inefficient labelling of arterial blood. Unfortunately, in an effort to limit the MRI examination to a total maximum of 60 min, we did not have time to perform Phase Contrast Angiography to compute the actual value of the peak blood velocity in carotid arteries.

Fourthly, the SNR of the perfusion scan would have also been compromised by the haematocrit of the subjects who on the whole, were of an advanced age (mean 63±39 years). It is well known that as the haematocrit changes (Silvennoinen et al. 2003), the value of the T1 of blood reduces and therefore the perfusion induced signal difference would decay more quickly for the same post-labelling delay.

Finally, a fundamental problem of performing ASL in this cohort is the fact that (as the data shows), perfusion is severely compromised in several regions around the lesion and therefore a longer post-labelling delay than the one used (we used 1500ms); may have been necessary to optimise the quantification of the CBF. However, from previous investigations on healthy, elderly control subjects (data not shown), lengthening of the post-labelling delay also induces further loss in SNR. As a compromise, we decided to use the value that we normally use in both young and elderly healthy controls (i.e. 1500ms). Future studies where perfusion assessment may be a higher priority would involve CBF mapping with a less motion sensitive version of PCASL (e.g. with an EPI readout) and an array of post labelling delays in

order to accommodate the greater heterogeneity in blood flow apparent in cerebrovascular disease.

12.7 Shortcomings of this study and future directions

Certain limitations and shortcomings have become evident over the course of this study. Where possible they were immediately addressed, such as the intolerance of acute patients to classical DTI sequence that was thence split into two shorter acquisitions. Other issues were beyond the control of the research team but should be taken into account for future studies.

12.7.1 Neuroimaging

In the acute stage, the allocated scanning time of one hour per subject is not sufficient. Patients are less mobile (due to hemiparesis) than controls and hence the transfer from chair to bed may take longer than anticipated. Also, medical impediments might delay or interrupt scanning if the patient does not feel well or becomes nauseous. In this patient cohort, in-scanner communication is more demanding than usual and quite often a member of the research team would go into the scanner room to check on the patient. Future studies of this sort, should allow up to 1.5 hours of scanning time to accommodate these specific needs.

Given the time constraints described above, the scanning protocol was not acquired in full for some of the patients and/or radiographers mistakenly chose a differently sliced T2-weighted image. Due to these irregularities the pre-processing for this study was not streamlined. For the perfusion imaging, the conventional T2-weighted imaging contrast is commonly used to co-register the ASL signal. In this study, using the T2-weighted scans was not possible and therefore the T1-weighted MR images were axially re-sliced and used instead.

For the diffusion imaging in the acute stage, the motion artefacts were substantial and we therefore implemented a split sequence that was later concatenated during the pre-processing. This split sequence allows for shorter scanning times and therefore adds to the patients' comfort whilst reducing the presence of artefacts at the same time. These changes were very successful and are now standard procedure in the currently planned stroke imaging studies in our centre.

Improvements can be applied to TBSS analyses. Lesion masking should be applied to interpret FA changes independent of the lesion. This can be achieved in the

latest version of fsl where the new script *setup_masks* is supplied to assist in using lesion masks (supplied by the user) in *randomise* to exclude (inconsistently located) lesions from group studies (http://fsl.fmrib.ox.ac.uk/fsl/fslwiki/randomise/UserGuide#Associated_Tools).

12.7.2 Logistics

Some issues that hampered the current study are no longer applicable as the Clinical Research Facilities are now implemented within King's College Hospital, making patient ambulance transport obsolete for future acute studies (http://www.kcl.ac.uk/iop/depts/neuroimaging/facilities/CRF/index.aspx).

As described in **Table 12** in chapter 6.5, ambulance transport was not efficient and often resulted in delayed arrival of the patients, which in turn lead to incomplete acquisitions. Should future studies chose a similar layout, instead of utilising the new facilities, study-dedicated transport ought to be in place.

Further, given the short target interval between admission and the baseline MRI scan, the absence of previous clinical notes is an obstacle. In this study, any possible effort was undertaken to obtain written notes by involving the next of kin of each patient or contacting the patients' General Practitioner and where necessary getting in contact with the hospitals that did perform the surgeries. Unfortunately, obtaining the clinical notes was not always possible and some patients had to be excluded from the study.

A further reduction in the sample size was due to the fast repatriation procedures at KCH. Ethical approval did not extend to other hospitals beyond KCH and therefore, patients that are not scanned within their inpatient stay at KCH were lost to the study.

12.7.3 Sample size and study cohort

The sample size is smaller than the initial target size due to the reasons specified above and in **Table 12** in chapter 6.5 as well as the strict exclusion criteria of the study. The inclusion criteria for this study can be considered restrictive but did allow us to exclude various potential nuisance variables, which would have otherwise reduced the power. The difficulties of recruiting acute stroke patients for advanced imaging studies often lead to the exclusion of the acute stage in longitudinal imaging studies (Cardebat et al. 2003; De Boissezon et al. 2005; Fernandez et al.

2004; Heiss et al. 1999; Léger et al. 2002). Future studies should aim to recruit higher numbers of participants to address these issues and possibly more than one full time person should be dedicated to recruitment and analysis.

Our study cohort can be considered selective as patients had to be medically stable enough to tolerate ambulance transport and be MRI compatible (i.e no claustrophobia, absence of metal, availability of previous medical history). Also, we recruited first-ever clinical strokes (although this can not exclude the presence of silent cerebral infarcts that have previously not been detected) which can be expected to occur in approximately 10% of the population (Das et al. 2008).

12.8 Overall Conclusion

Few images and concepts have achieved iconic status in the neurosciences. The classical view of the anatomy of language has, and rightly so. It is amongst the first theories to explain higher cortical functions in humans and it is applicable to the healthy and pathological population. Further, Broca's seminal work provided the foundation for cortical localisation theories. Over the centuries, challenges have been posed toward the classical model, yet it was never falsified but rather expanded and embedded into more a complex anatomy of language. It has been established, using various methods, that language processes involve more cortical and subcortical resources than merely Broca's and Wernicke's areas. Despite years of intense research, the entire complexity of language comprehension, language production and language disorders (such as aphasia) are still not fully understood. With regards to aphasia recovery, much of the improvement seen in language functions in the first three months can be related to neurophysiological factors, such as oedema reduction (Fazzini et al. 1986), resolution of diaschisis (Seitz et al. 1999), and reperfusion of salvageable tissue (A. E. Hillis et al. 2006; Fridriksson et al. 2012). However, little is known about the neurocognitive and psychological processes that might influence recovery (Code 2001).

The clinico-anatomical approach based on a narrow cortical localisationism attracted criticism since its beginning. In England John Hughlings Jackson was one of the first to point out that localisation of symptoms does not necessarily imply localisation of function. He argued that it is entirely possible that some symptoms can be explained by a secondary effect of the damage on other regions, such as, for example, some positive symptoms resulting from a 'release' mechanism (Catani, Dell'Acqua, Bizzi, et al. 2012a). Furthermore, he highlighted that many variables

intervene in the correlative process, such as the 'depth of the dissolution'; the 'onset and rapidity of the process'; the 'kind of brain' in which the dissolution occurs, and the 'influence of external and internal circumstances' upon the patient. Jackson's writings had little impact on his contemporaries, but were used some decades later as the ensign of the resurgent holistic movement. Crucial to holism was the assumption that all areas are mutually interconnected through short- and long-range fibres. According to the holistic theory, this architectural property of the brain explains the ability of other parts of the cortex to take over functions within the competence of the damaged area, a property designated by Karl Lashley as 'equipotentiality' of the cortex. Lesions, regardless of their location, always affect underlying connections that then lead to complex deficit patterns (Catani, Dell'Acqua, Bizzi, et al. 2012a). This variability of white matter damage might account for negative cortical case reports and the observed variability in clinical presentation and lesion-symptom mapping results (Cramer 2008). Future studies should also attempt multimodal imaging to comprehensively answer the pressing questions of temporal and connectional language networks (Conner et al. 2008; Ellmore et al. 2009; Thiebaut de Schotten, Dell'Acqua, et al. 2011a).

The current study by no means claims to solve this puzzle but was able to contribute novel ideas that hopefully will be taken into account in the future. The recovery of aphasia has to be re-investigated with multimodal methods embedded in a neurocognitive framework that is also accounting for compensation mechanisms at different levels (neurological, cognitive, and psychologically).

Figure 92 shows the current understanding of the left-hemispheric language network based on results from functional studies (fMRI, EEG) and connectional anatomy studies (DTI, post mortem dissections). The model contains the relevant anatomical structures from auditory language perception to comprehension as described by Friederici (2012; Hickok & Poeppel 2000) as well as the structures for language articulation (Shalom & Poeppel 2008; Price 2010). For articulation, the recently described frontal aslant tract connecting Broca's area with the pre-SMA is included in the model (Catani, Dell'Acqua, Vergani, et al. 2012b). The cross-modal association area of the inferior parietal lobe, especially implicated in semantic processing and reading, is recognised (Geschwind 1965a; Seghier 2012). The role of memory processes has been taken into account (Makuuchi & Friederici 2013; Seghier 2012). Likewise, the visual word form area (a key region for reading) and its white matter connections have been acknowledged (Dehaene & L. Cohen 2011;

Yeatman et al. 2013). This model of language function and aphasia is still work in progress.
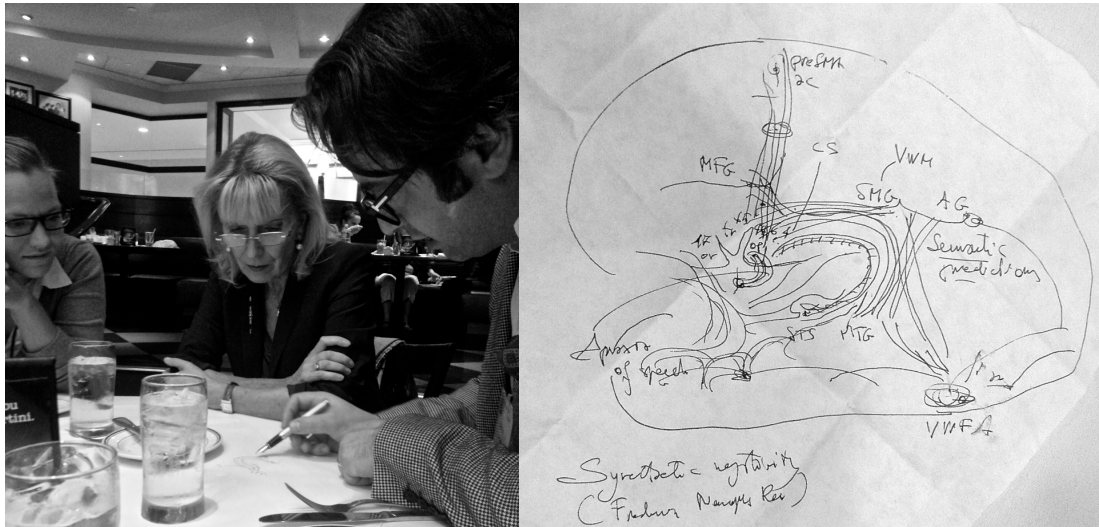
Figure 92   Anatomy of comprehension, articulation, reading, and aphasia

This figure shows Prof. Angela Friederici (middle), Dr. Marco Catani (right), and Stephanie Forkel (left), developing their neuroanatomical model of language and aphasia based on functional imaging results (Friederici) and connectional anatomy (Catani, Forkel). Picture taken at OHBM 2013 in Seattle, WA, US (courtesy of Arjun Sethi). The resulting model can be seen on the right. The pathways relevant to this figure are the uncinate, the anterior, posterior and long segments of the arcuate fasciculus, the frontal aslant tract, intra-insular connections, and temporal-occipital u-shaped fibres. MFG, middle frontal gyrus; STS, superior temporal sulcus; MTG, middle temporal gyrus; SMG, supramarginal gyrus; AG, angular gyrus; VWM, verbal working memory; ac, articulation; cs, central sulcus; or, pars orbitalis; tr, pars triangularis; op, pars opercularis; pre-SMA, pre-supplementary motor area; VWFA, visual word form area. Also indicated are BA47,45,44,6,4.

'The limits of my language mean the limits of my world'

(Ludwig Wittgenstein)

Abbott, R.D. et al., 1987. Diabetes and the Risk of Stroke. The Honolulu Heart Program. *JAMA : the journal of the American Medical Association*, 257(7), pp.949–952.

Abdul-Kareem, I.A. & Sluming, V., 2008. Heschl gyrus and its included primary auditory cortex: structural MRI studies in healthy and diseased subjects. *Journal of magnetic resonance imaging : JMRI*, 28(2), pp.287–299.

Abo, M. et al., 2004. Language-related brain function during word repetition in post-stroke aphasics. *NeuroReport*, 15(12), pp.1891–1894.

Aboitiz, F. & García, R., V, 1997. The evolutionary origin of the language areas in the human brain. A neuroanatomical perspective. *Brain Research Reviews*, 25(3), pp.381–396.

Aboitiz, F. & Montiel, J., 2003. One hundred million years of interhemispheric communication: the history of the corpus callosum. *Brazilian journal of medical and biological research*, 36(4), pp.409–420.

Aboitiz, F., Scheibel, A.B. & Zaidel, E., 1992a. Morphometry of the Sylvian fissure and the corpus callosum, with emphasis on sex differences. *Brain : a journal of neurology*, 115(5), pp.1521–1541.

Aboitiz, F., Scheibel, A.B., Fisher, R.S., et al., 1992b. Individual differences in brain asymmetries and fiber composition in the human corpus callosum. *Brain research*, 598(1-2), pp.154–161.

Abou-Khalil, B., 2007. An update on determination of language dominance in screening for epilepsy surgery: the Wada test and newer noninvasive alternatives. *Epilepsia*, 48(3), pp.442–455.

Abu-Zeid, H.A., Choi, N.W. & Nelson, N.A., 1975. Epidemiologic features of cerebrovascular disease in Manitoba: incidence by age, sex and residence, with etiologic implications. *Canadian Medical Association journal*, 113(5), pp.379–384.

Ackermann, H. & Riecker, A., 2004. The contribution of the insula to motor aspects of speech production: a review and a hypothesis. *Brain and language*, 89(2), pp.320–328.

Acosta-Cabronero, J. et al., 2010. Absolute diffusivities define the landscape of white matter degeneration in Alzheimer's disease. *Brain : a journal of neurology*,

133(Pt 2), pp.529–539.

Acosta-Cabronero, J. et al., 2011. Atrophy, hypometabolism and white matter abnormalities in semantic dementia tell a coherent story. *Brain : a journal of neurology*, 134(7), pp.1869–1871.

Addo, J. et al., 2011. Provision of acute stroke care and associated factors in a multiethnic population: prospective study with the South London Stroke Register. *British medical journal*, 342(10.1136/bmj.d744).

Akaike, H., 1974. A new look at the statistical model identification. *IEEE Transactions on Automatic Control*, 19(6), pp.716–723.

Alba-Ferrara, L.M. & de Erausquin, G.A., 2013. What does anisotropy measure? Insights from increased and decreased anisotropy in selective fiber tracts in schizophrenia. *Frontiers in integrative neuroscience*, 7, pp.10.3389–fnint.2013.00009.

Albers, G.W., 1998. Diffusion-weighted MRI for evaluation of acute stroke. *Neurology*, 51(3 Suppl 3), pp.S47–9.

Alekoumbides, A., 1978. Hemispheric dominance for language: quantitative aspects. *Acta neurologica Scandinavica*, 57(2), pp.97–140.

Alexander, M.P., Naeser, M.A. & Palumbo, C.L., 1987. Correlations of subcortical CT lesion sites and aphasia profiles. *Brain : a journal of neurology*, 110 (Pt 4), pp.961–991.

Alsop, D.C. & Detre, J.A., 1998. Multisection cerebral blood flow MR imaging with continuous arterial spin labeling. *Radiology*, 208(2), pp.410–416.

Amunts, K. & Zilles, K., 2012. Architecture and organizational principles of Broca's region. *Trends in Cognitive Sciences*, 16(8), pp.418–426.

Amunts, K. et al., 1999. Broca's region revisited: cytoarchitecture and intersubject variability. *The Journal of comparative neurology*, 412(2), pp.319–341.

Amunts, K. et al., 2010. Broca's Region: Novel Organizational Principles and Multiple Receptor Mapping D. Poeppel, ed. *PLoS Biology*, 8(9), p.e1000489.

Anderson, J.M. et al., 1999. Conduction Aphasia and the Arcuate Fasciculus: A Reexamination of the Wernicke–Geschwind Model. *Brain and language*, 70(1), pp.1–12.

Anon, 2003. *Aphasia and Its Therapy*, Oxford University Press, USA.

Anwander, A. et al., 2006. Connectivity-Based Parcellation of Broca's Area. *Cerebral cortex (New York, N.Y. : 1991)*, 17(4), pp.816–825.

Ardila, A., 2010. A proposed reinterpretation and reclassification of aphasic syndromes. *Aphasiology*, 24(3), pp.363–394.

Assaf, B.A. et al., 2003. Diffusion tensor imaging of the hippocampal formation in temporal lobe epilepsy. *AJNR. American journal of neuroradiology*, 24(9), pp.1857–1862.

Assaf, Y., 2008. Can we use diffusion MRI as a bio-marker of neurodegenerative processes? *BioEssays : news and reviews in molecular, cellular and developmental biology*, 30(11-12), pp.1235–1245.

Astrup, J., Siesjo, B.K. & Symon, L., 1981. Thresholds in cerebral ischemia - the ischemic penumbra. *Stroke; a journal of cerebral circulation*, 12(6), pp.723–725.

Avants, B.B. et al., 2008. Symmetric diffeomorphic image registration with cross-correlation: evaluating automated labeling of elderly and neurodegenerative brain. *Medical image analysis*, 12(1), pp.26–41.

Baddeley, A., 2003. Working memory: looking back and looking forward. *Nature Reviews Neuroscience*, 4(10), pp.829–839.

Badre, D. & Wagner, A.D., 2002. Semantic Retrieval, Mnemonic Control, and Prefrontal Cortex. *Behavioral and Cognitive Neuroscience Reviews*, 1(3), pp.206–218.

Baird, A.E. & Warach, S., 1998. Magnetic Resonance Imaging of Acute Stroke. *Journal of Cerebral Blood Flow & Metabolism*, 18(6), pp.583–609.

Baird, A.E. et al., 2001. A three-item scale for the early prediction of stroke recovery. *Lancet*, 357(9274), pp.2095–2099.

Barber, P.A. et al., 1998. Prediction of stroke outcome with echoplanar perfusion- and diffusion-weighted MRI. *Neurology*, 51(2), pp.418–426.

Barrett-Connor, E. & Khaw, K.T., 1988. Diabetes mellitus: an independent risk factor for stroke? *American journal of epidemiology*, 128(1), pp.116–123.

Barrick, T.R. et al., 2007. White matter pathway asymmetry underlies functional lateralization. *Cerebral cortex (New York, N.Y. : 1991)*, 17(3), pp.591–598.

Basser, P.J. & Le Bihan, D., 1992. Fiber orientation mapping in an aniosotropic medium with NMR diffusion spectroscopy. In ISMRM.

Basser, P.J. & Oezarslan, E., 2009. Introduction to diffusion MR. In H. Johansen-Berg & T. E. J. Behrens, eds. *Diffusion MRI*. Academic Press.

Basser, P.J. et al., 2000. In vivo fiber tractography using DT-MRI data. *Magnetic resonance in medicine : official journal of the Society of Magnetic Resonance in Medicine / Society of Magnetic Resonance in Medicine*, 44(4), pp.625–632.

Basser, P.J., Mattiello, J. & LeBihan, D., 1994. Estimation of the effective self-diffusion tensor from the NMR spin echo. *Journal of magnetic resonance. Series B*, 103(3), pp.247–254.

Basso, A., 1992. Prognostic factors in aphasia. *Aphasiology*, 6(4), pp.337–348.

Basso, A., 2000. The aphasias: fall and renaissance of the neurological model? *Brain and language*, 71(1), pp.15–17.

Basso, A. & Cubelli, R., 1999. Clinical aspects of aphasia. In G. Denes & L. Pizzamigliio, eds. *Handbook of Clinical and Experimental Neuropsychology*. East Sussex, UK: Psychology Press.

Basso, A. et al., 1987. Age and evolution of language area functions. A study on adult stroke patients. *Cortex*, 23(3), pp.475–483.

Basso, A. et al., 1985. Anatomoclinical correlations of the aphasias as defined through computerized tomography: exceptions. *Brain and language*, 26(2), pp.201–229.

Basso, A., Capitani, E. & Laiacona, M., 1980. Factors influencing type and severity of aphasia. *Cortex*, 16(4), pp.631–636.

Bastian, H.C., 1898. *A Treatise on Aphasia and Other Speech Defects*, Nabu Press.

Bastian, H.C., 1897. On a Case of Amnesia and other Speech Defects of Eighteen Years' Duration, with Autopsy. *Medico-chirurgical transactions*, 80, pp.61–86.3.

Bastian, H.C., 1887. On Different Kinds of Aphasia, with Special Reference to Their Classification and Ultimate Pathology. *British medical journal*, 2(1401), pp.985–990.

Bateman, F., 1870. *On Aphasia or Loss of Speech*, London: John Churchill & Sons.

Bates, E. et al., 2003. Voxel-based lesion–symptom mapping. *Nature neuroscience*, 6(5), pp.448–450.

Beaton, A.A., 1997. The Relation of Planum Temporale Asymmetry and Morphology of the Corpus Callosum to Handedness, Gender, and Dyslexia: A Review of the Evidence. *Brain and language*, 60(2), pp.255–322.

Beaulieu, C. et al., 1999. Longitudinal magnetic resonance imaging study of perfusion and diffusion in stroke: evolution of lesion volume and correlation with clinical outcome. *Annals of neurology*, 46(4), pp.568–578.

Becker, H. et al., 1979. CT fogging effect with ischemic cerebral infarcts. *Neuroradiology*, 18(4), pp.185–192.

Behrens, T.E.J., Johansen-Berg, H., et al., 2003a. Non-invasive mapping of connections between human thalamus and cortex using diffusion imaging. *Nature neuroscience*, 6(7), pp.750–757.

Behrens, T.E.J., Woolrich, M.W., et al., 2003b. Characterization and propagation of uncertainty in diffusion-weighted MR imaging. *Magnetic resonance in medicine : official journal of the Society of Magnetic Resonance in Medicine / Society of Magnetic Resonance in Medicine*, 50(5), pp.1077–1088.

Bello, L. et al., 2008. Motor and language DTI Fiber Tracking combined with intraoperative subcortical mapping for surgical removal of gliomas. *NeuroImage*, 39(1), pp.369–382.

Benbadis, S.R. et al., 1998. Is speech arrest during wada testing a valid method for determining hemispheric representation of language? *Brain and language*, 65(3), pp.441–446.

Benowitz, L.I. et al., 1983. Hemispheric specialization in nonverbal communication. *Cortex*, 19(1), pp.5–11.

Benson, D.F. & Geschwind, N., 1971. Aphasia and related cortical disturbances. In A. B. Baker & L. H. Baker, eds. *Clinical neurology*. New York: Harper and Row.

Benton, A.L., 1967. Problems of test construction in the field of aphasia. *Cortex*, 3(1), pp.32–58.

Benton, A.L., Hamsher, K.S.Sivan, AB, 1994. *Multilingual aphasia examination*, Iowa City: AJA.

Berman, J.I. et al., 2013. High Angular Resolution Diffusion Imaging Probabilistic Tractography of the Auditory Radiation. *American Journal of Neuroradiology*, 10.3174/ajnr.A3471.

Bernal, B. & Ardila, A., 2009. The role of the arcuate fasciculus in conduction aphasia. *Brain : a journal of neurology*, 132(Pt 9), pp.2309–2316.

Berndt, R.S. & Caramazza, A., 2008. A redefinition of the syndrome of Broca's aphasia: Implications for a neuropsychological model of language. *Applied Psycholinguistics*, 1(03), pp.225–2778.

Bernstein, M.A., King, K.F. & Zhou, X.J., 2004. *Handbook of MRI Pulse Sequences*, London: Elsevier Academic Press.

Berthier, M.L. et al., 2012. Arcuate fasciculus variability and repetition: the left sometimes can be right. *Cortex*, 48(2), pp.133–143.

Binder, J.R. et al., 1996. Determination of language dominance using functional MRI: a comparison with the Wada test. *Neurology*, 46(4), pp.978–984.

Biniek, R., 1997. *Akute Aphasien*, Stuttgart: Thieme.

Blanton, R.E. et al., 2004. Gender differences in the left inferior frontal gyrus in normal children. *NeuroImage*, 22(2), pp.626–636.

Bloch, F., 1946. Nuclear induction. *Physical review*, 70(7-8), pp.460–474.

Bodini, B. & Ciccarelli, O., 2009. Diffusion MRI in neurological disorders. In H. Johansen-Berg & T. E. J. Behrens, eds. *Diffusion MRI*. London: Academic Press.

Bogousslavsky, J., Van Melle, G. & Regli, F., 1988. The Lausanne Stroke Registry: analysis of 1,000 consecutive patients with first stroke. *Stroke; a journal of cerebral circulation*, 19(9), pp.1083–1092.

Bonhoeffer, K., 1902. Zur Kenntnis der Rueckbildung motorischen Aphasien. *Mitteilungen aus der Grenzgebieten der Medizin und Chirurgie*, 10, pp.203–224.

Bookheimer, S., 2002. Functional MRI of Language: New Approaches to Understanding the Cortical Organization of Semantic Processing. *Annual Review of Neuroscience*, 25(1), pp.151–188.

Bortz, J., 2005. *Statistik: Für Human- und Sozialwissenschaftler* 6 ed, Heidelberg: Springer Medizin Verlag.

Bowers, D. et al., 1987. Comprehension of emotional prosody following unilateral

hemispheric lesions: processing defect versus distraction defect. *Neuropsychologia*, 25(2), pp.317–328.

Brant-Zawadzki, M. et al., 1985. Basic principles of magnetic resonance imaging in cerebral ischemia and initial clinical experience. *Neuroradiology*, 27(6), pp.517–520.

Brant-Zawadzki, M. et al., 1983. NMR demonstration of cerebral abnormalities: comparison with CT. *AJR. American journal of roentgenology*, 140(5), pp.847–854.

Breier, J.I. et al., 2008. Language dysfunction after stroke and damage to white matter tracts evaluated using diffusion tensor imaging. *AJNR. American journal of neuroradiology*, 29(3), pp.483–487.

Brett, M., Johnsrude, I.S. & Owen, A.M., 2002. The problem of functional localization in the human brain. *Nature Reviews Neuroscience*, 3(3), pp.243–249.

Brott, T. et al., 1989. Measurements of acute cerebral infarction: a clinical examination scale. *Stroke; a journal of cerebral circulation*, 20(7), pp.864–870.

Brunner, E., Munzel, U. & Puri, M.L., 2002. The multivariate nonparametric Behrens–Fisher problem. *Journal of Statistical Planning and Inference*, 108(1-2), pp.37–53.

Brust, J.C. et al., 1976. Aphasia in acute stroke. *Stroke; a journal of cerebral circulation*, 7(2), pp.167–174.

Bruyn, R.P.M., 1989. Thalamic aphasia - A cenceptional critique. *Journal of neurology*, 236(1), pp.21–25.

Buckner, R.L., Raichle, M.E. & Petersen, S.E., 1995. Dissociation of human prefrontal cortical areas across different speech production tasks and gender groups. *Journal of neurophysiology*, 74(5), pp.2163–2173.

Burdach, C.-F., 1822. Von Baue und Leben des Gehirns. *Dyk*, pp.1–434.

Burdach, C.-F., 1826. *Von Baue und Leben des Gehirns*, Leipzig: Dyk.

Büchel, C. et al., 2004. White matter asymmetry in the human brain: a diffusion tensor MRI study. *Cerebral cortex (New York, N.Y. : 1991)*, 14(9), pp.945–951.

Bürgel, U. et al., 2006. White matter fiber tracts of the human brain: three-dimensional mapping at microscopic resolution, topography and intersubject variability. *NeuroImage*, 29(4), pp.1092–1105.

Bydder, G.M. et al., 1982. Clinical NMR imaging of the brain: 140 cases. *AJR. American journal of roentgenology*, 139, pp.215–236.

Cabeza, R. & Kingstone, A., 2001. Handbook of Functional Neuroimaging of Cognition. *MIT Press*.

Campbell, A.W., 1905. *Histological Studies on the Localisation of Cerebral Function*, Cambridge: Cambridge University Press.

Campbell, J.S.W. & Pike, G.B., 2013. Potential and limitations of diffusion MRI tractography for the study of language. *Brain and language*, 10.1016/j.bandl.2013.06.007.

Cappa, S.F., 2000. Neuroimaging of recovery from aphasia. *Neuropsychological rehabilitation*, 10(3), pp.365–376.

Cappa, S.F., 1997. Subcortical aphasia: still a useful concept? *Brain and language*, 58(3), pp.424–436.

Cappa, S.F. et al., 1997. A PET follow-up study of recovery after stroke in acute aphasics. *Brain and language*, 56(1), pp.55–67.

Caramazza, A., 1984. The logic of neuropsychological research and the problem of patient classification in aphasia. *Brain and language*, 21(1), pp.9–20.

Caramazza, A. & Badecker, W., 1991. Clinical syndromes are not God's gift to cognitive neuropsychology: a reply to a rebuttal to an answer to a response to the case against syndrome-based research. *Brain and cognition*, 16(2), pp.211–227.

Cardebat, D. et al., 2003. Behavioral and neurofunctional changes over time in healthy and aphasic subjects: a PET Language Activation Study. *Stroke; a journal of cerebral circulation*, 34(12), pp.2900–2906.

Carroll, K.A. & Chataway, J., 2006. Understanding stroke:Pathophysiology, presentation, and investigation. *student.bmj.com*, 14, pp.309–352.

Catani, M., 2006. Diffusion tensor magnetic resonance imaging tractography in cognitive disorders. *Current opinion in neurology*, 19(6), pp.599–606.

Catani, M. & ffytche, D.H., 2005. The rises and falls of disconnection syndromes. *Brain : a journal of neurology*, 128(10), pp.2224–2239.

Catani, M. & Mesulam, M.M., 2008a. The arcuate fasciculus and the disconnection theme in language and aphasia: History and current state. *Cortex*, 44(8), pp.953–961.

Catani, M. & Mesulam, M.M., 2008b. What is a disconnection syndrome? *Cortex*, 44(8), pp.911–913.

Catani, M. & Thiebaut de Schotten, M., 2008. A diffusion tensor imaging tractography atlas for virtual in vivo dissections. *Cortex*, 44(8), pp.1105–1132.

Catani, M. & Thiebaut de Schotten, M., 2012. *Atlas of Human Brain Connections*, OUP Oxford.

Catani, M. et al., 2013. A novel frontal pathway underlies verbal fluency in primary progressive aphasia. *Brain : a journal of neurology*, 136(8), pp.2619–2628.

Catani, M. et al., 2011. Altered integrity of perisylvian language pathways in schizophrenia: relationship to auditory hallucinations. *Biological psychiatry*, 70(12), pp.1143–1150.

Catani, M. et al., 2007. Symmetries in human brain language pathways correlate

with verbal recall. *Proceedings of the National Academy of Sciences of the United States of America*, 104(43), pp.17163–17168.

Catani, M. et al., 2002. Virtual in Vivo Interactive Dissection of White Matter Fasciculi in the Human Brain. *NeuroImage*, 17(1), pp.77–94.

Catani, M., Dell'Acqua, F., Bizzi, A., et al., 2012a. Beyond cortical localization in clinico-anatomical correlation. *Cortex*, 48(10), pp.1262–1287.

Catani, M., Dell'Acqua, F., Vergani, F., et al., 2012b. Short frontal lobe connections of the human brain. *Cortex*, 48(2), pp.273–291.

Catani, M., Forkel, S.J. & Thiebaut de Schotten, M., 2010. Asymmetry of White Matter Pathways. In K. Hugdahl & R. Westerhausen, eds. *The Two Halves of the Brain*. MIT Press (MA).

Catani, M., Jones, D.K. & ffytche, D.H., 2005. Perisylvian language networks of the human brain. *Annals of neurology*, 57(1), pp.8–16.

Chalela, J.A. & Kasner, S.E., 2000. The fogging effect. *Neurology*, 55(2), p.315.

Chalela, J.A. et al., 2000. Magnetic resonance perfusion imaging in acute ischemic stroke using continuous arterial spin labeling. *Stroke; a journal of cerebral circulation*, 31(3), pp.680–687.

Chenevert, T.L., Brunberg, J.A. & Pipe, J.G., 1990. Anisotropic diffusion in human white matter: demonstration with MR techniques in vivo. *Radiology*, 177(2), pp.401–405.

Chiarello, C. et al., 2004. Cerebral Asymmetries for Language: Evidence for Structural-Behavioral Correlations. *Neuropsychology*, 18(2), pp.219–231.

Chien, D. et al., 1992. MR diffusion imaging of cerebral infarction in humans. *AJNR. American journal of neuroradiology*, 13(4), pp.1097–1102.

Ciccarelli, O., 2007. Diffusion tensor MRI for the differentiation of Parkinson's disease and multiple system atrophy. *Nature Clinical Practice Neurology*, 3(10), pp.544–545.

Ciccarelli, O. et al., 2008. Diffusion-based tractography in neurological disorders: concepts, applications, and future developments. *Lancet neurology*, 7(8), pp.715–727.

Clark, W.E.L.G. & Russell, W.R., 1943. Cortical Deafness Without Aphasia. *The Journal of Nervous and Mental Disease*, 98(3), pp.375–383.

Clarke, E., 1963. Apoplexy in the Hipprocatic writings. *Bulletin of the history of medicine*, 37, pp.301–314.

Code, C., 2010. Aphasia. In J. Damico, N. Mueller, & M. J. Ball, eds. *The handbook of language and speech disorders*. Oxford, UK: Wiley Online Library.

Code, C., 2001. Multifactorial Processes in Recovery from Aphasia: Developing the Foundations for a Multileveled Framework. *Brain and language*, 77(1), pp.25–44.

Cohen, J., 1992. A power primer. *Psychological Bulletin*, 112(1), pp.155–159.

Cohen, J., 1990. Things I have learned (so far). *American psychologist*, 45(12), pp.1304–1312.

Commitee, I.A.N., 1989. *Nomina anatomica* 6 ed, Edinburgh, Scotland: Churchill Livingston.

Conner, C.R. et al., 2008. Repairing the human brain after stroke: I. Mechanisms of spontaneous recovery. *Annals of neurology*, 63(3), pp.272–287.

Conturo, T.E. et al., 1999. Tracking neuronal fiber pathways in the living human brain. *Proceedings of the National Academy of Sciences of the United States of America*, 96(18), pp.10422–10427.

Cook, P.A. et al., 2007. Optimal acquisition orders of diffusion-weighted MRI measurements. *Annals of neurology*, 25(5), pp.1051–1058.

Copen, W.A. et al., 2001. Ischemic stroke: effects of etiology and patient age on the time course of the core apparent diffusion coefficient. *Radiology*, 221(1), pp.27–34.

Courchesne, E. & Pierce, K., 2005. Why the frontal cortex in autism might be talking only to itself: local over-connectivity but long-distance disconnection. *Current Opinion in Neurobiology*, 15(2), pp.225–230.

Cox, A.M. et al., 2006. Socioeconomic status and stroke. *The Lancet Neurology*, 5(2), pp.181–188.

Craig, M.C. et al., 2009. Altered connections on the road to psychopathy. *Molecular Psychiatry*, (14), pp.946–953.

Cramer, S.C., 2008. Repairing the human brain after stroke: I. Mechanisms of spontaneous recovery. *Annals of neurology*, 63(3), pp.272–287.

Critchley, M., 1970. *Aphasiology and other aspects of language*, London: William Clowes and Sons.

Croquelois, A. et al., 2003. Aphasia in hyperacute stroke: language follows brain penumbra dynamics. *Annals of neurology*, 54(3), pp.321–329.

Crosson, B. et al., 1986. A case of thalamic aphasia with postmortem verification. *Brain and language*, 29(2), pp.301–314.

Curran, E.J., 1909. A new association fiber tract in the cerebrum with remarks on the fiber tract dissection method of studying the brain. *Journal of Comparative Neurology and Psychology*, 19(6), pp.645–656.

Damasio, A. et al., 1982. Aphasia with nonhemorrhagic lesions in the basal ganglia and internal capsule. *Archives of neurology*, 39(1), pp.15–24.

Damasio, H. & Damasio, A.R., 1980. The anatomical basis of conduction aphasia. *Brain : a journal of neurology*, 103(2), pp.337–350.

Das, R.R. et al., 2008. Prevalence and Correlates of Silent Cerebral Infarcts in the

Framingham Offspring Study. *Stroke; a journal of cerebral circulation*, 39(11), pp.2919–2920.

Davis, G., 1993. *A survey of adult aphasia*, Englewood Hills, NJ: Prentice Hall.

Davis, P.H. et al., 1987. Risk factors for ischemic stroke: a prospective study in Rochester, Minnesota. *Annals of neurology*, 22(3), pp.319–327.

De Boissezon, X. et al., 2005. Subcortical aphasia: a longitudinal PET study. *Stroke; a journal of cerebral circulation*, 36(7), pp.1467–1473.

de Laat, K.F. et al., 2010. Loss of white matter integrity is associated with gait disorders in cerebral small vessel disease. *Brain : a journal of neurology*, 134(1), pp.73–83.

De Witt Hamer, P.C. et al., 2011. Is the human left middle longitudinal fascicle essential for language? A brain electrostimulation study. *Human Brain Mapping*, 32(6), pp.962–973.

De Witte, E. & Mariën, P., 2012. The neurolinguistic approach to awake surgery reviewed. *Clinical neurology and neurosurgery*, 115(2), pp.127–145.

De Witte, L. et al., 2006. Impairment of syntax and lexical semantics in a patient with bilateral paramedian thalamic infarction. *Brain and language*, 96(1), pp.69–77.

Deacon, T.W., 1992. Cortical connections of the inferior arcuate sulcus cortex in the macaque brain. *Brain research*, 573(1), pp.8–26.

Dehaene, S. & Cohen, L., 2011. The unique role of the visual word form area in reading. *Trends in Cognitive Sciences*, 15(6), pp.254–262.

Deibler, A.R., Pollock, J.M., Kraft, R.A., Tan, H., Burdette, J.H. & Maldjian, J.A., 2008a. Arterial Spin-Labeling in Routine Clinical Practice, Part 2: Hypoperfusion Patterns. *American Journal of Neuroradiology*, 29(7), pp.1235–1241.

Deibler, A.R., Pollock, J.M., Kraft, R.A., Tan, H., Burdette, J.H. & Maldjian, J.A., 2008b. Arterial Spin-Labeling in Routine Clinical Practice, Part 3: Hyperperfusion Patterns. *American Journal of Neuroradiology*, 29(8), pp.1428–1435.

Dell'Acqua, F. & Catani, M., 2012. Structural human brain networks: hot topics in diffusion tractography. *Current opinion in neurology*, 25, pp.375–383.

Dell'Acqua, F. et al., 2010. A Modified Damped Richardson Lucy Algorithm to Reduce Isotropic Background Effects in Spherical Deconvolution. *NeuroImage*, 49(2), pp.1446–1458.

Dell'Acqua, F. et al., 2012. Can spherical deconvolution provide more information than fiber orientations? Hindrance modulated orientational anisotropy, a true-tract specific index to characterize white matter diffusion. *Human Brain Mapping*, pp.10.1002–hbm.22080.

Desmond, J.E. et al., 1995. Functional MRI measurement of language lateralization in Wada-tested patients. *Brain : a journal of neurology*, 118(6), pp.1411–1419.

Detre, J.A. & Alsop, D.C., 1999. Perfusion magnetic resonance imaging with continuous arterial spin labeling: methods and clinical applications in the central nervous system. *European Journal of Radiology*, 30(2), pp.115–124.

Démonet, J.-F., Thierry, G. & Cardebat, D., 2005. Renewal of the neurophysiology of language: functional neuroimaging. *Physiological reviews*, 85(1), pp.49–95.

Démonet, J.-F., Wise, R. & Frackowiak, R.S.J., 2004. Language functions explored in normal subjects by positron emission tomography: A critical review. *Human Brain Mapping*, 1(1), pp.39–47.

Dick, A.S. & Tremblay, P., 2012. Beyond the arcuate fasciculus: consensus and controversy in the connectional anatomy of language. *Brain : a journal of neurology*, 135(Pt 12), pp.3529–3550.

Dickey, L. et al., 2010. Incidence and profile of inpatient stroke-induced aphasia in Ontario, Canada. *Archives of physical medicine and rehabilitation*, 91(2), pp.196–202.

Dion, J.E. et al., 1987. Clinical events following neuroangiography: a prospective study. *Stroke; a journal of cerebral circulation*, 18(6), pp.997–1004.

Dirnagl, U., Iadecola, C. & Moskowitz, M.A., 1999. Pathobiology of ischaemic stroke: an integrated view. *Trends in neurosciences*, 22(9), pp.391–397.

Dogil, G. et al., 2002. The speaking brain: a tutorial introduction to fMRI experiments in the production of speech, prosody and syntax. *Journal of Neurolinguistics*, 15(1), pp.59–90.

Donnan, G.A. et al., 2008. Stroke. *Lancet*, 371, pp.1612–1623.

Doran, M. et al., 1990. Normal and abnormal white matter tracts shown by MR imaging using directional diffusion weighted sequences. *Journal of computer assisted tomography*, 14(6), pp.865–873.

Dronkers, N.F., 1996. A new brain region for coordinating speech articulation. *Nature*, 384(6605), pp.159–161.

Dronkers, N.F., 2000. The pursuit of brain-language relationships. *Brain and language*, 71(1), pp.59–61.

Dronkers, N.F. et al., 2007. Paul Broca's historic cases: high resolution MR imaging of the brains of Leborgne and Lelong. *Brain : a journal of neurology*, 130(Pt 5), pp.1432–1441.

Duffau, H., 2005. New insights into the anatomo-functional connectivity of the semantic system: a study using cortico-subcortical electrostimulations. *Brain : a journal of neurology*, 128(4), pp.797–810.

Duffau, H., 2008. The anatomo-functional connectivity of language revisited. New insights provided by electrostimulation and tractography. *Neuropsychologia*, 46(4), pp.927–934.

Duffau, H. et al., 2005. Contribution of intraoperative electrical stimulations in surgery of low grade gliomas: a comparative study between two series without

(1985-96) and with (1996-2003) functional mapping in the same institution. *Journal of neurology, neurosurgery, and psychiatry*, 76(6), pp.845–851.

Duffau, H. et al., 2009. Is the left uncinate fasciculus essential for language? A cerebral stimulation study. *Journal of neurology*, 256(3), pp.382–389.

Duffau, H., Capelle, L., et al., 2002a. Intraoperative mapping of the subcortical language pathways using direct stimulations. An anatomo-functional study. *Brain : a journal of neurology*, 125(Pt 1), pp.199–214.

Duffau, H., Denvil, D., et al., 2002b. Intraoperative mapping of the cortical areas involved in multiplication and subtraction: an electrostimulation study in a patient with a left parietal glioma. *Journal of neurology, neurosurgery, and psychiatry*, 73(6), pp.733–738.

Duffau, H., Leroy, M. & Gatignol, P., 2008a. Cortico-subcortical organization of language networks in the right hemisphere: an electrostimulation study in left-handers. *Neuropsychologia*, 46(14), pp.3197–3209.

Duffau, H., Peggy Gatignol, S.T., et al., 2008b. Intraoperative subcortical stimulation mapping of language pathways in a consecutive series of 115 patients with Grade II glioma in the left dominant hemisphere. *Journal of neurosurgery*, 109(3), pp.461–471.

EAFT, 1993. Secondary prevention in non-rheumatic atrial fibrillation after transient ischaemic attack or minor stroke. EAFT (European Atrial Fibrillation Trial) Study Group. *Lancet*, 342(8882), pp.1255–1262.

Eling, P., 1994. *Reader in the History of Aphasia: From Franz Gall to Norman Geschwind* P. Eling, ed., Amsterdam: John Benjamins B.V.

Ellmore, T.M. et al., 2009. Relationships between essential cortical language sites and subcortical pathways. *Journal of neurosurgery*, 111(4), pp.755–766.

Emde Boas van, W., 1999. Juhn A. Wada and the Sodium Amytal Test The first (and last?) 50 years. *Journal of the History of the Neurosciences*, 8(3), pp.286–292.

Enderby, P. et al., 1987. Aphasia after stroke: a detailed study of recovery in the first 3 months. *International Rehabilitation Medicine*, 8, pp.162–165.

Engelter, S.T. et al., 2006. Epidemiology of Aphasia Attributable to First Ischemic Stroke. *Stroke; a journal of cerebral circulation*, 37(6), pp.1379–1384.

Eslinger, P.J. & Damasio, A., 1981. Age and type of aphasia in patients with stroke. *Journal of neurology, neurosurgery, and psychiatry*, 44(5), pp.377–381.

Fadiga, L., Craighero, L. & Roy, A., 2006. Broca's Region: A Speech Area? In Y. Grodzinsky & K. Amunts, eds. *Broca's region*. Oxford: Oxford University Press.

Fazio, C., Sacco, G. & Bugiani, O., 1973. The Thalamic Hemorrhage. *Cerebrovascular Diseases*, 9(1), pp.30–43.

Fazzini, E., Bachman, D. & Albert, M.L., 1986. Recovery of function in aphasia. *Journal of Neurolinguistics*, 2(1-2), pp.15–46.

Fedorenko, E. & Kanwisher, N., 2009. Neuroimaging of Language: Why Hasn't a Clearer Picture Emerged? *Language and Linguistics Compass*, 3(4), pp.839–865.

Feigin, V.L. et al., 2003. Stroke epidemiology: a review of population-based studies of incidence, prevalence, and case-fatality in the late 20th century. *Lancet neurology*, 2(1), pp.43–53.

Fernandez, B. et al., 2004. Functional MRI follow-up study of language processes in healthy subjects and during recovery in a case of aphasia. *Stroke; a journal of cerebral circulation*, 35(9), pp.2171–2176.

Ferro, J.M. & Madureira, S., 1997. Aphasia type, age and cerebral infarct localisation. *Journal of neurology*, 244(8), pp.505–509.

Ferro, J.M., Mariano, G. & Madureira, S., 1999. Recovery from aphasia and neglect. *Cerebrovascular Diseases*, 9 Suppl 5, pp.6–22.

ffytche, D.H. & Catani, M., 2005. Beyond localization: from hodology to function. *Philosophical Transactions of the Royal Society B: Biological Sciences*, 360(1456), pp.767–779.

Fields, W.S. & Lemark, N.A., 1989. *A History of Stroke - Its Recognition and Treatment*, New York: Oxford University Press.

Finger, S., 1994. *Origins of Neuroscience: A History of Explorations Into Brain Function*, New York: Oxford University Press.

Forkel, S.J. et al., 2012. The anatomy of fronto-occipital connections from early blunt dissections to contemporary tractography. *Cortex*, 10.1016/j.cortex.2012.09.005.

Forssmann, W., 1929. Die Sondierung des rechten Herzens. *Journal of Molecular Medicine*, 8(45), pp.2085–2087.

Foundas, A.L. et al., 1998. MRI asymmetries of Broca's area: the pars triangularis and pars opercularis. *Brain and language*, 64(3), pp.282–296.

Frey, S. et al., 2008. Dissociating the human language pathways with high angular resolution diffusion fiber tractography. *The Journal of neuroscience : the official journal of the Society for Neuroscience*, 28(45), pp.11435–11444.

Fridriksson, J. et al., 2002. Aphasia severity: Association with cerebral perfusion and diffusion. *Aphasiology*, 16(9), pp.859–871.

Fridriksson, J. et al., 2012. Left hemisphere plasticity and aphasia recovery. *NeuroImage*, 60(2), pp.854–863.

Fridriksson, J., Baker, J.M. & Moser, D., 2009. Cortical mapping of naming errors in aphasia. *Human Brain Mapping*, 30(8), pp.2487–2498.

Fridriksson, J., Bonilha, L. & Rorden, C., 2007. Severe Broca"s aphasia without Broca"s area damage. *Behavioural neurology*, 18(4), pp.237–238.

Friederici, A.D., 1985. Levels of processing and vocabulary types: Evidence from

on-line comprehension in normals and agrammatics. *Cognition*, 19(2), pp.133–166.

Friederici, A.D., 2011. The brain basis of language processing: from structure to function. *Physiological reviews*, 91(4), pp.1357–1392.

Friederici, A.D., 2012. The cortical language circuit: from auditory perception to sentence comprehension. *Trends in Cognitive Sciences*, 16(5), pp.262–268.

Friederici, A.D., 2002. Towards a neural basis of auditory sentence processing. *Trends in Cognitive Sciences*, 6(2), pp.78–84.

Friederici, A.D., 2006. What's in control of language? *Nature neuroscience*, 9(8), pp.991–992.

Friederici, A.D., Brauer, J. & Lohmann, G., 2011. Maturation of the language network: from inter- to intrahemispheric connectivities. *PloS one*, 6(6), p.e20726.

Friederici, A.D., Pfeifer, E. & Hahne, A., 1993. Event-related brain potentials during natural speech processing: effects of semantic, morphological and syntactic violations. *Brain research. Cognitive brain research*, 1(3), pp.183–192.

Fuster, J., 1995. *Memory in the Cerebral Cortex*, Massachusetts: MIT Press.

Galaburda, A.M. et al., 1987. Planum temporale asymmetry, reappraisal since Geschwind and Levitsky. *Neuropsychologia*, 25(6), pp.853–868.

Gannon, P.J., 2010. Evolutionary depth of human brain language areas. In K. Hugdahl & R. Westerhausen, eds. *The Two Halves of the Brain: Information Processing in the Cerebral Hemispheres*. Cambridge, MA: MIT Press.

Gerstmann, J., 1940. Syndrome of finger agnosia, disorientation for right and left, agraphia and acalculia: Local diagnostic value. *Archives of Neurology & Psychiatry*, 44(2), pp.398–408.

Geschwind, N., 1971. Current concepts: Aphasia. *New England Journal of Medicine*, 284(12), pp.654–656.

Geschwind, N., 1965a. Disconnexion syndromes in animals and man. I. *Brain : a journal of neurology*, 88(2), pp.237–294.

Geschwind, N., 1965b. Disconnexion syndromes in animals and man. II. *Brain : a journal of neurology*, 88(3), pp.585–644.

Geschwind, N., 1970. The organization of language and the brain. *Science*, 170(3961), pp.940–944.

Geschwind, N. & Levitsky, W., 1968. Human brain: left-right asymmetries in temporal speech region. *Science*, 161(3837), pp.186–187.

Giles, M.F. & Rothwell, P.M., 2007. Risk of stroke early after transient ischaemic attack: a systematic review and meta-analysis. *Lancet neurology*, 6(12), pp.1063–1072.

Gillard, J.H. et al., 2001. MR diffusion tensor imaging of white matter tract disruption in stroke at 3 T. *The British journal of radiology*, 74(883), pp.642–647.

Gillum, L.A., Mamidipudi, S.K. & Johnston, S.C., 2000. Ischemic stroke risk with oral contraceptives: A meta-analysis. *JAMA : the journal of the American Medical Association*, 284(1), pp.72–78.

Glasser, M.F. & Rilling, J.K., 2008. DTI tractography of the human brain's language pathways. *Cerebral Cortex*, 18(11), pp.2471–2482.

Glassman, R.B. & Buckingham, H.W., 2007. David Hartley's neurophysiology of association. In H. A. Whitaker, C. U. M. Smith, & S. Finger, eds. *Brain, mind and medicine: Essays in eighteenthcentury neuroscience*. New York: Springer.

Goldenberg, G., 2003. Apraxia and Beyond: Life and Work of Hugo Liepmann. *Cortex*, 39(3), pp.509–524.

Goldenberg, G. & Spatt, J., 1994. Influence of size and site of cerebral lesions on spontaneous recovery of aphasia and on success of language therapy. *Brain and language*, 47(4), pp.684–698.

Goldstein, L.B. et al., 2006. Primary Prevention of Ischemic Stroke. *Stroke; a journal of cerebral circulation*, 37, pp.1583–1633.

González, R.G. et al., 1999. Diffusion-weighted MR imaging: diagnostic accuracy in patients imaged within 6 hours of stroke symptom onset. *Radiology*, 210(1), pp.155–162.

Good, C.D. et al., 2001. Cerebral asymmetry and the effects of sex and handedness on brain structure: a voxel-based morphometric analysis of 465 normal adult human brains. *NeuroImage*, 14(3), pp.685–700.

Goodglass, H. & Kaplan, E., 1983. *Boston diagnostic aphasia examination (BDAE)*, Philadelphia: Lea and Febiger.

Gouvea, A.C. et al., 2010. The linguistic processes underlying the P600. *Language and Cognitive Processes*, 25(2), pp.149–188.

Gralla, J. et al., 2006. Mechanical thrombectomy for acute ischemic stroke: thrombus-device interaction, efficiency, and complications in vivo. *Stroke; a journal of cerebral circulation*, 37(12), pp.3019–3024.

Greicius, M.D. & Kimmel, D.L., 2012. Neuroimaging insights into network-based neurodegeneration. *Current opinion in neurology*, 25(6), pp.727–734.

Group, I.S.T.C., 1997. The International Stroke Trial (IST): a randomised trial of aspirin, subcutaneous heparin, both, or neither among 19435 patients with acute ischaemic stroke. International Stroke Trial Collaborative Group., 349(9065), pp.1569–1581.

Gruber-Gerardy, K.F., Merz, W. & Sonnenberg, H., 2005. *Meilensteine aus der Geschichte des Schlaganfalls*, Ingelheim: Boehringer Ingelheim.

Haberman, S., Capildeo, R. & Clifford Rose, F., 1981. The seasonal variation in mortality from cerebrovascular disease. *Journal of the neurological sciences*,

52(1), pp.25–36.

Habib, M. et al., 1987. Age-related changes in aphasia type and stroke location. *Brain and language*, 31(2), pp.245–251.

Hacke, W. et al., 2008. Thrombolysis with alteplase 3 to 4.5 hours after acute ischemic stroke. *New England Journal of Medicine*, 359(13), pp.1317–1329.

Hackett, M.L. et al., 2005. Frequency of depression after stroke: a systematic review of observational studies. *Stroke; a journal of cerebral circulation*, 36(6), pp.1330–1340.

Hagmann, P. et al., 2006. Hand preference and sex shape the architecture of language networks. *Human Brain Mapping*, 27(10), pp.828–835.

Hagoort, P., 2005. On Broca, brain, and binding: a new framework. *Trends in Cognitive Sciences*, 9(9), pp.416–423.

Hahne, A. & Friederici, A.D., 1999. Electrophysiological evidence for two steps in syntactic analysis. Early automatic and late controlled processes. *Journal of cognitive neuroscience*, 11(2), pp.194–205.

Hajat, C. et al., 2011. Incidence of aetiological subtypes of stroke in a multi-ethnic population based study: the South London Stroke Register. *Journal of neurology, neurosurgery, and psychiatry*, 82(5), pp.527–533.

Hajnal, J.V. et al., 2001. Reduction of CSF artifacts on FLAIR images by using adiabatic inversion pulses. *AJNR. American journal of neuroradiology*, 22(2), pp.317–322.

Handley, R. et al., 2013. Acute effects of single-dose aripiprazole and haloperidol on resting cerebral blood flow (rCBF) in the human brain. *Human Brain Mapping*, 34(2), pp.272–282.

Hankey, G.J., 2007. *Stroke* 2nd ed, London: Churchill Livingstone.

Harasymiw, S.J., Halper, A. & Sutherland, B., 1981. Sex, age, and aphasia type. *Brain and language*, 12(1), pp.190–198.

Haymaker, W., 1953. *The founders of neurology: One hundred and thirty-three biographical sketches*, Springfield, IL: Thomas.

Häberling, I.S., Badzakova-Trajkov, G. & Corballis, M.C., 2013. Asymmetries of the arcuate fasciculus in monozygotic twins: genetic and nongenetic influences. *PloS one*, 8(1), p.e52315.

Head, H., 1926. *Aphasia and kindred disorders of speech*, New York: Macmillan.

Hecean, H. & Albert, M., 1978. *Human neuropsychology*, New York: Wiley.

Heide, Von Der, R.J. et al., 2013. Dissecting the uncinate fasciculus: disorders, controversies and a hypothesis. *Brain : a journal of neurology*, 136(Pt 6), pp.1692–1707.

Heim, S. & Friederici, A.D., 2003. Phonological processing in language production:

time course of brain activity. *NeuroReport*, 14(16), pp.2031–2033.

Heiss, W.D. et al., 1999. Differential capacity of left and right hemispheric areas for compensation of poststroke aphasia. *Annals of neurology*, 45(4), pp.430–438.

Henry, R.G. et al., 2004. Subcortical pathways serving cortical language sites: initial experience with diffusion tensor imaging fiber tracking combined with intraoperative language mapping. *NeuroImage*, 21(2), pp.616–622.

Hervé, P.-Y. et al., 2006. Handedness and cerebral anatomical asymmetries in young adult males. *NeuroImage*, 29(4), pp.1066–1079.

Hickok, G. & Poeppel, D., 2007. The cortical organization of speech processing. *Nature Reviews Neuroscience*, 8(5), pp.393–402.

Hickok, G. & Poeppel, D., 2000. Towards a functional neuroanatomy of speech perception. *Trends in Cognitive Sciences*, 4(4), pp.131–138.

Hier, D.B. et al., 1994. Gender and aphasia in the Stroke Data Bank. *Brain and language*, 47(1), pp.155–167.

Hier, D.B. et al., 1991. Stroke recurrence within 2 years after ischemic infarction. *Stroke; a journal of cerebral circulation*, 22(2), pp.155–161.

Highley, J.R. et al., 2002. Asymmetry of the uncinate fasciculus: a post-mortem study of normal subjects and patients with schizophrenia. *Cerebral cortex (New York, N.Y. : 1991)*, 12(11), pp.1218–1224.

Hill, M.D. et al., 2004. The high risk of stroke immediately after transient ischemic attack: A population-based study. *Neurology*, 62(11), pp.2015–2020.

Hillis, A. et al., 2000. MR perfusion imaging reveals regions of hypoperfusion associated with aphasia and neglect. *Neurology*, 55(6), pp.782–788.

Hillis, A.E. & Heidler, J., 2002. Mechanisms of early aphasia recovery. *Aphasiology*, 16(9), pp.885–895.

Hillis, A.E. et al., 2001. Hypoperfusion of Wernicke's area predicts severity of semantic deficit in acute stroke. *Annals of neurology*, 50(5), pp.561–566.

Hillis, A.E. et al., 2006. Restoring cerebral blood flow reveals neural regions critical for naming. *The Journal of neuroscience : the official journal of the Society for Neuroscience*, 26(31), pp.8069–8073.

Hillis, A.E. et al., 2002. Subcortical aphasia and neglect in acute stroke: the role of cortical hypoperfusion. *Brain : a journal of neurology*, 125(Pt 5), pp.1094–1104.

Hofer, S. & Frahm, J., 2006. Topography of the human corpus callosum revisited—comprehensive fiber tractography using diffusion tensor magnetic resonance imaging. *NeuroImage*, 32(3), pp.989–994.

Holtmannspötter, M. et al., 2005. Diffusion magnetic resonance histograms as a surrogate marker and predictor of disease progression in CADASIL: a two-year follow-up study. *Stroke; a journal of cerebral circulation*, 36(12), pp.2559–2565.

Hosomi, A. et al., 2009. Assessment of arcuate fasciculus with diffusion-tensor tractography may predict the prognosis of aphasia in patients with left middle cerebral artery infarcts. *Neuroradiology*, 51(9), pp.549–555.

Huber, W. et al., 1983. *Aachener Aphasie Test*, Goettingen: Hogrefe.

Huettel, S.A., Song, A.W. & McCarthy, G., 2009. *Functional magnetic resonance imaging* 2nd ed, Massachusetts, US: Sinauer Associates Inc.

Hugdahl, K. & Westerhausen, R., 2010. *The two halves of the brain*, Cambridge (MA): MIT Press.

Hurvich, C.M. & Tsai, C.-L., 1989. Regression and time series model selection in small samples. *Biometrika*, 76(2), pp.297–307.

Hutsler, J.J. & Gazzaniga, M.S., 1996. Acetylcholinesterase staining in human auditory and language cortices: regional variation of structural features. *Cerebral cortex (New York, N.Y. : 1991)*, 6(2), pp.260–270.

Inatomi, Y. et al., 2008. Aphasia during the Acute Phase in Ischemic Stroke. *Cerebrovascular Diseases*, 25(4), pp.316–323.

Indefrey, P. & Levelt, W.J.M., 2004. The spatial and temporal signatures of word production components. *Cognition*, 92(1-2), pp.101–144.

Inglese, M. & Bester, M., 2010. Diffusion imaging in multiple sclerosis: research and clinical implications J. H. Jensen & J. A. Helpern, eds. *NMR in Biomedicine*, 23(7), pp.865–872.

James, W., 1890. *The Principles of Psychology*, New York: Henry Holt.

Jimenez-Conde, J. et al., 2008. Weather as a Trigger of Stroke. *Cerebrovascular Diseases*, 26(4), pp.348–354.

Johnston, S.C. et al., 2000. Short-term prognosis after emergency department diagnosis of TIA. *JAMA : the journal of the American Medical Association*, 284(22), pp.2901–2906.

Jonas, S., 1982. The thalamus and aphasia, including transcortical aphasia: a review. *Journal of communication disorders*, 15(1), pp.31–41.

Jones, D.K., 2010. Challenges and limitations of quantifying brain connectivity in vivowith diffusion MRI. *Imaging in Medicine*, 2(3), pp.341–355.

Jones, D.K., 2003. Determining and visualizing uncertainty in estimates of fiber orientation from diffusion tensor MRI. *Magnetic resonance in medicine : official journal of the Society of Magnetic Resonance in Medicine / Society of Magnetic Resonance in Medicine*, 49(1), pp.7–12.

Jones, D.K., 2009. Gaussian modelling of the diffusion signal. In H. Johansen-Berg & T. E. J. Behrens, eds. *Diffusion MRI*. London: Academic Press.

Jones, D.K., 2008. Studying connections in the living human brain with diffusion MRI. *Cortex*, 44(8), pp.936–952.

Jones, D.K. & Cercignani, M., 2010. Twenty-five pitfalls in the analysis of diffusion MRI data J. H. Jensen & J. A. Helpern, eds. *NMR in Biomedicine*, 23(7), pp.803–820.

Jones, D.K. & Pierpaoli, C., 2005. Contribution of cardiac pulsation to variability of tractography results. *Proceedings International Society of Magnetic Resonance Medicine*, 13, p.222.

Jones, D.K. et al., 2002. Isotropic resolution diffusion tensor imaging with whole brain acquisition in a clinically acceptable time. *Human Brain Mapping*, 15(4), pp.216–230.

Jones, D.K. et al., 2005. The effect of filter size on VBM analyses of DT-MRI data. *NeuroImage*, 26(2), pp.546–554.

Jones, D.K., Knösche, T.R. & Turner, R., 2013. White matter integrity, fiber count, and other fallacies: the do"s and don"ts of diffusion MRI. *NeuroImage*, 73, pp.239–254.

Jung-Beeman, M., 2005. Bilateral brain processes for comprehending natural language. *Trends in Cognitive Sciences*, 9(11), pp.512–518.

Kaan, E. et al., 2000. The P600 as an index of syntactic integration difficulty. *Language and Cognitive Processes*, 15(2), pp.159–201.

Kaden, E., Knösche, T.R. & Anwander, A., 2007. Parametric spherical deconvolution: inferring anatomical connectivity using diffusion MR imaging. *NeuroImage*, 37(2), pp.474–488.

Kahle, K.T. et al., 2009. Molecular mechanisms of ischemic cerebral edema: role of electroneutral ion transport. *Physiology*, 24, pp.257–265.

Kakeshita, T., 1925. Zur Anatomie der operkularen Temporalregion. *Arbeiten aus dem Neurologischen Insitut der Universitaet Wien*, 27(292-326).

Kanaan, R.A.A. et al., 2009. Microstructural Organization of Cerebellar Tracts in Schizophrenia. *BPS*, pp.1–3.

Kandel, E.R., Schwartz, J.H. & Jessell, T.M., 2000. *Principles of neural science*, New York: McGraw Hill.

Kaplan, E. et al., 2010. Horizontal portion of arcuate fasciculus fibers track to pars opercularis, not pars triangularis, in right and left hemispheres: a DTI study. *NeuroImage*, 52(2), pp.436–444.

Kasper, S. et al., 1989. Epidemiological Findings of Seasonal Changes in Mood and Behavior: A Telephone Survey of Montgomery County, Maryland. *Archives of General Psychiatry*, 46(9), pp.823–833.

Katramados, A. & Vareals, P., 2007. Hemorrhagic stroke. In M. T. Torbey & M. H. Selim, eds. *The stroke book.* Cambridge University Press.

Kauhanen, M.L. et al., 2000. Aphasia, depression, and non-verbal cognitive impairment in ischaemic stroke. *Cerebrovascular Diseases*, 10(6), pp.455–461.

Keir, S.L. & Wardlaw, J.M., 2000. Systematic review of diffusion and perfusion imaging in acute ischemic stroke. *Stroke; a journal of cerebral circulation*, 31(11), pp.2723–2731.

Keller, S.S. et al., 2009. Broca's area: Nomenclature, anatomy, typology and asymmetry. *Brain and language*, 109(1), pp.29–48.

Keller, S.S. et al., 2007. Sulcal variability, stereological measurement and asymmetry of Broca's area on MR images. *Journal of Anatomy*, 211(4), pp.534–555.

Kemeny, S. et al., 2005. Comparison of continuous overt speech fMRI using BOLD and arterial spin labeling. *Human Brain Mapping*, 24(3), pp.173–183.

Kertesz, A., 1988a. Lesion size and location in recovery from aphasia. *Journal of Neurolinguistics*, 3(1), pp.49–61.

Kertesz, A., 2007. *Western Aphasia Battery Revised. Examiner's Manual*, San Antonio, TX: Harcourt Assessment, Inc.

Kertesz, A., 1988b. What do we learn from recovery from aphasia? *Advances in neurology*, 47, pp.277–292.

Kertesz, A. & McCabe, P., 1977. Recovery patterns and prognosis in aphasia. *Brain : a journal of neurology*, 100(1), pp.1–18.

Kertesz, A. & Phipps, J.B., 1977. Numerical taxonomy of aphasia. *Brain and language*, 4(1), pp.1–10.

Kertesz, A. & Poole, E., 1974. The aphasia quotient: the taxonomic approach to measurement of aphasic disability. *The Canadian journal of neurological sciences. Le journal canadien des sciences neurologiques*, 1(1), pp.7–16.

Kertesz, A. & Sheppard, A., 1981. The epidemiology of aphasic and cognitive impairment in stroke: age, sex, aphasia type and laterality differences. *Brain : a journal of neurology*, 104(Pt 1), pp.117–128.

Kertesz, A., Harlock, W. & Coates, R., 1979. Computer tomographic localization, lesion size, and prognosis in aphasia and nonverbal impairment. *Brain and language*, 8(1), pp.34–50.

Keyser, A., 1994. Carl Wernicke (1848–1905). In P. Eling, ed. *Reader in the history of aphasia*. Amsterdam: John Benjamins B.V.

Kinnunen, K.M. et al., 2011. White matter damage and cognitive impairment after traumatic brain injury. *Brain : a journal of neurology*, 134(Pt 2), pp.449–463.

Kinsbourne, M., 1975. The ontogeny of cerebral dominance. *Annals of the New York Academy of Sciences*, 263(1 Developmental), pp.244–250.

Klein, A. et al., 2009. Evaluation of 14 nonlinear deformation algorithms applied to human brain MRI registration. *NeuroImage*, 46(3), pp.786–802.

Kloska, S.P. et al., 2007. Color-coded perfused blood volume imaging using multidetector CT: initial results of whole-brain perfusion analysis in acute

cerebral ischemia. *European radiology*, 17(9), pp.2352–2358.

Koch, M.A., Norris, D.G. & Hund-Georgiadis, M., 2002. An investigation of functional and anatomical connectivity using magnetic resonance imaging. *NeuroImage*, 16(1), pp.241–250.

Kolk, H. & Heeschen, C., 1990. Adaptation symptoms and impairment symptoms in Broca's aphasia. *Aphasiology*, 4(3), pp.221–231.

Kontis, D. et al., 2009. Diffusion tensor MRI of the corpus callosum and cognitive function in adults born preterm. *NeuroReport*, 20(4), pp.424–428.

Kotten, A., 1997. *Lexikalische Störungen bei Aphasie*, Stuttgart: Thieme.

Kreindler, A., Mihailescu, L. & Fradis, A., 1980. Speech fluency in aphasics. *Brain and language*, 9(2), pp.199–205.

Kremer, C. et al., 2013. Prognosis of aphasia in stroke patients early after iv thrombolysis. *Clinical neurology and neurosurgery*, 115(3), pp.289–292.

Kubicki, M. et al., 2002. Uncinate fasciculus findings in schizophrenia: a magnetic resonance diffusion tensor imaging study. *The American journal of psychiatry*, 159(5), pp.813–820.

Kuehberger, A., 2006. *Statistik 2*, Salzburg: Paris-Lodron Univeristy Press.

Kumar, G. et al., 2010. Penumbra, the basis of neuroimaging in acute stroke treatment: current evidence. *Journal of the neurological sciences*, 288(1-2), pp.13–24.

Kummerer, D. et al., 2013. Damage to ventral and dorsal language pathways in acute aphasia. *Brain : a journal of neurology*, 136(2), pp.619–629.

Kumral, E., Evyapan, D. & Balkir, K., 1999. Acute caudate vascular lesions. *Stroke; a journal of cerebral circulation*, 30(1), pp.100–108.

Kussmaul, A., 1877. *Die Störungen der Sprache*, Leipzig: FCW Vogel.

Kutas, M. & Federmeier, K.D., 2011. Thirty years and counting: finding meaning in the N400 component of the event-related brain potential (ERP). *Annual review of psychology*, 62, pp.621–647.

Lansberg, M.G. et al., 2001. Evolution of apparent diffusion coefficient, diffusion-weighted, and T2-weighted signal intensity of acute stroke. *AJNR. American journal of neuroradiology*, 22(4), pp.637–644.

Larsen, B., Skinhøj, E. & Lassen, N.A., 1978. Variations in regional cortical blood flow in the right and left hemispheres during automatic speech. *Brain : a journal of neurology*, 101(2), pp.193–209.

Laska, A.C. et al., 2001. Aphasia in acute stroke and relation to outcome. *Journal of Internal Medicine*, 249(5), pp.413–422.

Latchaw, R.E. et al., 2009. Recommendations for imaging of acute ischemic stroke: a scientific statement from the American Heart Association. *Stroke; a journal of*

cerebral circulation, 40(11), pp.3646–3678.

Latour, L.L. & Warach, S., 2002. Cerebral spinal fluid contamination of the measurement of the apparent diffusion coefficient of water in acute stroke. *Magnetic resonance in medicine : official journal of the Society of Magnetic Resonance in Medicine / Society of Magnetic Resonance in Medicine*, 48(3), pp.478–486.

Lau, E. et al., 2006. The role of structural prediction in rapid syntactic analysis. *Brain and language*, 98(1), pp.74–88.

Lauterbur, P.C., 1973. Image Formation by Induced Local Interactions: Examples Employing Nuclear Magnetic Resonance. *Nature*, 241, pp.190–191.

Lawes, C.M.M. et al., 2004. Blood pressure and stroke: an overview of published reviews. *Stroke; a journal of cerebral circulation*, 35(4), pp.1024–785.

Lawes, N. et al., 2008. Atlas-based segmentation of white matter tracts of the human brain using diffusion tensor tractography and comparison with classical dissection. *NeuroImage*, 39(1), pp.62–79.

Lazar, R.M. et al., 2008. Variability in language recovery after first-time stroke. *Journal of neurology, neurosurgery, and psychiatry*, 79(5), pp.530–534.

Le Bihan, D., 2012. Diffusion, confusion and functional MRI. *NeuroImage*, 62(2), pp.1131–1136.

Le Bihan, D., 2003. Looking into the functional architecture of the brain with diffusion MRI. *Nature Reviews Neuroscience*, 4(6), pp.469–480.

Le Bihan, D., 1995. Molecular diffusion, tissue microdynamics and microstructure. *NMR in Biomedicine*, 8(7-8), pp.375–386.

Le Bihan, D. et al., 2006. Artifacts and pitfalls in diffusion MRI. *Journal of magnetic resonance imaging : JMRI*, 24(3), pp.478–488.

Le Bihan, D. et al., 1986. MR imaging of intravoxel incoherent motions: application to diffusion and perfusion in neurologic disorders. *Radiology*, 161(2), pp.401–407.

Lebel, C. & Beaulieu, C., 2009. Lateralization of the arcuate fasciculus from childhood to adulthood and its relation to cognitive abilities in children. *Human Brain Mapping*, 30(11), pp.3563–3573.

Leclercq, D. et al., 2010. Comparison of diffusion tensor imaging tractography of language tracts and intraoperative subcortical stimulations. *Journal of neurosurgery*, 112(3), pp.503–511.

Lecours, André Roch, Lhermitte, F. & Bryans, B., 1983a. *Aphasiology*, Bailliere Tindall Limited.

Lecours, André, Lhermitte, F. & Bryans, B., 1983b. *Aphasiology*, London: Bailliere Tindall Limited.

Lecours, André, Vanier, M. & Lhermitte, F., 1983c. The thalamus and linguistic

function. In A. R. Lecours, F. Lhermitte, & B. Bryans, eds. *Aphasia*. London: Bailliere Tindall Limited.

Lecours, AndréRoch et al., 1992. Paris 1908: The hot summer of aphasiology or a season in the life of a chair. *Brain and language*, 42(2), pp.105–152.

Lee, H. et al., 1984. Transfere of language dominance. *Annals of neurology*, 15(3), pp.304–307.

Lehéricy, S. et al., 2000. Functional MR evaluation of temporal and frontal language dominance compared with the Wada test. *Neurology*, 54(8), pp.1625–1633.

Lendrem, W. & Lincoln, N.B., 1985. Spontaneous recovery of language in patients with aphasia between 4 and 34 weeks after stroke. *Journal of neurology, neurosurgery, and psychiatry*, 48(8), pp.743–748.

Lennox, B.R. et al., 2000. The functional anatomy of auditory hallucinations in schizophrenia. *Psychiatry research*, 100(1), pp.13–20.

Leonard, C.M. et al., 1998. Normal variation in the frequency and location of human auditory cortex landmarks. Heschl's gyrus: where is it? *Cerebral cortex (New York, N.Y. : 1991)*, 8(5), pp.397–406.

Levelt, W.J.M., 1989. *Speaking: From Intention to Articulation*, Cambridge, MA: MIT Press.

Lezak, M.D., Howieson, D. & Loring, D., 2004. *Neuropsychological Assessment*, New York: Oxford University Press, USA.

Léger, A. et al., 2002. Neural Substrates of Spoken Language Rehabilitation in an Aphasic Patient: An fMRI Study. *NeuroImage*, 17(1), pp.174–183.

Lieberman, P., 2002. On the nature and evolution of the neural bases of human language. *American Journal of Physical Anthropology*, 119(S35), pp.36–62.

Liepmann, H., 1900. Das Krankheitsbild der Apraxie ("motorischen Asymbolie") auf Grund eines Falles von einseitiger Apraxie. *Monatsschrift fuer Psychiatry und Neurologie*, 8(1), pp.15–44.

Lindell, A.K., 2006. In Your Right Mind: Right Hemisphere Contributions to Language Processing and Production. *Neuropsychology review*, 16(3), pp.131–148.

Lissauer, H., 1890. Ein Fall von Seelenblindheit nebst einem Beitrage zur Theorie derselben. *Archiv für Psychiatrie und Nervenkrankheiten*, 21(2), pp.222–270.

Lomas, J. & Kertesz, A., 1978. Patterns of spontaneous recovery in aphasic groups: A study of adult stroke patients. *Brain and language*, 5(3), pp.388–401.

London, H.F., 2009. Healthcare for London. *NHS Commissioning support for London*. Available at: http://www.londonhp.nhs.uk/wp-content/uploads/2011/03/Stroke-Commissioning-and-Tariff-Guidance.pdf [Accessed August 5, 2009].

Lovett, J.K. et al., 2003. Very early risk of stroke after a first transient ischemic

attack. *Stroke; a journal of cerebral circulation*, 34(8), pp.e138–40.

Lövblad, K.O. et al., 1997. Ischemic lesion volumes in acute stroke by diffusion-weighted magnetic resonance imaging correlate with clinical outcome. *Annals of neurology*, 42(2), pp.164–170.

Luppino, G. et al., 1991. Multiple representations of body movements in mesial area 6 and the adjacent cingulate cortex: an intracortical microstimulation study in the macaque monkey. *The Journal of comparative neurology*, 311(4), pp.463–482.

Luria, A.R., 1958. Brain disorders and language analysis. *Language and speech*, 1(1), pp.14–34.

Luria, A.R., 1966. *Higher cortical functions in man*, New York: Basic Books.

Luria, A.R. & Hutton, J.T., 1977. A modern assessment of the basic forms of aphasia. *Brain and language*, 4(2), pp.129–151.

Lythgoe, M.F. et al., 1997. Effects of diffusion anisotropy on lesion delineation in a rat model of cerebral ischemia. *Magnetic resonance in medicine : official journal of the Society of Magnetic Resonance in Medicine / Society of Magnetic Resonance in Medicine*, 38(4), pp.662–668.

Maas, L.C. & Mukherjee, P., 2005. Diffusion MRI: Overview and clinical applications in neuroradiology. *Applied Radiology*, 34(11), pp.44–60.

Maas, M. et al., 2012. The Prognosis for Aphasia in Stroke. *Journal of Stroke and Cerebrovascular Diseases*, 21(5), pp.350–357.

MacMahon, S. et al., 1990. Blood pressure, stroke, and coronary heart disease. Part 1, Prolonged differences in blood pressure: prospective observational studies corrected for the regression dilution bias. *Lancet*, 335(8692), pp.765–774.

Macmillan, M., 2012. Alfred Walter Campbell and the visual functions of the occipital cortex. *Cortex*, pp.10.1016–j.cortex.2012.10.007.

Magalhães, R. et al., 2011. Are Stroke Occurrence and Outcome Related to Weather Parameters Results from a Population-Based Study in Northern Portugal. *Cerebrovascular Diseases*, 32(6), pp.542–551.

Makris, N. et al., 2009. Delineation of the middle longitudinal fascicle in humans: a quantitative, in vivo, DT-MRI study. *Cerebral Cortex*, 19(4), pp.777–785.

Makris, N. et al., 2005. Segmentation of subcomponents within the superior longitudinal fascicle in humans: a quantitative, in vivo, DT-MRI study. *Cerebral Cortex*, 15(6), pp.854–869.

Makuuchi, M. & Friederici, A.D., 2013. Hierarchical functional connectivity between the core language system and the working memory system. *Cortex*, 10.1016/j.cortex.2013.01.007.

Maldonado, I.L., Moritz-Gasser, S. & Duffau, H., 2011. Does the left superior longitudinal fascicle subserve language semantics? A brain electrostimulation

study. *Brain structure & function*, 216(3), pp.263–274.

Mandonnet, E. et al., 2007. Does the left inferior longitudinal fasciculus play a role in language? A brain stimulation study. *Brain : a journal of neurology*, 130(Pt 3), pp.623–629.

Mansfield, P. & Pykett, I.L., 1978. Biological and medical imaging by NMR. *Journal of Magnetic Resonance*, 29(2), pp.355–373.

Mant, J. et al., 2007. Warfarin versus aspirin for stroke prevention in an elderly community population with atrial fibrillation (the Birmingham Atrial Fibrillation Treatment of the Aged Study, BAFTA): a randomised controlled trial. *Lancet*, 370(9586), pp.493–503.

Manual, W.S.S.World Health Organization, 2006. The WHO STEPwise approach to stroke surveillance. *World Health Organization. Ge*.

Marchina, S. et al., 2011. Impairment of speech production predicted by lesion load of the left arcuate fasciculus. *Stroke; a journal of cerebral circulation*, 42(8), pp.2251–2256.

Marie, P., 1883. De l'aphasie, cecité verbale, surdité verbale, apasie motire, agraphie. *Revue Medicale*, 3, pp.693–703.

Marie, P., 1926. *Travaux et Memoires*, Paris: Masson et Cie.

Mariën, P. et al., 2004. Adult crossed aphasia in dextrals revisited. *Cortex*, 40(1), pp.41–74.

Marks, M.P. et al., 1999. Evaluation of early reperfusion and IV tPA therapy using diffusion- and perfusion-weighted MRI. *Neurology*, 52(9), pp.1792–1792.

Markus, H.S. et al., 2007. Differences in stroke subtypes between black and white patients with stroke: the South London Ethnicity and Stroke Study. *Circulation*, 116(19), pp.2157–2164.

Marshall, J., 2010. Classification of aphasia: Are there benefits for practice? *Aphasiology*, 24(3), pp.408–412.

Marslen-Wilson, W. & Tyler, L.K., 1980. The temporal structure of spoken language understanding. *Cognition*, 8(1), pp.1–71.

Mathers, C.D., Boerma, T. & Ma Fat, D., 2009. Global and regional causes of death. *British Medical Bulletin*, 92, pp.7–32.

Matsumoto, R. et al., 2004. Functional connectivity in the human language system: a cortico-cortical evoked potential study. *Brain : a journal of neurology*, 127(Pt 10), pp.2316–2330.

Matsumoto, R. et al., 2008. Hemispheric asymmetry of the arcuate fasciculus. *Journal of neurology*, 255(11), pp.1703–1711.

Matsumoto, R. et al., 2011. Left anterior temporal cortex actively engages in speech perception: A direct cortical stimulation study. *Neuropsychologia*, 49(5), pp.1350–1354.

Maxwell, S.E., 2000. Sample size and multiple regression analysis. *Psychological methods*, 5(4), pp.434–458.

McDermott, F.B., Horner, J. & DeLong, E.R., 1996. Evolution of acute aphasia as measured by the Western Aphasia Battery. *Clinical Aphasiology*, 24, pp.159–172.

Medina, L.S. et al., 2004. Functional MR imaging versus Wada test for evaluation of language lateralization: cost analysis. *Radiology*, 230(1), pp.49–54.

Mega, M.S. & Alexander, M.P., 1994. Subcortical aphasia: the core profile of capsulostriatal infarction. *Neurology*, 44(10), pp.1824–1829.

Mega, M.S. et al., 1997. The limbic system: an anatomic, phylogenetic, and clinical perspective. *The Journal of neuropsychiatry and clinical neurosciences*, 9(3), pp.315–330.

Meijer, F.J.A. et al., 2013. Update on diffusion MRI in Parkinson's disease and atypical parkinsonism. *Journal of the neurological sciences*, 332(1-2), pp.21–29.

Mesulam, M.-M., 1990. Large-scale neurocognitive networks and distributed processing for attention, language, and memory. *Annals of neurology*, 28(5), pp.597–613.

Mesulam, M.M., 1982. Slowly progressive aphasia without generalized dementia. *Annals of neurology*, 11(6), pp.592–598.

Mesulam, M.M. & Pandya, D.N., 1973. The projections of the medial geniculate complex within the sylvian fissure of the rhesus monkey. *Brain research*, 60(2), pp.315–333.

Metter, E.J. et al., 1990. Temporoparietal cortex in aphasia. Evidence from positron emission tomography. *Archives of neurology*, 47(11), pp.1235–1238.

Metzler-Baddeley, C., Hunt, S., et al., 2012a. Temporal association tracts and the breakdown of episodic memory in mild cognitive impairment. *Neurology*, 79(23), pp.2233–2240.

Metzler-Baddeley, C., O'Sullivan, M.J., et al., 2012b. How and how not to correct for CSF-contamination in diffusion MRI. *NeuroImage*, 59(2), pp.1394–1403.

Meyer, A., 1970. Karl Friedrich Burdach and his place in the history of neuroanatomy. *Journal of neurology, neurosurgery, and psychiatry*, 33(5), pp.553–561.

Meynert, T., 1885. *Psychiatry—Clinical Treatise on Diseases of the Fore-Brain based upon a study of its structure, functions, and nutrition (B. Sachs, Trans.)*, New York: Putnam.

Miceli, G. et al., 1981. Influence of age, sex, literacy and pathologic lesion on incidence, severity and type of aphasia. *Acta neurologica Scandinavica*, 64(5), pp.370–382.

Mohan, K.M. et al., 2009. Frequency and predictors for the risk of stroke recurrence up to 10 years after stroke: the South London Stroke Register. *Journal of*

neurology, neurosurgery, and psychiatry, 80(9), pp.1012–1018.

Mohr, J.P., 2004. *Stroke* 4 ed. J. P. Mohr et al., eds., Philadelphia, PA: Churchill Livingston.

Mohr, J.P. et al., 1978. Broca aphasia: pathologic and clinical. *Neurology*, 28(4), pp.311–324.

Mohr, J.P. et al., 1995. Magnetic resonance versus computed tomographic imaging in acute stroke. *Stroke; a journal of cerebral circulation*, 26(5), pp.807–812.

Monakow, von, C., 1905. *Gehirnpathologie: I. Allgemeine Einleitung. II. Lokalisation. III. Gehirnblutungen*, Wien: Hoelder.

Morel, A., Magnin, M. & Jeanmonod, D., 1997. Multiarchitectonic and stereotactic atlas of the human thalamus. *The Journal of comparative neurology*, 387(4), pp.588–630.

Mori, S. & van Zijl, P.C.M., 2002. Fiber tracking: principles and strategies - a technical review. *NMR in Biomedicine*, 15(7-8), pp.468–480.

Mori, S. et al., 1999. 3D reconstruction of axonal fibers from diffusion tensor imaging using fiber assignment by continuous tracking (FACT). In In 8th Annual Meeting of the ISMRM. Philadelphia, PA.

Morosan, P. et al., 2001. Human primary auditory cortex: cytoarchitectonic subdivisions and mapping into a spatial reference system. *NeuroImage*, 13(4), pp.684–701.

Moscovitch, M., 1976. On the representation of language in the right hemisphere of right-handed people. *Brain and language*, 3(1), pp.47–71.

Moscovitch, M., 1981. Right-hemisphere language. *Topics in Language Disorders*, 1(4), pp.41–61.

Moscovitch, M., 1983. The linguistic and emotional functions of the noraml right hemisphere. In E. Perceman, ed. *Cognitive Processing in the right hemipshere*. Academic Press.

Moseley, M.E. et al., 1990. Diffusion-weighted MR imaging of acute stroke: correlation with T2-weighted and magnetic susceptibility-enhanced MR imaging in cats. *AJNR. American journal of neuroradiology*, 11(3), pp.423–429.

Mukherjee, P., 2005. Diffusion Tensor Imaging and Fiber Tractography in Acute Stroke. *Neuroimaging clinics of North America*, 15(3), pp.655–665.

Murdoch, B.E., 1988. Computerized tomographic scanning: Its contributions to the understanding of the neuroanatomical basis of aphasia. *Aphasiology*, 2(5), pp.437–462.

Murray, L. & Coppens, P., 2011. Formal and informal assessment of aphasia. In I. Papathanasiou, P. Coppens, & C. Potagas, eds. *Aphasia and Related Neurogenic Communication Disorders*. Burlington, MA: Jones & Bardett Learning, LLC.

Müsseler, J. & Prinz, W., 2002. *Allgemeine Psychologie*, Heidelberg: Spektrum Akademischer Verlag.

Myint, P.K. et al., 2007. Winter excess in hospital admissions, in-patient mortality and length of acute hospital stay in stroke: a hospital database study over six seasonal years in Norfolk, UK. *Neuroepidemiology*, 28(2), pp.79–85.

Nadeau, S., 2008. Subcortical Language Mechanisms. In B. Stemmer & H. A. Whitaker, eds. *Handbook of the neuroscience of language*. London: Academic Press.

Nadeau, S.E. & Crosson, B., 1997. Subcortical Aphasia. *Brain and language*, 58(3), pp.355–402.

Naeser, M.A. et al., 1982. Aphasia with predominantly subcortical lesion sites: description of three capsular/putaminal aphasia syndromes. *Archives of neurology*, 39(1), pp.2–14.

Naidich, T.P. et al., 2001. Anatomic substrates of language: emphasizing speech. *Neuroimaging clinics of North America*, 11(2), pp.305–341.

Nicholas, M.L. et al., 1993. Evolution of severe aphasia in the first two years post onset. *Archives of physical medicine and rehabilitation*, 74(8), pp.830–836.

Nichols, T.E. & Holmes, A.P., 2002. Nonparametric permutation tests for functional neuroimaging: a primer with examples. *Human Brain Mapping*, 15(1), pp.1–25.

Nieuwenhuys, R. et al., 2008. *The human central nervous system*, Springer.

Nixon, P. et al., 2004. The inferior frontal gyrus and phonological processing: an investigation using rTMS. *Journal of cognitive neuroscience*, 16(2), pp.289–300.

Nogueira, R.G. et al., 2012. Trevo versus Merci retrievers for thrombectomy revascularisation of large vessel occlusions in acute ischaemic stroke (TREVO 2): a randomised trial. *Lancet*, 380(9849), pp.1231–1240.

Norman, B.D., 1988. The Effects of Aging on the Word Fluency Subtest of the Western Aphasia Battery. *Human Communication Canada*, 12(4), pp.39–42.

O'Sullivan, M. et al., 2005. Damage within a network of white matter regions underlies executive dysfunction in CADASIL. *Neurology*, 65(10), pp.1584–1590.

Obler, L.K. et al., 1978. Aphasia type and aging. *Brain and language*, 6(3), pp.318–322.

Ochfeld, E. et al., 2010. Ischemia in Broca Area Is Associated With Broca Aphasia More Reliably in Acute Than in Chronic Stroke. *Stroke; a journal of cerebral circulation*, 41, pp.325–330.

Ohyama, M. et al., 1996. Role of the Nondominant Hemisphere and Undamaged Area During Word Repetition in Poststroke Aphasics : A PET Activation Study. *Stroke; a journal of cerebral circulation*, 27(5), pp.897–903.

Oishi, K. et al., 2008. Human brain white matter atlas: identification and assignment of common anatomical structures in superficial white matter. *NeuroImage*,

43(3), pp.447–457.

Ojemann, G.A., 2003. The neurobiology of language and verbal memory: observations from awake neurosurgery. *International Journal of Psychophysiology*, 48(2), pp.141–146.

Olsen, T.S., BRUHN, P. & Oberg, R.G., 1986. Cortical hypoperfusion as a possible cause of 'subcortical aphasia'. *Brain : a journal of neurology*, 109 (Pt 3), pp.393–410.

Onufrowicz, W., 1887. Das balkenlose Mikrocephalengehirn Hofmann. *Archiv für Psychiatrie und Nervenkrankheiten*, 18(2), pp.305–328.

Osterhout, L., Holcomb, P.J. & Swinney, D.A., 1994. Brain potentials elicited by garden-path sentences: evidence of the application of verb information during parsing. *Journal of experimental psychology. Learning, memory, and cognition*, 20(4), pp.786–803.

Pagani, E. et al., 2007. Diffusion MR imaging in multiple sclerosis: technical aspects and challenges. *AJNR. American journal of neuroradiology*, 28(3), pp.411–420.

Pai, B.S. et al., 2007. Microsurgical anatomy of the posterior circulation. *Neurology India*, 55(1), pp.186–190.

Pajevic, S. & Pierpaoli, C., 1999. Color schemes to represent the orientation of anisotropic tissues from diffusion tensor data: application to white matter fiber tract mapping in the human brain. *Magnetic resonance in medicine : official journal of the Society of Magnetic Resonance in Medicine / Society of Magnetic Resonance in Medicine*, 42(3), pp.526–540.

Paolucci, S. et al., 1998. Functional outcome in stroke inpatient rehabilitation: predicting no, low and high response patients. *Cerebrovascular Diseases*, 8(4), pp.228–234.

Papagno, C., 2011. Naming and the role of the uncinate fasciculus in language function. *Current neurology and neuroscience reports*, 11(6), pp.553–559.

Papagno, C. et al., 2011. What is the role of the uncinate fasciculus? Surgical removal and proper name retrieval. *Brain : a journal of neurology*, 134, pp.405–414.

Papathanassiou, D. et al., 2000. A common language network for comprehension and production: a contribution to the definition of language epicenters with PET. *NeuroImage*, 11(4), pp.347–357.

Park, H.-J. et al., 2004. White matter hemisphere asymmetries in healthy subjects and in schizophrenia: a diffusion tensor MRI study. *NeuroImage*, 23(1), pp.213–223.

Parker, G.J.M. et al., 2005. Lateralization of ventral and dorsal auditory-language pathways in the human brain. *NeuroImage*, 24(3), pp.656–666.

Parsons, M.W. et al., 2002. Diffusion- and perfusion-weighted MRI response to thrombolysis in stroke. *Annals of neurology*, 51(1), pp.28–37.

Patel, B. & Markus, H.S., 2011. Magnetic resonance imaging in cerebral small vessel disease and its use as a surrogate disease marker. *International Journal of Stroke*, 6(1), pp.47–59.

Paulesu, E. et al., 1997. Functional heterogeneity of left inferior frontal cortex as revealed by fMRI. *NeuroReport*, 8(8), pp.2011–2016.

Paus, T. et al., 1999. Structural maturation of neural pathways in children and adolescents: in vivo study. *Science*, 283(5409), pp.1908–1911.

Pedelty, L. & Gorelick, P., 2007. Stroke risk factors: impact and management. In M. T. Torbey & M. H. Selim, eds. *The Stroke Book*. Cambridge: Cambridge University Press.

Pedersen, P.M. et al., 1995. Aphasia in acute stroke: Incidence, determinants, and recovery. *Annals of neurology*, 38(1), pp.129–130.

Pedersen, P.M., Vinter, K. & Olsen, T.S.O.J., 2004. Aphasia after Stroke: Type, Severity and Prognosis. *Cerebrovascular Diseases*, 17(1), pp.35–43.

Penfield, W. & Roberts, L., 1959. *Speech and Brain-Mechanisms*, Princton, New Jersey: Princton University Press.

Penhune, V.B. et al., 1996. Interhemispheric anatomical differences in human primary auditory cortex: probabilistic mapping and volume measurement from magnetic resonance scans. *Cerebral cortex (New York, N.Y. : 1991)*, 6(5), pp.661–672.

Penhune, V.B. et al., 2003. The morphometry of auditory cortex in the congenitally deaf measured using MRI. *NeuroImage*, 20(2), pp.1215–1225.

Petersen, S.E. et al., 1988. Positron emission tomographic studies of the cortical anatomy of single-word processing. *Nature*, 331(6157), pp.585–589.

Petitti, D.B. et al., 1996. Stroke in users of low-dose oral contraceptives. *New England Journal of Medicine*, 335(1), pp.8–15.

Pfefferbaum, A. & Sullivan, E.V., 2003. Increased brain white matter diffusivity in normal adult aging: Relationship to anisotropy and partial voluming. *Magnetic resonance in medicine : official journal of the Society of Magnetic Resonance in Medicine / Society of Magnetic Resonance in Medicine*, 49(5), pp.953–961.

Pfefferbaum, A. et al., 2000. Age-related decline in brain white matter anisotropy measured with spatially corrected echo-planar diffusion tensor imaging. *Magnetic resonance in medicine : official journal of the Society of Magnetic Resonance in Medicine / Society of Magnetic Resonance in Medicine*, 44(2), pp.259–268.

Pierpaoli, C. & Basser, P.J., 1996. Toward a quantitative assessment of diffusion anisotropy. *Magnetic resonance in medicine : official journal of the Society of Magnetic Resonance in Medicine / Society of Magnetic Resonance in Medicine*, 36(6), pp.893–906.

Pierpaoli, C. et al., 2003. Analyzing the contribution of cardiac pulsation to the variability of quantities derived from the diffusion tensor. *Proceedings of the*

11th Annual Meeting of ISMRM, Toronto, Canada, p.70.

Pierpaoli, C. et al., 1996. High temporal resolution diffusion MRI of global cerebral ischemia and reperfusion. *Journal of Cerebral Blood Flow & Metabolism*, 16(5), pp.892–905.

Plowman, E., Hentz, B. & Ellis, C., 2012. Post-stroke aphasia prognosis: a review of patient-related and stroke-related factors. *Journal of evaluation in clinical practice*, 18(3), pp.689–694.

Poeppel, D. & Hickok, G., 2004. Towards a new functional anatomy of language. *Cognition*, 92(1-2), pp.1–12.

Poncelet, B.P. et al., 1992. Brain parenchyma motion: measurement with cine echo-planar MR imaging. *Radiology*, 185(3), pp.645–651.

Powell, H.W.R. et al., 2006. Hemispheric asymmetries in language-related pathways: A combined functional MRI and tractography study. *NeuroImage*, 32(1), pp.388–399.

Price, C.J., 2012. A review and synthesis of the first 20years of PET and fMRI studies of heard speech, spoken language and reading. *NeuroImage*, 62(2), pp.816–847.

Price, C.J., 2010. The anatomy of language: a review of 100 fMRI studies published in 2009. *Annals of neurology*, 1191, pp.62–88.

Price, C.J., 2000. The anatomy of language: contributions from functional neuroimaging. *Journal of Anatomy*, 197(03), pp.335–359.

Price, C.J. et al., 1996. Hearing and saying. The functional neuro-anatomy of auditory word processing. *Brain : a journal of neurology*, 119 (Pt 3), pp.919–931.

Prodoehl, J. et al., 2013. Diffusion tensor imaging of Parkinson's disease, atypical parkinsonism, and essential tremor. *Movement Disorders*, doi: 10.1002/mds.25491.

Pujol, J. et al., 2006. Myelination of language-related areas in the developing brain. *Neurology*, 66(3), pp.339–343.

Purcell, E.M., Torrey, H.C. & Pound, R.V., 1946. Resonance absorption by nuclear magnetic moments in a solid. *Physical review*, 69(1-2), pp.37–38.

Raboyeau, G. et al., 2008. Right hemisphere activation in recovery from aphasia. *Neurology*, 70(4), pp.290–298.

Rademacher, J., Bürgel, U. & Zilles, K., 2002. Stereotaxic localization, intersubject variability, and interhemispheric differences of the human auditory thalamocortical system. *NeuroImage*, 17(1), pp.142–160.

Ramadan, N.M., Deveshwar, R. & Levine, S.R., 1989. Magnetic resonance and clinical cerebrovascular disease. An update. *Stroke; a journal of cerebral circulation*, 20(9), pp.1279–1283.

Rauschecker, J.P. et al., 1997. Serial and parallel processing in rhesus monkey auditory cortex. *The Journal of comparative neurology*, 382(1), pp.89–103.

Reil, J.C., 1809a. Das Balken-System oder die Hirnschenkel-Organisation im großen Gehirn. *Archiv für die Physiologie*, 9, pp.172–195.

Reil, J.C., 1809b. Die Sylvische Grube oder das Thal, das gestreifte große Hirnganglium, dessen Kapsel und die Seitentheile des großen Gehirns. *Archiv für die Physiologie*, 9, pp.195–208.

Reil, J.C., 1809c. Die sylvische Grube. *Archiv für Physiologie*, 9, pp.196–208.

Reil, J.C., 1812a. Die vördere Commissur im großen Gehirn. *Archiv für Physiologie*, 11, pp.89–100.

Reil, J.C., 1812b. Nachträge zur Anatomie des großen und kleinen Gehirns. *Archiv für Physiologie*, 12, pp.129–135.

Reil, J.C., 1809d. Untersuchungen über den Bau des grossen Gehirns im Menschen. *Archiv für Physiologie*, 9(1), pp.136–208.

Reil, J.C., 1808. Untersuchungen über den Bau des grossen Gehirns im Menshen 2. Fortsetzung. Über die Organisation der Lappen und Läppchen, oder der Stämme, Äste, Zweige und Blättchen des kleinen Gehirns, die auf dem Kern desselbben aufsitzen. *Archiv für die Physiologie*, 8, pp.385–426.

Riese, W. & Hoff, E.C., 1951. A history of the doctrine of cerebral localization. II. Methods and main results. *Journal of the history of medicine and allied sciences*, 6(4), pp.439–470.

Ringo, J.L. et al., 1994. Time is of the essence: a conjecture that hemispheric specialization arises from interhemispheric conduction delay. *Cerebral cortex (New York, N.Y. : 1991)*, 4(4), pp.331–343.

Roberts, D. et al., 1994. Quantitative magnetic resonance imaging of human brain perfusion at 1.5 T using steady-state inversion of arterial water. *Proceedings of the National Academy of Sciences of the United States of America*, 91(1), pp.33–37.

Roberts, P., Code, C. & McNeil, M., 2003. Describing participants in aphasia research: Part 1. Audit of current practice. *Aphasiology*, 17(10), pp.911–932.

Rodrigo, S. et al., 2007. Uncinate fasciculus fiber tracking in mesial temporal lobe epilepsy. Initial findings. *European radiology*, 17(7), pp.1663–1668.

Roehmholdt, M.E. et al., 1983. Transient ischemic attack and stroke in a community-based diabetic cohort. *Mayo Clinic proceedings. Mayo Clinic*, 58(1), pp.56–58.

Rorden, C. & Karnath, H.-O., 2004. Opinion: Using human brain lesions to infer function: a relic from a past era in the fMRI age? *Nature Reviews Neuroscience*, 5(10), pp.812–819.

Rorden, C., Bonilha, L. & Nichols, T.E., 2007a. Rank-order versus mean based statistics for neuroimaging. *NeuroImage*, 35(4), pp.1531–1537.

Rorden, C., Karnath, H.-O. & Bonilha, L., 2007b. Improving Lesion-Symptom Mapping. *Journal of cognitive neuroscience*, 19(7), pp.1081–1088.

Ross, E.D. & Mesulam, M.M., 1979. Dominant language functions of the right hemisphere? Prosody and emotional gesturing. *Archives of neurology*, 36(3), pp.144–148.

Ross, E.D., Edmondson, J.A. & Seibert, G.B., 1988. Acoustic analysis of affective prosody during right-sided wada test: A within-subject verification of the right hemisphere's role in language. *Brain and language*, 33, pp.128–145.

Rothwell, P.M. et al., 1996. Is stroke incidence related to season or temperature? *The Lancet*, 347(9006), pp.934–936.

Röntgen, W.C., 1898. *Über eine neue Art von Strahlen.* In: *Sitzungsberichte der Würzburger Physik.-Medic.-Gesellschaft*. In Würzburger Physik.-Medic.-Gesellschaft.

Rudrauf, D. et al., 2008. Rapid Interactions between the Ventral Visual Stream and Emotion-Related Structures Rely on a Two-Pathway Architecture. *The Journal of ….*

Rutten, G.J.M. et al., 2002. FMRI-determined language lateralization in patients with unilateral or mixed language dominance according to the Wada test. *NeuroImage*, 17(1), pp.447–460.

Ryalls, J., 2003. Where does the term "aphasia" come from? *Brain and language*, 21(2), pp.358–363.

Sacco, R.L. et al., 2001. High-density lipoprotein cholesterol and ischemic stroke in the elderly: the Northern Manhattan Stroke Study. *JAMA : the journal of the American Medical Association*, 285(21), pp.2729–2735.

Sacco, R.L. et al., 1999. The protective effect of moderate alcohol consumption on ischemic stroke. *JAMA : the journal of the American Medical Association*, 281(1), pp.53–60.

Saka, O., McGuire, A. & Wolfe, C., 2009. Cost of stroke in the United Kingdom. *Age and ageing*, 38(1), pp.27–32.

Sakai, K.L., 2005. Language acquisition and brain development. *Science*, 310(5749), pp.815–819.

Salis, C. & Edwards, S., 2004. Adaptation theory and non-fluent aphasia in English. *Aphasiology*, 18(12), pp.1103–1120.

Salter, K. et al., 2006. Identification of aphasia post stroke: a review of screening assessment tools. *Brain injury : [BI]*, 20(6), pp.559–568.

Sarubbo, S. et al., 2012. Complete recovery after surgical resection of left Wernicke's area in awake patient: a brain stimulation and functional MRI study. *Neurosurgical review*, 35(2), pp.287–292.

Saur, D. et al., 2010. Combining functional and anatomical connectivity reveals brain networks for auditory language comprehension. *NeuroImage*, 49(4),

pp.3187–3197.

Saur, D. et al., 2006. Dynamics of language reorganization after stroke. *Brain : a journal of neurology*, 129(Pt 6), pp.1371–1384.

Saur, D. et al., 2008. Ventral and dorsal pathways for language. *PNAS*, 105(46), pp.18035–18040.

Saver, J.L. et al., 2013. Time to Treatment With Intravenous Tissue Plasminogen Activator and Outcome From Acute Ischemic StrokeTime to Treatment With IV tPA and Ischemic Stroke. *JAMA : the journal of the American Medical Association*, 309(23), pp.2480–2488.

Scharf, J.H., 1960. Johann Christian Reil als Anatom. In H. Eulner, ed. *Nova Acta Leopoldina*. Halle: Abhandlungen der Deutschen Akademie der Naturforscher

Leopoldina, pp. 51–97.

Schäffler, L. et al., 1993. Comprehension deficits elicited by electrical stimulation of Broca's area. *Brain : a journal of neurology*, 116 (Pt 3), pp.695–715.

Schellinger, P.D. et al., 2010. Evidence-based guideline: The role of diffusion and perfusion MRI for the diagnosis of acute ischemic stroke: Report of the Therapeutics and Technology Assessment Subcommittee of the American Academy of Neurology. *Neurology*, 75(2), pp.177–185.

Schiller, F., 1970. Concepts of stroke before and after Virchow. *Medical history*, 14(2), pp.115–131.

Schmahmann, J.D. & Pandya, D.N., 2006. *Fiber Pathways of the Brain*, Oxford: Oxford University Press, USA.

Schmithorst, V.J. & Holland, S.K., 2007. Sex differences in the development of neuroanatomical functional connectivity underlying intelligence found using Bayesian connectivity analysis. *NeuroImage*, 35(1), pp.406–419.

Schmülling, S. et al., 2008. Notwendigkeit eines Trainings für den Gebrauch der NIH Stroke Scale. *Aktuelle Neurologie*, 26(01), pp.31–34.

Schneider, P. et al., 2005. Structural and functional asymmetry of lateral Heschl's gyrus reflects pitch perception preference. *Nature neuroscience*, 8(9), pp.1241–1247.

Schofield, T.M., 2013. On my way to being a scientist. *Nature*, 497(7448), pp.277–278.

Seashore, R.H. & Eckerson, L.D., 1940. The measurement of individual differences in general English vocabularies. *Journal of Educational Psychology*, 31(1), pp.14–38.

Seghier, M.L., 2008. Laterality index in functional MRI: methodological issues. *Magnetic Resonance Imaging*, 26(5), pp.594–601.

Seghier, M.L., 2012. The Angular Gyrus: Multiple Functions and Multiple Subdivisions. *The Neuroscientist : a review journal bringing neurobiology,*

neurology and psychiatry, 19(1), pp.43–61.

Seghier, M.L. et al., 2008. Lesion identification using unified segmentation-normalisation models and fuzzy clustering. *NeuroImage*, 41(4), pp.1253–1266.

Seitz, R.J. et al., 1999. The role of diaschisis in stroke recovery. *Stroke; a journal of cerebral circulation*, 30(9), pp.1844–1850.

Selnes, O.A., 2001. Recovery from aphasia: activating the "right" hemisphere. *Annals of neurology*, 45(4), pp.419–420.

Selya, A.S. et al., 2012. A Practical Guide to Calculating Cohen's f(2), a Measure of Local Effect Size, from PROC MIXED. *Frontiers in psychology*, 3, pp.10.3389–fpsyg.2012.00111.

Seung, S., 2012. *Connectome: How the Brain's Wiring Makes Us Who We Are* None, Houghton Mifflin Harcourt Trade.

Sexton, C.E., Mackay, C.E. & Ebmeier, K.P., 2009. A Systematic Review of Diffusion Tensor Imaging Studies in Affective Disorders. *Biological psychiatry*, 66(9), pp.814–823.

Shalom, D.B. & Poeppel, D., 2008. Functional anatomic models of language: assembling the pieces. *The Neuroscientist : a review journal bringing neurobiology, neurology and psychiatry*, 14(1), pp.119–127.

Shapiro, B.E. & Danly, M., 1985. The role of the right hemisphere in the control of speech prosody in propositional and affective contexts. *Brain and language*, 25(1), pp.19–36.

Shenton, M.E. et al., 2012. A review of magnetic resonance imaging and diffusion tensor imaging findings in mild traumatic brain injury. *Brain Imaging and Behavior*, 6(2), pp.137–192.

Shinton, R. & Beevers, G., 1989. Meta-analysis of relation between cigarette smoking and stroke. *BMJ*, 298(6676), pp.789–794.

Sidtis, J.J. et al., 1981. Variability in right hemisphere language function after callosal section: evidence for a continuum of generative capacity. *The Journal of neuroscience : the official journal of the Society for Neuroscience*, 1(3), pp.323–331.

Siesjö, B.K., 2008. Pathophysiology and treatment of focal cerebral ischemia. Part I: Pathophysiology. (1992). *Journal of neurosurgery*, 108(3), pp.616–631.

Signoret, J.-L. et al., 1984. Rediscovery of Leborgne's brain: Anatomical description with CT scan. *Brain and language*, 22(2), pp.303–319.

Simon, G., 1991. Prevention of stroke in older persons with isolated systolic hypertension. *JAMA : the journal of the American Medical Association*, 266(20), pp.2829–2830.

Small, S.L. et al., 2002. Cerebellar hemispheric activation ipsilateral to the paretic hand correlates with functional recovery after stroke. *Brain : a journal of neurology*, 125(Pt 7), pp.1544–1557.

Smith, C., 2007a. Brain and mind in the "long" eighteenth century. In H. A. Whitaker, C. U. M. Smith, & S. Finger, eds. *Brain, mind and medicine: Essays in eighteenth-century neuroscience*. New York: Springer US, pp. 15–28.

Smith, S.M. et al., 2007. Acquisition and voxelwise analysis of multi-subject diffusion data with tract-based spatial statistics. *Nature protocols*, 2(3), pp.499–503.

Smith, S.M. et al., 2004. Advances in functional and structural MR image analysis and implementation as FSL. *NeuroImage*, 23 Suppl 1, pp.S208–19.

Smith, S.M. et al., 2009. Correspondence of the brain's functional architecture during activation and rest. *Proceedings of the National Academy of Sciences of the United States of America*, 106(31), pp.13040–13045.

Smith, S.M. et al., 2006. Tract-based spatial statistics: Voxelwise analysis of multi-subject diffusion data. *Brain and language*, 31(4), pp.1487–1505.

Smith, W.S., 2007b. Intra-arterial thrombolytic therapy for acute basilar occlusion: pro. *Stroke; a journal of cerebral circulation*, 38(2 Suppl), pp.701–703.

Sondhaus, E. & Finger, S., 1988. Aphasia and the CNS from Imhotep to Broca. *Neuropsychology*, 2(2), pp.87–110.

Sotak, C.H., 2002. The role of diffusion tensor imaging in the evaluation of ischemic brain injury - a review. *NMR in Biomedicine*, 15(7-8), pp.561–569.

Spreen, O. & Risser, A.H., 2003. *Assessment of Aphasia*, Oxford: Oxford Univeristy Press.

Spreen, O. & Strauss, E., 1998. *A Compendium of Neuropsychological Tests: Administration, Norms, and Commentary*, New York: Oxford Univeristy Press.

Srinivasan, A. et al., 2006. State-of-the-Art Imaging of Acute Stroke. *Radiographics : a review publication of the Radiological Society of North America, Inc*, 26(Supplement 1), pp.S75–S95.

Steele, J., 2002. The Speciation of Modern Homo sapiens. In Proceedings of the British Academy.

Stefani, M.A. et al., 2000. Anatomic variations of anterior cerebral artery cortical branches. *Clinical anatomy (New York, N.Y.)*, 13(4), pp.231–236.

Steffens, H., 1815. *Johann Christian Reil: eine Denkschrift*, Halle: In der Gurtschen Buchhandlung.

Stehling, M.K., Turner, R. & Mansfield, P., 1991. Echo-planar imaging: magnetic resonance imaging in a fraction of a second. *Science*, 254(5028), pp.43–50.

Steinhauer, K. & Friederici, A.D., 2001. Prosodic boundaries, comma rules, and brain responses: the closure positive shift in ERPs as a universal marker for prosodic phrasing in listeners and readers. *Journal of Psycholinguistic Research*, 30(3), pp.267–295.

Steinmetz, H. & Seitz, R.J., 1991. Functional anatomy of language processing:

Neuroimaging and the problem of individual variability. *Neuropsychologia*, 29(12), pp.1149–1161.

Stemmer, B. & Whitaker, H.A., 2008. *Handbook of the Neuroscience of Language*, London: Academic Press.

Steno, N., 1669. Discours de Monsieur Stenon, sur l'anatomie du cerveau. *Ninville*.

Stewart, J.A. et al., 1999. Ethnic differences in incidence of stroke: prospective study with stroke register. *BMJ*, 318(7189), pp.967–971.

Stirling, W., 1902. *Some Apostles of Physiology*, London: Waterlow.

Sturm, J.W. et al., 2004. Determinants of handicap after stroke: the North East Melbourne Stroke Incidence Study (NEMESIS). *Stroke; a journal of cerebral circulation*, 35(3), pp.715–720.

Suk, S.-H. et al., 2003. Abdominal obesity and risk of ischemic stroke: the Northern Manhattan Stroke Study. *Stroke; a journal of cerebral circulation*, 34(7), pp.1586–1592.

Swindell, C.S., Holland, A.L. & Fromm, D., 1984. Classification of aphasia: WAB type versus clinical impression. In Clinical Aphasiology Conference: Clinical Aphasiology Conference (1984 : 14th : Seabrook Island, SC : May 20-24, 1984). In Clinical Aphasiology Conference. pp. 48–54.

Szaflarski, J.P. et al., 2006. fMRI study of language lateralization in children and adults. *Human Brain Mapping*, 27(3), pp.202–212.

Sztriha, L.K. et al., 2011. Safety and clinical outcome of thrombolysis in ischaemic stroke using a perfusion CT mismatch between 3 and 6 hours. *PloS one*, 6(10), p.e25796.

Talairach, J., 1988. *Talairach: Co-planar stereotaxic atlas of the human*, Stuttgart: Thieme.

Temkin, O., 1947. Gall and the phrenological movement. *Bulletin of the history of medicine*, 21(3), pp.275–321.

Tesak, J. & Code, C., 2008. *Milestones in the History of Aphasia: Theories and Protagonists* C. Code, ed., Hove: Psychology Press.

Thiebaut de Schotten, M. & Bartolomeo, P., 2011. New insights into neurocognition provided by brain mapping: visuospatial cognition. In H. Duffau, ed. *Brain Mapping: From Neural Basis of Cognition to Surgical Applications*. Vienna: Springer.

Thiebaut de Schotten, M. et al., 2008. Visualization of disconnection syndromes in humans. *Cortex*, 44(8), pp.1097–1103.

Thiebaut de Schotten, M., Cohen, L., et al., 2012a. Learning to Read Improves the Structure of the Arcuate Fasciculus. *Cerebral Cortex*, 10.1093/cercor/bhs383.

Thiebaut de Schotten, M., Dell'Acqua, F., et al., 2011a. A lateralized brain network for visuospatial attention. *Nature neuroscience*, 14(10), pp.1245–1246.

Thiebaut de Schotten, M., Dell'Acqua, F., et al., 2012b. Monkey to human comparative anatomy of the frontal lobe association tracts. *Cortex*, 48(1), pp.82–96.

Thiebaut de Schotten, M., ffytche, D.H., et al., 2011b. Atlasing location, asymmetry and inter-subject variability of white matter tracts in the human brain with MR diffusion tractography. *NeuroImage*, 54(1), pp.49–59.

Thiebaut de Schotten, M., Tomaiuolo, F., et al., 2012c. Damage to White Matter Pathways in Subacute and Chronic Spatial Neglect: A Group Study and 2 Single-Case Studies with Complete Virtual "In Vivo" Tractography Dissection. *Cerebral Cortex*, pp.10.1093–cercor–bhs351.

Thomalla, G., 2005. Time course of wallerian degeneration after ischaemic stroke revealed by diffusion tensor imaging. *Journal of neurology, neurosurgery, and psychiatry*, 76(2), pp.266–268.

Thompson-Schill, S.L., 2005. Dissecting the language organ: A new look at the role of Broca's area in language processing. In A. Cutler, ed. *Twenty-first Century Psycholinguistics: Four Cornerstones*. Hillsdale, NJ, : Lawrence Erlbaum Associates.

Toga, A.W., John C Mazziotta, M.D.P.D. & Frackowiak, R.S.J., 2000. *Brain Mapping: The Methods* 2nd ed, London: Academic Press.

Tomandl, B.F. et al., 2003. Comprehensive imaging of ischemic stroke with multisection CT. *Radiographics : a review publication of the Radiological Society of North America, Inc*, 23(3), pp.565–592.

Tong, D.C. et al., 1998. Correlation of perfusion- and diffusion-weighted MRI with NIHSS score in acute (<6.5 hour) ischemic stroke. *Neurology*, 50(4), pp.864–869.

Torbey, M.T. & Selim, M.H., 2007. *The Stroke Book*, New York, NY: Cambridge University Press.

Travers, B.G. et al., 2012. Diffusion Tensor Imaging in Autism Spectrum Disorder: A Review. *Autism Research*, 5(5), pp.289–313.

Triarhou, L.C., 2007. The Economo-Koskinas atlas revisited: cytoarchitectonics and functional context. *Stereotactic and functional neurosurgery*, 85(5), pp.195–203.

Troyer, A.K., 2000. Normative Data for Clustering and Switching on Verbal Fluency Tasks. *Journal of Clinical and Experimental Neuropsychology*, 22(3), pp.370–378.

Turgeon, Y. & Macoir, J., 2008. Classical and contemporary assessment of aphasia and acquired disorders of language. In B. Stemmer & H. A. Whitaker, eds. *Handbook of the neuroscience of language*. London: Academic Press.

Turin, T.C. et al., 2008. Higher stroke incidence in the spring season regardless of conventional risk factors: Takashima Stroke Registry, Japan, 1988-2001. *Stroke; a journal of cerebral circulation*, 39(3), pp.745–752.

Turken, A.U. & Dronkers, N.F., 2011. The neural architecture of the language

comprehension network: converging evidence from lesion and connectivity analyses. *Frontiers in systems neuroscience*, 5, pp.10.3389–fnsys.2011.00001.

Turner, R. et al., 1990. Echo-planar imaging of intravoxel incoherent motion. *Radiology*, 177(2), pp.407–414.

Türe, U. et al., 1999. Topographic anatomy of the insular region. *Journal of neurosurgery*, 90(4), pp.720–733.

Vallar, G. et al., 1988. Recovery from aphasia and neglect after subcortical stroke: neuropsychological and cerebral perfusion study. *Journal of neurology, neurosurgery, and psychiatry*, 51(10), pp.1269–1276.

van Ewijk, H. et al., 2012. Diffusion tensor imaging in attention deficit/hyperactivity disorder: A systematic review and meta-analysis. *Neuroscience & Biobehavioral Reviews*, 36(4), pp.1093–1106.

van Rossum, C.T. et al., 2001. Seasonal variation in cause-specific mortality: are there high-risk groups? 25-year follow-up of civil servants from the first Whitehall study. *International journal of epidemiology*, 30(5), pp.1109–1116.

Vernooij, M.W. et al., 2007. Fiber density asymmetry of the arcuate fasciculus in relation to functional hemispheric language lateralization in both right- and left-handed healthy subjects: A combined fMRI and DTI study. *NeuroImage*, 35(3), pp.1064–1076.

Versnick, E.J. et al., 2005. Mechanical thrombectomy for acute stroke. *AJNR. American journal of neuroradiology*, 26(4), pp.875–879.

Vigneau, M. et al., 2006. Meta-analyzing left hemisphere language areas: phonology, semantics, and sentence processing. *NeuroImage*, 30(4), pp.1414–1432.

Wada, J., 1949. A new method for the determination of the side of cerebral speech dominance. A preliminary report on the intracarotid injection of sodium Amytal in man (published in Japanese). *Iguku to Seibutsugaku (Medicine and Biology)*, 14, pp.221–222.

Wada, J. & Rasmussen, T., 1960. Intracarotid injection of sodium amytal for the lateralization of cerebral speech dominance. 1960. *Journal of neurosurgery*, 17(2), pp.266–282.

Wada, J.A., Clarke, R. & Hamm, A., 1975. Cerebral Hemispheric Asymmetry in Humans: Cortical Speech Zones in 100 Adult and 100 Infant Brains. *Archives of neurology*, 32(4), pp.239–246.

Wade, D.T. et al., 1986. Aphasia after stroke: natural history and associated deficits. *Journal of neurology, neurosurgery, and psychiatry*, 49(1), pp.11–16.

Wahl, M. et al., 2008. The human thalamus processes syntactic and semantic language violations. *Neuron*, 59(5), pp.695–707.

Wakana, S. et al., 2004. Fiber Tract–based Atlas of Human White Matter Anatomy. *Radiology*, 230(1), pp.77–87.

Warach, S. et al., 1995. Acute human stroke studied by whole brain echo planar diffusion-weighted magnetic resonance imaging. *Annals of neurology*, 37(2), pp.231–241.

Warach, S. et al., 1992. Fast magnetic resonance diffusion-weighted imaging of acute human stroke. *Neurology*, 42(9), pp.1717–1723.

Warach, S. et al., 1996. Time Course of Diffusion Imaging Abnormalities in Human Stroke. *Stroke; a journal of cerebral circulation*, 27(7), pp.1254–1255.

Warach, S., Boska, M.D. & Welch, K.M., 1997. Pitfalls and potential of clinical diffusion-weighted MR imaging in acute stroke. *Stroke; a journal of cerebral circulation*, 28(3), pp.481–481.

Wehmeyer, M. & Groetzbach, H., 2010. *Aphasie. Wege aus dem Sprachdschungel* 4 ed. M. M. Thiel & C. Ewerbeck, eds., Berlin: Springer.

Weigl, E. & Bierwisch, M., 1970. Neuropsychology and Linguistics: Topics of common research. *Foundations of language*, 6, pp.1–18.

Weintraub, S., Mesulam, M.M. & Kramer, L., 1981. Disturbances in prosody. A right-hemisphere contribution to language. *Archives of neurology*, 38(12), pp.742–744.

Weisenburg, T.H. & McBride, K.E., 1935. *Aphasia, a clinical and psychological study*, New York: Commonwealth Fund.

Welch, K.M.A. et al., 1995. A Model to Predict the Histopathology of Human Stroke Using Diffusion and T2-Weighted Magnetic Resonance Imaging. *Stroke; a journal of cerebral circulation*, 26, pp.1983–1989.

Wernicke, C., 1874. *Der Aphasische Symptomencomplex: Ein psychologische Studie auf anatomischer Basis*, Breslau: Cohn & Weigert.

Wernicke, C., 1906. *Grundrisse der Psychiatrie*, Leipzig: Thieme.

Wheeler-Kingshott, C.A.M. & Cercignani, M., 2009. About "axial" and 'radial' diffusivities. *Magnetic resonance in medicine : official journal of the Society of Magnetic Resonance in Medicine / Society of Magnetic Resonance in Medicine*, 61(5), pp.1255–1260.

Williamson, P.C. & Allman, J.M., 2012. A framework for interpreting functional networks in schizophrenia. *Frontiers in human neuroscience*, 6, pp.10.3389–fnhum.2012.00184.

Wise, R. et al., 1991. Distribution of cortical neural networks involved in word comprehension and word retrieval. *Brain : a journal of neurology*, 114 (Pt 4), pp.1803–1817.

Wise, R.J. et al., 2001. Separate neural subsystems within 'Wernicke's area'. *Brain : a journal of neurology*, 124(Pt 1), pp.83–95.

Wolf, P.A., Abbott, R.D. & Kannel, W.B., 1991. Atrial fibrillation as an independent risk factor for stroke: the Framingham Study. *Stroke; a journal of cerebral circulation*, 22(8), pp.983–988.

Wolfe, C., 2000. The impact of stroke. *British Medical Bulletin*, 56(2), pp.275–286.

Wolfe, C.D.A., 2002. Incidence and case fatality rates of stroke subtypes in a multiethnic population: the South London Stroke Register. *Journal of neurology, neurosurgery, and psychiatry*, 72(2), pp.211–216.

Wolfgang, R. & Michael, N., 2008. [Franz Joseph Gall and his "talking skulls" established the basis of modern brain sciences]. *Wiener medizinische Wochenschrift (1946)*, 158(11-12), pp.314–319.

Wong, E.C., Buxton, R.B. & Frank, L.R., 1999. Quantitative perfusion imaging using arterial spin labeling. *Neuroimaging clinics of North America*, 9(2), pp.333–342.

Wu, O. et al., 2011. Diffusion in Acute Stroke. In D. K. Jones, ed. *Diffusion MRI*. Oxford: Oxford University Press.

Wundt, W., 1904. *Principles of physiological psychology (E.B. Titchener, Trans: translated from the fifth German edition (1902)*, London: Swan Sonnenschein.

Yamada, K. et al., 2007. MR tractography depicting damage to the arcuate fasciculus in a patient with conduction aphasia. *Neurology*, 68(10), p.789.

Yamada, K. et al., 2009. MR tractography: a review of its clinical applications. *Magnetic resonance in medical sciences : MRMS : an official journal of Japan Society of Magnetic Resonance in Medicine*, 8(4), pp.165–174.

Yeatman, J.D. et al., 2011. Anatomical Properties of the Arcuate Fasciculus Predict Phonological and Reading Skills in Children. *Journal of cognitive neuroscience*, 23(11), pp.3304–3317.

Yeatman, J.D., Rauschecker, A.M. & Wandell, B.A., 2013. Anatomy of the visual word form area: adjacent cortical circuits and long-range white matter connections. *Brain and language*, 125(2), pp.146–155.

Yetkin, F.Z. et al., 1998. Functional MR of frontal lobe activation: comparison with Wada language results. *AJNR. American journal of neuroradiology*, 19(6), pp.1095–1098.

Yoo, S.-S. et al., 2005. Functional asymmetry in human primary auditory cortex: identified from longitudinal fMRI study. *Neuroscience letters*, 383(1-2), pp.1–6.

York, G.K., 2009. Localization of language function in the twentieth century. *Journal of the History of the Neurosciences*, 18(3), pp.283–290.

Yoshida, S. et al., 2013. Diffusion tensor imaging of normal brain development. *Pediatric Radiology*, 43(1), pp.15–27.

Zatorre, R.J. et al., 1996. PET studies of phonetic processing of speech: review, replication, and reanalysis. *Cerebral cortex (New York, N.Y. : 1991)*, 6(1), pp.21–30.

Zatorre, R.J., Belin, P. & Penhune, V.B., 2002a. Structure and function of auditory cortex: music and speech. *Trends in Cognitive Sciences*, 6(1), pp.37–46.

Zatorre, R.J., Bouffard, M., et al., 2002b. Where is" where"in the human auditory

cortex? *Nature neuroscience*, 5(9), pp.905–909.

Zilles, K. et al., 2002. Architectonics of the human cerebral cortex and transmitter receptor fingerprints: reconciling functional neuroanatomy and neurochemistry. *European neuropsychopharmacology : the journal of the European College of Neuropsychopharmacology*, 12(6), pp.587–599.

Zola-Morgan, S., 1995. Localization of Brain Function: The Legacy of Franz Joseph Gall (1758-1828). *Annual Review of Neuroscience*, 18(1), pp.359–383.

APPENDIX A. CARDIAC GATING PROTOCOL

Cardiac gating scanner settings for DTIstroke

Scan A: 8.30 min, 4B0, 29DWI, 93.5
Scan B: 8.45 min, 3B0, 31DWI, 93.5

heart rate	scanner value	max slices	scan time (min)
40	9	63	7.39
41	9	63	7.28
42	10	60	8.06
43	10	60	7.54
44	10	60	7.44
45	10	60	7.30
46	10	60	7.24
47	10	60	7.14
48	10	60	7.05
49	12	60	8.20
50	12	60	8.10
51	12	60	8.00
52	12	60	7.51
53	12	60	7.42
54	12	60	7.33
55	12	60	7.25
56	12	60	7.17
57	12	60	7.10
58	12	60	7.02
59	15	60	8.39
60	15	60	8.30
61	15	60	8.32
62	15	60	8.14
63	15	60	8.03
64	15	60	7.58
65	15	60	7.51
66	15	60	7.44
67	15	60	7.37
68	15	60	7.30
69	15	60	7.24
70	15	60	7.17
71	15	60	7.17
72	15	60	7.05
73	15	60	9.19
74	20	60	9.11
75	20	60	9.04
76	20	60	8.57
77	20	60	8.50
78	20	60	8.43
79	20	60	8.37
80	20	60	8.30
81	20	60	8.24
82	20	60	8.18
83	20	60	8.12
84	20	60	8.06
85	20	60	8.00
86	20	60	7.54
87	20	60	7.49
88	20	60	7.44
89	20	60	7.30
90	20	60	7.38

APPENDIX B. NATIONAL HEALTH INSTITUTE STROKE SCALE (NIHSS)

Occupational Therapy/Physiotherapy/Speech and Language Therapy Hyper Acute Stroke Screening Proforma

Triager & profession	OT/PT/SLT	Date of Screening	
Patient Name		Local Area	
Hosp Number		Language	
HPC/ MEDICAL HISTORY	Time of stroke onset _____ Thrombolysed Y/N Time _____ Date of admission to KCH _____		

King's Adapted NIH Stroke Scale		Trigger cross-referral
Level of Consciousness	0 = **Alert**; keenly responsive. 1 = **Not alert**; but arousable by minor stimulation to obey, answer, or respond. 2 = **Not alert**; requires repeated stimulation to attend, or is obtunded and requires strong or painful stimulation to make movements (not stereotyped). 3 = Responds only with reflex motor or autonomic effects or totally unresponsive, flaccid, and areflexic.	≥1 OT, PT & SLT
LOC question	0 = **Answers** both questions correctly. 1 = **Answers** one question correctly. 2 = **Answers** neither question correctly	≥ 1 OT & SLT
LOC command	0 = Performs both tasks correctly. 1 = Performs one task correctly. 2 = Performs neither task correctly	≥ 1 OT & SLT
Best Gaze	0 = **Normal**. 1 = **Partial gaze palsy**; gaze is abnormal in one or both eyes, but forced deviation or total gaze paresis is not present. 2 = **Forced deviation**, or total gaze paresis	≥ 1 OT
Visual	0 = **No visual loss**. 1 = **Partial hemianopia**. 2 = **Complete hemianopia**. 3 = **Bilateral hemianopia** (blind including cortical blindness).	≥ 1 OT
Facial	0 = **Normal** symmetrical movements. 1 = **Minor paralysis** (flattened nasolabial fold, asymmetry on smiling). 2 = **Partial paralysis** (total or near-total paralysis of lower face). 3 = **Complete paralysis** of one or both sides (absence of facial movement in the upper and lower face).	≥ 1 SLT ≥ 2 PT & SLT
Arm	0 = **No drift**; limb holds 90 (or 45) degrees for full 10 seconds. 1 = **Drift**; limb holds 90 (or 45) degrees, but drifts down before full 10 seconds; does not hit bed or other support. 2 = **Some effort against gravity**; limb cannot get to or maintain (if cued) 90 (or 45) degrees, drifts down to bed, but has some effort against gravity. 3 = **No effort against gravity**; limb falls. 4 = **No movement**. UN = **Amputation** or joint fusion, explain: _____ **5a. Left Arm** **5b. Right Arm**	≥ 1 OT & PT
Leg	0 = **No drift**; leg holds 30-degree position for full 5 seconds. 1 = **Drift**; leg falls by the end of the 5-second period but does not hit bed. 2 = **Some effort against gravity**; leg falls to bed by 5 seconds, but has some effort against gravity. 3 = **No effort against gravity**; leg falls to bed immediately. 4 = **No movement**. UN = **Amputation** or joint fusion, explain: _____ **6a. Left Leg** **6b. Right Leg**	≥ 1 OT & PT
Ataxia	0 = **Absent**. 1 = **Present in one limb**. 2 = **Present in two limbs**. UN = **Amputation** or joint fusion, explain: _____	≥ 1 OT & PT
Sensory	0 = **Normal**; no sensory loss. 1 = **Mild-to-moderate sensory loss**; patient feels pinprick is less sharp or is dull on the affected side; or there is a loss of superficial pain with pinprick, but patient is aware of being touched. 2 = **Severe to total sensory loss**; patient is not aware of being touched in the face, arm, and leg.	≥ 1 OT & PT

Aphasia	0 = **No aphasia**; normal. 1 = **Mild-to-moderate aphasia**; some obvious loss of fluency or facility of comprehension, without significant limitation on ideas expressed or form of expression. Reduction of speech and/or comprehension, however, makes conversation about provided materials difficult or impossible. For example, in conversation about provided materials, examiner can identify picture or naming card content from patient's response. 2 = **Severe aphasia**; all communication is through fragmentary expression; great need for inference, questioning, and guessing by the listener. Range of information that can be exchanged is limited; listener carries burden of communication. Examiner cannot identify materials provided from patient response. 3 = **Mute, global aphasia**; no usable speech or auditory comprehension.	≥ 1 SLT
Dysarthria	0 = **Normal**. 1 = **Mild-to-moderate dysarthria**; patient slurs at least some words and, at worst, can be understood with some difficulty. 2 = **Severe dysarthria**; patient's speech is so slurred as to be unintelligible in the absence of or out of proportion to any dysphasia, or is mute/anarthric. UN = **Intubated** or other physical barrier, explain: _____	≥ 1 SLT
Extinction and Inattention (formerly Neglect)	0 = **No abnormality**. 1 = **Visual, tactile, auditory, spatial, or personal inattention** or extinction to bilateral simultaneous stimulation in one of the sensory modalities. 2 = **Profound hemi-inattention or extinction to more than one modality**; does not recognize	≥ 1 OT and PT
Respiratory	SaO2 < 95%, on more than 2 litres oxygen, pyrexia, Coughing or staff report problems clearing secretion, history of aspiration.	**Liaise with physio urgently**
Swallow	Has the patient had a swallow screen? Y ☐ N ☐ (nursing need to screen) What was the result of the screen? Pass ☐ / Fail ☐ (if fail, refer to SLT) Are they eating and drinking a normal diet? Y☐ /N ☐ (if no, state what they are having and the reason and refer to SLT)	
Cognition and Mood	Does the patient appear easily distracted? Y☐ N☐ Is the patient orientated to time, place and person? Y☐ N☐ Does the patient appear to have difficulty recalling information? Y☐ N☐ Is there a delay in the patient's response to questions/tasks? Y☐ N☐ Does the patient's mood appear consistent with what has happened? Y☐ N☐ Does the patient have any concerns or anxieties re returning home? Y☐ N☐ If yes to any of the above, please refer to OT	
SH	Lives alone ☐ with partner ☐with children ☐with friend ☐ other ☐ In a house ☐ flat ☐ maisonette ☐ bungalow ☐ Stairs internal ☐ external ☐ Working ☐ Retired ☐ Unemployed ☐ Other ☐ Other:	
Function Observed	Sat on edge of bed Independently ☐ Assistance 1 ☐ Assistance 2 ☐ Stood Independently ☐ Assistance 1 ☐ Assistance 2 ☐ Walked Independently ☐ Assistance 1 ☐ Assistance 2 ☐ Picked up drink/glasses Independently ☐ Assistance 1 ☐ Assistance 2 ☐ Liaise with OT & PT if need for assistance noted	
Other/Comments		
Decision	TIA no impairments ☐ ⟶ Impairments noted ☐ ⟶	No therapy input required **Document on EPR** Liaise and refer to appropriate disciplines To be repatriated ☐ Non local but aim home from KCH ☐ Local aim home from KCH ☐ Local further ax needed re: d/c plans ☐ Requires OT ☐ PT ☐ SLT ☐ **Document decision on EPR and liaise**

King's Therapy Services/March 2010

APPENDIX C. WESTERN APHASIA BATTERY REVISED (WAB-R)

	Year	Month	Day
Date of Test	2006	9	22
Date of Birth	1936	2	11
Chronological Age	70	7	11

Record Form Part 1

Western Aphasia Battery™ REVISED

Name: _Bob Duncan (B.J.)_   ID Number: _160706_

Sex: ☒M ☐F Age: _70_ Address: _96 S. Main, Cincinnati, OH 45121_

Phone Number: _(512) 555-5555_   Years of Education: _12_ Native Language: _English_

Present/Former Occupation: _Retired farmer_

Examiner's Name: _P. Palison_

Referral Source: _Dr. David Whales_

Date of Onset: _9/20/06_

Hemiparesis:	Side of Hemiparesis:	Severity of Hemiparesis:	Hemianopia (loss of visual field):	Neglect:	Handedness:
☒Yes	☒Right	☐Mild	☒None	☐None	☒Right
☐No	☐Left	☒Moderate	☐Right	☒Right	☐Left
		☐Severe	☐Left	☐Left - _a little_	☐Ambidextrous

Site of lesion (or attach report): _See attached (LCVA)_

Site of lesion established by: ☐CT Scan ☒MRI ☐Other (specify): _____

Contact Person(s): _Marla Duncan (wife)_   Phone Number: _____

Address: _SAME AS ABOVE_

Notes:

General Recording and Scoring Directions

1. Unless otherwise indicated, score 1 point for a correct response and 0 points for an incorrect response.
2. Write NR if the patient does not respond and score as 0.
3. Unless otherwise indicated, the maximum point value for each item is in parentheses in the lower, right-hand corner of the score column.
4. If the patient's response is different from the target, write it verbatim in the space provided.

Figure 3.2 Example of a Completed and Scored WAB–R Record Form Part 1

Chapter 3: Administration and Scoring Directions 39

Spontaneous Speech

A. Conversational Questions   *Materials:* Audio- or Video-tape Recorder (Optional)

Directions: Read the stimulus as written or substitute similar questions as appropriate (e.g., "What *was* your occupation?"). If you substitute a question, write it next to the question replaced.

Repetition: Repeat the question if the patient requests or does not appear to understand.

Recording Responses: Write the patient's response verbatim in the Response column. Place a checkmark (✓) in the Correct or Incorrect columns as appropriate.

Optional: Audiotape or videotape the patient's responses for later review.

Item	Response	Correct	Incorrect
1. How are you today?	50-50	✓	
2. Have you been here before?	No	✓	
3. What is your first and last name? (For incomplete responses, probe for first or last name.)	First Name *Bob* Last Name *Robert*		✓
4. What is your full address? (For incomplete responses, probe for the street, city, or state. No ZIP code is needed.)	Number & Street *96 S. Main St.* City *Cincinnati* State (Country) *OH*	✓	
5. What is your occupation?	*Farmer*	✓	
6. Why are you here (in the hospital)? *or* What seems to be the trouble?	*My wife brought me*		✓

B. Picture Description   *Materials:* Stimulus Book

Directions: Turn to page 1 in the Stimulus Book, and say, **Tell me what is happening in this picture.** If the patient lists single words, say, **Try to talk in sentences.** Ask for a more complete response if he or she produces only a few words. Encourage the patient to pay attention to all aspects of the picture. Move the picture toward the patient's intact visual field if necessary.

Recording Responses: Write the patient's response verbatim.

He's reading a book, car at the house

the girl is pouring, tree

there are shoes, he's running, a dog

2   ✓ Spontaneous Speech

Figure 3.2 Example of a Completed and Scored WAB–R Record Form Part 1 *(continued)*

40   ✓ Western Aphasia Battery-Revised

Scoring Information Content of Spontaneous Speech Tasks A and B

Directions: Circle the point value corresponding to the statement that best describes the information content of the patient's speech on Tasks A and B. Count recognizable phonemic paraphasias as correct.

0 = No information.
1 = Incomplete responses only (e.g., first name or last name only).
2 = Correct response to any 1 item in Task A.
3 = Correct responses to any 2 items in Task A.
4 = Correct responses to any 3 items in Task A.
5 = Correct responses to any 3 of the items in Task A plus some response to the picture in Task B.
6 = Correct responses to any 4 of the items in Task A plus some response to the picture in Task B.
(7) = Correct responses to any 4 of the items in Task A and a mention of at least 6 things in the picture in Task B.
8 = Correct responses to any 5 of the items in Task A and an incomplete description of the picture in Task B.
9 = Correct responses to all items in Task A and an almost complete description of the picture in Task B; at least 10 people, objects, or actions should be named. Circumlocution may be present.
10 = Correct responses to all of the items in Task A and a reasonably complete description of the picture in Task B. Sentences of normal length and complexity, referring to most of the items and activities.

Information Content Score | 7 |

Scoring Fluency, Grammatical Competence, and Paraphasias of Spontaneous Speech Tasks A and B

Directions: Review the point values and corresponding statements. Circle the point value that best represents the fluency, grammatical competence, and occurrence of paraphasias in the patient's speech during Tasks A and B.

0 = No words or short, meaningless utterances.
1 = Recurrent, brief, stereotypic utterances with varied intonation; the emphasis or prosody may convey some meaning.
2 = Single words, often paraphasias, effortful and hesitant.
3 = Longer, recurrent stereotypic or automatic utterances without information, or mumbling.
4 = Halting, telegraphic speech; mostly single words; paraphasias; occasional prepositional phrases; severe word-finding difficulty. No more than two complete sentences with the exception of automatic sentences (e.g., "Oh I don't know."); characteristic of agrammatic, nonfluent aphasia.
5 = Often telegraphic but more fluent speech with some grammatical organization; marked word-finding difficulty. Paraphasias may be prominent; few, but more than two propositional sentences.
6 = More propositional sentences with normal syntactic patterns; may have paraphasias; significant word-finding difficulty and hesitations may be present.
7 = Phonemic jargon with semblance to English syntax and rhythm with varied phonemes and neologisms. May talk excessively; must be fluent; characteristic of severe Wernicke's aphasia.
(8) = Circumlocutory, fluent speech; moderate word-finding difficulty; with or without paraphasias; may have semantic jargon. The sentences are often complete but may be irrelevant.
9 = Mostly complete, relevant sentences; occasional hesitations and/or paraphasias; some word-finding difficulty; near normal, but still perceptibly aphasic.
10 = Sentences of normal length and complexity, without definite slowing, halting, or paraphasias.

Fluency, Grammatical Competence, and Paraphasias Score | 8 |

Spontaneous Speech ✔ 3

Figure 3.2 Example of a Completed and Scored WAB–R Record Form Part 1 *(continued)*

Chapter 3: Administration and Scoring Directions ✔ 41

Auditory Verbal Comprehension

A. Yes/No Questions

Materials: None

Directions: Say, **I'm going to ask you some questions. Answer Yes or No.** If the patient cannot respond consistently verbally or gesturally, train the patient to close his or her eyes to indicate Yes responses. Because aphasics often elaborate and circumlocute, it is particularly important to remind and reinforce the patient to respond Yes or No as requested.

Repetition: Repeat the directions and the question if the patient gives an ambiguous or confabulatory response.

Scoring: Indicate the type of response given by checking (✓) the box in the appropriate column. Score 3 points for each correct response and 0 points for each incorrect (ambiguous or confabulatory) response. If the patient self-corrects, score the last response he or she gives.

Item	Target Response	Verbal	Gestural	Eye Blink	NR	Correct	Incorrect
1. Is your name Smith?	No	✓				③	0
2. Is your name Brown?	No	✓				③	0
3. Is your name ____? (Patient's last name) *Duncan*	Yes	✓				③	0
4. Do you live in ____? (Nearby city/town where patient does not live) *Covington*	No	✓				③	0
5. Do you live in ____? (Patient's city/town of residence) *Cincinnati*	Yes	✓				③	0
6. Do you live in ____? (Another nearby city/town where patient does not live) *Dayton*	No	✓				③	0
7. Are you a man/woman?	Yes	✓				③	0
8. Are you a doctor?	No	✓				③	0
9. Am I a man/woman?	Yes	✓				③	0
10. Are the lights on in this room?	Yes	✓				③	0
11. Is the door closed?	Yes	✓				③	0
12. Is this a hotel?	No	✓				3	⓪
13. Is this ____? (Actual location) *a hospital*	Yes	✓				3	⓪
14. Are you wearing red pajamas?	No	✓				③	0
15. Will paper burn in fire?	Yes	✓				③	0
16. Does March come before June?	Yes	✓				3	⓪
17. Do you eat a banana before you peel it?	No	✓				③	0
18. Does it snow in July?	No	✓				3	⓪
19. Is a horse larger than a dog?	Yes	✓				3	⓪
20. Do you cut the grass with an ax?	No	✓				③	0

(handwritten left margin: personal orientation; environment; more general)

(handwritten right margin: increased linguistic complexity (syntax) but semantically simple)

Yes/No Questions Score [45] (Max = 60)

4 Auditory Verbal Comprehension

Figure 3.2 Example of a Completed and Scored WAB–R Record Form Part 1 *(continued)*

42 Western Aphasia Battery-Revised

B. Auditory Word Recognition *Materials:* Stimulus Book, cup, matches, pencil, flower, comb, screwdriver

Directions: Refer to the specific directions for each set of items (e.g., Items 1–6; Items 7–36).

Repetition: Repeat each item one time if the patient requests or does not respond.

Scoring: Score correct responses as 1 point and incorrect responses as 0 points. If the patient points to more than one choice, score as 0, unless it is clear that the patient is self-correcting.

For Items 1–6, place objects in a random cluster, making sure they are within the patient's intact visual field if hemianopia is present. Say, **Point to the ___,** or **Show me the ___.**

Real Objects	Score
1. Cup	1
2. Matches	1
3. Pencil	1
4. Flower	1
5. Comb	1
6. Screwdriver	1

For Items 7–36, begin with page 2 in the Stimulus Book. Say, **Point to the ___,** or **Show me the ___.**

Pictured Objects	Score
7. Matches	1
8. Cup	1
9. Comb	1
10. Screwdriver	1
11. Pencil	1
12. Flower	1

Forms	Score
13. Square	1
14. Triangle	1
15. Circle	1
16. Arrow *NR*	0
17. Cross	1
18. Cylinder *NR*	0

Letters	Score
19. J	1
20. F	1
21. B	1
22. K	1
23. M	1
24. D	1

Numbers	Score
25. 5	1
26. 61	1
27. 500	1
28. 1867 *NR*	0
29. 32	1
30. 5000 *500*	0

Colors	Score
31. Blue	1
32. Brown	1
33. Red	1
34. Green	1
35. Yellow	1
36. Black	1

→ detect category-specific loss of comprehension

For Items 37–42, if an object is not in the room, substitute a comparable item and note the substituted item. Say, **Point to the ___,** or **Show me the ___.**

Furniture	Score
37. Window	1
38. Chair	1
39. ⊘Desk⊘ Bed	1
40. Light	1
41. Door	1
42. Ceiling	1

Body Parts	Score
43. Ear	1
44. Nose	1
45. Eye	1
46. Chest	1
47. Neck	1
48. Chin	1

Fingers	Score
49. Thumb	1
50. Ring Finger	1
51. Index Finger	1
52. Little Finger *Index finger*	0
53. Middle Finger	1

Gerstmann's Syndrom
parietal lobe + partial angular gyrus lesion
⇒ finger agnosia + R/L confusion

For Items 54–60, the patient must get both the side (right or left) *and* body part correct to receive credit.

Right-Left on Body	Score
54. Right Ear *Lf. ear*	0
55. Right Shoulder	1
56. Left Knee *Rt knee*	0
57. Left Ankle	1
58. Right Wrist	1
59. Left Elbow	1
60. Right Cheek	1

Auditory Word Recognition Score ⟨ 53 ⟩ (Max = 60)

Note. Add the scores for Letters Items 19–24 and transfer the score (Max = 6) to the Letter Discrimination score box on page 5 of Record Form Part 2.

Auditory Verbal Comprehension ⌣ 5

Figure 3.2 Example of a Completed and Scored WAB–R Record Form Part 1 *(continued)*

Chapter 3: Administration and Scoring Directions ⌣ 43

C. Sequential Commands

length kept within WM span!

Materials: Pen, comb, book   *most diff. task within WAB and crucial for Diagnosis*

Directions: Say, **I am going to ask you to do some things.** Read each item.

Repetition: Repeat each item in its entirety one time if the patient requests or appears confused.

Scoring: Score the maximum point value if the patient correctly executes the entire command. If not, score each underlined segment of a multi-part command separately according to the number above the segment.

Item	Score	
1. Raise your hand. [2]	*2*	(2)
2. Shut your eyes. [2]	*2*	(2)
3. Point to the chair. [2]	*2*	(2)
4. Point to the window, [2] then to the door. [2]	*4*	(4)

Arrange the pen, comb, and book (from left to right) on the table in front of the patient. Point to each and say, **See the pen, the comb, and the book? I will ask you to point to them and do things with them. Are you ready?** Proceed to Item 5. If the patient does not understand Item 5 say, **If I ask you to point to the pen with the comb, you would do this...** (demonstrate). Repeat Item 5.

Item	Score	
5. Point to the pen [2] and the book. [2]	*4*	(4)
6. Point with the pen [4] to the book. [4]	*8*	(8)
7. Point to the pen [4] with the book. [4]	*8*	(8)
8. Point to the comb [4] with the pen. [4]	*4*	(8)
9. With the book [4] point to the comb. [4]	*0*	(8)
10. Put the pen [4] on top of the book, [6] then give it to me. [4]	*8*	(14)
11. Put the comb [5] on the other side of the pen [5] and turn over the book. [5]	*5*	(20)

increasing complexity of sequential commands →

Sequential Commands Score **47** (Max = 80)

→ measures auditory comprehension span

6 Auditory Verbal Comprehension

Figure 3.2 Example of a Completed and Scored WAB–R Record Form Part 1 *(continued)*

44 Western Aphasia Battery-Revised

Repetition → *distinguish conduction / transcortical aphasia*

kept within WM span to reduce memory & executive deficits interference!

Materials: None

Directions: Say, **Repeat these words. Say** _____. Present the words in the order listed.

Repetition: Repeat each item one time if the patient requests or does not appear to hear the stimulus.

Scoring: Score the maximum point value if the patient correctly repeats the target word or phrase. Score 2 points for each recognizable word. Deduct 1 point for each phonemic paraphasia (e.g., shindow for window) and each error in word sequence. Give credit for responses that differ due to dysarthria (e.g., slurring), dialectal variations (e.g., winder/window), or word contractions (e.g., "He isn't coming back.").

Verbal Apraxia Rating: Rate phonemic substitutions, stuttering, repetition, segmentation, dysprosody and other features of verbal apraxia as absent, mild, moderate, or severe.

Item	Score	
1. bed	2	(2)
2. nose	2	(2)
3. pipe	2	(2)
4. window	2	(2)
5. banana	2	(2)
6. snowball *slowball*	3	(4)
7. forty-five	4	(4)
8. ninety-five percent	6	(6)
9. sixty-two and a half	4	(10)
10. The pastry cook was satisfied.	10	(10)
11. The telephone is ringing.	8	(8)
12. He is not coming back.	9	(10)
13. delicious freshly baked bread	6	(8)
14. no ifs, ands, or buts	6	(10)
15. Pack my box with five dozen jugs of liquid detergent.	12	(20)

oral agility item

only monosyllabic words

all letters of the alphabet

Repetition Total | 78 | (Max = 100)

Verbal Apraxia Rating:
☒ Absent   ☐ Mild   ☐ Moderate   ☐ Severe

Repetition ❧ 7

Figure 3.2 Example of a Completed and Scored WAB–R Record Form Part 1 *(continued)*

determine severity of aphasia but not

Naming and Word Finding

A. Object Naming

→ *measurement of lexical access*

Materials: Book, ball, knife, cup, safety pin, hammer, toothbrush, eraser, (pad)lock, pencil, screwdriver, key, paper clip, watch, comb, rubber band, spoon, tape, fork, matches

Directions: Present the objects in the order listed. Say, **What is this?** or **What is the name of this object?** If the patient does not respond or responds incorrectly, ask him or her to hold the object (tactile cue) and to tell you what it is. If the patient still does not respond or responds incorrectly, present the first phoneme of the word (phonemic cue), or, if it is a compound word, the first half of the word (semantic cue).

Time Limit: Allow 20 seconds maximum for each item.

Scoring: Score 3 points if the object is named correctly or with a minor articulatory error (e.g., dysarthric slurring) and no cue is needed. Score 2 points if the object name is recognizable, but with a phonemic paraphasia (e.g., "fife" for "knife") and no cue is needed. If a tactile, phonemic, or semantic cue is needed, circle the *T*, the *P*, or the *S* in the Tactile, Phonemic, or Semantic column and score as 1 point. Score an incorrect or no response after cueing as 0 points.

Item	Other Response	Tactile	Phonemic	Semantic	Score			
1. Book		T	P	S	③	2	1	0
2. Ball		T	P	S	③	2	1	0
3. Knife		T	P	S	③	2	1	0
4. Cup		T	P	S	③	2	1	0
5. Safety Pin		T	P	S	③	2	1	0
6. Hammer		T	P	S	③	2	1	0
7. Toothbrush		Ⓣ	Ⓟ	Ⓢ	3	2	1	⓪
8. Eraser		T	P	S	③	2	1	0
9. (Pad)lock		T	P	S	③	2	1	0
10. Pencil		T	P	S	③	2	1	0
11. Screwdriver	*hammer*	Ⓣ	Ⓟ	Ⓢ	3	2	1	⓪
12. Key		T	P	S	③	2	1	0
13. Paper Clip		T	P	S	③	2	1	0
14. Watch		T	P	S	③	2	1	0
15. Comb	*brush*	Ⓣ	Ⓟ	Ⓢ	3	2	1	⓪
16. Rubber Band		T	P	S	③	2	1	0
17. Spoon		T	P	S	③	2	1	0
18. Tape		T	P	S	③	2	1	0
19. Fork	*spoon, knife*	Ⓣ	Ⓟ	Ⓢ	3	2	1	⓪
20. Matches		T	P	S	③	2	1	0

Object Naming Score **48** (Max = 60)

8 ✌ Naming and Word Finding

Figure 3.2 Example of a Completed and Scored WAB–R Record Form Part 1 *(continued)*

46 ✌ Western Aphasia Battery-Revised

type of aphasia!!

B. Word Fluency

*measure of lexical
access + component
of executive system*

*lexical/semantic
fluency*

Materials: None
Directions: Say, **Name as many animals as you can in one minute.** If the patient is hesitant, cue him or her by saying, **Think of a domestic animal like the horse, or a wild animal like the tiger.** After 30 seconds, prompt the patient to continue if necessary.
Scoring: Score 1 point for each unique animal named (except for *horse* or *tiger* if given as an example), even if distorted by phonemic paraphasias.
Recording Responses: Write the patient's responses verbatim on the lines provided below.

cow, horse, pig, ~~cow~~, dog, ~~pat~~,
elephant, birds, ~~cow~~, tiger

Word Fluency Score **7** (Max = 20)

C. Sentence Completion

*contextual setting
automatic lexical
access in over-
learned sentences*

Materials: None
Directions: Say, **Complete what I say. For example, ice is . . .** (cold). Present the test items.
Scoring: Score 2 points if the target response or a reasonable response is given (e.g., Sugar is . . . fattening). Score 1 point for a phonemic paraphasia or off-target alternative responses (e.g., Grass is . . . brown). Score 0 points for an unreasonable response (e.g., Grass is . . . cold).

Item	Target Response	Other Response	Score		
1. The grass is ____.	green		(2)	1	0
2. Sugar is ____.	(sweet)/white		(2)	1	0
3. Roses are red, violets are ____.	blue		(2)	1	0
4. They fought like cats and ____.	dogs		(2)	1	0
5. Christmas is in the month of ____.	December	*May*	2	1	(0)

Sentence Completion Score **8** (Max = 10)

D. Responsive Speech

word fluency in

*near spontaneous
speech but
controlled setting*

Materials: None
Directions: Say, **Answer the following questions.** Present the items.
Scoring: Score 2 points if the target response or a reasonable alternative response is given (e.g., Nurses work in a . . . clinic). Score 1 point for a phonemic paraphasia or off-target alternative responses (e.g., Nurses work in an...office). Score 0 points for an unreasonable response (e.g., Nurses work in a...store).

Item	Target Response	Other Response	Score		
1. What do you write with?	pen/(pencil)		(2)	1	0
2. What color is snow?	white	*NR*	2	1	(0)
3. How many days are in a week?	seven		(2)	1	0
4. Where do nurses work?	hospital	*here*	(2)	1	0
5. Where can you get stamps?	post office/store		(2)	1	0

Responsive Speech Score **8** (Max = 10)

Naming and Word Finding **9**

Figure 3.2 Example of a Completed and Scored WAB–R Record Form Part 1 *(continued)*

Chapter 3: Administration and Scoring Directions **47**

Score Summary Worksheet — Western Aphasia Battery REVISED

Spontaneous Speech | Patient's Score

Information Content: 7 (10) p. 3

Fluency, Grammatical Competence, and Paraphasias: 8 (10) p. 3

Spontaneous Speech Total: 15 (20)

15 (20) **Spontaneous Speech Score** (Use to calculate AQ, LQ, and CQ)

Auditory Verbal Comprehension

A. Yes/No Questions: 45 (60) p. 4

B. Auditory Word Recognition: 53 (60) p. 5

C. Sequential Commands: 47 (80) p. 6

Auditory Verbal Comprehension Total: 145 (200)

÷ 20

7.25 (10) **Auditory Verbal Comprehension Score** (Use to calculate AQ)

÷ 10

14.5 (20) **Auditory Verbal Comprehension Score** (Use to calculate LQ and CQ)

Repetition

Repetition Total: 78 (100) p. 7

÷ 10

7.8 (10) **Repetition Score** (Use to calculate AQ, LQ, and CQ)

Naming and Word Finding

A. Object Naming: 48 (60) p. 8

B. Word Fluency: 7 (20) p. 9

C. Sentence Completion: 8 (10) p. 9

D. Responsive Speech: 8 (10) p. 9

Naming and Word Finding Total: 71 (100)

÷ 10

7.1 (10) **Naming and Word Finding Score** (Use to calculate AQ, LQ, and CQ)

Aphasia Quotient (AQ)

15 (20) Spontaneous Speech Score

7.25 (10) Auditory Verbal Comprehension Score for AQ

7.8 (10) Repetition Score

7.1 (10) Naming and Word Finding Score

37.15 (50)

× 2

74.3 (100) Aphasia Quotient (AQ)

WAB–R Aphasia Classification Criteria

Numbers in the Fluency column represent the Fluency, Grammatical Competence, and Paraphasias score. Numbers in the Auditory Verbal Comprehension, Repetition, and Naming and Word Finding columns represent section scores used to determine the Aphasia Quotient.

Directions: Compare the patient's four scores with the row of scores associated with each aphasia type to determine the WAB–R Aphasia Classification.

Aphasia Type	Fluency	Auditory Verbal Comprehension	Repetition	Naming & Word Finding
Global	<5	0–3.9	0–4.9	<7
Broca's	<5	4–10	0–7.9	<9
Isolation	<5	0–3.9	5–10	<7
Transcortical Motor	<5	4–10	8–10	<9
Wernicke's	>4	0–6.9	0–7.9	<10
Transcortical Sensory	>4	0–6.9	8–10	<10
Conduction	>4	7–10	0–6.9	<10
Anomic	>4	7–10	7–10	<10

Adapted with permission from Kertesz & Poole, 1974, *The Canadian Journal of Neurological Science, 1*(1), 7–16.

AQ = Aphasia Quotient   LQ = Language Quotient   CQ = Cortical Quotient

Figure 3.2 Example of a Completed and Scored WAB–R Record Form Part 1 *(continued)*

48 Western Aphasia Battery-Revised

1.   Getting the data from the scanner and conversion into readable format

1.1.   Project data storage

Data stored on two different servers:

Analysed data: /home/username (30GB with Biostats department) and

Raw data: /data/research/username (100GB with CNS)

Data collection from CNS 3T scanner

ssh –X username@server

cd /home/mri_data/CNSCNSB (CNSCNSA= 1.5T, CNSCNSB = 3T)

cp –r NAME /home/username/studyname/

-r copies all the subfolders

1.2.   Uncompressing and converting DICOM to NIFTI files

cd subject folder/DICOM/subfolder/

Two files should be ending in ~03. Those are the DTI sequences, i.e. 008160.0403.tar.bz2. This identifies that the fourth scan is the DWI series.

bunzip2 008169.0004.tar.bz2

(first set of 30 directions, then second set of 30 directions)

tar –xvf 008169.0004.tar

This produces a series of DICOM files.

In separate window (still UNIX):

cd /home/K0919341/PROG/mricron

./dcm2niigui

Navigate to the previously created folder: File, DICOM to NIFTI, username, study name, subject folder, DICOM, Diffusion folder, first set of directions and repeat for second set of directions, select first DICOM file (000001) and click open.

The first conversion will have 33 directions, the second 34 directions. Both files need to be renamed and moved into a NIFTI folder for further processing: 34 directions=b and 33 directions=a

mv 20100319_102611s004a1001.nii subjectID.nii

cp DTISTROKE05a.nii /home/username/Diffusion/NIFTI_preconcat/

2.   Diffusion tensor imaging pre-processing

2.1.   Concatenate nifty files

In matlab: set path (if necessary): file, set path with subfolders, Users/stephanieforkel/Applications/Exp2Trk/

Or *addpath(' /user/folder/subforlder/programme/',path)*

Select the folder with the two NIFTI files (a,b,) in the left panel

NBL_concat (2, {'name_a.nii', 'name_b.nii'}, {'name_a.bval', "name_b.bval'}, {'name_a.bvec', 'name_b.bvec'}, 1, 0, 'outputname.nii')

NBL_concat: order has to be nii/bval/bvec

NOTE: bval is OK, bvec is broken so it is possible to change the input/output names accordingly but keep bval/bvec identical.

2.2.   Voxel fix (data-dependent)

Collect concatenated files in one NIFTI folder.

Load matlab from home not within the folder:

navigate into the NIFIT concatenated directory

voxelsize_fix

→ Creats: SubjectID_C.nii

2.3.   ExploreDTI

Connect to CNS server ssh –X username@server

In matlab: set path (if necessary): file, set path with subfolders, Users/stephanieforkel/Applications/Exp2Trk/

addpath(' /user/folder/subforlder/programme/',path)

Calculate DTI mat file

Format diffusion weighted data: 4DNIFTI

Permute spatial dimensions: AP RL IS

Flip spatial orientations: AP RL IS

Perform visual check: No

Diffusion tensor estimation: Linear (high speed-low accuracy)

Format diffusion information: text file (*.txt)

Background masking approach: automatic

Permute gradient components: Y X Z

Flip sign of gradient components: X Y –Z (study specific!)

Data processing mode: multiple or single data set

b-vlaue, voxel size, nr B0, nr DWI, matrix size: 1500, 2.4x2.4x2.4, 7, 60, 128x128x60 (study specific!)

Convert raw data to mat file

Input folder: NIFTI_done

Gradient table in DTIinfo/DTISTROKE_60.txt

Output folder: MAT

Check for fibre orientation

Load DTI from MAT and select Y view

Seed around the corpus callosum and Calculate.

Draw and check reconstruction. Ctrl + click closes drawings

If fibre orientation is correct, run for multiple datasets.

→ Creates DTISTROKEXX_C.mat in MAT folder

Motion & Eddy Current corrections and tensor estimation

Plugins, Motion/distortion correction

Change (same window as below):

Tensor estimation =3 (for special subjects set to 5 in V.4.8.1)

Transform DTI to MNI =0

(~ 50min per subject)

→ Creates: subjectID_C_MD_C_E.mat

Tensor-based tracking

Plugins

Whole brain tractography

DTItensor interpolation – high memory needs

Multiple data sets/ single data set

analyse for FA thresholds 15 and 20!

Long computing time (let run over night)

Seedpoint: 2.4x2.4x2.4

Seed FA threshold: 0.2

FA threshold: 0.2 1

MD tracking: 0 0.002

Linear tracking threshold: 0 1

Planar tracking threshold: 0 1

Spherical tracking threshold: 0 1

Fibre length range: 25 500

Angle threshold: 45

Step size: 0.5

Interpolation: 2

Input mat file: CMD_C_E.mat

→ Creates: subjectID _C_MD_C_E.mat & subjectID _C_MD_C_E_tracts.mat

put both in separate folder

Export to TrackVis

matlab

FLA_ExpDti2TrackV(0,1)

Select folder with ~MC_C_E.mat and Tracts.mat

→ Creates a folder with the trk file and all the maps (FA, FA colour, MD/ADC etc)

3.   Lesion Analysis (simple overlay)

3.1.   Lesion size and lesion volume

Lesion size always to be drawn in native space not standaradised. Classically, drawn on a plain structural T1. In our case we need to reslice the aquired coronal SPGRs (T1) into axial slices (see below). Volume of interest (.voi) are then drawn on the re-sliced axial T1.

FSL, BET

Input: concatinated file

Advanced options: tick output binary brain mask

Fraction threshold: 0.5

Robust brain centre estimation → GO

Fslview: check coregistration visually

gunzip and copy

fslstats filename.nii(.gz) –V displays all voxels of the lesion not considering the) voxels (i.e. non touched voxels)

3.2.   MNI normalization of lesion volume

MRICRON

Open: axial_cut_T1

Save: axial_cut_T1.voi convert to .nii with mricron in draw creates binary map

FSL

FLIRT, Utils, Apply FLIRT

Matrix: MNI_T1reg.mat

Input: volume.nii

Ref: normalized

Out: subjectID_lesion_norm.nii

fslmath DTIXX_MNIlesion.nii –bin–div 255 DTIXX_MNIlesion_binarised.nii

-div 255 = divided by 255 as image was between 0-255 but binarised needs to be between 0-1

3.3.   Percentage overlay maps

SPM, fMRI, BATCH, SPM, UTIL, Image Calculator

Input: MNIlesions (n=13)

fslmerge –t tmpbin '$FSLDIR /bin/imglab *.nii.gz'

Concatenates all files together

fslmaths tempbin.nii.gz –Tmean 'percentage.nii'

0.9 – 1	90%
0.75-0.8	75%
0.5 – 0.51	50%
0-1	total overlay 100%

4.   Axial re-slicing of coronal SPGRs (manual)

in PROG

./dcm2nii(sp) –e N –d N –I N –o
/data/research/username/subjectID/DICOM/007986/0009/.dcm(sp) *.dcm*

Produces three files:

co….	=	cut axial SPGR
oo…	=	axial SPGR
oo…210=		?

Re-slice coronal SPGR to axially cut T1

Original zipped DICOM SPGR files

mkdir NIFTI

tar -xjf sequence.tar.bz2 -C ./ NIFTI /

dcm2nii -e N -d N -i N -o 0000.dcm*

or in PROG:

./dcm2nii –e N –d N –I N –o /data/research/username/studyfolder/ subjectID
/DICOM/0007986/SPGR sequence folder/.dcm *.dcm*

Results in a series of DICOMS plus three files:

co0000….nii.gz =		cut axial SPGR
o00000….nii.gz =		axial SPGR
000…210.nii.gz =		coronal SPGR??

Strip T2prop

bet DTISTROKEXX_T2prop DTISTROKEXX_T2prop_stripped -f 0.4 -g 0 -m

Co-register T1 to stripped T2 (affine) and write a matrix only

flirt -in DTISTROKEXX_axial_cut_T1.nii.gz -ref DTISTROKEXX_T2prop_stripped.nii.gz -omat DTISTROKEXX_T2reg_T1.mat -dof 12

Invert matrix

convert_xfm -omat inv_ DTISTROKEXX_T2reg_T1.mat -inverse DTISTROKEXX_T2reg_T1.mat

Register T2 brain mask to axial cut T1 using inverted matrix

flirt -in DTISTROKEXX_T2prop_stripped_mask.nii.gz -ref DTISTROKEXX_axial_cut_T1.nii.gz -applyxfm -init inv_ DTISTROKEXX_T2reg_T1.mat -out DTISTROKEXX_T2reg_toT1_brain_mask

Binarise the registered brain mask

fslmaths DTISTROKEXX_T2reg_toT1_brain_mask.nii.gz –bin bin_DTISTROKEXX_T2reg_toT1_brain_mask.nii.gz

Strip T1 using the binarised T2_brainmask

fslmaths DTISTROKEXX_axial_cut_T1.nii.gz –mul bin_DTISTROKEXX_T2reg_toT1_brain_mask.nii.gz stripped_axial_cut_T1_DTISTROKEXX

fslview filename

MNI normalisation of brain scans

standard_space_roi DTISTROKEXX_axial_cut.nii.gz DTISTROKEXX_axial_cut_brain.nii.gz –b

default is affine

strip T1 again with –f 0.1 and flirt to MNI

5.   Continuous arterial spin labelling

Setting the origin manually on T1s and pCASL.

Segmenting the T1s using the spm clinical toolbox

Co-reg smoothed pCASL to smoothed GM and apply transformation to non-smoothedpCASL:

GM = strtrim('/Users/stephanie/Dropbox/Structural/1/T1_Axial_cut/Orginial

T1/c1DTISTROKE18_axial_cut_T1.nii') %specify target volume (GM)

seg_params = '/Users/stephanie/Dropbox/Structural/1/T1_Axial_cut/Orginial

T1/DTISTROKE18_axial_cut_T1_seg_sn.mat'

pCASL_file = 'CBF_1_18.img' %specify ASL

```matlab
pCASL_dir  = '/Users/stephanie/Dropbox/RAW/1/' %pCASL directory

pCASL=strtrim(strcat(pCASL_dir, pCASL_file));% specify ASL image


tmpl = GM

spm_smooth(tmpl,'GM_temp.nii',[6 6 6]) %create temporary smoothed GM image (6mm
kernel)

vg=spm_vol('GM_temp.nii'); %load temp GM into matlab

flags.regtype='rigid' % specify that registration will be rigid body

f = pCASL

spm_smooth(f,'temp.nii',[6 6 6]); %created smoothed ASL image

vf=spm_vol('temp.nii'); %load smoothed ASL into matlab

[M,scal] = spm_affreg(vg,vf,flags); %register two smoothed images together

M3=M(1:3,1:3); %select the first 3 rows and columns from transformation matrix

[u s v]=svd(M3); %calculate SVD

M3=u*v';

M(1:3,1:3)=M3;

N=nifti(f); %create a new nifti header for ASL image

N.mat=M*N.mat; % apply the translations and rotations

create(N); %write out the registered pCASL as a nifti (same name, only header has
changed)

% apply spatial normalization parameters from segmentat iob

matlabbatch{1}.spm.spatial.normalise.write.subj.matname{1} = seg_params % specify
segmentation params

matlabbatch{1}.spm.spatial.normalise.write.subj.resample{1} = strcat(pCASL,',1'); %specify
image to be normalized

matlabbatch{1}.spm.spatial.normalise.write.roptions.preserve = 0;

matlabbatch{1}.spm.spatial.normalise.write.roptions.bb = [-78 -112 -50

                              78 76 85];

matlabbatch{1}.spm.spatial.normalise.write.roptions.vox = [2 2 2];

matlabbatch{1}.spm.spatial.normalise.write.roptions.interp = 1;

matlabbatch{1}.spm.spatial.normalise.write.roptions.wrap = [0 0 0];
```

```
matlabbatch{1}.spm.spatial.normalise.write.roptions.prefix = 'w'; % new prefix

% use imcalc to mask the brain

matlabbatch{2}.spm.util.imcalc.input{1} = strcat(pCASL_dir,'w',pCASL_file) % first image is
normalized pCASL

matlabbatch{2}.spm.util.imcalc.input{2} = '/Applications/spm8/apriori/brainmask.nii,1' %
specify brain mask

matlabbatch{2}.spm.util.imcalc.output = strcat(pCASL_dir, 'mask_w',pCASL_file); % specify
output (masked) filename

matlabbatch{2}.spm.util.imcalc.outdir = {''};

matlabbatch{2}.spm.util.imcalc.expression = 'i1.*(i2>0.8)'; % multiply pCASL by binarised
brain mask (80% probability of being brain)

matlabbatch{2}.spm.util.imcalc.options.dmtx = 0;

matlabbatch{2}.spm.util.imcalc.options.mask = 0;

matlabbatch{2}.spm.util.imcalc.options.interp = 1;

matlabbatch{2}.spm.util.imcalc.options.dtype = 4;

% smooth the masked images

matlabbatch{3}.spm.spatial.smooth.data(1) = cfg_dep; % configure dependency to grab
output from imcalc

matlabbatch{3}.spm.spatial.smooth.data(1).tname = 'Images to Smooth';

matlabbatch{3}.spm.spatial.smooth.data(1).tgt_spec{1}(1).name = 'filter';

matlabbatch{3}.spm.spatial.smooth.data(1).tgt_spec{1}(1).value = 'image';

matlabbatch{3}.spm.spatial.smooth.data(1).tgt_spec{1}(2).name = 'strtype';

matlabbatch{3}.spm.spatial.smooth.data(1).tgt_spec{1}(2).value = 'e';

matlabbatch{3}.spm.spatial.smooth.data(1).sname = 'Image Calculator: Imcalc Computed
Image: output.img';

matlabbatch{3}.spm.spatial.smooth.data(1).src_exbranch = substruct('.','val', '{}',{2}, '.','val',
'{}',{1}, '.','val', '{}',{1});

matlabbatch{3}.spm.spatial.smooth.data(1).src_output = substruct('.','files');

matlabbatch{3}.spm.spatial.smooth.fwhm = [8 8 8]; %specify smoothing kernel to be applied
to mask_pCASL

matlabbatch{3}.spm.spatial.smooth.dtype = 0;

matlabbatch{3}.spm.spatial.smooth.im = 0;
```

```
matlabbatch{3}.spm.spatial.smooth.prefix = 's';

spm_jobman('run',matlabbatch) %run the batch

clear matlabbatch %clear batch in anticipation of the next subject
```

Remask to include GM only (>30%)

Using spm imcalc expression i1.*(i2>0.3)

Input 1: smoothed masked CBF from step before

Input 2: GM prior from spm

Split MNI mask and binarise

```
fslmaths MNI152_T1_1mm.nii.gz -roi 0 89 0 218 0 182 0 1 R_MNI_mask

fslmaths MNI152_T1_1mm.nii.gz -roi 89 90 0 218 0 182 0 1 L_MNI_mask


foreach i ( *nii.gz )

foreach? fslmaths $i -thr 0.2 -bin 1bit_20_${i}

foreach? echo $i

foreach? end
```

Apply bin split MNI mask to CBF maps

```
matlabbatch{1}.spm.util.imcalc.input = {

                        '/Users/stephanie/Dropbox
(NBLdisk)/RAW/L_R_Split/GM30_1_XX.img,1'

                        '/Users/stephanie/Dropbox
(NBLdisk)/RAW/L_R_Split/1bit_20_L_MNI_mask.img,1'

                        };

matlabbatch{1}.spm.util.imcalc.output = 'LH_GM30_smask_1_XX.img';

matlabbatch{1}.spm.util.imcalc.outdir = {'/Users/stephanie/Dropbox (NBLdisk)/RAW/'};

matlabbatch{1}.spm.util.imcalc.expression = 'i1.*i2';

matlabbatch{1}.spm.util.imcalc.options.dmtx = 0;

matlabbatch{1}.spm.util.imcalc.options.mask = 0;

matlabbatch{1}.spm.util.imcalc.options.interp = 1;
```

matlabbatch{1}.spm.util.imcalc.options.dtype = 4;

Extract globals from segmented GM data and create output

foreach i (LH/RH_GM30_smask thresholded CBF maps)

foreach? echo $i >> $i.txt

foreach? fslstats $i -M>>$i.txt

foreach? end

paste -d , *.txt >> FINAL_SPLIT_BRAIN_PERFUSION.csv

6.   TBSS analysis acute vs. chronic patient data

In a first step all FA maps were zipped (gzip) and saved in a folder "Acute" with all FA maps labelled as "identifier.nii.gz"; same procedure for chronic FA maps (exactly the same name as for acute). The analysis steps then included co-registering the chronic FA maps to the acute maps before subtracting them. The maps were then averaged and the TBSS script available online from the FSL web site was applied.

```
echo "Registering Chronic with Acute FA (linear)"
mkdir temp
mkdir sub
cd Acute
for a in *.nii.gz
do echo $a
cd ..
flirt -in Chronic/$a -ref Acute/$a -out Chronic/Reg_$a -omat temp/2acute_$a.mat -bins 256 -cost corratio -searchrx -90 90 -searchry -90 90 -searchrz -90 90 -dof 6 -schedule /usr/local/fsl/etc/flirtsch/sch3Dtrans_3dof

% NOTE: six degrees of freedom are sufficient as it is a repeated within-subject scan. (3 DOF translation, 6 DOF plus rotation)

echo "Subtracting Chronic with Acute FA (linear)"
fslmaths Chronic/Reg_$a -sub Acute/$a sub/$a

echo "Averaging and masking all FAs"
fslmaths Acute/$a -add Chronic/Reg_$a -div 2 $a
cd Acute
done

echo "TBSS job now"
```

cd ..

tbss_1_preproc *.nii.gz % prepares FA data in TBSS working directory in the right format

tbss_2_reg –T % elastic and affine registration of all FA images into standard space (Oxford template (-T) or own template (-t))

tbss_3_postreg –S % creates mean FA image and skeletonizes it. –S to use study-specific template

tbss_4_prestats 0.2 % projects all subject's FA data onto the mean FA skeleton with

an FA threshold of 0.2

tbss_non_FA sub % L2 in the original script was changed for the folder 'sub' containing all the subtraction maps

echo "TBSS preprocessing finished – be happy the script run and move on to statistical analysis!"

Next step is to define the model.

Glm_gui or alternatively open FSL, MISC, GLM Setup

Number of EVs is equivalent to the number of regressors. In this case I used 5 regressors: EV1: age, EV2: sex, EV3:TPA, EV4: lesion size, EV5: AQ (Chronic-Acute).

Define the model as 'higher level/non-time series design', define the contrasts to be used and save model in TBSS stats folder.

randomise -i all_FA_skeletonise -o tbss -m mean_FA_skeleton_mask -d design.mat -t design.con –n 1000 –T2 -V

Design here is defined as GLMrecovery.mat -t GLMrecovery.con

Number of iterations is set to -n 1000

Given that FSL uses non-paramtric stats the number of iterations can be added. Default is -n 500 however this depends on the data. More details here: http://fsl.fmrib.ox.ac.uk/fsl/fslwiki/Randomise/Theory.

Open FA_mean as background (min 0, max 0.1), add overlay: tbss_tfce_corrp_tstat1

NOTE to express p<0.5, set the min to 0.95 and the max to 1, as fslview does not display the p-value but (1-p-value).

The more regressors one uses the lower the significance drops due to the multiple comparison correction! For example, when adding 5 regressors into the model, the default stats p-value of 0.05 is decided by five rendering the significant level to 0.01. Meaning that we now do not accept variable that are significant at 0.05 but only if they reach the corrected significance level of p=0.01.

n	Confidence limits for p=0.05
100	0.0500 ± 0.0436
1,000	0.0500 ± 0.0138
5,000	0.0500 ± 0.0062
10,000	0.0500 ± 0.0044
50,000	0.0500 ± 0.0019

More info to be found here: http://fsl.fmrib.ox.ac.uk/fsl/fslwiki/FEAT/UserGuide

7.   Export data to local hard drive

Export pre-processed data using FileZilla 3.3.4.1 (http://filezilla-project.org).

8.   UNIX commands used

-r	everything below, i.e. subfolders
-rw	read & write
!(nr)	repeats commands nr=244
??	Matches exactle 2 characters whereas * just matches any length (e.g. DTIstroke??.T1.gz)
./	within current directory or execute command labeled *
Bg	has it run in the background
bunzip *.bz2	Unzip every .bz2 file in given directory
bzip2	zip up to *.bz2
cat name.txt	opens text files (DON'T use with big files)
chmod 777	Activate script (indicated with *)
Ctrl c	stops commands
Ctrl z	suspends commands
df –h	disk free human readable, i.e. check for disk space
fsl_sub	send files to cue and uses all networks (→ very fast ☺)
fslchfiletype	Change file type (e.g. fslchfiletype NIFTI *name*.hdr)
fslstats filename –V	Volume in voxels of ROI (i.e. lesion size)
gzip	zip up to *.gz
history	shows all previous used commands
History >> history.txt	Writes context into file
ls –lh	display authorisations
ls –Ltr	lists files in timely order to find the latest
ls *.voi >> VOI.txt	Lists everything ending in .voi and writes into text files
ls lgrep –v DTISTROKE01	Shows all that is not DTIstroke01
ls lgrep DTISTROKE01	Only show DTIstroke01
Man	manual
pwd	print working directory, i.e. displays current directory
q	quit
qstat	Shows all currently running jobs at a time(r=done, qw=quewe)
rm -r yourdir	Delete directory, icl. subfolders
rm *.*	removes everything
slicesdir –p	Shows overlay
slicesdir 'file'	Visualises files quickly in firefox
unc2analyze	Convert UNC to ANALYZE
x	executable
xdispunc name	To identify different sequences

Education

Post-Doc *Clinical* *Neuroimaging*	**University College London, UK (from Oct 2013)** Multimodal imaging of body awareness after stroke and the psychosocial and neurobiological correlates of anosognosia
PhD *Clinical* *Neuroimaging*	**King's College London, UK (2009-13)** Identification of anatomical predictors of language recovery of stroke-induced aphasia investigated with Diffusion Tensor Imaging (DTI)
MSc *Neuroscience*	**King's College London, UK (2008/9)** Anatomy of the fronto-occipital networks ***Distinction***
Undergraduate *Psychology*	**National University of Ireland (2007/8)** ***First class honours*** **University of Salzburg, Austria (2005-8)** ***Vordiplom 2.2***

G r a n t s

2012	Maudsley Charity (PI: Stephanie Forkel, £10.358)
2011	Hardship fund (£4.000)
	Chaplaincy Discretionary Fund (£200)
2010	University of London teaching initiative funding (£1.000)
2008	MSc/PhD Bursary from the Guy's and St. Thomas's Charity Trust (£60.000)
2007	Denominated Erasmus student for full academic year (€21.000)

H o n o u r s   &   A w a r d s

2013	OHBM Trainee Abstract Award (700$)
	Guarantors of Brain Travel Grant (£800)
	King's College London, Graduate School Conference Fund (£450)
2012	Guarantors of Brain Travel Grant (£800)
	King's College London, Graduate School Conference Fund (£400)
	King's College Sargeaunt Travel Fund (£300)
	American Academy of Neurology nomination for Neurology Highlights in the field (non-monetary award)
2011	Graduate School Conference Fund (£300)
2010	Erasmus Operational Mobility award (£500)
	Guarantors of Brain Travel Grant (£500)
2009	Nominated Master thesis of reference (non-monetary award)

G r a n t s

Memberships

Current   **The British Neuropsychological Society**

The BNS is dedicated to the clinical investigations of patients with neuropsychological impairments and basic cognitive science

Organisation for Human Brain Mapping

The Organization for Human Brain Mapping (OHBM) is the primary international organization dedicated to neuroimaging research.

DAAD UK Network of German Academics

The German Academic Exchange Service (DAAD) is the German national agency for the support of international academic cooperation.

Committee International School of Clinical Neuroanatomy

ISOCN offers a unique opportunity for neurologists, neuroradiologists, psychologists, neurosurgeons and psychiatrists to share their knowledge and integrate complementary approaches to clinical neuroanatomy.

Previous   **American Stroke Association (2011-13)**

The German and Austrian Psychological Societies (2005-07)

Memberships

Publications: Articles under review/in prep

Forkel SJ, Thiebaut de Schotten M, Dell'Acqua F, Kalra L, Murphy D, Williams S, Catani M. Right hemispheric arcuate volume predicts aphasia recovery (submitted to Brain)

Fernández-Andújar M, Thiebaut de Schotten M, **Forkel SJ** et al. Attention and response inhibition: a spherical deconvolution study of the Frontal Aslant Tract (in prep)

Forkel SJ, Thiebaut de Schotten M, Dell'Acqua F, Kalra L, Murphy D, Williams S, Catani M. The anatomy of repetition form a topological and hodological perspective (in prep)

Publications: Peer reviewed Articles

(IF 6.08) Forkel SJ, Thiebaut de Schotten M, Kawadler JM, Dell'Acqua F, Danek A, Catani M. Anatomy of fronto-occipital connections from early blunt dissections to contemporary neuroimaging. *Cortex doi: 10.1016/j.cortex.2012.09.005*.

(IF 6.08) Catani M, Dell'Acqua F, Bizzi A, **Forkel SJ** et al., Beyond cortical localisation in clinico-anatomical correlation. *Cortex*, doi: 10.1016/j.cortex.2012.07.001. 2012

(IF 15.531) Thiebaut de Schotten M, Dell'Acqua F, **Forkel SJ,** et al. A Lateralized Brain Network for Visuo-Spatial Attention. *Nature Neuroscience*, 18;14(10):1245-6. 2011

(IF 6.619) Catani M, Craig M, **Forkel SJ**, et al. Altered integrity of perisylvian language pathways in schizophrenia: relationship to auditory hallucinations. *British Journal of Psychiatry* 15;70(12):1143-50. 2011

Book Chapter

Forkel SJ. Identification of anatomical predictors of post stroke aphasia recovery with DTI. Doctoral dissertation. King's College London, UK. 2013

Catani M, **Forkel SJ**, Thiebaut de Schotten M. Asymmetry of white matter pathways in the brain. In The Two Halves Of The Brain: Information Processing In The Cerebral Hemispheres (Eds, Hugdahl, K & Davidson, RJ). MIT Press. 2010

Forkel SJ. The anatomy of fronto-occipital connections. Master Thesis. King's College London, UK. 2009

Published Conference Contributions

Forkel SJ, Dell'Acqua F, Kalra L, Williams SC, Catani M. Lateralisation of the arcuate fasciculus predicts aphasia recovery at 6 months. *Procedia Social and Behavioral Sciences* 23:164-166. 2011

Forkel SJ, Danek, A, Catani, M. Are direct connections between occipital and frontal lobes unique to the human brain? *Journal of Neurology* 255 (Suppl.2):140-140. 2008

Sürer F, **Forkel S**, et al. Towers of Hanoi and London on a tablet-PC Correlations with other executive tests. *Aktuelle Neurologie* 34:122. 2007

R e v i e w e r

Biological Psychiatry, Neuroradiology, Clinical Anatomy, Cortex, and OHBM conference

V o l u n t e e r i n g

Current **Erasmus co-ordinator for Max-Planck-Institute Leipzig (since 2012) & LMU Munich (since 2010)**

Erasmus allows us to closely work with the MPI Leipzig and the LMU Munich through common workshops and the short-term exchange of academic staff

DAAD UK Network of German Academics (since 2012)

The German Academic Exchange Service (DAAD) is the German national agency for the support of international academic cooperation

NIHR Health Technology Assessment programme (since 2011)

HTA programme is part of the National Institute for Health Research. It produces independent research information about the effectiveness, costs and broader impact of healthcare treatments and tests for those who plan, provide or receive care in the NHS

Committee International School of Clinical Neuroanatomy (since 2011)

ISOCN offers a unique opportunity for neurologists, neuroradiologists, psychologists, neurosurgeons and psychiatrists to share their knowledge and integrate complementary approaches to clinical neuroanatomy (www.isocn.eu)

Chair Clinical Neuroanatomy Seminars (since 2010)

Monthly lecture series highlighting and integrating current topics relevant to clinical neuroanatomy (www.clinicalneuroanatomyseminars.com)

T e a c h i n g

Current **Associate Fellow of the Higher Education Academy (GCAP)**

Graduate Certificate in Academic Practice is the first qualification in academic practice. The programme is mapped against the anticipated UK Professional Standards Framework Standard Descriptor 2 (Fellowship) and is comprised of Enhancing Academic Practice.

Module co-ordinator MSc Neuroscience

The MSc has a specialised module on Neuroimaging and tractography. My responsibilities for this module include: timetabling, lecturing, and student support (2009-13).

SSC Psychiatry Research & Intercalated BSc Cognitive

Neuropsychology

SSC Psychiatry Research aims to introduce medical students to the excitement and challenges of academic research psychiatry (2012).

The aim of the iBSc is to provide medical and dental students with an in-depth, critical understanding of research, theory and empirical findings in core areas of psychology (2010-12).

Diffusion Tensor Imaging (DTI) Workshop

The Natbrainlab is hosting regular practical workshops where delegates learn methodological and practical aspects about diffusion tensor tractography.

Skills & Competencies

Core Skills

Highly structured and organised working style

Solid Data Management background

Solid Data pre-processing, processing and analysing background

Teaching experience in Higher Education and Adult Education

Soft skills

Target oriented team player

Excellent interaction skills with internal & external collaborators

Open-minded and friendly personality

Highly committed, reliable employee

Pro-active approach to problem solving

Clinical training

MRI Safety Training

NIH Stroke Scale – Certification (A+B)

Thrombolysis Training, St. George's Hospital

EEG Attentional Blink and Posner Paradigms

Memory Clinic, LMU Munich Klinikum Grosshadern

NHS & SLaM Mental Capacity & DoLS Awareness Training

Imaging software

FSL, SPM, Matlab, ExploreDTI, Trackvis, Diffusion Toolkit, Mricron, Superlab

References

Academic Supervisor	**Prof. Steve Williams**
	Head of Dept. for Neuroimaging Sciences
	Institute of Psychiatry,
	King's College London, PO89
	SE5 8AF London, UK
	Steve.Williams@kcl.ac.uk
Clinical Supervisor	**Prof. Lalit Kalra**
	Head of Stroke Medicine
	King's College Hospital
	SE5 9RS London, UK
	Lalit.Kalra@nhs.net
Academic Co-Supervisor	**Dr. Marco Catani**
	Senior Lecturer
	Institute of Psychiatry,
	King's College London, PO50
	SE5 8AF London, UK
	Marco.1.Catani@kcl.ac.uk